# Evolutions des systèmes GR*H* et des hormones glycoprotéiques dans les contrôles endocrine et paracrine de la spermatogénèse chez la roussette, Scyliorhinus canicula.

Fabian Jeanne

▶ **To cite this version:**

Fabian Jeanne. Evolutions des systèmes GR*H* et des hormones glycoprotéiques dans les contrôles endocrine et paracrine de la spermatogénèse chez la roussette, Scyliorhinus canicula.. Biologie de la reproduction. Normandie Université, 2024. Français. NNT : 2024NORMC225 . tel-04822856

**HAL Id: tel-04822856**

**https://theses.hal.science/tel-04822856v1**

Submitted on 6 Dec 2024

**HAL** is a multi-disciplinary open access archive for the deposit and dissemination of scientific research documents, whether they are published or not. The documents may come from teaching and research institutions in France or abroad, or from public or private research centers.

L'archive ouverte pluridisciplinaire **HAL**, est destinée au dépôt et à la diffusion de documents scientifiques de niveau recherche, publiés ou non, émanant des établissements d'enseignement et de recherche français ou étrangers, des laboratoires publics ou privés.

Normandie Université

UNIVERSITÉ CAEN NORMANDIE

# THÈSE

**Pour obtenir le diplôme de doctorat**

Spécialité **ASPECTS MOLECULAIRES ET CELLULAIRES DE LA BIOLOGIE**

Préparée au sein de l'**Université de Caen Normandie**

## Evolutions des systèmes GNRH et des hormones glycoprotéiques dans les contrôles endocrine et paracrine de la spermatogénèse chez la roussette, Scyliorhinus canicula.

Présentée et soutenue par

**FABIAN JEANNE**

**Thèse soutenue le 12/11/2024**

devant le jury composé de :

| | | |
|---|---|---|
| M. PASCAL SOURDAINE | Professeur des universités - Université de Caen Normandie (UCN) | Directeur de thèse |
| M. CHRISTELLE DELALANDE-LECAPITAINE | Professeur des universités - Université de Caen Normandie (UCN) | Président du jury |
| MME PASCALE CREPIEUX | Directrice de recherche - CNRS | Membre du jury |
| MME CHARLOTTE LECUREUIL | Maître de conférences HDR - Universite de Tours | Membre du jury |
| M. JEAN-JACQUES LAREYRE | Directeur de recherche - Institut National de Recherche pour l'Agriculture, l'alimentation et l'environnement | Rapporteur du jury |
| M. CHARLES PINEAU | Directeur de recherche - Institut national de la santé et de la recherche médicale | Rapporteur du jury |

Thèse dirigée par **PASCAL SOURDAINE** (Biologie des organismes et ecosystèmes aquatiques (Caen))

ED 497 NBISE
Normande de Biologie Intégrative, Santé, Environnement

BOREA
Biologie des organismes et écosystèmes aquatiques

Normandie Université

# THÈSE

**Pour obtenir le diplôme de doctorat**

**Spécialité Aspects Moléculaires et Cellulaires de la Biologie**

**Préparée au sein de l'université de Caen Normandie**

# Évolution des systèmes GnRH et des hormones glycoprotéiques dans les contrôles endocrine et paracrine de la spermatogenèse chez la roussette, *Scyliorhinus canicula*


**Présentée et soutenue par**
**Fabian JEANNE**


| Thèse soutenue publiquement le 12/11/2024 devant le jury composé de | | |
|---|---|---|
| M. PASCAL SOURDAINE | Professeur des universités, Université de Caen Normandie | Directeur de thèse |
| MME. CHRISTELLE DELALANDE | Professeur des universités, Université de Caen Normandie | Membre du jury |
| MME. PASCALE CRÉPIEUX | Directrice de recherche, CNRS | Membre du jury |
| MME. CHARLOTTE LÉCUREUIL | Maître de conférences, Université de Tours | Membre du jury |
| M. JEAN-JACQUES LAREYRE | Directeur de recherche, INRAE | Rapporteur du jury |
| M. CHARLES PINEAU | Directeur de recherche, INSERM | Rapporteur du jury |

**Thèse dirigée par Pascal SOURDAINE (Biologie des organismes et des écosystèmes aquatiques, BOREA)**

UNIVERSITÉ CAEN NORMANDIE

ED 497 NBISE
Normande de Biologie Intégrative, Santé, Environnement

BOREA
Biologie des organismes et écosystèmes aquatiques

**« *La nature fait les choses sans se presser, et pourtant tout est accompli.* »**

Lao Tseu (李耳)

Le livre de la voie et de la vertu, Tao Tê Ching (道德經), II$^{e}$ siècle avant notre ère

*En hommage à Jean-Paul Rault-Verpre et Louis Jeanne*

## Financeurs et Partenaires

Ces travaux de recherches ont été réalisés au sein de l'école doctorale Normande de Biologie Intégrative, Santé, Environnement (ED 497 NBISE, France) et de la tutelle Université de Caen Normandie du laboratoire de Biologie des ORganismes et Écosystèmes Aquatiques, UMR 8067 (BOREA, France).

Cette thèse a été financée par une allocation doctorale d'établissement (Normandie Université), et les programmes suivants :

« Manche 2021 - Plateformes d'exploitation de ressources marines », Programme opérationnel FEDER/FSE – Région Normandie 2014-2020;

« NeUropeptides et régulation de la spermatogenèse chez un Élasmobranche, la roussette *Scyliorhinus canicula* (Nuée) », Projet fédérateur du Département AVIV 2020 du MNHN;

« RIN Emergent CauSy : Le Système NeuroSécréteur Caudal (SNSC) chez un requin: un rôle essentiel dans l'adaptation physiologique aux changements globaux ? », Région Normandie 2022-2024.

**Nuee**
**NeU**ropeptides and regulation of spermatogenesis in an **E**lasmobranch, the dogfish *Scyliorhinus canicula*

**CauSy**
The **Cau**dal Neurosecretory **Sy**stem of a shark: a key role in physiological adaptation to global change ?

Parmi les animaux utilisés à des fins de recherches, une partie a été capturée en Mer de Manche par le Lycée Maritime et Aquacole de Cherbourg (France) et une autre lors de la campagne CGFS (Channel Ground Fish Survey) de l'IFREMER (France) en 2022. Les animaux ont été maintenus à la station marine de l'Université de Caen Normandie (Centre de Recherches en Environnement Côtier (CREC), Luc-sur-Mer, France). Les installations expérimentales du CREC ont été approuvées par le département de la protection de la population sous le numéro B14384001 (Préfecture du Calvados, France). Un dernier groupe

d’animaux a été obtenu en collaboration avec la Station Biologique de Roscoff (CNRS, Sorbonne Université, France). Les expérimentations réalisées sur les animaux ont été approuvées par le ministère de l'enseignement supérieur et de la recherche sous le numéro APAFIS #43519-2023021509345442 v4.

L’emploi de certaines méthodologies a été permis grâce à des collaborations avec :

la plateforme PROTEOGEN de l’US EMerode, Université de Caen Normandie (France), pour la réalisation d’analyses protéomiques ;

l’UMR 7247 – INRAE 0085 - Physiologie de la Reproduction & des Comportements, CNRS, (France), pour la réalisation de tests fonctionnels en conditions cellulaires *in vitro* avec les financements du GIS FC3R gérés par l’Inserm (France) [numéro de subvention 22FC3R-008] ;

l’INSERM U1086 "ANTICIPE" Unité de Recherche Interdisciplinaire pour la Prévention et le Traitement des Cancers, Centre de Lutte Contre le Cancer Francois Baclesse (France), pour la quantification de stéroïdes par spectrométrie de masse.

# Remerciements

*Comme le veut la coutume, il apparaît être le bon moment et le lieu judicieux pour remercier l'ensemble des personnes qui ont constitué mon entourage professionnel, amical et familial durant ces quelques années de doctorat. Rien qu'à l'idée de remercier toutes ces personnes, je sens l'impossibilité de le faire d'une façon concise. En effet, par bien des aspects, le contexte de cette thèse fut à l'origine des moments les plus intenses et les plus enrichissants de ma jeune existence.*

*Ces remerciements vont débuter par les personnes qui ont bien voulu se pencher sur la lecture et l'évaluation de la pertinence de l'ensemble du travail qui est présenté tout au long de ce manuscrit de thèse. Je tiens donc à remercier en premier lieu les deux rapporteurs de notre travail, le Dr. Jean-Jacques Lareyre et le Dr. Charles Pineau. Le jury de thèse a également la chance de bénéficier des expertises du Dr. Pascale Crépieux, du Dr. Charlotte Lécureuil et du Pr. Christelle Delalande, en qualité de membres examinateurs. Pour finir, c'est avec plaisir que nous accueillons le Dr. Sylvie Dufour et le Dr. Yves Combarnous en tant que membres invités.*

*Ces remerciements vont se poursuivre par la personne qui a rendu possible ces quatre années de travail scientifique, le professeur des universités Pascal Sourdaine. C'est sous sa direction que tout a commencé, dans un contexte où le monde pouvait sembler éteint. En effet, nous avons réalisé mon stage de Master 1 pendant le premier confinement dû à la pandémie de la COVID 19 de 2020. Cette expérience unique m'a montré la pédagogie, la sympathie et l'investissement de Pascal. Je me suis donc naturellement fait cette remarque : je veux travailler avec lui. C'est ainsi que mon stage de Master 2 a débuté sous sa direction, stage qui s'est conclu par l'évaluation des rapporteurs Guillaume Rivière et Pascal Favrel. Une marche importante restait à gravir, celle de l'obtention de l'allocation établissement indispensable au financement du projet de thèse. Le soutien de Pascal concernant la réalisation de la présentation et de l'entraînement aux questions fut indispensable, d'autant que j'avais atteint un niveau de fatigue important puisque c'est en moins de deux semaines que nous avons réalisé la rédaction de mon mémoire de Master 2, préparé la soutenance correspondante puis la soutenance pour l'obtention de la bourse doctorale, cette dernière ayant été montée en moins de 4 jours. C'est alors que nous avons constaté, avec satisfaction, l'obtention de cette allocation. Au sein de mes années de thèse, Pascal a joué un rôle unique, plus proche d'un*

*interlocuteur d'une grande pertinence que d'un directeur au sens strict, au travers de nombreux challenges scientifiques, comme la réalisation de méthodologies riches, complexes et diversifiées, de la mise en place d'un CV, avec la réalisation de formations en vue des futurs postes, de la mise en avant auprès des pairs et pendant les congrès, de la quête de rédactions parachevées, et bien d'autres choses encore. Et c'est pour cette somme de raisons que je considère mon expérience de thèse comme l'expérience la plus enrichissante de ma vie. En effet, ce contexte m'a permis de développer mon esprit critique au travers de la mise en place de raisonnements scientifiques et de leur présentation par des productions manuscrites et orales. Les bienfaits culturels et sociaux furent de même envergure. Par exemple, c'est en thèse que j'ai réalisé mon premier voyage en dehors de la métropole et que j'ai rencontré des personnes de toutes origines, aussi bien européennes, asiatiques que du nouveau monde. Bien sûr, j'ai également rencontré des chercheurs « avec de la bouteille » qui m'ont également abreuvé de conseils et de retours d'expériences que je garde précieusement en tête.*

*Pour continuer, je tiens à remercier le personnel de direction et administratif de BOREA qui joue un rôle central dans le développement de nos projets. Je tiens donc à remercier Céline Gaudin, Catherine Eude, Sandrine Soro et surtout Sylvia Forte, qui a résolu nombre de mes problèmes. Dans cette continuité, je tiens à remercier l'école doctorale EdNBISE, en particulier le Directeur Alain Rincé ainsi que le personnel administratif avec Annie Collin et surtout Sandrine Maviel (du collège des écoles doctorales) qui a su trouver une solution pour la formation obligatoire à l'éthique scientifique.*

*Je tiens également à remercier les membres de mon comité de suivi de thèse qui ont accueilli sympathiquement notre travail et qui n'ont pas hésité à prodiguer des conseils et proposer des discussions enrichissantes. Je pense notamment à Sylvie Mazan qui nous a partagé une base de données très riche et à Hervé Tostivint qui a répondu à toutes mes questions, y compris lors de notre rencontre en congrès. Bien sûr, je remercie également le représentant du CSP, Antoine Ouvrard-Pascaud, et la représentante des Doctorants, Lucie Thorel, à qui je souhaite une bonne continuation.*

*Par ailleurs, la thèse a débuté dans un relatif isolement scientifique dû à la réalisation en duo du projet de thèse, impliquant seulement Pascal et moi. Cependant, pour des raisons méthodologiques, nous avons interagi avec Benoît Bernay et Julien Pontin de la plateforme PROTEOGEN ainsi que Raphaël Delépée et Stéphanie Lagadu de l'unité ANTICIPE. De plus, suite*

*à une présentation au congrès GDR Repro, j'ai eu l'occasion de rencontrer Yves Combarnous, puis Danièle Klett. Pour terminer, à la suite d'une demande de Pascal nous avons sollicité Pascal Favrel et Sylvie Dufour et organisé le recrutement de Stanislas Pilet. Je tiens particulièrement à remercier l'ensemble de ces coauteurs qui ont tous pris avec sérieux nos travaux, qui ont participé avec pertinence, rapidité et sympathie à l'obtention de résultats et à la rédaction des manuscrits. C'est avec un plaisir franc que j'ai vu grandir notre projet, depuis notre huile de coude, à Pascal et moi-même, jusqu'à l'huile de coude de tous ceux qui ont rejoint le bateau de la « couille de roussette » avec entrain, dans un contexte de collaboration très riche d'enseignements pour moi ! Avec un peu plus de détails, les importantes expertises de Pascal Favrel, Sylvie Dufour et de Yves Combarnous ont enrichi nos approches des différentes thématiques, Benoît Bernay a permis la réalisation des approches protéomiques avec un grain de folie qui égaye le quotidien (de MTG au mini-ping sous couvert de blagues à n'en plus finir), et Stanislas Pilet fut d'abord le collègue, et maintenant ami, avec qui j'ai formé un duo pouvant être indépendant, efficient et performant autant que rigolard, joueur de Soccer Random et fin adorateur de la vertigineuse diversité des organismes marins.*

*Nombre de méthodes se sont déroulées en interaction plus ou moins étroites avec le personnel technique que je remercie ici, incluant Marie-Pierre Dubos, et notamment Nadège Villain-Naud qui a été de bonne humeur et de bons conseils pour la réalisation des approches histologiques et d'immunohistochimie.*

*Tout au long de ces trois années, j'ai rencontré un bon nombre de personnes qui me sont toutes restées en tête. En effet, sans trop savoir pourquoi, j'ai toujours aimé discuter, ce qui créait un nombre important de bons souvenirs. En suivant l'ordre chronologique, je tiens à remercier Asrar de m'avoir soutenu lors de mon stage de Master 1, Paul, Céline, Mélissa et Élisabeth avec qui j'ai formé une fine équipe de rigolards pendant mon stage de Master 2, Julie, Émilie et Lorane qui ont juste eu le temps de me donner des conseils avant de quitter le laboratoire, Marie, Élise, Quentin, Baptiste, Amélie et bien sûr Claire qui ont été des amis proches pendant mes premières années de thèse ainsi que Paula, Laura, Élisa, Marine et Rémy qui nous ont rejoints le temps de 4 à 6 mois seulement, Hélène et Anna, Robberto qui est devenu un réel ami pour former un duo qui se soutenait et s'entraînait fréquemment aux fléchettes, je remercie également Maureen de m'avoir accompagné durant ma deuxième année, Morgane et Laurie qui ont égayé notre quotidien et Laurie continue de le faire, bien sûr Natacha et*

*Solène qui sont les meilleures « collègues » de bureau que j'aurais pu avoir, après les tristes départs de Claire et Élise, Sean, une autre Maureen et Victor avec qui je discute depuis plus récemment et qui font vivre le laboratoire, Carine qui était ma collègue de gonade et qui a su apporter un certain nombre d'excellents conseils, Bérénice avec qui j'ai pu partager les joies de travailler sur un modèle requin sous couvert d'une excellente ambiance, et une liste encore longue de stagiaires et contractuels que l'on croise trop peu de temps mais qui font la richesse et la diversité de nos quotidiens. Je tiens donc à tous les remercier pour leur amitié et leur souhaite à tous de réussir à entreprendre ce qu'ils/elles souhaitent !*

*Je tiens également à remercier tous mes groupes d'amis, notamment le Totoro Clan, la compagnie des joyeux lurons et la communauté de la piche parfaite qui, derrière ces noms, cache un grand nombre de personnes qui m'ont tous influencé positivement depuis bien longtemps maintenant. Et voici quelques autres amis qui me sont chers et que je souhaiterais remercier tout particulièrement pour leur présence : Yann, un fin plantologue qui est remercié par son Fabacé préféré, Nathan, un vrai ami de chemin depuis 5 ans maintenant, et bien sûr Charlotte, entre raison et folie, et Erwann, mon colocataire déjanté avec qui je chante et danse beaucoup trop souvent.*

*Évidemment, je remercie ma famille qui est toujours là en support et notamment ma mère, qui est probablement la seule à avoir fait le travail de comprendre ma thématique de recherche, notamment en passant outre la somme colossale de blagues douteuses qui peut en être faite. J'ai une pensée particulière pour elle qui doit encore se demander comment un gamin qui détestait à ce point l'école a pu finir par atteindre le bout d'un des parcours universitaires les plus longs. J'en profite pour embrasser mes toutes jeunes nièces, Anastasia et Camélia. De plus, comme le chien est le meilleur ami de l'homme, j'en profite également pour avoir une pensée vers notre Pitchou familial.*

*Durant cette dernière année de thèse j'ai eu la chance d'être accompagné d'Asrar qui a su composer avec mes prises de paroles interminables sur le caractère féerique de la nature et de sa compréhension.*

*Toutes ces lignes de remerciement correspondent à quelqu'un qui, dans les exigences et les difficultés de la thèse, s'est vraiment bien amusé culturellement, professionnellement, scientifiquement et socialement. Et c'est après avoir présenté cet ensemble riche et dont je suis*

*pleinement satisfait que j'accorde mes dernières pensées à mes grands-pères, Jean-Paul et Louis.*

*Merci à toutes et tous*

# Liste des Abréviations

**2R :** second whole-genome duplication

**3β-HSD :** 3β-HydroxySteroid Dehydrogenase

**17β-HSD :** 17β-HydroxySteroid Dehydrogenase

**20β-HSD :** 20β-HydroxySteroid Dehydrogenase

**3R :** third whole-genome duplication

**ACTH :** AdrenoCorTicotropic Hormone

**Ad1 :** type A1 differentiated spermatogonia

**ADH :** AntiDiuretic Hormone

**ADN :** Acide DésoxyriboNucléique

**ancgphβ :** ancestral glycoprotein hormone beta polypeptide

**ancgthß :** ancestral gonadotropin hormone beta polypeptide

**anctshß :** ancestral thyrotropin hormone beta polypeptide

**APPL1 :** Adaptor protein, Phosphotyrosine interacting with PH domain and Leucine zipper 1

**Apr :** type A paired undifferentiated spermatogonia

**ARC :** ARCuate nucleus

**ARNm :** Acide RiboNucléique messager

**As :** type A single undifferentiated spermatogonia

**Aund :** undifferentiated spermatogonia

**ATP :** Adenosine TriPhosphate

**AVPV :** AnteroVentral PeriVentricular nucleus

**c20S :** Constitutive proteasome

**cAMP/AMPc :** cyclic Adenosine MonoPhosphate

**CB :** Chromatoid Body

**CGβ/CGB :** Chorionic Gonadotrophin Beta

**CGA :** Glycoprotein hormones, alpha polypeptide

**CGH :** Corticotroph-derived Glycoprotein Hormone

**CRH :** Corticotrophin-Releasing Hormone

**CRZ :** CoRaZonin

**CUL3 :** CULlin 3

**CUL4 :** CULlin 4

**CUL4B :** CULlin 4B

**CYP11A :** Cholesterol side-chain cleavage enzyme, mitochondrial

**CYP17 :** Steroid 17-alpha-hydroxylase/17,20 lyase

**D1 :** type 1 iodothyronine Deiodinase

**D2 :** type 2 iodothyronine Deiodinase

**DCAF :** DDB1- and CUL4- associated factor

**DDB1 :** Damage specific DNA Binding protein 1

**DHP :** 5α-DiHydroProgesterone

**E1 :** Estrone

**E2 :** Estradiol

**$EC_{50}$ :** half maximal Effective Concentration

**EL :** Extracellular Loop

**FSHβ (βFSH) :** Follicle-Stimulating Hormone beta polypeptide

**FSH :** Follicle-Stimulating Hormone

**FSHR :** Follicle-Stimulating Hormone Receptor

**GAP :** GnRH Associated Peptide

**GDNF :** Glial cell line-Derived Neurotrophic Factor

**GFRα1 :** GDNF Family Receptor alpha-1

**GH :** Growth Hormone

**GHR :** Growth Hormone Receptor

**GnIH :** Gonadotropin-Inhibitory Hormone

**GnRH :** Gonadotropin-Releasing Hormone

**GnRHR :** Gonadotropin-Releasing Hormone Receptor

**GO :** Gene Ontology

**GPA :** ancestral GlycoProtein hormone Alpha

**GPA2 :** GlycoProtein hormone Alpha 2

**GPB :** ancestral GlycoProtein hormone Beta

**GPB5 :** GlycoProtein hormone Beta 5

**GPHβ :** GlycoProtein Hormone beta polypeptide

**GPH :** GlycoProtein Hormone

**GPHR :** GlycoProtein Hormone Receptor

**GtH :** Gonadotropin Hormone

**GtHR :** Gonadotropin Hormone Receptor

**GRTH :** Gonadotropin-Regulated Testicular Helicase

**hCGR :** human Chorionic Gonadotropin Receptor

**HHG :** axe Hypothalamo-Hypophyso-Gonadique

**HHS :** axe Hypothalamo-Hypophyso-Somatotrope

**HHT :** axe Hypothalamo-Hypophyso-Thyroïdien

**ICC :** ImmunoCytoChemistry

**IGF-I :** Insulin-like Growth Factor 1

**IGF-IR :** Insulin-like Growth Factor 1 Receptor

**IHC :** ImmuHistoChemistry

**IL :** Intracellular Loop

**IP3 :** Inositol triPhosphate

**ISH :** *In Situ* Hybridisation

**KEGG :** Kyoto Encyclopedia of Genes and Genomes

**KNDy :** Kisspeptin, Neurokinine B, and Dynorphin neurons

**KO :** Knock-Out

**LGR :** Leucine-rich repeat-containing G-protein-coupled Receptor

**LHβ (βLH) :** Luteinizing Hormone beta polypeptide

**LH :** Luteinizing Hormone

**LHCGR :** Luteinizing Hormone / ChorioGonadotropin Receptor

**LHR :** Luteinizing Hormone Receptor

**miARN :** micro Acide RiboNucléique

**MSH :** Melanocyte-Stimulating Hormone

**PA28γ :** Proteasome Activator 28γ

**PCR:** Polymerase Chain Reaction

**PKA :** Protein Kinase A

**PL :** PreLeptotene spermatocyte

**PLZF :** Promyelocytic Leukemia Zinc Finger

**PRL :** PRoLactin

**PRP3 :** U4/U6 small nuclear ribonucleoprotein

**PSMA8 :** Proteasome 20S subunit alpha 8

**PSME3 :** Proteasome activator complex subunit 3

**RCPG :** Récepteur Couplé aux Protéines G

**REGɣ :** REGulator complex subunit gamma

**RNP :** RiboNucléoProtéine

**s20S :** spermatoprotéasome

**SCF :** Stem Cell Factor

***sc*X :** protein X of *Scyliorhinus canicula*

**SNRPA1 :** Small Nuclear Ribonucleoprotein Polypeptide A

**StAR :** Steroidogenic Acute Regulatory protein

**T :** Testosterone

**T3 :** Triiodothyronine

**T4 :** Thyroxine

**TM :** TransMembrane alpha-helices

**TMAO :** TriMethylAmine-N-Oxide

**TRα :** Thyroid hormone Receptor alpha

**TRβ :** Thyroid hormone Receptor beta

**TRH :** Thyrotropin-Releasing Hormone / thyréolibérine

**TSHß1 :** Thyroid-Stimulating Hormone beta 1 polypeptide

**TSHβ1a :** Thyroid-Stimulating Hormone beta 1a polypeptide

**TSHβ1b :** Thyroid-Stimulating Hormone beta 1b polypeptide

**TSHß2 :** Thyroid-Stimulating Hormone beta 2 polypeptide

**TSHβ3 :** Thyroid-Stimulating Hormone beta 3 polypeptide

**TSHβ (βTSH) :** Thyroid-Stimulating Hormone beta polypeptide

**TSH :** Thyroid-Stimulating Hormone

**TSHR :** Thyroid-Stimulating Hormone Receptor

**U2A :** U2 small nuclear ribonucleoprotein A

**UBE2G2 :** UBiquitin conjugating enzyme E2 G2

**UBE4B :** UBiquitination factor E4B

**Zone A- :** Zone containing the germinal zone

**Zone A0 :** Zone containing the cysts with spermatogonia

**Zone A :** Zone containing the germinal zone and cysts with spermatogonia

**Zone B :** Zone containing the cysts with spermatocytes

**Zone C :** Zone containing the cysts with round spermatids

**Zone D :** Zone containing the cysts with elongated spermatids

# Table des matières

**Introduction générale ..... 2**

I. Phylogénie des Métazoaires ..... 2

II. Les Chondrichtyens, des Vertébrés à squelette cartilagineux ..... 4

II.1. Généralités ..... 4

II.2. La petite roussette *Scyliorhinus canicula*, un modèle d'étude des Élasmobranches 11

II.3. Vulnérabilité des Chondrichtyens ..... 12

III. La spermatogenèse et les tractus génitaux chez les Vertébrés ..... 16

III.1. Généralités ..... 16

III.2. Les différentes organisations testiculaires ..... 16

III.3. Régulations et coordinations des processus biologiques et des voies de signalisations au niveau testiculaire ..... 22

III.4. Anatomie du testicule et spermatogenèse chez les Élasmobranches ..... 28

III.5. Les tractus génitaux mâles ..... 36

IV. Origines évolutives et approche comparée des axes endocrines cerveaux-hypophyse-testicule impliquant les hormones glycoprotéiques ..... 40

IV.1. Généralités sur les axes cerveau-hypophyse-gonade (HHG) et glande thyroïde (HHT) ..... 40

IV.2. Origine et diversité des GnRHs et de leurs récepteurs chez les Vertébrés ..... 44

IV.3. Un rôle paracrine des GnRHs au niveau testiculaire chez les Vertébrés ..... 49

IV.4. Origine et évolution des hormones glycoprotéiques chez les Vertébrés ..... 50

IV.5. Acquisition, évolution et fonctions de l'axe hypothalamo-hypophyso-gonadique . 56

IV.6. Les tractus génitaux mâles et leurs modulations par les hormones gonadotropes 69

V. Objectifs ..... 70

VI. Annexes de l'introduction générale ..... 76

**Comparative Proteome Analysis of Four Stages of Spermatogenesis in the Small-Spotted Catshark (*Scyliorhinus canicula*), Using High-Resolution NanoLC-ESI-MS/MS .....102**

I. Annexes chapitre I : Données supplémentaires ..... 156

**Characterization of gonadotropins and their receptors in a chondrichthyan, *Scyliorhinus canicula*, fills a gap in the understanding of their coevolution.....170**

I. Annexes chapitre II : Données supplémentaires ..... 228

II. Annexes chapitre II : La folliculogenèse chez *Scyliorhinus canicula* ..... 244

**Pleiotropic signaling of thyrostimulin (GPA2/GPB5) on Glycoprotein Hormone Receptors (FSHR, LHR, TSHR) in the elasmobranch *Scyliorhinus canicula* reproduction .....250**

I. Annexes chapitre III : Données supplémentaires ..... 302

II. Annexes chapitre III : Perspectives et analyses préliminaires ..... 316

**Characterization of a direct endocrine role of GnRHs in testicular regulation in the small-spotted catshark *Scyliorhinus canicula*: a GnRH signaling in the control of spermiogenesis and steroidogenesis in early gnathostomes .....324**

I. Annexes chapitre IV : Données supplémentaires ..... 376

**Discussion générale et perspectives .....392**

II. Caractérisation de processus moléculaires et de voies de signalisation au cours de la spermatogenèse chez *S. canicula* ..... 392

III. Les axes hypothalamo-hypophyso-gonadique et hypothalamo-hypophyso-thyroïdien chez *S. canicula*, une lacune comblée dans l'histoire évolutive des Vertébrés ..... 398

IV. Proposition d'un modèle couplant les régulations endocrine et paracrine de la spermatogenèse chez *S. canicula* : une redondance et/ou une compensation fonctionnelle dans la modulation d'une spermatogenèse relativement indépendante ..... 412

**Conclusion générale.....414**

**Références bibliographiques .....420**

# Table des figures et des tableaux

**Introduction générale**

Fig. 1. Phylogénie des Métazoaires……1

Fig. 2. Arbre phylogénétique des Chondrichtyens indexé sur l'échelle des temps géologiques..3

Fig. 3. Phylogénie mitogénomique bayésienne des chondrichtyens……5

Fig. 4. Bibliométrie : cumule du nombre d'articles publiés par clades de Vertébrés s entre 2000 et 2024……7

Fig. 5. Transitions évolutives entre les modes de reproduction chez les Chondrichtyens……9

Fig. 6. Représentation schématique de la répartition des statuts IUCN associés aux espèces de chondrichtyens, comparaison des évaluations de 2014 et 2021……..13

Fig. 7. Représentation schématique de la spermatogenèse……15

Fig. 8. Représentation schématique des organisations testiculaires de types non cystique (exemple de la souris) et cystique (exemple du poisson zèbre)……17

Fig. 9. Organisation testiculaire chez les Vertébrés……19

Fig. 10. Coupes histologiques de testicules de téléostéens de type restreint et non restreint..21

Fig. 11. Représentation schématique de l'organisation et du devenir des corps chromatoïdes (CB) au cours de la spermiogenèse, exemple de la souris……..25

Fig. 12. Représentation schématique des interactions entre les hormones de croissance et les hormones gonadiques au niveau testiculaire……25

Fig. 13. Représentations schématiques des différentes organisations testiculaires chez les Élasmobranches……27

Fig. 14. Présentation des différents stades de la spermatogenèse chez la petite roussette, *Scyliorhinus canicula*……29

Fig. 15. Morphologie et ultrastructure des spermatozoïdes des raies *R. javanica* et *T. meyeni* ……31

Fig. 16. Système des canaux intratesticulaires, de l'épididyme et de la glande de Leydig du tractus génital mâle chez les Élasmobranches.....33

Fig. 17. Représentation schématique du tractus génital mâle chez différents clades de Vertébrés.....35

Fig. 18. Le tractus génital mâle chez la petite roussette *Scyliorhinus canicula*.....37

Fig. 19. Représentation schématique des axes hypothalamo-hypophyso-gonadique (HHG) et -thyroïdien (HHT), exemple des Mammifères.....41

Fig. 20. Représentation schématique des organisations anatomiques de l'hypophyse.....43

Fig. 21. Représentation schématique du scénario évolutif de la famille des GnRHs chez les Vertébrés.....45

Fig. 22. Représentation schématique de l'évolution des types des récepteurs au GnRH (GnRHR) chez les Gnathostomes.....47

Fig. 23. Représentation schématique des événements de duplications de gènes, de génomes et de perte de gènes liés aux sous-unités des hormones glycoprotéiques.....51

Fig. 24. Répartition des sous-unités des hormones glycoprotéiques identifiées chez des représentant des différents clades de Vertébrés.....51

Fig. 25. Représentation schématique de la structure en nœud cystéine et des sous-unités des hormones glycoprotéiques.....53

Fig. 26. Identification des LGRs et des GPHs chez les Bilatériens.....53

Fig. 27. Représentation schématique de la coévolution des hormones glycoprotéiques et de leurs récepteurs.....55

Fig. 28. Représentation schématique de la structure du FSHR de l'humain.....55

Fig. 29. Représentation schématique de l'évolution des axes neuroendocriniens chez les chordés.....57

Fig. 30. Représentation schématique des fonctions des systèmes GnRHergiques chez les invertébrés.....67

**VI. Annexes de l'introduction générale**

Fig. 1 Testicular transverse section in *Scyliorhinus canicula*……79

Fig. 2 Illustration of the male genital tract in *Scyliorhinus canicula*……79

Fig. 3 Anatomy of testis……81

Fig. 4 Stages of spermatogenesis in *Scyliorhinus canicula*……83

Fig. 5 Ultrastructure of spermatogonia associated to Sertoli cells at stage II……83

Fig. 6 A network of tubules……87

**Comparative Proteome Analysis of Four Stages of Spermatogenesis in the Small-Spotted Catshark (*Scyliorhinus canicula*), Using High-Resolution NanoLC-ESI-MS/MS**

Figure 1. Review of databases considering number of identified proteins, of gene ontologies and Kegg pathways for species regarded as representative of a clade……113

Figure 2. Mapping, using venn diagram, of the 2969 mouse putative homologs proteins obtained by blastp according to the four testicular zones……117

Figure 3. Best 10 hits of gene ontology for the 401 mice putative homologs of the zone A, 146 of the continuum B, 97 of the continuum C and 242 of the zone D……119

Figure 4. Expression patterns of clusters based on the 1284 catshark proteins expressed in all four zones according to testicular zones……121

Figure 5. Best 10 hits of gene ontology for the five clusters, obtained by hierarchical ascending classification with Euclidean distance and ward method for the 1284 catshark proteins found in all four zones……123

Figure 6. Pathway of the catshark proteasome based on mouse putative homologs identification and proteasome pathway (mmu03050)……127

Figure 7. Pathway of the catshark ubiquitin mediated proteolysis based on mouse putative homologs identification and ubiquitin mediated proteolysis pathway (mmu04120)……129

Figure 8. Pathway of the catshark spliceosome based on mouse putative homologs identification and spliceosome pathway (mmu03040)……131

Figure 9. Pathway of the catshark steroidogenesis based on mouse putative homologs identification and ovarian steroidogenesis pathway (mmu04913).....133

**I. Annexes chapitre I : Données supplémentaires**

Figure S1. Histological section of the testis.....158

Figure S2. Overall workflow of proteome analysis.....159

Figure S3. Sample quality control of biological replicates.....160

Figure S4. Principal component analysis of proteins found in all four zones.....161

Figure S5. Venn diagram of proteins identified in the four testicular zones.....162

Figure S6. Blastp results against *C. milii*, *D. rerio*, *G. gallus*, *X. leavis*, *M. musculus*, *H. sapiens*.....163

Figure S7. Analysis of *S.canicula* PA28β-like.....164

**Characterization of gonadotropins and their receptors in a chondrichthyan, *Scyliorhinus canicula*, fills a gap in the understanding of their coevolution**

Figure 1. Synteny and *in silico* analysis of the 3D structures of the GTHs/GTHRs interaction complexes, in *S. canicula*, based on the *H. sapiens* templates.....187

Figure 2. Dose-responses of HEK293T cells co-expressing *sc*GPHR/*hs*G$\alpha_{16}$ induced by recombinant *sc*FSHβ-*sc*CGA (*sc*FSH) or *sc*LHβ-*sc*CGA (*sc*LH).....189

Figure 3. Relative expression profiles of *cga*, *fshβ* and *lhβ* transcripts in different tissues of *S. canicula*.....189

Figure 4. Relative expression profiles of *fshr* and *lhr* transcripts in *S. canicula* tissues focused on the testis (zones A-D), male genital tract and other male and female tissues.....191

Figure 5. Immunocytofluorescence on HEK293T cells expressing *S. canicula gthrs.* HEKT293T cells were transfected with pTarget-*scfshr*, pTarget-*sclhr* or empty pTarget plasmids.....193

Figure 6. Immunohistochemistry and RNA *in situ* hybridization of GTHRs and *gthrs* in *S. canicula* testicular sections.....195

Figure 7. Immunohistochemistry and RNA *in situ* hybridization of FSHR, LHR, *fshr* and *lhr* in *S. canicula* vitellogenic flollicle sections and other organs associated with the male genital tract.....197

Figure 8. A proposed analysis of the co-evolution between gonadotropin hormones, their receptors and gonad structures in vertebrates.....203

**I. Annexes chapitre II : Données supplémentaires**

Table S1. List of the primers used for real-time PCR and *in situ* hybridization.....227

Table S2. Supporting information for the model prediction of *S. canicula*, *C. milii* and *H. sapiens* GTHs/GTHRs interaction complexes.....228

Fig. S1. Validation of the 5SRNA as reference gene for the real-time PCR normalization.....229

Fig. S2. Molecular phylogeny of gnathostomes CGA subunits.....230

Fig. S3. Molecular phylogeny of gnathostomes GTHβ subunits. Identified elasmobranch LHβs and FSHβs are highlighted in blue.....231

Fig. S4. Molecular phylogeny of gnathostomes GTHRs.....232

Fig. S5. Multiple alignment of chondrichthyan CGA subunit protein sequences.....233

Fig. S6. Multiple alignment of chondrichthyan FSHβ and protein LHβ sequences.....234

Fig. S7. Multiple alignment of chondrichthyan FSHR protein sequences.....235

Fig. S8. Multiple alignment of chondrichthyan LHR protein sequences.....236

Fig. S9. In vitro mLTC bioassay. mLTC cells expressing endogeneous murine LH receptors (mLHR), were transfected with *scfshr* then stimulated by scFSH, scLH and scTSH ligands expressed in CHO cells (10µl of 5X concentrated supernatant).....237

Fig. S10. Immunohistochemistry targeting FSHR and *in situ* control in *S. canicula* testicular sections.....238

Fig. S11. *In situ* control in *S. canicula* vitellogenic follicle sections and other organs associated with the male genital tract.....240

**II. Annexes chapitre II : La folliculogenèse chez *Scyliorhinus canicula***

Fig. 1. Le tractus génital femelle chez la petite roussette *Scyliorhinus canicula*……241

Fig. 2. Histologie de l'ovaire et des différents stades folliculaires chez la petite roussette *Scyliorhinus canicula*……241

**Pleiotropic signaling of thyrostimulin (GPA2/GPB5) on Glycoprotein Hormone Receptors (FSHR, LHR, TSHR) in the elasmobranch *Scyliorhinus canicula* reproduction**

Fig. 1. *In silico* characterization of elasmobranchian GPA2 and GPB5……263

Fig. 2. *In silico* characterization of elasmobranchian TSHR and TSHβ2……265

Fig. 3. *In silico* analysis of the 3D structures of *S. canicula, C. milii* and *H. sapiens* TSHβ, GPA2, GPB5 and TSHR……267

Fig.4. Dose-responses of cells expressing *sc*FSHR, *sc*LHR or *sc*TSHR induced by recombinant *sc*GPA2, *sc*GPB5 or single-chain *sc*GPB5-*sc*GPA2……267

Fig. 5. Relative expression profiles of *tshr*, *gpa2*, *gpb5* and *tshβ* transcripts in *S. canicula* tissues with a focus on the male genital tract……269

Fig. 6. Western blot analysis and relative quantification of TSHR in *S. canicula* tissues with a focus in the male genital tract……271

Fig. 7. Immunocytofluorescence on HEK293T cells expressing *S. canicula tshr*. HEK293T cells were transfected with p-target-*Sc-tshr* (HEK293T *tshr*+) or empty plasmids (HEK293T *gphr*-)……271

Fig. 8. Immunohistochemistry and RNA *in situ* hybridization of TSHR, *tshr*, *gpa2* and *gpb5* in *S. canicula* testicular sections……273

Fig. 9. Immunohistochemistry and RNA *in situ* hybridization of TSHR, t*shr*, *gpb5* and *gpa2* in the male genital tract and in vitellogenic follicle of *S. canicula*……275

**I. Annexes chapitre III : Données supplémentaires**

Table S1. List of the primers used for RT-qPCR and *in situ* hybridization……301

Table S2. Supporting information for the model prediction of *S. canicula*, *C. milii* and *H. sapiens* TSHβ, GPA2, GPB5 and TSHR……302

Table S3. Analysis of the supporting information for the model prediction of *S. canicula*, *C. milii* and *H. sapiens* TSHβ, GPA2, GPB5 and TSHR……303

Fig. S1. Validation of the 5sRNA as reference gene for the real-time PCR……304

Fig. S2. Multiple alignment of chondrichthyan TSHβ2 subunit protein sequences……305

Fig. S3. Multiple alignment of chondrichthyan GPA2 and GPB5 protein sequences……306

Fig. S4. Multiple alignment of chondrichthyan TSHR protein sequences……307

Fig. S5. (A1-G2) Immunohistochemistry controls were performed with using the rabbit IgG polyclonal isotype control (human) antibody (1:2000, Abcam, ab37415)……308

Fig. S6. *In situ* control in *S. canicula* vitellogenic follicle sections and other organs of the male genital tract……310

**II. Annexes chapitre III : Perspectives et analyses préliminaires**

Fig. 1. Contrôle de l'homogénéité des réplicats expérimentaux (N = 3)……313

Fig. 2. Analyse protéomique des explants de la zone testiculaire D de *S. canicula* stimulés par les protéines recombinantes *Sc*GPA2, *Sc*GPB5 ou *Sc*GPB5-*Sc*GPA2……315

**Characterization of a direct endocrine role of GnRHs in testicular regulation in the small-spotted catshark *Scyliorhinus canicula*: a GnRH signaling in the control of spermiogenesis and steroidogenesis in early gnathostomes**

Fig. 1. A schematic diagram showing the evolution model of GnRHs orthologs……337

Fig. 2. *In silico* characterization of elasmobranch GnRHRs and GnIH……339

Fig. 3. Relative expression profiles of *gnrh1*, *gnrh2* and *gnrh3* transcripts in *S. canicula* tissues with a focus on stages of spermatogenesis……341

Fig. 4. Relative expression profiles of *gnrhrI1*, *gnrhrIIb2*, *gnrhrIIa1* and *gnrhrIIa2* transcripts in *S. canicula* tissues with a focus on stages of spermatogenesis……343

Fig. 5. *In situ* hybridization of *gnrhrI1* and *gnrhrIIb2* mRNAs in *S. canicula* testicular sections……..345

Fig. 6. Proteomic analysis of *S. canicula* testicular zone D explants stimulated with 0 nM, 10 nM or 100 nM of ScGnRH2 or ScGnRH3……347

Fig. 7. Expression analyses of *ghr*, *17ϐhsd3* and *17ϐhsd12* transcripts in spermatogenesis stages……..351

**I. Annexes chapitre IV : Données supplémentaires**

Table S1. List of the primers used for real-time PCR and *in situ* hybridization……373

Table S2. Data on steroids assayed by LC-HRMS……374

Fig. S1. Validation of the 5sRNA as reference gene for the real-time PCR……375

Fig. S2. Molecular phylogeny of gnathostomes GnRHs and GnRHRs……376

Fig. S3. *In situ* hybridization controls were performed using sense riboprobes of *gnrhrI1* (A1-F1) and *gnrhrIIb2* (A2-F2)……378

Fig. S4. *In situ* hybridization controls were performed using sense riboprobes of *ghr* (A1-F1), *17ϐhsd3* (A2-F2) and *17ϐhsd12* (A3-F3)……..380

**Discussion générale et perspectives**

Fig. 31 Représentation schématique de la dynamique du protéome testiculaire de *S. canicula*, en fonction des stades de la spermatogenèse……389

Fig. 32 Représentation schématique des axes neuroendocrines chez la roussette *S. canicula*……393

Fig. 33 Représentation schématique de l'axe hypophyso-tractus génital mâle chez *S. canicula*……399

Fig. 34 Représentation schématique de la régulation paracrine GPA2/GPB5 au niveau du tractus génital mâle chez *S. canicula*……405

Fig. 35 Proposition d'un modèle de régulation de la spermatogenèse couplant les régulations endocrine et paracrine au cours de la spermatogenèse chez *S. canicula*…… 407

# Introduction générale

# Introduction générale

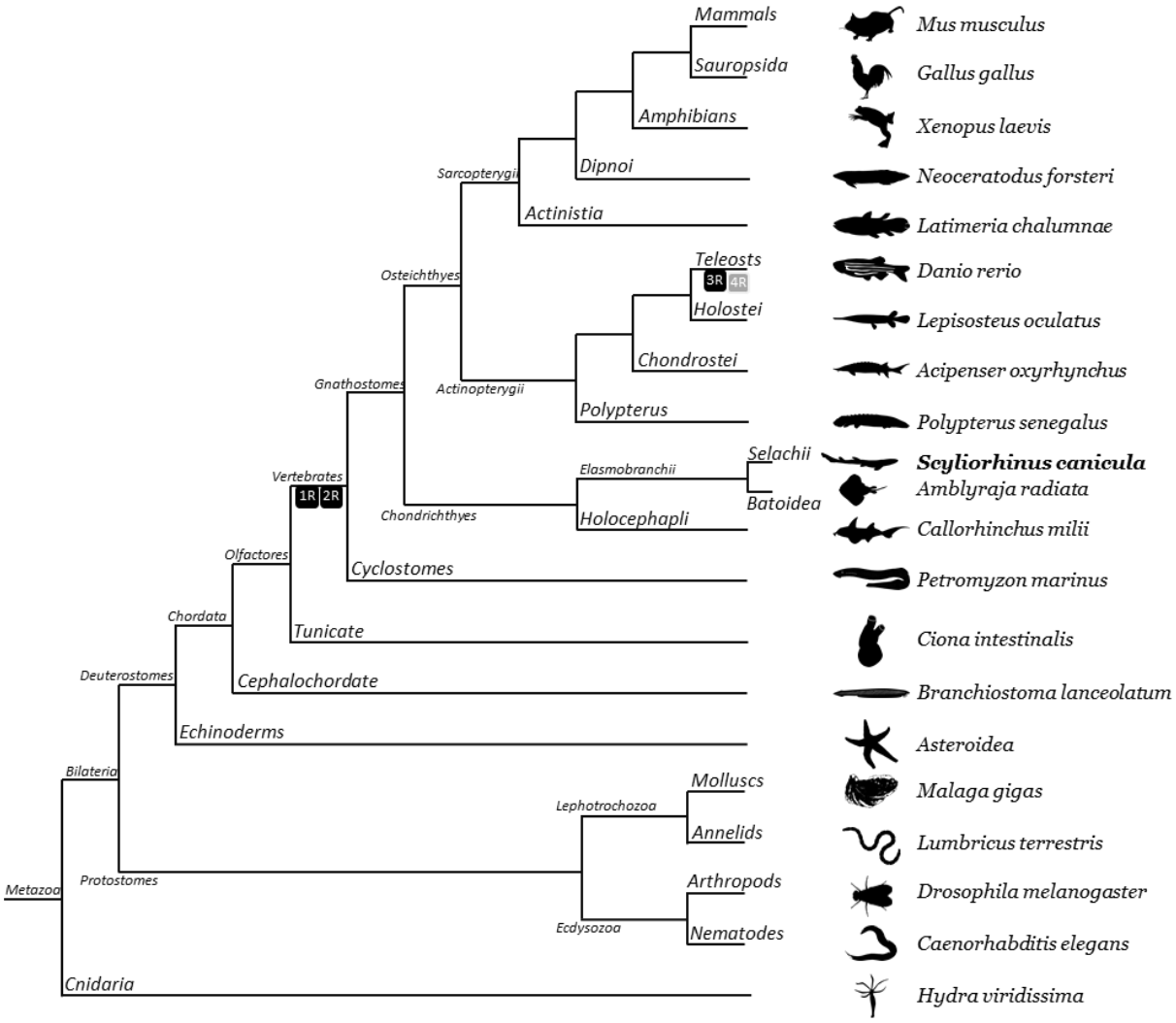


Fig. 1. **Phylogénie des Métazoaires.** Les Cnidaires représentent le groupe le plus basal des Métazoaires. Parmi les Bilatériens, les Protostomiens sont le clade frère des Deutérostomiens et se subdivisent en deux clades que sont les Lophotrochozoaires (Annélides, Mollusques, …) et les Ecdysozoaires (vers plats, insectes, crustacés, …). Au niveau des Deutérostomiens, les Tuniciers sont considérés comme le clade frère des Vertébrés qui regroupe les Chondrichtyens (Vertébrés à squelette cartilagineux avec les chimères, les raies et les requins) et les Ostéichtyens (Vertébrés à squelette osseux). Le clade des Ostéichtyens est subdivisé en deux groupes, celui des Actinoptérygiens (Cladistiens, Chondrostéens, Ginglymodes, Halécomorphes, Téléostéens) et des Sarcoptérygiens (Cœlacanthe, amphibiens, oiseaux, Mammifères, …). Au cours de l'évolution, deux duplications globales du génome (1R et 2R) ont eu lieu à la base de la lignée des Vertébrés. Une troisième duplication globale du génome (3R) s'est produite à la base de la lignée des Téléostéens et une quatrième (4R) s'est produite à la base de la lignée des Salmonidés. Les illustrations d'animaux sont utilisées avec l'autorisation de http://phylopic.org. Communication personnelle.

# Introduction générale

## I. Phylogénie des Métazoaires

La caractérisation des systèmes neuroendocrines impliqués dans la régulation de la reproduction au niveau de groupes phylogénétiques peu étudiés est un axe de recherche à part entière. Les données obtenues par l'étude d'une espèce modèle peuvent être extrapolées aux autres espèces du même clade et être inclues dans un contexte évolutif. Ce type d'approche permet d'appréhender l'histoire évolutive des systèmes, de leur émergence à la mise en place des structures les plus complexes. Afin de présenter les différentes données issues de la bibliographie sous forme d'une approche comparée et évolutive, il apparait nécessaire de présenter l'arbre phylogénétique des Métazoaires. Les Métazoaires regroupent les Cnidaires (anémones, méduses et coraux) et les Bilatériens (Fig. 1). Les Bilatériens sont le principal clade des Métazoaires et rassemblent des espèces à symétrie bilatérale (au moins au stade embryonnaire) et à trois couches de tissus embryonnaires (endoderme, mésoderme, ectoderme), d'où leurs appellations de triploblastiques. Les Bilatériens sont subdivisés en deux clades majeurs, celui des Deutérostomiens comprenant les Chordés (Céphalochordés, Tuniciers et Vertébrés) et celui des Protostomiens comprenant les larges groupes des Ecdysozoaires (vers plats, insectes, crustacés, …) et des Lophotrochozoaires (annélides, mollusques, …) (Nosenko et al., 2013). Les Vertébrés, quant à eux, regroupent plusieurs groupes d'espèces dont le groupe le plus basal est celui des Cyclostomes (anciennement Agnathes), regroupant les lamproies et les myxines. Ce dernier est le clade frère des Gnathostomes qui est caractérisé par un ensemble d'innovations évolutives incluant notamment une mâchoire complète. Les Gnathostomes regroupent les Vertébrés à squelette cartilagineux (Chondrichtyens) et à squelette osseux (Ostéichthyens) dont la divergence s'est produite il y a environ 450 millions d'années (Irisarri et al., 2017). Les Chondrichtyens regroupent les Holocéphales (chimères) et les Élasmobranches (raies et requins). Les Ostéichthyens sont divisés en Actinoptérygiens et Sarcoptérygiens. Les Actinoptérygiens regroupent les « poissons » à nageoires rayonnées avec, dans l'ordre évolutif, les Cladistiens, les Chondrostéens, les Ginglymodes, les Halécomorphes et les Téléostéens. Les Téléostéens constituent le plus grand groupe d'Actinoptérygiens et de Vertébrés avec plus de 25 000 espèces répertoriées. Les Sarcoptérygiens comprennent les « poissons » à nageoires charnues

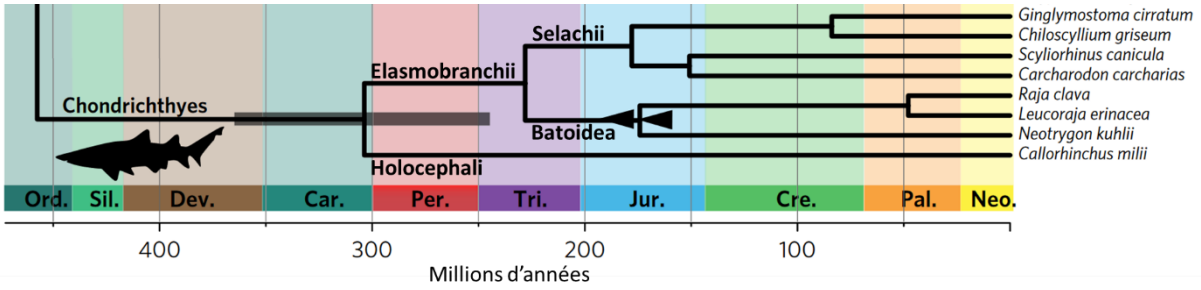


Fig. 2. **Arbre phylogénétique des Chondrichtyens indexé sur l'échelle des temps géologiques.** Les principales périodes géologiques sont mises en évidence. La divergence entre les Holocéphales et les Élasmobranches a eu lieu il y a environ 300 millions d'années. Un exemple d'espèce est indiqué pour chaque clade. La divergence entre les *Selachii*, représentés par le requin nourrice *Ginglymostoma cirratum*, le requin-chabot *Chiloscyllium griseum*, la petite roussette *Scyliorhinus canicula* et le grand requin blanc *Carcharodon carcharias*, et les *Batoidea*, représentés par la raie bouclée *Raja clava*, la raie hérisson *Leucoraja erinacea* et la raie pastenague *Neotrygon kuhlii*, a eu lieu il y a environ 225 millions d'années. Car., carbonifère ; Cre., crétacé ; Dev., dévonien ; Jur., jurassique ; Neo., néogène ; Ord., ordovicien ; Pal., paléogène ; Per., permien ; Sil., silurien, Tri., trias. Modifié d'après Irisarri et al., 2017.

(Actinistiens), les « poissons » pulmonés (Dipneustes) et les Tétrapodes regroupant les Sauropsidés (Amphibiens, Aves et « reptiles ») et les Mammifères (Irisarri et al., 2017). Cette organisation phylogénétique illustre le caractère paraphylétique du terme « poisson » qui regroupe des espèces d'appartenance phylogénétique très distincte. L'usage du terme « poisson » est donc impropre en l'absence de précision d'ordre phylogénétique. Par l'utilisation de cette vision large de la phylogénie, il est possible d'appréhender l'origine et l'évolution des systèmes endocrines qui sont des innovations évolutives au fondement de la mise en place de nouvelles communications intercellulaires « longues distances » au sein d'individus pluricellulaires.

## II. Les Chondrichtyens, des Vertébrés à squelette cartilagineux[1]

### II.1. Généralités

L'émergence des Gnathostomes a marqué un événement majeur dans l'évolution des Vertébrés. Cette transition s'est accompagnée de nombreuses innovations morphologiques et physiologiques telles qu'une mâchoire complète, des appendices pairs, un système immunitaire acquis et une diversification couplée à une spécialisation d'acteurs hormonaux comme les hormones glycoprotéiques (Buechi and Bridgham, 2017). Comment ces nouveautés sont-elles apparues et comment ont-elles facilité la divergence, l'adaptation et la domination des Gnathostomes en tant que principal groupe (99,9 %) de Vertébrés vivants ? Ces questions essentielles restent ouvertes (Venkatesh et al., 2014). De par la position phylogénétique clef des Chondrichtyens, à la fois à la base des Gnathostomes et comme clade frère des Vertébrés osseux, leur étude constitue une base essentielle à l'exploration des phénotypes qui leur sont propres et permettra de donner un aperçu de l'état ancestral des caractéristiques morphologiques et des systèmes physiologiques spécifiques aux Gnathostomes (Venkatesh et al., 2014).

[1] Ce chapitre s'inspire en partie du chapitre d'encyclopédie suivant : Sourdaine and Jeanne, 2024 (Annexe I)

Le groupe des Chondrichtyens est une lignée de Vertébrés aquatiques dont l'origine remonte à la limite entre les périodes géologiques silurienne et dévonienne, il y a environ 450 millions d'années (Amaral et al., 2018). Cependant, les formes contemporaines des Chondrichtyens

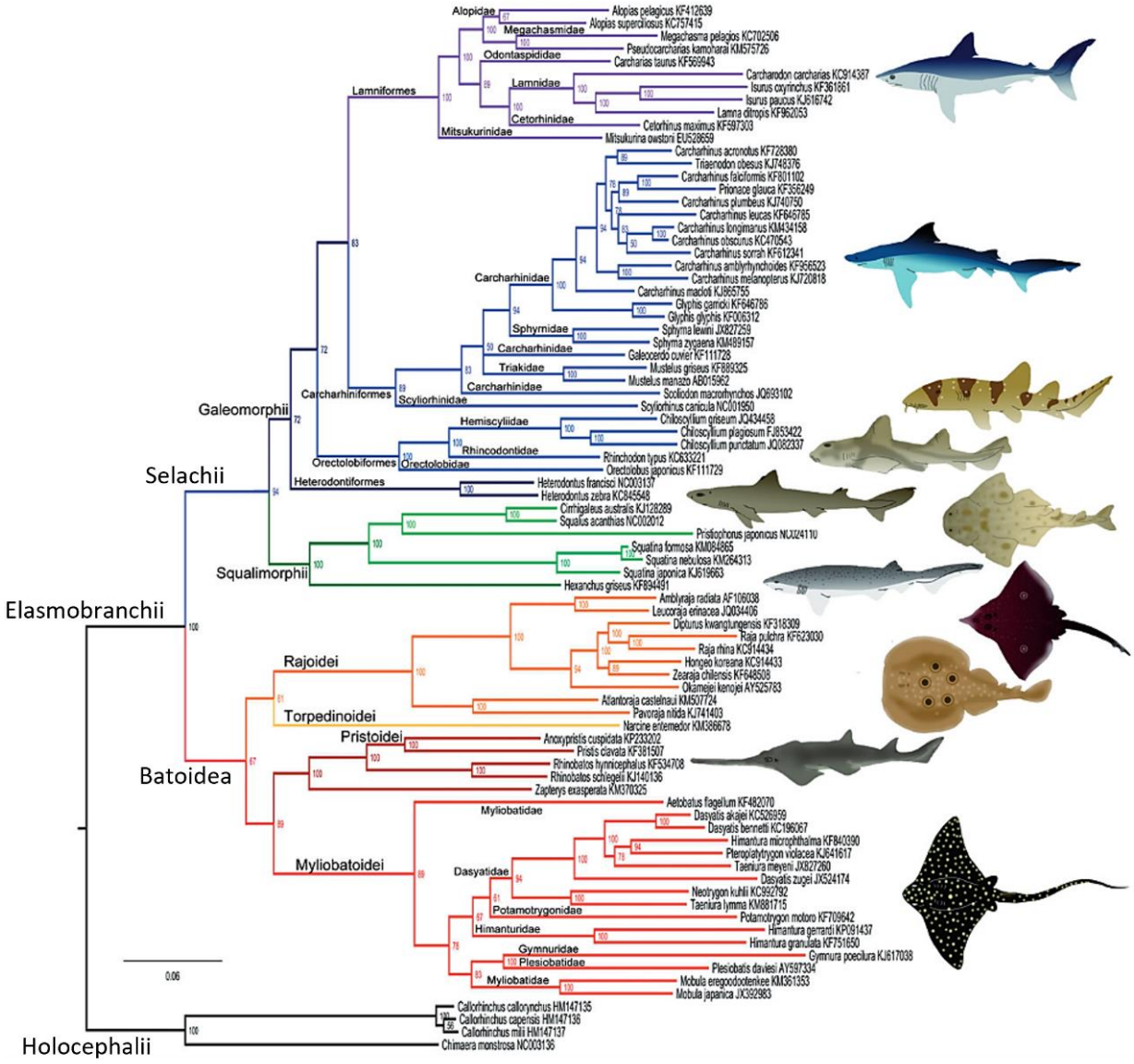


Fig. 3. **Phylogénie mitogénomique bayésienne des Chondrichtyens.** Les différents ordres sont mis en avant par des couleurs différentes. Les probabilités *a posteriori* sont représentées au-dessus des nœuds. Modifié d'après Amaral et al., 2018.

remonteraient au Jurassique (Leuzinger et al., 2017). Aujourd'hui, ce groupe est le second groupe de Vertébrés aux origines les plus anciennes et pourrait être le plus diversifié sur le plan écologique, avec des représentants répartis dans les océans, les mers et les eaux intérieures du monde entier (Dulvy et al., 2014 ; Weigmann, 2016). La divergence entre les Holocéphales (chimères) et les Élasmobranches (requins et raies) se serait produite très tôt à la base de l'arbre des Chondrichtyens, il y a environ 300 millions d'années (Fig. 2) (Irisarri et al., 2017). Les Chondrichtyens regroupent environ 1477 espèces dont 96% sont des Élasmobranches tandis que les Holocéphales constituent un groupe moins diversifié, avec 57 espèces (Fricke et al., 2024) (Fig. 3). Au sein des Élasmobranches, les Batoïdes constituent le groupe le plus important (environ 800 espèces regroupées en 23 familles) avec une grande variété d'habitats et une importante diversité morphologique et anatomique. Le terme "raie" est un terme générique qui englobe une variété d'espèces telles que les pocheteaux (skates), les mantas, les poissons-guitares, les poissons-scies et les raies pastenagues, entre autres. D'autre part, le groupe des *Selachii* englobe toutes les espèces de requins (environ 600 espèces regroupées en 35 familles), allant des espèces les plus grandes, tel le requin-baleine *Rhyncodon typus* (18 m), aux requins les plus petits, tel le requin Sagre *Etmopterus perryi* (20 cm), avec des espèces emblématiques tel le requin-marteau *Sphyrna tiburo* capable de parthénogenèse accidentelle (Chapman et al., 2007) ou le requin du Groenland *Somniossus microcephalus* dont la longévité est proche de 400 ans (Nielsen et al., 2016).

Les Chondrichtyens sont caractérisés par deux synapomorphies distinctives : la minéralisation de leur squelette et la présence d'organes copulateurs mâles (Nelson et al., 2016). Le terme Chondrichtyens, qui signifie littéralement poisson cartilagineux (du grec classique khóndros, cartilage et ikhthús, poisson), fait référence à leur nature aquatique et à leur endosquelette cartilagineux, par opposition à l'endosquelette osseux de la plupart des Vertébrés (Hall, 2005). Le mode de minéralisation de ce squelette est précisément la synapomorphie qui définit le groupe, avec des structures calcifiées polygonales appelées tessères qui renforcent l'endosquelette, lui conférant des qualités mécaniques uniques (Seidel et al., 2016). La deuxième synapomorphie correspond à une modification de l'endosquelette de la ceinture pelvienne en ptérygopodes, ou claspers, qui permettent le transfert du sperme dans l'oviducte des femelles au cours de l'accouplement (Grogan et al., 2012; Jones et al., 2005). Il a été récemment proposé que la diversité morphologique des ptérygopodes, importante

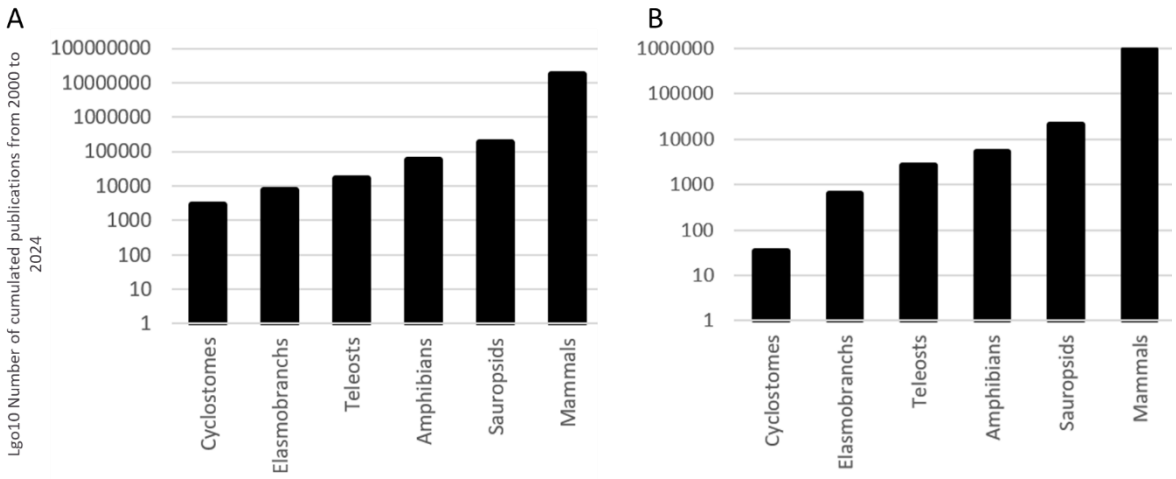


Fig. 4. **Bibliométrie : cumule du nombre d'articles publiés par clades de Vertébrés entre 2000 et 2024. A.** Dénombrement des articles recherchés avec les termes *Cyclostome*, *Elasmobranch*, *Teleost*, *Amphibian*, *Reptile* et *Bird*, et *Mammal*. **B.** Dénombrement des articles recherchés avec les termes précédents cumulés avec le terme *Reproduction*. Cette analyse a été réalisée sur la base de données NCBI (https://www.ncbi.nlm.nih.gov/). Communication personnelle.

notamment chez les Scyliorhinidés, pourrait être utilisée dans les études phylogénétiques des Chondrichtyens (Soares, 2020). Le développement de ces claspers est dépendant d'une régulation androgénique stimulant la voie de signalisation *Sonic hedgehog* chez la raie *Leucoraja erinacea* (O'Shaughnessy et al., 2015). Les requins possèdent plusieurs autres caractéristiques anatomiques notables comme la présence d'écailles placoïdes, d'orifices des canaux endolymphatiques des oreilles internes à l'arrière des évents, et d'ampoules de Lorenzini qui contiennent des cellules sensorielles pourvues de récepteurs électromagnétiques localisées sur la tête. Les Élasmobranches présentent également des particularités physiologiques comme une forte concentration en urée dans le sang, contribuant au maintien d'une pression osmotique élevée d'environ 900 mOsm/kg, et son effet toxique est compensé par la synthèse endogène de TMAO (trimethylamine-N-oxide) (Laxson et al., 2011). Les caractéristiques physico-chimiques du plasma sanguin ont été prises en compte pour la mise au point d'un milieu de culture spécifique appelé « milieu de Gautron » (Gautron, 1978; Loir and Sourdaine, 1994). Les Élasmobranches possèdent également un système immunitaire acquis complexe basé sur l'expression lymphocytaire d'une grande diversité de récepteurs aux antigènes (Boehm, 2011) et présentent des immunoglobulines (Ig) de type IgM, IgW et IgNAR (*new antigen receptor*). Ces dernières, par leur petite taille, leur résistance à la dénaturation et leur capacité à reconnaitre plusieurs épitopes avec une haute affinité, sont aujourd'hui au cœur du développement de différentes biotechnologies (Matz and Dooley, 2019).

Malgré leur position phylogénétique clef et leur importance écologique, les études sur les Chondrichtyens demeurent sous-représentées dans la littérature. Une analyse bibliométrique rapide de la base de données NCBI (https://www.ncbi.nlm.nih.gov/genome/) a mis en évidence la fraction très faible de publication contenant le terme « *elasmobranch* », avec environ 7 500 publications sur la période 2000-2024 (représentant 0,04% du nombre total de publication dénombré), par comparaison aux autres groupes de Vertébrés Sarcoptérygiens, avec pas moins de 56 000 publications dénombrées (Fig. 4A). Si le terme « *reproduction* » est cumulé aux termes correspondant aux différents groupes de Vertébrés, seulement 632 publications (représentant 0,07% du nombre total des publications dénombrées) ont été associées aux Élasmobranches, par comparaison aux autres groupes de Vertébrés Sarcoptérygiens où 2 556 publications ont été associées aux poissons téléostéens, 5 273 aux

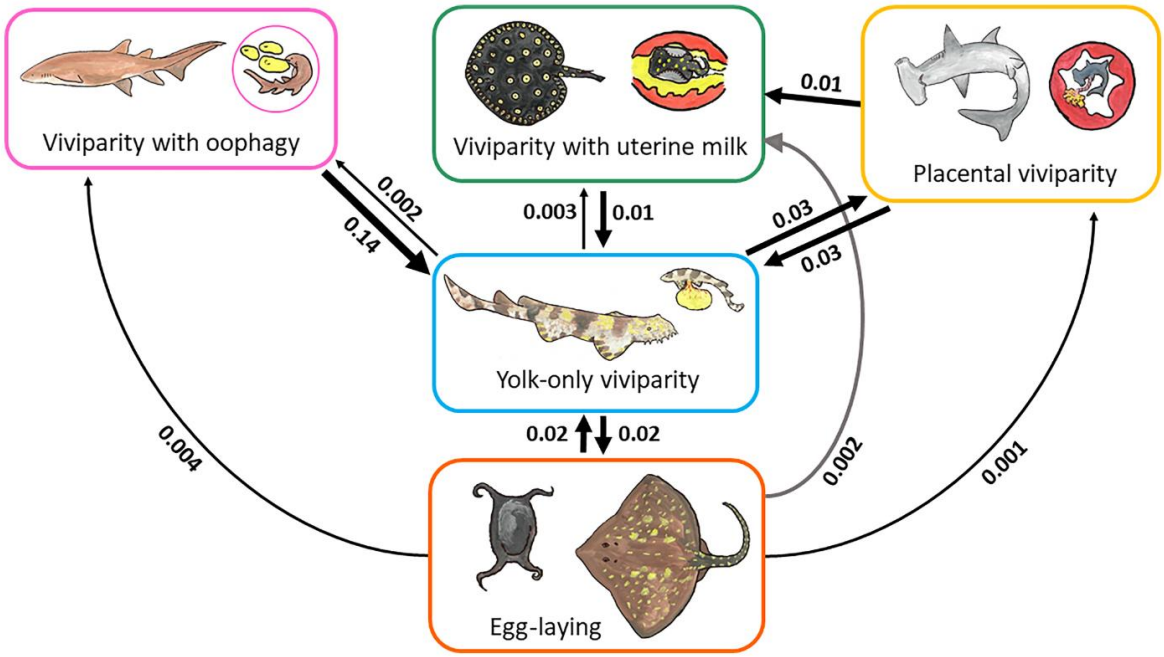


Fig. 5. **Transitions évolutives entre les modes de reproduction chez les Chondrichtyens.** Les nombres représentent les fréquences relatives de transition d'un mode de reproduction à un autre pour chaque transition de mode de reproduction observé dans l'arbre phylogénétique des Élasmobranches (le nombre de transitions d'un mode de reproduction à un autre a été divisé par le nombre d'occurrences de l'état initial). Modes de reproduction et espèces illustrées : oviparité, raie bouclée (*Raja clavata*, Rajidae) ; viviparité lécithotrophe, Requin-tapis paste (*Orectolobus ornatus*, Orectolobidae), viviparité oophage, requin-nourrice fauve (*Nebrius ferrugineus*, Ginglymostomatidae) ; viviparité histotrophe, raie du fleuve Xingu (*Potamotrygon leopoldi*, Potamotrygonidae) ; viviparité placentaire, requin-marteau lisse (*Sphyrna zygaena*, Sphyrnidae) (Katona et al., 2023).

Amphibiens, 20 663 aux Sauropsidés et 926 990 aux Mammifères (Fig. 4B), ce qui illustre la méconnaissance de la physiologie de la reproduction des Élasmobranches. Cependant, des avancées récentes ont amené à la publication de génomes séquencés et assemblés, à commencer par celui de la chimère éléphant *Callorhinchus milii* (Venkatesh et al., 2014), puis du requin bambou *Chiloscyllium punctatum*, de la roussette nuageuse *Scyliorhinus torazane*, du requin-baleine *Rhincodon typus* (Hara et al., 2018) et du grand requin blanc *Carcharodon carcharias* (Marra et al., 2019). Ces publications constituent des bases essentielles à la réalisation d'approches « -omiques » qui ont exploré les transcriptomes de plusieurs tissus et organes de la roussette nuageuse *Scyliorhinus torazame* (Hara et al., 2018), du requin épineux *Squalus acanthias* (Chana-Munoz et al., 2017) et de la petite raie *Leucoraja erinacea* (Wang et al., 2012) ainsi que les protéomes du plasma sanguin du requin nourrice *Ginglymostoma cirratum* (Bakke et al., 2022) et du plasma séminal et des spermatozoïdes de la petite roussette *Scyliorhinus canicula* (Muñoz-Baquero et al., 2024). De plus, une récente publication a mis à disposition une importante base de données couplant génomique, transcriptomique et analyse morphologique chez la petite roussette *S. canicula* (Mayeur et al., 2024). Par ailleurs, un certain nombre de données génomiques et transcriptomiques associées à d'autres espèces d'Élasmobranches sont accessibles mais demeurent non publiées comme les assemblages des génomes complets de la raie radiée *Amblyraja radiata* (sAmbRad1.1.pri), du requin-chabot *Chiloscyllium plagiosum* (ASM401019v1), du requin-scie *Pristis pectinata* (sPriPec2.1.pri) et de la petite roussette *Scyliorhinus canicula* (sScyCan1.2), disponibles dans les bases de données NCBI (https:// www.ncbi.nlm.nih.gov/genome/), et de la raie pastenague *Hemitrygon akajei* (sHemAka1.1), disponible dans la base de données Squalomix (https://transcriptome.riken.jp/squalomix/blast/). Malgré l'acquisition de ces nouvelles données « -omiques », les mécanismes de régulation de la reproduction des Élasmobranches restent largement inexplorés. De plus, l'édition génétique n'a pas encore été développée mais des progrès sur le transfert de gènes émergent (Fujimori et al., 2022).

Les requins et les raies présentent une variété inhabituelle de modes de reproduction et constituent un groupe idéal pour tester les facteurs à l'origine de l'évolution de la complexité de la reproduction. Chez les Chondrichtyens, le mode de reproduction le plus ancestral est l'oviparité et quatre modes de viviparités sont également distingués en fonction du mode d'apport en nutriments à l'embryon, avec : la lécithotrophie basée sur la consommation des

seules réserves vitellines lors de la gestation interne, retrouvée par exemple chez le requin-baleine ; l'oophagie où l'embryon est alimenté par des œufs ou des embryons supplémentaires, retrouvée chez le requin-taureau ; l'histotrophie, où les sécrétions maternelles sous forme de lait utérin constituent une source de nourriture, retrouvée chez le grand requin blanc ; et la viviparité placentaire avec un placenta choriovitellin retrouvé par exemple chez le requin-marteau (Fig. 5). Des corrélations entre les traits de vie, l'environnement et le mode de reproduction seraient retrouvées avec, par exemple, une taille corporelle adulte et une longévité plus importantes chez les lécithotrophes par rapport aux ovipares et une progéniture moins nombreuse chez les matrotrophes par rapport aux lécitothrophes (Blackburn and Hughes, 2024; Katona et al., 2023).

### II.2. La petite roussette *Scyliorhinus canicula*, un modèle d'étude des Élasmobranches[2]

La petite roussette *Scyliorhinus canicula* appartient au groupe des Sélaciens, à l'ordre des Carcharhiniformes, et à la famille des Scyliorhinidés qui est la plus grande famille d'Élasmobranches avec 170 espèces répertoriées. Les caractéristiques morphologiques communes aux Scyliorhinidés sont la présence d'une nageoire anale et de deux dorsales, la présence de cinq paires de fentes branchiales et le positionnement des yeux au-dessus de la bouche ventrale. Plusieurs noms vernaculaires ont été donnés à la petite roussette avec « saumonette » qui est associé à sa forme commerciale et *dogfish* puis *catshark* utilisés par la communauté scientifique. Cette espèce est classée *least concern* dans la liste rouge des espèces menacées de l'IUCN (*International Union for Conservation of Nature*) (Field et al., 2009). La petite roussette a une répartition spatiale qui s'étend du nord du Sénégal au sud de la Norvège et vit à des profondeurs pouvant aller jusqu'à 400 mètres maximum, associée de préférence à des substrats sablo-rocheux. C'est un prédateur nocturne avec un sex-ratio légèrement en faveur de la femelle (Ivory et al., 2004) et elle semble se reproduire en eau peu profonde à proximité des côtes, là où la densité de femelles matures est la plus importante et où sont retrouvés les juvéniles. Les mâles sont quant à eux retrouvés en plus forte densité dans les eaux plus profondes (Martin et al., 2012). La petite roussette a une espérance de vie comprise entre 10 et 12 ans et atteint la maturité sexuelle à 6,6 ans pour les mâles et 7,9 ans

[2] Cette partie s'inspire en partie du chapitre d'encyclopédie suivant : Sourdaine and Jeanne, 2024 (Annexe I)

pour les femelles, en moyenne (Ivory et al., 2004). Les mâles atteignent la maturité sexuelle pour une taille supérieure à 57 cm en mer de Manche, 52 cm en Atlantique (Capapé et al., 2014), 39 cm en mer Egée (Kousteni et al., 2010) et 37 cm en Méditerranée (Capapé et al., 2014). De même, il a été observé un dimorphisme entre des mâles du nord de la mer Adriatique, qui présentent un tractus génital plus développé, et des mâles du détroit de Sicile ; ce qui suggère l'existence d'une compétition spermatique plus forte dans le premier site (Finotto et al., 2015).

Comme la majorité des Scyliorhinidés, la petite roussette est ovipare avec une fécondation interne de l'ovule au niveau de la glande nidamentaire, ou glande oviducale, de la femelle. Par ailleurs, la femelle développe différentes stratégies de contrôle du sperme reçu, ce qui explique l'indice de paternité multiple compris entre 85 et 92% chez cette espèce, par comparaison à d'autres Chondrichtyens comme l'aiguillat tacheté *Squalus acanthias* où l'indice est compris entre 17 et 30% (Fitzpatrick et al., 2012). Après la fécondation, l'œuf est entouré d'enveloppes complexes telles que la gelée et la coque qui sont sécrétées par les glandes nidamentaires de la femelle. L'œuf sera pondu entre 5 et 15 jours post-fécondation pour une température comprise entre 10°C et 18°C (Ballard et al., 1993). L'œuf est accroché par ses vrilles sur un support fixe lors de l'oviposition et l'éclosion s'effectue entre 170 jours et 220 jours plus tard (Mellinger, 1994).

### II.3. Vulnérabilité des Chondrichtyens

Récemment, Dulvy et al., 2021 ont présenté une réévaluation mondiale du statut UICN de 1 199 espèces de Chondrichtyens, dans le but de révéler l'ampleur et les moteurs de la perte de biodiversité marine. La première évaluation mondiale (en 2014) avait conclu qu'un quart (24%) des espèces était menacées (Fig. 6) (Dulvy et al., 2014). Aujourd'hui, ce sont un tiers (32,6%) des espèces (soit 391 espèces) qui sont menacées d'extinction, nombre qui pourrait être étendu à 37,5% si les espèces non répertoriées où les données manquantes étaient ajoutées. La surpêche constitue la seule menace pour 67,3% des espèces et interagit avec trois autres menaces, expliquant le tiers restant, qui sont la perte et la dégradation d'habitats (31,2% des espèces menacées), le dérèglement climatique (10,2%) et la pollution (6,9%).

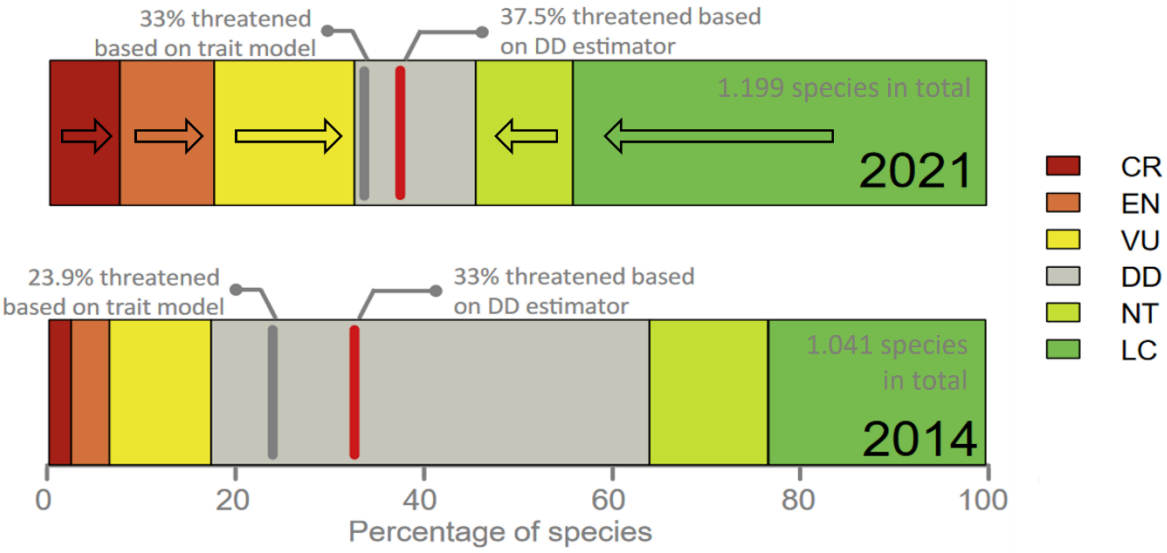


Fig. 6. **Représentation schématique de la répartition des statuts IUCN associés aux espèces de Chondrichtyens, comparaison des évaluations de 2014 et 2021.** Différence de statut dans la liste rouge de l'IUCN entre l'évaluation de 2021 (barre supérieure) et celle de 2014 (barre inférieure). Entre ces deux évaluations, le nombre d'espèces prises en compte a augmenté et davantage de données acquises sont représentées comme le montre l'augmentation des fractions comprenant les statuts NT (vert clair) et LC (vert foncé). Il en résulte une augmentation du nombre d'espèces menacées associées aux trois statuts CR (rouge), EN (orange) et VU (jaune). CR, en danger critique ; EN, en danger ; VU, vulnérable ; DD, données insuffisantes ; NT, Quasi menacée ; LC, préoccupation mineure. Modifié d'après Dulvy et al., 2021.

Pour faire face au risque d'extinction de plusieurs espèces d'Élasmobranches, la reproduction assistée est actuellement développée en aquarium (Penfold and Wyffels, 2019). Ces développements incluent la publication de méthodes de collecte et de cryoconservation du sperme (García-Salinas et al., 2021a), d'insémination artificielle (Luer et al., 2007) et d'évaluation non invasive des paramètres andrologiques (De Oliveira Camilo et al., 2023). Des études sur les comparaisons des profils hormonaux chez les individus captifs par rapport aux individus sauvages sont également entreprises dans le but de développer la conservation *in situ* (Becerril-García et al., 2020; Muñoz-Baquero et al., 2024). Paradoxalement, la reproduction assistée est également susceptible de bénéficier du développement de méthodes contraceptives visant à réduire l'agressivité en captivité, en utilisant notamment des antagonistes de la GnRH, ce qui pourrait permettre de comprendre les particularités du contrôle neuroendocrinien de la reproduction chez les Élasmobranches (Sailler et al., 2023).

La reproduction est un processus biologique qui permet la production de nouveaux organismes d'une espèce à partir d'individus de cette espèce. Chez les Vertébrés, les gamètes mâles (spermatozoïdes) et femelles (ovules) sont produits à partir de cellules souches qui prolifèrent et se différencient au niveau des gonades avant de finir leurs maturations dans les autres organes des tractus génitaux. Le succès reproductif des espèces dépend du bon déroulement de la gamétogenèse puisque la fécondation, à l'origine d'un zygote, n'est possible que si les gamètes ont été produits de façon qualitative, quantitative et coordonnée avec le cycle biologique de l'individu. L'une des principales innovations évolutives des Vertébrés est l'acquisition d'un système endocrinien spécialisé dans le contrôle de la reproduction et, plus spécifiquement, de la gamétogenèse : l'axe hypothalamo-hypophyso-gonadique (HHG). Parallèlement, un système neuroendocrine spécialisé dans la régulation du métabolisme, appelé axe hypothalamo-hypophyso-thyroïdien (HHT), a également été acquis. Ces deux axes impliquent les hormones glycoprotéiques.

Dans la suite de cette introduction, nous aborderons les différents types d'organisation des testicules et des tractus mâles retrouvés chez les Vertébrés puis la mise en place des axes hypothalamo-hypophyso gonadiques.

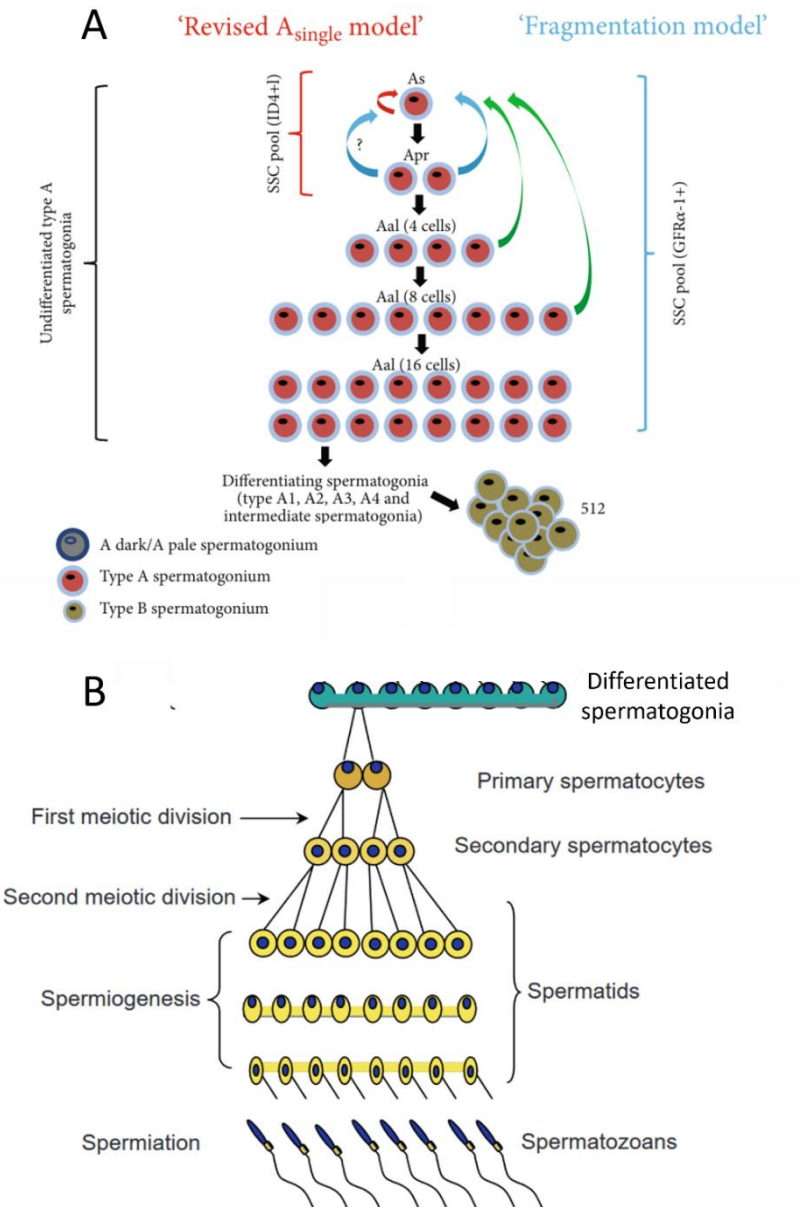


Fig. 7. **Représentation schématique de la spermatogenèse.** **A.** Compartiment souche. Les spermatogonies indifférenciées isolées ($A_s$) ont la capacité de s'autorenouveler et de se différencier en spermatogonies indifférenciées paires ($A_{pr}$) qui se divisent pour donner les spermatogonies indifférenciées A alignées ($A_{al4}$ à $A_{al16}$). Les $A_{pr}$ et $A_{al4-8}$ peuvent redonner des spermatogonies $A_s$ par fragmentation clonale (flèche verte). Les spermatogonies indifférenciées $A_{al}$ peuvent, sans division, donner les premières spermatogonies différenciées de type A1, A2, A3, A4 qui donneront les spermatogonies intermédiaires puis B. D'après Song et al., 2022. **B.** Schéma de la spermatogenèse. Les spermatogonies donnent les spermatocytes pré-leptotènes qui donneront les spermatocytes primaires. Après la division réductionnelle de méiose, les spermatocytes secondaires sont obtenus et donnent les spermatides rondes après la division équationnelle. Au cours de la spermiogenèse, les spermatides rondes se différencient en spermatides allongées matures qui seront relargués dans les canaux collecteurs lors de la spermiation. D'après Goodman, 2009.

# III. La spermatogenèse et les tractus génitaux chez les Vertébrés

## III.1. Généralités

La gamétogenèse conduit à la formation d'un gamète haploïde (n) à partir d'une cellule diploïde (2n). La spermatogenèse se déroule au sein du testicule et comprend trois grandes étapes conservées au cours de l'évolution. La première est l'étape de prolifération mitotique et de différenciation des spermatogonies souches, ou indifférenciées, en spermatogonies différenciées puis en spermatocytes primaires pré-leptotènes (Fig. 7A) (Song et al., 2022). La deuxième est celle de la méiose avec une prophase de longue durée qui permet de différencier les différents spermatocytes primaires qui, lors de la division réductionnelle, donnent les spermatocytes secondaires qui se divisent ensuite lors de la division équationnelle pour donner les jeunes spermatides haploïdes ou spermatides rondes. La troisième étape est la spermiogenèse qui correspond à la transformation des spermatides rondes en spermatides allongées, hautement différenciées (Goodman, 2009) (Fig. 7B). Les spermatozoïdes seront ensuite relargués, au cours de la spermiation, dans un réseau de canaux connecté à d'autres organes du tractus génital mâle, si celui-ci est différencié, où la maturation des spermatozoïdes se poursuivra.

## III.2. Les différentes organisations testiculaires

Alors que la spermatogenèse apparait comme un processus extrêmement conservé au cours de l'évolution, l'organisation anatomique du testicule varie en fonction des clades de Vertébrés. Néanmoins, le testicule reste composé de deux compartiments principaux : le compartiment interstitiel et le compartiment séminifère. Le compartiment séminifère est délimité par les cellules myoïdes et contient les cellules germinales en différenciation associées aux cellules de Sertoli. Chez les Vertébrés, deux organisations du compartiment séminifère ont été décrites : l'organisation cystique et non-cystique. L'organisation cystique apparait comme l'organisation la plus ancestrale et est observée chez les Vertébrés anamniotes comme les Cyclostomes, les Chondrichtyens, les Actinoptérygiens et certains Sarcoptérygiens, à l'exception des Sauropsidés et Synapsides. Cette structure se met en place par l'association initiale d'une cellule de Sertoli avec une spermatogonie indifférenciée (Fig.

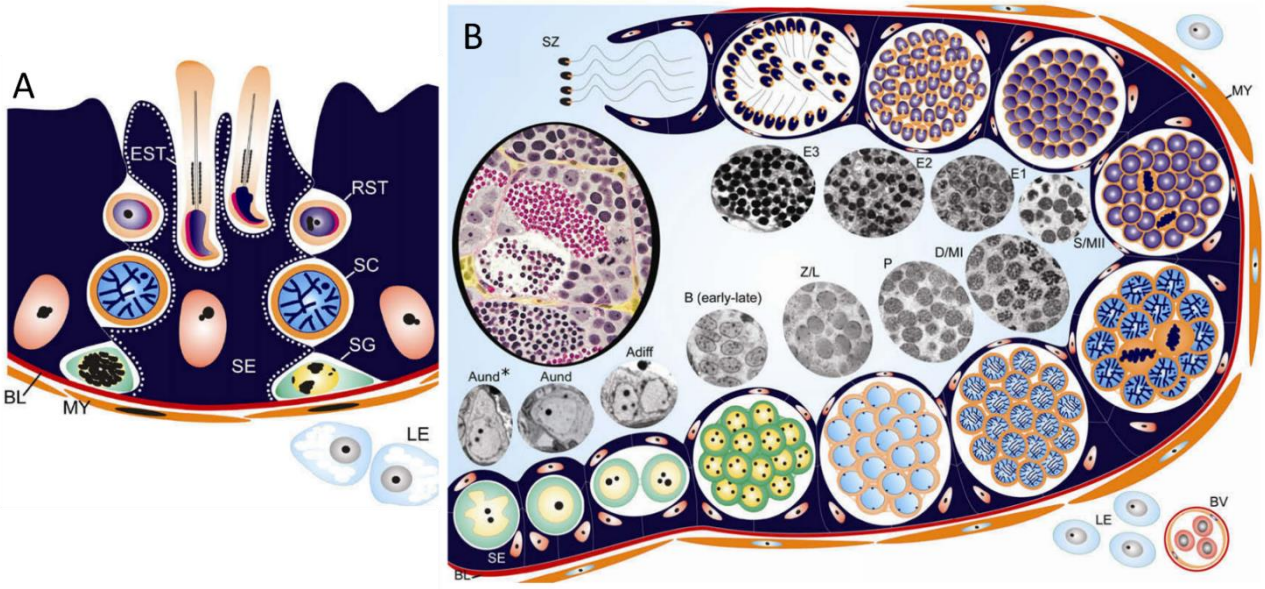


Fig. 8. **Représentation schématique des organisations testiculaires de types non cystique (exemple de la souris) et cystique (exemple du poisson zèbre).** Des segments de tubules séminifères sont représentés pour illustrer les différents types d'association entre les cellules de Sertoli et les cellules germinales, dans le cas d'une organisation non-cystique (**A**) et cystique (**B**). L'épithélium séminifère (A) contient des cellules de Sertoli (SE) associées aux cellules germinales à différents stades de la spermatogenèse avec les spermatogonies en position basales et les spermatides allongées en position adluminale. Cet épithélium séminifère est délimité par une lame basale (LB) et des cellules myoïdes péritubulaires (MY). Les cellules de Leydig interstitielles (LE) et les vaisseaux sanguins (BV) sont représentés. SG, Spermatogonies ; SC, spermatocytes ; RST, spermatides rondes ; EST, spermatides allongées. Si l'organisation testiculaire est cystique (B), les prolongements cytoplasmiques des cellules de Sertoli vont envelopper un groupe unique de cellules germinales, ce qui forme un spermatocyste. Au sein d'un spermatocyste, l'évolution des cellules germinales est synchrone. Aund*, spermatogonies indifférenciées* de type A ; Aund, spermatogonies indifférenciées de type A ; Adiff, spermatogonies différenciées de type A ; B, spermatogonies de type B ; L/Z, spermatocytes primaires leptotènes/zygotènes ; P, spermatocytes primaires pachytènes ; D/MI, spermatocytes diplotènes/métaphase I ; S/MII, spermatocytes secondaires/métaphase II ; E1, spermatides précoces ; E2, spermatides intermédiaires ; E3, spermatides finales ; SZ, spermatozoïdes (Schulz et al., 2010).

8B). Au cours des proliférations cellulaires, sertoliennes et germinales, les cellules de Sertoli associées à la lignée issue de la spermatogonie d'origine forment ainsi un spermatocyste (cyste) où l'évolution des cellules germinales, connectées entre elles par des ponts cytoplasmiques, est synchrone, d'où l'appellation de clone germinal. À l'inverse, l'organisation non-cystique n'est présente que chez les Vertébrés amniotes (Sauropsidés et Synapsides). Le testicule est composé de nombreux tubules séminifères pourvus d'une lumière centrale et d'un épithélium séminifère où les cellules de Sertoli sont associées à des cellules germinales à différents stades de développement et qui sont organisées en assises successives depuis le compartiment basal, où sont localisées les spermatogonies, jusqu'au compartiment adluminal, où sont localisées les spermatides allongées (Fig. 8A). De plus, les cellules de Sertoli sont reliées entre elles par des jonctions spécialisées qui constituent l'un des éléments de la barrière hémato-testiculaire à l'origine de la compartimentation de l'épithélium séminifère (basal, intermédiaire et adluminal) (Wong and Cheng, 2009). Que ce soit au niveau d'une organisation cystique ou non-cystique, le compartiment interstitiel est défini entre les compartiments séminifères et c'est à ce niveau que sont retrouvées les cellules de Leydig productrices de testostérone, les macrophages, les cellules péritubulaires myoïdes, les télocytes ainsi que les vaisseaux sanguins et lymphatiques (Pawlicki et al., 2024).

Chez les lamproies, l'organisation testiculaire est cystique et les cystes ne semblent pas ordonnés. Le compartiment interstitiel apparait très peu développé mais contient des cellules interstitielles qui ressemblent à des précurseurs mésenchymateux, dont l'activité stéroïdogène reste à être mise en évidence, qui pourraient correspondre à des cellules Leydig-*like* (Engel and Callard, 2007).

Chez les Actinoptérygiens, l'organisation testiculaire est également cystique et les cystes peuvent être contenus dans des tubules séminifères, comme observé chez les Téléostéens appartenant au groupe des Osteoglossiformes, ou des lobules séminifères, comme observé chez les Néotéléostéens (Fig. 9) (Pecio, 2019; Song et al., 2022; Vizziano et al., 2008). Le compartiment interstitiel est localisé entre les lobules/tubules séminifères et comprend notamment les cellules de Leydig stéroïdogènes (Rupik et al., 2011). Trois structures lobulaires/tubulaires ont été différenciées sur la base de la répartition des spermatogonies. Le premier est le type restreint, présent par exemple chez Le fondule *Fundulus grandis* (Fig.

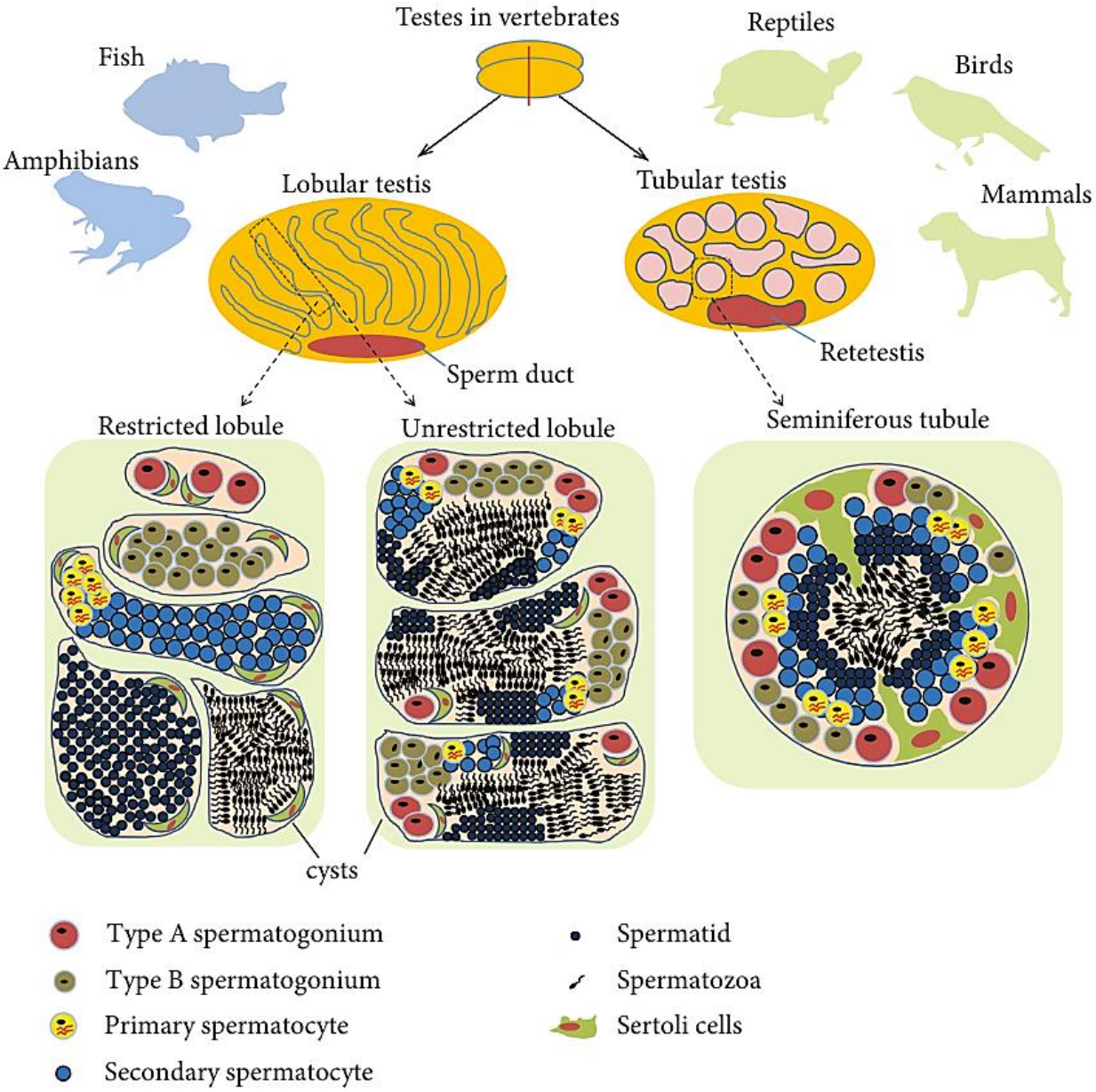


Fig. 9. **Organisation testiculaire chez les Vertébrés**. Les Amphibiens et les Téléostéens ont des testicules constitués de lobules (ou de tubules) renfermant des cystes et à organisation restreintes et non restreintes. Au niveau du testicule restreint, les cystes à spermatogonies de type A sont positionnées à un pôle du lobule testiculaire. Au sein d'un cyste, la spermatogenèse est synchrone et les cellules germinales sont à un même stade de maturité (clones germinaux). Au niveau du testicule non-restreint, les spermatogonies de type A sont positionnées en périphérie des cystes qui contiennent plusieurs stades de maturité de cellules germinales. Chez les Sauropsidés et les Synapsides, le testicule a une organisation en tubules séminifères constitués d'un épithélium séminifère où les cellules germinales sont étroitement associées aux cellules de Sertoli et sont à différents stades de développement, avec une localisation des spermatogonies dans le compartiment basal et des spermatides dans le compartiment adluminal (Song et al., 2022).

10A), le second est le type non restreint, observé par exemple chez le poisson zèbre *Danio rerio* (Fig. 10B), et le troisième est le type intermédiaire, comme observé chez le tilapia *Oreochromis niloticus* (Parenti and Grier, 2004; Schulz et al., 2010). Dans un testicule de type non restreint, les cystes sont dépourvus de lumière, ne migrent pas au cours de leur développement et évoluent autour de la lumière centrale du lobule/tubule. Cette dernière peut être anastomosée avec les lumières des autres lobules/tubules et débouchée dans les canaux collecteurs des spermatozoïdes. En conséquence, les différents stades de la spermatogenèse sont dispersés le long des lobules/tubules séminifères et les spermatogonies indifférenciées sont localisées sur toute la longueur et la périphérie des lobules (Leal et al., 2009) (Fig. 9, Fig. 10B). La distribution non restreinte des spermatogonies est considérée comme un modèle plus primitif que l'on retrouve dans des groupes taxonomiques comme les Cypriniformes, les Characiformes et les Salmoniformes (Parenti and Grier, 2004). Au niveau du type intermédiaire, les spermatogonies indifférenciées se trouvent de préférence, mais pas exclusivement, à proximité de la tunique albuginée. Chez la morue *Gadus morhua*, les spermatogonies proviennent d'une zone germinative située à la périphérie du parenchyme testiculaire (Almeida et al., 2008). Par conséquent, il y a une zonation du testicule où les stades précoces se situent à la périphérie et les stades avancés près du canal collecteur, une situation qui résulte d'une croissance appositionnelle alimentée par l'activité de génération de cystes de la zone germinative. Quant au testicule de type restreint, il est constitué de lobules séminifères connectés par une extrémité aux canaux évacuateurs et les cystes à spermatogonies indifférenciées sont localisés à leurs opposés (Fig. 9, Fig. 10A). Au cours de la spermatogenèse, les cystes migrent de la périphérie vers les canaux collecteurs où les spermatozoïdes seront relargués (Iwai et al., 2006). Ce type d'arrangement se retrouve chez les Téléostéens supérieurs, comme dans l'ordre des Athériniformes, des Cyprinodontiformes et des Béloniformes (Parenti and Grier, 2004).

Chez les Sarcoptérygiens anamniotes, les testicules peuvent avoir une organisation cystique ou non-cystique. En effet, chez le triton *Taricha granulosa*, le testicule est lobé et ses lobes sont reliés par des ponts interlobaires où sont localisées les niches germinatives constituées de spermatogonies prolifératives et indifférenciées et de précurseurs somatiques. Au cours de leurs différenciations, les spermatogonies et les précurseurs sertoliens vont s'associer pour

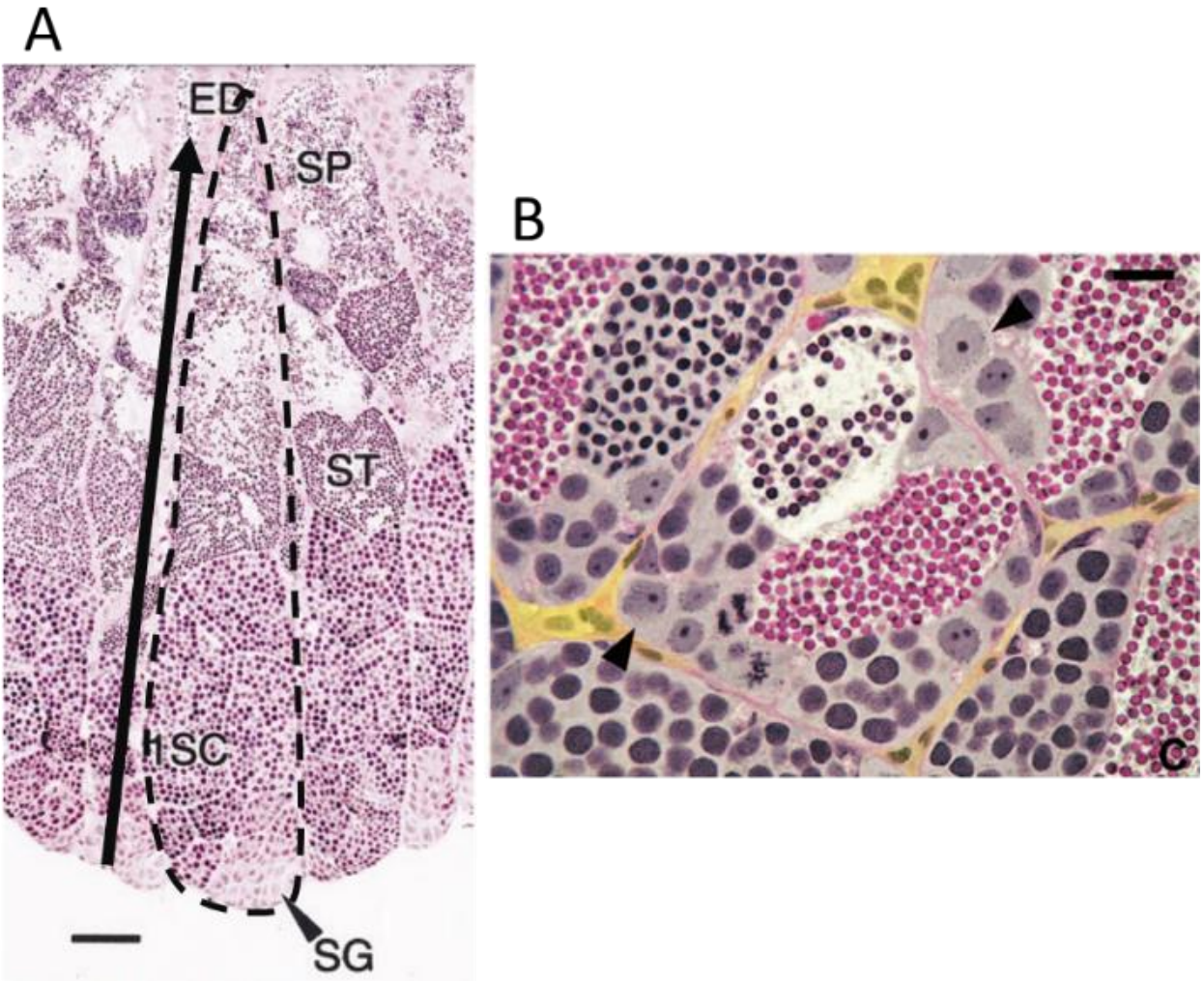


Fig. 10. **Coupes histologiques de testicules de téléostéens de type restreint et non restreint. A.** Restreint. Coupe transversale du testicule du fondule du golfe *Fundulus grandis* à organisation testiculaire restreinte. Les tubules séminifères (pointillés) s'étendent jusqu'à la périphérie du testicule, où se trouvent les spermatogonies. Au cours de leur différenciation, les spermatocystes migrent en suivant l'onde spermatogénétique (flèche). ED, canaux efférents ; 1SC, spermatocyte primaire ; SP, sperm ; ST, spermatid. Barre d'échelle : 50 µm. D'après Parenti, 2004. **B.** Non-restreint. Coupe transversale de tubules séminifères du poisson zèbre *Danio rerio* à organisation testiculaire non-retreinte et contenant des cystes à différents stades de développement. Les spermatogonies indifférenciées de type A (têtes de flèches) sont positionnées à la périphérie du tubule, au regard de l'interstitium (jaune). Barre d'échelle = 10 µm. D'après Nóbrega et al., 2010.

former les cystes qui sont localisés dans de nombreux lobes. À l'intérieur des lobes, les cystes se développent selon une onde spermatogénétique longitudinale céphalo-caudale. Chez les Sarcoptérygiens amniotes, l'organisation du testicule est de type non-cystique. Les spermatogonies indifférenciées sont réparties dans des régions spécifiques du compartiment basal et sont à l'origine de clones de cellules germinales qui vont se différencier du compartiment basal vers le compartiment adluminal (Miyaso et al., 2022) comme, par exemple, chez le lézard *Sceloporus t. torquatus* (Grier et al., 2016). La spermatogenèse étant continue, plusieurs clones à différents stades de développement sont retrouvés au contact d'une même cellule de Sertoli. L'onde spermatogénétique s'effectue dans le sens transversal et dans le sens longitudinal du tubule séminifère. Chez les rongeurs, cette onde spermatogénétique particulière fut à l'origine de la définition de plusieurs stades de l'épithélium séminifère. Ainsi, douze et quatorze stades d'association de cellules germinales à une cellule de Sertoli donnée ont été initialement établis chez la souris et le rat, respectivement. Chaque association différenciable sur une section transversale d'un tubule séminifère définit un stade du cycle de l'épithélium séminifère. Sur la longueur des tubules, la succession chronologique d'une série complète de ces douze ou quatorze stades, d'un point donné du tubule jusqu'à la réapparition du premier stade, constitue un cycle de l'épithélium séminifère (Perey et al., 1960). Chez les primates non-humains, le nombre de stades qui a été défini est de douze pour le singe rhésus et le babouin, de neuf pour le marmouset et de six pour le chimpanzé. Chez l'homme, la présence de trois vagues spermatogénétiques simultanées imbriquées les unes dans les autres sous forme de spirale a rendu plus difficile l'analyse des stades par rapport à l'onde spermatogénétique linéaire observée pour les rongeurs (Muciaccia et al., 2013).

### III.3. Régulations et coordinations des processus biologiques et des voies de signalisations au niveau testiculaire

Le testicule est un organe unique où sont réalisées des fonctions hautement spécialisées au cours d'événements progressifs et coordonnés. Cette spécificité du testicule est illustrée par le fait que c'est l'organe qui contient le plus grand nombre de gènes spécifiquement exprimés par comparaison aux autres tissus, au moins chez l'homme (Djureinovic et al., 2014). Trois exemples de processus biologiques seront décrits par la suite afin d'illustrer ces particularités

de la fonction testiculaire. Notre choix a été motivé par les résultats obtenus dans les différents chapitres de cette thèse et par le fait que des acteurs des régulations endocrines sont exprimés localement au niveau du testicule.

### III.3.1 Exemple du protéasome spécifique au testicule, le spermatoprotéasome

Les protéines inutiles ou endommagées qui sont présentes dans les cellules sont dégradées par le protéasome suite à leur marquage par des ubiquitines ou l'ajout de groupes acétyles. La dégradation protéasomale des protéines est un mécanisme essentiel pour de nombreux processus, dont la spermatogenèse. Chez les Mammifères, le protéasome spécifique du testicule, où spermatoprotéasome, est l'un des trois protéasomes spécifiques à un tissu avec l'immunoprotéasome et le thymoprotéasome. Ce spermatoprotéasome est caractérisé par une protéine homologue de la sous-unité α4 (PSMA7), appelée α4s (PSMA8), exprimée au cours de la méiose et son importance au cours de la spermatogenèse a été mise en évidence chez une lignée de souris déficiente en *psma8* qui a présenté une infertilité avec l'observation de spermatides rondes apoptotiques et l'absence de spermatides allongées (Gómez-H et al., 2019). Plus récemment, il a été montré que le spermatoprotéasome (s20S) était fortement activé lorsque les cellules germinales entrent en méiose par une augmentation de l'activation des protéines du complexe protéique activeur 19S qui lui est associé. De plus, le protéasome au niveau des spermatogonies est initialement composé à 98% de protéines protosomales constitutives (c20S) avant d'évoluer vers une nouvelle composition de 82% puis de 92% de s20S au niveau des spermatocytes pachytènes et des spermatides, respectivement, probablement en raison de l'augmentation de l'expression de α4s par rapport à α4 (Živković et al., 2022).

### III.3.2 Exemple du découplage temporel entre la transcription et la traduction.

Au cours de la spermiogenèse, les spermatides deviennent transcriptionnellement inactives en raison du remodelage des nucléosomes par le remplacement des histones par les protamines. Pour permettre la production de protéines au sein de cellules transcriptionnellement inactives, un découplage temporel entre les processus de transcription et de traduction au sein de la lignée germinale est mis en place. En effet, les premiers stades

de la spermatogenèse sont marqués par une transcription active et certains ARNm *de novo* sont transportés et stockés transitoirement dans des granules cytoplasmiques ribonucléoprotéiques appelés "corps chromatoïdes" (CB), en attente de traduction au cours des derniers stades de la spermatogenèse (Fig. 11). Au sein de ces CB, la stabilité des ARNm peut être régulée afin de permettre la synchronisation correcte entre l'expression des protéines et les différents stades de formation des spermatozoïdes. Un acteur protéique essentiel est la GRTH (*Gonadotropin-regulated testicular helicase*) qui transporte les ARNm du noyau vers le cytoplasme et la phospho-GRTH qui transporte les ARNm du cytoplasme vers les CB (Sato et al., 2010). La GRTH régule les protéines du complexe microprocesseur, Drosha et DGCR8 (biogenèse des miARN), au niveau des ARNm et des protéines. Il a été démontré que les protéines de la voie des miARN s'accumulent dans les CB des spermatides rondes haploïdes, ce qui suggère que le GRTH et les CB jouent un rôle dans la régulation des gènes dépendant des miARN (Dai et al., 2011). Par ailleurs, la GRTH se lie à des ARNm spécifiques en tant que composant intégral des RNPs (complexe ribonucleoprotéique) en s'associant aux polyribosomes pour réguler la traduction des gènes cibles pendant la différenciation des cellules germinales (Dufau and Kavarthapu, 2019). L'importance de la GRTH a notamment été mise en évidence par la mise en place de lignée de souris GRTH *knock-out* qui ont présenté une stérilité avec une spermiogenèse interrompue au stade 8 des spermatides (Anbazhagan et al., 2022; Kavarthapu et al., 2019).

### III.3.3 Exemple d'une boucle paracrine ultracourte

Un système de régulation paracrine impliquant des interactions croisées entre des acteurs des axes Hypothalamo-Hypophyso-Gonadique (HHG) et Hypothalamo-Hypophyso-Somatotrope (HHS) est présent au niveau testiculaire. L'hormone de croissance (GH) et le facteur de croissance apparenté à l'insuline 1 (IGF-I), qui sont des acteurs centraux de l'axe HHS, sont également synthétisés localement par les cellules de Leydig et les cellules de Sertoli sous l'influence des hormones gonadotropes systémiques FSH et LH (Fig. 12). La GH et l'IGF-I génèrent de nombreux signaux paracrines et autocrines impliqués dans la régulation de la spermatogenèse et de la stéroïdogenèse *via l'activation* des récepteurs GHR et IGF-IR exprimés par les cellules de Leydig, de Sertoli et par les spermatocytes primaires et secondaires. En effet, l'IGF-I stimulerait la p rolifération et la différenciation des progéniteurs

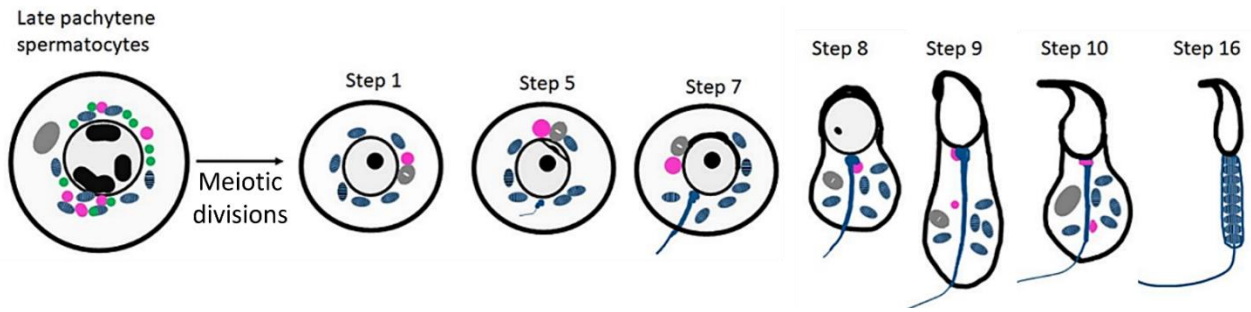


Fig. 11. **Représentation schématique de l'organisation et du devenir des corps chromatoïdes (CB) au cours de la spermiogenèse, exemple de la souris.** Le ciment inter-mitochondrial (IMC ; vert) entremêlé de mitochondries (bleu) et les précurseurs des CB (rose) coexistent dans les spermatocytes en fin de stade pachytène. L'appareil de Golgi est représenté en gris. Le CB est condensé sous sa forme finale au niveau des spermatides rondes précoces. À l'étape 8 de la spermiogenèse, le CB se trouve à la base du flagelle. Plus tard, il se sépare en deux structures distinctes (à partir de l'étape 9) et finit par disparaître. D'après Anbazhagan et al., 2022.

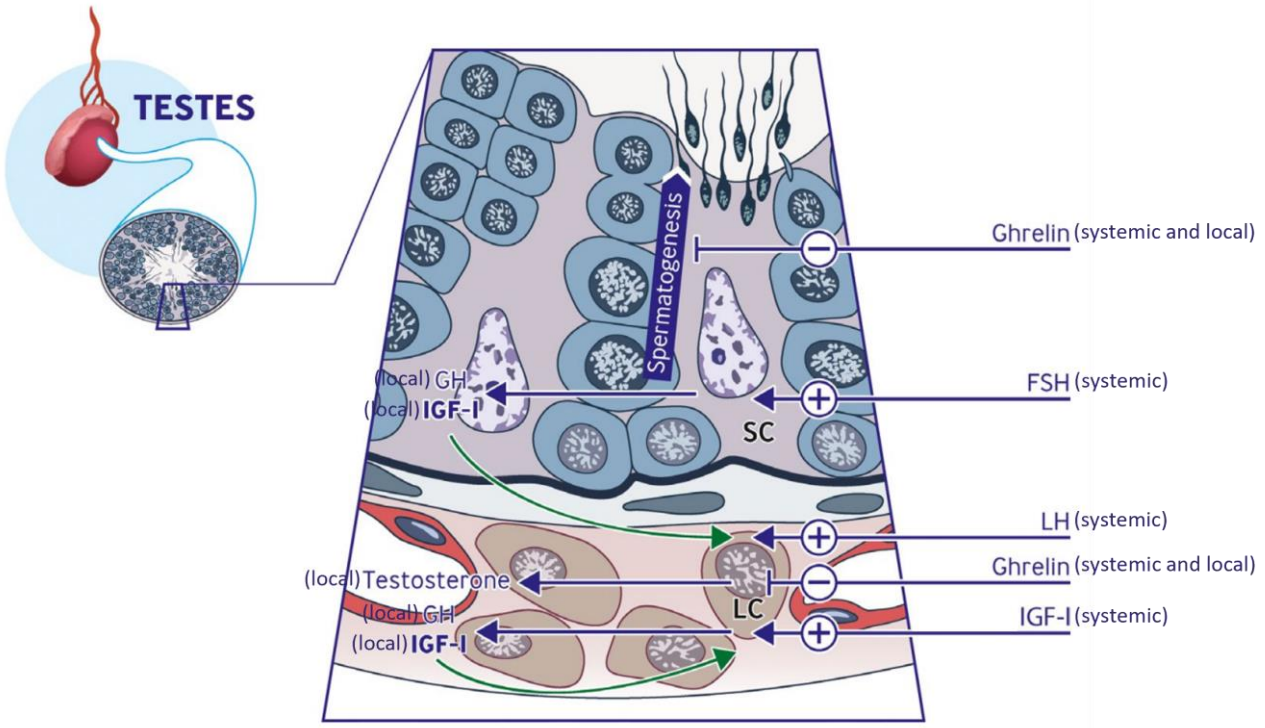


Fig. 12. **Représentation schématique des interactions entre les hormones de croissance et les hormones gonadiques au niveau testiculaire (résultats provenant de modèles mammaliens).** Les cellules de Leydig (LC) et de Sertoli (SC) sont capables de produire la GH et l'IGF-I localement, sous le contrôle de la FSH et de la LH systémiques. L'IGF-I produit localement est capable de générer de nombreux signaux paracrines et autocrines impliqués dans la spermatogenèse et la stéroïdogenèse (flèches vertes). L'IGF-I locale stimule la prolifération et la différenciation des progéniteurs des cellules de Leydig ; la GH locale renforce la protéine régulatrice aiguë de la stéroïdogenèse (StAR) et accroît l'expression du gène codant pour la 3β-HSD dans les cellules de Leydig ; la ghréline locale et systémique inhibe la libération de GH par les cellules de Leydig et de Sertoli et inhibe la spermatogenèse. Il est important de noter que l'action de l'IGF-I sur la spermatogenèse n'est pas encore totalement confirmée. D'après Tenuta et al., 2021.

des cellules de Leydig et augmenterait la motilité des spermatozoïdes chez la souris (Chatelain et al., 1991). La GH stimulerait la stéroïdogenèse en augmentant l'expression de la protéine StAR, permettant le transport du cholestérol de la membrane externe vers la membrane interne mitochondriale, et de la 3βHSD, d'où une augmentation de la production d'androgène par les progéniteurs leydigiens chez le rat (Kanzaki and Morris, 1999). L'importance de la GH a notamment été mise en évidence par la mise en place de lignées de souris *Ghr* $^{-/-}$ dont les mâles ont présenté une diminution du pouvoir fécondant des spermatozoïdes sans pour autant observer un arrêt de la spermatogenèse, probablement en raison d'une production d'IGF-I indépendante de la GH dans les tubes séminifères (Chandrashekar et al., 1999). Ce système paracrine testiculaire est également modulé par la ghréline, produite localement par les cellules adultes de Leydig ou provenant du système circulatoire général, qui agit sur les cellules de Leydig et de Sertoli qui expriment le récepteur à la ghréline (GHS-R). La ghréline inhibe la sécrétion de testostérone, ce qui module la prolifération des cellules de Leydig ainsi que l'expression de gènes comme le *scf* (*stem cell factor*) chez le rat (Tena-Sempere, 2005). Ce système qui implique une production testiculaire de GH, IGF-I, ghréline et testostérone modulerait localement la stéroïdogenèse et la spermatogenèse en synergie avec les actions liées aux hormones systémiques FSH, LH, GH et ghréline. Ce système illustre l'existence d'une boucle paracrine ultra-courte qui impliquerait une interconnexion entre les acteurs des axes HHG et HHS (Tenuta et al., 2021).

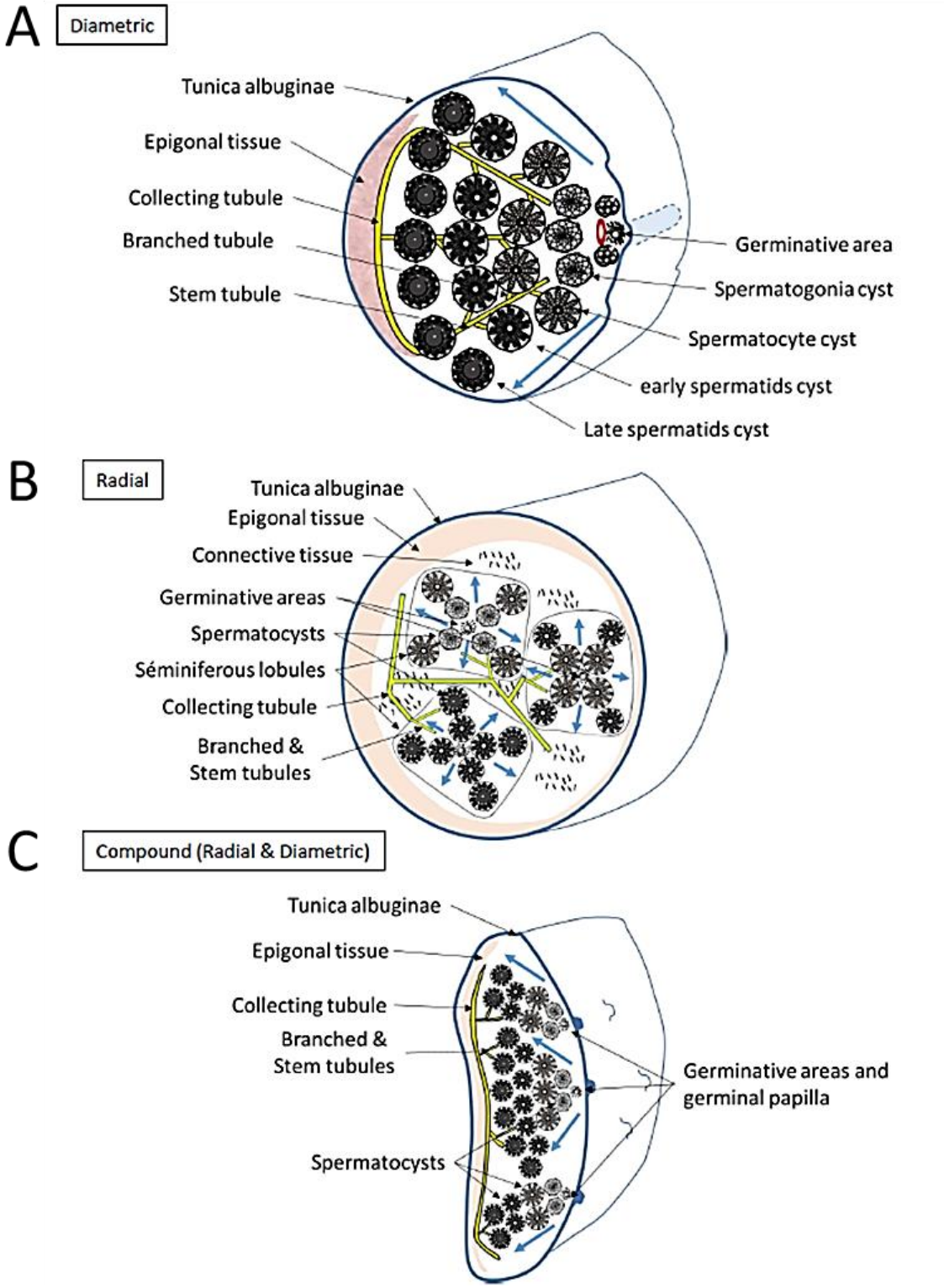


Fig. 13. **Représentations schématiques des différentes organisations testiculaires chez les Élasmobranches.** Les organisations testiculaires des Élasmobranches sont classées en trois types : **A.** le type diamétral où la zone germinative s'étend sur la longueur dorsale du testicule ; **B.** le type radial où la zone germinative est positionnée au centre de lobules séminifères, lesquels contiennent des cystes ; **C.** le type composé où le testicule est subdivisé en lobes, chacun contenant une zone germinative formant une papille. Sourdaine et al., 2018 et modifié d'après Pratt, 1988.

### III.4. Anatomie du testicule et spermatogenèse chez les Élasmobranches[3]

Chez les Élasmobranches, selon l'espèce et le type de testicule, l'aire germinative est unique ou multiple. Chez les espèces de requins Squalomorphes, Galeomorphes et Carcharhiniformes, l'aire germinative est constituée d'une bande située entre l'albuginée et le vaisseau sanguin testiculaire principal qui s'étend sur la longueur dorsale du testicule. Cette structure testiculaire a été classée en type diamétral (Pratt, 1988) (Fig. 13A). Les Squaliformes, tels que *Centroscymnes coelolepes* et *Centrophorus squamosus*, peuvent présenter des testicules lobés et chaque lobe a une structure diamétrale (Girard et al., 2000). Chez les Lamniformes, le testicule est de type radial et comprend des lobules séminifères présentant en leur centre une zone germinative à partir de laquelle le développement des cystes s'effectue radialement (Fig. 13B). Chez les Batoïdes, le testicule combine une structure radiale et une structure diamétrale et a été qualifié de « composé » par Pratt, 1988 (Fig. 13C). Ils peuvent comporter des divisions lobées, comme cela a été observé chez *Rhinoptera bonasus* (Poulakis and Grier, 2014). Les zones germinatives sont multiples et forment des protubérances ou papilles sur la surface dorsale du testicule et le développement des cystes se fait de manière diamétrale à partir de chaque zone germinative.

Chez *Scyliorhinus canicula*, une classification de la spermatogenèse a été initialement développée par Stanley, 1966, puis affinée par Loir et al., 1995 (Fig. 14). Le stade I, retrouvé dans la zone germinative, correspond à des spermatogonies de grandes tailles (10 µm de diamètre nucléaire), entourées de cellules somatiques allongées qui correspondent aux précurseurs des cellules de Sertoli. Dans les différentes sous-parties de la zone germinative, réparties de l'albuginée au vaisseau sanguin, les spermatogonies sont successivement isolées, par paire ou en groupes de 4 et peuvent être qualifiées respectivement de spermatogonies A isolées (As), A paires (Apr) et A indifférenciées (Aund). Leurs ultrastructures révèlent un noyau avec une chromatine d'aspect marbré, un nucléole et un cytoplasme contenant de nombreuses mitochondries et un matériel dense, le nuage germinatif (Loppion et al., 2008). Dès la première division mitotique, les spermatogonies seront reliées par des ponts cytoplasmiques pour former un syncytium. En quittant la zone germinative, les précurseurs

[3] Cette partie s'inspire en partie du chapitre d'encyclopédie suivant : Sourdaine and Jeanne, 2024 (Annexe I)

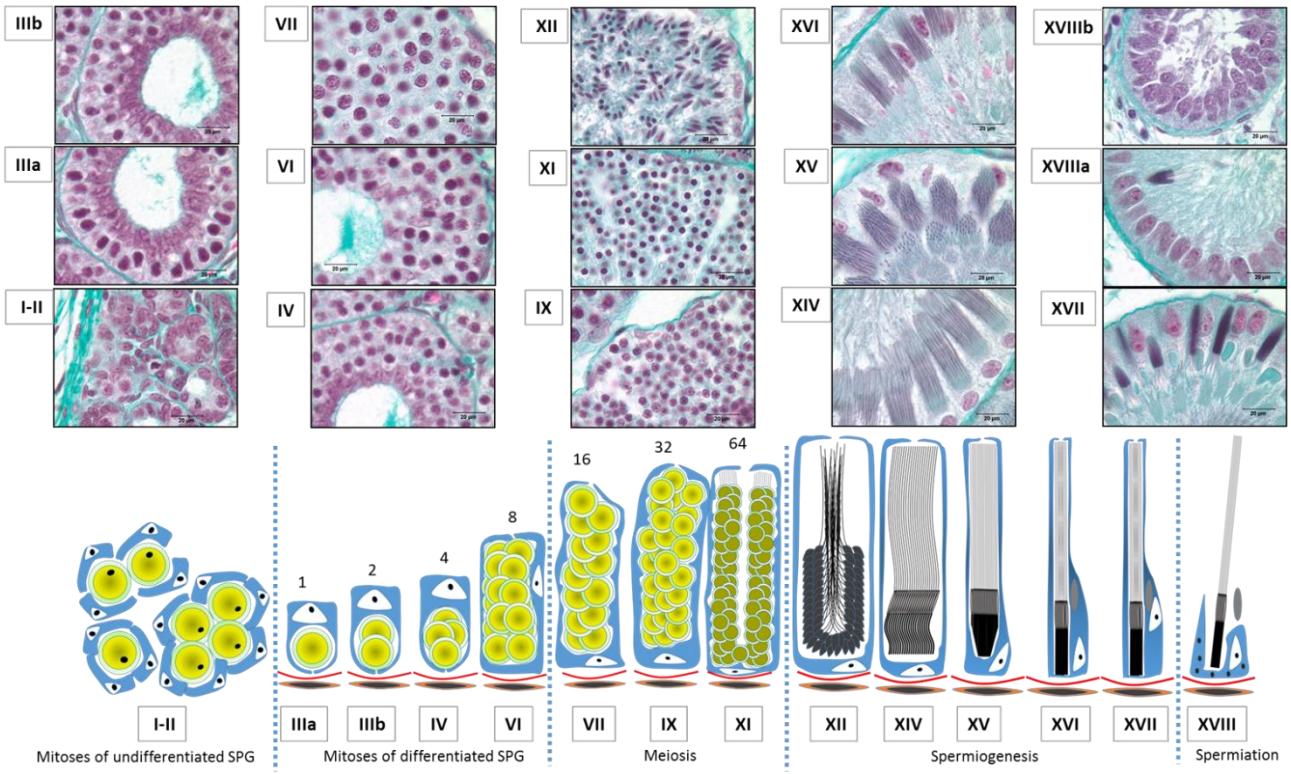


Fig. 14. **Présentation des différents stades de la spermatogenèse chez la petite roussette, *Scyliorhinus canicula*.** Partie supérieure : histologie des différents stades de la spermatogenèse (I à XVIII). Partie inférieure : représentation schématique des associations entre les cellules de Sertoli (en bleu) et les cellules germinales (en jaune, puis en noir) au cours des stades de la spermatogenèse. I-II : zones germinatives et de transition. IIIa à XVIII : schémas de l'évolution d'un spermatoblaste dans des cystes contenant des spermatogonies (IIIa à VI), des spermatocytes (VII, IX), des spermatides (XI-XVIII) (Sourdaine et al., 2018).

des cellules de Sertoli et les spermatogonies en prolifération se regroupent progressivement pour former des cystes sphériques avec une lumière qui apparaît progressivement (stade II). Le stade III correspond à la fin de la formation du cyste avec une seule assise de cellules de Sertoli dont les noyaux sont en position adluminale et une assise de spermatogonies en position basale (stade IIIa). À ce stade, il y aurait une cellule de Sertoli pour une spermatogonie et l'association de ces deux types cellulaires constituerai l'unité de base du cyste ou spermatoblaste. La formation du cyste (stade IIIa) coïncide avec la fin des divisions des cellules de Sertoli et quatre mitoses supplémentaires des spermatogonies différenciées ont ensuite lieu (stades IIIb à VI). Au cours des stades IV à VI, ce dernier correspondant à la dernière génération de spermatogonies ou spermatocytes pré-leptotène, le noyau sertolien est progressivement repoussé de sa position adluminale vers une position basale. Le nombre de cellules germinales par spermatoblaste est de 4, 8 et 16 pour les stades IV, V et VI, respectivement. En considérant le ratio de 1 cellule de Sertoli pour une spermatogonie au stade IIIa, et le nombre de noyaux de cellules de Sertoli par cyste (reflétant également le nombre de spermatoblastes par cyste), le nombre de mitoses a été évalué à 9 pour les spermatogonies indifférenciées (de As à Aund 512) et à 4 pour les spermatogonies différenciées (de Ad1 aux spermatocytes PL) (Bosseboeuf et al., 2014). Cette phase de forte prolifération permet de produire un grand nombre de spermatozoïdes à partir d'un petit nombre de cellules souches germinales. La différence entre le nombre théorique (512) et observé (469) de spermatoblastes (Holstein, 1968) suggère un contrôle de l'homéostasie testiculaire par apoptose comme observé chez tous les Vertébrés et étudié chez le requin *S. acanthias* (McClusky, 2012). Cette capacité à observer ces différentes générations de spermatogonies a permis d'établir une signature moléculaire pour chacune d'entre elles avec, par exemple, une expression du récepteur GFRα1 au GDNF par les spermatogonies indifférenciées (Bosseboeuf et al., 2014). La méiose se déroule des stades VII à XI. Le stade VII correspond aux cystes contenant les spermatocytes primaires en prophase méiotique et tous les noyaux des cellules de Sertoli sont observés contre la lame basale. Le stade VIII correspond à la première division méiotique (métaphase, anaphase, télophase) qui donne les spermatocytes secondaires (stades IX et X). À la fin de la méiose, le nombre de spermatides précoces (ou spermatides rondes) est de 64 par spermatoblaste (stade XI). Les spermatides précoces vont ensuite évoluer en spermatides matures au cours de la spermiogenèse. Au cours de ce processus, les principales transformations cellulaires sont la formation de

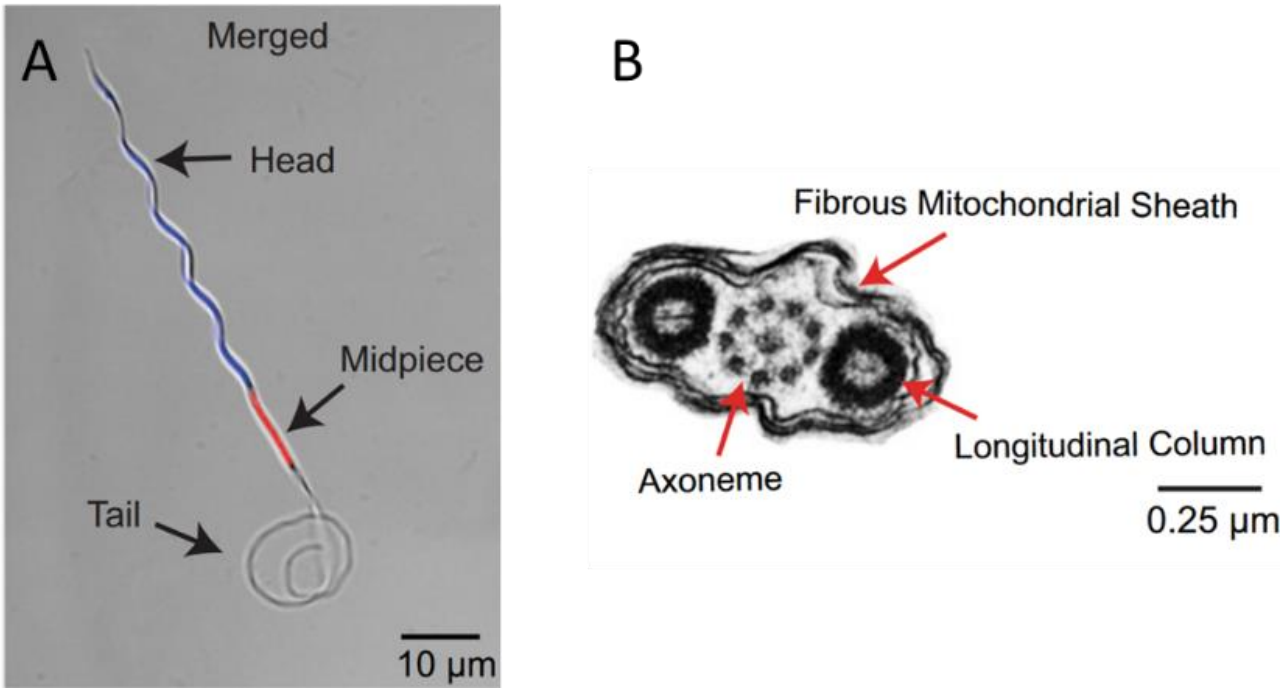


Fig. 15. **Morphologie et ultrastructure des spermatozoïdes des raies *R. javanica* et *T. meyeni*. A.** Image d'un spermatozoïde de raie observé au microscope à fluorescence. L'ADN nucléaire marqué par le Hoechst figure en bleu et les mitochondries marquées par le MitoTracker figurent en rouge. **B.** Ultrastructure d'une coupe transversale du flagelle d'un spermatozoïde de raie. Modifié d'après Wang et al., 2021.

l'acrosome, la compaction de la chromatine avec le remplacement des histones par des protéines de transition puis des protamines, l'assemblage du flagelle et la réorganisation du cytoplasme. Au cours de celle-ci, la majeure partie du cytoplasme et des organites sont éliminés pour conserver un cytoplasme principalement limité à la pièce intermédiaire contenant des mitochondries. Chez *S. canicula*, le stade XI correspond à des cystes avec de jeunes spermatides rondes disposées en « feston » avec des noyaux présentant des plages de chromatine dense et des flagelles visibles. Au stade XII, la condensation de la chromatine est bien avancée et l'allongement de la tête spermatique et du flagelle sont observables sur coupes histologiques. Au cours des stades suivants, le développement de la tête hélicoïdale, caractéristique des spermatozoïdes de Chondrichtyens, se produit et s'achève au stade XIV. À ce stade, les spermatides sont disposées en faisceaux parallèles perpendiculaires à la lame basale du cyste. La torsion hélicoïdale de la spermatide, qui comprend la tête, la pièce intermédiaire et les éléments flagellaires, joue un rôle dans la motilité des spermatozoïdes. Ceux-ci, tournent autour de leur grand axe en utilisant leur tête et leur queue pour une propulsion bidirectionnelle, comme observé chez la raie *Taeniura meyeni* (Wang et al., 2021). Le flagelle du spermatozoïde présente la particularité d'avoir, en plus de la gaine fibreuse classiquement observée, deux colonnes fibreuses longitudinales se développant à partir de l'anneau et s'étendant de chaque côté de l'axonème (Stanley, 1971; Wang et al., 2021). Ces colonnes joueraient un rôle dans la propulsion bidirectionnelle du spermatozoïde (Fig. 15) (Wang et al., 2021). Au cours des stades XV à XVII, les noyaux des cellules de Sertoli migrent vers le cytoplasme intermédiaire de la cellule et les faisceaux de spermatides deviennent plus compacts et plus proches de la lame basale. La pièce intermédiaire de la spermatide est également bien visible à l'arrière de la tête. Au niveau de l'ultrastructure, chez l'aiguillat *Squalus suckleyi*, des granules de glycogène sont présents et dispersés entre les mitochondries, l'acrosome forme une coiffe étendue sur le noyau de la spermatide et un court perforatorium se développe entre le noyau et l'acrosome (dans l'espace subacrosomique) (Pudney, 1995; Stanley, 1971). Classiquement, un perforatorium permet la pénétration du spermatozoïde à travers le chorion de l'ovule lors de la fécondation. Un autre trait caractéristique des étapes de la spermiogenèse chez les Élasmobranches est l'apparition d'un corps protéique dans le cytoplasme intermédiaire de la cellule de Sertoli (stade XVI), le corps de Semper. Sa fonction n'est pas claire et il sera libéré avec les faisceaux de spermatozoïdes lors de la spermiation. Comme il contient des gouttelettes lipidiques et des organites

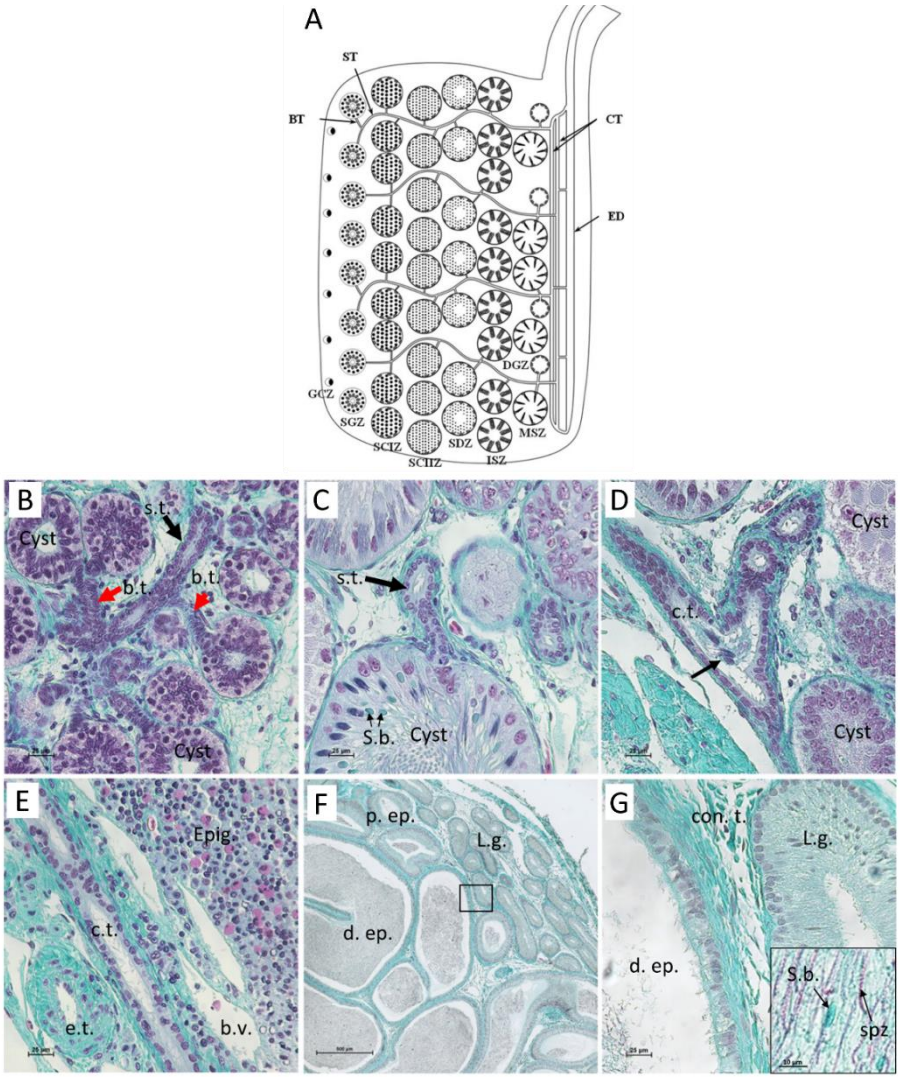


Fig. 16. **Système des canaux intratesticulaires, de l'épididyme et de la glande de Leydig du tractus génital mâle chez les Élasmobranches.** **A.** Schéma du système de canaux intratesticulaires chez *Mustelus manazo*. BT, tubule ramifié ; ST, tubule souche ; CT, tubule collecteur ; ED, canal efférent ; GCZ, zone germinative ; SGZ, zone des cystes à spermatogonies ; SCIZ, zone des cystes à spermatocytes primaires ; SCIIZ, zone des cystes à spermatocytes secondaires ; SDZ, zone des cystes à spermatides rondes ; ISZ, zone des cystes à spermatides allongées ; DGZ, zone des cystes post-spermiants. D'après Park et al., 2013. **B-C.** Tubules intratesticulaires. B : Au cours de leur développement, les cystes sont connectés très tôt à des tubules ramifiés (b.t.) qui convergent en tubules souches (s.t.). C : histologie d'un cyste en spermiation avec son tubule ramifié ouvert et connecté à un tubule souche ; S.b. : corps de Semper. **D-E**. Tubules collecteurs et canaux efférents. D : tubule collecteur (c.t.) contenant un faisceau de spermatozoïdes (flèche). E : réseau de tubules au niveau de la connexion entre les tubules collecteurs (c.t.) et les tubules efférents (e.t.). Ce réseau est positionné sur la bordure testiculaire adjacente au tissu épigonal (Epig.). b.v. : vaisseau sanguin. **F.** Histologie des tubules positionnés à la jonction entre les segments proximal (p. ep.) et distal (d. ep.) de l'épididyme et de la glande de Leydig adjacente (L.g.). **G.** Vue agrandie du carré de la Fig. 16F illustrant les épithéliums de l'épididyme et de la glande de Leydig qui sont séparés par un tissu conjonctif (con. t.). Dans la lumière de l'épididyme sont retrouvés les spermatozoïdes (spz) et corps de Semper (S.b.) (insert Fig. 16G) (Sourdaine and Jeanne, 2024).

(mitochondries, ribosomes, réticulum endoplasmique), dont certains sont associées à la synthèse des stéroïdes, Pudney et Callard (1986) ont émis l'hypothèse qu'il pourrait contribuer à la synthèse des stéroïdes présents dans le sperme et qu'il serait nécessaire à la maturation et à la survie des spermatozoïdes dans les tractus génitaux. Une autre hypothèse serait que le corps de Semper est l'équivalent du corps résiduel des spermatides de Mammifères ; sa fonction reste à étudier. Le stade XVIII correspond à la spermiation qui se déroule par le détachement des faisceaux de spermatides et de la partie adluminale du cytoplasme sertolien. Les faisceaux de spermatozoïdes sont ensuite évacués par les canaux collecteurs cystiques (tubules ramifiés), préalablement fermés par un bouchon cellulaire. En prenant en compte le nombre de 500 spermatoblastes par cyste chez *S. canicula*, 32 000 spermatozoïdes seraient produits par cyste pour cette espèce. Le cyste post-spermiation contenant les cytoplasmes basaux et les noyaux sertoliens serait résorbé dans le tissu épigonal (McClusky and Sulikowski, 2014; Park et al., 2013). Cependant, le tissu épigonal n'étant pas observé chez plusieurs requins squaloïdes des grands fonds (Girard et al., 2000), sa fonction dans la résorption des cystes reste à confirmer. Une autre caractéristique intéressante de cette association est l'effet inhibiteur du tissu épigonal sur la synthèse de l'ADN des cystes pré-méiotiques, ce qui suggère une interaction entre les deux organes pour réguler le cycle spermatogénique (Piferrer and Callard, 1995).

Chez les amniotes, la barrière hémato-testiculaire est essentielle à la spermatogenèse et se met en place au cours de la puberté lorsque les cellules de Sertoli cessent de se diviser. Classiquement, les barrières hémato-tissulaires limitent ou contrôlent l'entrée des molécules présentes dans la circulation dans un tissu ou un compartiment. La barrière hémato-testiculaire est constituée en partie de jonctions spécialisées entre les cellules de Sertoli et crée un microenvironnement spécifique au développement des cellules haploïdes et permet également la production du fluide testiculaire utile, notamment, au transport des spermatozoïdes. Cette barrière hémato-testiculaire peut être visualisée par exclusion d'un colorant fluorescent de haut poids moléculaire (10 kDa). En utilisant cette approche, McClusky a montré qu'elle s'établissait et était fonctionnelle dans les cystes à spermatides chez l'aiguillat *S. acanthias* (McClusky, 2006). Ce résultat est en accord avec la description plus ancienne de jonctions serrées entre les cellules de Sertoli des cystes à spermatides

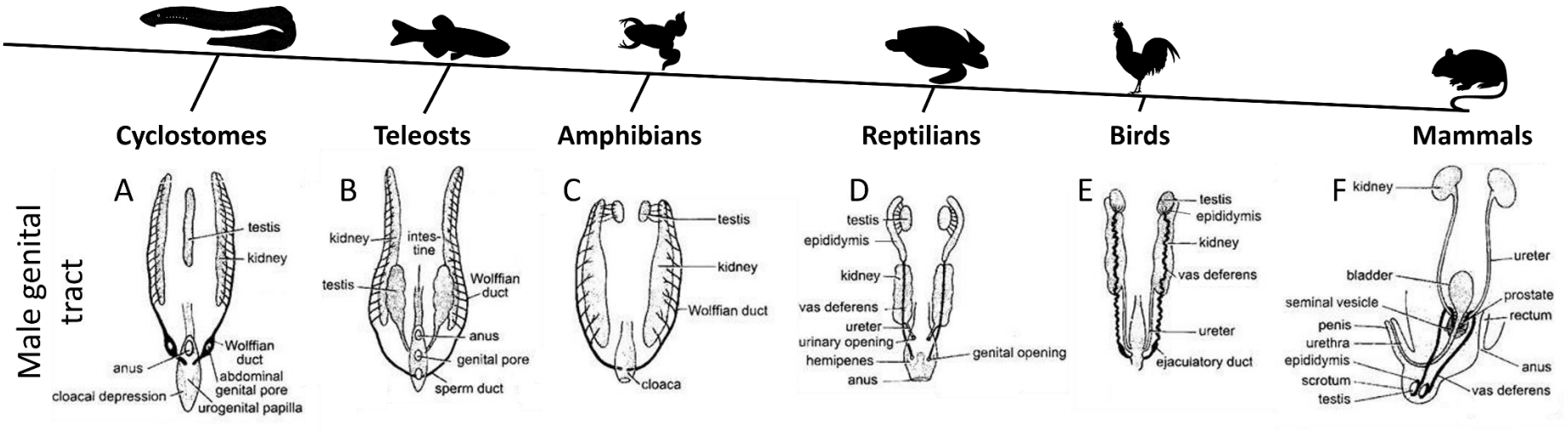


Fig. 17. **Représentation schématique du tractus génital mâle chez différents clades de Vertébrés.** (A) Chez les Cyclostomes, les gonades ne sont pas paires et ne sont connectés à aucun canal. Au niveau des tractus génitaux mâles, les Gnathostomes ont des testicules pairs connectés aux canaux de Wolff, en position postérieure des reins, eux-mêmes connectés aux mésonéphros (reins définitifs des poissons Téléostéens et des Amphibiens) et aux testicules lui donnant la fonction d'urospermiducte (B-C). Chez les amniotes (reptiles, oiseaux et Mammifères), le mésonéphros n'est représenté que par l'épididyme et le canal déférent (*vas deferens*) ce qui lui donne la fonction de spermiducte (D-F). Modifié d'après Bhavya, 2017.

(Collenot and Damas, 1980) ; la structure détaillée de cette barrière hémato-testiculaire reste à être étudiée.

La structure d'un réseau intratesticulaire ramifié de tubules a été bien décrite chez le requin *Mustelus manazo* (Park et al., 2013). Ce système est composé de tubules ramifiés reliés aux cystes et qui, *via* un réseau secondaire de tubules souches, débouchent dans les tubules collecteurs. Les tubules ramifiés et souches peuvent être observés très tôt dans la zone de formation des cystes (stade II) et les cystes sont connectés aux tubules ramifiés tout au long de la spermatogenèse (Fig. 16). Cela implique que les cystes et les tubules migreront simultanément de la zone spermatogoniale vers la zone mature du testicule, impliquant sans aucun doute des mécanismes de régulation encore inconnus. Lors de la spermiation, le bouchon cellulaire qui obstruait le tubule ramifié à sa jonction avec le cyste est éliminé et permet le transfert des faisceaux de spermatozoïdes dans les tubules souches puis les tubules collecteurs. Le transport des spermatozoïdes serait réalisé grâce à la présence de cellules épithéliales ciliées au niveau des différents tubules, et à la contraction des cellules myoïdes entourant les tubules intratesticulaires.

### III.5. Les tractus génitaux mâles

Après leur production et émission par les testicules, les spermatozoïdes vont poursuivre leur maturation dans d'autres organes du tractus génital lorsque celui-ci est différencié. En effet, les tractus génitaux ont également évolué et possèdent leurs propres spécificités en fonction des différents clades de Vertébrés. Chez les Cyclostomes, les gonades ne sont pas paires et les canaux collecteurs sont absents (Fig. 17A), les gamètes étant directement relarguées dans le cœlome avant d'être extrudées vers le milieu extérieur. Au niveau des tractus génitaux mâles, les Gnathostomes ont des testicules pairs et leurs spermatozoïdes sont relargués dans les canaux de Wolff. Chez les anamniotes, les canaux de Wolff sont en position caudale et sont connectés aux mésonéphros (reins définitifs des Téléostéens et des Amphibiens) et aux testicules et jouent le rôle d'urospermiducte (Fig. 17B,C). Chez les amniotes (Sauropsidés et Mammifères), le mésonéphros et les canaux de Wolff ont évolué en canaux déférents, épididyme et canal déférent, lequel joue uniquement le rôle de spermiducte (Fig. 17D-F). Chez les amniotes, l'épididyme permet le transport, la maturation (acquisition de la motilité

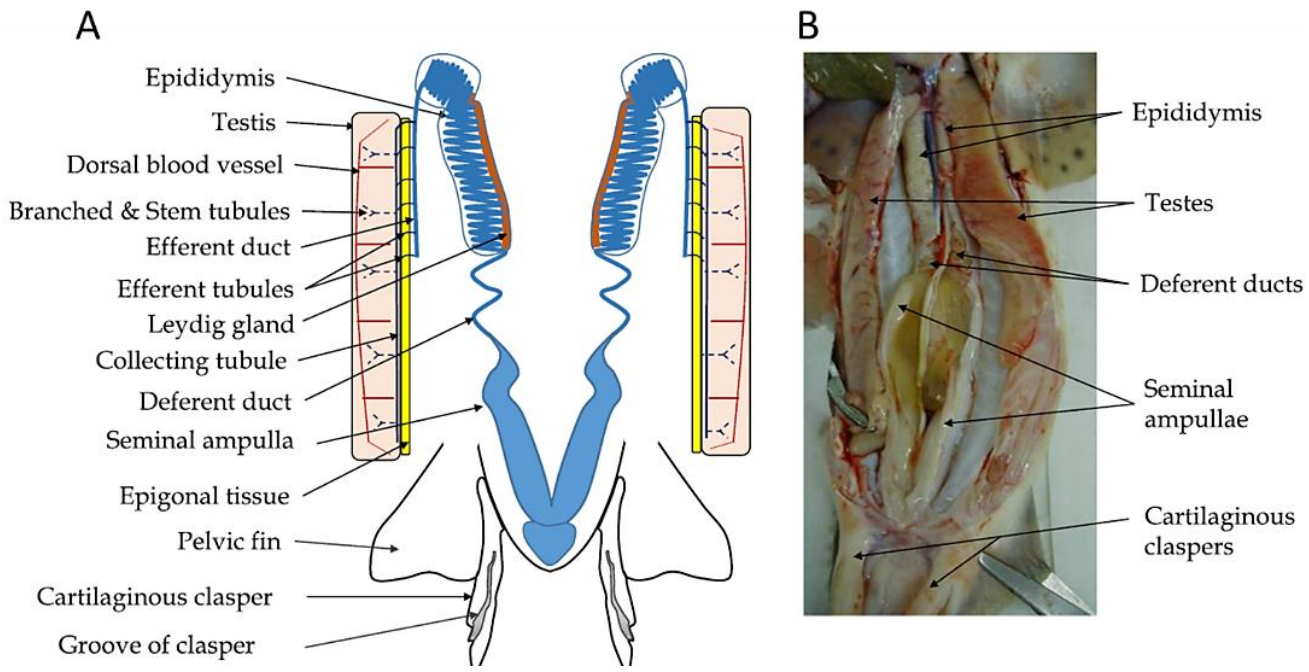


Fig. 18. **Le tractus génital mâle chez la petite roussette *Scyliorhinus canicula*.** Représentation schématique du tractus génital mâle (A) et photo anatomique correspondante (B) (Sourdaine and Jeanne, 2024).

et de l'aptitude à féconder) et le stockage des spermatozoïdes notamment par la sécrétion de protéines et de stéroïdes qui conduisent à la mise en place d'un microenvironnement unique (James et al., 2020; Johnston et al., 2005; Sullivan and Mieusset, 2016).

Chez les Élasmobranches, le tractus génital mâle est anatomiquement élaboré (Fig. 18). Deux testicules allongés ont la particularité d'être étroitement associés au tissu épigonal, un tissu lymphomyéloïde produisant des leucocytes, des granulocytes et des lymphocytes. Les spermatozoïdes sont collectés par un système de canaux associé à chaque testicule et composé de tubules intra-testiculaires (tubules souches et tubules ramifiés), de canaux collecteurs et de deux à six canaux efférents (homologue du *rete testis*) selon les espèces de requins. Les canaux efférents sont suivis de l'épididyme, composé d'un segment proximal et d'un segment distal, qui se prolonge par le canal déférent. Ce dernier enveloppe la vésicule séminale interne et est élargi à son extrémité pour former l'ampoule séminale utilisée pour le stockage des spermatozoïdes. Les parties postérieures des deux ampoules séminales convergent et le sperme passe du sinus urogénital à la papille urogénitale qui forme un sillon au niveau du clasper pelvien ou ptérygopode. Les Élasmobranches mâles possèdent également des structures uniques associées à la reproduction avec la glande de Leydig et les sacs à siphon (Del Mar Pedreros-Sierra and Ramírez-Pinilla, 2015). La glande de Leydig se présente sous la forme d'un canal parallèle accolé à la partie distale de l'épididyme et séparé de celle-ci par du tissu conjonctif. Elle est connectée à son extrémité à l'épididyme et au canal déférent et sécrète une partie du liquide séminal. Même si leurs fonctions restent à clarifier, les sacs à siphons des requins pourraient soit faciliter le transfert des spermatozoïdes dans le tractus génital de la femelle en induisant des contractions utérines, soit aider à la compétition des spermatozoïdes en lavant le tractus génital femelle avant l'éjaculation par l'émission d'un flux d'eau (Gilbert and Heath, 1972; Whitney et al., 2004). Chez les raies, des glandes supplémentaires associées aux claspers, et absentes chez les requins, produiraient un lubrifiant et un fluide coagulant avec l'eau de mer (Pratt and Carrier, 2001).

L'épididyme a été peu étudié chez les Élasmobranches, ce qui est surprenant compte tenu de sa taille et de son apparente similitude avec celui des Mammifères. Des études sur le requin *Heterodontus portusjacksoni* (Jones et al., 1984), sur la raie *Raja eglanteria* (Jones et al., 2005; Jones and Hamlett, 2006) et sur la raie *Potamotrygon motorothe* (Dzyuba et al., 2019) ont montré que l'épididyme participe effectivement aux modifications du fluide séminal avec

notamment une réabsorption du sodium et une sécrétion de potassium et de protéines. Ces études ont également montré que les spermatozoïdes, immotiles dans le segment proximal épididymaire, acquièrent leur motilité dans le segment distal épididymaire. Chez la raie *R. eglanteria*, les cellules épithéliales de l'épididyme et de la glande de Leydig présentent différentes activités de synthèse de glucides (glucosamine, galactosamines, acide sialique) et de structures glycanes (N-linked glycans, N-acetyl galactosamine) qui pourraient contribuer à la maturation des spermatozoïdes mais également à la formation d'une matrice glycosylée impliquée dans la réagrégation des spermatozoïdes (Jones and Hamlett, 2002). En effet, lors de leurs transports depuis le cyste, où ils étaient agrégés en faisceaux, jusqu'au segment distal de l'épididyme, les faisceaux de spermatozoïdes sont dissociés et les spermatozoïdes se réagrègent en spermatophores ou en spermatozeugmatas, selon les espèces, au niveau des ampoules séminales (Pratt and Tanaka, 1994). Les spermatozoïdes sont stockés dans un état motile dans les ampoules séminales et une hyperactivation a lieu dans l'appareil reproducteur femelle, leur permettant de progresser dans des environnements visqueux (utérus, glande oviducale et oviducte) grâce à leur propulsion rotationnelle particulière (Wang et al., 2021).

# IV. Origines évolutives et approche comparée des axes endocrines cerveaux-hypophyse-testicule impliquant les hormones glycoprotéiques

## IV.1. Généralités sur les axes cerveau-hypophyse-gonade (HHG) et glande thyroïde (HHT)

Chez les Vertébrés, le contrôle neuroendocrine de la reproduction et du métabolisme sont assurés par les axes hypothalamo-hypophyso-gonadique et -thyroïdien, respectivement (Zubeyde et al., 2021). Ces deux axes impliquent l'hypothalamus qui est une petite région du cerveau inclue dans le système limbique et qui fait le lien entre le système nerveux central et le système endocrinien. Chez les Mammifères, l'hypothalamus est directement relié par un mince pédoncule, nommé éminence médiane ou *infundibulum*, à l'hypophyse ou glande pituitaire. L'hypophyse est composée de trois régions distinctes que sont les lobes antérieurs, intermédiaire et postérieur. L'hypophyse antérieure ou adénohypophyse dérive du tissu épithélial de la cavité buccale embryonnaire dont la partie bulbeuse, appelée *pars distalis*, est dans le prolongement du lobe tubéral (*pars tubelaris*) de l'*infundibulum*. Le lobe intermédiaire ou *pars intermedia* est plus ou moins développé selon les espèces et se présente généralement sous la forme d'une fine bande de tissu qui délimite les hypophyses antérieure et postérieure. L'hypophyse postérieure, ou neurohypophyse, est constituée par les prolongements axonaux des neurones hypothalamiques formant la tige infundibulaire et se terminant par une région bulbeuse ou *pars nervosa*. La neurohypophyse est à l'origine de neurohormones telles la vasopressine ou hormone antidiurétique (ADH) et l'ocytocine. L'adénohypophyse produit une large variété d'hormones qui régulent l'activité de nombreuses glandes endocrines périphériques. Les cellules hormonogènes de l'adénohypophyse sont généralement classées en cinq grands types selon la nature des hormones synthétisées : les cellules somatotropes à somatotropine (hormone de croissance) ; les cellules lactotropes à prolactine (PRL) ; les cellules thyréotropes à thyréostimuline (TSH) ; les cellules corticotropes aux hormones adrénocorticotropes (ACTH) ; les cellules mélanotropes à mélanotropine (MSH) ; et les cellules gonadotropes qui sécrètent l'hormone folliculostimulante (FSH) et l'hormone lutéinisante (LH). La synthèse de ces hormones de l'adénohypophyse est contrôlée par le système nerveux central, intégrant notamment les informations physiologiques et environnementales, *via* l'hypothalamus et la neurosécrétion de peptides régulateurs. Dans le cadre de la régulation de la reproduction, l'hypothalamus

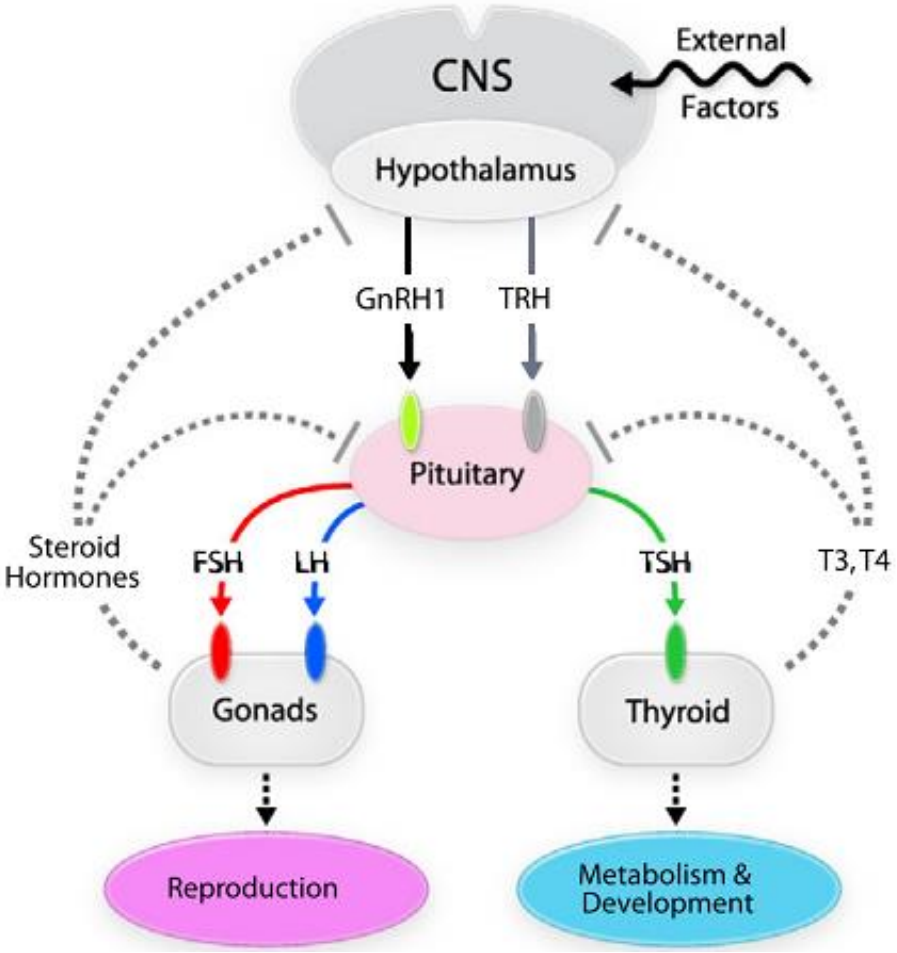


Fig. 19. **Représentation schématique des axes hypothalamo-hypophyso-gonadique (HHG) et -thyroïdien (HHT), exemple des Mammifères.** L'axe HHG fait intervenir la gonadolibérine (GnRH) hypothalamique. La GnRH stimule les sécrétions hypophysaires des hormones gonadotropes, FSH et LH, qui régulent les fonctions gonadiques par l'activation de leurs récepteurs spécifiques, FSHR et LHR. L'axe HHT fait intervenir la thyréolibérine (TRH) hypothalamique qui stimule la synthèse et la sécrétion hypophysaire de la thyréostimuline (TSH) ayant pour fonction de stimuler la production des hormones thyroïdiennes T4 (thyroxine) et T3 (triiodothyronine) par activation de son récepteur TSHR. Les hormones stéroïdiennes et thyroïdiennes agissent en rétrocontrôles négatifs au niveau de l'hypophyse et du système nerveux central (CNS). Modifié d'après de Sower, 2018.

synthétise et libère le neurodécapeptide GnRH, ou gonadolibérine, qui est acheminé vers l'adénohypophyse par le biais du système porte, lorsqu'il est présent, afin de stimuler la synthèse et la libération des hormones gonadotropes, FSH et LH. Ces gonadotrophines (GTHs) sont acheminées, par le biais du système circulatoire général, vers les gonades où elles stimuleront la gamétogenèse et la stéroïdogenèse après interaction avec leurs récepteurs spécifiques, FSHR et LHR (Fig. 19).

En ce qui concerne la régulation du métabolisme, l'hypothalamus synthétise et libère thyréolibérine (TRH) qui stimule la production de thyrotropine (TSH) hypophysaire qui, à son tour, stimulera la production et la sécrétion des hormones thyroïdiennes, la thyroxine (T4) et la triiodothyronine (T3). La T3 étant la forme active se liant aux récepteurs TRα et TRβ, elle est obtenue par conversion de la T4 par les déionidases D1 et D2 au niveau des tissus cibles. Au niveau de l'organisme, l'expression ubiquiste des récepteurs permet une action pléiotrope de la T3 notamment sur la croissance, le développement et le maintien des fonctions basales des systèmes cardiovasculaire, respiratoire, squelettique et nerveux central. Pour chaque axe, les glandes périphériques exercent un rétrocontrôle sur leur propre sécrétion en agissant soit directement sur l'adénohypophyse, soit indirectement *via* le système nerveux central et l'hypothalamus (Sower, 2018).

L'hypothalamus et l'hypophyse sont présents chez tous les Vertébrés, des Cyclostomes aux Mammifères (Fig. 20A) (Santiago-Andres et al., 2021). Les Protochordés et les autres invertébrés sont dépourvus d'hypophyse. Au cours de l'évolution des Vertébrés, les caractéristiques structurales de l'hypophyse et de l'hypothalamus ont évolué, ce qui a pu optimiser la communication entre ces tissus. Les vertébrés sont devenus plus grands et plus complexes, et la distance entre l'hypothalamus et l'hypophyse a augmenté de manière significative. Classiquement, chez les Vertébrés, il existe généralement 3 modèles de contrôle anatomique de l'hypophyse : le système porte *via* l'éminence médiane (Tétrapodes), l'innervation directe (Téléostéens) et la diffusion (Cyclostomes) (Gorbman, 1995; Sower, 2015). Cependant, une particularité des Élasmobranches est la localisation d'une partie des cellules hormonogènes, notamment les cellules gonadotropes au sein du lobe ventral hypophysaire qui n'est pas alimenté par un système porte ou des projections neuronales (Fig. 20B) (Santiago-Andres et al., 2021). Cette hypothèse a été étayée par le dosage du GnRH dans

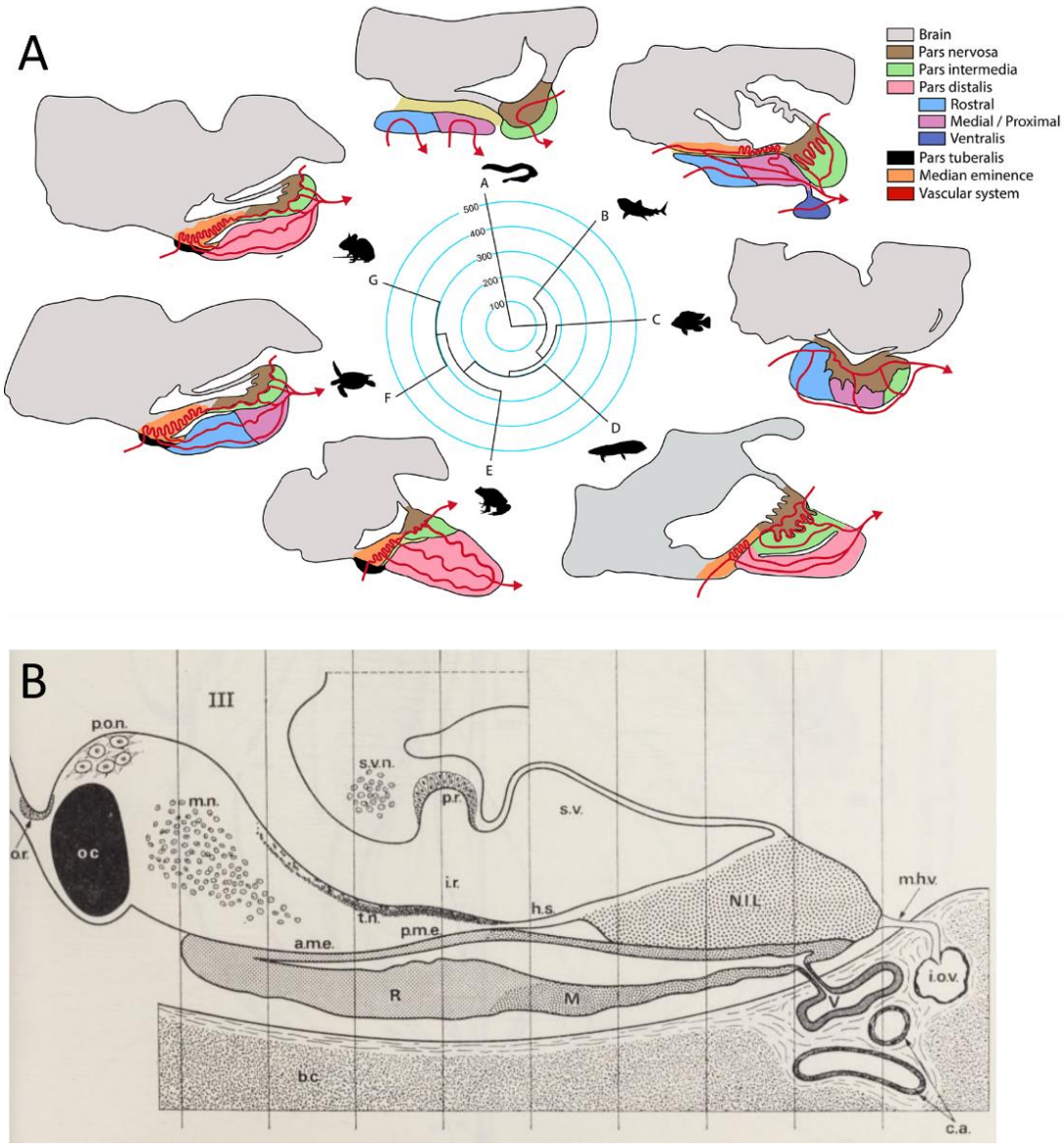


Fig. 20. **Représentation schématique des organisations anatomiques de l'hypophyse.** **A.** Organisations anatomiques de l'hypophyse de plusieurs espèces représentatives des principaux clades de Vertébrés. Les branches terminales de l'arbre phylogénétique montrent un organisme représentatif de chaque clade (A, Cyclostome ; B, Chondrichtyen ; C, poisson téléostéen ; D, dipneuste ; E, amphibien ; F, Sauropsidé ; G, Mammifère) et la représentation sagittale des principales structures de l'hypophyse. La base de données TimeTree a été utilisée pour construire l'arbre et les nombres dans la phylogénie sont en millions d'années (Santiago-Andres et al., 2021). **B.** Organisation anatomique de l'hypophyse et de l'hypothalamus chez la petite roussette *Scyliorhinus canicula*. a.m.e., éminence médiane antérieure ; b.c., base du crâne ; c.a., artères carotides ; h.s., tige hypophysaire ; i.o.v., veine interorbitaire ; i.r., creux infundibulaire ; M, lobe médian de l'hypophyse ; m.n., noyau médian ; m.h.v., veine hypophysaire médiane ; N.I.L., lobe neuro-intermédiaire ; o.c., chiasma optique ; o.r., cavité préoptique ; p.m.e., éminence médiane postérieure ; p.o.n., noyau préoptique ; p.r., creux postérieur ; R, lobe rostral de l'hypophyse, s.v., *saccus vasculosus* ; s.v.n., noyau du *saccus vasculosus ;* t.n., noyau tubéral ; V, lobe ventral de l'hypophyse (Knowles et al., 1975).

la circulation systémique à des concentrations physiologiques (D'antonio et al., 1995; Knowles et al., 1975; Sherwood and Lovejoy, 1993).

## IV.2. Origine et diversité des GnRHs et de leurs récepteurs chez les Vertébrés

### IV.2.1 Diversité des GnRHs chez les Vertébrés

Avant l'émergence des Vertébrés, deux duplications globales des génomes (1R et 2R) et de multiples et indépendantes pertes de gènes ont conduit à l'émergence de trois orthologues du GnRH, correspondant aux GnRH1, GnRH2 et GnRH3 (Gaillard et al., 2018). Chez les espèces possédant plusieurs formes de GnRHs, une distribution particulière dans le cerveau peut être associée à chaque forme. Chez les Gnathostomes, trois grands systèmes neuronaux à GnRH ont été identifiés (Dubois et al., 2002). Le premier, appelé système GnRH du cerveau antérieur ventral, est composé de neurones principalement situés dans l'aire préoptique de l'hypothalamus et qui projettent vers les cellules gonadotropes de l'hypophyse. La forme moléculaire de la GnRH généralement synthétisée par ces neurones est la GnRH1 et correspond à la forme hypophysiotrope. Le gène codant pour la GnRH1 est conservé chez les Gnathostomes, à l'exception de quelques Téléostéens, alors qu'il a été perdu chez les Cyclostomes (Fig. 21). Le second système GnRH, appelé système GnRH mésencéphalique, est composé de neurones situés dans le tegmentum mésencéphalique, près du troisième ventricule. Ces neurones se projettent dans tout le cerveau, en particulier vers le mésencéphale et le cerveau postérieur, mais aussi vers l'hypophyse chez certaines espèces de Téléostéens et d'Amphibiens. Ils produisent la GnRH2 qui est conservée chez tous les Vertébrés à l'exception de quelques Mammifères. Le troisième système, appelé système GnRH du nerf terminal, n'a été identifié que chez les Téléostéens. Les neurones de ce système sont principalement situés dans le ganglion terminal central près du bulbe olfactif et se projettent principalement vers le télencéphale mais aussi plus largement dans l'ensemble du cerveau, y compris la rétine et l'épithélium olfactif. Ils expriment spécifiquement la GnRH3 (Okubo and Nagahama, 2008) qui n'a pas été identifiée chez les Tétrapodes et les Holocéphales alors qu'elle a été maintenue chez les Téléostéens, les Élasmobranches et a été dupliquée chez les Cyclostomes pour donner les paralogues GnRHI et GnRHIII. Enfin, la GnRH4 putative aurait probablement disparu peu après la 2R sans laisser de traces chez les espèces

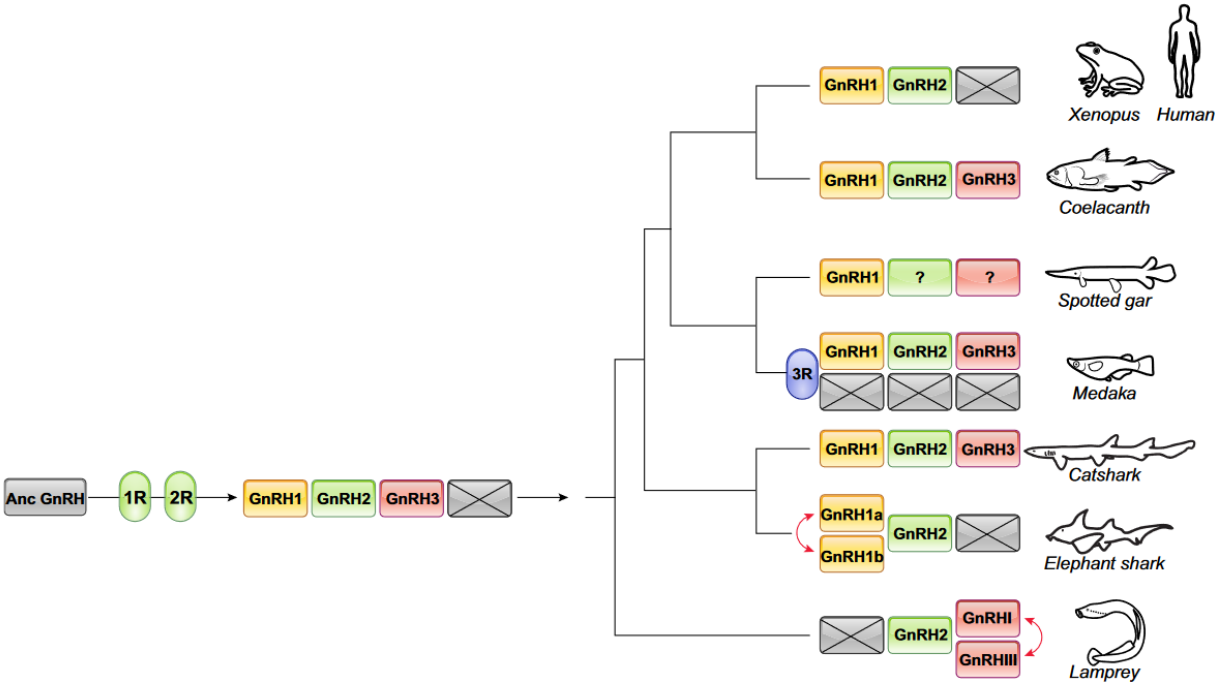


Fig. 21. **Représentation schématique du scénario évolutif de la famille des GnRHs chez les Vertébrés.** Après la première (1R) et la deuxième (2R) duplication globale des génomes, le gène ancestral des GnRHs (Anc GnRH) a donné les gènes codant pour la GnRH1, la GnRH2, la GnRH3 et la GnRH4 (laquelle a rapidement été perdue). La troisième duplication du génome (3R) n'a pas été à l'origine de nouveaux gènes. Les croix noires correspondent aux gènes perdus et les flèches rouges aux duplications locales de gènes (Dufour et al., 2020).

encore vivantes. En dehors de ces considérations générales, d'autres pertes de GnRHs, spécifiques à une espèce, à un genre ou à une famille, se sont produites. Par exemple, certains Téléostéens ont perdu la GnRH1, notamment le saumon, la truite, le poisson zèbre et le poisson rouge, ou la GnRH3, comme par exemple l'anguille et le poisson-chat (Dufour et al., 2020). Chez la chimère éléphant *C. milii*, deux paralogues de la GnRH1 ont été identifiés (GnRH1a et GnRH1b) et la GnRH3 a aussi été perdue (Gaillard et al., 2018). De même, certains Mammifères ont perdu, en plus de la GnRH3, la GnRH2, comme les Murins et les Bovins, et ne possèdent plus que la GnRH1. Par ailleurs, il peut être noté qu'aucun effet de la 3R n'a été observé sur le nombre actuel de GnRHs chez les Téléostéens, ce qui suggère des pertes massives de gènes après celle-ci. En revanche, deux GnRH3s sont présentes chez le saumon *Salmo salar* probablement en raison de la quatrième duplication globale du génome (4R) spécifique aux Salmonidés (Dufour et al., 2020).

Les gènes des GnRHs codent pour des précurseurs inactifs nommés preproGnRHs, dont le peptide signal sera clivé pour donner les proGnRHs qui seront ensuite clivés, par des proprotéines convertases, en peptides actifs qui seront sécrétés. À noter que la séquence située dans la région carboxy-terminale des proGnRHs correspond au GAP (*GnRH-associated protein*) (Wetsel and Srinivasan, 2002) et aurait un effet positif sur la production de 17α, 20β-dihydroxy-4-pregnen-3-one (DHP) et sur le frai, comme observé chez le poisson rouge *Carassius auratus* traité *in vivo* par un recombinant GnRH-GAP (Mohammadzadeh et al., 2020). Les GnRHs sont constituées de 10 acides-aminés avec une conservation au cours de l'évolution des acides-aminés en position 1-4 (QHWS), 9 (P) et 10 (G), la présence d'un pyroglutamate en position N-terminal et d'une glycine-amide en position C-terminal. Ces acides aminés sont indispensables à la mise en place de l'interaction et à l'activation des récepteurs aux GnRHs (GnRHR) (Millar, 2005). Une glycine en position 6 est souvent conservée et augmente la flexibilité globale de la séquence, ce qui favorise la mise en place de l'interaction ligand-récepteur. Plus de 10 séquences différentes (isoformes) de GnRH1 ont été identifiées chez les Vertébrés alors que les GnRH2 et GnRH3 apparaissent nettement plus conservées avec des séquences majoritaires QHWSHGWYPG et QHWSYGWLPG, respectivement (Choi, 2018).

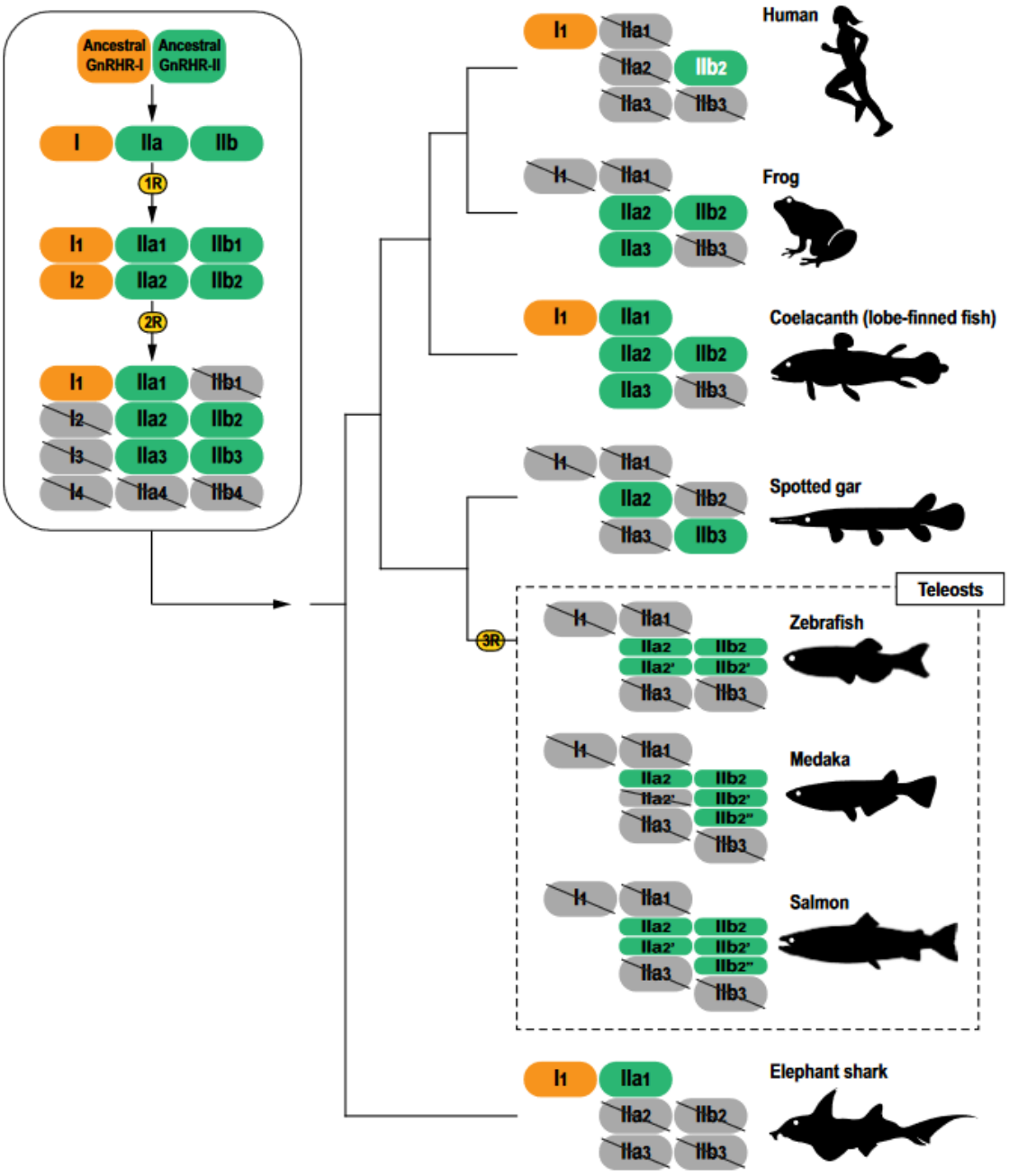


Fig. 22. **Représentation schématique de l'évolution des types de récepteurs aux GnRHs (GnRHR) chez les Gnathostomes.** Ce modèle a été construit sur la base d'analyses de synténie des gènes. Six orthologues de récepteurs aux GnRHs (GnRHR-I, -IIa1, -IIa-2, -IIa3, -IIb2 et -IIb3) seraient dérivés des GnRHR-I et GnRHR-II ancestraux *via* les deux cycles de duplication du génome (1R et 2R). Les GnRHRs de types -I2, -I3,-I4, -IIa4, -IIb1 et -IIb4 auraient été perdus dans la lignée ancestrale des Vertébrés (encadré de gauche). Chez les Téléostéens (encadré en pointillé), la 3R aurait contribué à générer les sous-types supplémentaires GnRHR-IIa2' et -IIb2', puis une duplication locale supplémentaire serait à l'origine du sous-type -IIb2'' (Ogawa et al., 2022).

### IV.2.2 Diversité des récepteurs aux GnRHs (GnRHRs)

En parallèle de l'évolution des GnRHs, leurs récepteurs ont également coévolué et se seraient diversifiés à partir d'un GnRHR ancestral lors des différentes duplications globales des génomes (Ogawa et al., 2022). La famille des récepteurs aux GnRHs a été catégorisée en deux grands groupes correspondant aux GnRHR type-I et GnRHR type-II avec six sous-familles correspondant aux types -I, -IIa1, -IIa2, -IIa3, -IIb2 et -IIb3 (Fig. 22). Des événements multiples de pertes de gènes ont conduit au maintien d'un à cinq types de GnRHRs selon les espèces avec, par exemple, uniquement le GnRHR-I chez l'humain et les GnRHR-I1, GnRHR-IIa1, GnRHR-IIa2, GnRHR-IIa3 et GnRHR-IIb2 chez le cœlacanthe *Latimeria chalumnae*. Chez les Chondrichtyens étudiés, seuls les GnRHR-I1 et IIa1 ont été maintenus chez la chimère *C. milii* alors que quatre récepteurs ont été identifiés chez le requin *S. torazame*, sans que leurs types aient été déterminés (Hara et al., 2018). Chez certains Téléostéens comme *D. rerio*, seuls deux types de GnRHR, le -IIa2 et le -IIb2, ont été maintenus mais la 3R a conduit à l'émergence de deux paralogues nommés GnRHR-IIa2' et GnRHR-IIb2'.

Chez les Tuniciers, neuf GnRH-*like* et quatre GnRHRs ont été identifiés (Roch et al., 2011; Sakai et al., 2020). Plus ancestralement, chez le céphalochordé *Branchiostoma floridae*, deux peptides GnRH-*like* (Roch et al., 2014; Sakai et al., 2020) et quatre GnRHR-*like* ont été identifiés avec les GnRHR-1 et -2 qui sont des membres du groupe des GnRHRs de Vertébrés et les GnRHR-3 et -4 qui sont des membres du groupe des ancêtres moléculaires des récepteurs d'invertébrés nommés « CRZ receptor/invertebrate GnRHR ». Ces peptides et ces récepteurs pourraient correspondre aux séquences ancestrales ou à l'état de transition entre les CRZ (corazonine) d'invertébrés et les GnRHs (Sakai et al., 2020).

D'un point de vue fonctionnel, tous les GnRHRs sont activés par les différentes GnRHs, avec cependant une efficacité variable, comme observé chez le cœlacanthe *L. chalumnae* (Sefideh et al., 2014), la cione *Ciona intestinalis* (Tello et al., 2005), la carpe *Ctenopharyngodon idellus* et chez l'humain (Li et al., 2022).

Au niveau de leurs structures, les récepteurs aux GnRHs présentent les caractéristiques des récepteurs couplés aux protéines G (RCPG) (Millar, 2003). Le domaine N-terminal est suivi de sept domaines transmembranaires (TM) hélicoïdaux reliés par trois boucles extracellulaires (EL) et trois boucles intracellulaires (IL). Les domaines extracellulaires sont généralement impliqués dans la liaison du ligand et les TM seraient impliqués dans le changement de

conformation induisant l'activation de la cascade de signalisation. Les domaines intracellulaires sont quant à eux impliqués dans l'interaction avec les protéines de la signalisation cellulaire dont les protéines G (Sakai et al., 2020).

### IV.3. Un rôle paracrine des GnRHs au niveau testiculaire chez les Vertébrés

En dehors de leurs rôles régulateurs de l'axe HHG, les GnRHs possèdent des fonctions extra-cérébrales qui ont été décrites ces dernières décennies. En effet, les gènes codant les GnRHs et les GnRHRs sont exprimés au niveau de glandes périphériques tel le testicule, comme cela a été observé chez la grenouille *Rana esculenta* (Chianese et al., 2012), chez *D. rerio* (Fallah et al., 2020) et chez l'humain (Ciaramella et al., 2015). Cette coexpression est à l'origine d'une régulation autocrine/paracrine de la fonction testiculaire. Il a été notamment montré chez le porc *Sus domesticus*, que les niveaux de GnRH2 et de GnRHR-2 testiculaires étaient plus élevés que les niveaux hypophysaire et hypothalamique, avec une immunolocalisation du GnRH2 dans les cellules germinales et du GnRHR-2 dans les cellules de Leydig. Des traitements par la GnRH2 ont stimulé la sécrétion de testostérone par des explants testiculaires en culture, et également *in vivo*, avec des concentrations comparables à celles obtenues pour des stimulations *in vitro* par la gonadotrophine chorionique humaine (hCG) ou *in vivo* par la GnRH1 (Desaulniers et al., 2015). Dans cette étude, l'absence d'élévation de la LH plasmatique en réponse à la GnRH2, contrairement à la stimulation in vivo par la GnRH1, suggérait également un rôle paracrine de GnRH2 chez le verrat (Desaulniers et al., 2015). Chez *D. rerio*, les gènes *gnrh2*, *gnrh3*, *gnrhr1*, *gnrhr2*, *gnrhr3* et *gnrhr4* sont exprimés au niveau testiculaire et les GnRHs ont été immunolocalisés au niveau des spermatogonies, des cellules germinales méiotiques et post-méiotiques, des cellules de Sertoli et des cellules de Leydig. Des cultures d'explants testiculaires traités avec la GnRH2 et la GnRH3 ont montré une stimulation de la spermatogenèse basale en augmentant le nombre de spermatogonies indifférenciées et de spermatozoïdes avec également une augmentation de la production de testostérone (Fallah et al., 2020). L'ensemble de ces résultats soutient fortement l'hypothèse selon laquelle les GnRHs gonadiques feraient partie d'un système complexe de régulation multifactorielle qui contrôlerait la gamétogenèse et la stéroïdogenèse de manière autocrine et/ou paracrine chez les Vertébrés. Cependant, ces fonctions n'ont été caractérisées que chez un nombre restreint d'espèces dont des Mammifères et un Téléostéen, ce qui soulève la question de la

conservation de ces rôles autocrines/paracrines des GnRHs au cours de l'évolution des Vertébrés.

Chez les Élasmobranches, les gènes *gnrhr1a*, *gnrhr1b* et *gnrhr2b* sont exprimés au niveau testiculaire, comme observé chez *S. torazame*, alors que les *gnrhs* ne semblent pas l'être (Hara et al., 2018). D'un point de vue fonctionnel, des études antérieures ont montré que la GnRH agit directement sur les ovaires de la petite raie *Leucoraja erinacea* pour stimuler la stéroïdogenèse (Callard et al., 1993), notamment en augmentant la production de testostérone, ce qui est en accord avec les concentrations physiologiques des GnRHs trouvées dans le plasma (D'antonio et al., 1995; Knowles et al., 1975; Sherwood and Lovejoy, 1993). Ces résultats suggèrent l'existence d'une régulation de la gamétogenèse par les GnRHs circulantes d'origine hypothalamique, ce qui reste à être caractérisé.

### IV.4. Origine et évolution des hormones glycoprotéiques chez les Vertébrés

Les hormones glycoprotéiques constituent une famille d'hormones clefs dans la régulation de la reproduction et du métabolisme.

Au début des années 2000, deux gènes supplémentaires, *gpa2* et *gpb5*, apparentés aux sous-unités *cga*, *lhβ*, *fshβ* et *tshβ*, ont été identifiés à partir du génome humain (Hsu et al., 2002). Sur la base de la capacité de la protéine humaine recombinante GPA2/GPB5 à augmenter la production de thyroxine par activation du TSHR humain et de rat, la GPH correspondante a été nommée thyrostimuline ou hormone glycoprotéique dérivée des corticotrophes (CGH) (Nagasaki *et al*., 2006; Nakabayashi et al., 2002). Cette découverte a apporté un nouveau regard sur l'évolution des hormones glycoprotéiques. En effet, des orthologues de *gpa2* et *gpb5* ont été identifiés chez d'autres Vertébrés (Buechi and Bridgham, 2017; Cahoreau et al., 2015; Hara et al., 2018; Levavi-Sivan et al., 2010; Sower et al., 2015) et des orthologues ancestraux, renommés récemment GPA et GPB (Dufour et al., 2020; Querat, 2021), ont été identifiés chez plusieurs Protostomiens (Heyland et al., 2012; Kudo et al., 2000; Sudo et al., 2005; Wahl et al., 2022), Chordés primitifs (Dong et al., 2013; P. Wang et al., 2018; Yang et al., 2023), mais pas chez les Cnidaires (Dos Santos et al., 2009). De plus, les hormones GPA/GPB recombinantes peuvent activer les GpHRs ancestraux présents chez les Protostomiens (Kenis et al., 2023; Rocco and Paluzzi, 2020; Sudo et al., 2005; P. Wang et al., 2018) et les Chordés

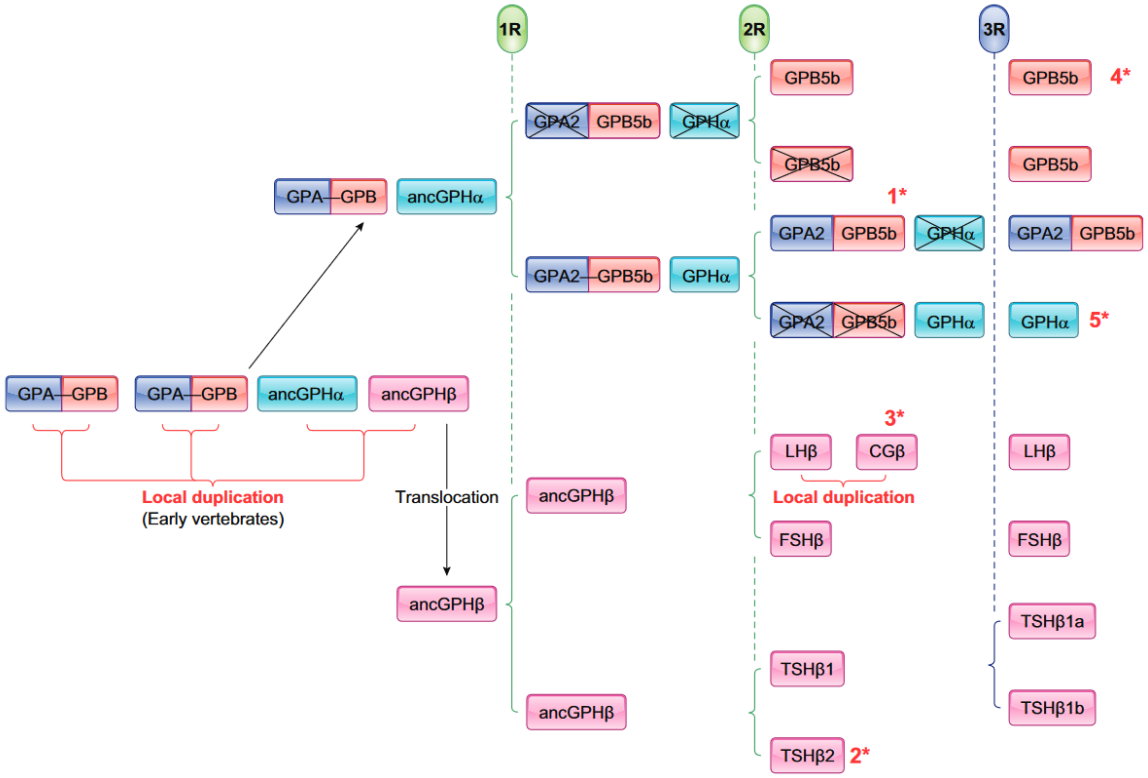


Fig. 23. **Représentation schématique des événements de duplications de gènes, de génomes et de perte de gènes liés aux sous-unités des hormones glycoprotéiques.** 1R, première duplication du génome, 2R, deuxième duplication du génome, 3R, troisième duplication du génome. 1*, le locus *gpa2-gpb5a* a été maintenu chez les Téléostéens et le cœlacanthe alors que le gène *gpb5a* a été perdu chez les Tétrapodes. 2*, la sous-unité TSHβ2 a été conservée chez les Sarcoptérygiens basaux (cœlacanthes et dipneustes) et les Chondrichtyens alors qu'il a été perdu chez les Téléostéens et les Tétrapodes. 3*, le gène codant pour la sous-unité LHβ a été dupliqué pendant la radiation des primates pour générer plusieurs copies de gènes codant la sous-unité CGβ. 4*, après la 3R, seule la sous-unité TSHβ1b a été conservée. 5*, certains Téléostéens peuvent avoir deux copies de la sous-unité CGA résultant d'événements de tétraploïdisation récents et spécifiques (Dufour et al., 2020).

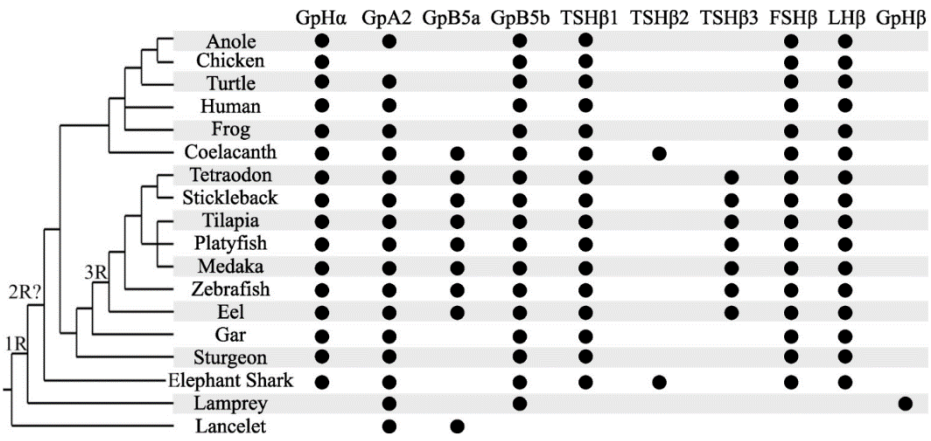


Fig. 24. **Répartition des sous-unités des hormones glycoprotéiques identifiées chez des représentants des différents clades de Vertébrés.** Les gènes codant pour des homologues des sous-unités des hormones glycoprotéiques identifiés à ce jour dans les organismes listés (à l'exception des CGβ spécifiques des primates) sont indiqués par un cercle noir (Hausken and Levavi-Sivan, 2019).

primitifs (Dos Santos et al., 2009; P. Wang et al., 2018; Yang et al., 2023) alors que c'est l'hormone GPA2/GPB5 recombinante qui active les GpHRs ancestraux des Cyclostomes (Hausken et al., 2018). Cela souligne la coévolution de la signalisation GpH/GpHR au cours de l'évolution des Bilatériens.

La famille des hormones glycoprotéiques aurait donc pour origine un gène unique présent chez l'ancêtre commun des Bilatériens. Une première duplication locale de ce gène aurait permis l'émergence des deux gènes ancestraux *gpa* et *gpb* (Fig. 23). Chez les Protostomiens comme les Lophotrochozoaires et les Ecdysozoaires, ces deux gènes ont été conservés et la duplication du locus *gpa-gpb* avant la radiation des Vertébrés serait à l'origine des gènes *gpa2* et *gpb5* et des homologues ancestraux *ancgphα* et *ancgphβ* codant les sous-unités α et β ancestrales. Le gène *ancgphα* a été maintenu à proximité du locus *gpa2-gpb5*, tandis que le gène *ancgphβ* a été transloqué peu après la duplication. Après la 1R, une copie de *gpa2* et une copie de *gphα* ont été perdues alors que les deux copies de *gpb5* ont été conservées avec le *gpb5a* retrouvé dans le locus *gpa2-gpb5a-gphα* et le *gpb5b* retrouvé isolé. La 1R serait également à l'origine de la duplication du gène *ancgphβ*, donnant les gènes *ancgthß* et *anctshß*. Après la 2R, une seule copie de *gpb5b*, du locus *gpa2-gpb5a* et de *gphα* ont été conservées. L'organisation en tandem de g*pa2-gpb5a* a été maintenue chez les Téléostéens et le cœlacanthe alors que *gpb5a* a été perdu chez les Tétrapodes, qui n'ont donc conservé que *gpb5b*. Chez les Cyclostomes, la sous-unité ancestrale GpHβ a été identifiée en plus de GPA2 et GPB5b. Par ailleurs, c'est à la racine des Gnathostomes que la 2R a dupliqué le gène *ancgthß* pour générer les gènes *fshß* et *lhß*, et le gène *anctshß* pour générer les gènes *tshß1* et *tshß2*. Le gène *tshß2* a été conservé chez les Chondrichtyens, les dipneustes et le cœlacanthe, mais a été perdu chez les Téléostéens et les Tétrapodes. Après la 3R spécifique des Téléostéens, tous les gènes dupliqués codants les sous-unités des hormones glycoprotéiques ont été perdus à l'exception de ceux issus de *tshβ1*, donnant *tshβ1a* et *tshβ1b* (ou TSHβ3) (Dos Santos et al., 2011; Dufour et al., 2020; Maugars et al., 2014). D'une façon indépendante, une duplication en tandem supplémentaire du gène *lhβ* s'est produite pendant la radiation des primates et a conduit à l'émergence des sous-unités CGβ (Henke and Gromoll, 2008; Maston and Ruvolo, 2002). Cette histoire évolutive des sous-unités des hormones glycoprotéiques est à l'origine de leurs diversités au sein des différents clades de Vertébrés, comme cela a été répertorié par Hausken and Levavi-Sivan, 2019 (Fig. 24).

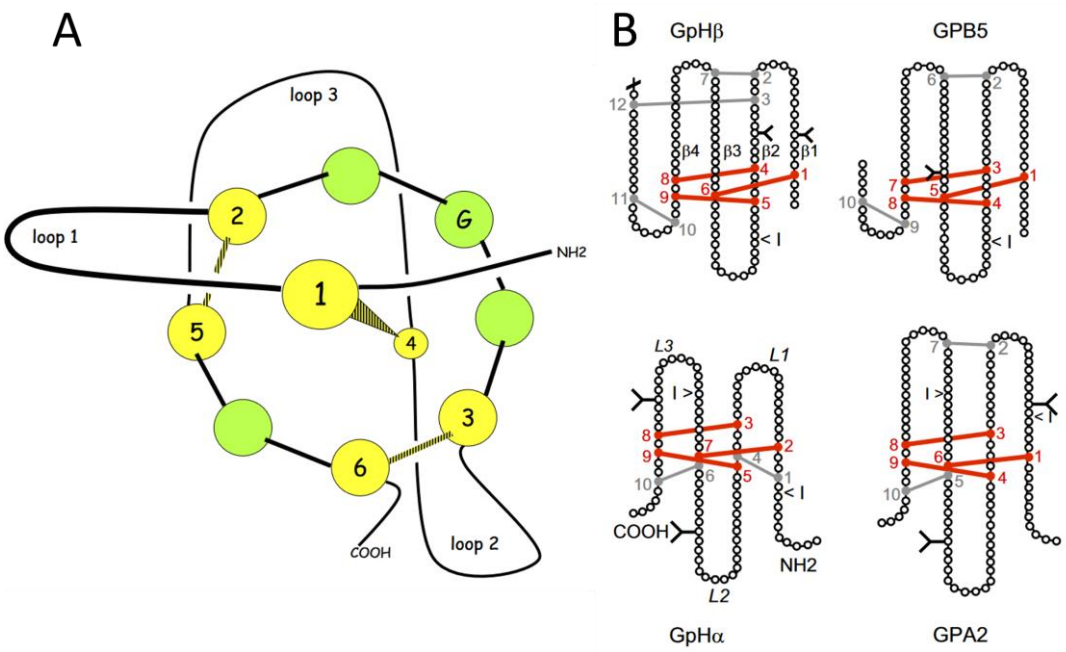


Fig. 25. **Représentation schématique de la structure en nœud cystéine et des sous-unités des hormones glycoprotéiques.** **A**. Les six cystéines appartenant au nœud cystéine sont représentées en jaune. Les quatre acides aminés restants qui appartiennent à l'anneau de huit résidus sont représentés en vert. Le G représente la glycine qui est conservée dans toutes les sous-unités des hormones glycoprotéiques. Les segments noirs et jaunes représentent les trois ponts disulfures formant le nœud cystéine (Alvarez et al., 2009). **B**. Les acides aminés constituant les sous-unités des hormones glycoprotéiques sont représentés par des cercles. Les chaînes de glycosylation sont représentées par des Y. Les ponts disulfures sont symbolisés par des barres (rouge pour celles qui sont responsables de la structure en nœud et grises pour les autres). Les cystéines conservées sont numérotées. Les emplacements des brins (β1-β4) et des boucles (L1-L3) sont indiqués (Dufour et al., 2020).

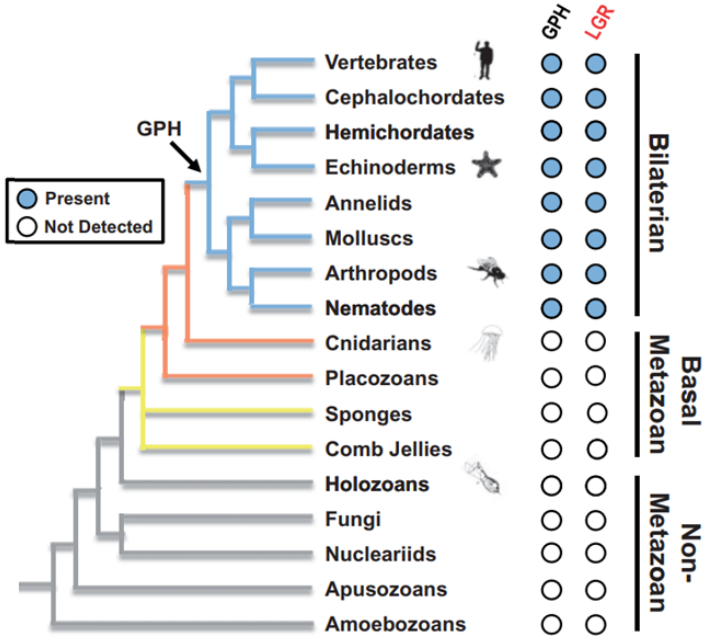


Fig. 26. **Identification des LGRs et des GPHs chez les Bilatériens.** Des représentants des familles des GPHs et des LGRs ont été identifiés (cercles bleues) dans chacun des principaux clades de Bilatériens (Roch and Sherwood, 2014).

Au niveau structural, ces différentes sous-unités s'associent de façon non covalente pour former les hormones glycoprotéiques hétérodimériques (GpHs). Les GpHs sont composées de la sous-unité commune CGA et de la sous-unité spécifique FSHβ, LHβ, TSHβ ou CGβ, qui confère la spécificité biologique. Les sous-unités α et β appartiennent à la grande famille des protéines à nœuds de cystéines, caractérisée par un anneau de huit résidus fermés par deux ponts disulfures et traversé par un troisième pont disulfure (Fig. 25A). Les sous-unités α contiennent dix résidus cystéines au total alors que les sous-unités β en possèdent douze (Fig. 25B). De plus, le dernier résidu cystéine du côté de l'extrémité C-terminal des sous-unités β forme un pont disulfure avec la troisième cystéine, constituant ainsi la boucle nommée "ceinture de sécurité" qui, en enserrant l'extrémité C-terminale de la sous-unité α, stabilise le dimère aux faibles concentrations, rencontrées notamment dans la circulation systémique (Xing et al., 2004). Il a été suggéré que cette "ceinture de sécurité" détermine la spécificité d'interaction en inhibant la liaison de chaque hétérodimère aux autres GPHRs selon le modèle dit de spécificité négative (Combarnous, 1992; Combarnous and Hengé, 1981). Les sous-unités CGBs et GPB5s sont quant à elles dépourvues de ceinture de sécurité en l'absence de la cystéine 12, ce qui pose la question de la stabilité, voire de l'existence de l'hétérodimère GPA2/GPB5 dans la circulation systémique. Il a donc été suggéré que la thyrostimuline possèderait des fonctions autocrines et/ou paracrines, plutôt que les fonctions endocrines classiquement associées aux GpHs (Alvarez et al., 2009). Les récepteurs aux hormones glycoprotéiques (GpHRs) se sont également diversifiés en trois types au cours de l'évolution. Ces GpHRs appartiennent au sous-type A de la famille des récepteurs couplés aux protéines G à domaines riches en leucine (LGR) (Hsueh and Feng, 2020). La présence de gènes appartenant aux familles des LGRs et des GPHs a été identifiée au sein de tous les principaux clades de Bilatériens (Roch and Sherwood, 2014) (Fig. 26). Une hypothèse de l'origine évolutive des GpHRs a été proposée avec un récepteur ancestral qui interagirait avec une GpH ancestrale monomérique ou homodimérique. Par la suite, la duplication du récepteur ancestral aurait conduit à l'émergence du récepteur à la TSH, le TSHR, et du récepteur à la gonadotrophine ancestrale, le GTHR. Cette étape a été suivie par la duplication du gène *gthr* à l'origine de l'émergence des récepteurs FSHR et LHR (Fig. 27). Les structures protéiques des GPHRs sont caractérisées par un grand ectodomaine N-terminal constitué d'un solénoïde incurvé avec des domaines de répétitions riches en leucines (LRR), des sites de N-glycosylation et une région "charnière" contenant une tyrosine sulfatée (Fig. 28). Leurs domaines transmembranaires

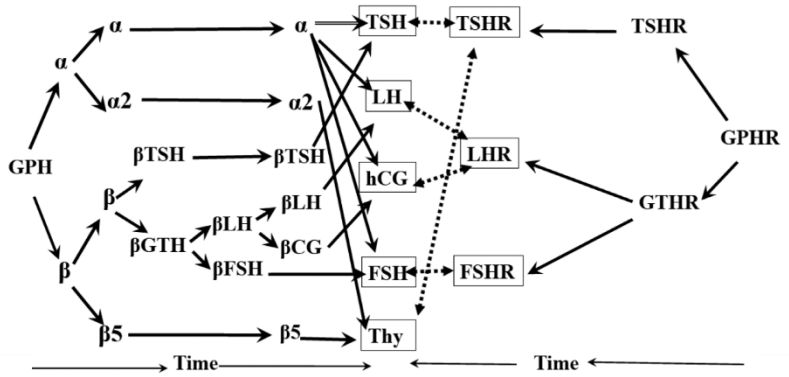


Fig. 27. **Représentation schématique de la coévolution des hormones glycoprotéiques et de leurs récepteurs.** La duplication et la néo-fonctionnalisation des gènes ancestraux des hormones glycoprotéiques et de leurs récepteurs sont illustrées au cours de l'évolution. GPH : hormones glycoprotéiques ; GTH : hormone gonadotrope ; Thy : thyrostimuline ; GTHR : récepteur à l'hormone gonadotrope ancestrale ; GPHR : récepteur à l'hormone glycoprotéique ancestrale (Hsueh and He, 2018).

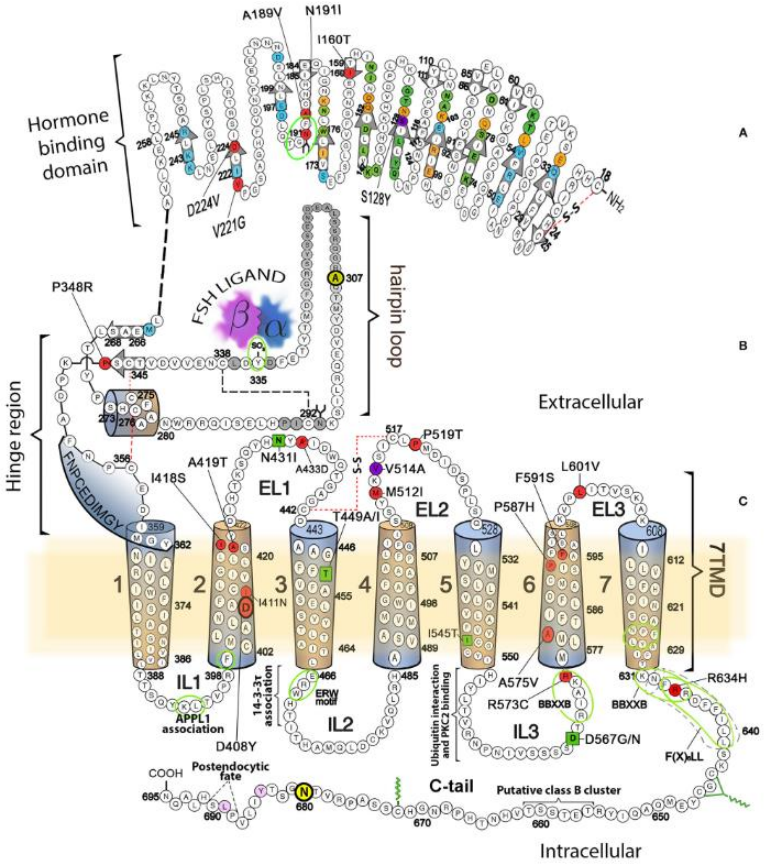


Fig. 28. **Représentation schématique de la structure du FSHR de l'humain. A.** Domaine extracellulaire impliqué dans l'interaction spécifique à l'hormone. Les résidus impliqués dans l'interaction avec la sous-unité CGA uniquement sont représentés en vert, avec la sous-unité FSHβ uniquement, en bleu et avec les deux sous-unités, en orange. Les feuillets bêta situés dans la surface concave du domaine extracellulaire (correspondant aux répétitions riches en leucine) sont indiqués par les flèches grises. **B.** Région charnière. Une tyrosine sulfatée en position 335 est impliquée dans la liaison aux sous-unités CGA et FSHβ (ovale vert). **C.** Domaine transmembranaire constitué de sept hélices α transmembranaires (représentées sous forme de cônes). Les séquences et résidus des faces intracellulaires sont impliqués dans l'activation du récepteur, l'association du récepteur avec des protéines d'interactions et dans le trafic cellulaire du récepteur (Ulloa-Aguirre et al., 2018).

sont caractérisés par sept hélices α transmembranaires (TM), trois boucles extracellulaires (EL) interagissant avec la région " charnière " et trois boucles intracellulaires (IL) impliquées dans l'activation de la voie Gαs/adenylyl cyclase/cAMP/PKA *via* les motifs ERW et BBXXB et dans l'activation de la voie Gαq11/$Ca^{2+}$/IP3 *via* l'adaptateur APPL1 (Johnson and Jonas, 2020). Le domaine C-terminal est caractérisé par un second motif BBXXB, un motif $F(X)_6LL$ impliqué dans le trafic intracellulaire, un motif riche en sérine/thréonine (S/T) de classe B qui est impliqué dans la désensibilisation, le recyclage et la signalisation médiée par ERK1/2 de façon indépendante de la protéine Gs (Kara et al., 2006; Marion et al., 2006).

## IV.5. Acquisition, évolution et fonctions de l'axe hypothalamo-hypophyso-gonadique

Dans la littérature, l'axe HHG des Mammifères est le plus étudié et sert de socle de connaissances générales pour l'exploration de ses homologues présents au niveau d'autres clades de Vertébrés (Fig. 29A).

### IV.5.1 Chez les Mammifères

L'activité sécrétoire des neurones à GnRH est pulsatile et la fréquence et l'amplitude des épisodes de sécrétion sont essentielles pour la libération et la synthèse des GTHs hypophysaires. En effet, des fréquences croissantes de sécrétion de GnRH entraînent une sécrétion préférentielle de LH, tandis que les fréquences décroissantes entraînent une sécrétion préférentielle de FSH (Thompson and Kaiser, 2014). Classiquement chez les Tétrapodes, comme décrit précédemment, une population de neurones à GnRH est localisée dans l'aire préoptique et l'éminence arquée-médiane hypothalamique et leurs axones se projettent vers l'éminence médiane. Ces neurones à GnRH seraient les intégrateurs finaux d'un ensemble de neurofacteurs cérébraux, incluant par exemple des peptides RF-amides et des monoamines, qui constituent des intermédiaires aux signaux métaboliques et environnementaux. Ils permettraient de moduler la sécrétion de GnRH afin de réguler la reproduction en fonction du statut métabolique de l'individu et/ou de la saison. Parmi ces réseaux de neurones, deux populations de neurones à kisspeptines ont été bien étudiées chez les rongeurs. La première population présente des corps cellulaires localisés dans le noyau antéroventral-périventriculaire (AVPV) et exprime le gène *KISS1* codant pour les kisspeptines. Le précurseur des kisspeptines est composé de 145 acides aminés et il sera clivé en un peptide actif de 54, 14, 13 ou 10 acides aminés, partageant une région C-terminale commune RFamide,

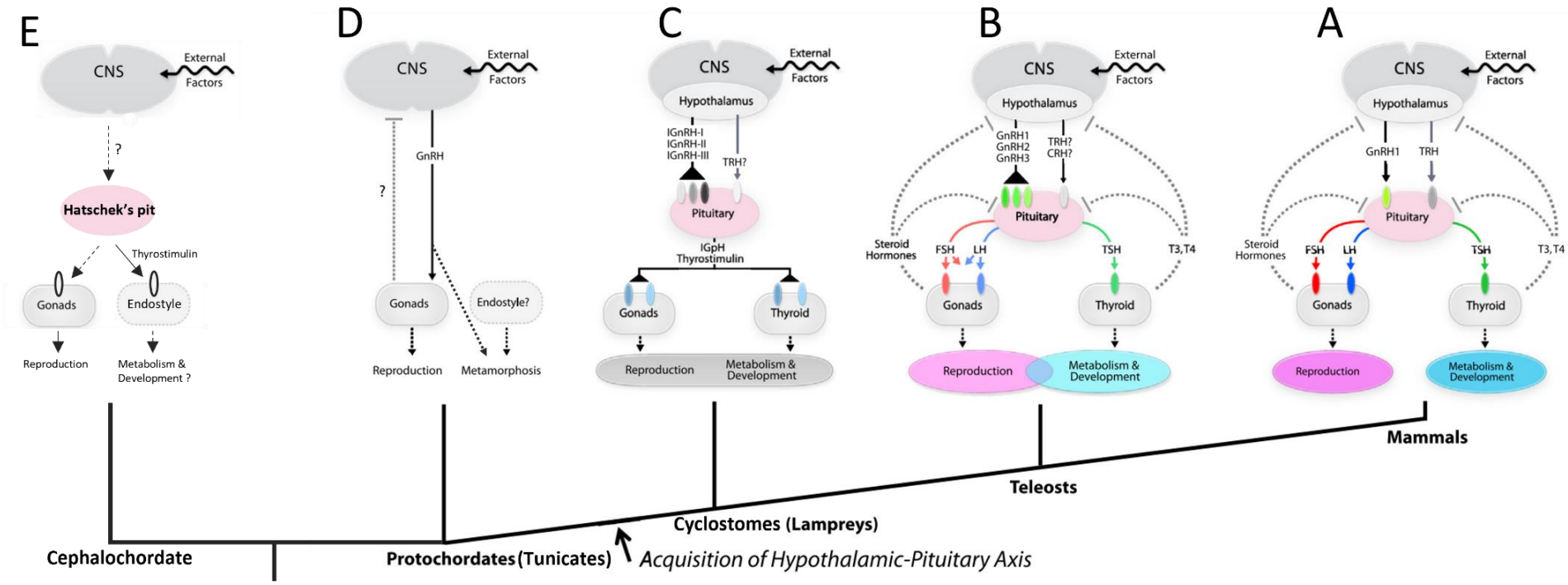


Fig. 29. **Représentation schématique de l'évolution des axes neuroendocriniens chez les Chordés.** Les systèmes Hypothalamo-Hypophyso-Gonadiques (HHG) et Hypothalamo-Hypophyso-Thyroïdien (HHT) auraient évolué à partir d'un système ancestral pré-Vertébrés exclusivement neuroendocrinien, par l'émergence progressive des composants d'un nouveau niveau de contrôle (hormones glycoprotéiques/récepteurs hormonaux glycoprotéiques) en même temps que le développement des structures anatomiques correspondantes (hypothalamus et hypophyse). Les Céphalocordés (**E**) (Modifié d'après Wang et al., 2018) et les Protochordés (**D**) (Modifié d'après Satake and Sasakura, 2024; Sower, 2018) ne semblent pas avoir d'axes neuroendocriniens spécifiques. Le contrôle endocrine des fonctions reproductives et thyroïdiennes chez la lamproie (**C**) pourrait refléter un stade évolutif intermédiaire vers les axes HPG et HPT, partiellement redondants chez les Téléostéens (**B**) ou hautement spécialisés chez les Tétrapodes (**A**) (Modifié d'après Sower, 2018). CRH, hormone de libération de la corticotrophine ; CNS, système nerveux central ; FSH, hormone folliculostimulante ; LH, hormone lutéinisante ; GnRH, hormone de libération des gonadotrophines ; lGnRH, hormone de libération des gonadotrophines de lamproie ; lGpH, hormone glycoprotéique de lamproie ; lGpH-R, récepteur de l'hormone glycoprotéique de la lamproie ; T3, triiodothyronine ; T4, thyroxine ; TRH, thyréolibérine; TSH, thyrotropine ; TSHR, récepteur à la thyrotropine.

responsable de la synthèse et la libération de GnRH. La deuxième population, composée des neurones KNDy localisés dans le noyau arqué (ARC), exprime la neurokinine B et la dynorphine en plus des kisspeptines. Les neurones KNDy sont régulés par les mécanismes combinés de rétroaction positive et négative médiés par la neurokinine B et la dynorphine, respectivement, ce qui permet au réseau de neurones de fonctionner comme un oscillateur et d'être impliqué dans la pulsatilité de la sécrétion de GnRH et, en réponse, des gonadotrophines (Plain et al., 2022; Sonigo and Binart, 2012; Xie et al., 2022). Une autre population de neurones régulateurs des neurones à GnRH est localisée dans l'aire hypothalamique dorsomédiane et exprime un inhibiteur de la synthèse et de la sécrétion de GnRH qu'est le peptide RF-amide GnIH (*Gonadotropin-inhibitory hormone*). Le GnIH module également les neurones à kisspeptines et les cellules gonadotropes hypophysaires (Tsutsui and Ubuka, 2021). Les stéroïdes gonadiques vont exercer un rétrocontrôle sur la sécrétion de GnRH et des gonadotrophines en agissant directement au niveau des neurones à kisspeptines, des neurones KDNy (Plain et al., 2022), des neurones à GnIH (Ubuka et al., 2012) et au niveau des cellules gonadotropes hypophysaires (Acevedo-Rodriguez et al., 2018).

Les hormones gonadotropes de Tétrapodes interagissent spécifiquement avec leurs récepteurs. La LH induit la prolifération et la maturation des cellules de Leydig qui expriment LHR et stimule la production de testostérone (T). La testostérone en combinaison avec la FSH déclenche et maintient la spermatogenèse en agissant sur les cellules de Sertoli qui expriment FSHR et le récepteur aux androgènes (Oduwole et al., 2021). S'il était bien admis que la production de testostérone stimulée par LH était essentielle au maintien d'une spermatogenèse quantitative et qualitative, en régulant la méiose et la spermiogenèse, le rôle spécifique de FSH a été plus discuté, notamment chez le rat et la souris (Huhtaniemi, 2015). C'est l'étude de souris knock-out pour *lhr* (LuRKO), qui présentaient un arrêt de la spermatogenèse au stade des spermatides rondes, qui a permis de redéfinir les rôles de LH, FSH et de la testostérone dans le contrôle de la spermatogenèse (Oduwole et al., 2021). En effet, la supplémentation en testostérone à hauteur de seulement 1,4% des concentrations en testostérone testiculaire s'est avérée suffisante pour restaurer une spermatogenèse complète chez les souris LuRKO, d'où la conclusion que des niveaux élevés en testostérone n'étaient pas nécessaires pour la spermatogenèse. Par la suite, il a été montré que des souris n'exprimant pas LHR mais avec une surexpression de FSHR dans les cellules de Sertoli (double

mutant *Fshr-CAM/Lhr*$^{-/-}$) avaient une spermatogenèse normale, même en présence d'un anti-androgène, le flutamide (Huhtaniemi, 2018). La conclusion de ces études est qu'une stimulation forte de FSH était suffisante pour maintenir la spermatogenèse en absence de LH et de concentrations élevées de testostérone. Ces résultats ont également été discutés au regard de la régulation hormonale de la spermatogenèse au cours de l'évolution, avec une régulation FSH prépondérante chez les Téléostéens tandis que c'est la régulation LH/T qui est dominante chez les Mammifères (Huhtaniemi, 2015).

En ce qui concerne les fonctions de GPA2/GPB5, la thyrostimuline serait également impliquée dans la formation osseuse (Bassett et al., 2015), la réponse immunitaire (Suzuki et al., 2009), le développement larvaire (Vandersmissen et al., 2014) et la reproduction (Sun et al., 2010). Ce dernier rôle a été mis en évidence chez l'humain en tant qu'hormone à fonction paracrine sécrétée par l'ovocyte et modulant les cellules de la granulosa et de la thèque qui expriment TSHR (Sun et al., 2010).

### IV.5.2 Chez les Téléostéens

Chez les poissons Téléostéens, l'axe HHG présente un nombre important de particularités par rapport à celui des Tétrapodes (Fig. 29B). Par exemple, les neurones à GnRH se projettent directement vers l'hypophyse et la GnRH1 est le principal peptide hypophysiotrope, sauf chez certains poissons comme le poisson zèbre où ce rôle est assumé par la GnRH3. En effet, chez le poisson zèbre *D. rerio*, ce sont les neurones à GnRH2 et à GnRH3 qui se projettent vers l'hypophyse. Cependant, une double invalidation des gènes *gnrh2* et *gnrh3* n'a pas affecté la fertilité des animaux, ce qui suggère que *D. rerio* semble être capable de se reproduire sans système GnRH (Kanda, 2019; Marvel et al., 2018). De plus, il a été montré que les kisspeptines stimulent la synthèse et la sécrétion des gonadotrophines chez différentes espèces de Téléostéens mais leur mode d'action ne semble pas être médié par les neurones à GnRH. Chez le poisson zèbre et le médaka, au moins, les neurones à GnRH hypophysiotropes n'expriment pas de récepteurs aux Kisspeptines et les neurones à Kisspeptines se projettent directement vers les cellules gonadotropes à LH chez certaines espèces, ce qui suggère une action hypophysiotrope directe (Somoza et al., 2020).

Chez les poissons Téléostéens, FSH régule la prolifération des cellules de Sertoli ainsi que la prolifération des cellules germinales et la LH module les fonctions des cellules de Leydig et stimule la synthèse des androgènes, régulant les étapes finales de la spermatogenèse (Li and

Ge, 2020; Xie et al., 2017). Contrairement aux modèles mammaliens, les cellules de Leydig expriment FSHR, en plus de LHR, et la FSH peut réguler la stéroïdogenèse et les étapes de la spermatogenèse dépendantes et indépendantes des stéroïdes (García-López et al., 2009; Sambroni et al., 2013). De plus, les cellules de Sertoli expriment également FSHR et LHR chez le poisson zèbre, ce qui suggère une redondance fonctionnelle (García-López et al., 2010). Ceci a été validé par des approches *knock-out* chez le poisson zèbre où les mâles *lhr;fshr* double-KO avaient des testicules sous-développés et étaient infertiles (Zhang et al., 2015) mais l'expression d'un seul récepteur était suffisante pour maintenir une spermatogenèse complète (Xie et al., 2017). De plus, les concentrations plasmatiques de testostérone (T) et d'estradiol (E2) étaient normales chez les poissons zèbres mutants LHB, ce qui suggère que la FSH peut maintenir la stéroïdogenèse gonadique grâce à l'activation croisée du LHR (Shang et al., 2019). En effet, les interactions ligands-récepteurs sont moins discriminantes avec le LHR qui peut être activé par la LH et la FSH, comme observé chez la truite arc-en-ciel *Oncorhynchus mykiss* (Sambroni et al., 2007), le medaka *Oryzias latipes* et *D. rerio* et, plus marginalement, le FSHR qui peut être activé par la FSH et la LH, comme observé chez *D. rerio* et *O. latipes* (Burow et al., 2020; Xie et al., 2017). De manière intéressante, chez *O. latipes*, les phénotypes *lhr* KO, *fshr* KO et *lhr;fshr* double-KO présentaient des mâles fertiles avec des testicules histologiquement normaux contenant tous les stades de la spermatogenèse et sans différence marquée des niveaux en hormones stéroïdiennes (Kitano et al., 2022).

### IV.5.3 Chez les Chondrichtyens[4]

Chez les Chondrichtyens, la régulation des fonctions gonadiques par les hormones de l'axe hypothalamo-hypophyso-gonadique (HPG) est très peu documentée. Des analyses biochimiques anciennes ont identifié plusieurs formes immunoréactives de GnRHs dont deux correspondaient aux GnRH2 et GnRH3 (King et al., 1992). Par ailleurs, au moins trois autres formes ont été observées mais leurs séquences n'ont pas été caractérisées (Sherwood and Lovejoy, 1993). Comme nous l'avons indiqué précédemment, les différentes GnRHs actuellement identifiées sont : chez la chimère éléphant la GnRH2, la GnRH1a et la GnRH1b ; et chez la roussette la GnRH1, la GnRH2 et la GnRH3 (Gaillard et al., 2018). Les GnRHs sont exprimés dans l'hypothalamus (Hara et al., 2018) et leur transport se fait *via* la circulation générale en l'absence d'une vascularisation directe entre l'hypothalamus et le lobe ventral

[4] Cette partie s'inspire en partie du chapitre d'encyclopédie suivant : Sourdaine and Jeanne, 2024 (Annexe I)

hypophysaire (D'antonio et al., 1995). Par ailleurs, quatre GnRHRs ont été identifiés par analyse transcriptomique de quelques individus de la roussette nuageuse *S. torazame* (Hara et al., 2018).

Les hormones gonadotropes ont été identifiées chez la roussette *S. canicula* et, avec les progrès sur les séquençages des génomes, les séquences de FSH, LH et de leurs récepteurs ont également été identifiés chez quelques autres espèces (Arimura et al., 2024; Hara et al., 2018). Chez *S. torazame*, les sous-unités des hormones gonadotropes, CGA, FSHβ et LHβ sont majoritairement exprimées au niveau du lobe ventral hypophysaire (Arimura et al., 2024; Hara et al., 2018), où sont localisées les cellules gonadotropes (Knowles et al., 1975), et FSHR et LHR sont exprimés dans le testicule et l'ovaire (Arimura et al., 2024; Hara et al., 2018). Cependant, les rôles et les modes d'actions des hormones gonadotropes restent largement inexplorés hormis, par exemple, une publication ancienne montrant que des extraits du lobe ventral hypophysaire étaient capables de stimuler d'un facteur 1,5 la production d'androgènes par des explants testiculaires de *S. canicula* (Sourdaine et al., 1990). Plus récemment, parallèlement à la réalisation de ce travail de thèse, Arimura et al., 2024 ont publié la caractérisation fonctionnelle de FSHR et LHR chez *S. torazame*, un requin proche de *S. canicula*, avec notamment un variant de LHR dépourvu de l'exon 10 codant pour une partie de la région charnière et qui présente une activité AMPc basale. De plus, des extraits hypophysaires ont stimulé de façon dose-dépendante la signalisation AMPc *via* l'activation de FSHR et LHR de *S. torazame* en condition *in vitro* (Arimura et al., 2024). Chez la chimère éléphant *C. milii*, les interactions GTH-GTHR ont été analysées et FSH et LH apparaissaient spécifiques de FSHR et LHR, respectivement (Buechi and Bridgham, 2017), ce qui se rapproche plus du profil d'interaction ligand-récepteur des Mammifères que de celui des Téléostéens. En ce qui concerne la thyrostimuline (GPA2-GPB5), il a été montré que celle de *C. milii* n'active aucun des trois récepteurs aux GpHRs (FSHR, LHR ou TSHR) (Buechi and Bridgham, 2017). Par ailleurs, l'analyse transcriptomique réalisée chez *S. torazame* a mis en évidence une coexpression des gènes *gpa2* et *gpb5* au niveau testiculaire (Hara et al., 2018), ce qui laisse suggérer une régulation paracrine de la spermatogenèse médiée par la thyrostimuline.

À l'heure actuelle, le contrôle de la spermatogenèse chez les Élasmobranches repose essentiellement sur l'étude ciblée des niveaux d'expression d'ARNm ou de protéines en fonction du développement ou des stades de la spermatogenèse, ou sur l'analyse de niveaux

hormonaux en fonction de la saisonnalité. La présence de cellules de Leydig fonctionnelles chez les Élasmobranches est encore débattue. Chez les amniotes, les cellules de Leydig sont associées à la production d'androgènes et présentent une ultrastructure associée à la synthèse des stéroïdes avec la présence de mitochondries à crêtes tubulo-vésiculaires, d'un réticulum endoplasmique lisse et de gouttelettes lipidiques. De plus, elles expriment des enzymes clés impliquées dans la biosynthèse des stéroïdes telles la 3β-hydroxystéroïde déshydrogénase (3β-HSD) et la 17β-hydroxystéroïde déshydrogénase (17β-HSD) (Zirkin and Papadopoulos, 2018). Chez les Élasmobranches, les cellules de Leydig ont été décrites comme absentes ou présentes selon les auteurs et/ou les stades de développement et/ou la saisonnalité. Des études antérieures ont suggéré soit l'absence de cellules de Leydig chez *Scyliorhinus stellaris* et *Squalus acanthias* (Holstein, 1968; Simpson and Wardle, 1967), soit la présence de quelques cellules indifférenciées mésenchymateuses de type *Leydig-like* chez *S. canicula* (Loir et al., 1995) et *S. acanthias* (Pudney and Callard, 1984a). Par contre, des cellules de Leydig différenciées ont été identifiées chez la raie *Torpedo mormorata* (Prisco et al., 2008) et le requin-marteau *Sphyrna tiburo* (Tyminski et al., 2015). Ces cellules pourraient correspondre aux précurseurs ancestraux des cellules de Leydig des Vertébrés osseux (Callard, 1991; Engel and Callard, 2007). Dans tous les cas, il semblerait que ces cellules de Leydig soient faiblement impliquées dans la synthèse des stéroïdes testiculaires qui serait assurée par les cellules de Sertoli. En effet, les cellules de Sertoli de ces espèces présentent des caractéristiques d'ultrastructures stéroïdogènes et des cystes isolés chez *S. acanthias* et chez *S. canicula* ont la capacité de synthétiser des androgènes (Cuevas and Callard, 1992a; Loir et al., 1995; Pudney and Callard, 1984b; Sourdaine and Garnier, 1993). Chez la raie *T. marmorata*, les cellules de Leydig ne sont pas réparties uniformément dans le testicule, elles sont plus développées et plus nombreuses à proximité des cystes en méiose et à jeunes spermatides et moins nombreuses au niveau des cystes à spermatogonies et à spermatides âgées (Prisco et al., 2008). Cependant, sur la base de l'immunolocalisation de la 3β-HSD et de la 17β-HSD, les différents types cellulaires suivants seraient stéroïdogènes chez la raie : les spermatogonies aux stades précoces ; les cellules de Sertoli des cystes contenant des spermatogonies ; les cellules de Leydig associées aux stades méiotiques ; et les cellules de Sertoli des cystes à spermatides (Prisco et al., 2008).

Plusieurs études, examinées par Becerril-García et al., 2020, ont analysé les niveaux de stéroïdes en relation avec le cycle de reproduction saisonnier et les étapes spermatogénétiques. Il en ressort que chez les individus matures, les androgènes (principalement la testostérone au lieu de la 11-kétotestostérone) régulent le développement et la maturation des cystes ainsi que le stade final de la maturation des spermatozoïdes. Le récepteur aux androgènes a été principalement localisé aux stades préméiotiques dans les testicules de *S. acanthias*, suggérant une régulation du développement des premiers stades par les androgènes. Cette localisation préméiotique du récepteur aux androgènes a également été observé chez *S. tiburo* (Tyminski et al., 2015) mais avec une expression, et donc une fonction potentielle, étendue aux canaux gonadiques. De plus, les augmentations du développement du tractus génital et du nombre de spermatozoïdes matures sont corrélés à une augmentation du taux de testostérone plasmatique chez les animaux saisonniers, comme observé chez *S. tiburo* (Gonzalez De Acevedo et al., 2020) ou chez *C. taurus* (Wyffels et al., 2020). La progestérone et la 17α, 20β dihydroxyprogestérone (DHP) ont également été identifiées et associées à des cystes contenant des spermatides tardives (Sourdaine and Garnier, 1993). De plus, le récepteur de la progestérone a été identifié dans les canaux extratesticulaires de la raie *P. wallacei*, suggérant un rôle potentiel de la progestérone dans la maturation des spermatozoïdes (Morales-Gamba et al., 2023).

La spermatogenèse peut montrer peu ou pas de changements saisonniers chez les Élasmobranches, comme c'est le cas pour *S. canicula* qui montre une spermatogenèse continue tout au long de l'année. Mais chez l'aiguillat *S. acanthias* la spermatogenèse est interrompue par l'apoptose des cellules germinales lors de la transition mitose-méiose aux mois d'avril-mai, conduisant à la formation d'une zone de dégénérescence (ZD) temporaire. Par l'étude de cette zone de dégénérescence, la durée de la spermatogenèse a été évaluée à environ 2 années avec une durée de l'évolution du stade préleptotène en stade spermatide de 9 à 10 mois chez *S. acanthias* (McClusky, 2006). Cette interruption de la spermatogenèse entrainera une diminution de la production de spermatozoïdes qui aura lieu 9 à 10 mois plus tard, soit aux mois de février-mars de l'année suivante (McClusky, 2005). À l'inverse, le nombre plus élevé de cystes contenant des spermatides matures s'observe entre octobre et janvier et coïncide avec la période ou les femelles sont fécondes (décembre à février) (McClusky, 2012). Chez *S. canicula*, les cystes à spermatides matures sont en plus grand

nombre d'avril à août et le plus grand nombre de spermatozoïdes par ampoule séminale a été observé de mars à mai chez les individus capturés en Mer de Manche (Garnier et al., 1999). Cette zone de dégénérescence observée chez *S. acanthias* peut être induite expérimentalement chez *S. canicula* par hypophysectomie partielle couplée à une augmentation de la température, ce qui suggère que cette transition mitotique-méiose est une étape critique de la spermatogenèse sous un double contrôle, hormonal (hormones gonadotropes) et environnemental (Dobson and Dodd, 1977a, 1977b). Par conséquent, le caractère saisonnier de la reproduction peut être plus marqué chez les espèces qui habitent des régions où les conditions environnementales varient fortement entre les saisons.

### IV.5.4 Chez les Cyclostomes

Chez les Cyclostomes, les trois GnRHs (GnRHI, GnRHII et GnRHIII) sont synthétisées au niveau hypothalamique et deux sites de fixation aux GnRHs ont été mis en évidence au niveau hypophysaire (Fig. 29C) (Sower, 2018). Par ailleurs des injections *in vivo* de GnRH ont montré une augmentation des niveaux plasmiques de 15α-hydroxytestostérone et de 15α-hydroxyprogestérone, ce qui suggère un rôle stimulateur de la stéroïdogenèse directe ou indirecte exercé par la GnRH (Young et al., 2007). Par ailleurs, comme les hormones gonadotropes, thyréotrope et leurs récepteurs se sont diversifiés à la base des Gnathostomes, ils sont absents chez les Cyclostomes (Buechi and Bridgham, 2017). À la place, deux récepteurs aux hormones glycoprotéiques ont été identifiés et correspondent aux GpHRI et GpHRII. Le GpHRI est majoritairement exprimé au niveau testiculaire et le GpHRII au niveau de la glande thyroïde (Hausken et al., 2018). GpHRI et GpHRII peuvent être activés par les hormones glycoprotéiques GPA2/GPB5 (thyrostimuline) et GPA2/GpHβ ou seulement GPA2/GPB5, respectivement (Hausken et al., 2018). Cela met en avant l'hypothèse d'une mise en place progressive des axes HHG et HHT au cours de l'évolution, qui s'est produite en parallèle de la coévolution des paires ligand/récepteur, avec l'acquisition progressive des hautes affinités et spécificités d'interactions. De plus, comme GPA2/GPB5 active GpHRI et GpHRII, la séparation entre les axes régulateurs de la reproduction et du métabolisme ne serait pas encore établie chez les lamproies (Sower, 2018).

### IV.5.5 Chez les Pro- et Céphalo-chordés

Plus ancestralement, avant l'acquisition de l'axe HHG et en l'absence d'hypothalamus et d'hypophyse différenciés et de gènes codant les hormones gonadotropes, les peptides

apparentés aux GnRHs seraient des régulateurs directs de tissus cibles (Sakai et al., 2020). Chez les Tuniciers, douze GnRH-*like* ont été identifiées et les gènes associés codent pour des précurseurs contenant plusieurs copies de GnRH-*like*, contrairement aux gènes GnRHs des Vertébrés et des invertébrés non ascidiens, qui codent pour une seule séquence GnRH (Kawada et al., 2013). L'analyse des neurones immunoréactifs à une GnRH-*like* a montré une distribution de ceux-ci au niveau du plexus du cordon dorsal, du ganglion cérébral jusqu'aux gonades le long du faisceau nerveux dorsal de *C. intestinalis* (Terakado, 2001). De même, les expressions des ARNm des GnRH-*like* sont spécifiques des tissus nerveux et sont notamment retrouvées au niveau du ganglion cérébral (Kavanaugh et al., 2005). Les GnRHRs identifiés sont exprimés au niveau du faisceau nerveux dorsal associé à la glande neurale, préfigurant l'ébauche d'un axe hypothalamo-hypophysaire, mais également dans divers autres tissus tels la gonade, le cœur, l'intestin, l'endostyle et le sac branchial (Tello et al., 2005). Cela suggère que la signalisation GnRH-*like* des Tuniciers est capable de réguler différentes fonctions biologiques en plus de celles liées à la reproduction. L'un des premiers exemples illustrant une implication d'une GnRH-*like* dans la reproduction a été l'effet stimulateur sur la contraction du corps de *C. intestinalis*, induisant ainsi la libération des gamètes (Terakado, 2001). Plus récemment chez la cione *Ciona robusta*, l'étude anatomique et fonctionnelle du système nerveux à l'aide d'un gène rapporteur exprimé spécifiquement au niveau des neurones a montré que les neuropeptides du ganglion cérébral sont sécrétés vers l'ovaire par les neurones du plexus dorsal et/ou les nerfs viscéraux et réguleraient sa croissance et sa maturation (Osugi et al., 2017). En présentant la cartographie détaillée de l'innervation des différents tissus périphériques comme par exemple celle du gonoducte et de l'organe cupulaire constitué de cellules sensorielles ciliées au niveau du siphon exhalant, ce travail s'inscrit dans l'étude de l'évolution du système neuroendocrine chez les Chordés (Osugi et al., 2017). Par ailleurs, il a été observé chez l'ascidie *Styela clava*, une coexpression des gènes *gpa*, *gpb* et *gphr* (anciennement nommés *gpa2*, *gpb5* et *tshr*) au niveau gonadique (Yang et al., 2023), mettant en avant le rôle paracrine ancestral de GPA2 et GPB5.

Chez les Céphalocordés, la distribution tissulaire des GnRH-*like* et des GnRHRs ne semble pas avoir été publiée, à l'exception d'une immunohistochimie des GnRH-*like* chez l'amphioxus *Branchiostoma floridae* qui a mis en évidence un immunomarquage à proximité ou à l'intérieur du canal central de la vésicule cérébrale (Roch et al., 2014). Même si les fonctions biologiques de la signalisation GnRHergique chez *B. floridae* restent encore à explorer, une

hypothèse a été émise sur la base de l'axe HHG des Gnathostomes. Dans cette hypothèse, la base de la vésicule cérébrale, la fosse de Hatschek (*Hatschek's pit*) et l'endostyle seraient, respectivement, les homologues potentiels de l'hypothalamus, de l'hypophyse et de la thyroïde des Gnathostomes (Wang et al., 2017). Si la régulation de la reproduction par cet axe reste à étudier, il apparait que le métabolisme des amphioxus serait régulé par la thyrostimuline (GPA2/GPB5) produite par l'*Hatchek's pit* en stimulant la production d'hormones thyroïdiennes endostylaires *via* l'interaction avec le seul LGR caractérisé, nommé « TSHR » (P. Wang et al., 2018). De plus, une coexpression des gènes *gpa*, *gpb* et *gphr* a été décrite au niveau gonadique chez *Branchiostoma belcheri japonicum* (P. Wang et al., 2018).

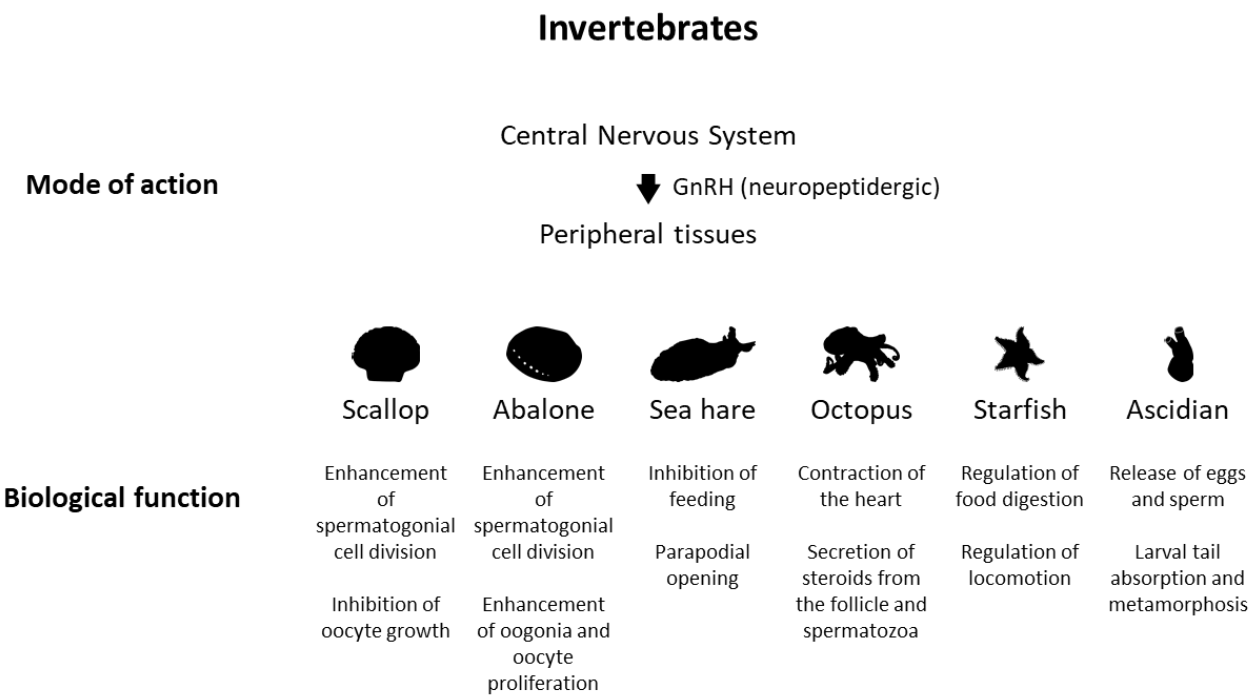


Fig. 30. **Représentation schématique des fonctions des systèmes GnRHergiques chez les non-vertébrés.** La GnRH produite par le système nerveux central agit directement sur les organes périphériques, dont les gonades, comme cela a été mis en évidence chez les pétoncles, l'ormeau, le poulpe, l'étoile de mer et l'ascidie (Sakai et al., 2020).

### IV.5.6 Chez les Ecdysozoaires

Plus généralement chez les Ecdysozoaires, les peptides apparentés aux GnRHs ont des fonctions associées à la reproduction et à d'autres fonctions biologiques plus larges selon les espèces (Fig. 30). Il est très probable que les GnRH-*like* des Ecdysozoaires agissent directement sur les gonades d'une manière neuropeptidergique, compte tenu de l'expression des GnRHRs au niveau des gonades. Il a été également démontré que les GnRH-*like* induisaient la prolifération des cellules germinales précoces (gonies) chez le Gastéropode *Haliotis discus hannai* et le Bivalve *Mizuhopecten yessoensis* (Sakai et al., 2020) et induisaient la méiose ovocytaire chez le Malacostracé *Eriocheir sinensis* (Luo et al., 2023), ce qui suggère un rôle direct des GnRHs-*like* dans la croissance et la maturation des gonades mâles.

Par ailleurs, les hormones glycoprotéiques GPA et GPB possèderaient un rôle régulateur de la reproduction comme cela a été mis en évidence par l'utilisation d'ARNs interférents ciblant leurs LGR associés (portant des noms différents selon les espèces). Ainsi, l'inhibition de l'expression du GPHR de *Caenorhabditis elegans* ou du LGR1 du moustique *Aedes aegypti* a provoqué une absence de renouvellement des cellules germinales (Cho et al., 2007) ou une spermatogenèse anormale (Rocco et al., 2019, 2017), respectivement. De plus, les gènes *gpa*, *gpb* et les LGR associés sont coexprimés dans les gonades de plusieurs Protostomiens comme la mouche *Drosophila melanogaster* (Vandersmissen et al., 2014), le pétoncle japonais *Patinopecten yessoensis* (M. Zhang et al., 2020) ou la crevette *Macrobrachium rosenbergii* (Wahl et al., 2022).

Cette présentation de l'origine et de l'évolution des systèmes de régulations de la reproduction met en lumière la diversité des systèmes régulateurs qui ont tous pour objectif final de permettre le bon déroulement d'une gamétogenèse qualitative, quantitative et coordonnée avec le cycle biologique de l'individu.

### IV.6. Les tractus génitaux mâles et leurs modulations par les hormones gonadotropes

Les fonctions épididymaires sont régulées par les hormones gonadotropes au regard des expressions de FSHR et LHCGR observées aux niveaux des différents segments de l'épididyme de rat et de l'homme (Shayu and Rao, 2006; Świder-Al-Amawi et al., 2010), du singe *Maccaca radiata* (Dahia and Rao, 2006) et de l'écureuil *Spermophilus dauricus* (Wang et al., 2019). D'un point de vue fonctionnel, des lignées de cellules souches embryonnaires de souris KO LHR/hCGR ont été mises en place et les adultes étaient infertiles et présentaient une diminution importante du poids du tractus génital, incluant une diminution de la taille et du poids des épididymes (Lei et al., 2001). Par ailleurs, un traitement par la FSH de cellules épithéliales épididymaires de rat provoque une augmentation de la synthèse d'œstradiol (Świder-Al-Amawi et al., 2010), ce qui a également été le cas avec un traitement à l'hCG qui module l'expression de l'aromatase (Awider-Al-Amawi et al., 2007). De plus, il a été montré chez l'écureuil *S. dauricus* que les niveaux d'expression épididymaire des gènes *lhr* et *fshr* fluctuaient en fonction du cycle saisonnier avec des niveaux plus élevés lors de la période de reproduction (Wang et al., 2019). Les études sur la caractérisation du rôle des hormones gonadotropes sur les tractus génitaux, en dehors des gonades, demeurent peu nombreuses et se sont portées essentiellement sur les Mammifères. Cependant, elles tendent à mettre en évidence la présence d'un axe « hypothalamo-hypohyso-tractus génital », qui intègre un nombre d'organes plus large que les gonades.

## V. Objectifs

L'objectif de cette thèse est d'explorer les régulations endocrines et paracrines exercées par les acteurs de l'axe hypothalamo-hypophyso-ganodique sur la spermatogenèse chez un modèle Élasmobranche, la petite roussette *Scyliorhinus canicula*. Ce travail a été étendu aux hormones glycoprotéiques GPA2 et GPB5 ainsi qu'à des organes autres que le testicule. Les résultats sont présentés en quatre chapitres rédigés sous la forme de manuscrits scientifiques.

**Chapitre I** : Comparative Proteome Analysis of Four Stages of Spermatogenesis in the Small-Spotted Catshark (*Scyliorhinus canicula*), Using High-Resolution NanoLC-ESI-MS/MS (Jeanne et al., 2023)

L'organisation particulière du testicule de *S. canicula* permet d'accéder facilement aux principaux stades de la spermatogenèse, ce qui facilite leurs caractérisations. L'objectif de cette étude est de faire une analyse descriptive de l'évolution du protéome testiculaire en fonction des quatre stades de la spermatogenèse qui correspondent à la prolifération mitotique, la méiose et les phases précoces et tardives de la spermiogenèse. Les protéomes associés aux différents stades ont fait l'objet d'annotations fonctionnelles sur la base des données de *Gene Ontology* et des voies de signalisation *KEGG*. Ce travail a permis de mettre en lumière un nombre non-négligeable de processus biologiques et de voies de signalisations dont un certain nombre sont classiquement régulés par les acteurs de l'axe hypothalamo-hypophyso-gonadique. Les protéomes obtenus ont été publiés afin d'augmenter le nombre de données disponibles chez les Élasmobranches, un clade à forts enjeux de conservation.

**Chapitre II** : Characterization of gonadotropins and their receptors in a chondrichthyan, *Scyliorhinus canicula*, fills a gap in the understanding of their coevolution

L'axe hypothalamo-hypophyso-gonadique constitue le principal système régulateur de la reproduction chez les Vertébrés. Cependant, malgré les intérêts multiples d'étudier les Élasmobranches, leur axe HHG reste largement inexploré, ce qui souligne la méconnaissance

de leur physiologie et met en évidence une lacune dans l'histoire évolutive de cet axe. L'objectif principal est donc ici de caractériser les hormones gonadotropes et leurs récepteurs chez les Élasmobranches par l'étude de leurs structures protéiques, de leurs profils d'expression, notamment au niveau du testicule de *S. canicula*, et des profils d'interaction ligand-récepteur en utilisant des protéines recombinantes en système cellulaire *in vitro*.

**Chapitre III** : Pleiotropic signaling of thyrostimulin (GPA2/GPB5) on Glycoprotein Hormone Receptors (FSHR, LHR, TSHR) in the elasmobranch *Scyliorhinus canicula* reproduction

Compte tenu des fonctions ancestrales de la thyrostimuline, ou des glycoprotéines GPA2 et GPB5, de son action paracrine dans la régulation de différents organes et de son rôle potentiel dans la régulation de la reproduction, nous avons voulu davantage caractériser son rôle chez les Élasmobranches. L'objectif est donc ici de caractériser les structures protéiques de GPA2 et de GPB5, d'étudier leurs profils d'expression, notamment au niveau du testicule de *S. canicula*, et d'étudier les interactions ligand-récepteur en système *in vitro* par l'utilisation de protéines recombinantes.

**Chapitre IV** : Characterization of a direct endocrine role of GnRHs in testicular regulation in the small-spotted catshark *Scyliorhinus canicula*: a GnRH signaling in the control of spermiogenesis and steroidogenesis in early gnathostomes

En dehors du rôle hypophysiotrope de la GnRH, une fonction paracrine des GnRHs sur la spermatogenèse et la stéroïdogenèse testiculaire a été mise en évidence chez les Mammifères et les Téléostéens. Cette fonction soulève un questionnement plus général sur l'évolution d'une régulation paracrine *versus* une régulation endocrine de la fonction testiculaire mais aussi par rapport à un rôle direct de la GnRH sur le testicule des Élasmobranches, compte tenu de la sécrétion systémique de la GnRH chez ces espèces. L'objectif de ce chapitre est par conséquent de mettre en évidence ce rôle direct par la caractérisation des séquences protéiques des GnRHs et de leurs récepteurs chez les Élasmobranches, de leurs profils

d'expression au niveau du testicule de *S. canicula*, et la réalisation d'une approche fonctionnelle en analysant le protéome d'explants testiculaires stimulés *in vitro* par des GnRHs synthétiques.

L'ensemble de ces chapitres a pour objectif général d'enrichir les données actuelles sur la reproduction des Élasmobranches dans le but de mieux comprendre leur physiologie si particulière, ce qui constitue un levier d'importance pour la protection des individus sauvages et la maitrise de leur reproduction en captivité. Par ailleurs, les données obtenues servent également à compléter l'histoire évolutive des systèmes régulateurs de la reproduction à l'échelle des Vertébrés et des Bilatériens.

# Annexe de l'introduction générale

## Spermatogenesis in Elasmobranchs

**Pascal Sourdaine[1], et Fabian Jeanne[1]**

[1] Université de Caen Normandie, MNHN, SU, UA, CNRS, IRD, Laboratoire de Biologie des Organismes et Ecosystèmes Aquatiques (BOREA), UMR 8067, 14032 Caen cedex 5, France.

*Encyclopedia of Reproduction, 3d Edition. Elsevier*

Sourdaine, P., Jeanne, F. 2024. Spermatogenesis in Elasmobranchs. In M. K. SKINNER & I. DOBRINSKI (Eds.), Encyclopedia of Reproduction, 3d edition. vol. 6, chapter 14, pp. 1–13. Academic Press: Elsevier.

DOI: https://doi.org/10.1016/B978-0-443-21477-6.00014-6

Note : Il s'agit d'une mise à jour de Pascal Sourdaine, Aude Gautier, Laura Gribouval, Spermatogenesis and Spermiogenesis in Elasmobranchs, a Short Overview, Editor(s): Michael K. Skinner, Encyclopedia of Reproduction (Second Edition), Academic Press, 2018, Pages 305–312, ISBN 9780128151457, https://doi.org/10.1016/B978-0-12-809633-8.20572-4.

## VI. Annexes de l'introduction générale

# Spermatogenesis in Elasmobranchs

**Pascal Sourdaine[1], et Fabian Jeanne[1]**

[1] Université de Caen Normandie, MNHN, SU, UA, CNRS, IRD, Laboratoire de Biologie des Organismes et Ecosystèmes Aquatiques (BOREA), UMR 8067, 14032 Caen cedex 5, France.

*Encyclopedia of Reproduction, 3d Edition. Elsevier*

Sourdaine, P., Jeanne, F. 2024. Spermatogenesis in Elasmobranchs. In M. K. SKINNER & I. DOBRINSKI (Eds.), Encyclopedia of Reproduction, 3d edition. vol. 6, chapter 14, pp. 1–13. Academic Press: Elsevier.

DOI: https://doi.org/10.1016/B978-0-443-21477-6.00014-6

Note : Il s'agit d'une mise à jour de Pascal Sourdaine, Aude Gautier, Laura Gribouval, Spermatogenesis and Spermiogenesis in Elasmobranchs, a Short Overview, Editor(s): Michael K. Skinner, Encyclopedia of Reproduction (Second Edition), Academic Press, 2018, Pages 305–312, ISBN 9780128151457, https://doi.org/10.1016/B978-0-12-809633-8.20572-4.

**CHAPTER00014 Spermatogenesis in Elasmobranchs (Accepted version)**

**Pascal Sourdaine, Fabian Jeanne**

Normandy University, UNICAEN, Caen, France

Sorbonne University, France

MNHN, UPMC Univ Paris 06, UA, CNRS, IRD, Caen, France

Biology of Aquatic Organisms and Ecosystems Joint Unit, UMR 8067, Caen, France

**Abstract**

Elasmobranchs (Skates, rays and sharks) are interesting models because the anatomical organization of their testes allows easy access to the main stages of spermatogenesis, facilitating their characterization. Moreover, as they belong to the chondrichthyans, the sister clade of bony vertebrates, the study of elasmobranchs is essential for a complete understanding of the regulation of spermatogenesis during evolution. In this brief overview, a descriptive presentation of spermatogenesis and the male genital tract in elasmobranchs is presented, highlighting their specific features.

This is an update of Pascal Sourdaine, Aude Gautier, Laura Gribouval, Spermatogenesis and Spermiogenesis in Elasmobranchs, a Short Overview, Editor(s): Michael K. Skinner, Encyclopedia of Reproduction (Second Edition), Academic Press, 2018, Pages 305–312, ISBN 9780128151457, https://doi.org/10.1016/B978-0-12-809633-8.20572-4.

**Key Points**

- The aim of this chapter is to present an overview of spermatogenesis in Elasmobranchs, a clade of phylogenetic interest.

**Introduction**

Elasmobranchs, comprising batoids (skates and rays) and sharks, belong to chondrichthyans which also include chimaeras (Holocephalans). Chondrichthyans (Cartilaginous fishes) are the sister group of bony vertebrates with a time of divergence estimated between 462 and 421 million years ago (MYA). Recent knowledge on fossilized chondrichthyans suggests that the last common ancestor of elasmobranchs and holocephalans lived about 370–380 MYA.

Despite the phylogenetic interest of chondrichthyans and their high number of species (around 1200), they have been the subject of few publications, notably concerning their reproduction. However, spermatogenesis in elasmobranchs is at the origin of old observations, particularly at the middle of the 19th century with the advent of microscopy, because of the advantages associated with the anatomical organization of their testis. In 1841, (Lallemand, 1841) observed that spermatozoa formation occurs in “spherical ampullae”, what we name presently spermatocysts, in rays and, in 1875, Semper gave a first description of the different stages of spermatogenesis in dogfish. La Valette St George (1878) was the first to describe the close association between germ cells and Sertoli cells to give what he called “spermatogennum”, currently called “spermatoblast”. A century later, the stages of spermatogenesis were more precisely classified and quantified by works of Mellinger (1965), Stanley (1966) or Holstein (1969) in the lesser spotted dogfish *Scyliorhinus canicula* (Carcharhiniformes) and the spiny dogfish *Squalus acanthias* (Squaliformes). For all elasmobranchs, the unit structure of the testis is the spheroidal spermatocyst (cyst) (terms used by previous authors were ampulla or follicle), defining their testicular structure as polyspermatocystic type. Each cyst is made up of spermatoblasts in which one Sertoli cell is associated to a clone of synchronously developing germ cells, from 1 spermatogonium initially to 64 mature spermatids. Cysts originate from the germinative zone located at fixed sites on the dorsal or dorsal-lateral margins of the testis according to species. Because new cysts are being formed and added continually, older cysts are moved in sequential order leading to a zonate arrangement according to the spermatogenetic wave as for example in *Scyliorhinus canicula* (Fig. 1). Therefore, a transverse section of the testis displays a dorsoventrally oriented succession of zones corresponding to spermatogonial, spermatocytes, early spermatids, late spermatids and degeneration zones.

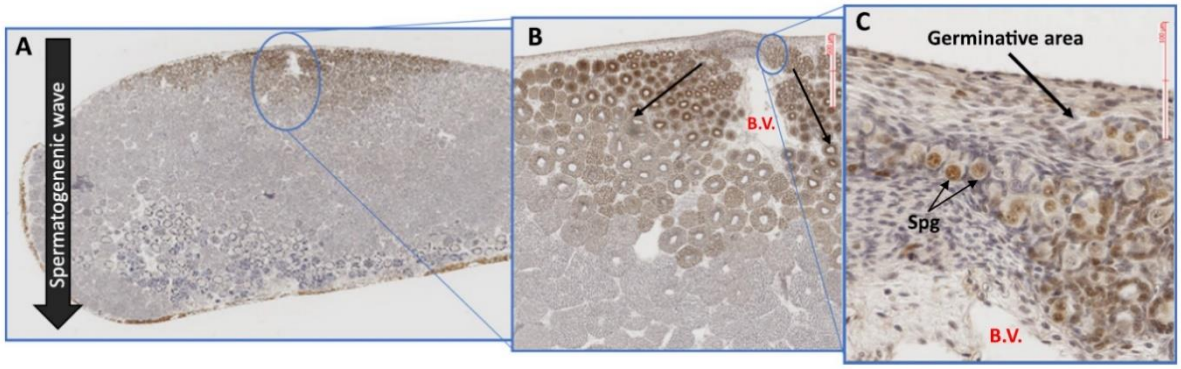


Fig. 1 **Testicular transverse section in *Scyliorhinus canicula*. A:** Spermatogenic wave (arrow) in transverse section of a diametric testis in Scyliorhinus canicula. **A-C:** immunodetection of PCNA was done (brown color) as an indicator of cell proliferation. **B-C:** corresponding enlarged views showing the progressive formation of cysts (black arrows) on either side of the blood vessel (B.V.) from the germinative area (B).Spg: spermatogonia.

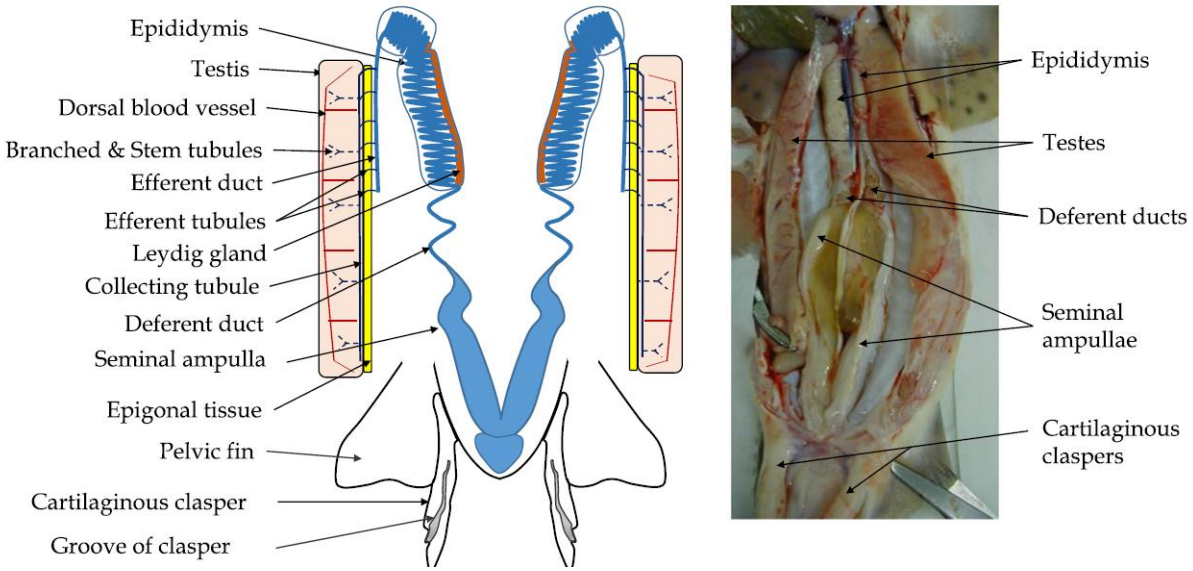


Fig. 2 **Illustration of the male genital tract in *Scyliorhinus canicula*.**

**The Male Genital Tract**

Anatomically, the male genital tract of elasmobranchs is elaborate (Fig. 2). Two elongated testes have the particularity to be closely associated to the epigonal tissue, a lymphomyeloid tissue producing leukocytes, granulocytes and lymphocytes. Spermatozoa are collected through a paired duct system associated to each testis and made of intra-testicular tubules (branched and stem tubules), collecting tubules and from two to six efferent ducts (rete testis homolog) in sharks or one efferent duct in batoids. Efferent ducts are followed by an epididymis, composed of a proximal and distal segment, which extends into the deferent duct, enlarged at its tip to form the seminal ampulla used for sperm storage (referred to as a sperm sac in some early publications), enveloping the internal seminal vesicle. The two seminal ampullae converge in their posterior region. Sperm passes from the urogenital sinus to the urogenital papilla which consists of the groove of pelvic clasper, the copulatory organs of chondrichthyans used for internal fertilization. The male chondrichthyans are the only vertebrates possessing claspers and their different morphologies can be useful in phylogenetic studies (Soares, 2020). Male elasmobranchs also possess unique reproduction- associated structures: the Leydig's gland, the siphon sacs in sharks or the clasper glands in batoids, and the alkaline gland unique to batoids (Pedreros-Sierra and Ramírez-Pinilla, 2015). Leydig's gland is closely associated and connected to the deferent duct and secretes part of the seminal fluid. The alkaline glands appear as diverticula in the posterior region of the seminal ampulla and have openings into the urogenital papilla and their precise function, notably a positive effect on sperm activation, still being discussed (Dzyuba et al., 2019). Since their functions also remain to be clarified, siphon sacs in sharks could either facilitate the transfer of sperm to the female by inducing uterine contractions or assist sperm competition by the washing female genital tract before ejaculation with a water flux (Whitney et al., 2004). The clasper gland in batoids can also facilitate copulation by providing a lubricant and a fluid coagulating with sea water that could seal the groove of the clasper to form a tube.

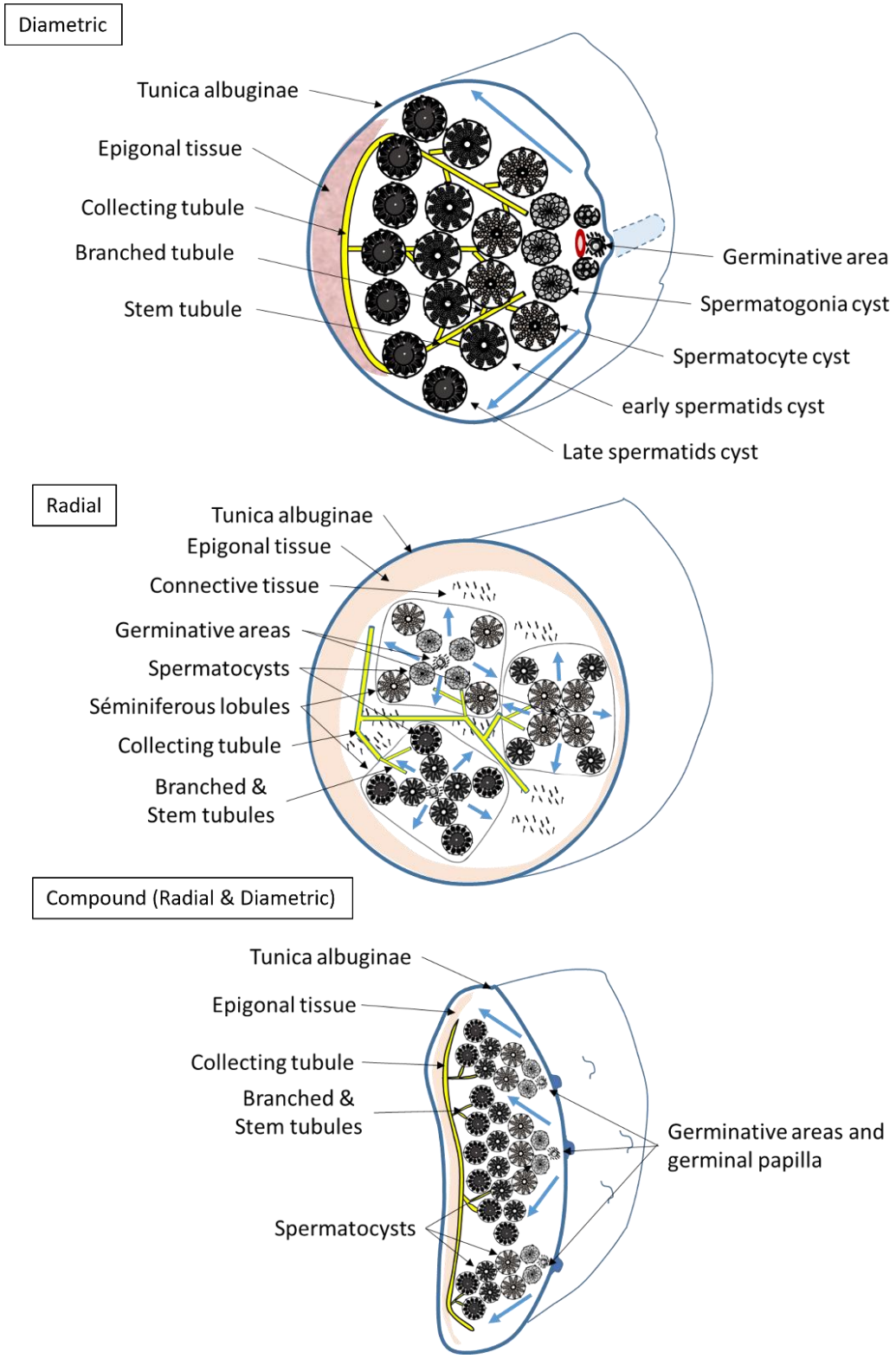


Fig. 3 **Anatomy of testis.** The testicular structure of elasmobranchs is classified as diametric, radial or compound. In diametric-type testis, the germinative area runs the dorsal length of the testis. In radial-type testis, the germinative area is in the center of seminiferous lobules. In compound-type testis, testis is subdivided in lobes, each containing a germinative area forming papilla. Adapted from Pratt, H.L., 1988. Elasmobranch gonad structure: A description and survey. *Copeia* 3, 719–729.

**Anatomy of Testis**

According to species and testicular type, germinative area is unique or multiple. In Squalomorph, Galeomorph and Carcharhinidae shark species, the germinative area consists of one band located between albuginea and the main testicular blood vessel which runs the dorsal length of the testis. This testicular structure has been classified as diametric-type testis (Pratt, 1988) (Fig 1, Fig. 3). Squaliformes, such as *Centroscymnes coelolepe*s and *Centrophorus squamosus* may present lobate testis and each lobe has a diametric structure (Girard *et al*., 2000). In Lamniformes, testis comprises seminiferous lobules (Radial-type testis) with a germinative area in the center of each seminiferous lobule and cyst development proceeds radially from the germinal area (Fig. 3). In batoids, testis combines radial and diametric structure and was termed “compound” by Pratt. Their testis may comprise lobate divisions as observed for the Cownose Ray, *Rhinoptera bonasus* (Poulakis and Grier, 2014). Germinative areas originate from the germinal papilla that appears as a small projection at the dorsal surface of the testis and cyst development proceeds diametrically from each germinative area (Fig. 3).

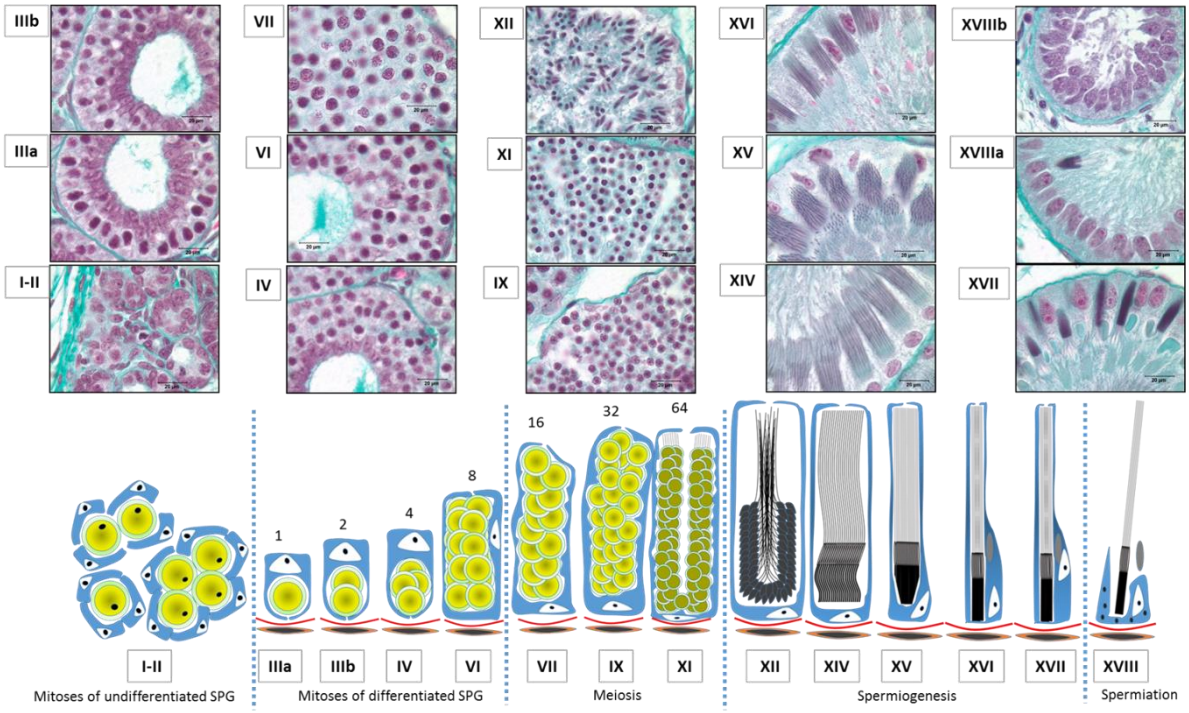


Fig. 4 **Stages of spermatogenesis in *Scyliorhinus canicula*.** Associations between Sertoli cells (in blue) and germ cells (in yellow, then black) are illustrated during stages of spermatogenesis (I to XVIII). I-II: germinative and transition zones. IIIa to XVIII: schemes of the evolution of a single spermatoblast in cysts containing spermatogonia (IIIa to VI), spermatocytes (VII, IX), spermatids (XI-XVIII) are represented in the lower part of the figure. Corresponding histology is in the upper part of the figure.

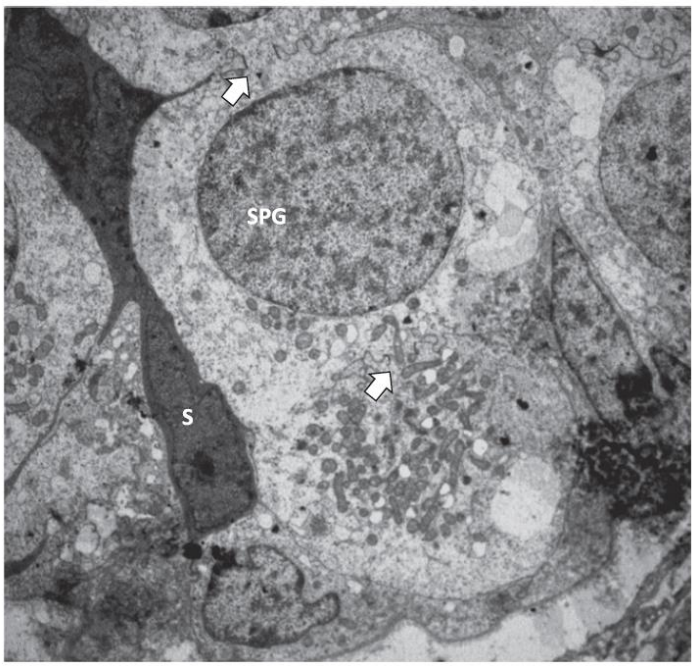


Fig. 5 **Ultrastructure of spermatogonia associated to Sertoli cells at stage II.** Intercellular bridges between spermatogonia (SPG) are indicated by arrows. S:Sertolicell.

**The mitotic Proliferative Phase of Spermatogenesis**

To describe precisely the different stages of spermatogenesis, the example of *Scyliorhinus canicula* will be detailed below (Fig. 4). Stage I corresponds to large spermatogonia (10 µm in nuclear diameter) of the germinative zone, surrounded by elongated somatic cells which correspond to Sertoli cell precursors. In the different subparts of the germinative zone, from the area just behind the fibrous albuginea toward the blood vessel, spermatogonia are isolated, paired or in clusters of 4 and they can be qualified as A single (As), A paired (Apr) and A undifferentiated (Aund) spermatogonia, respectively. Their ultrastructure observed by transmission electron microscopy reveals a nucleus with chromatin of a mottled appearance, a nucleolus and a cytoplasm containing numerous mitochondria and a dense material, the germinative nuage. From the first mitotic division, all spermatogonia will be connected with intercellular bridges to form a germ cell syncytium (Fig. 5). While leaving the germinative area, both Sertoli cell precursors and spermatogonia proliferate and both types of cells regroup progressively to form spherical cysts with a lumen that progressively appears (stage II). Stage III corresponds to the end of the cyst formation with a single layer of Sertoli cell nuclei around the central lumen and a single layer (stage IIIa) or two layers (stage IIIb) of spermatogonia toward the basal lamina. Here, it is important to notice that the cyst formation (stage IIIa) coincides with the end of Sertoli cell divisions and to the further four mitoses of differentiated spermatogonia (stages IIIb to VI). Stage IV has four layers of spermatogonia and Sertoli cell nuclei remaining at the adluminal position. Stage V presents five layers of spermatogonia and the Sertoli cell nuclei are at an adluminal (majority) or at an intermediate position. Stage VI exhibits about six layers of spermatogonia (corresponding to pre-leptotene spermatocytes) and Sertoli cell nuclei are in an intermediate (majority) or basal position. The number of germ cells per spermatoblast is 4, 8 and 16 for stages IV, V and VI, respectively. Considering the ratio of 1 Sertoli cell for 1 spermatogonium at stage IIIa, and the number of Sertoli cell nuclei per cyst (reflecting also the number of spermatoblasts per cyst), it is possible to evaluate the number of cell mitotic divisions for undifferentiated spermatogonia. Holstein (1969) has determined 469 spermatoblasts per cysts in *Squalus acanthias* and this number is about 500 in *Scyliorhinus canicula* cysts and about 250 in Torpedo marmorata cysts. In *S. canicula and S. acanthias*, this will correspond to 9 cell cycle divisions for undifferentiated spermatogonia (from As to Aund 512) and to 4 more divisions for differentiated spermatogonia (from Ad1 to

PL spermatocytes), considering that no division occurs between the last stage of undifferentiated spermatogonia and the first stage of differentiated ones. Concerning T. marmorata, the total number of spermatogonial mitotic divisions is 12 instead of 13. This high proliferative phase allows to produce a large number of spermatozoa from a small number of germinal stem cells. Otherwise, the difference between the theoretical (512) and observed (469) number of spermatoblasts suggests an apoptosis control of testicular homeostasis as observed for all vertebrates and studied in the shark *S. acanthias* (McClusky, 2012) or in the ray *T. Marmorata*.

This ability to observe these different generations of spermatogonia is also of interest for studying spermatogonial stem cells and their progeny by establishing a molecular signature for each of them using in situ hybridization and immunocytochemistry approaches. Such studies have shown, for example, that one of the most universal spermatogonial stem cell regulator, the GDNF family receptor GFRa1, is expressed in undifferentiated spermatogonia (Bosseboeuf et al., 2014).

**Meiosis**

In the dogfish *S. canicula*, meiosis proceeds from stages VII to XI (Fig. 4). Stage VII corresponds to cysts containing the primary spermatocytes at the meiotic prophase and all the Sertoli cell nuclei are observed against the basal lamina. Stage VIII corresponds to the first meiotic division (metaphase, anaphase, telophase) which gives secondary spermatocytes (stages IX and X). At the end of meiosis, the number of early spermatids (or round spermatids) is of 64 per spermatoblast (stage XI).

**Spermiogenesis**

Spermiogenesis is the development of spermatids into mature spermatozoa. During this process, the main cell transformations are the acrosome formation, the compaction of chromatin with the replacement of histones by transition proteins and then protamines, the flagella assembly and the cytoplasm reorganization with elimination of its major part and of its organelles to keep a cytoplasm mainly restricted to the midpiece containing mitochondria.

In *S. canicula*, stage XI corresponds to cysts with young round spermatids arranged as "a festoon figure" with nuclei showing patches of dense chromatin and flagella which are noticeable (Fig. 4). In stage XII, condensation of the chromatin is well advanced and elongation of the spermatic head and the flagellum are observable on histological sections. During the following stages, the development of the helical head, a characteristic feature of chondrichthyan spermatozoa, occurs and is completed at stage XIV. At this stage spermatids are arranged in parallel bundles which are perpendicular to the basal lamina of the cyst. The helical twisting of the spermatid which includes the head, the midpiece and flagellar elements, has a function in spermatozoa motility achieved by revolving around their long axis by using both their head and tail for helical propulsion (Wang et al., 2021). During stages XV to XVII, the nuclei of Sertoli cell migration towards the intermediate cytoplasm of the cell and spermatid bundles become more compact and closer to the basal lamina. The midpiece of spermatid is also well noticeable at the back of the head. At the ultrastructure level, for the spiny dogfish, glycogen granules are present and dispersed between mitochondria, the acrosome forms an elongated cap over the nucleus of the spermatid and a short perforatorium develops between the nucleus and the acrosome (in the subacrosomal space). Classically, the function of the perforatorium is the penetration of the sperm through the egg chorion during fertilization. The flagellar apparatus of spermatozoa is also characterized by the presence of flagellar roots which form the axis of the midpiece and the existence of two longitudinal columns associated with the axoneme. Once again, given the particular motility of spermatozoa in elasmobranchs, column function could be associated with the process of changing their bidirectional motion (forward only, backward and forward, backward only) as observed for sperm of the Javanese Cownose Ray (Wang et al., 2021).

Another characteristic feature during the stages of spermiogenesis in elasmobranchs, is the apparition of a large protein body in the intermediate cytoplasm of Sertoli cell (stage XVI), the Semper's body. Its function is unclear and it will be released with bundles of spermatozoa during spermiation. A similar body has been found in the semen of the spiny dogfish and named "Sertoli cell cytoplast". As it contains organelles (mitochondria, ribosomes, endoplasmic reticulum) and lipid droplets, some of them associated to steroid synthesis, Pudney and Callard hypothesized that it could contribute to the steroids found in the semen and necessary for maturation and maintenance of spermatozoa in the reproductive ducts

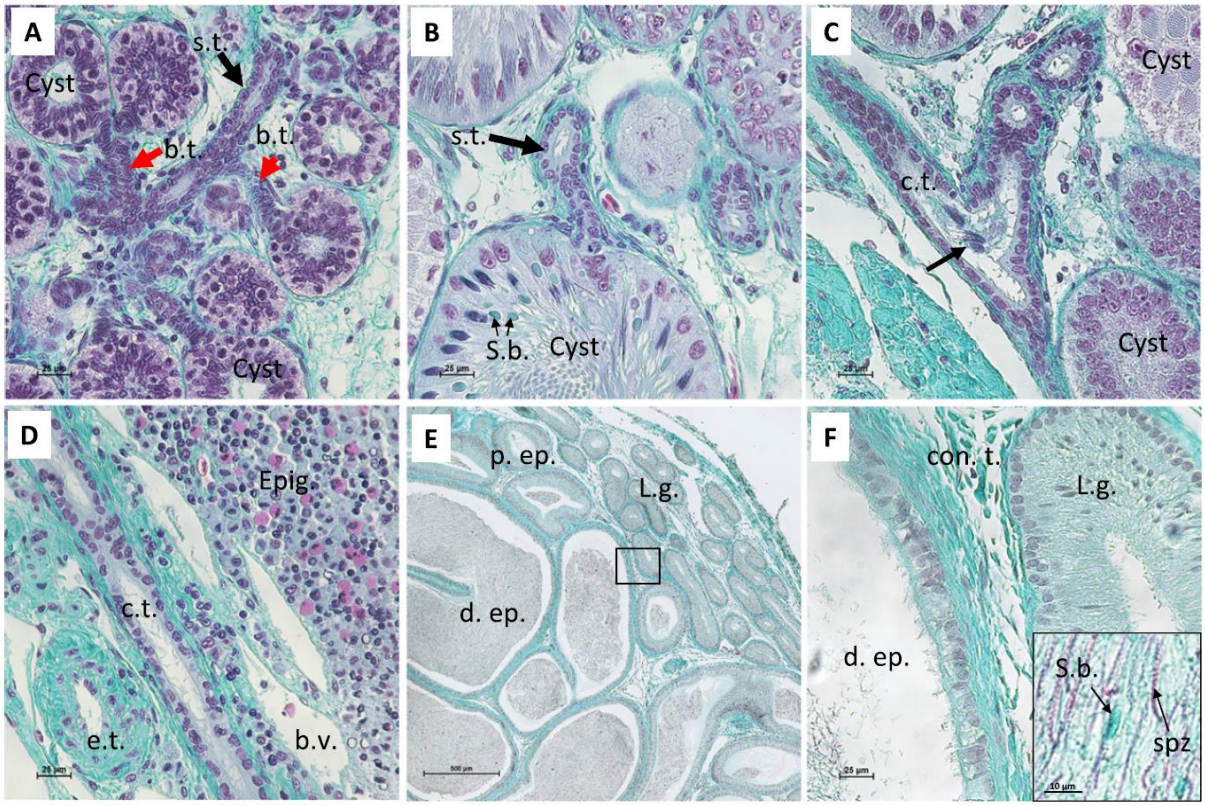


Fig. 6 **A network of tubules.** **A-D:** Intratesticular tubules. **E-F:** Epididymal and Leydig's gland tubules. **A:** During their development ,cysts are connected early to branched tubules (b.t.) which converge into stem tubules (s.t.). **B:** illustration of a cyst in spermiation with its branched tubule open and connected to a stem tubule; S.b.: Semper's bodies. **C:** collecting tubule (c.t.) containing a bundle of spermatozoa (arrow). **D:** network of tubules at the connection between collecting tubules (c.t.) and efferent tubules (e.t.) on the mature margin of the testis adjacent to the epigonal tissue (Epig.); b.v.: blood vessel. **E:** Illustration of tubules at the junction of the proximal (p.ep.) and distal (d.ep.) segments of epididymis, containing spermatozoa, and of the adjacent Leydig's gland (L.g.). **F:** Enlarged view of the square in Fig. 6E illustrating epithelia of epididymis and of Leydig's gland which are separated by a connective tissue (con.t.) Fig. 6E insert: spermatozoa (spz) and Semper's body (S.b.) in the lumen of epididymis.

(Pudney and Callard, 1986). Another hypothesis may be that the Semper's body is equivalent to the residual body observed for mammalian spermatids. Its function remains to be studied. Stage XVIII corresponds to the spermiation which takes place by the detachment of the spermatid bundle which carries with it the adluminal part of the Sertolian cytoplasm. Bundles of spermatozoa are then evacuated through the cystic collecting ductule (branched tubules), previously closed by a cellular plug (Fig. 6). By taking into account the number of 500 spermatoblasts in *S. canicula* and of 250 in *T. marmorata*, it could be calculated that 32,000 and 16,000 spermatozoa will be produced per cyst, respectively, for these species.

The post-spermiation cyst contains the remaining basal cytoplasms and nuclei of Sertoli cells and will be resorbed in the epigonal organ, underlying this characteristic feature of the close association between this lymphomyeloid tissue and the testis in elasmobranchs. However, there are a few exceptions, as epigonal organs have not been observed associated with gonads in several deep-sea squaloid sharks (Girard et al., 2000). Another interesting feature about this association was the inhibitory effect on DNA synthesis of premeiotic cysts by epigonal cytosolic extracts, suggesting a crosstalk between the two organs to regulate the spermatogenic cycle. Involvement of growth factors (GDNF, IGF1, bFGF…) and cytokines (IL1, G-CSF…) in the regulation of spermatogonial proliferation is now well documented in several species.

**Blood-Testis Barrier**

In amniotes, the blood-testis barrier (BTB) is essential for spermatogenesis and forms during puberty when Sertoli cells stop mitosis. Classically, blood–tissue barriers restrict or control the entry of molecules present in circulation from entering a tissue or compartment. This barrier partially made of specialized junctions between Sertoli cells "protects" haploid cells in a specific microenvironment and allows also the production of the testicular fluid useful, in particular, for transporting spermatozoa. This blood-testis barrier can be visualized by exclusion of a high molecular weight (10 kDa) fluorescent dye. Using this approach, McClusky has shown that living post-meiotic cysts are impermeant, suggesting a functional blood-testis barrier in cysts containing spermatids in the spiny dogfish (McClusky, 2006). Furthermore, in

spermatid cysts, tight junctions have been observed between Sertoli cells, reinforcing the presence of a BTB but the precise description of its ultrastructural components remains to be done.

**Sperm Transport, Maturation and Storage**

Structure of a branching intratesticular network of ductules has been well described in the starspotted smooth-hound *Mustelus manazo* (Park *et al*., 2013). This system is composed of branched tubules, linked to cysts, which are connected via a secondary network of stem tubules to the collecting tubules. Branched and stem tubules can be observed early in the cyst-forming area (stage II) and during the spermatogenetic wave, cysts are still attached to branched tubules (Fig. 6). This implies that both cyst and tubules will move together from the germinal to the mature zone of the testis, undoubtedly involving regulatory mechanisms not yet known. During spermiation, branched tubules open at their junction with the cyst allowing the flow of bundles of spermatozoa into the stem tubules. Transport of spermatozoa will be achieved thanks to the presence of ciliated epithelial cells lining the lumen of branched, stem and collecting tubules (Fig. 6). Contraction of myoid cells surrounding the intratesticular tubules probably also contributes to the transport of spermatozoa towards the epididymis where maturation occurs (Fig. 6). In mammals, spermatozoa acquire their motility and fertilizing properties during their epididymal transit. Epididymis has been poorly studied in elasmobranchs, which is surprising considering its size and its apparent similarity to that of mammals. Studies in the Port Jackson Shark, *Heterodontus portusjacksoni* (Jones *et al*., 1984), in the Clearnose Skate *Raja eglanteria* (Jones and Hamlett, 2006) and in the ocellate river stingray *Potamotrygon motorothe* (Dzyuba *et al*., 2019) have shown that epididymis effectively participates in luminal fluid modifications, including sodium resorption, and that spermatozoa, immotile in the proximal segment, acquired their motility during their transit in the distal segment of epididymis. In *Raja eglanteria*, the glycosylation activity of the Leydig's gland (Fig. 6), connected to epididymis and to the deferent duct, is associated to spermatozoa aggregation. During their transport from the cyst, where they were aggregated into bundles, to the distal segment of epididymis, bundles of spermatozoa are dissociated and spermatozoa reaggregate into the seminal vesicle where they are embedded in a mucoid matrix. Two basic types of spermatozoa aggregation are described for elasmobranchs: spermatozeugmata and

spermatophores. In spermatophores, bundles of spermatozoa are embedded in a matrix with the heads inside and the flagella projected out the matrix. Spermatophores are found in Alopidae, Odontaspididae and Lamnidae. Spermatozeugmata are un-encapsulated masses of naked spermatozoa. Spermatozeugmata may consist of different architectures: simple aligned bundles of spermatozoa (*Squalus acanthias*, *Hydrolagus colliei*); radially aligned bundles of spermatozoa (*Charcharinus plumbeus*); several layers of sperm bundles (*Sphyrna lewini*). Spermatozoa are stored in a motile state within seminal ampullae and increase their velocity in the female reproductive tract, where they are able to swim through a wide range of viscous environments (uterus, oviducal gland and oviduct) thanks to their peculiar rotational propulsion mechanism (Wang et al., 2021).

**Seasonality of Spermatogenesis**

Spermatogenesis can show little or no seasonal changes in Elasmobranchs, as this is the case for *S. canicula* or the ray *T. marmorata* showing continuous spermatogenesis throughout the year. But in the spiny dogfish *S. acanthias*, caught along the United States Atlantic coast, the spermatogenic cycle is interrupted by germ cell apoptosis at the mitosis–meiosis transition in April-May, leading to a zone of degeneration. By studying this zone of degeneration, several pieces of information of interest can be found. Firstly, because this interruption is temporary, the resumption of the mitosis-meiosis transition will give new cysts that will lead to a displacement of the zone of degeneration (ZD) towards the mature side of the testis. So, the observation of this zone of degeneration along the time will give an idea of the duration of spermatogenesis. In the spiny dogfish, McClusky (2006) has thus established that the spermatogenic cycle spans about 2 years and that the duration from the Preleptotene stage to the more mature spermatid stage is of 9–10 months, underlining the long time required for spermatogenesis in that shark. In terms of sperm production, the displacement of the ZD at the mature side of the testis will lead to the absence of mature cysts and consequently the decrease of sperm production 9–10 months later, in February-March of the following year. Conversely, the higher number of cysts containing mature spermatids is observed between October and January and coincides with the matting period (December to February). Secondly, this zone of degeneration was experimentally reproduced in the dogfish *S. canicula* by partial hypophysectomy coupled with an increase of temperature, suggesting that this mitotic-

meiosis transition is a critical stage of spermatogenesis under gonadotrophin and environmental control. Consequently, seasonality of reproduction can be more marked in species that inhabit regions where environmental conditions vary widely with season.

A ZD has also been observed in the blue shark *Prionace glauca*, the Atlantic stingray *Hypanus sabinus*, in the skate *Raja erinacea* or in the ray *Urobatis halleri* for examples. Apart from the presence or absence of a ZD, it has been reported that the relative abundance of cysts at different stages of spermatogenesis varies seasonally according to species. As observed for *S. acanthias*, higher number of cysts containing mature spermatids or higher number of spermatozoa in seminal ampullae generally correlate with the mating period for sharks. In *S. canicula* (Carcharhiniformes, wide geographic range, Northeast Atlantic), mature spermatids containing cysts increase from April through to August and the greatest number of spermatozoa per seminal ampulla was observed from March through to May in species caught in the English Channel. In Epaulet shark, *Hemiscyllium ocellatum* (Orectolobiformes, tropical, Western Pacific), a higher degree of sperm storage occurs from August through to November, preceding mating period in December. In Starspotted smooth-hound *Mustelus manazo* and in Spotless smooth-hound *Mustelus griseus*, two Carcharhiniformes tropical species (Western Indian Ocean and Western Pacific), the highest number of cysts containing mature spermatids was observed in March and May, respectively, and accumulation of spermatozoa was greatest from December through to May. In both Mustelus species, it appears that spermatozoa production was at maximum before the June-August mating period. Among sharks, the Bonnethead *Sphyrna tiburo* (Carchariniformes, subtropical, Western Atlantic) appears as a special case since all stages of spermatogenesis are not present at all time of the year, a complete testicular regression and recrudescence is observed (Parsons and Grier, 1992). All the reports cited above concern sharks, what about rays ? In the subtropical Myliobatiforms Atlantic stingray *Hypanus sabinus* (Western Atlantic) and round stingrays *Urobatis halleri* (Eastern Pacific), inactive phase of spermatogenesis was observed from March through to July and maximum production of mature cysts in winter (from August through to January in *H. sabinus*, December in *U.halleri*) preceding spring mating period when sperm stored in seminal vesicles will be used (Tricas et al., 2000). In lesser guitar fish *Rhinobatus annulatus* (Rhinopristiformes, subtropical, Southeast Atlantic), no spermatogenetic resting period was

observed since all stages were found in the testes throughout the year. However, a peak in sperm production was observed from November through to January (Rossouw, 2014).

**Control of Spermatogenesis**

In Elasmobranchs, like in other vertebrates, the testicular function is hormonally controlled via a hypothalamus–pituitary–gonadal (HPG) axis involving the GnRH (Gonadotropin-releasing hormone) hypothalamic neuropeptide, pituitary gonadotropins LH (luteinizing hormone) and FSH (follicle stimulating hormone) and gonadal steroids. GnRH and gonadotropins act by binding to their specific G-protein coupled-receptor (GnRHR, FSHR, LHR) expressed by their target cells. Three groups of GnRH (GnRH-I, GnRH-II, GnRH-III) have been identified in brain but it is classically considered that control of synthesis and release of gonadotropins is regulated by the GnRH-I localized in diencephalon. In Elasmobranchs, the transport of GnRH-I to pituitary occurs via the general circulation in absence of a direct vasculature such as the portal system found in mammals. Gonadotropins are heteromeric glycoproteins made of one common α subunit and one specific β subunit (β-LH or β-FSH). The three subunits have been first identified in *S. canicula* and with advances in elasmobranch genome sequencing, sequences of hormones and their receptors have been identified in several species. Presently, interactions between glycoprotein hormones (LH, FSH, TSH) and their receptors have been only studied in the elephant shark *Callorhinchus milii* (Buechi and Bridgham, 2017), a chondrichthyan belonging to holocephalans which have diverged early from elasmobranchs (around −400/−350 MYA). However, the expression profiles and functions of FSH and LH receptors have not yet been studied in elasmobranchs, underscoring the work that remains to be done in these species. At present, the control of spermatogenesis in elasmobranchs is essentially based on the targeted study of mRNA or protein expression levels as a function of development or stages of spermatogenesis, or on the analysis of hormone levels as a function of seasonality. Gene editing has not yet been developed, but recent advances in gene transfer are emerging (Fujimori et al., 2022).

**The Case of Leydig Cells**

When testicular anatomy is presented, it is usual to present the seminiferous compartment in which spermatogenesis occurs and the interstitial compartment, which includes the Leydig cells. This pattern is probably true for amniotes but the presence of functional Leydig cells in elasmobranchs is still questioned. In amniotes, the Leydig cells are associated to androgen production and they show an ultrastructure classically associated to steroid synthesis such as presence of mitochondria with tubular cristae, agranular endoplasmic reticulum and lipid droplets. In addition, they express key enzymes involved in the biosynthesis of steroids such as the 3β-hydroxysteroid dehydrogenase (3β-HSD) and 17β-hydroxysteroid dehydrogenase (17β-HSD). In elasmobranchs, Leydig cells have been described as absent or present according to authors and/or stages of development and/or seasonality. For example, Leydig cells have been described as absent from the interstitial tissue of *Scyliorhinus stellaris* or rare in *Cetorhinus maximus* and *Scyliorhinus canicula* or present but undifferentiated in *Squalus acanthias*. Furthermore, Sertoli cells in these species show steroidal ultrastructure features and isolated cysts in *Squalus acanthias* or in *Scyliorhinus canicula* have the abilities to synthesize androgens. However, interesting studies conducted in the ray *T. marmorata* (Prisco et al., 2008) have shed new light on the question. In fact, in this species, typical Leydig cells are observed in the interstitial compartment adjacent to cysts engaged in spermatogenesis but they have reduced cellular components when they are associated to cysts containing spermatogonia and, at the other end, when they are associated to cysts engaged in spermiation. Immunolocalization of 3β-HSD and 17β-HSD has confirmed a distinctive stage-related involvement of cells in steroid production: spermatogonia of the early stages, Sertoli cells of cysts containing spermatogonia, Leydig cells associated to meiotic stages and Sertoli cells in late spermatids stages.

Several studies, reviewed by Becerril-Garcia et al. (2020), have analyzed steroid levels in relation with the seasonal reproductive cycle and spermatogenetic stages. Briefly, in mature individuals, androgens (mainly testosterone instead of 11-ketotestosterone) regulate development and maturation of cysts as well as the final stage of sperm maturation. Androgen receptor was primarily localized in premeiotic stages in the testis of *S. acanthias*, suggesting that androgens regulate the development of early stages of spermatogenesis, which has also been observed in the bonnethead *Sphyrna tiburo* (Tyminski et al., 2015) but with an

expression, and therefore a potential function, extended to gonadal ducts. In agreement, increased male genital tract development and mature sperm count correlate with increased plasma testosterone in seasonal animals as observed, for example, for the bonnethead (Gonzalez De Acevedo et al., 2020) or for the sand tiger shark *Carcharias taurus* (Wyffels et al., 2020). Among other steroids, progesterone and 17α, 20β dihydroxyprogesterone (OHP) have also been identified and associated with cysts containing late spermatids (Sourdaine and Garnier, 1993). In addition, the progesterone receptor has been identified in the extratesticular ducts of the Amazonian stingray *Potamotrygon wallacei*, suggesting a potential role for progesterone in sperm maturation (Morales-Gamba et al., 2023).

**Reproductive Science in Elasmobranchs**

The science of assisted reproduction in elasmobranchs is currently being developed in aquaria in an attempt to address the risk of extinction of several species (Penfold and Wyffels, 2019). These developments include the publication of methods for semen collection adapted to species, for sperm cryopreservation (García-Salinas et al., 2021) and for non-invasive evaluation of andrological parameters (de Oliveira Camilo et al., 2023). Studies on comparisons of hormonal profiles in captive versus wild individuals are also being undertaken with the aim of developing in situ conservation (Becerril-Garcia et al., 2020). Paradoxically, assisted reproduction is also likely to benefit from the development of contraceptive methods to reduce aggressiveness in captivity, using GnRH antagonists in particular, which could help to understand the particularities of the neuroendocrine control of reproduction in elasmobranchs (Sailler et al., 2023).

**Conclusion**

Elasmobranchs present a remarkable male genital tract that by some aspects, appears more related to the genital tract of amniotes than of anamniote species (epididymis for example). They have also characteristic features like the close association between the testis and the epigonal tissue or the diversity of testicular cells involved in steroidogenesis. What is the evolutionary meaning of these features? Endocrine and paracrine control of spermatogenesis

are still poorly understood while knowledge on the reproduction of elasmobranchs is still a challenge because of their vulnerability.

**References**

Becerril-Garcia, E.E., et al., 2020. Steroid hormones and chondrichthyan reproduction: physiological functions, scientific research, and implications for conservation. PeerJ 8, e9686.

Bosseboeuf, A., et al., 2014. Characterization of spermatogonial markers in the mature testis of the dogfish (Scyliorhinus canicula L.). Reproduction 147 (1), 125–139.

Buechi, H.B., Bridgham, J.T., 2017. Evolution of specificity in cartilaginous fish glycoprotein hormones and receptors. General and Comparative Endocrinology 246, 309–320.

Dzyuba, V., et al., 2019. Sperm motility in ocellate river stingrays: Evidence for post-testicular sperm maturation and capacitation in Chondrichthyes. Journal of Zoology 307, 9–16.

Fujimori, C., et al., 2022. In vitro and in vivo gene transfer in the cloudy catshark Scyliorhinus torazame. Development, Growth & Differentiation 64 (9), 558–565.

García-Salinas, P., Gallego, V., Asturiano, J.F., 2021. Development of sperm cryopreservation protocols for sharks and rays: New tools for elasmobranch conservation. Frontiers in Marine Science 8, 689089.

Girard, M., Rivalan, P., Sinquin, G., 2000. Testis and sperm morphology in two deep-water squaloid sharks, Centroscymnus coelolepis and Centrophorus squamosus. Journal of Fish Biology 57, 1575–1589.

Gonzalez De Acevedo, M., et al., 2020. Reproductive cycle and fecundity of the bonnethead Sphyrna tiburo L. from the northwest Atlantic Ocean. Journal of Fish Biology 97 (6), 1733–1747.

Holstein, A., 1969. On the problem of the local control of the spermatogenesis of the spiny dogfish (Squalus acanthias L.). Zeitschrift für Zellforschung und Mikroskopische Anatomie 93, 265–281.

Jones, C.J.P., Hamlett, W.C., 2006. Ultrastructure of the male genital ducts of the clearnose skate Raja eglanteria. Journal of Experimental Zoology 305A, 1018–1029.

Jones, R.C., Jones, N., Djakiew, D., 1984. Luminal composition and maturation of spermatozoa in the male genital ducts of the Port Jackson shark, , Heterodontus portusjacksoni. The Journal of Experimental Zoology 230, 417–426.

La Valette St George, A., 1878. Dissertatio de spermatosomatum evolutione in plagiostomis. formis Caroli Georgi univ. typogr, Bonnae.

Lallemand, F., 1841. Observations sur le développement des zoospermes de la raie. Annales des Sciences Naturelles Zoologie 15, 257–262.

McClusky, L.M., 2006. Stage-dependency of apoptosis and the blood–testis barrier in the dogfish shark (Squalus acanthias): Cadmium-induced changes as assessed by vital fluorescence techniques. Cell and Tissue Research 325 (3), 541–553.

McClusky, L.M., 2012. Coordination of spermatogenic processes in the testis: Lessons from cystic spermatogenesis. Cell and Tissue Research 349 (3), 703–715.

Mellinger, J., 1965. Stades de la spermatogénèse chez Scyliorhinus caniculus (L.): Description, données histochimiques, variations normales et expérimentales. Zeitschrift für Zellforschung und Mikroskopische Anatomie 67, 653–673.

Morales-Gamba, R.D., et al., 2023. Progesterone receptors in extratesticular ducts of the Amazonian stingray Potamotrygon wallacei: A potential role in sperm maturation and aggregate formation. General and Comparative Endocrinology 344, 114375.

Oliveira Camilo, L., et al., 2023. Andrology of shortnose guitarfish Zapteryx brevirostris (Müller & Henle, 1841) (Chondrichthyes, Trygonorrhinidae). Journal of Fish Biology 103 (3), 635–645.

Park, J.C., et al., 2013. Structure of the intratesticular duct system for sperm emission in the starspotted smooth-hound Mustelus manazo. Fisheries Science 79 (2), 203–211.

Parsons, G.R., Grier, H.J., 1992. Seasonal changes in shark testicular structure and spermatogenesis. Journal of Experimental Zoology 261 (2), 173–184.

Pedreros-Sierra, T.M., Ramírez-Pinilla, M.P., 2015. Morphology of the reproductive tract and acquisition of sexual maturity in males of Potamotrygon magdalenae (Elasmobranchii: Potamotrygonidae). Journal of Morphology 276 (3), 273–289.

Penfold, L.M., Wyffels, J.T., 2019. Reproductive Science in Sharks and Rays. Advances in Experimental Medicine and Biology 1200, 465–488.

Poulakis, G.R., Grier, H.J., 2014. Ontogenetic testicular development and spermatogenesis in rays: The Cownose Ray, Rhinoptera bonasus, as a model. Environmental Biology of Fishes 97 (9), 1013–1029.

Pratt, H.L., 1988. Elasmobranch gonad structure: A description and survey. Copeia 1988 (3), 719–729.

Prisco, M., et al., 2008. Immunolocalization of 3beta-HSD and 17beta-HSD in the testis of the spotted ray Torpedo marmorata. General and Comparative Endocrinology 155 (1), 157–163.

Pudney, J., Callard, G.V., 1986. Sertoli cell cytoplasts in the semen of the spiny dogfish Squalus acanthias. Tissue and Cell 18 (3), 375–382.

Rossouw, G.J., 2014. Maturity, spermatogenesis and seasonal reproductive cycle of male Rhinobatos annulatus (Muller & Henle, 1841) from Algoa Bay, South Africa, and a novel description for sperm release from the spermatocyst. African Zoology 49 (1), 128–139.

Sailler, A., Laidebeure, S., Lécu, A., 2023. ). Effects of a GnRH vaccine and Deslorelin acetate implants in male freshwater stingrays (Potamotrygon sp.). Journal of zoo and Wildlife Medicine: Official Publication of the American Association of Zoo Veterinarians 54 (1), 40–48.

Soares, K.D., 2020. Comparative anatomy of the clasper of catsharks and its phylogenetic implications (Chondrichthyes: Carcharhiniformes: Scyliorhinidae). Journal of Morphology 281 (6), 591–607.

Sourdaine, P., & Garnier, D.H. (1993). Stage-dependent modulation of Sertoli cell steroid production in dogfish (Scyliorhinus canicula). . Journal of Reproduction and Fertility , 97(1), 133–142.

Stanley, H.P. (1966). The structure and development of the seminiferous follicle in Scyliorhinus caniculus and Torpedo marmorata (Elasmobranchii). . Zeitschrift fiir Zellforschung , 75, 453–468.

Tricas, T.C., Maruska, K.P., & Rasmussen, L.E. (2000). Annual cycles of steroid hormone production, gonad development, and reproductive behavior in the atlantic stingray. . General and Comparative Endocrinology , 118(2), 209–225.

Tyminski, J. P., Gelsleichter, J. J., & Motta, P. J. (2015). Androgen receptors in the bonnethead, Sphyrna tiburo: cDNA cloning and tissue-specific expression in the male reproductive tract. General and comparative endocrinology, 224, 235–246.

Wang, P., et al., (2021). Self-adaptive and efficient propulsion of Ray sperms at different viscosities enabled by heterogeneous dual helixes. Proceedings of the National Academy of Sciences of the United States of America, 118(23), e2024329118.

Whitney, N.M., Pratt, H.L., Carrier, J.C. (2004). Group courtship, mating behaviour and siphon sac function in the whitetip reef shark, Triaenodon obesus, Animal Behaviour, 68(6), 1435-1442.

Wyffels, J. T., et al., (2020). Testosterone and semen seasonality for the sand tiger shark Carcharias taurus. Biology of reproduction, 102(4), 876–887.

# Chapitre I

## Comparative Proteome Analysis of Four Stages of Spermatogenesis in the Small-Spotted Catshark (Scyliorhinus canicula), Using High-Resolution NanoLC-ESI-MS/MS

**Fabian Jeanne, Benoît Bernay, et Pascal Sourdaine**

*Journal of Proteome Research 2023, 22, 2477-2492*

DOI: https://doi.org/10.3390/ani14091281

# Chapitre I

## Comparative Proteome Analysis of Four Stages of Spermatogenesis in the Small-Spotted Catshark (*Scyliorhinus canicula*), Using High-Resolution NanoLC-ESI-MS/MS

**Fabian Jeanne, Benoît Bernay, et Pascal Sourdaine**

*Journal of Proteome Research 2023, 22, 2477-2492*

DOI: **https://doi.org/10.3390/ani14091281**

## Analyse comparée des protéomes des quatre stades de la spermatogenèse chez la petite roussette (*Scyliorhinus canicula*), par l'utilisation d'un NanoLC-ESI-MS/MS à haute résolution

Le testicule est l'organe qui exprime le plus grand nombre de gènes enrichis au niveau tissulaire (Djureinovic et al., 2014) et des efforts sont actuellement déployés pour caractériser les fonctions de ces gènes (Vandenbrouck et al., 2020). Dans ce but, l'analyse des expressions spécifiques aux types cellulaires et dépendantes du stade est fondamentale pour caractériser les événements se déroulant au cours de la spermatogenèse. Dans ce contexte, l'analyse des protéomes testiculaires de la petite roussette *Scyliorhinus canicula* présente des intérêts du fait de sa position phylogénétique unique à la racine des Gnathostomes (Irisarri et al., 2017) et de la possession des répertoires de gènes régulant l'homéostasie et la reproduction (Hara et al., 2018). Le testicule de *S. canicula* possède une organisation cystique où chaque cyste est constitué de spermatoblastes eux-mêmes constitués d'une association entre une cellule de Sertoli et une lignée de cellules germinales à développement synchrone (Stanley, 1966). La spermatogenèse se déroule sur tout le diamètre du testicule, ainsi, une coupe transversale du testicule montre une succession de zones correspondant à la zone germinative et la zone des cystes à spermatogonies (zone A), puis des cystes à spermatocytes (zone B), des cystes à jeunes spermatides (zone C) et des cystes à spermatides matures (zone D), qui sont facilement distinguables et accessibles (Loir and Sourdaine, 1994). De plus, l'absence de cellules de Leydig différenciées renforce le rôle essentiel des cellules de Sertoli chez cette espèce (Engel and Callard, 2007).

L'objectif de cette étude est de caractériser, pour la première fois chez un Vertébrés cartilagineux, les protéomes des quatre principales zones testiculaires afin d'établir les changements protéiques en fonction des stades de la spermatogenèse.

Après microdissections des quatre zones testiculaires de la roussette *S. canicula*, les protéomes ont été analysés par NanoLC-ESI-MS/MS à haute résolution et les protéines identifiées ont été annotées par Blastp contre le protéome prédit de *S. canicula*. Les protéines annotées ont fait l'objet d'une annotation homologue par Blastp contre le protéome de la souris *Mus musculus*. Les protéines spécifiques de chaque zone ont été identifiées et illustrées par un diagramme de Venn avant de faire l'objet d'une annotation fonctionnelle par ontologie

génétique. D'autre part, les abondances des protéines exprimées dans les quatre zones testiculaires ont été analysées par k-clustering (k = 5) et représentées par une carte de chaleur avant de faire également l'objet d'une annotation fonctionnelle par ontologie génétique. À partir des termes obtenus, trois voies de signalisation ont fait l'objet d'une analyse approfondie incluant l'identification des différents acteurs impliqués ainsi que l'analyse de leurs profils d'expression en fonction des stades de la spermatogenèse. L'analyse de la stéroïdogenèse a été inclue sur la base du rôle cruciale des stéroïdes dans la régulation de la spermatogenèse.

En termes de protéines spécifiques aux zones, cette étude a mis en évidence que les deux zones avec le plus de protéines spécifiques étaient la zone A, avec 401 protéines, et la zone D avec 242 protéines.

Des termes d'intérêt ont été mis en avant au niveau des différentes zones testiculaires. Les termes obtenus pour la zone A sont liés aux processus métaboliques des ARNm, à l'épissage des ARNm et à la réplication de l'ADN alors que les termes obtenus pour la zone D sont liés au développement du flagelle des spermatides ainsi qu'à son activité.

En termes de protéines montrant des changements significatifs d'abondance entre les zones, les 1284 protéines différentiellement exprimées entre les quatre zones testiculaires ont été partitionnées sur la base des différents profils d'expression observés, qui sont au nombre de cinq. L'ontologie génétique associée a mis en évidence que le terme « Rho-GTPase activate PKNs » apparait majoritairement associé à la zone A. Cette famille de protéines a été peu étudiée au niveau testiculaire mais des données récentes ont montré que la protéine PKN1 pourrait être essentielle à la croissance et la migration des cellules cancéreuses ovariennes (Zeng et al., 2020). Par ailleurs, le métabolisme du glucose apparait majoritairement associé à la zone D ce qui est en accord avec le fait qu'il est l'une des principales sources de production d'ATP au niveau des spermatozoïdes (Amaral, 2022). Les protéines associées aux processus de traduction et de traitement des ARNm diminuent en abondance de la zone A vers la zone D, ce qui est en accord avec les régulations transcriptionnelles et post-transcriptionnelles au cours de la spermatogenèse et le fait que les cellules germinales mâles expriment le plus grand nombre d'épissages alternatifs d'ARN messagers (Li et al., 2020).

Par la suite, quatre voies de signalisation ont été analysées avec : le protéasome et la protéolyse dépendante de l'ubiquitine, compte tenu de leurs mises en évidence par l'analyse d'ontologie génétique, le splicéosome ; compte tenu de son importance particulière dans l'épissage des ARNm au cours de la spermatogenèse ; et la stéroïdogenèse, compte tenu de la disponibilité des données sur les stéroïdes testiculaires chez différents Élasmobranches.

Les protéines du protéasome sont plus abondantes en zone A et D et la protéine α4s (PSMA8), caractéristique du spermatoprotéasome, est plus abondante dans la zone des cystes à spermatogonies. Ce résultat indique une expression plus précoce de PSMA8 par rapport à des études chez la souris où elle est exprimée dans les spermatocytes primaires et interagit avec les composants du complexe synaptonémal (Gómez-H et al., 2019; Živković et al., 2022). Parmi les protéines associées à la protéolyse ubiquitine-dépendante, UBE2G2 et UBE4B sont les deux seules enzymes dont l'abondance est plus élevée dans la zone B. Leurs rôles au cours de la spermatogenèse ont été peu étudiés, à l'exception de publications montrant des différences dans les niveaux d'UBE2G2 chez les hommes subfertiles (Laqqan and Hammadeh, 2018) et la surexpression de l'UBE4B dans les spermatides allongées chez la souris (M. Li et al., 2020). Concernant les composants du splicéosome, ils sont majoritairement associés à la zone A, d'où un rôle possible du splicéosome plus important au cours des premiers stades de la spermatogenèse. Une autre possibilité serait une synthèse de ceux-ci au cours des premiers stades mais avec une activation du splicéosome aux stades suivants, notamment au niveau des spermatocytes primaires qui présentent l'activité transcriptionnelle la plus importante avec la synthèse des variants testiculaires. Pour terminer, la voie de la stéroïdogenèse présente une forte abondance de la 17β-HSD en zone D, ce qui est en accord avec les concentrations en androgènes plus élevées dans cette zone (Sourdaine and Garnier, 1993).

Pour conclure, cette analyse devrait permettre d'enrichir les données disponibles chez les Élasmobranches et de mieux comprendre la régulation de la spermatogenèse au cours de l'évolution. Nos résultats sont cohérents avec le fait que les répertoires de gènes régulant la spermatogenèse seraient présents au moins à la racine des Gnathostomes et qu'ils ont évolué lentement. Cependant, notre étude a montré que le nombre le plus élevé de protéines spécifiques à une zone a été retrouvé pour les zones A et D, ce qui correspond aux étapes contrôlant la phase d'amplification cellulaire qui déterminera le nombre final de gamètes produits (zone A) et l'étape finale de différenciation et de libération des gamètes (zone D). Ces

deux étapes correspondent à des traits variables d'une espèce à l'autre, tels que le taux de production de spermatozoïdes et la morphologie des spermatozoïdes. Pour terminer, notre étude a mis en évidence que le plus grand nombre de protéines non caractérisées était associé à la zone D, dont une protéine avec une signature lipocaline et une protéine avec un site *ATP-dependent DNA ligase AMP-binding site*. Le fait de retrouver des protéines non caractérisées associées à la spermiogenèse peut être mis en relation avec une publication récente qui a montré que l'évolution du testicule a été guidée, au moins en partie, par l'émergence de nouveaux gènes associés à la spermiogenèse (Murat et al., 2023).

**Comparative proteome analysis of four stages of spermatogenesis in the small-spotted catshark (*Scyliorhinus canicula*), using high-resolution nanoLC-ESI-MS/MS**

Fabian Jeanne[1], Benoît Bernay[2], and Pascal Sourdaine[1,*]

[1] Université de Caen Normandie, MNHN, SU, UA, CNRS, IRD, Laboratoire de Biologie des Organismes et Ecosystèmes Aquatiques (BOREA), UMR 8067, 14032 Caen cedex 5, France.

[2] Université de Caen Normandie - Plateforme PROTEOGEN, US EMerode, 14032 Caen cedex 5, France.

*Corresponding Author: orcid.org/0000-0001-9811-2876; Email: pascal.sourdaine@unicaen.fr

## ABSTRACT

Spermatogenesis is a highly specialized process of cell proliferation and differentiation leading to the production of spermatozoa from spermatogonial stem cells. Due to its testicular anatomy, *Scyliorhinus canicula* is an interesting model to explore stage-based changes in proteins during spermatogenesis. The proteomes of four testicular zones corresponding to the germinative niche and to spermatocysts (cysts) with spermatogonia (zone A), cysts with spermatocytes (zone B), cysts with young spermatids (zone C) and cysts with late spermatids (zone D) have been analyzed by nanoLC-ESI-MS/MS. Gene ontology and KEGG annotations were also performed. A total of 3346 multiple protein groups were identified. Zone-specific protein analyses highlighted RNA-processing, chromosome-related processes, cilium organisation and cilium activity in zones A, B, C and D, respectively. Analyses of proteins with zone-dependent abundance revealed processes related to cellular stress, ubiquitin-dependent degradation by the proteasome, post-transcriptional regulation and regulation of cellular homeostasis. Our results also suggest that the roles of some proteins, such as ceruloplasmin, optineurin, the pregnancy zone protein, PA28β or the Culling-RING ligase 5 complex as well as some uncharacterized proteins, during spermatogenesis could be further explored. Finally, the study of this shark species allows to integrate these data in an evolutionary context of the regulation of spermatogenesis. Mass spectrometry data are freely

accessible via iProX-integrated Proteome resources (https://www.iprox.cn/) for reuse purposes.

Key words: Spermatogenesis, Chondrichthyes, Elasmobranchs, testicular proteome, shark

## INTRODUCTION

The small-spotted catshark belongs to the cartilaginous fishes (Chondrichthyes) comprising the Holocephalans (Chimaeras) and the Elasmobranchs (Sharks, rays and skates) which occupy a unique phylogenetic position as a result of their divergence from Osteichthyes (Bony Vertebrates) estimated have occurred around 450-million years ago (Mya)(Irisarri et al., 2017). Due to their key position near the base of phylogeny, the Chondrichthyans are of interest for the evolutionary study of various biological processes or systems such as the adaptive immune system(Almeida et al., 2021; Matz et al., 2021), various developmental processes(Criswell et al., 2021; Schmidt et al., 2022) or the endoskeleton evolution(Atake and Eames, 2021). Among the recent advances in the whole genome sequencing of several species, those concerning the elephant shark *Callorhinchus milii* are the first to have opened new vistas regarding the molecular underpinnings of various cellular processes in Chondrichthyans(Hara et al., 2018; King et al., 2011; Marra et al., 2019; Read et al., 2017; Venkatesh et al., 2007). The genomes of sharks are characterized by reduced molecular evolution rates and their relatively large size, from 974 Mb length for *C. milii* to 4600 Mb length for *Carcharodon carcharias* and feature large introns and a large content of transposable elements rather than massive gene duplication(Hara et al., 2018; Marra et al., 2019; Tan et al., 2021; Weber et al., 2020). Analysis of origins and losses of vertebrate gene families showed that a significant number of gene families were present at the root of the Gnathostomata branch, establishing the gene families present in bony vertebrates and cartilaginous fishes(Tan et al., 2021; Weber et al., 2020). So, the jawed vertebrate ancestor was found to possess the gene repertories regulating homeostasis and reproduction(Hara et al., 2018) and Chondrichthyes are the most basal extant jawed vertebrates with glycoprotein hormones differentiated into gonadotropins (FSH and LH), thyrotropins (TSH1 and TSH2) and thyrostimulin (GPHA2B5)(Buechi and Bridgham, 2017). However, several gains and losses of genes have been described between

Elasmobranchs and Osteichthyes(Joyce et al., 2023; Marra et al., 2019; Neves et al., 2022; Tan et al., 2021; Y. Zhang et al., 2020) but also between Elasmobranchs and the Holocephalans in the Chondrichthyes, two groups which diverged early after the estimated divergence time of Chondrichthyes and Osteichthyes(Kuraku, 2021; Neves et al., 2022; Tan et al., 2021). In addition to the importance of identifying chondrichthyan genomes for the understanding of genome evolution, these data are also fundamental for large-scale -omic analyses and several transcriptomic and proteomic data elements are now available for Elasmobranchs(Bakke et al., 2022; Chana-Munoz et al., 2017; Krishnaswamy Gopalan et al., 2014; Machado et al., 2018; Mulley et al., 2014; Nazarian et al., 2007; Onimaru et al., 2018; Stavrianakou et al., 2017), providing important molecular tools for physiological studies in Chondrichthyans. In the present study, we explored the proteome of the testis using a high-resolution nanoLC-ESI-MS/MS approach to study the evolution of the regulation of spermatogenesis and to enrich the proteomic data for Elasmobranchs.

Spermatogenesis is a highly conserved and orderly process under endocrine and paracrine regulation that allows production of spermatozoa from undifferentiated spermatogonial stem cells. Classically, spermatogenesis is divided into three main stages: mitotic proliferation and spermatogonia differentiation, meiosis, leading to the formation of young haploid spermatids from primary spermatocytes and spermiogenesis corresponding to the cellular transformation of round spermatids into mature elongated spermatids. The testis expresses the largest number of tissue-enriched genes and efforts are currently directed towards characterizing their functions(Ahn et al., 2017; Djureinovic et al., 2014; Vandenbrouck et al., 2020). For this purpose, the analysis of cell-specific and stage-dependent expressions is fundamental to characterize specific events during spermatogenesis. This is why the testis of the small-spotted catshark is of specific interest. The testes of this and other chondrichthyans consist of spermatocysts (cysts), each housing spermatoblasts in which one Sertoli cell is associated with synchronously-developing germ cells, from 1 spermatogonium initially to 64 mature spermatids(Gomes do Rêgo et al., 2016; Grier, 1992; Grier et al., 2016; Pratt, 1988; Stanley, 1966). In the small-spotted catshark testis, during spermatogenic development which proceeds across the diameter, cysts originate from the germinative zone on the dorsolateral margins of the testis and, as new cysts are continuously formed, older cysts are displaced in a sequential order leading to a zonal arrangement according to the spermatogenetic wave.

Thus, a cross section of the testis shows a succession of dorsoventrally oriented zones corresponding to the germinal area, the zone of spermatogonial cysts, the zone of spermatocyte cysts, the zone of early spermatid cysts and the zone of late spermatid cysts, which are easily distinguishable and accessible(Bosseboeuf et al., 2014; Gautier et al., 2014; Loir and Sourdaine, 1994; Loppion et al., 2008). In addition, the absence of differentiated Leydig cells reinforces the essential role of the Sertoli cells, whose structure evolves specifically in relation to the germ cell stage. These cells are the main steroidogenic cells of the testis for *S. canicula* as well as for *Squalus acanthias*(Cuevas et al., 1993; Cuevas and Callard, 1992a; Loir et al., 1995; Pudney and Callard, 1984b, 1984a; Sourdaine and Garnier, 1993). Furthermore, testicular homeostasis appears to be controlled by germ cell and Sertoli cell apoptosis, as has been shown in *S. acanthias* and other Elasmobranch species(McClusky, 2022, 2013, 2012; Prisco et al., 2003; Ricchiari et al., 2006). The close relationship between the testis and the epigonal tissue, a lymphomyeloid tissue unique in Elasmobranchs, suggests a crosstalk between the two organs to regulate the spermatogenic cycle(Piferrer and Callard, 1995). And lastly, the size of testes allows for easy access to cells from a non-endangered species belonging to the Carcharhiniforms, the largest family of sharks.

The aim of this current study is to characterize the proteome of the four main testicular zones of *S. canicula* to establish stage-related protein changes in the cellular microenvironment during spermatogenesis. We reported the Gene Ontology annotation and enriched pathways information of proteins exclusive to each zone and proteins showing significant stage-related changes in abundance. The results of this study highlight some of the evolutionarily conserved proteomic aspects of spermatogenesis, with a particular focus on the proteasome and the ubiquitin-mediated proteolysis, the spliceosome and steroidogenesis.

## EXPERIMENTAL PROCEDURES

### Animals and samples collection

Small-spotted Catshark *Scyliorhinus canicula* has been assessed for the IUCN (International Union for Conservation of Nature) red list of threatened species in 2020 and listed as a least concern species. Mature male catsharks were fished off Cherbourg (Manche, France) by the *Lycée Professionnel Maritime et Aquacole Daniel Rigolet*, then starved in natural sea water outflow tanks at the marine station of the University of Caen Normandy (*Centre de Recherche*

*en Environnement Côtier* (CREC), Luc sur Mer, France). The CREC experimental facilities were approved by the council department of population care under the A14384001 number (*Préfecture du Calvados*, France). No project agreement by the Regional Ethical Committee (Cenomexa, committee agreement number 54) was required since animals were used only for tissue sampling. Catsharks were allowed to acclimate at least 2 weeks before collection of the samples. Animals were killed by percussive blow to the head followed by sectioning and pithing of the spinal cord and brain and exsanguination according to the European directive 2010/63/UE for care and use of animals. Testes were sampled and transferred into Gautron's buffer (pH 7.8, 890 mosmol kg-1)(Gautron, 1978) complemented by 58 mM trimethylamine-N-oxide (TMAO, Sigma, France). As previously described(Loir and Sourdaine, 1994), fresh testicular cross sections (2 mm) were microdissected into four zones corresponding to the germinative area and spermatocysts (cysts) with spermatogonia (zone A), cysts with spermatocytes (zone B), cysts with early spermatids (zone C) and cysts with late spermatids (zone D) (Figure S1). Samples were stored in RNAzol RT (Sigma) at -80°C until protein extraction.

### Protein extraction

Protein extraction was performed separately on the 4 testicular zones from 3 catsharks (n=12). Frozen tissues were crushed in liquid nitrogen, extracted with 2.5 volumes of ice-cold lysis buffer (Urea 6M, Thiourea 2M, Tris-Base 40mM, CHAPS 2%, EDTA 1 mM, DTT 0.5 mM, AEBSF 1 mM and E64 10 µM protease inhibitors), then sonicated and stayed 1 hr on ice before being centrifuged at 15000 g for 30 min at 4 °C. Supernatants were then ultracentrifuged at 105000 g for 1 hr at 4 °C. Protein concentration of resulting supernatants was determined using the bicinchoninic acid protein assay (Sigma-Aldrich, Merck, France).

### NanoLC-ESI-MS/MS analysis

From each sample, 5 µg of proteins were prepared using a modified GASP protocol (Gel-aided sample preparation with a gel plug cut into two pieces only)(Fischer and Kessler, 2015) before an overnight hydrolysis at 37°C with a mix solution of trypsin/lysine-C (400 ng per sample; V5073 Promega). Resulting peptides samples were first desalted and concentrated onto a C18 microcolumn (Omix C18 10µl, Agilent) then fractionated onto a NanoElute ultrahigh-pressure nanoflow chromatography system (nanoLC, Bruker Daltonics) with a C18 pepmap 100 (5mm

x 300µm i.d.) precolumn (Thermo Scientific) and separated at 50°C onto a reversed phase Reprosil column (25cm x 75µm i.d.) packed with 1.6µm C18 coated porous silica beads (Ionopticks). The mobile phases consisted of 0.1% formic acid in water (solvent A) and 0.1% formic acid in acetonitrile (solvent B). The nanoflow rate was set at 400 nL/min with a gradient profile from 2% to 15% solvent B within 60 min, then an increase to 25% solvent B within 30 min and to 37% solvent B within 10 min, followed by a 95% solvent B washing step before reequilibration.

ESI-MS analyses were realized on a TIMS-TOF Pro mass spectrometer (Bruker Daltonics) with a nanoelectrospray ion source (Captive Spray, Bruker Daltonics). The system was calibrated weekly and the mass accuracy was better than 1 ppm. A 1600 spray voltage with a capillary temperature of 180 °C was carried out for ionizing and MS spectra acquired in the 100 to 1700 m/z mass range in PASEF mode.

### Database searching

The nanoLC-ESI-MS/MS mass spectra from each 12 samples were analysed using the Preview program (ProteinMetrics)(Kil et al., 2011) to estimate digestion quality and posttranslational modifications. The database searching was carried out using PeaksXPro software (Bioinformatics Solutions Inc.; Waterloo, Canada) against the NCBI predicted proteome from *S. canicula* genome. The search parameters used were as follows: trypsin parameter was selected with a maximum of 2 miss cleavage; the variable modifications allowed were methionine-oxidation, lysine-acetylation and asparagine-/glutamine-deamidation. Propionamide modification on the cysteine residues was set as fix. Mass accuracy was set to 20 ppm and 0.05 Da for MS and MS/MS modes, respectively. Data were filtered according to a false discovery rate (FDR) of 1% at the peptide level. Label-free analysis was done using ANOVA in order to filter results to proteins with a peak significance greater than 10 and a minimum ratio of 1.5. From database search results, 6744 proteins/accession numbers were retrieved and corresponded to 3346 protein groups. The overall workflow of the proteome analysis is presented as supplementary information (Figure S2).

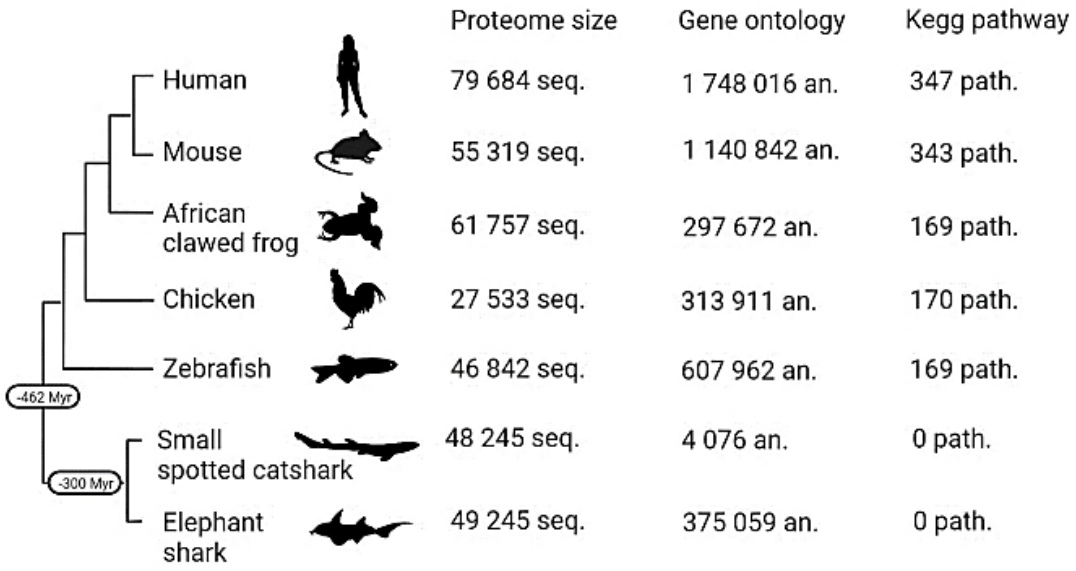


Figure 1. Review of databases considering number of identified proteins, of gene ontologies and Kegg pathways for species regarded as representative of a clade with elephant shark for Chondrichthyes, zebrafish for teleost fishes, chicken for Aves, African clawed frog for Amphibians, mouse and human for Mammals (In date of the 06/2020). an., annotations; Myr, Million years ago; path., pathways; seq. sequences. Animal illustrations are used with permission from http://phylopic.org.Figure.

### Sample quality control

The quantification values of the 1284 catshark proteins common to the four zones were converted into log2ratio (abundance values of proteins in a sample divided by the mean abundance value in all samples) and used as matrix for a principal component analysis (PCA), using the FactomineR package(Lê et al., 2008) of Rstudio software (https://www.rstudio.com/). Then, PCA results were treated by k-mean clustering using the Factoextra package(Kassambara and Mundt, 2020), the best sample segregation parameter was searched and found for 4 clusters with the highest BSS/TSS ratio of 0.75, and the replicates were grouped into their corresponding clusters (Figure S3).

### Bioinformatics and functional annotation

Due to the limited number of correctly-annotated proteins (48 245 sequences, as of 06/2020), the limited number of gene ontologies (4076 annotations, as of 06/2020) and the absence of kegg pathways in *S. canicula*, identified proteins were blasted against *Homo sapiens* proteome (Proteome ID: UP000005640), *Mus musculus* proteome (Proteome ID: UP000000589), *Xenopus laevis* proteome (Proteome ID: UP000186698), *Gallus gallus* proteome (Proteome ID: UP000000539), *Danio rerio* proteome (Proteome ID: UP000000437) and *Callorhincus milii* proteome (Proteome ID: UP000314986). Proteomes were uploaded from Uniprot (https://www.uniprot.org/) and species were selected as representative of a clade, notably on the basis of the availability of their databases.

BLASTp were carried out using the Galaxy web resource (https://usegalaxy.org/) with hits filtering proteins showing more than 40% of identity and coverage, and e-value below $1e^{-05}$. For each catshark protein and against each proteome, hits with lowest e-value and higher percentage of identity were retained. Then, distribution of identity percentages, e-values and coverage percentages of retained hits were analysed. Mice was chosen as a reference because of the richness of available databases (55 319 sequences for proteome, 1 140 842 GO annotations with 61 459 annotations validated by mutant phenotypes and 343 Kegg pathways; as of 06/2020) (Figure 1) and the obtained distribution of e-values, identity percentages and coverage considered as control indicators for blastp hit results. In absence of mice putative homologs, catshark proteins were analysed using blastp results against all proteins referenced on NCBI (https://www.ncbi.nlm.nih.gov/genome/).

Protein mapping according to testicular zones has been done by using the ggvenn package on the Rstudio software (https://www.rstudio.com/)(Yan, 2021). Protein mapping resulted in several protein groups from those retrieved in only one testicular zone (i.e., zone A, zone B, zone C, zone D) to those retrieved in all zones (i.e., common to zones A, B, C, D) and those retrieved in intermediate groups (i.e., common between zones A and B, common between zones A, B, C, …).

Changes in abundance of proteins during stages of spermatogenesis were analysed for proteins retrieved in all zones with a quantification value different than 0, where 0 means no significant difference between the protein quantification and background noise. Then, a principal component analysis (PCA) on abundance values (means of triplicates) was done before a hierarchical ascending classification with Euclidean distance and ward method using the function HCPC (Hierarchical Clustering on Principal Components) of the FactoMineR package(Lê et al., 2008). Although the dendrogram obtained showed that the highest inertia loss was between clusters 3 and 4 (inertia-loss$_{3\text{-}4}$ = 0.2), a division into five clusters was retained in order to differentiate profiles more in line with the four testicular zones (Figure S4). The inertia loss due to the division in five clusters instead of three has been of 36%. Abundance distributions were represented with the ComplexHeatmap package(Gu et al., 2016).

Gene Ontology (GO), reactome pathway and wiki pathway-based functional annotation of protein groups were carried out for mice putative homologs by using Cluego, a Cytoscape plug-in (https://apps.cytoscape.org/apps/cluego)(Bindea et al., 2009). The following parameters were applied: GO tree between 3-8; cluster with a minimum of 3 accessions associated by term; genes association higher than 4%; Term P-value corrected with Bonferroni step down < 0.05; Go Term fusion parameter selected. Corrected P-values were converted into -log2(P-value) and the 10 most significant terms have been kept for each queried database and each sample.

For KEGG annotation, K-numbers were found based on putative homologs mice uniprot accession using the Retrieve/IDmapping tool of uniprot (https://www.uniprot.org/id-mapping/) for pathway identification with the Kegg mapper – Search tool (https://www.genome.jp/kegg/mapper.html). The dataset of k-numbers retrieved in all zones was used for the identification of pathways based on the high number of retrieved proteins,

proteins with abundance values and their link with the spermatogenesis. Ubiquitin-mediated proteolysis (mmu04120), Proteasome (mmu03050), Spliceosome (mmu03040) and Ovarian steroidogenesis (mmu04913) were selected, abundance values were added before the inclusion of involved proteins not retrieved in all zones. To be noticed: p68 was identified by manual blastp as Q61656, an isoform of Q8BTS0 present in the spliceosome pathway; PA28β (psme2) was identified as G3X9V0, an isoform of P97372 present in the proteasome pathway; Cul4b and Ube4a were present in the ubiquitin mediated proteolysis pathway and identified as E9PXY1, an isoform of A2A432, and G3X9Y5, an isoform of E9Q735, respectively.

### Data Availability Statement

Mass spectrometry data have been deposited into the iProX - integrated Proteome resources (https://www.iprox.cn/) with the data set identifier IPX0006196000.

## RESULTS AND DISCUSSION

### Proteomic profile of small-spotted catshark during spermatogenesis

The nanoLC-ESI-MS/MS analysis of the different testicular zones using the predicted proteome from the *S. canicula* genome allowed to identify 6744 proteins/accession numbers included in 3346 multiple protein groups typically represented by isoforms (Table S1). Of these proteins, 5552 were found expressed in zone A (representing 82.35% of total proteins) with 1011 (15%) exclusively identified in A; 3745 proteins were expressed in zone B (55.56%) with 25 (0.4%) exclusively identified in B; 3643 proteins were expressed in zone C (54.02%) with 33 (0.5%) exclusively identified in C; 5192 proteins were expressed in zone D (77.02%) with 795 (11.8%) exclusively identified in D (Figure S5). The number of proteins common to the 4 zones was 2876, representing 42.6% of total proteins, of which 1284 (19.0%) have shown abundance values. These last set of proteins was used for sample quality control, and further analysed during spermatogenesis (see below paragraph PCA, Heatmap). Since spermatogenesis proceeds continuously from zone A to zone D, and given the above results showing a small number of proteins expressed exclusively in zones B and C, the proteins were grouped for functional analysis as follows: (i) specific proteins identified in zone A (1011 proteins) corresponding to the start of the spermatogenic wave; (ii) proteins specific to zone B (25 proteins) and common ones between zones B and A (252 proteins), and between zones B and

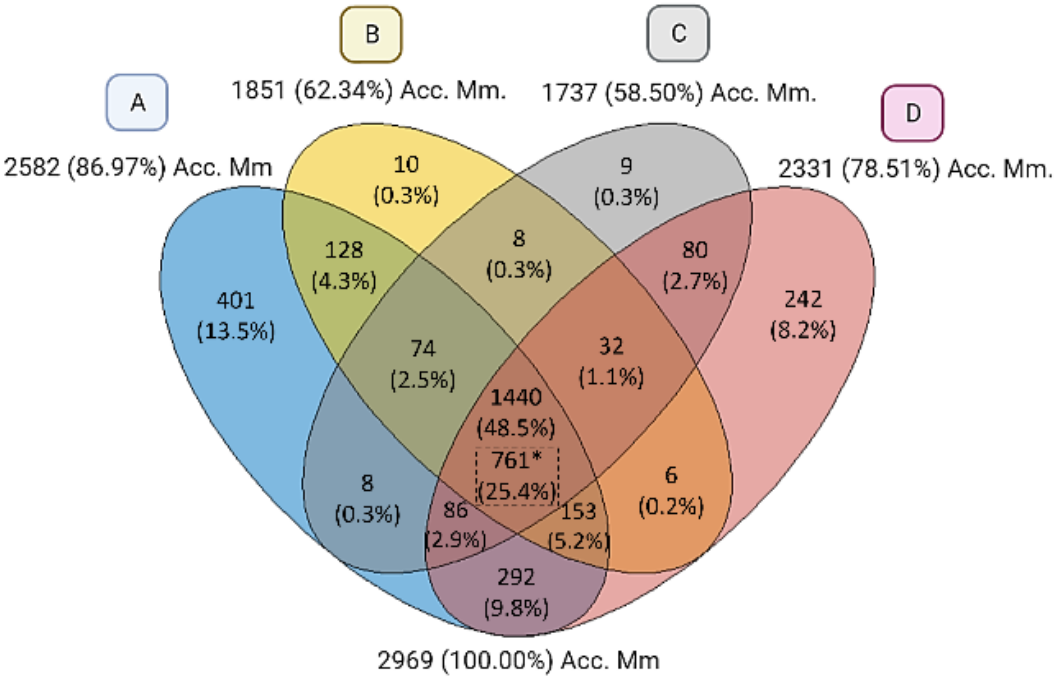


Figure 2. Mapping, using venn diagram, of the 2969 mouse putative homologs proteins obtained by blastp according to the four testicular zones. A: zone A; B: zone B; C: zone C; D: zone D; Acc. Mm.: accessions of *Mus musculus*; *: putative homologs retrieved in all four zones with abundance values.

C (22 proteins), illustrating the meiotic progression of spermatogenesis, which we have named "continuum B"; (iii) proteins specific to zone C (33 proteins) and common proteins between zones B and C (22 proteins) and between zones C and D (218 proteins) illustrating the early spermiogenesis progression and named "continuum C"; (iiii) specific proteins identified in zone D (795 proteins), illustrating the end of the spermatogenic wave.

The BLASTp results for the 6744 proteins against the proteins of the six species have shown that between 6150 (*G. gallus*) and 6285 (*H. Sapiens*) proteins were retrieved with an e-value equal to 0 for 61% (*C. milii*) to 55% (*H. sapiens*, *M. musculus*, *X. leavis*, *G. gallus*, *D. rerio*) of proteins, a percentage of identity between 80% and 100% for 55% (*C. milii*) to 32% (*D. rerio*, *M. musculus*) of proteins, a percentage of identity between 60% and 80% for 45% (*G. gallus*, *X. leavis*, *M. musculus*) to 34% (*C. milii*) of proteins and a percentage of coverage between 80 and 100% for 87% (*M. musculus*) to 73% (*C. milii*) of proteins (Figure S6). Because of the lack of marked differences between species observed here, and thanks to the large number of functional annotations available in mice, this species was further used for functional annotation of catshark proteins. Interestingly, the number of proteins completely conserved between species appeared similar (i.e., 34 with *C. milii*; 39 with *M musculus*; 40 with *H. sapiens*) and corresponds to 22 protein groups for *C.milii* and around 10 for *H. sapiens*, *M. musculus*, *X. leavis*, *G. gallus* and *D. rerio*. On the other hand, between 291 (4.3%) and 600 (8.8%) proteins were not identified when blasted against *C. milii* and *D. rerio* proteomes, respectively. These results are in agreement with genome analyses showing that around 50% of genes have ancient origins(Tan et al., 2021; Weber et al., 2020).

## Functional analysis of testicular stage-specific proteins during spermatogenesis

Blastp against mice proteome identified 2969 (89%) mice putative homologs with unique annotation to the 3346 multiple protein groups identified in testicular zones of *S. canicula*. Protein mapping according to the zones of spermatogenesis revealed 2582 mice homologs expressed in the zone A (86.97%), 1851 in the zone B (62.34%), 1737 in the zone C (58.50%) and 2331 proteins in the zone D (78.51%) (Figure 2). Among them, 1440 mice homologs (48.5%) were common to the 4 zones, 401 (13.5%) were exclusively identified in zone A, 146 (4.9%) were identified in continuum B, 97 (3.26%) were identified in continuum C and 242 (8.2%) were exclusively identified in zone D. The proteins of zone A, continuum B, continuum

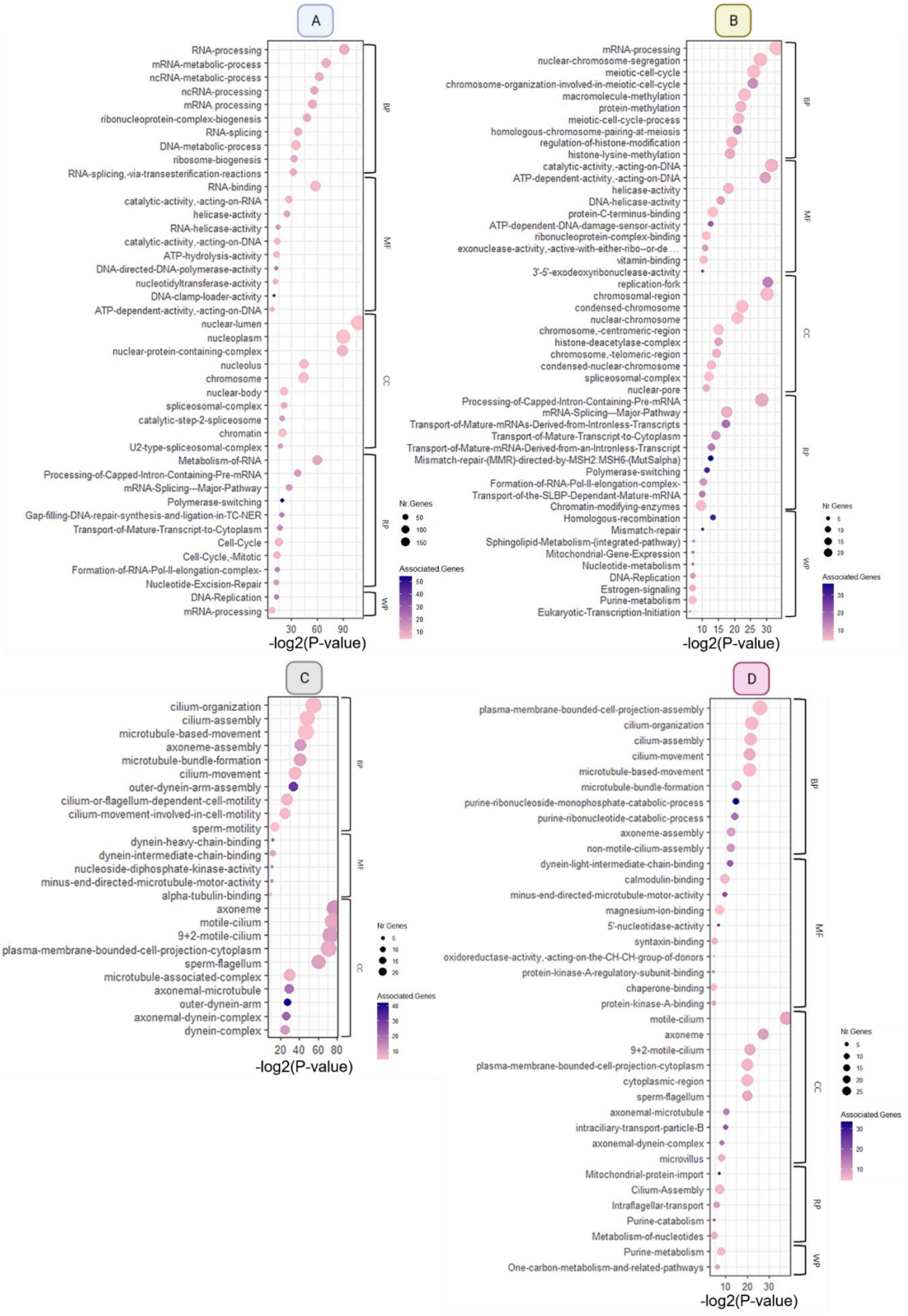


Figure 3. Best 10 hits of gene ontology for the 401 mice putative homologs of the zone A, 146 of the continuum B, 97 of the continuum C and 242 of the zone D. BP: biological process; MF: molecular function; CC: cellular function; RP: reactome pathway; WP: wikipathway; Nr. Genes: number of genes.

C and zone D contributed to 206, 184, 37 and 86 functional annotations, respectively. The number of associated terms was higher in the zone A, corresponding to stages of proliferation and differentiation of spermatogonia, and in the continuum B, corresponding to meiosis, than in continuum C and zone D, reflecting a lower diversity of biological functions during stages of spermiogenesis. Furthermore, no or few terms associated to reactome and wiki pathways were retrieved for these zones corresponding to spermiogenesis.

The ten most significant terms for each biological function revealed that unique proteins of zone A were related to RNA processing including, among others, mRNA and ncRNA metabolic processes and RNA splicing and were also related to DNA replication and mitotic cell cycle (Figure 3). Terms related to mRNA processing and DNA replication were kept in the meiotic zone (continuum B) but completed by chromosome-related process in accordance with meiosis (i.e., nuclear chromosome segregation and meiotic cell cycle in biological process; chromosomal region and condensed chromosome in cellular component; homologous recombination and mismatch repair in wiki pathway). Interestingly, biological process related to methylation and histone modifications were also retrieved, which could be associated to the establishment of a specific regulation of gene expression during spermatogenesis(Burlibaşa et al., 2019; M. Li et al., 2020; Naro et al., 2017; Paronetto and Sette, 2010). Sphingolipid metabolism was also noticed in wiki pathway and this could be related to male meiotic cytokinesis(Kunduri et al., 2022; Rabionet et al., 2015). Oestrogen signalling was also highlighted which is in agreement with one of the pioneering works of G.V. Callard on the paracrine function of oestrogens during spermatogenesis in a shark species(Callard et al., 1985). Proteins associated to spermiogenesis (continuum C and zone D) were unsurprisingly related to the spermatid flagellum development (i.e. for continuum C: cilium organisation in biological process; cilium in cellular component; dynein in molecular function) and completed by cilium activity (i.e. for zone D: motile cilium in cellular component; calmodulin and magnesium binding in molecular function; mitochondrial protein import in reactome pathway and purine metabolism in wiki pathway).

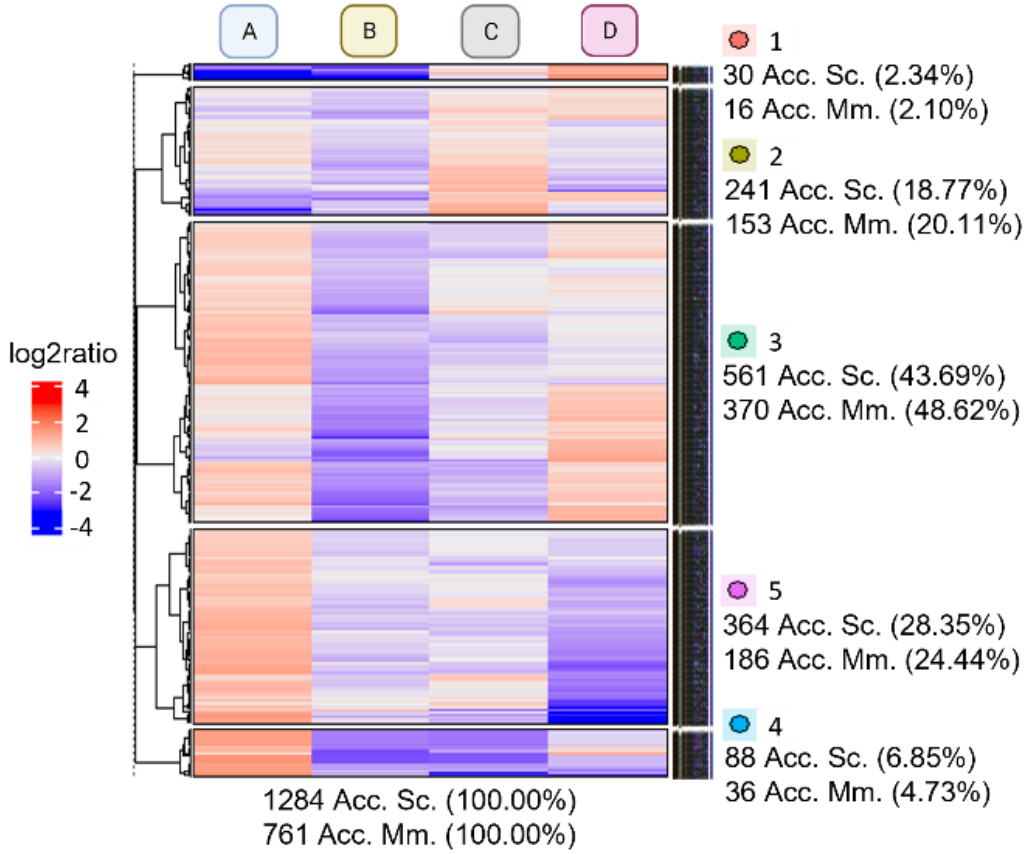


Figure 4. Expression patterns of clusters based on the 1284 catshark proteins expressed in all four zones according to testicular zones. Acc. Sc.: accessions of *Scyliorhinus canicula*; Acc. Mm: accessions of *Mus musculus*.

## Variations in protein levels during spermatogenesis

From the 2876 proteins identified in *S. canicula* and common to the 4 zones, 1284 proteins corresponding to 807 protein groups have shown a significant difference in abundance. The hierarchical clustering of the 1248 proteins allowed us to define five clusters corresponding roughly to proteins at the highest levels in zone D (Cluster 1) and the highest levels in zone C (Cluster 2), the lowest levels in zone B (Cluster 3), the highest levels in zone A (Cluster 4) and the lowest levels in zone D (Cluster 5) (Figure 4). The number of proteins per cluster was 30, 241, 561, 88 and 364 in cluster 1, 2, 3, 4 and 5, respectively. The number of identified mice homologs, corresponding to 761 protein groups, was 16, 153, 370, 36 and 186 in clusters 1, 2, 3, 4 and 5, respectively.

The ten most significant terms (Figure 5) according to biological functions (biological process, cellular component, molecular function, reactome pathway, wiki pathway) revealed that those found in cluster 1 were related to: glucose metabolism; binding of sperm to zona pellucida, also found in cluster 2; HSP90-mediated steroid hormone receptor activation; HSF1-mediated controls. These results are in agreement with a higher expression profile in the zone of cysts with late spermatids as glycolysis is one of the main ATP-producing pathways, with oxidative phosphorylation, in spermatozoa(Amaral, 2022) and the roles of heat shock transcription factors (HSF1 and HSF2) during spermatogenesis(Dietrich et al., 2019; Widlak and Vydra, 2017). HSP90-mediated activation of glucocorticoid and oestrogen receptors involves a network of co-chaperone proteins(Backe et al., 2022), which does not yet appear to have been studied during spermatogenesis. It may also be noted that the term associated with the import of peroxisomal proteins can be related to the fact that a defect in peroxisomes induces spermatogenesis arrest at the spermatid stage in mice(Brauns et al., 2019).

Concerning cluster 2, several metabolic and biosynthesis processes are highlighted, associated with cytoplasmic translation, with several terms related to ribosomes and RNAs, protein folding, transmembrane transporters, cellular trafficking, biogenesis and maintenance of organelles and cilium assembly. All these terms appear to be in agreement with the deep cellular remodelling which occurs during spermiogenesis, although it should be kept in mind that the zone C analysed also included somatic cells associated with spermatids. Regarding the reactome pathway, the term “L13a-mediated translational silencing of ceruloplasmin expression”, found also in clusters 4 and 5, refers to ceruloplasmin which has been identified

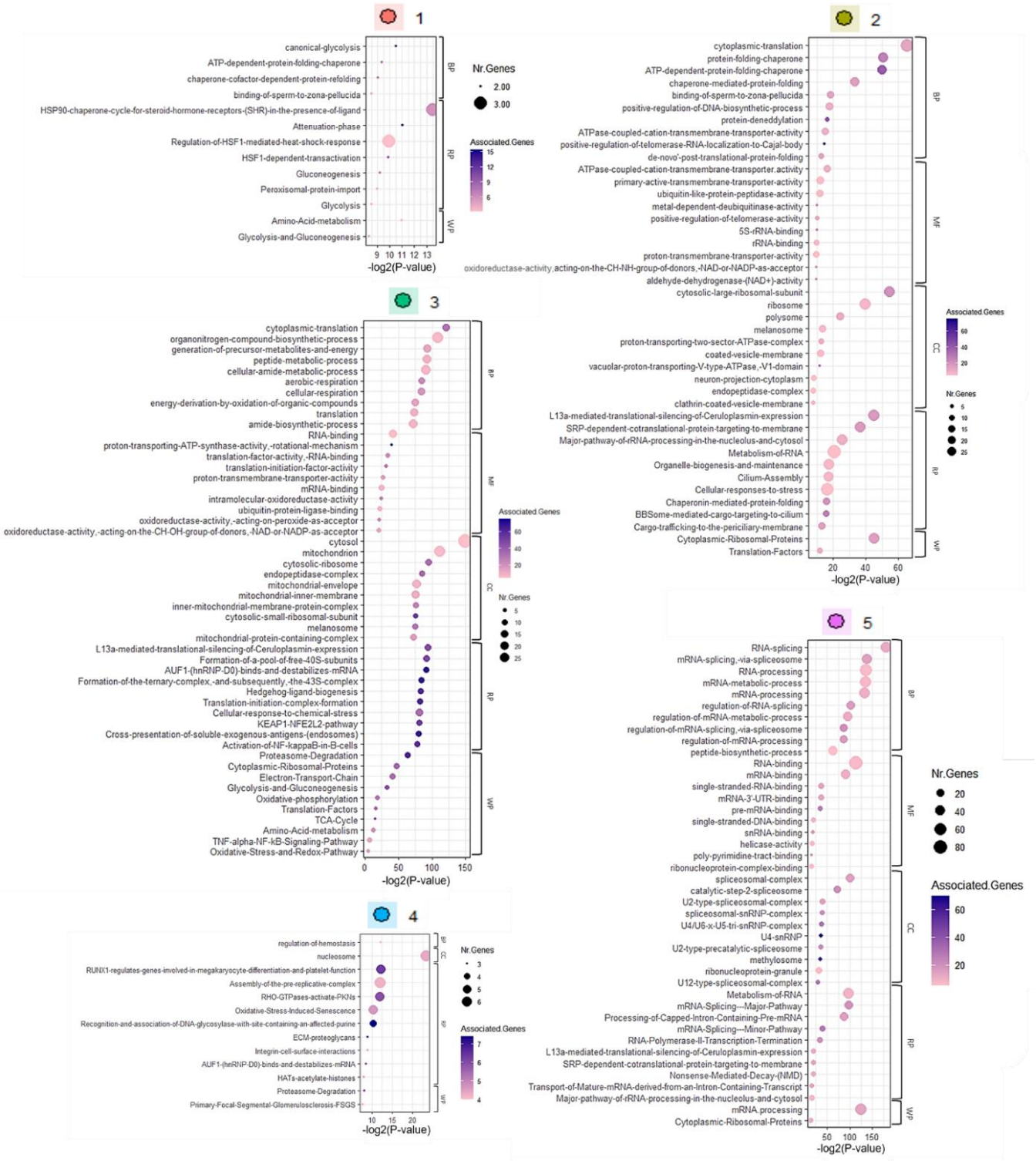


Figure 5. Best 10 hits of gene ontology for the five clusters, obtained by hierarchical ascending classification with Euclidean distance and ward method for the 1284 catshark proteins found in all four zones. BP: biological process; MF: molecular function; CC: cellular function; RP: reactome pathway; WP: wikipathway; Nr. Genes: number of genes.

as a Sertoli cell secretory protein for a long time(Onoda and Djakiew, 1990) but its functional importance during spermatogenesis has been the object of relatively few studies apart from its role as a potential copper transporter(Ogórek et al., 2019).

Concerning cluster 3, several terms appeared similar to those of cluster 2 such as cytoplasmic translation or transmembrane transporters but the proteins associated with these processes differed between the two clusters. Cluster 3 is also characterised by a stronger representation of terms associated with energy metabolism in relation to mitochondria and oxidative, peptide and amide-related metabolic processes. From the heat map (Figure 4), one can only observe that proteins associated with these processes are expressed in zones A and D, less so in zone C and clearly reduced in zone B corresponding to meiotic cysts. Indeed, it has long been established that meiotic and post-meiotic cells use lactate rather than glucose as an energy source and that spermatids differ from each other in their energy metabolism(Nakamura et al., 1984), so the overall expression profile of cluster 3 is rather consistent with changes in energy metabolism processes during spermatogenesis. Functional annotations related to the reactome pathway revealed several terms. One was related to mRNA stability through the AU-rich binding protein AUF1 (hnRNP-D0 or HNRPD), also found in cluster 5 and of which several variants have been identified in mice testis(Lu and Schneider, 2004). “Hedgehog ligand biogenesis” was also noticed where Hh could sustain spermatogonial cells proliferation(Sahin et al., 2014; Zhao et al., 2022). The NF-KappaB signaling and Keap1/Nfe2l2 pathways were also highlighted, which could have a protective effect against oxidative stress in the testis(Feng et al., 2020).

Cluster 4, which corresponds to a set of proteins with a higher expression level in the testicular zone A, appeared characterized by terms associated to the “regulation of homeostasis” (Biological process), the “nucleosome” (Cellular function) or to the “Rho-GTPase activate PKNs” and “the assembly of the pre-replicative complex” (Reactome pathway) which does not seem aberrant given that this zone includes the germinative zone comprising spermatogonial and somatic stem cells, and also corresponds to the establishment of cysts which involve both germ cells and somatic cells proliferations as well as cell-cell and cell-ECM interactions(Bosseboeuf et al., 2014; Loppion et al., 2008). Interestingly, the Protein Kinase N family proteins, comprising three isoforms, have been little studied in the testis whereas recent data have shown that PKN1 may be essential for anchorage-independent growth and

migration of ovarian cancer cells(Zeng et al., 2020). Gene regulation by RUNX1 was also highlighted in the reactome pathway category and no data seems to be available concerning its function during spermatogenesis excepted as a transcriptional cofactor, with CEBPβ, of the androgen receptor in human epididymis epithelial cells(Browne et al., 2019). The term "primary focal segmental glomerulosclerosis (FSGS)" evidenced in the wiki pathway is questionable and remains to be explored. However, a study of glomerular transcriptomes in patients has revealed that up-regulated genes in FSGS were involved in, among other things, spermatogenesis and gamete generation, and related for example to cell cycle and proliferation, TGF-β superfamily signaling and RNA processing(Tong et al., 2015).

Cluster 5 appeared to be characterized by translation and mRNA processing, including mRNA splicing, in all of the five biological categories, which is in accordance with the fact that factors controlling spermatogenesis are controlled at transcriptional and posttranscriptional levels, resulting in male germ cells expressing the widest array of transcript variants(Li et al., 2020; Naro et al., 2017; Paronetto and Sette, 2010; Soumillon et al., 2013). According to the heatmap profile of cluster 5, actors in mRNA processing exhibit a higher expression level in the zone of cysts with spermatogonia, then levels decreased during spermatogenesis to be at the lowest in the zone of late spermatids.

Overall, it can be noticed that terms related to the proteasome regulation appeared in three of the five clusters as: "protein-deneddylation" (Biological process, cluster 2) that regulate Cul1 and Cul3 protein accumulation(Wu et al., 2005); "ubiquitin-like protein peptidase activity" and "metal-dependent deubiquitinase activity" (Molecular function, cluster 2); "ubiquitin protein ligase binding" (Molecular function, cluster 3) and "proteasome degradation" (wikipathway, cluster 3 and 4). This led us to explore the ubiquitin-proteasome pathway during spermatogenesis using the kegg mapper (see below).

### Catshark testicular proteins with no positive blast against mice proteome

From the 3346 proteins groups identified in the catshark testis, 377 had no positive blast against the mice proteome. Among these 377 protein groups, 140 protein groups showed variations according to the testicular zone where 20 were specific to the zone A, 1 to the zone B, 4 to the zone C, 76 to the zone D and 39 were found in all zones but with variations in their levels. By only taking into account this set of 140 protein groups, a blastp search against the

proteome of the other species was done. Results have shown that 22 proteins groups had homologs only with *C. milii*, 4 only with *D. rario*, 5 only with *X. laevis*, 2 only with *G. gallus*, 2 only with *H. sapiens*, 9 with all of the five species except *M. musculus* and 46 protein groups still had no positive blast (Table S1). The lack of positive blast was due to the fact that the proteins did not satisfy the filtering parameters used and was mainly due to less than 40% identity, reflecting less evolutionarily conserved sequences. Out of the 140 protein groups, 19 were annotated as "uncharacterized" at the date of writing of the manuscript.

From these 22 protein groups, it could be noticed the following proteins whose annotation may suggest a gonadal function. The "scaffold attachment factor B2" (SAFB2) belongs to the type B scaffold attachment factor proteins first identified as binder of the nuclear matrix and involved in a large variety of nucleic acid-related biological functions(Norman et al., 2016). In mice testis, SAFB2 is expressed in spermatogonial stem cells end Sertoli cell nuclei(Zheng et al., 2014) and SAFB-/- mice showed an increase number of Sertoli cells(Jiang et al., 2015). Expression of SAFB2 in the catshark testis may be consistent with a conserved role for SAFB2 in Sertoli cell and spermatogonial differentiation. The "prothymosin alpha-A" (PTMA) which is a highly acidic nuclear protein was found in the late stage of spermatogenesis that is in accordance with its nuclear localization in spermatids of another cartilaginous fish, *Torpedo marmorata*(Prisco et al., 2009) and in other species(Venditti and Minucci, 2017). Roles of other proteins such as "optineurin", a ubiquitin-binding adaptor protein; the "pregnancy zone protein", a chaperone protein maintaining protein homeostasis during pregnancy, the "Programmed cell death 6-interacting protein" or "Testis, prostate and placenta-expressed protein" or "Maestro heat-like repeat family member 1" during spermatogenesis remain to be clarified. While for others, a role during spermatogenesis has been explored such as for prosaposin (PSAP) involved in the development of the reproductive system(Guo et al., 2007), cofilin as an actin depolymerizing factor(Park et al., 2021), progranulin (PGRN) an acrosomal glycoprotein synthesized during spermatogenesis(Baba et al., 1993), centrin 3 a member of the centrosome protein family(Xiaodong et al., 2002) or "Spermatogenesis-associated protein 6" (SPATA6)(Lin et al., 2021).

Among the 19 uncharacterized proteins, 2 were specific to zone A, 1 to zone B, 13 to zone D and 3 found with level variations in the four zones. For the two proteins of zone A, searching

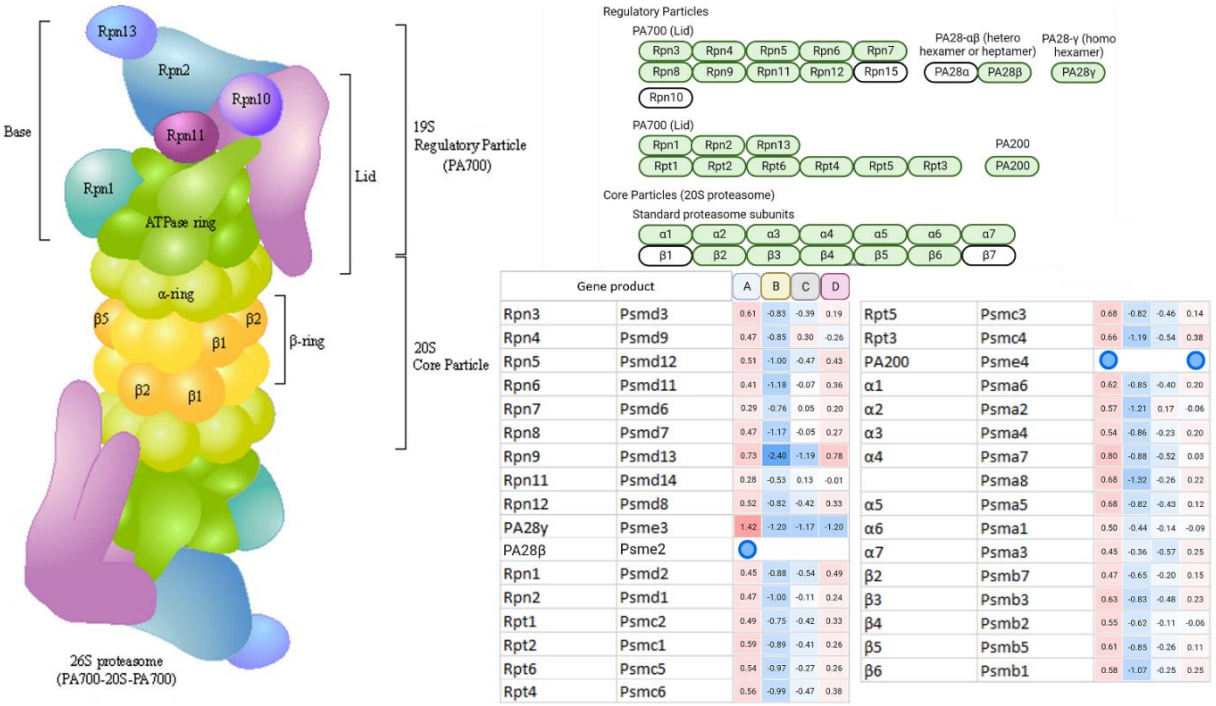


Figure 6. Pathway of the catshark proteasome based on mouse putative homologs identification and proteasome pathway (mmu03050). Green boxes corresponded to identified proteins and white boxes to no protein identification. Blue circles corresponded to identified proteins as specific in a zone. A: zone A; B: zone B; C: zone C; D: zone D.

for protein domains and homologs in UniProtKB revealed three zinc-finger domains (two C3H1 type and one CHY type) and homologs in bony fishes, Coelacanth and Amphibia but no other Tetrapoda for XP_038640217.1; height zinc-finger C2H2 type domains and homologs in *C. milii* and Dermophiidae amphibians for XP_038640519.1. No significant hit was found in the search for protein domains of the protein of the zone B (XP_038676215.1). For uncharacterized proteins in zone D, only two protein domains were found, such as a Lipocalin signature for XP_038638045.1 and an ATP-dependent DNA ligase AMP-binding site for XP_038633879.1. For proteins found in the four zones, a zinc finger C2H2 type domain signature was found for XP_038653542.1 with homologs in Chondrichthyes and the protein XP_038663142.1 appeared homologous to cadherin-like beta sandwich domain-containing protein which appeared well conserved from *Ciona intestinalis* to bony fishes and Amphibia but with no homologs in other Tetrapoda.

### Enriched pathways

From the 2969 mice putative homologs identified, 2584 k-numbers were retrieved before a kegg pathway mapping. Pathways were selected then completed by including stage-related protein abundances. Because of the results obtained on changes in the testicular proteome during spermatogenesis in the catshark highlighted processes associated to proteasome and ubiquitin-mediated proteolysis, a first investigation on theses pathways was performed. A second and third investigation were done by taking into account spliceosome and mRNA processing due to their particular importance during the spermatogenesis process. A fourth pathway was detailed concerning steroidogenesis, which was motived by the availability of previous studies on steroids analysed in the catshark testis, or in other Elasmobranchs(Becerril-García et al., 2020).

#### Proteasome and ubiquitin-mediated proteolysis

Within the ubiquitin-mediated proteolysis pathway we identified 31 factors, of which 27 were preferentially associated with zone A and 26 with zone D. A similar expression pattern was observed for the core and regulatory proteins of the proteasome with higher values in zones A and D for most of the 33 proteins found. The standard proteasome subtypes, forming the constitutive 20S core particle (c20S), were found (α1 to α6 and β2 to β6) with the exception of β1 and β7 (Figure 6). The α4s (PSMA8) characterising the spermatoproteasome (s20S

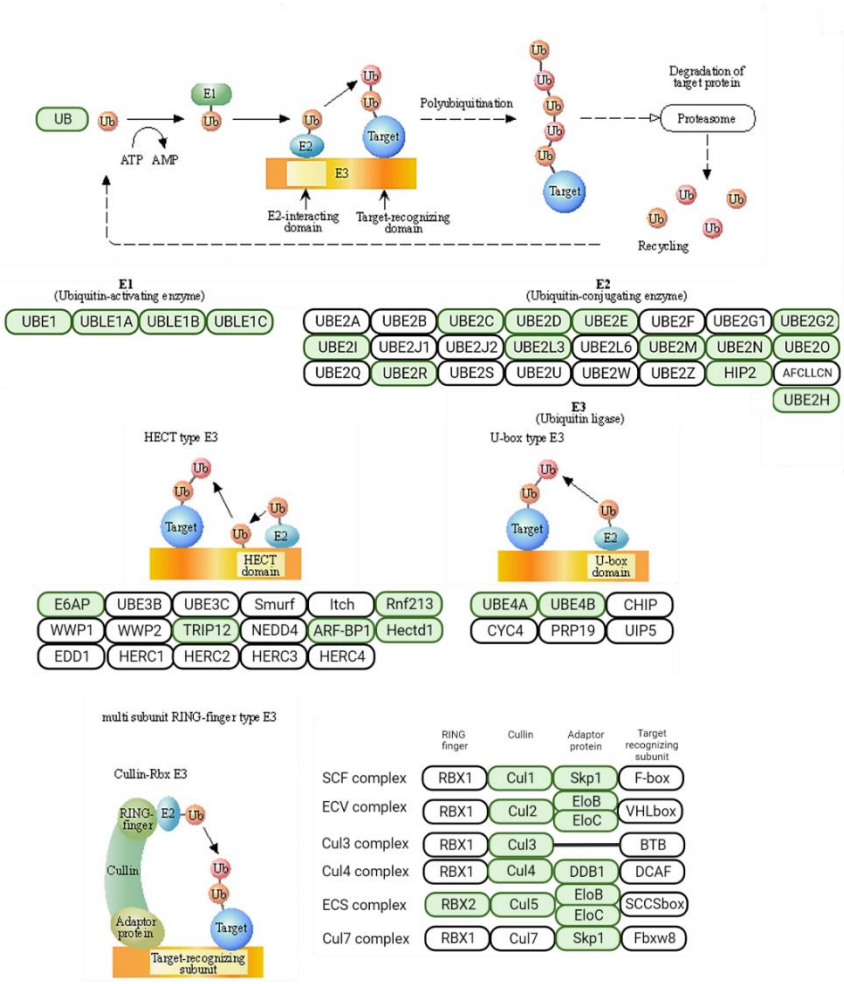


| Gene product | | A | B | C | D |
|---|---|---|---|---|---|
| UB | Rps27a | 0.70 | -0.60 | -0.64 | 0.11 |
| UBE1 | Uba1 | 0.58 | -0.89 | -0.29 | 0.20 |
| | Uba6 | -0.85 | -1.81 | 0.36 | 0.91 |
| UBLE1A | Sae1 | 1.16 | -0.51 | -0.07 | -3.12 |
| UBLE1B | Uba2 | 0.98 | -1.01 | -0.92 | ● |
| UBE1c | Uba3 | 0.45 | ● | | -0.65 |
| UBE2C | Ube2c | | | ● | |
| UBE2D | Ube2d2a | ● | ● | ● | ● |
| UBE2E | Ube2e1 | ● | | | |
| UBE2G2 | Ube2g2 | -0.16 | 0.37 | -0.18 | -0.10 |
| UBE2H | Ube2h | | | 0.38 | -0.51 |
| UBE2I | Ube2i | ● | | | |
| UBE2L3 | Ube2l3 | 0.78 | -1.33 | 0.11 | -0.30 |
| UBE2M | Ube2m | 0.70 | -0.85 | 0.24 | -0.66 |
| UBE2N | Ube2n | 0.58 | -1.10 | 0.05 | -0.00 |
| UBE2O | Ube2o | | | | ● |
| UBE2R | Ube2r2 | | | | ● |
| HIP2 | Ube2k | -0.57 | -2.52 | 0.67 | 0.64 |
| E6AP | Ube3a | -0.42 | -1.58 | 0.65 | 0.43 |
| Cul5 | Rnf13 | ● | | | |
| TRIP12 | Trip12 | ● | | | ● |
| ARF-BP1 | Huwe1 | 0.00 | -0.97 | 0.67 | -0.15 |
| Cul5 | Hectd1 | ● | ● | | ● |
| Cul3 | Ube4A | ● | | | ● |
| UBE4B | Ube4b | -0.32 | 0.26 | | |
| Cul1 | Cul1 | -1.72 | | ● | 0.77 |
| Skp1 | Skp1 | 0.41 | -0.60 | -0.43 | 0.34 |
| Cul2 | Cul2 | -1.49 | -0.82 | 1.43 | -1.37 |
| EloB | Elob | 0.23 | -0.93 | -0.25 | 0.55 |
| EloC | Eloc | -0.10 | -1.12 | 0.31 | 0.46 |
| Cul3 | Cul3 | -1.73 | -1.06 | 0.82 | 0.54 |
| Cul4 | Cul4b | ● | | | ● |
| DDB1 | Ddb1 | 0.83 | -0.42 | -0.23 | -0.67 |
| RBX2 | Rnf7 | ● | | | |
| Cul5 | Cul5 | ● | | | ● |

Figure 7. Pathway of the catshark ubiquitin mediated proteolysis based on mouse putative homologs identification and ubiquitin mediated proteolysis pathway (mmu04120). Green boxes corresponded to identified proteins and white boxes to no protein identification. Blue circles corresponded to identified proteins as specific in a zone. A: zone A; B: zone B; C: zone C; D: zone D.

particle) was also observed with higher expression in zone A while in mice it is expressed in primary spermatocytes and interact with components of the synaptonemal complex (Gómez-H et al., 2019; Živković et al., 2022). Proteins from both subcomplexes of the 19S regulator particle were found: Rpn3-9 and Rpn11, Rpn12 for the Lid subcomplex (PA700); Rpn1, Rpn2, Rpn13 and Rpt1-6 for the base subcomplex. The regulators PA200 and PA28ɣ were also found in zones A and D and only in zone A, respectively. This is consistent with their potential roles in the maturing process and oxidative stress response of spermatozoa(Dietrich et al., 2019; Huang et al., 2016) but also with a more recent finding of the role of PA28ɣ on the regulation of spermatogonia(Gao et al., 2019). The regulators PA28β and PA28α that assemble as heterotetrametric have functions associated with the process of MHC class I antigen presentation. Only PA28β was found with zone A-specific expression, which raises questions about its roles at this stage and whether it is active as a monomer or a homoheptamer as suggested in structure studies(Cascio, 2021). An analysis of PA28 precursors was performed and suggested the presence of a single precursor that appears to be more homologous to mouse PA28β than to PA28α (Figure S7).

The analysis of the factors of ubiquitin-mediated proteolysis showed that the ubiquitin activating enzymes UBE1, UBLEA1A, UBLEA1B, UBE1c were most abundant in zone A while Uba6 was most abundant in zone D (Figure 7). Thirty-one ubiquitin-conjugating enzymes were found with a higher abundance of 11 in zone A, 4 identified only in zone A and 7 in the zones C and/or D. UBE2G2 and UBE4B were the only two enzymes showing higher abundance in zone B corresponding to cysts with spermatocytes. Their role during spermatogenesis has been little studied, with the exception of publications showing differences in levels of UBE2G2 in subfertile men(Laqqan and Hammadeh, 2018) and overexpression of UBE4b in elongated spermatids in mice(M. Li et al., 2020). Relatively few E3 ubiquitin ligases were found in the present study while many isoforms are expressed in the testis(Richburg et al., 2014; Xiong et al., 2022). Of the E3 substrates identified, CUL3 was most abundant in the spermatid zones, which is in agreement with its previously reported profile in mice(Richburg et al., 2014), while CUL2 appeared to be most abundant only in the early spermatid zone, although its expression has been reported to regulate meiotic entry in the *C. elegans* germline(Burger et al., 2013). Other E3 substrates playing an important role during spermatogenesis are the isoforms CUL4A and CUL4B(Kopanja et al., 2011; Yin et al., 2021, 2016) but only CUL4B was found in Zone A

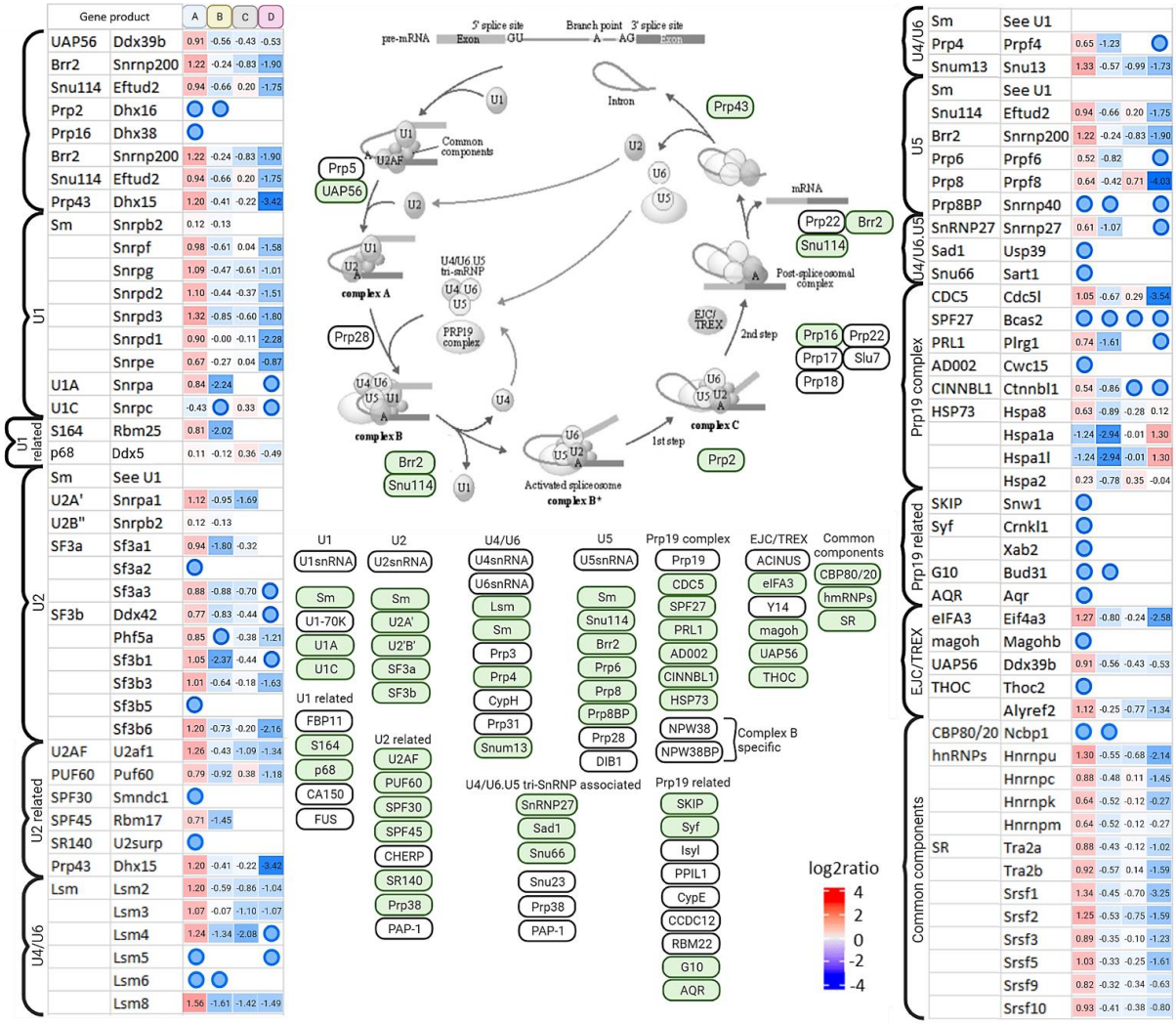


Figure 8. Pathway of the catshark spliceosome based on mouse putative homologs identification and spliceosome pathway (mmu03040). Green boxes corresponded to identified proteins and white boxes to no protein identification. Blue circles corresponded to identified proteins as specific in a zone. A: zone A; B: zone B; C: zone C; D: zone D.

and D. However, the Ddb1 adaptor of Cul4 was found to be more abundant in zone A, which may be consistent with the importance of the CUL4-DDB1 complex for germ-cell cycle progression, cell proliferation and survival(Yin et al., 2021). Four proteins (Cul5, RBX2/rnf7, Elob, Eloc) of the potential Cullin-RING ligase 5 (CRL5) complex were also found in zone A, which may be of interest for a new study topic, given the lack of data available concerning them during spermatogenesis.

Spliceosome

During spermatogenesis, the transcriptionally active germ-cell stages are the mitotic and meiotic stages and alternative splicing controls the temporally specific use of transcripts required for spermiogenesis(Li et al., 2020) including, in particular, meiotic intron-retaining transcripts mechanisms(Naro et al., 2017). Eighty-four factors involved in the spliceosome pathway were found in the present analysis with a large majority of proteins showing a higher abundance in zone A (Figure 8). These factors are linked to the different U1-U6, Prp19 and EJC/TREK complexes. The early expression of these factors at stages corresponding to the zone of differentiation and proliferation of spermatogonia is questionable as the spliceosome would be expected to be established in spermatocytes. However, some studies have shown that spliceosome factors were required for early stages of spermatogenesis such as U2A/snrpa1(Wu et al., 2016) and Prp3(Chen et al., 2019) in *Drosophila* and Bud31 in mice(Qin et al., 2023), which are required for spermatogonial stem cell self-renewal and spermatogonial differentiation. Our results raise the question of whether spliceosome factors may either have more roles during the early stages of spermatogenesis or be expressed in the early stages but the spliceosome is activated later. On the other hand, only two factors related to the Prp19 complex were more abundant in zone D corresponding to cysts with late spermatids. These proteins are Hspa1a and Hspa1l which are members of the heat shock protein family A (Hsp70), member 1A and member 1-like, respectively. As Hsp70 proteins are pleiotropic and involved in a wide range of cellular processes as molecular chaperones, it would be speculative to focus on their function here, however it has been reported that HSPA1L is localized in mouse spermatids and human spermatozoa, albeit with no clear explanation of its function(Liu et al., 2022; Wang et al., 2020).

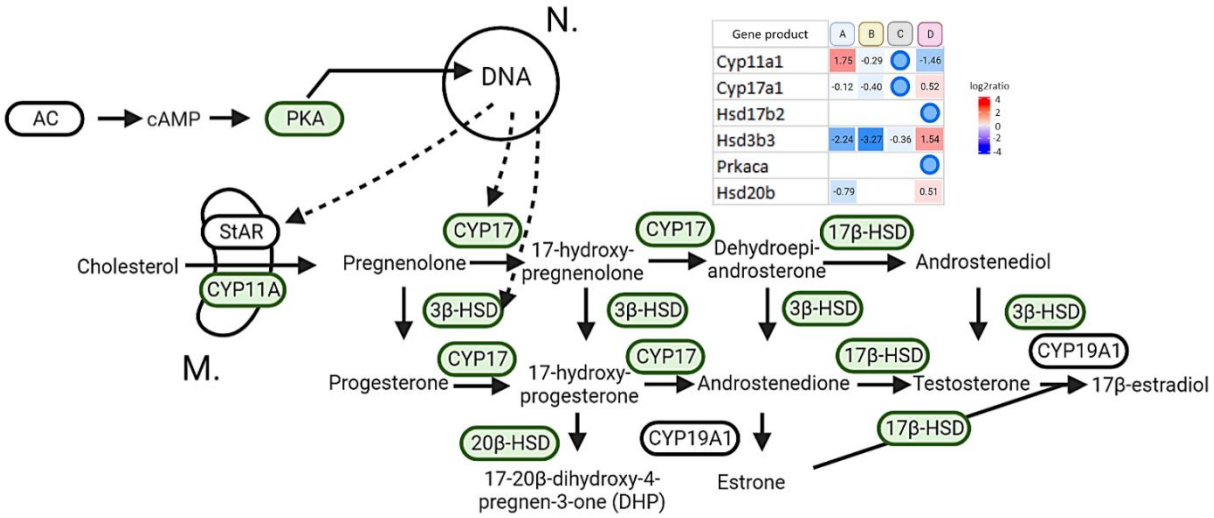


Figure 9. Pathway of the catshark steroidogenesis based on mouse putative homologs identification and ovarian steroidogenesis pathway (mmu04913). Green boxes corresponded to identified proteins and white boxes no protein identification. Blue circles corresponded to identified proteins as specific in a zone. A: zone A; B: zone B; C: zone C; D: zone D; N.: Nucleus; M.: Mitochondria.

Post-transcriptional regulation

During spermiogenesis, spermatids become transcriptionally inactive due to extensive remodelling of their nuclei by replacing histones with protamines. This may raise the question of the proteins identified in zones C and D being primarily derived from Sertoli cells and not from spermatids. However, several spermatid proteins were found to be expressed in zones C and D, such as a spermatid perinuclear RNA-binding protein isoform, sperm-associated antigen16 protein-like, sperm acrosome-associated protein9 isoforms, sperm surface protein Sp17, spermatogenesis-associated protein6-like or spermidine synthase. Therefore, although the relative abundance of proteins identified in zones C and D cannot be attributed to Sertoli cells and spermatids, it is clear that spermatid-associated proteins are present despite their transcriptional inactivation. In fact, gene expression in haploid spermatids requires a temporal uncoupling of transcription and translation. During the early stages, mRNAs are actively transcribed and stored in specialized cytoplasmic assemblies of ribonucleoproteins (RNPs) including chromatoid bodies (CBs). They serve as storehouses and processing centers of mRNAs awaiting translation during the post-meiotic stages of spermatogenesis(Anbazhagan et al., 2022). In our study, Ddx4, Ddx6, EiF4e, Marcks and Piwil1 were found in all zones, in zones A, B and C for Tdrd7, in zones A and B for Nsun2 and only in zone A for Piwil2. These eight proteins are constitutive of the chromatoid bodies, suggesting their effectiveness as facilitators of compartmentalization and coordination of mRNAs regulatory pathways in the male germline.

Steroidogenesis

All enzymes involved in the "classical" pathway of gonadal steroid synthesis were found in our study with the exception of aromatase (CYP19A1) (Figure 9). The relative abundance of proteins according to the stages of spermatogenesis would suggest that pregnenolone would be preferentially synthesised in zone A by CYP11A and preferentially metabolised in zone D to delta-5 steroids by CYP17 or to progesterone by 3β-HSD, and then to 17OH-progesterone and androstenedione by CYP17 and testosterone by the 17β-HSD. The transformation of 17OH-progesterone to 17α-20β-dihydroxyprogesterone (DHP) by 20β-HSD also appears to occur preferentially in zone D. PKA was also found in abundance in zone D, suggesting that stimulation of steroidogenesis occurs mainly in the late stages of spermatogenesis. These results are in agreement with our previous publications showing higher concentrations of

androstenedione, testosterone and DHP in cysts containing late spermatids(Sourdaine and Garnier, 1993). High concentrations of androgens have been also associated with advanced stages of spermatogenesis in other Elasmobranchs such as *Squalus acanthias*(Cuevas et al., 1993), *Dasyatis sabina*(Tricas et al., 2000) and *Cephaloscyllium laticeps*(Awruch, 2013). In the present study, the abundance of CYP11A in zone A would not be consistent with the fact that progesterone concentrations were also higher in zone D(Sourdaine and Garnier, 1993). This discrepancy could be explained by the stage-related patterns of steroid secretion *versus* steroid retention(Cuevas and Callard, 1992a) and/or the rate at which progesterone was converted into downstream steroid metabolites(Awruch, 2013). Another discrepancy in our results is the absence of aromatase (CYP19), contrasting with previously reported testicular activities in *Squalus acanthias*(Callard et al., 1985) but in agreement with the low concentrations measured in testicular zones of *S. canicula*(Sourdaine et al., 1990), probably reflecting a very low level of the proteins.

## CONCLUSIONS

This analysis of the dogfish testicular proteome should enrich the data available for the Elasmobranchs, a phylogenetically and environmentally important group in which many species are currently considered as threatened. Our study adds to the interest of this organism for the study of proteins according to the stages of spermatogenesis and for a better understanding of the regulation of spermatogenesis during evolution. Although the divergence between Chondrichthyes and Osteichthyes is estimated to have happened around 450 million years ago, only 11% of the catshark testicular proteins did not have a positive blast compared to the mouse proteome under the filtering parameters used in our study. This result is rather consistent with the fact that the repertoires of genes regulating spermatogenesis would be present at least at the root of Gnathostomata and that they have evolved slowly. However, our study showed that the highest number of zone-specific proteins was found in zone A and zone D, corresponding to the fundamental steps of spermatogenesis controlling the cell amplification phase that will determine the final number of gametes produced (zone A) and controlling the final step of gamete differentiation and release (zone D). These two steps correspond to variable traits across species, such as the rate of sperm production and the morphology of the spermatozoa. Furthermore, in our study, the largest number of uncharacterized proteins was found in zone D, including a protein with lipocalin signature and

a protein with an ATP-dependent DNA ligase AMP-binding site. Thus, these results highlight the proteome of spermiogenesis and it is interesting to relate this with a recent publication that showed that the evolution of the testis was driven, at least, by the emergence of new genes associated with spermiogenesis(Murat et al., 2023). Among other uncharacterized proteins, our study showed that several zing-finger proteins and a cadherin-like beta sandwich domain-containing protein would be not conserved in Tetrapods except in Amphibians, suggesting the identification of ancient players in the regulation of testicular function. Our results also highlight specific processes along the spermatogenic wave such as mRNA and ncRNA metabolic process and regulation of homeostasis in zone A; chromosome-related, methylation and histone modifications process as well as changes in metabolic process in zone B; cilium organisation and cytoplasmic translation in zone C; cilium activity and cytoplasmic translation in zone D. Factors related to proteasome and ubiquitin-dependent proteolysis were found to be more abundant in zone D, consistent with the maturation process during spermiogenesis. However, the α4s subunit of the spermatoproteasome, the regulators PA200 and PA28ɣ as well as several Culling-RING ligase complexes were also found in abundance in zone A, which might be associated with the regulation of spermatogonia and Sertoli cells, which, in this shark testis model, differentiate and proliferate from the germinative area and progressively form spermatocysts. While these processes are already known to be important during spermatogenesis, our study points to actors whose testicular function remains poorly explored, such as for the import of peroxisomal proteins, ceruloplasmin, optineurin, the pregnancy zone protein, PA28β or the Culling-RING ligase 5 complex. Our results also suggest that spliceosome factors are expressed earlier during spermatogenesis, as early as the spermatogonial stages, although it is generally accepted that they are expressed at the spermatocyte stage.

## ■ ASSOCIATED CONTENT

Complete list of proteins identified in the nanoLC-ESI-MS/MS analysis of the four testicular zones (Table S1) (XLSX).

Supplementary figures corresponding to: Overall workflow of the proteome analysis (Fig. S1); Sample quality control (Fig. S2); Principal component analysis of proteins found in all four zones (Fig. S3); Venn diagram of proteins identified in the four testicular zones (Fig. S4); Blastp results against *C. milii*, *D. rerio*, *G. gallus*, *X. leavis*, *M. musculus*, *H. sapiens* (Fig. S5) (PDF).

## AUTHOR INFORMATION


### Corresponding Author

**Pascal Sourdaine** – Université de Caen Normandie, MNHN, SU, UA, CNRS, IRD, Laboratoire de Biologie des Organismes et Ecosystèmes Aquatiques (BOREA), UMR 8067, 14032 Caen cedex 5, France ; orcid.org/0000-0001-9811-2876 ; Email : pascal.sourdaine@unicaen.fr

### Authors

**Fabian Jeanne** – Université de Caen Normandie, MNHN, SU, UA, CNRS, IRD, Laboratoire de Biologie des Organismes et Ecosystèmes Aquatiques (BOREA), UMR 8067, 14032 Caen cedex 5, France

**Benoit Bernay** – Université de Caen Normandie - Plateforme PROTEOGEN, US EMerode, 14032 Caen cedex 5, France


### Authors Contributions

The manuscript was written by P.S., F.J. and B.B. and all authors have given approval to its final version. P.S. supervised and managed the study, performed dissection. B.B. performed mass spectrometry analyses. F.J. prepared samples for mass spectrometry, performed data analyses, analyzed and discussed the results with B.B. and P.S..


### Fundings

French Ministry for Higher Education and Research, the European Union and the Normandy Region within the Operational Programme ERDF/ESF 2014-2020 under the project

"Manche 2021– *Plateformes d'exploitation de ressources marines*" and the *Muséum National d'Histoire Naturelle* (MNHN) under the project "NeUropeptides and regulation of spermatogenesis in an elasmobranch, the dogfish *Scyliorhinus canicula* (Nuée).

### Note

The authors declare no competing financial interest.

## ACKNOWLEDGEMENTS

The authors are grateful to Mr Faliguerho and Mr Lequenne of the "Lycée Maritime et Aquacole de Cherbourg" (France) for capturing the dogfish specimens, the aquarium "La Cité de la Mer" staff and particularly Mr Faure, Mr Bouis and Mr Cauvin (Cherbourg, France) and Mr Guyon of the "Centre de Recherches en Environnement Côtier" (Luc sur Mer, France) for the care given to catsharks. The authors wish also to thank Mrs Gauvin for enriching discussions concerning statistical analyses and Pr. L.M. McClusky for helpful comments and Mr C. Joubel for the English proofreading.

## REFERENCES

(1) Irisarri, I.; Baurain, D.; Brinkmann, H.; Delsuc, F.; Sire, J.-Y.; Kupfer, A.; Petersen, J.; Jarek, M.; Meyer, A.; Vences, M.; Philippe, H. Phylotranscriptomic Consolidation of the Jawed Vertebrate Timetree. Nat. Ecol. Evol. 2017, 1, 1370–1378. https://doi.org/10.1038/s41559-017-0240-5.

(2) Almeida, T.; Ohta, Y.; Gaigher, A.; Muñoz-Mérida, A.; Neves, F.; Castro, L. F. C.; Machado, A. M.; Esteves, P. J.; Veríssimo, A.; Flajnik, M. F. A Highly Complex, MHC-Linked, 350 Million-Year-Old Shark Nonclassical Class I Lineage. J. Immunol. 2021, 207 (3), 824–836. https://doi.org/10.4049/jimmunol.2000851.

(3) Matz, H.; Munir, D.; Logue, J.; Dooley, H. The Immunoglobulins of Cartilaginous Fishes. Dev. Comp. Immunol. 2021, 115, 103873. https://doi.org/10.1016/j.dci.2020.103873.

(4) Criswell, K. E.; Roberts, L. E.; Koo, E. T.; Head, J. J.; Gillis, J. A. Hox Gene Expression Predicts Tetrapod-like Axial Regionalization in the Skate, Leucoraja Erinacea. Proc. Natl. Acad. Sci. 2021, 118, e2114563118. https://doi.org/10.1073/pnas.2114563118.

(5) Schmidt, P.; Leman, E.; Lagadec, R.; Schubert, M.; Mazan, S.; Reshef, R. Evolutionary Transition in the Regulation of Vertebrate Pronephros Development: A New Role for Retinoic Acid. Cells 2022, 11, 1304. https://doi.org/10.3390/cells11081304.

(6) Atake, O. J.; Eames, B. F. Mineralized Cartilage and Bone-Like Tissues in Chondrichthyans Offer Potential Insights Into the Evolution and Development of Mineralized Tissues in the Vertebrate Endoskeleton. Front. Genet. 2021, 12, 762042. https://doi.org/10.3389/fgene.2021.762042.

(7) Venkatesh, B.; Kirkness, E. F.; Loh, Y.-H.; Halpern, A. L.; Lee, A. P.; Johnson, J.; Dandona, N.; Viswanathan, L. D.; Tay, A.; Venter, J. C.; Strausberg, R. L.; Brenner, S. Survey Sequencing and Comparative Analysis of the Elephant Shark (Callorhinchus Milii) Genome. PLoS Biol. 2007, 5, e101. https://doi.org/10.1371/journal.pbio.0050101.

(8) King, B. L.; Gillis, J. A.; Carlisle, H. R.; Dahn, R. D. A Natural Deletion of the HoxC Cluster in Elasmobranch Fishes. Science 2011, 334, 1517–1517. https://doi.org/10.1126/science.1210912.

(9) Read, T. D.; Petit, R. A.; Joseph, S. J.; Alam, Md. T.; Weil, M. R.; Ahmad, M.; Bhimani, R.; Vuong, J. S.; Haase, C. P.; Webb, D. H.; Tan, M.; Dove, A. D. M. Draft Sequencing and Assembly of the Genome of the World's Largest Fish, the Whale Shark: Rhincodon Typus Smith 1828. BMC Genomics 2017, 18, 532. https://doi.org/10.1186/s12864-017-3926-9.

(10) Hara, Y.; Yamaguchi, K.; Onimaru, K.; Kadota, M.; Koyanagi, M.; Keeley, S. D.; Tatsumi, K.; Tanaka, K.; Motone, F.; Kageyama, Y.; Nozu, R.; Adachi, N.; Nishimura, O.; Nakagawa, R.; Tanegashima, C.; Kiyatake, I.; Matsumoto, R.; Murakumo, K.; Nishida, K.; Terakita, A.; Kuratani, S.; Sato, K.; Hyodo, S.; Kuraku, S. Shark Genomes Provide Insights into Elasmobranch Evolution and the Origin of Vertebrates. Nat. Ecol. Evol. 2018, 2, 1761–1771. https://doi.org/10.1038/s41559-018-0673-5.

(11) Marra, N. J.; Stanhope, M. J.; Jue, N. K.; Wang, M.; Sun, Q.; Pavinski Bitar, P.; Richards, V. P.; Komissarov, A.; Rayko, M.; Kliver, S.; Stanhope, B. J.; Winkler, C.; O'Brien, S. J.; Antunes,

A.; Jorgensen, S.; Shivji, M. S. White Shark Genome Reveals Ancient Elasmobranch Adaptations Associated with Wound Healing and the Maintenance of Genome Stability. Proc. Natl. Acad. Sci. 2019, 116, 4446–4455. https://doi.org/10.1073/pnas.1819778116.

(12) Weber, J. A.; Park, S. G.; Luria, V.; Jeon, S.; Kim, H.-M.; Jeon, Y.; Bhak, Y.; Jun, J. H.; Kim, S. W.; Hong, W. H.; Lee, S.; Cho, Y. S.; Karger, A.; Cain, J. W.; Manica, A.; Kim, S.; Kim, J.-H.; Edwards, J. S.; Bhak, J.; Church, G. M. The Whale Shark Genome Reveals How Genomic and Physiological Properties Scale with Body Size. Proc. Natl. Acad. Sci. 2020, 117 (34), 20662–20671. https://doi.org/10.1073/pnas.1922576117.

(13) Tan, M.; Redmond, A. K.; Dooley, H.; Nozu, R.; Sato, K.; Kuraku, S.; Koren, S.; Phillippy, A. M.; Dove, A. D.; Read, T. The Whale Shark Genome Reveals Patterns of Vertebrate Gene Family Evolution. eLife 2021, 10, e65394. https://doi.org/10.7554/eLife.65394.

(14) Buechi, H. B.; Bridgham, J. T. Evolution of Specificity in Cartilaginous Fish Glycoprotein Hormones and Receptors. Gen. Comp. Endocrinol. 2017, 246, 309–320. https://doi.org/10.1016/j.ygcen.2017.01.007.

(15) Zhang, Y.; Gao, H.; Li, H.; Guo, J.; Ouyang, B.; Wang, M.; Xu, Q.; Wang, J.; Lv, M.; Guo, X.; Liu, Q.; Wei, L.; Ren, H.; Xi, Y.; Guo, Y.; Ren, B.; Pan, S.; Liu, C.; Ding, X.; Xiang, H.; Yu, Y.; Song, Y.; Meng, L.; Liu, S.; Wang, J.; Jiang, Y.; Shi, J.; Liu, S.; Sabir, J. S. M.; Sabir, M. J.; Khan, M.; Hajrah, N. H.; Ming-Yuen Lee, S.; Xu, X.; Yang, H.; Wang, J.; Fan, G.; Yang, N.; Liu, X. The White-Spotted Bamboo Shark Genome Reveals Chromosome Rearrangements and Fast-Evolving Immune Genes of Cartilaginous Fish. iScience 2020, 23, 101754. https://doi.org/10.1016/j.isci.2020.101754.

(16) Joyce, W.; Ripley, D. M.; Gillis, T.; Black, A. C.; Shiels, H. A.; Hoffmann, F. G. A Revised Perspective on the Evolution of Troponin I and Troponin T Gene Families in Vertebrates. Genome Biol. Evol. 2023, 15, evac173. https://doi.org/10.1093/gbe/evac173.

(17) Neves, F.; Muñoz-Mérida, A.; Machado, A. M.; Almeida, T.; Gaigher, A.; Esteves, P. J.; Castro, L. F. C.; Veríssimo, A. Uncovering a 500 Million Year Old History and Evidence of Pseudogenization for TLR15. Front. Immunol. 2022, 13, 1020601. https://doi.org/10.3389/fimmu.2022.1020601.

(18) Kuraku, S. Shark and Ray Genomics for Disentangling Their Morphological Diversity and Vertebrate Evolution. Dev. Biol. 2021, 477, 262–272. https://doi.org/10.1016/j.ydbio.2021.06.001.

(19) Nazarian, J.; Hathout, Y.; Vertes, A.; Hoffman, E. P. The Proteome Survey of an Electricity-Generating Organ (Torpedo Californica Electric Organ). PROTEOMICS 2007, 7, 617–627. https://doi.org/10.1002/pmic.200600686.

(20) Krishnaswamy Gopalan, T.; Gururaj, P.; Gupta, R.; Gopal, D. R.; Rajesh, P.; Chidambaram, B.; Kalyanasundaram, A.; Angamuthu, R. Transcriptome Profiling Reveals Higher Vertebrate Orthologous of Intra-Cytoplasmic Pattern Recognition Receptors in Grey Bamboo Shark. PLoS ONE 2014, 9, e100018. https://doi.org/10.1371/journal.pone.0100018.

(21) Mulley, J. F.; Hargreaves, A. D.; Hegarty, M. J.; Heller, R. S.; Swain, M. T. Transcriptomic Analysis of the Lesser Spotted Catshark (Scyliorhinus Canicula) Pancreas, Liver and Brain Reveals Molecular Level Conservation of Vertebrate Pancreas Function. BMC Genomics 2014, 15, 1–18. https://doi.org/10.1186/1471-2164-15-1074.

(22) Stavrianakou, M.; Perez, R.; Wu, C.; Sachs, M. S.; Aramayo, R.; Harlow, M. Draft de Novo Transcriptome Assembly and Proteome Characterization of the Electric Lobe of Tetronarce Californica: A Molecular Tool for the Study of Cholinergic Neurotransmission in the Electric Organ. BMC Genomics 2017, 18, 611. https://doi.org/10.1186/s12864-017-3890-4.

(23) Chana-Munoz, A.; Jendroszek, A.; Sønnichsen, M.; Kristiansen, R.; Jensen, J. K.; Andreasen, P. A.; Bendixen, C.; Panitz, F. Multi-Tissue RNA-Seq and Transcriptome Characterisation of the Spiny Dogfish Shark (Squalus Acanthias) Provides a Molecular Tool for Biological Research and Reveals New Genes Involved in Osmoregulation. PLOS ONE 2017, 12, e0182756. https://doi.org/10.1371/journal.pone.0182756.

(24) Machado, A. M.; Almeida, T.; Mucientes, G.; Esteves, P. J.; Verissimo, A.; Castro, L. F. C. De Novo Assembly of the Kidney and Spleen Transcriptomes of the Cosmopolitan Blue Shark, Prionace Glauca. Mar. Genomics 2018, 37, 50–53. https://doi.org/10.1016/j.margen.2017.11.009.

(25) Onimaru, K.; Tatsumi, K.; Shibagaki, K.; Kuraku, S. A de Novo Transcriptome Assembly of the Zebra Bullhead Shark, Heterodontus Zebra. Sci. Data 2018, 5, 180197. https://doi.org/10.1038/sdata.2018.197.

(26) Bakke, F. K.; Gundappa, M. K.; Matz, H.; Stead, D. A.; Macqueen, D. J.; Dooley, H. Exploration of the Nurse Shark (Ginglymostoma Cirratum) Plasma Immunoproteome Using High-Resolution LC-MS/MS. Front. Immunol. 2022, 13, 873390. https://doi.org/10.3389/fimmu.2022.873390.

(27) Djureinovic, D.; Fagerberg, L.; Hallström, B.; Danielsson, A.; Lindskog, C.; Uhlén, M.; Pontén, F. The Human Testis-Specific Proteome Defined by Transcriptomics and Antibody-Based Profiling. MHR Basic Sci. Reprod. Med. 2014, 20, 476–488. https://doi.org/10.1093/molehr/gau018.

(28) Ahn, J.; Park, Y.-J.; Chen, P.; Lee, T. J.; Jeon, Y.-J.; Croce, C. M.; Suh, Y.; Hwang, S.; Kwon, W.-S.; Pang, M.-G.; Kim, C.-H.; Lee, S. S.; Lee, K. Comparative Expression Profiling of Testis-Enriched Genes Regulated during the Development of Spermatogonial Cells. PLOS ONE 2017, 12, e0175787. https://doi.org/10.1371/journal.pone.0175787.

(29) Vandenbrouck, Y.; Pineau, C.; Lane, L. The Functionally Unannotated Proteome of Human Male Tissues: A Shared Resource to Uncover New Protein Functions Associated with Reproductive Biology. J. Proteome Res. 2020, 19, 4782–4794. https://doi.org/10.1021/acs.jproteome.0c00516.

(30) Stanley, H. P. The Structure and Development of the Seminiferous Follicle in Scyliorhinus Caniculus and Torpedo Marmorata (Elasmobranchii). Z. Für Zellforsch. Mikrosk. Anat. 1966, 75, 453–468. https://doi.org/10.1007/BF00336875.

(31) Pratt, H. L. Elasmobranch Gonad Structure: A Description and Survey. Copeia 1988, 1988, 719. https://doi.org/10.2307/1445394.

(32) Grier, H. J. Chordate Testis: The Extracellular Matrix Hypothesis. J. Exp. Zool. 1992, 261, 151–160. https://doi.org/10.1002/jez.1402610206.

(33) Grier, H. J.; Uribe, M. C.; Lo Nostro, F. L.; Mims, S. D.; Parenti, L. R. Conserved Form and Function of the Germinal Epithelium through 500 Million Years of Vertebrate Evolution:

Vertebrate Germinal Epithelium. J. Morphol. 2016, 277, 1014–1044. https://doi.org/10.1002/jmor.20554.

(34) Gomes do Rêgo, M.; Fitzpatrick, J. L.; Hissa V. Hazin, F.; Araujo, M. Lucia. G.; Barros, M. E. G.; Evêncio Neto, J. Comparison of the Morphology and Histomorphometry of Spermatogenic Cyst of Three Sharks Species With Diametric Testes: Morphology of Cysts of Three Sharks. Anat. Rec. 2016, 299, 759–768. https://doi.org/10.1002/ar.23326.

(35) Loir, M.; Sourdaine, P. Testes Cells: Isolation and Culture. In: Hochachka PW, Mommsen TP (Eds) Biochemistry and Molecular Biology of Fishes: Analytical Techniques; Elsevier: New York, 1994; pp 219–272.

(36) Loppion, G.; Crespel, A.; Martinez, A.-S.; Auvray, P.; Sourdaine, P. Study of the Potential Spermatogonial Stem Cell Compartment in Dogfish Testis, Scyliorhinus Canicula L. Cell Tissue Res. 2008, 332, 533–542. https://doi.org/10.1007/s00441-008-0590-z.

(37) Bosseboeuf, A.; Gautier, A.; Auvray, P.; Mazan, S.; Sourdaine, P. Characterization of Spermatogonial Markers in the Mature Testis of the Dogfish (Scyliorhinus Canicula L.). REPRODUCTION 2014, 147, 125–139. https://doi.org/10.1530/REP-13-0316.

(38) Gautier, A.; Bosseboeuf, A.; Auvray, P.; Sourdaine, P. Maintenance of Potential Spermatogonial Stem Cells In Vitro by GDNF Treatment in a Chondrichthyan Model (Scyliorhinus Canicula L.)1. Biol. Reprod. 2014, 91, 91–105. https://doi.org/10.1095/biolreprod.113.116020.

(39) Pudney, J.; Callard, G. V. Development of Agranular Reticulum in Sertoli Cells of the Testis of the DogfishSqualus Acanthias during Spermatogenesis. Anat. Rec. 1984, 209, 311–321. https://doi.org/10.1002/ar.1092090309.

(40) Pudney, J.; Callard, G. V. Identification of Leydig-like Cells in the Testis of the DogfishSqualus Acanthias. Anat. Rec. 1984, 209, 323–330. https://doi.org/10.1002/ar.1092090310.

(41) Cuevas, M. E.; Callard, G. In Vitro Steroid Secretion by Staged Spermatocysts (Sertoli/Germ Cell Units) of Dogfish (Squalus Acanthias) Testis. Gen. Comp. Endocrinol. 1992, 88, 151–165. https://doi.org/10.1016/0016-6480(92)90204-W.

(42) Cuevas, M. E.; Collins, K.; Callard, G. V. Stage-Related Changes in Steroid-Converting Enzyme Activities in Squalus Testis: Synthesis of Biologically Active Metabolites via 3fl-Hydroxysteroid Dehydrogenase/ Isomerase and 5ce-Reductase. Steroids 1993, 58, 87–94. https://doi.org/10.1016/0039-128X(93)90058-U.

(43) Sourdaine, P.; Garnier, D. H. Stage-Dependent Modulation of Sertoli Cell Steroid Production in Dogfish (Scyliorhinus Canicula). Reproduction 1993, 97, 133–142. https://doi.org/10.1530/jrf.0.0970133.

(44) Loir, M.; Sourdaine, P.; Mendis-Handagama, S. M. L. C.; Jégou, B. Cell-Cell Interactions in the Testis of Teleosts and Elasmobranchs: CELL-CELL INTERACTIONS IN THE TESTIS. Microsc. Res. Tech. 1995, 32, 533–552. https://doi.org/10.1002/jemt.1070320606.

(45) McClusky, L. M. The Caspase-Dependent Apoptosis Gradient in the Testis of the Blue Shark, Prionace Glauca. REPRODUCTION 2013, 145, 297–310. https://doi.org/10.1530/REP-12-0216.

(46) McClusky, L. M. Coordination of Spermatogenic Processes in the Testis: Lessons from Cystic Spermatogenesis. Cell Tissue Res. 2012, 349, 703–715. https://doi.org/10.1007/s00441-011-1288-1.

(47) McClusky, L. M. Several Routes of Cell Death to Secondary Necrosis in the Elasmobranch Testis. Apoptosis 2022, 27, 454–464. https://doi.org/10.1007/s10495-022-01733-0.

(48) Prisco, M.; Liguoro, A.; Comitato, R.; Cardone, A.; D'Onghia, B.; Ricchiari, L.; Angelini, F.; Andreuccetti, P. Apoptosis during Spermatogenesis in the Spotted RayTorpedo Marmorata. Mol. Reprod. Dev. 2003, 64, 341–348. https://doi.org/10.1002/mrd.10267.

(49) Ricchiari, L.; Liguoro, A.; Andreuccetti, P.; Angelini, F.; Prisco, M. The Fas/FasL System Is a Possible Regulator of Germ Cell Apoptosis in the Testis of Torpedo Marmorata. J. Fish Biol. 2006, 69, 1779–1787. https://doi.org/10.1111/j.1095-8649.2006.01248.x.

(50) Piferrer, F. C.; Callard, G. V. Inhibition of Deoxyribonucleic Acid Synthesis during Premeiotic Stages of Spermatogenesis by a Factor from Testis-Associated Lymphomyeloid Tissue in the Dogfish Shark (Squalus Acanthias)1. Biol. Reprod. 1995, 53, 390–398. https://doi.org/10.1095/biolreprod53.2.390.

(51) Gautron, J. Effet Du Calcium et de La Stimulation Sur Les Terminaisons Nerveuses Des Fonctions Nerf-Électroplaque de La Torpille. Biol Cell 1978, 31, 31–44.

(52) Fischer, R.; Kessler, B. M. Gel-aided Sample Preparation (GASP)—A Simplified Method for Gel-assisted Proteomic Sample Generation from Protein Extracts and Intact Cells. PROTEOMICS 2015, 15, 1224–1229. https://doi.org/10.1002/pmic.201400436.

(53) Kil, Y. J.; Becker, C.; Sandoval, W.; Goldberg, D.; Bern, M. Preview: A Program for Surveying Shotgun Proteomics Tandem Mass Spectrometry Data. Anal. Chem. 2011, 83, 5259–5267. https://doi.org/10.1021/ac200609a.

(54) Lê, S.; Josse, J.; Husson, F. FactoMineR: An R Package for Multivariate Analysis. J Stat Softw 2008, 25, 1–18. https://doi.org/10.18637/jss.v025.i01.

(55) Kassambara, A.; Mundt, F. Factoextra: Extract and Visualize the Results of Multivariate Data Analyses. 2020, R Package Version 1.0.7.

(56) Yan, L. Ggvenn: Draw Venn Diagram by Ggplot2. 2021, R package version 0.1.9.

(57) Gu, Z.; Eils, R.; Schlesner, M. Complex Heatmaps Reveal Patterns and Correlations in Multidimensional Genomic Data. Bioinformatics 2016, 32, 2847–2849. https://doi.org/10.1093/bioinformatics/btw313.

(58) Bindea, G.; Mlecnik, B.; Hackl, H.; Charoentong, P.; Tosolini, M.; Kirilovsky, A.; Fridman, W.-H.; Pagès, F.; Trajanoski, Z.; Galon, J. ClueGO: A Cytoscape Plug-in to Decipher Functionally Grouped Gene Ontology and Pathway Annotation Networks. Bioinformatics 2009, 25, 1091–1093. https://doi.org/10.1093/bioinformatics/btp101.

(59) Paronetto, M. P.; Sette, C. Role of RNA-Binding Proteins in Mammalianspermatogenesis. Cancer Res. 2010, 70, 229–239. https://doi.org/10.1111/j.1365-2605.2009.00959.x.

(60) Naro, C.; Jolly, A.; Di Persio, S.; Bielli, P.; Setterblad, N.; Alberdi, A. J.; Vicini, E.; Geremia, R.; De la Grange, P.; Sette, C. An Orchestrated Intron Retention Program in Meiosis Controls Timely Usage of Transcripts during Germ Cell Differentiation. Dev. Cell 2017, 41, 82-93.e4. https://doi.org/10.1016/j.devcel.2017.03.003.

(61) Burlibaşa, L.; Ionescu, A. C.; Dragusanu, D.-M. Histone Hyperacetylation and DNA Methylation Interplay during Murine Spermatogenesis. Zygote 2019, 27, 305–314. https://doi.org/10.1017/S0967199419000303.

(62) Li, M.; Li, H.; Yang, H.; Cheng, R.; Zheng, P.; Guo, R. Comparative Proteomic Analysis of Round and Elongated Spermatids during Spermiogenesis in Mice. Biomed. Chromatogr. 2020, 34. https://doi.org/10.1002/bmc.4799.

(63) Rabionet, M.; Bayerle, A.; Jennemann, R.; Heid, H.; Fuchser, J.; Marsching, C.; Porubsky, S.; Bolenz, C.; Guillou, F.; Gröne, H.-J.; Gorgas, K.; Sandhoff, R. Male Meiotic Cytokinesis Requires Ceramide Synthase 3-Dependent Sphingolipids with Unique Membrane Anchors. Hum. Mol. Genet. 2015, 24, 4792–4808. https://doi.org/10.1093/hmg/ddv204.

(64) Kunduri, G.; Le, S.-H.; Baena, V.; Vijaykrishna, N.; Harned, A.; Nagashima, K.; Blankenberg, D.; Yoshihiro, I.; Narayan, K.; Bamba, T.; Acharya, U.; Acharya, J. K. Delivery of Ceramide Phosphoethanolamine Lipids to the Cleavage Furrow through the Endocytic Pathway Is Essential for Male Meiotic Cytokinesis. PLOS Biol. 2022, 20, e3001599. https://doi.org/10.1371/journal.pbio.3001599.

(65) Callard, G. V.; Pudney, J. A.; Mak, P.; Canick, J. A. Stage-Dependent Changes in Steroidogenic Enzymes and Estrogen Receptors during Spermatogenesis in the Testis of the Dogfish, Squalus Acanthias*. Endocrinology 1985, 117, 1328–1335. https://doi.org/10.1210/endo-117-4-1328.

(66) Amaral, A. Energy Metabolism in Mammalian Sperm Motility. WIREs Mech. Dis. 2022, 14. https://doi.org/10.1002/wsbm.1569.

(67) Widlak, W.; Vydra, N. The Role of Heat Shock Factors in Mammalian Spermatogenesis. Adv Anat Embryol Cell Biol 2017, 222, 45–65. https://doi.org/10.1007/978-3-319-51409-3_3.

(68) Dietrich, M. A.; Nynca, J.; Ciereszko, A. Proteomic and Metabolomic Insights into the Functions of the Male Reproductive System in Fishes. Theriogenology 2019, 132, 182–200. https://doi.org/10.1016/j.theriogenology.2019.04.018.

(69) Backe, S. J.; Sager, R. A.; Regan, B. R.; Sit, J.; Major, L. A.; Bratslavsky, G.; Woodford, M. R.; Bourboulia, D.; Mollapour, M. A Specialized Hsp90 Co-Chaperone Network Regulates

Steroid Hormone Receptor Response to Ligand. Cell Rep. 2022, 40, 111039. https://doi.org/10.1016/j.celrep.2022.111039.

(70) Brauns, A.-K.; Heine, M.; Tödter, K.; Baumgart-Vogt, E.; Lüers, G. H.; Schumacher, U. A Defect in the Peroxisomal Biogenesis in Germ Cells Induces a Spermatogenic Arrest at the Round Spermatid Stage in Mice. Sci. Rep. 2019, 9, 9553. https://doi.org/10.1038/s41598-019-45991-6.

(71) Onoda, M.; Djakiew, D. Modulation of Sertoli Cell Secretory Function by Rat Round Spermatid Protein(s). Mol. Cell. Endocrinol. 1990, 73, 35–44. https://doi.org/10.1016/0303-7207(90)90042-7.

(72) Ogórek, M.; Herman, S.; Pierzchała, O.; Bednarz, A.; Rajfur, Z.; Baster, Z.; Grzmil, P.; Starzyński, R. R.; Szudzik, M.; Jończy, A.; Lipiński, P.; Lenartowicz, M. Molecular Machinery Providing Copper Bioavailability for Spermatozoa along the Epididymial Tubule in Mouse. Biol. Reprod. 2019, 100, 1505–1520. https://doi.org/10.1093/biolre/ioz028.

(73) Nakamura, M.; Okinaga, shoichi; ARAI, K. Metabolism of Pachytene Primary Spermatocytes from Rat Testes: Pyruvate Maintenance of Adenosine Triphosphate Level. Biol Reprod 1984, 30, 1187–1197.

(74) Lu, J.-Y.; Schneider, R. J. Tissue Distribution of AU-Rich MRNA-Binding Proteins Involved in Regulation of MRNA Decay. J. Biol. Chem. 2004, 279, 12974–12979. https://doi.org/10.1074/jbc.M310433200.

(75) Sahin, Z.; Szczepny, A.; McLaughlin, E. A.; Meistrich, M. L.; Zhou, W.; Ustunel, I.; Loveland, K. L. Dynamic Hedgehog Signalling Pathway Activity in Germline Stem Cells. Andrology 2014, 2, 267–274. https://doi.org/10.1111/j.2047-2927.2014.00187.x.

(76) Zhao, C.; Zhang, Z.; Qu, X.; Bai, X.; Liu, X.; Tao, W.; Zhou, L.; Wang, D.; Wei, J. Desert Hedgehog Mediates the Proliferation of Medaka Spermatogonia through Smoothened Signaling. Reproduction 2022, 163, 209–218. https://doi.org/10.1530/REP-21-0468.

(77) Feng, J.; He, Y.; Shen, Y.; Zhang, G.; Ma, S.; Zhao, X.; Zhang, Y. Protective Effects of Nuclear Factor Erythroid 2-Related Factor on Oxidative Stress and Apoptosis in the Testis of Mice before Adulthood. Theriogenology 2020, 148, 112–121. https://doi.org/10.1016/j.theriogenology.2020.03.002.

(78) Zeng, R.; Wang, Z.; Li, X.; Chen, Y.; Yang, S.; Dong, J. Cyclin-Dependent Kinase 1-Mediated Phosphorylation of Protein Kinase N1 Promotes Anchorage-Independent Growth and Migration. Cell. Signal. 2020, 69, 109546. https://doi.org/10.1016/j.cellsig.2020.109546.

(79) Browne, J. A.; Leir, S.; Yin, S.; Harris, A. Transcriptional Networks in the Human Epididymis. Andrology 2019, 7, 741–747. https://doi.org/10.1111/andr.12629.

(80) Tong, J.; Xie, J.; Ren, H.; Liu, J.; Zhang, W.; Wei, C.; Xu, J.; Zhang, W.; Li, X.; Wang, W.; Lv, D.; He, J. C.; Chen, N. Comparison of Glomerular Transcriptome Profiles of Adult-Onset Steroid Sensitive Focal Segmental Glomerulosclerosis and Minimal Change Disease. PLOS ONE 2015, 10, e0140453. https://doi.org/10.1371/journal.pone.0140453.

(81) Soumillon, M.; Necsulea, A.; Weier, M.; Brawand, D.; Zhang, X.; Gu, H.; Barthès, P.; Kokkinaki, M.; Nef, S.; Gnirke, A.; Dym, M.; de Massy, B.; Mikkelsen, T. S.; Kaessmann, H. Cellular Source and Mechanisms of High Transcriptome Complexity in the Mammalian Testis. Cell Rep. 2013, 3, 2179–2190. https://doi.org/10.1016/j.celrep.2013.05.031.

(82) Li, Q.; Li, T.; Xiao, X.; Ahmad, D. W.; Zhang, N.; Li, H.; Chen, Z.; Hou, J.; Liao, M. Specific Expression and Alternative Splicing of Mouse Genes during Spermatogenesis. Mol. Omics 2020, 16, 258–267. https://doi.org/10.1039/C9MO00163H.

(83) Wu, J.-T.; Lin, H.-C.; Hu, Y.-C.; Chien, C.-T. Neddylation and Deneddylation Regulate Cul1 and Cul3 Protein Accumulation. Nat. Cell Biol. 2005, 7, 1014–1020. https://doi.org/10.1038/ncb1301.

(84) Norman, M.; Rivers, C.; Lee, Y.-B.; Idris, J.; Uney, J. The Increasing Diversity of Functions Attributed to the SAFB Family of RNA-/DNA-Binding Proteins. Biochem. J. 2016, 473, 4271–4288. https://doi.org/10.1042/BCJ20160649.

(85) Zheng, B.; Zhou, Q.; Guo, Y.; Shao, B.; Zhou, T.; Wang, L.; Zhou, Z.; Sha, J.; Guo, X.; Huang, X. Establishment of a Proteomic Profile Associated with Gonocyte and Spermatogonial Stem Cell Maturation and Differentiation in Neonatal Mice. PROTEOMICS 2014, 14, 274–285. https://doi.org/10.1002/pmic.201300395.

(86) Jiang, S.; Katz, T. A.; Garee, J. P.; DeMayo, F. J.; Lee, A. V.; Oesterreich, S. Scaffold Attachment Factor B2 (SAFB2) Null Mice Reveal Non-Redundant Functions Compared to Its Paralog SAFB1. Model Mec 2015, 8, 1121–1127. https://doi.org/10.1242/dmm.019885.

(87) Prisco, M.; Donizetti, A.; Aniello, F.; Locascio, A.; Del Giudice, G.; Agnese, M.; Angelini, F.; Andreuccetti, P. Expression of Prothymosin Alpha during the Spermatogenesis of the Spotted Ray Torpedo Marmorata. Gen. Comp. Endocrinol. 2009, 164, 70–76. https://doi.org/10.1016/j.ygcen.2009.05.005.

(88) Venditti, M.; Minucci, S. Prothymosin Alpha Expression in the Vertebrate Testis: A Comparative Review. Zygote 2017, 25, 760–770. https://doi.org/10.1017/S096719941700065X.

(89) Guo, F.; Huang, X.; Li, S.; Sun, L.; Li, Y.; Li, H.; Zhou, Y.; Chu, Y.; Zhou, T. Identification of Prosaposin as a Novel Interaction Partner for Rhox5. J. Genet. Genomics 2007, 34, 392–399. https://doi.org/10.1016/S1673-8527(07)60042-3.

(90) Park, J.; Kim, S. W.; Cho, M. C. The Role of LIM Kinase in the Male Urogenital System. Cells 2021, 11, 78. https://doi.org/10.3390/cells11010078.

(91) Baba, T.; Hoff III, H. B.; Nemoto, H.; Lee, H.; Orth, J.; Arai, Y.; Gerton, G. L. Acrogranin, an Acrosomal Cysteine-Rich Glycoprotein, Is the Precursor of the Growth-Modulating Peptides, Granulins, and Epithelins, and Is Expressed in Somatic as Well as Male Germ Cells. Mol Reprod Dev 1993, 34, 233–243. https://doi.org/10.1002/mrd.1080340302.

(92) Xiaodong, S.; Yehua, G.; Jing, M.; Zuoren, Y.; Sai, L.; Yongchao, W.; Shepu, X.; Daishu, H. The Cloning and Expression Characterization of the Centrosome Protein Genes Family (Centrin Genes) in Rat Testis. Sci. China C Life Sci. 2002, 45, 655 662. https://doi.org/10.1007/BF02879754.

(93) Lin, C.-J.; Jeng, S.-R.; Lei, Z.-Y.; Yueh, W.-S.; Dufour, S.; Wu, G.-C.; Chang, C.-F. Involvement of Transforming Growth Factor Beta Family Genes in Gonadal Differentiation in Japanese Eel, Anguilla Japonica, According to Sex-Related Gene Expressions. Cells 2021, 10, 3007. https://doi.org/10.3390/cells10113007.

(94) Becerril-García, E. E.; Arellano-Martínez, M.; Bernot-Simon, D.; Hoyos-Padilla, E. M.; Galván-Magaña, F.; Godard-Codding, C. Steroid Hormones and Chondrichthyan Reproduction: Physiological Functions, Scientific Research, and Implications for Conservation. PeerJ 2020, 8, e9686. https://doi.org/10.7717/peerj.9686.

(95) Gómez-H, L.; Felipe-Medina, N.; Condezo, Y. B.; Garcia-Valiente, R.; Ramos, I.; Suja, J. A.; Barbero, J. L.; Roig, I.; Sánchez-Martín, M.; de Rooij, D. G.; Llano, E.; Pendas, A. M. The PSMA8 Subunit of the Spermatoproteasome Is Essential for Proper Meiotic Exit and Mouse Fertility. PLOS Genet. 2019, 15, e1008316. https://doi.org/10.1371/journal.pgen.1008316.

(96) Živković, D.; Sanchez Dafun, A.; Menneteau, T.; Schahl, A.; Lise, S.; Kervarrec, C.; Toste Rêgo, A.; da Fonseca, P. C. A.; Chavent, M.; Pineau, C.; Burlet-Schiltz, O.; Marcoux, J.; Bousquet, M.-P. Proteasome Complexes Experience Profound Structural and Functional Rearrangements throughout Mammalian Spermatogenesis. Proc. Natl. Acad. Sci. 2022, 119, e2116826119. https://doi.org/10.1073/pnas.2116826119.

(97) Huang, L.; Haratake, K.; Miyahara, H.; Chiba, T. Proteasome Activators, PA28γ and PA200, Play Indispensable Roles in Male Fertility. Sci. Rep. 2016, 6, 23171. https://doi.org/10.1038/srep23171.

(98) Gao, X.; Chen, H.; Liu, J.; Shen, S.; Wang, Q.; Clement, T. M.; Deskin, B. J.; Chen, C.; Zhao, D.; Wang, L.; Guo, L.; Ma, X.; Zhang, B.; Xu, Y.; Li, X.; Li, L. The REGγ-Proteasome Regulates Spermatogenesis Partially by P53-PLZF Signaling. Stem Cell Rep. 2019, 13, 559–571. https://doi.org/10.1016/j.stemcr.2019.07.010.

(99) Cascio, P. PA28γ: New Insights on an Ancient Proteasome Activator. Biomolecules 2021, 11, 228. https://doi.org/10.3390/biom11020228.

(100) Laqqan, M.; Hammadeh, M. E. Alterations in DNA Methylation Patterns and Gene Expression in Spermatozoa of Subfertile Males. Andrologia 2018, 50, e12934. https://doi.org/10.1111/and.12934.

(101) Richburg, J. H.; Myers, J. L.; Bratton, S. B. The Role of E3 Ligases in the Ubiquitin-Dependent Regulation of Spermatogenesis. Semin. Cell Dev. Biol. 2014, 30, 27–35. https://doi.org/10.1016/j.semcdb.2014.03.001.

(102) Xiong, Y.; Yu, C.; Zhang, Q. Ubiquitin-Proteasome System–Regulated Protein Degradation in Spermatogenesis. Cells 2022, 11, 1058. https://doi.org/10.3390/cells11061058.

(103) Burger, J.; Merlet, J.; Tavernier, N.; Richaudeau, B.; Arnold, A.; Ciosk, R.; Bowerman, B.; Pintard, L. CRL2LRR-1 E3-Ligase Regulates Proliferation and Progression through Meiosis in the

Caenorhabditis Elegans Germline. PLoS Genet. 2013, 9, e1003375. https://doi.org/10.1371/journal.pgen.1003375.

(104) Kopanja, D.; Roy, N.; Stoyanova, T.; Hess, R. A.; Bagchi, S.; Raychaudhuri, P. Cul4A Is Essential for Spermatogenesis and Male Fertility. Dev. Biol. 2011, 352, 278–287. https://doi.org/10.1016/j.ydbio.2011.01.028.

(105) Yin, Y.; Liu, L.; Yang, C.; Lin, C.; Veith, G. M.; Wang, C.; Sutovsky, P.; Zhou, P.; Ma, L. Cell Autonomous and Nonautonomous Function of CUL4B in Mouse Spermatogenesis. J. Biol. Chem. 2016, 291, 6923–6935. https://doi.org/10.1074/jbc.M115.699660.

(106) Yin, Y.; Zhu, L.; Li, Q.; Zhou, P.; Ma, L. Cullin4 E3 Ubiquitin Ligases Regulate Male Gonocyte Migration, Proliferation and Blood-Testis Barrier Homeostasis. Cells 2021, 10, 2732. https://doi.org/10.3390/cells10102732.

(107) Wu, H.; Sun, L.; Wen, Y.; Liu, Y.; Yu, J.; Mao, F.; Wang, Y.; Tong, C.; Guo, X.; Hu, Z.; Sha, J.; Liu, M.; Xia, L. Major Spliceosome Defects Cause Male Infertility and Are Associated with Nonobstructive Azoospermia in Humans. Proc. Natl. Acad. Sci. 2016, 113, 4134–4139. https://doi.org/10.1073/pnas.1513682113.

(108) Chen, X.; Luan, X.; Zheng, Q.; Qiao, C.; Chen, W.; Wang, M.; Yan, Y.; Xie, B.; Shen, C.; He, Z.; Zhang, J.; Liu, M.; Hu, X.; Li, H.; Zheng, B.; Fang, J.; Yu, J. Precursor RNA Processing 3 Is Required for Male Fertility, and Germline Stem Cell Self-Renewal and Differentiation via Regulating Spliceosome Function in Drosophila Testes. Sci. Rep. 2019, 9, 9988. https://doi.org/10.1038/s41598-019-46419-x.

(109) Qin, J.; Huang, T.; Wang, Z.; Zhang, X.; Wang, J.; Dang, Q.; Cui, D.; Wang, X.; Zhai, Y.; Zhao, L.; Lu, G.; Shao, C.; Li, S.; Liu, H.; Liu, Z. Bud31-Mediated Alternative Splicing Is Required for Spermatogonial Stem Cell Self-Renewal and Differentiation. Cell Death Differ. 2023, 30, 184–194. https://doi.org/10.1038/s41418-022-01057-1.

(110) Wang, X.; Xie, W.; Yao, Y.; Zhu, Y.; Zhou, J.; Cui, Y.; Guo, X.; Yuan, Y.; Zhou, Z.; Liu, M. The Heat Shock Protein Family Gene Hspa1l in Male Mice Is Dispensable for Fertility. PeerJ 2020, 8, e8702. https://doi.org/10.7717/peerj.8702.

(111) Liu, X.; Teng, Z.; Wang, Z.; Zhu, P.; Song, Z.; Liu, F. Expressions of HSPA1L and HSPA9 Are Associated with Poor Sperm Quality of Low-Motility Spermatozoa in Fertile Men. Andrologia 2022, 54, e14321. https://doi.org/10.1111/and.14321.

(112) Anbazhagan, R.; Kavarthapu, R.; Dufau, M. L. Chromatoid Bodies in the Regulation of Spermatogenesis: Novel Role of GRTH. Cells 2022, 11, 613. https://doi.org/10.3390/cells11040613.

(113) Tricas, T. C.; Maruska, K. P.; Rasmussen, L. E. L. Annual Cycles of Steroid Hormone Production, Gonad Development, and Reproductive Behavior in the Atlantic Stingray. Gen. Comp. Endocrinol. 2000, 118, 209–225. https://doi.org/10.1006/gcen.2000.7466.

(114) Awruch, C. A. Reproductive Endocrinology in Chondrichthyans: The Present and the Future. Gen. Comp. Endocrinol. 2013, 192, 60–70. https://doi.org/10.1016/j.ygcen.2013.05.021.

(115) Sourdaine, P.; Garnier, D. H.; Jégou, B. The Adult Dogfish (Scyliorhinus Canicula L.) Testis: A Model to Study Stage-Dependent Changes in Steroid Levels during Spermatogenesis. J. Endocrinol. 1990, 127, 451–460. https://doi.org/10.1677/joe.0.1270451.

(116) Murat, F.; Mbengue, N.; Winge, S. B.; Trefzer, T.; Leushkin, E.; Sepp, M.; Cardoso-Moreira, M.; Schmidt, J.; Schneider, C.; Mößinger, K.; Brüning, T.; Lamanna, F.; Belles, M. R.; Conrad, C.; Kondova, I.; Bontrop, R.; Behr, R.; Khaitovich, P.; Pääbo, S.; Marques-Bonet, T.; Grützner, F.; Almstrup, K.; Schierup, M. H.; Kaessmann, H. The Molecular Evolution of Spermatogenesis across Mammals. Nature 2023, 613, 308–316. https://doi.org/10.1038/s41586-022-05547-7.

# Annexes Chapitre I

## Supporting Information

**Comparative proteome analysis of four stages of spermatogenesis in the small-spotted catshark (*Scyliorhinus canicula*) using high-resolution nanoLC-ESI-MS/MS**

Fabian Jeanne[1], Benoît Bernay[2], and Pascal Sourdaine[1,*]

[1] Université de Caen Normandie, MNHN, SU, UA, CNRS, IRD, Laboratoire de Biologie des Organismes et Ecosystèmes Aquatiques (BOREA), UMR 8067, 14032 Caen cedex 5, France.

[2] Université de Caen Normandie - Plateforme PROTEOGEN, US EMerode, 14032 Caen cedex 5, France.

*Corresponding Author: orcid.org/0000-0001-9811-2876; Email: pascal.sourdaine@unicaen.fr

# I. Annexes chapitre I : Données supplémentaires

**Supplementary material**

**Comparative proteome analysis of four stages of spermatogenesis in the small-spotted catshark (*Scyliorhinus canicula*) using high-resolution nanoLC-ESI-MS/MS**

Fabian Jeanne[1], Benoît Bernay[2], and Pascal Sourdaine[1,*]

[1] Université de Caen Normandie, MNHN, SU, UA, CNRS, IRD, Laboratoire de Biologie des Organismes et Ecosystèmes Aquatiques (BOREA), UMR 8067, 14032 Caen cedex 5, France.

[2] Université de Caen Normandie - Plateforme PROTEOGEN, US EMerode, 14032 Caen cedex 5, France.

*Corresponding Author: orcid.org/0000-0001-9811-2876; Email: pascal.sourdaine@unicaen.fr

**Supporting Information**

**Table of Contents**

**Figure S1.** Histological section of the testis ..... **S1**

**Figure S2.** Overall workflow of proteome analysis ..... **S2**

**Figure S3.** Sample quality control of biological replicates ..... **S3**

**Figure S4.** Principal component analysis of proteins found in all four zones ..... **S4**

**Figure S5.** Venn diagram of proteins identified in the four testicular zones ..... **S5**

**Figure S6.** Blastp results against *C. milii*, *D. rerio*, *G. gallus*, *X. leavis*, *M. musculus*, *H. sapiens* ..... **S6**

**Figure S7.** Analysis of *S.canicula* PA28β-like ..... **S7**

**Reference** ..... **S8**

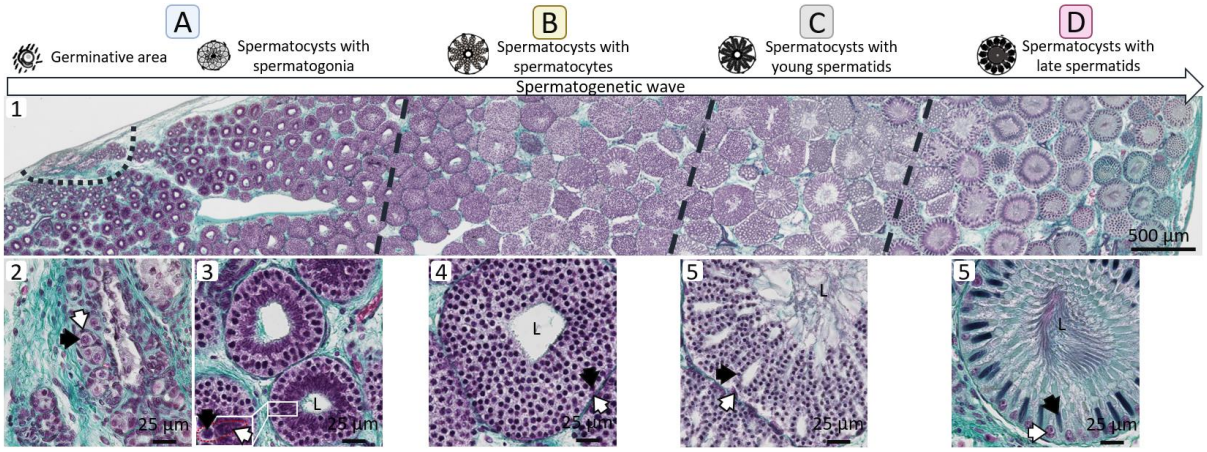


**Figure S1.** Histological section of the testis. Histological section of the small-spotted catshark testis. (1): Representative view of a testis section from the germinative area (small dotted line) to the opposite margin of the testis where spermiation occurs; the arrow represents the spermatogenic wave from zone A to zone D; large dotted lines represent margins between the four zones A, B, C and D. (2): Germinative area showing somatic cell precursors (whitehead arrow) and undifferentiated spermatogonia (blackhead arrow), the two types of cells proliferate and progressively aggregate to form spherical spermatocysts (cysts) with a progressively emerging lumen (L). (3): illustration of the zone A with a stage corresponding to the end of cyst formation with a single layer of Sertoli cell nuclei (whitehead arrow) in adluminal position and a single layer of spermatogonia (blackhead arrow) in basal position of the cyst. At this stage, the Sertoli cells stop proliferating and form a spermatoblast consisting of one Sertoli cell associated with one spermatogonia (Insert). (4): illustration of zone B with a cyst containing about six layers of primary spermatocytes (blackhead arrow), the Sertoli cell nuclei are in a basal position (whitehead arrow). (5): illustration of zone C with a cyst containing round spermatids arranged in a “festoon” pattern (blackhead arrow) and Sertoli cell nuclei in basal position (whitehead arrow). (6): illustration of zone D with a cyst containing parallel bundles of late spermatids (blackhead arrow) and Sertoli cell nuclei in basal position (whitehead arrow).

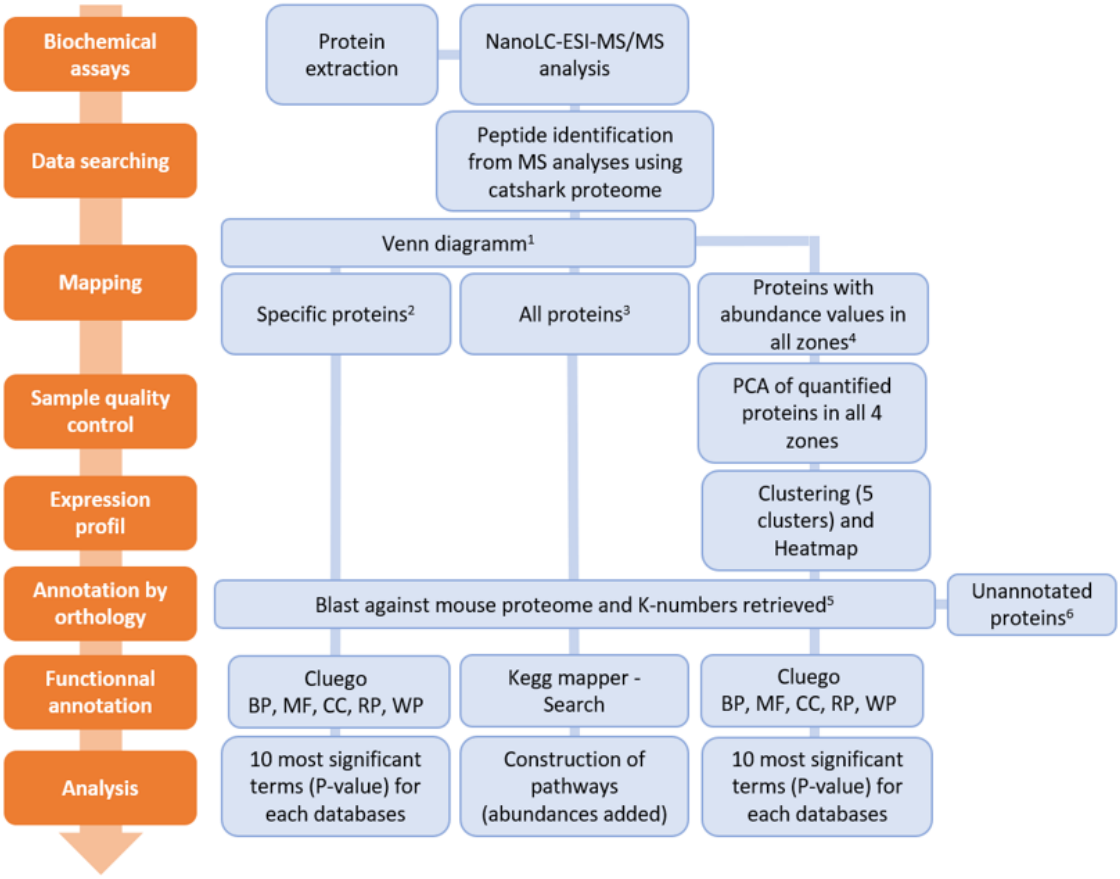


**Figure S2**. Overall workflow of proteome analysis based on the total proteins identified by NanoLC-ESI-MS/MS in the four testicular zones of the catshark, *Scyliorhinus canicula*. Number of corresponding accessions: [1]: 6744 Acc. Sc.; [2]: 1011 Acc. Sc. (ZoneA), 299 Acc. Sc. (ContinuumB), 273 Acc. Sc. (ContinuumC), 795 Acc. Sc. (Zone D); [3]: 6744 Acc. Sc.; [4]: 1284 Acc. Sc.; [5]: 2969 Acc. Mm., 2584 k-numbers; [6]: 377 Prot. Gr. Sc.. Acc. Sc.: Accessions of *Scyliorhinus canicula*; Acc. Mm.: Accessions of *Mus musculus*; Prot. Gr. Sc.: protein groups of *Scyliorhinus canicula*; BP: biological process; MF: molecular function; CC: cellular component; RP: reactome pathway; WP: wikipathway.

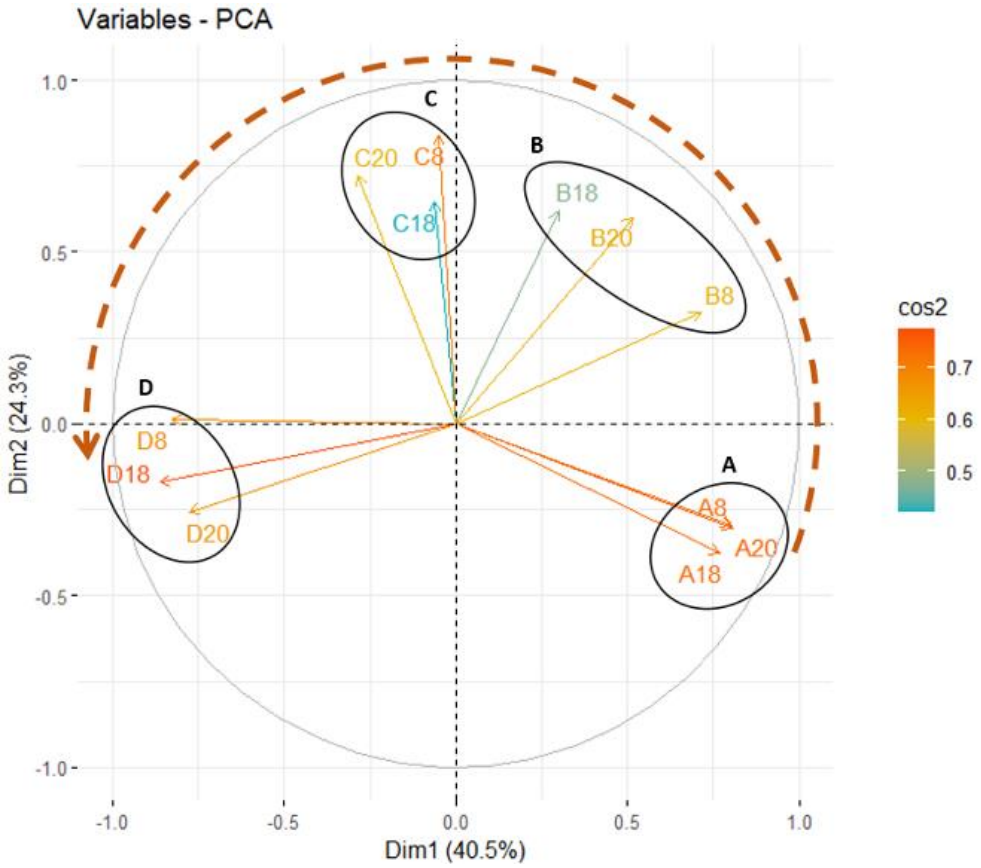


**Figure S3**. Sample quality control of biological replicates (N = 3), considering only the 1284 catshark proteins retrieved in all four zones, by principal component analysis and k-means clustering. Cos2 color gradient indicate the representation qualities of samples considering both selected dimension for representation. Black circles represent the clusters obtained for biological replicates for zone A, zone B, zone C and zone D (for the highest BSS/TSS ratio obtained of 0.75). The brown arrow represents the spermatogenetic wave.

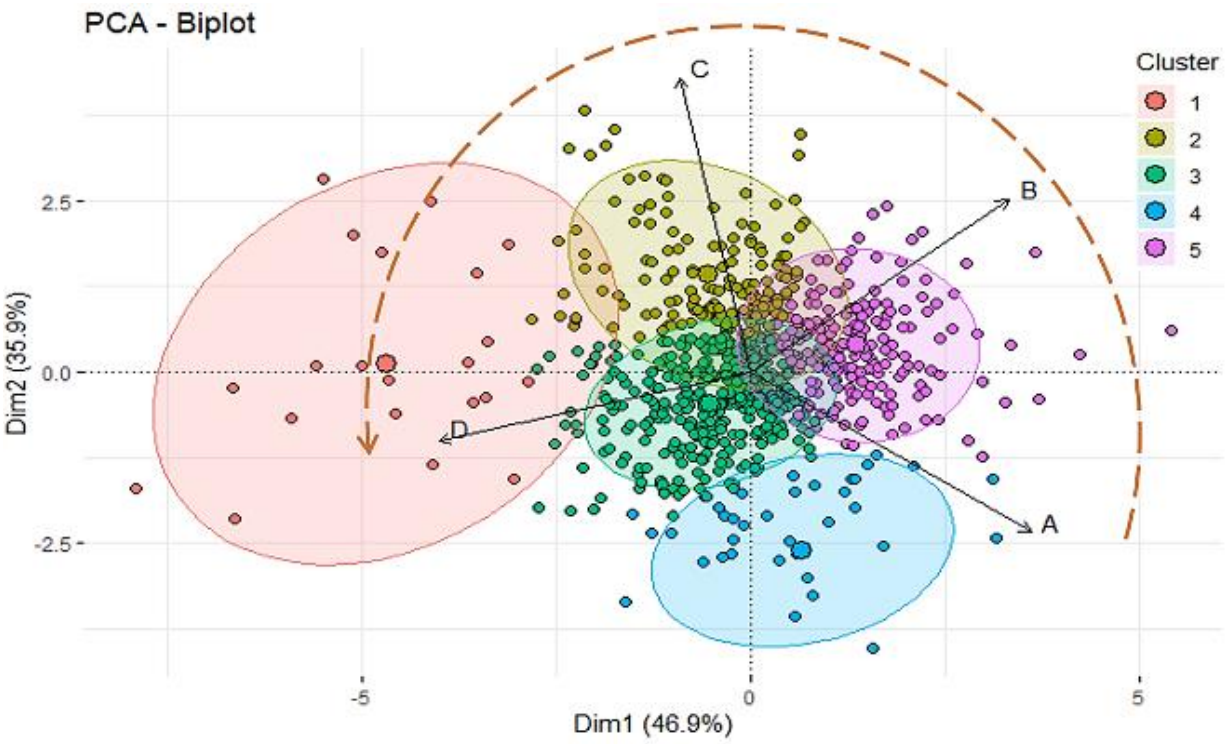


**Figure S4.** Principal component analysis of testicular zones (Means of replicates, N = 3) with clustering, using hierarchical ascending classification with euclidean distance and ward method, of the 1284 catshark proteins found in the four zones. The cluster 1 (red) is composed by 30 catshark proteins, the cluster 2 (yellow) by 241, the cluster 3 (green) by 561, the cluster 4 (blue) by 88 and the cluster 5 (pink) by 364 proteins represented by the smallest points. The larger points represent centers of clusters and the elipse represent confidence interval of 95%. The brown arrow represents the spermatogenetic wave.

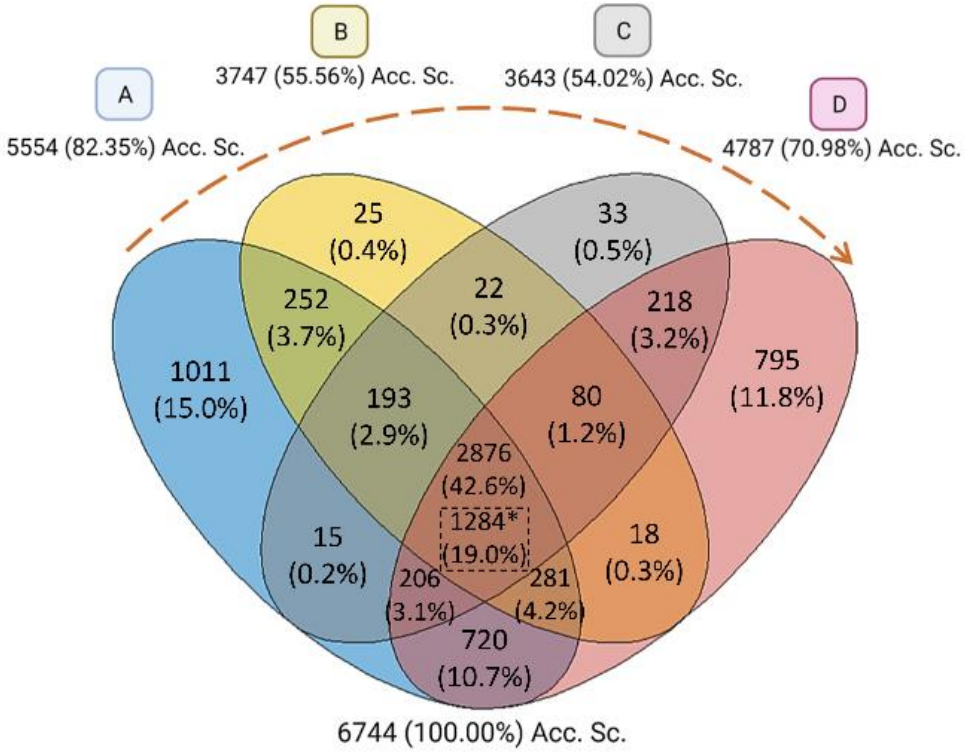


**Figure S5**. Mapping, using venn diagram, of the 6744 catshark proteins obtained by NanoLC-ESI-MS/MS analysis according to the four testicular zones. A: zone A; B: zone B; C: zone C; D: zone D; Acc. Mm.: accessions of Mus musculus; *: putative homologs retrieved in all four zones with abundance values. The brown arrow represents the spermatogenetic wave.

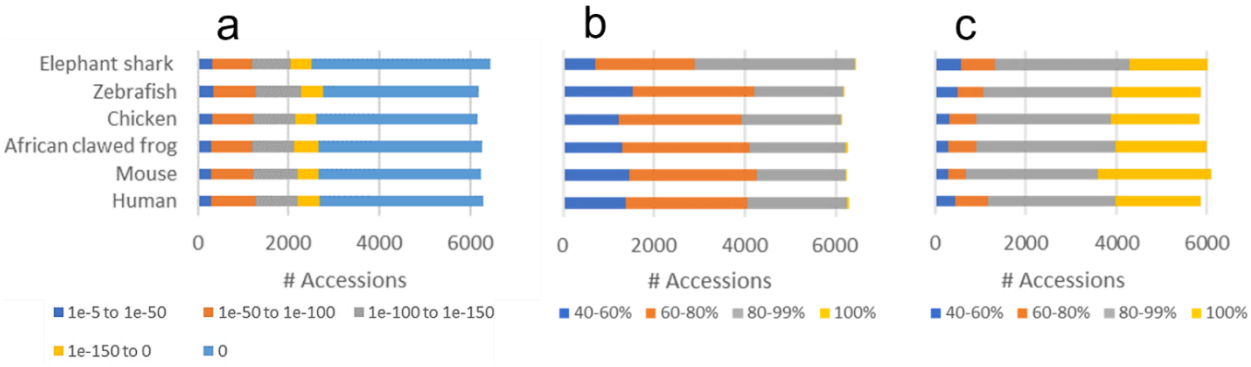


**Figure S6**. Control indicators analysis after the blastp of the 3346 catshark protein groups (6744 proteins) against the *Mus musculus* proteome where 2969 putative homologs proteins were obtained. a: e-value distribution; b: percentage of identity distribution; c: percentage of coverage distribution.

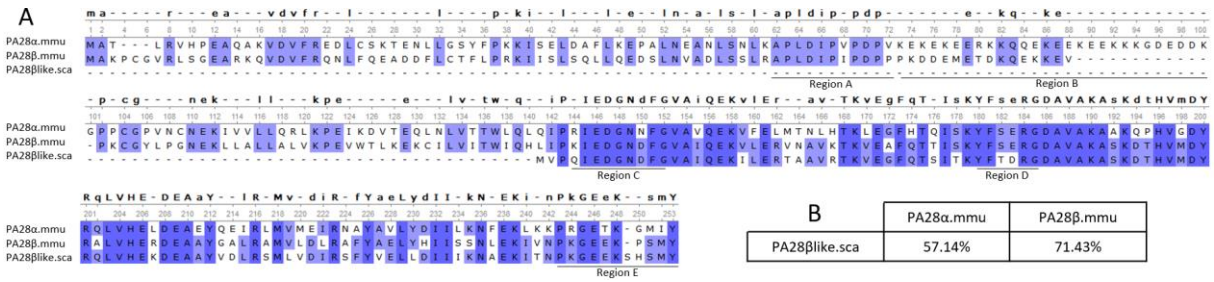


B

| | PA28α.mmu | PA28β.mmu |
|---|---|---|
| PA28βlike.sca | 57.14% | 71.43% |

**Figure S7.** Analysis of *S.canicula* PA28β-like. (A): Multiple alignment of *Mus musculus* PA28α (P97371), *Mus musculus* PA28β (P97372) and *Scyliorhinus canicula* PA28β-like (XP_038630988.1). The characteristic regions were placed, based on the work of Tan *et al.*[1], with the proline-rich motif (Region A, position 62-72), the KEKE motif (Region B, position 73-100), the potential protein kinase C recognition site (Region C, 144-152), the activation loop (Region D, position 180-185) and the C-terminal region (Region E, position 243-253). (B): Percentage of identities between catshark and mouse sequences.

Reference

(1) Tan, Y.; Lu, Q.; Li, L.; Zhu, Y.; Fu, B. Molecular cloning and tissue transcriptional analysis of a novel gene encoding proteasome activator PA28-α from common carp (Cyprinus carpio L.). *Fish. Sci.* **2010**, *76*, 511-519. https://doi.org/10.1007/s12562-010-0226-6.

# Chapitre II

## Characterization of gonadotropins and their receptors in a chondrichthyan, *Scyliorhinus canicula*, fills a gap in the understanding of their coevolution

**Fabian Jeanne, Stanislas Pilet, Danièle Klett, Yves Combarnous, Benoît Bernay, Sylvie Dufour, Pascal Favrel et Pascal Sourdaine**

# Chapitre II

## Characterization of gonadotropins and their receptors in a chondrichthyan, *Scyliorhinus canicula*, fills a gap in the understanding of their coevolution

**Fabian Jeanne, Stanislas Pilet, Danièle Klett, Yves Combarnous, Benoît Bernay, Sylvie Dufour, Pascal Favrel et Pascal Sourdaine**

*General and Comparative Endocrinology, Accepted*

# Caractérisation des gonadotrophines et de leurs récepteurs chez un Chondrichtyen, *Scyliorhinus canicula*, une lacune comblée dans la compréhension de leur coévolution

Chez les Vertébrés à mâchoire complète, la reproduction est principalement contrôlée par l'axe hypothalamo-hypophyso-gonadique (HHG), *via* les hormones folliculo-stimulante (FSH) et lutéinisante (LH). Ces hormones gonadotropes (GtHs) sont produites par l'adénohypophyse et activent leurs récepteurs associés, FSHR et LHR, exprimés au niveau des gonades. Chaque GTH est constituée d'une sous-unité α commune et d'une sous-unité spécifique, βFSH ou βLH. Au cours de l'évolution, la FSH, la LH et leurs récepteurs se seraient différenciés avant la divergence des Chondrichtyens (Holocéphales et Élasmobranches), ce qui rend ce groupe frère des vertébrés osseux essentiel à la compréhension de l'évolution des systèmes régulateurs de la reproduction. Cependant, compte tenu de leur intérêt, Il est surprenant de constater que la caractérisation des gonadotrophines et de leurs récepteurs est encore limitée chez les Chondrichtyens.

C'est dans ce contexte que cette étude a eu pour objectif d'identifier les séquences des sous-unités des GTHs (CGA, FSHβ et LHβ) et des GTHRs chez plusieurs espèces d'Élasmobranches, d'analyser leurs structures ainsi que leurs profils d'expression par PCR en temps réel et par des approches *in situ*, notamment au cours de la spermatogenèse, chez *Scyliorhinus canicula*. Les profils d'interactions ligand-récepteur ont également été étudiés à l'aide de protéines recombinantes en système de coexpression *in vitro*. L'ensemble des résultats obtenus a été discuté dans une perspective d'analyse de la co-évolution GTH/GTHR chez les Vertébrés.

Cette étude a mis en évidence la conservation des structures des sous-unités CGA, FSHβ et LHβ et des récepteurs FSHR et LHR chez les Élasmobranches, avec néanmoins une sous-unité LHβ structuralement plus proche de FSHβ que de la LHβ humaine. De plus, cette étude a mis en évidence la spécificité d'activation du LHR par la LH alors que FSHR apparait moins discriminant, puisqu'il peut être activé par la FSH et la LH. Ces résultats divergent des profils d'interactions spécifiques FSH/FSHR et LH/LHR identifiés chez la chimère éléphant *Callorhincus milii*, un Holocéphale. Ce profil d'interaction identifié chez les Élasmobranches apparait plus proche de celui des Téléostéens que de celui des Holocéphales et des Mammifères du fait que, chez les Téléostéens, FSHR apparait également moins discriminant,

ainsi que LHR qui peut être aussi activé par FSH chez la truite arc-en-ciel, le poisson zèbre et le médaka, mais pas chez l'anguille. Par ailleurs, l'analyse de l'expression des récepteurs a montré des niveaux plus élevés de FSHR dans les gonades et de LHR dans les tractus génitaux et les organes lymphomyéloïdes. Les deux récepteurs sont exprimés au cours de la spermatogenèse au niveau des cellules germinales et somatiques, avec une expression plus élevée dans les stades précoces, ce qui soulève la question de l'implication des gonadotrophines dans la différenciation des spermatogonies indifférenciées et/ou des progéniteurs somatiques. Enfin, notre étude a cherché à inclure les résultats obtenus dans une perspective d'évolution parallèle des signalisations endocrines et des structures gonadiques. Pour cela, un modèle a été proposé dans lequel, chez les mâles, les cellules de Sertoli seraient les cellules somatiques fondamentalement associées à la spermatogenèse et les cellules de Leydig seraient des cellules somatiques de support, alors que, chez les femelles, les cellules de la thèque et de la granulosa se seraient différenciées avant l'émergence des Gnathostomes et seraient toutes les deux indispensables à la folliculogenèse.

Ce travail a donc permis de caractériser les séquences, les profils d'expressions et d'interactions des sous-unités des GTHs et de leurs récepteurs, ce qui a mis en évidence les spécificités physiologiques des Élasmobranches, possédant notamment un FSHR moins discriminant. De plus, par l'inclusion d'un nombre non-négligeable d'organes des tractus génitaux mâle et femelle, les expressions retrouvées de *Ihr* au niveau de l'épididyme, des ampoules séminales, des glandes nidamentaires et des oviductes suggèrent l'existence d'un axe hypothalamo-hypophyso-tractus génital. En plus de cette première exploration des régulations endocrines passant par les GTHs chez un Élasmobranche, ces données permettent de combler, au moins partiellement, le fossé de connaissances qui séparait les Cyclostomes des Ostéichtyens et donc, d'améliorer notre compréhension de l'origine et de l'histoire évolutive des régulations endocrines dépendantes des GTHs chez les Vertébrés.

**Characterization of gonadotropins and their receptors in a chondrichthyan, *Scyliorhinus canicula*, fills a gap in the understanding of their coevolution.**

Fabian Jeanne[1], Stanislas Pilet[1], Danièle Klett[2], Yves Combarnous[2], Benoît Bernay[3], Sylvie Dufour[1], Pascal Favrel[1] and Pascal Sourdaine*[1]

[1] Université de Caen Normandie, MNHN, SU, UA, CNRS, IRD, Laboratoire de Biologie des Organismes et Ecosystèmes Aquatiques (BOREA), UMR 8067, 14032 Caen cedex 5, France.

[2] INRAE, CNRS, UMR Physiologie de la Reproduction & des Comportements, 37380 Nouzilly, France

[3] Université de Caen Normandie - Plateforme PROTEOGEN, US EMerode, 14032 Caen cedex 5, France.

*Corresponding Author: orcid.org/0000-0001-9811-2876; Email: pascal.sourdaine@unicaen.fr

ABSTRACT

In Gnathostomes, reproduction is mainly controlled by the hypothalamic-pituitary-gonadal (HPG) axis, with the involvement of the pituitary gonadotropic hormones (GTH), follicle-stimulating hormone (FSH) and luteinizing hormone (LH), which activate their cognate receptors, FSHR and LHR, expressed in gonads. Each GTH consists of a common α subunit and of a specific FSHβ or LHβ subunit. Chondrichthyes (holocephalans and elasmobranchs) is a sister group of bony vertebrates. This position is highly favorable for the understanding of the evolution of endocrine regulations of reproduction among gnathostomes. Surprisingly, the characterization of gonadotropins and their receptors is still limited in chondrichthyes. In the present study, GTH and GTHR sequences have been identified from several chondrichthyan genomes, and their primary structures were analyzed relative to human orthologs. 3D models of GTH/GTHR interaction were built, highlighting the importance of the receptor hinge region for ligand recognition. Functional hormone-receptor interactions have been studied in HEK cells using the small-spotted catshark (*Scyliorhinus canicula*) recombinant proteins and

showed that LHR was specifically activated by LH whereas FSHR was activated by both FSH and LH. Expression profiles of GTHs and their receptors were explored by real-time PCR*, in situ* hybridization and immunohistochemistry during spermatogenesis, along the male genital tract and other tissues, as well as in some female tissues for comparison. Tissue-expression analyses showed that the highest levels were observed for *fshr* transcripts in testis and ovary and for *lhr* in specific extragonadal tissues. The two receptors were expressed at all stages of spermatogenesis by both germ cells and somatic cells, including undifferentiated spermatogonia, spermatocytes, spermatids, somatic precursors and Sertoli cells; differentiated Leydig cells being absent in the testis of *S. canicula*. Receptors were also expressed by the lymphomyeloid epigonal tissue and the testicular tubules. These results, suggest a wide range of gonadotropin-regulated functions in Elasmobranchs, as well as functional redundancy during spermatogenesis. These extended functions are discussed in an evolutionary context in which the specificity of gonadotropin signaling must have contributed to the evolution of gonadal cells' morphology and function.

Keywords: Gonadotropins, Gonadotropin receptors, Follicle-stimulating hormone, Luteinizing hormone, Spermatogenesis, Chondrichthyes, Elasmobranchs, Shark, Evolution, Testis, Epididymis.

## 1. Introduction

Gonadotropic hormones (GTH) and their receptors (GTHR) of the hypothalamic-pituitary-gonadal (HPG) axis play a crucial role in the endocrine regulation of reproduction (Campbell, 2004). GTHs belong to the glycoprotein hormones (GPHs) family, also including thyroid-stimulating hormone (TSH). They comprise a common α-subunit (CGA) and a specific β-subunit (LHβ, FSHβ or TSHβ) that are non-covalently associated, and interact with their cognate leucine-rich repeat G protein-coupled receptors (LGRs) (Hsueh and Feng, 2020). They are classic examples of the coevolution of ligand-receptor interaction complexes following their ancient evolutionary origin (Kudo et al., 2000). In fact, an ancestral form of LGRs has been identified in Placozoa and its subsequent evolution has given rise to three types of receptors, including subtype A LGRs found as early as in cnidaria, which could be considered the GPH receptor (GPHR) ancestral form (Van Hiel et al., 2012). In the same way, an early tandem duplication of a single ancestral gene encoding a cystine knot protein led to the first two GPHs subunit genes, *gpa2* and *gpb5* identified in ecdysozoans (Kudo et al., 2000; Sudo et al., 2005) and lophotrochozoans (Heyland et al., 2012) and which can be considered the ancestors of the α- and β-subunits families. In the oldest lineage of vertebrates (cyclostomata), GPA2 and GPB5 were identified at the same time as the ancestral GpHβ has emerged concomitantly (at the evolution scale) with a first diversification of GPHRs, as shown by the identification of GpHRI and GpHRII, in the lamprey (Hausken et al., 2018; Hsueh and He, 2018). Furthermore, the recombinant heterodimer GPA2/GPB5 could activate the two receptors while GPA2/GpHβ activated only GpHRI (Hausken et al., 2018). Then, the two differentiated GTHs corresponding to the follicle stimulating hormone (FSH) and luteinizing hormone (LH), with their respective receptors, FSHR and LHR, would have emerged in chondrichthyes, before their divergence in osteichthyes (bony vertebrates) estimated to have occurred around 450-million years ago (Buechi and Bridgham, 2017). The chondrichthyes include holocephalans (chimeras) and elasmobranchs (sharks and rays) which diverged around 300-million years ago (Irisarri et al., 2017). In the chimaera *Callorhinchus milii,* which was the first sequenced chondrichthyan genome (Venkatesh et al., 2014), all the genes encoding GPH subunits or subunits' ancestors (GPA2, CGA, GPB5, LHβ, FSHβ and two TSHβ, TSHβ1 and TSHβ2) and their receptors (FSHR, LHR and TSHR) were identified for the first time (Buechi and Bridgham, 2017; Maugars et al., 2014; Maugars and Dufour, 2015). Advances in the sequencing of elasmobranchian genomes

(from 5 sharks and 4 rays, notably) are now making it possible to include elasmobranchs more widely in evolutionary analyses of GPHs/GTHs and their receptors, sequences of which have been identified in some sharks (e.g., *Scyliorhinus torazame* (Hara et al., 2018; Arimura et al., 2024)). In actinopterygians, tandem gene duplication of *lhr* led to duplicated *lhr1* and *lhr2*, conserved in teleosts (Maugars and Dufour, 2015). The teleost-specific whole genome duplication (3R) had no impact on the number of GTHR in teleosts, due to paralog gene losses early after 3R, leading to only one or two *lhr* and a single *fshr* (Chauvigné et al., 2010; Dufour et al., 2020; Maugars and Dufour, 2015). In primates, a particular feature has been the specific tandem gene duplication of *Lhb* at the origin of the chorionic gonadotropin subunit β (CGB) expressed in the placenta, giving the human chorionic gonadotropin (hCG) which has the ability to bind to LHR (Maston and Ruvolo, 2002). Interestingly, while the specificity of LHR and FSHR has long been established in mammals, and recently in the holocephalan *C. milii* (Buechi and Bridgham, 2017), FSHR appeared less discriminating in various teleosts and can be activated by LH in addition to FSH (Andersson et al., 2009; García-López et al., 2009; Kazeto et al., 2008; Suzuki et al., 2020). It has also been reported that LHR may also be activated by FSH in the rainbow trout, the zebrafish and the medaka (Burow et al., 2020; Sambroni et al., 2007; Xie et al., 2017) but not in the eel (Suzuki et al., 2020), suggesting that LH and FSH specificity might have varied during evolution.

The specificity of the GTHRs activation by GTHs is determined by their structures, which are mainly studied in humans. Alpha and β subunits are cystine-knot proteins containing disulfide bonds (SS) arranged in such a way that one SS bond crosses the ring formed by the other SS bridges (Lapthorn et al., 1994). Heterodimerization of the α and β subunits involves a low-affinity interaction between two regions named “seat”, followed by wrapping of the α subunit by the “seat-belt” consisting of the C-terminus of the β subunit and finally locking of the specific SS bridge, called “buckle”, involved in dynamic stability of the heterodimer (Belghazi et al, 2006; Burova et al, 2001; Galet et al. 2004; Hiro’oka et al., 2000; Jiang et al., 2014a; Lapthorn et al., 1994).

GTHRs are characterized by a large N-terminal ectodomain presenting a curved solenoid (horseshoe) with leucine-rich repeats domains (LRR), N-glycosylation sites and a “hinge” region containing a potentially sulfated tyrosine residue (reviewed in Helenius and Aebi, 2004; Vassart, 2004). Their transmembrane domain is characterized by seven transmembrane α-

helix (7TM), three extracellular loops (EL) interacting with the “hinge” region (Jiang et al., 2014a) and three intracellular loops (IL) involved in the activation of G protein-dependent signaling pathways (reviewed in Johnson and Jonas, 2020; Nechamen et al., 2007). The C-terminal domain is characterized by various motifs involved in intracellular trafficking (reviewed in Dong et al., 2007), receptor desensitization, recycling and $G_s$-independent ERK1/2-mediated signaling in several mammals (Kara et al., 2006; Marion et al., 2006; Troispoux et al., 1999; Wehbi et al., 2010).

The study of the biological functions of gonadotropins and their receptors has been the subject of extensive research in vertebrates for many years. Classically, in osteichthyes, including actinopterygians such as teleosts and sarcopterygians (mammals, birds, amphibians), FSH and LH are secreted by pituitary gonadotroph cells into the general bloodstream to regulate gametogenesis and steroidogenesis in males and females (reviewed in Oduwole et al., 2021). Extra-pituitary expression of LH and FSH as well as of their receptors in extragonadal tissues have been also reported (Dufour et al., 2020; Johnson and Jonas, 2020). Surprisingly, few studies have been carried out on gonadotropins functions in the chondrichthyes, despite this group occupies an interesting phylogenetic position as the sister group to the osteichthyes. In chondrichthyes, *cga*, *fshβ* and *lhβ* were shown to be mainly expressed in the ventral lobe of the pituitary, and *fshr* and *lhr* expressed in the gonads as studied in the catshark *S. torazame* (Hara et al., 2018). However, these data are still insufficient to understand GTH functions in elasmobranchs, hence the present study during spermatogenesis in the small-spotted catshark *Scyliorhinus canicula*. In this species, spermatogenesis occurs in spermatocysts made up of synchronously-developing germ cells associated with Sertoli cells, forming a zonal arrangement of the spermatogenetic wave. Thus, on a cross section of the testis, zones corresponding to different stages of spermatogenesis are easily distinguishable and accessible (Bosseboeuf et al., 2014; Gautier et al., 2014; Loppion et al., 2008). A particular feature of the elasmobranch testis is the absence of differentiated Leydig cells, which, nevertheless, is a matter of debate. Indeed, previous studies showed rare undifferentiated “Leydig-like” cells in the testes of the sharks *Squalus acanthias* (Pudney and Callard, 1984) and *S. canicula* (Loir et al., 1995), but differentiated Leydig cells in the ray *Torpedo mormorata* (Prisco et al., 2002), which may correspond to the forerunners of true vertebrate Leydig cells of bony vertebrates (Callard, 1991; Engel and Callard, 2007). Another

unique feature in elasmobranchs is the epigonal tissue, a lymphomyeloid tissue at the ventral testicular, where spermiation occurs (Manca et al., 2019). Anatomically, the male genital tract of elasmobranchs is complex. Spermatozoa converge through collecting tubules into efferent ducts, subsequently forming the epididymis, which also receives fluid from its adjacent Leydig's gland. The epididymis is followed by a deferent duct which is enlarged at its end and forms the seminal ampullae where spermatozoa are stored (Park et al., 2013).

In the present study, sequences of GTH subunits, including CGA, FSHβ and LHβ and of corresponding GTHRs have been identified in several elasmobranch species. Protein structures have been analyzed and expression patterns explored by real-time PCR and *in situ* approaches during spermatogenesis and in different tissues in the small spotted catshark as a model species. Functional hormone-receptor interactions have also been studied using recombinant proteins and *in vitro* bioassays. The results are discussed from an evolutionary perspective of the parallel evolution of endocrine signaling systems and gonadal structures.

## 2. Materials and Methods

### *2.1. Animals and Tissue Sampling*

In 2020, the catshark *Scyliorhinus canicula* was assessed as a least concern species in the red list of threatened species by the IUCN (International Union for Conservation of Nature). Sexually mature male (608 ± 137 g; 58± 3 cm) and adult female (647 ± 90 g; 57 ± 4 cm) catsharks were fished during a CGFS (Channel Ground Fish Survey) campaign by IFREMER in the East Manche in September 2022 (Giraldo et al., 2022). Although females have an extended breeding season, with maximum egg-laying frequency from December to June (Sumpter and Dodd, 1979), females caught in September had their lowest gonadosomatic index and their ovaries consisted of post-ovulatory follicles and a few early vitellogenic follicles. Animals were maintained in natural seawater tanks at the marine station of the University of Caen Normandy (*Centre de Recherches en Environnement Côtier* (CREC), Luc-sur-Mer, France). The CREC experimental facilities were approved by the council department of population care under the A14384001 number (*Préfecture du Calvados*, France). Catsharks were allowed to acclimate at least 2 weeks before collection of the samples. Animals were killed by percussive blow to the head followed by sectioning and pithing of the spinal cord and exsanguination

according to the European directive 2010/63/UE for care and use of animals. Testes, epigonal tissues, proximal and distal epididymis, seminal ampullae, myelencephalons, cerebellum, midbrains corresponding to diencephalon and mesencephalon and including pituitaries, forebrains, olfactory bulbs, eyes, thyroid glands, Leydig organs, spleens, livers, pancreas, duodenums, kidneys, rectal glands, gills, hearts and muscles were sampled from 14 males and myelencephalons, cerebellum, midbrains, forebrains, olfactory bulbs, ovaries, nidamental glands, oviducts, uterus and thyroid glands from 7 females and were transferred directly in liquid nitrogen before being stored at -80°C until RNA extractions. Fresh testicular cross sections were transferred into ice-cold Gautron's buffer (pH 7.8, 890 mOsmol kg-1) (Gautron, 1978) completed by 58 mM trimethylamine-N-oxide (TMAO, Sigma, 317594), then microdissected into zones A, B, C and D corresponding to the zone of undifferentiated spermatogonia and cysts with spermatogonia, the zone of cysts with spermatocytes, the zone of cysts with early spermatids and the zone of cysts with late spermatids, respectively (Loir and Sourdaine, 1994). Tissues used for IHC and ISH were fixed in Gautron's buffer with paraformaldehyde 4% before alcoholic dehydration and stocked in butan-1-ol at -20°C.

*2.2. Sequence searches*

Protein sequences of CGA, FSHβ and LHβ subunits and their receptors were identified using BLAST searches, based on *C. milii* sequences (Buechi and Bridgham, 2017), against genomes of *Amblyraja radiata* (sAmbRad1.1.pri), *Carcharodon carcharias* (Marra et al., 2019), *Chiloscyllium plagiosum* (ASM401019v1), *Chiloscyllium punctatum* (Hara et al., 2018), *Pristis pectinata* (sPriPec2.1.pri), *Rhincodon typus* (Read et al., 2017), *S. canicula* (sScyCan1.2) and *S. torazame* (Hara et al., 2018) on NCBI (https://www.ncbi.nlm.nih.gov/genome/); of *Hemitrygon akajei* (sHemAka1.1) on Squalomix Blast Server (https://transcriptome.riken.jp/squalomix/blast/); and of *Leucoraja erinacea* (Wang et al., 2012) on Skatebase (http://skatebase.org). To assess the relationship between obtained sequences and their putative families, phylogenetic trees were built based on the previous work of Buechi and Bridgham, 2017 using the MAFFT (Multiple Alignment using Fast Fourier Transform) program, BMGE (Block Mapping and Gathering with Entropy) alignment curation and PhylML tree inference on NGPhylogeny online services (https://ngphylogeny.fr/workflows/oneclick/, Lemoine et al., 2019) with a bootstrap of 1000. Obtained trees were finalized using iTOL online tool (https://itol.embl.de/, Letunic and Bork,

2021). Synteny analyses of *fshβ* and *lhβ* genes in *H. sapiens* and *S. canicula* were performed to verify the orthologs identified. The genes were mapped using NCBI's Genome Data Viewer (https://www.ncbi.nlm.nih.gov/genome/gdv/).

*2.3. Structural analyses and 3D model building*

Multiple alignments were performed using Clustal Omega package (https://www.ebi.ac.uk/Tools/msa/clustalo/, Sievers et al., 2011) with manual corrections to identified conserved structures (based on the knowledge in *H. sapiens* sequences). Signal peptides were predicted using predisi software (http://www.predisi.de/). Predictive models of GTHs/GTHRs interaction complexes of *S. canicula* α, β-subunits and the ectodomain of GTHRs were built using SWISS-MODEL (https://swissmodel.expasy.org/, Waterhouse et al., 2018), using the 4mqw.1 and 7fii.1 templates of *Homo sapiens*, and finalized using Swiss PDB Viewer program (Johansson et al., 2012). Obtained models were evaluated by retaining global sequence identities with the template, the highest GMQE score (Global Model Quality Estimate, Waterhouse et al., 2018), which depends on coverage, and the highest QMEANDisCo Global score (Studer et al., 2020), which evaluates the model "as is" without explicit coverage dependency. The same procedure was performed with *H. sapiens* sequences, as control, and for *C. milii* sequences. Using Swiss-PdbViewer (Johansson et al., 2012), predicted models were superimposed and the Root Mean Square Deviation (RMSD) were calculated and averaged by GTHs and by GTHRs.

*2.4. Functional hormone-receptor interaction in* in vitro *assays*

Synthetic pTarget plasmids containing *S. canicula* cDNA sequences for *fshr* (*sc-fshr*) or *lhr* (*sc-lhr*) were obtained from Twist Bioscience (San Francisco, USA) and synthetic pTarget plasmids containing fusion construct *gphβ-cga* were obtained from GenScript Biotech (Rijswijk, Netherlands). Human embryonic kidney (HEK293T) cells were transiently transfected with the synthetic plasmid using FuGENE HD (Promega) according to the manufacturer's instructions. Co-transfection was done with *gphr*/pTarget construct and a pTarget expression construct for the human $G\alpha_{16}$ subunit, a promiscuous G protein which can direct intracellular signaling of GPCRs to the release of calcium *via* the phospholipase Cβ pathway, regardless of the endogenous G protein coupling of the receptor. The pTarget ligand constructs were transfected in HEK293T cells at around 80% confluence in 150 $cm^2$ flasks, then after 24 h of

culture, the media were collected and concentrated using Amicon® 3K filters (Millipore). Cells for negative control experiments were transfected with empty pTarget or *hs*Gα16 and empty pTarget. Activation of the *S. canicula* GTHRs by GTHs was monitored using a fluorescence-based calcium mobilization assay according to (Schwartz, 2021). Briefly, transfected HEK293T cells were loaded with Fluo-4 Direct (Invitrogen) for 1 day at 37°C with 5% $CO_2$. Excitation of the fluorophore was done at 488 nm. The calcium response was measured at 525 nm for 2 min using a Flexstation 3 (Molecular Devices) at 37°C and analyzed using SoftMax Pro (Molecular Devices). For analysis of the activation of the Gαs/adenylyl cyclase/cAMP/PKA pathway, transfected cells were incubated with Glosensor cAMP reagent (4% final concentration in media) (Promega) for 2 h at room temperature prior the injection of the ligands (*sc*FSHβ-*sc*CGA, *sc*LHβ-*sc*CGA or *sc*TSHβ-*sc*CGA, as negative control and intracellular cAMP concentration was estimated by the luminescence response measured at 37°C for 30 min using the Flexstation 3.

To determine the absolute concentration of the ligand produced, an initial proteomic analysis of the ligand-containing media was carried out using high-resolution nanoLC-ESI-MS/MS to identify a peptide resulting from trypsin digestion of the common α-subunit (CGA). The criteria for the choice of this peptide were the absence of cysteine residue, the absence of post-translational modifications, and a number of amino acids superior to 5. The selected peptide (VTLMGNLK) was synthesized by CliniSciences (Nanterre, France) and used as an internal quantity marker. The standard curve was established, ranging from 16.3 pg/µl to 666 pg/µl, and the equation obtained was y = 400,05x - 6339,1 ($R^2$ = 0,9967) where “y” was the peak area of the peptide and “x” the concentration. Half maximum effective concentrations ($EC_{50}$ values) and activation percentages were calculated with 95% confidence intervals (profile likelihood) from sigmoidal dose-response equations which were constructed with a nonlinear regression analysis using Prism 5.0 (GraphPad Software, USA). A more sensitive *in vitro* bioassay has also been used, according to Klett and Combarnous, 2021. Developed to measure luteinizing hormone and chorionic gonadotropin concentrations in the plasma of most mammalian species, this system used mLTC Leydig cell line (ATCC CRL-2065) transiently co-transfected with the cAMP Glosensor reporter gene (Promega) and the *gthr* of interest. The scGTHb-scCGA ligands were produced in CHO-K1 cell line (ATCC CCL-61), and the supernatants were tested on mLTC cells previously preincubated for 2 hours in the presence of $10^{-3}$M IBMX (3-isobutyl-

1-methylxanthine), $10^{-5}$M forskolin, $10^{-8}$M oxytocin (OXT) and 1% Glosensor cAMP reagent. Intracellular cAMP concentration was estimated by the luminescence response measured at 28°C for 60 min using a Polarstar Optima (BMG Labtech Sarl, Champigny sur Marne, France).

*2.5. Reverse Transcription and real-time PCR*

Total RNAs were extracted from *S. canicula* tissues using Tri-Reagent (Sigma-Aldrich, 93289) before purification with the NucleoSpin RNAII columns kit (Machery-Nagel). They were quantified on a NanoDrop™ 2000 (Thermo Scientific) and their qualities were analyzed on an Agilent 2100 Bioanalyzer (Agilent). Obtained RINs (RNA integrity number) were greater than 7. For tissue distribution, real-time PCR was performed independently for three animals (N=3) in triplicate (n=3) except for testes (zone A, B, C and D) and epigonal tissues where six animals were used (N=6, n=18). The CFX Connect Detection System (Bio-Rad) was used for real-time PCR analyses. Two hundred and seventy ng of total RNAs were treated with 1U of RQ1 DNase (Promega, M6101) (37°C/20min) following by the reverse transcription using 1 ng of random hexanucleotide primers (Promega, C1181), 0.5 mM dNTPs and 200 U of M-MLV Reverse Transcriptase (Promega, M1701) then the reactions were stopped (70°C/5min). The gene-specific primers were designed using Primer-BLAST (https://www.ncbi.nlm.nih.gov/tools/primer-blast/, Ye et al., 2012) with manual corrections to take into account the following criteria: length between 18-22 bp, GC content over 50%, Tm close to 60°C and generation of an 150-200 bp amplicon (supplementary data Table S1). The real-time PCR monitoring of amplifications (5 ng of cDNA, 40 cycles: 95°C/15s, 60°C/45s), the GoTaq®qPCR Master Mix (Promega, A6001) was used and melt curve analysis and efficiency tests were carried out to ensure the primers amplified a single product with 90-110% efficiency. The Ct values were read at 200 relative fluorescence units and normalized against the 5S RNA (Redon et al., 2010), using the $\Delta C_t$ method (Schefe et al., 2006). The $2^{-\Delta\Delta Ct}$ method (Livak and Schmittgen, 2001) allowed to calculate the expression variations based on the mean $\Delta C_t$ of all tissues. Comparison of the Ct 5SRNA/total RNA ratio between tissues shown no significant difference using none parametric Kruskal-Wallis test with a P-value of 0.11 (supplementary data Fig. S1). Statistical analyses were performed using the non-parametric Mann-Whitney U (based on the previous Shapiro-wilk test results) test for P-value $< 0.05$.

*2.6. In situ hybridization (ISH)*

Digoxigenin-conjugated riboprobes were synthesized from cDNA clones produced with specific primers (supplementary data Table S1). The resulting amplicons were cloned in pCR™II-TOPO™ Vector by TA cloning and then transformed in chemically competent *E. coli* using the TOPO TA Cloning kit (Invitrogen, k461020). After cultures, plasmids were purified using the Wizard® Plus SV Minipreps (Promega, A1340) then the digoxigenin-conjugated riboprobes were generated using M13 PCR on 100 ng of plasmids with 1 mM $MgCl_2$, 0.2 mM of each dNTPs, 0.4 µM M13 primer and 0.625 U GoTaq® Flexi DNA Polymerase (Promega, M8291). The cycling parameters were as follows: 1X(95°C, 5min), 30X[(95°C, 30s), (60°C, 45s), (72°C, 1min30s)], 1X(72°C, 5min). PCR products were quantified using Nanodrop 2000 spectrophotometer (Thermo Scientific) and then purified using the NucleoSpin RNA Clean-up (Marcherey-Nagel, 740948.50). The size checking was done using gel migration. *In vitro* transcriptions were carried out for 3 h at 37°C on 1.2 µg PCR products with 25 U RNAsin, 25 U T7 or SP6 polymerase, 10 mM dithiothreitol, 1 mM rATP, rCTP and rGTP, 0.65 rUTP, and 0.35 digoxigenin-UTP (Roche, 03359247910) using the Riboprobe® Combination Systems (Promega, P1460). DNAs were digested with 2 U RQ1 DNAse (Promega, M6101) for 30 min at 37°C. The resulting riboprobes were purified and their qualities were checked by dot blots on PVDF membrane. Paraffin slices (5 µm) were incubated at 61°C to facilitate deparaffinization using Roti-histol (sigma, 6640.6). Hydration was achieved by successive ethanol baths (100%, 95% and 70%), then by PBS. Between each of the following treatments, slices were washed into PBS. Slices were treated with 4% PFA in PBS, with 5 µg/ml proteinase k in Tris buffer for 4 min, with 4% PFA in PBS, with 100 mM Triethanolamine in 25 % acetic acid, then with 100 mM glycine in tris buffer. Tissues were incubated for 1 h at 65°C with the hybridization mix (50% deionized formamide, 1X saline-sodium citrate (SSC), 0.5 M Ethylenediaminetetraacetic acid (EDTA), 10% Tween 20, 1X Denhardt'solution, 28 mg/ml Dextran sulphate, 0.1 mg/ml heparin, 10% Chaps, 0.5 mg/ml tRNA). Then, 0.1-0.5 ng/µl riboprobes in hybridization mix were incubated overnight at 65°C. Slices were washed using successive baths of SSC (1X and 1.5X at 65°C, 2X at 37°C, 2X with 0.2 µg/ml of RNAse A (Promega, A797C) at 37°C, 2X, and 0.2X at 60°C) before maleic acid buffer baths with 0.3 % triton (MABT). For immunostaining and revelation, the DIG Nucleic Acid Detection kit (Roche, 11175041910) was used. Tissues were incubated 3 h in blocking solution then, overnight at 4°C, with 100 µl per slice of 1/2000 v/v anti-digoxigenin-AP-conjugate antibody 750 U/ml. According to the kit guidelines, slices were washed in MABT baths before being developed overnight at 4°C in NBT/BCIP. Finally, slices

were mounted in Mowiol mounting medium and then dried for 48 h at 4°C, before being observed using a Nikon eclipse 80i microscope.

*2.7. Immunohistochemistry (IHC)*

Tissues embedded in paraffin were cut into 5 µm sections with a microtome (Leica, Histocore Autocut R). The slices were deparaffined in roti-histol baths (Roth, 6640.2), rehydrated using successive ethanol dilutions (100%, 96%, 75% and 50%) and washed in PBS before antigen unmasking (2x 90s, micro-waves 600W followed by a 1 h cooling period). Endogenous peroxidase activities were blocked with 3% hydrogen peroxide in PBS, and non-specific labeling was blocked using PBS with 0.1% Triton and 1% BSA. Diluted primary antibodies in Antibody Diluent (Abcam, ab64211) were incubated overnight at 4°C then washed in PBS before a 2h incubation with the corresponding secondary antibodies at room temperature. After washing, the DAB Substrate Kit (3.3'-Diaminobenzidine, Abcam, ab64238) was applied until staining (2-60 min). Then, the slices were counterstained with Groat's haematoxylin and rinsed with running water. They were dehydrated into successive ethanol baths (50%, 75%, 96% and 100%), then into roti-histol (Roth, 6640.2) before to be mounted into roti®histokit media (Roth, 6638.1). Images were taken using an optical microscope (Nikon, eclipse 80i) equipped with NIS-Elements D 3.0 software (Nikon Instruments). The primary antibody targeting PCNA (proliferating cell nuclear antigen, Mouse monoclonal PCNA (rat) antibody, 1:500, Invitrogen, 13-3900 PC-10) was used as quality control for testes tissues and the same results as Loppion et al., 2008 were obtained (not shown). Primary antibodies were used at the indicated dilution: mouse monoclonal anti-human FSHR antibody (1:500, Abcam, ab219312), rabbit polyclonal anti-human FSHR antibody (1:500, Abcam, ab137695), mouse monoclonal anti-human LHR antibody (1:100, Abcam, ab218447). Secondary antibodies were used at the indicated dilution: Goat Anti-Mouse IgG H&L, horseradish peroxidase (HRP) polymer (1:1, Abcam, ab214879) and Goat Anti-Rabbit IgG H&L, HRP polymer (1:1, Abcam, ab214880).

*2.8. Immunocytofluorescence (ICF)*

Immunocytofluorescence detections were performed to verify the expression of recombinant proteins and the antibodies' specificity used in IHC analyses. HEKT293T cells transfected with pTarget-*scfshr* or pTarget-*sclhr* plasmids were washed twice using PBS with 1% BSA, collected

and fixed with 4% PFA for 15 min before attachment to polysine slides (Epredia). The cells were permeabilized with 0.1% Triton in PBS buffer with 1% BSA for 5 min then incubated with primary antibodies, overnight, at 4°C. The cells were then washed and incubated for 2 h with secondary antibodies, at room temperature. After washes, the cells were mounted in Prolong™ Gold Antifade Mountant with 40,6-diamidino-2-phenylindole (DAPI) (P36935). Images were taken using an optical microscope (Nikon, eclipse 80i) equipped with NIS-Elements D 3.0 software (Nikon Instruments) with the same exposure time for each antibody, independently of the sample tested. The same primary antibodies as in IHC experiments were used: mouse monoclonal anti-human FSHR antibody (1:100, Abcam, ab219312), rabbit polyclonal anti-human FSHR antibody (1:100, Abcam, ab137695) and mouse monoclonal anti-human LHR antibody (1:100, Abcam, ab218447). Secondary antibodies were used at the indicated dilution: Goat anti-Rabbit IgG (H+L), Alexa Fluor™ 488 (1:250, Invitrogen, A-11008) and Goat anti-Mouse IgI (H+L), Alexa Fluor™ 488 (1:250, Invitrogen, A-11001).

## 3. Results

### *3.1. Genome searches of GTHs and GTHRs in Elasmobranchs*

Sequence searches were carried out on the basis of sequences identified in *C. milii* and some predicted sequences available in the NCBI database for *S. canicula*. A first analysis using the *C. milii* FSHR sequence blasted the LHR isoform XP_038666531.1 of *S. canicula* (loci LOC119973089), whereas the LHR sequence of *C. milii* blasted another LHR-like sequence of *S. canicula* (XP_038650550.1, loci LOC119964708). Further analyses of the *S. canicula* genome (sScyCan1.2) with sequences from a transcriptome library (S. Mazan, personal communication) enabled us to identify the FSHR and LHR sequences of *S. canicula* and the incorrect annotation of the LHR isoform XP_038666531.1, which in fact corresponded to FSHR. Then, the subsequent phylogenetic analysis, including sequences of 159 GTH subunits and 91 GTHRs, validated their annotations. Molecular phylogeny of the CGA subunits (supplementary data Fig. S2) showed that the chondrichthyan sequences are grouped in accordance of species phylogeny and that the holocephalan CGA rooted with the elasmobranchian sequences (batoidea and selachii groups). In addition, chondrichthyan CGA sequences are grouped with those of the sarcopterygii and segregated from those of the actinopterygii. Molecular phylogeny of the β subunits sequences (supplementary data Fig. S3) showed that the chondrichthyan FSHβs sequences segregated between the actinopterygian and

sarcopterygian FSHβs sequences. The holocephalan FSHβ sequence was found between the batoidea and Selachii sequences. Contrary to what was obtained for chondrichthyan FSHβ sequences, the chondrichthyan LHβ sequences rooted with the actinopterygian and sarcopterygian sequences. As observed for FSHβ sequences, the holocephalan LHβ sequence was found between the batoidea and Selachii sequences. In the GTHRs phylogenetic tree (supplementary data Fig. S4), both chondrichthyan FSHRs and LHRs sequences are grouped with those of the sarcopterygii and segregated from those of the actinopterygii. The holocephalan GTHR sequences rooted with the corresponding elasmobranch (batoidea and selachii) sequences.

*3.2. Predicted structural domains of GTHs and GTHRs*

The primary structures of elasmobranchs GTHs and GTHRs were analyzed in relation to knowledge of human orthologs. Alignment of the chondrichthyan CGA sequences has shown 10 conserved cysteines (C), 2 putative N-glycosylation sites and a 'seat' region conserved in all elasmobranchs with a lysine (K) residue instead of a valine (V) in the holocephalan sequence (supplementary data Fig. S5). The alignment of the chondrichthyan β-subunit sequences, evidences 12 conserved C residues, including the three characteristic cysteines of the "seat-belt" (C10, C11, C12), and 1 (LHβ) or 2 (FSHβ) N-glycosylation sites (supplementary data Fig. S6). The "seat" region (amino acids 55 to 59) is conserved in selachii FSHβs with an alanine (A) instead of a serine (S) in the holocephalan and batoidea sequences. In the 'seat' region of elasmobranchs LHβs, the threonine (T) of the holocephalan was substituted by a serine (S), except in *S. canicula* where it was substituted by a glycine (G).

Multiple alignments of the protein sequences of FSHR (supplementary data Fig. S7) and LHR (supplementary data Fig. S8) have shown, in their large extracellular domains, 35 well-conserved leucine (L) residues, 3 (FSHR) or 5 (LHR) putative N-glycosylation sites, 10 (FSHR) or 2 (LHR) conserved cysteines (C) and the perfectly conserved putatively sulfated tyrosine in the FSHR and LHR sequences. The putative limit between the solenoid and the "hinge" region was predicted. The transmembrane region of the chondrichthyan GTHRs was composed of 7 putative α-helical transmembrane domains (TM), 2 conserved cysteines, one APPL1, one ERW, one Ubiquitin interaction and PKC2 binding domain, and one BXXBB putative motif. A putative L-palmitoyl site was identified in the TM helix 7 of FSHRs. The C-terminal region of GTHRs

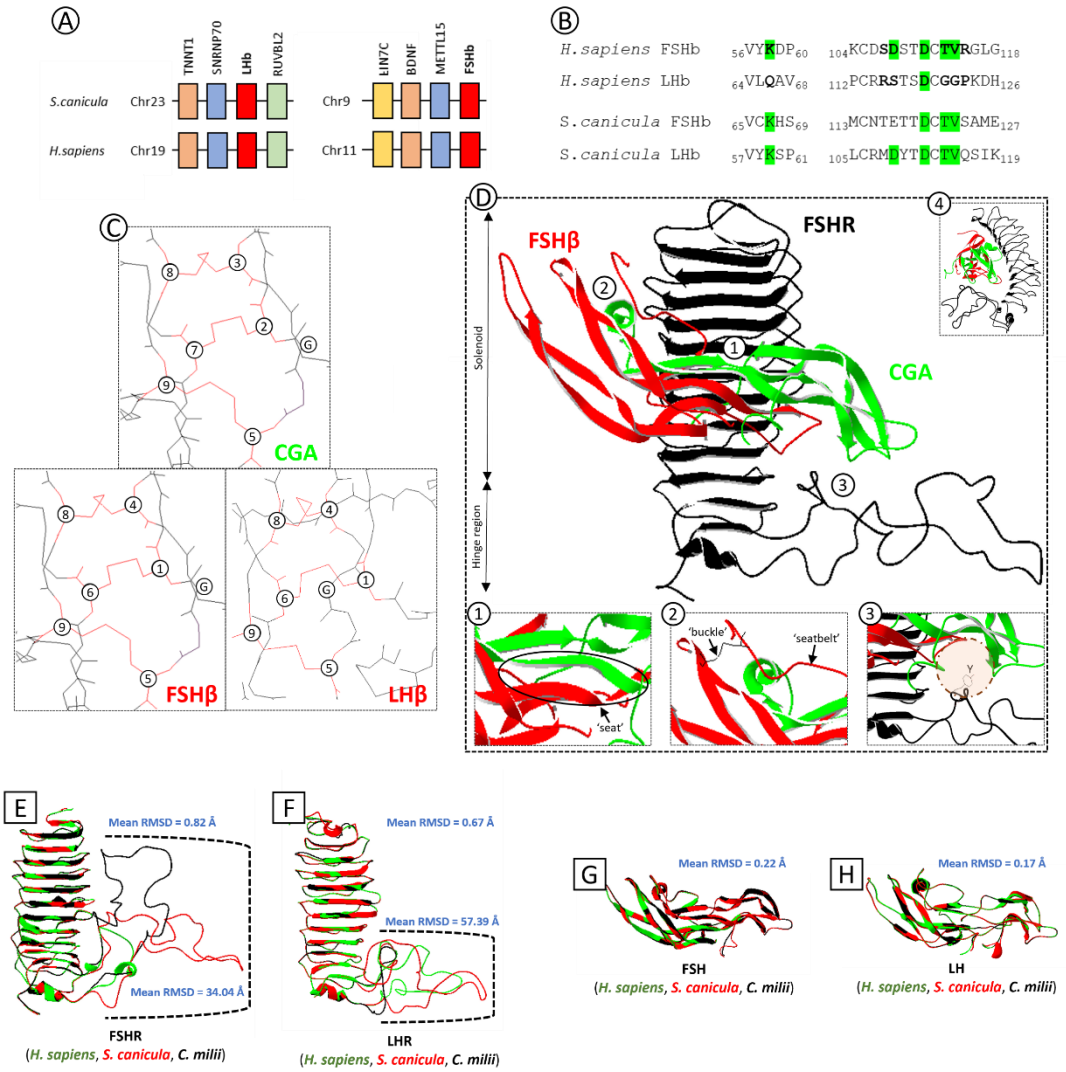


**Figure 1.** Synteny and *in silico* analysis of the 3D structures of the GTHs/GTHRs interaction complexes, in *S. canicula*, based on the *H. sapiens* templates. (A) Synteny of the genomic region flanking *fshβ* and *lhβ* genes in *H. sapiens* and *S. canicula*. The chromosome numbers are indicated. The *H. sapiens* genomic regions were used as templates. (B) Multiple alignments of FSHβ and LHβ receptor-binding sites. Residues known to be involved in ligand-receptor interaction are shown in bold. Corresponding conserved residues are highlighted in green. (C) Predictive models of the 8-aa-ring cystine-knot structure for *S. canicula* CGA, FSHβ and LHβ. The conserved cysteines and the glycine are underlined by circled numbers and G, respectively. (D) The model of the 3D FSHβ-CGA/FSHR interaction complex in *S. canicula*. FSHβ is colored in red, CGA in green and the FSHR N-terminal ectodomain (solenoid and hinge) in black. The inserts correspond to part of the global view identified by numbers: (1) the interaction between the FSHβ and CGA 'seat' interface regions, (2) the 'seatbelt' region which wrap the CGA and forming the 'buckle' disulfide bond (SS), (3) the putative sulfotyrosine residue found in the FSHR hinge which is oriented toward the FSH pocket (brown area) and (4) the lateral view of the interacting complex with the FSH positioned between the concave surface of the solenoid and the hinge. 3D interacting models were constructed from the *H. sapiens* 4mqw.1 template for FSHβ-CGA/FSHR and from the 7fii.1 for LHβ-CGA/LHR (data not shown). (E-F) Superimpositions of the predicted models of the *S. canicula*, *C. milii* and *H. sapiens* FSHRs and LHRs. G-H. Superimpositions of the predicted models of the *S. canicula*, *C. milii* and *H. sapiens* FSHs and LHs. The mean of Root Mean Square Deviations (RMSD), in ångström (Å), were calculated to illustrate the global superimposition correspondences. The dotted brackets highlight the hinge regions.

exhibits a putative $F(X)_6LL$ motif, a S/T cluster, a second BXXBB and a second L-palmitoyl site. *S. canicula* FSHβ and LHβ annotations were validated by synteny (Fig. 1A). Amino acid residues involved in the FSHβ or LHβ binding specificity to their receptors were analyzed and appeared conserved between *S. canicula* FSHβ, *S. canicula* LHβ and *H. sapiens* FSHβ sequences (Fig. 1B).

*3.3 Predicted models of the GTHs/GTHRs interacting complexes*

The FSH/FSHR interacting models, obtained with SWISS-MODEL and using the 4mqw.1 and 7fii.1 templates of *H. sapiens*, showed overall sequence identities relative to the 4mqw.1 template of 56.20% and 51.55% for *C. milii* and *S. canicula*, respectively (Table 1). However, compared with the human model, the GMQE scores were 0.08 lower for both, and the QMEANDisCo Global scores were 0.08 and 0.09 lower for the *C. milii* and *S. canicula* models, respectively, reinforcing the models obtained. Better scores were obtained for the LH/LHR interacting models with 66.42% and 67.07% global sequence identities compared to the *H. sapiens* 7fii.1 template, a GMQE score 0.03 and 0.09 lower, and a QMEANDisCo Global score 0.05 and 0.10 lower compared to the human model, for the *C. milii* and *S. canicula* models, respectively (Table 1). The predicted FSH/FSHR model obtained for *S. canicula* showed that the main characteristic 3D structures involved in αβ subunits interactions were conserved with the cystine-knot (Fig. 1C1), the "seat" (Fig. 1D1) and the "seatbelt" (Fig. 1D2) structures. The solenoid and the "hinge" regions of the FSHR ectodomain were also represented (Fig 1D). The CGA/GTHβ dimers showed the interaction between the two "seat" regions (Fig. 1D1), the "seatbelt" girdling the CGA subunit and the "buckle" in place (Fig. 1D2). FSH was positioned between the concave surface of the solenoid and the "hinge" of the receptor (Fig. 1D4) with the putative sulfotyrosine residue of the "hinge" towards the hormone binding pocket (Fig. 1D3). Similar results were obtained for LH/LHR interaction (data not shown). Superimpositions of the 3D structures between the three species were realized for the two receptors and the two hormones in order to analyze the most variable protein structure. The results showed that the GTHR models had very low and similar Root Mean Square Deviations (rmsd), ranging from 0.67 to 0.82 Å, for the solenoids, but very high rmsd for the "hinge" regions, ranging from 34.04 to 57.39 Å (Fig. 1E,F). The superimpositions of the GTHs models have shown highly similar rmsd, ranging from 0.17 to 0.22 Å (Fig. 1G,H).

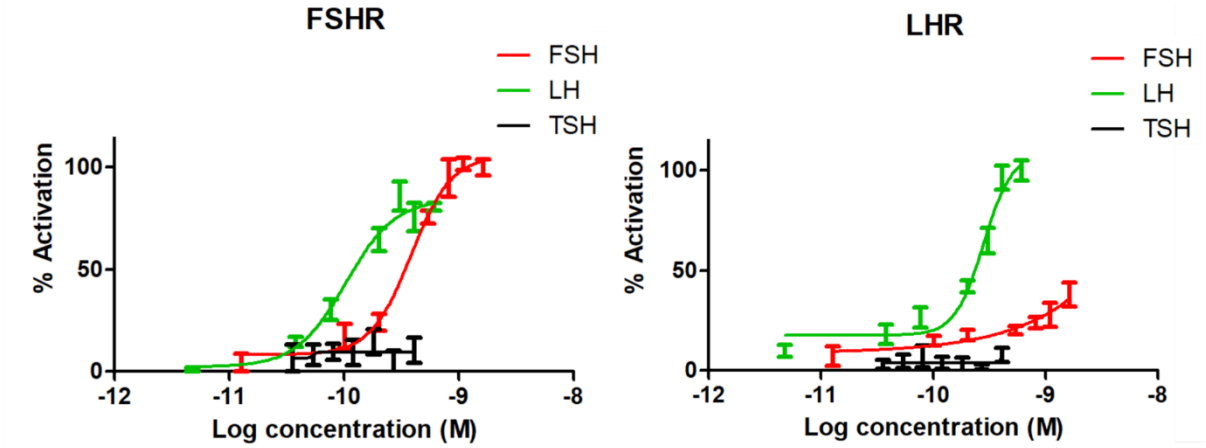


**Figure 2.** Dose-responses of HEK293T cells co-expressing *sc*GPHR/*hs*Gα$_{16}$ induced by recombinant *sc*FSHβ-*sc*CGA (*sc*FSH) or *sc*LHβ-*sc*CGA (*sc*LH). (A-B) Dose-dependent calcium responses of HEK293T cells co-expressing *sc*GPHR/*hs*Gα$_{16}$ treated with serial dilutions of conditionned medium from HEK293T transfected with corresponding pTarget *ghpβ-cga* plasmids. All experiments were performed in duplicate and the most representative was selected for ligand absolute quantification using high-resolution nanoLC-ESI-MS/MS. Data are shown as relative (%) to the highest value (100% activation) for a given ligand and represent the mean of an experiment (n = 3).

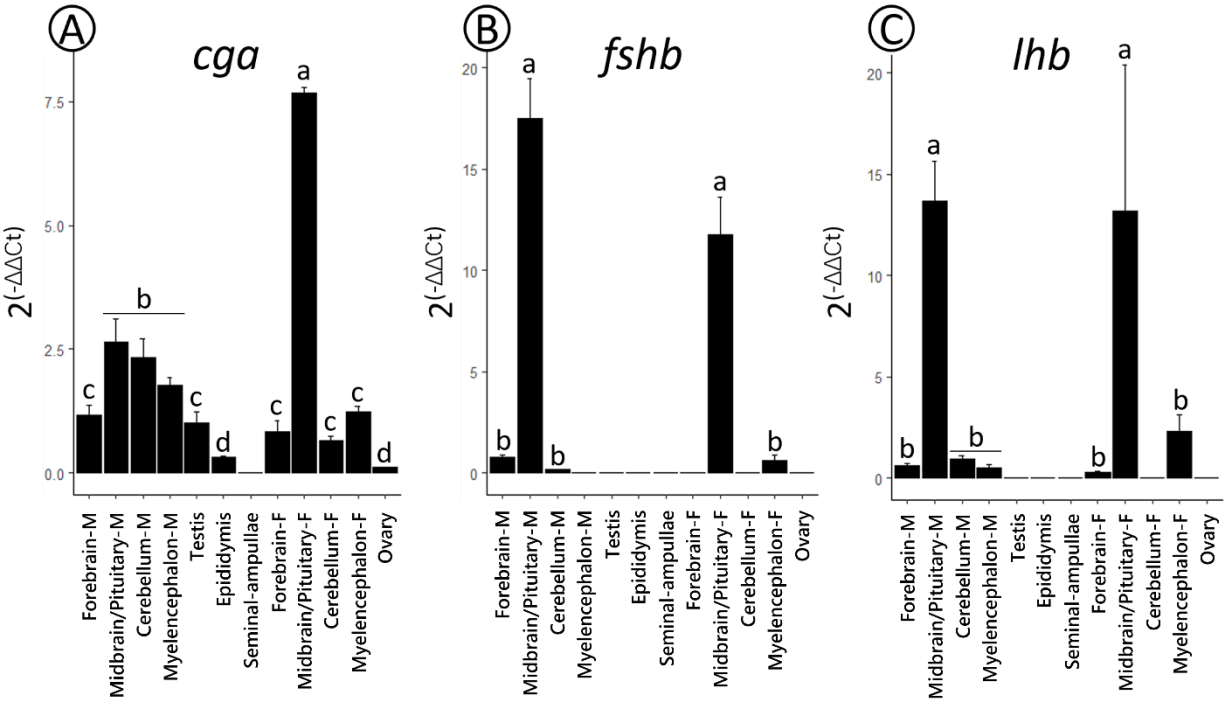


**Figure 3.** Relative expression profiles of *cga*, *fshβ* and *lhβ* transcripts in different tissues of *S. canicula*. Messenger RNA levels were assayed for *cga* (A), *fshβ* (B) and *lhβ* (C) by real-time PCR in various tissues of adult catshark: forebrain, midbrain/pituitary, cerebellum, myelencephalon, testis, epididymis, seminal ampullae, ovary. Each tissue was analyzed in triplicates from three animals (N=3; n=9). M, Male; F, Female.

*3.4. Functional hormone-receptor interactions in vitro assays*

HEK293T cells co-expressing *sc*FSHR/*hs*G$\alpha_{16}$ subunit or *sc*LHR/*hs*G$\alpha_{16}$ were stimulated by serial dilutions of conditioned medium from cells expressing the monocatenary recombinant protein *sc*FSHβ-*sc*CGA, *sc*LHβ-*sc*CGA or, as control, *sc*TSHβ-*sc*CGA (Fig. 2) (Table1). Dose-response analyses based on $Ca^{2+}$ detection have shown that *sc*FSHβ-*sc*CGA and *sc*LHβ-*sc*CGA were able to activate *sc*FSHR-expressing cells with a higher $EC_{50}$ with *sc*FSH (0.383 ± 0.019 nM) than with *sc*LH (0.103 ± 0.005 nM) (Fig. 2A; Table1). However, the maximum response for *sc*FSHR was higher with *sc*FSHβ-*sc*CGA (100.00 ± 3.58 %) than with *sc*LHβ-*sc*CGA (78.18 ± 4.15 %). The recombinant *sc*TSHβ-*sc*CGA protein was unable to activate *sc*FSHR. Cells expressing *sc*LHR were activated by the recombinant *sc*LHβ-*sc*CGA protein, with an $EC_{50}$ of 0.279 ± 0.014 nM, but not with *sc*FSHβ-*sc*CGA or *sc*TSHβ-*sc*CGA (Fig. 2B; Table1). Analyses of cAMP production in response to recombinant proteins in HEK293T cells expressing *sc*FSHR or *sc*LHR, without co-transfection with the human *hs*G$\alpha_{16}$ subunit, didn't allow to detect any significant responses. However, using the highly sensitive *in vitro* bioassay in mLTC Leydig cell line, dose-response was obtained for *sc*FSHβ-*sc*CGA after transfection with *scfshr*. In this system, *sc*FSHβ-*sc*CGA and also *sc*LHβ-*sc*CGA in a lesser extent but not *sc*TSHβ-*sc*CGA activated cAMP accumulation through *sc*FSHR (supplementary data Fig. S9).

*3.5. Relative expression profiles of cga, fshβ and lhβ transcripts in S. canicula tissues*

The expression profiles of transcripts of the genes coding for gonadotropins subunits were explored by real-time RT-PCR in 12 tissues including the male genital tract (testis, epididymis with Leydig's gland, seminal ampulla), ovary, and different parts of male and female brains. As expected, the highest expression of all transcripts was observed in the midbrain (including the pituitary gland) of males and females with a three-fold lower relative value for *cga* mRNAs in the male midbrain (2.6±0.9) than in the female midbrain (7.7± 0.4) (Fig. 3). Expression of *cga* was also observed in others parts of the brain in both males and females, in the testis and at low levels in epididymis and ovary (Fig. 3A). Both *fshβ* and *lhβ* were highly expressed in the midbrain/pituitary in both sexes, about fifteen times less in other parts of the brain and not detectable in the male tract and ovary (Fig. 3B,C).

*3.6. Relative expression profiles of fshr and lhr transcripts in S. canicula tissues with a focus in the male genital tract*

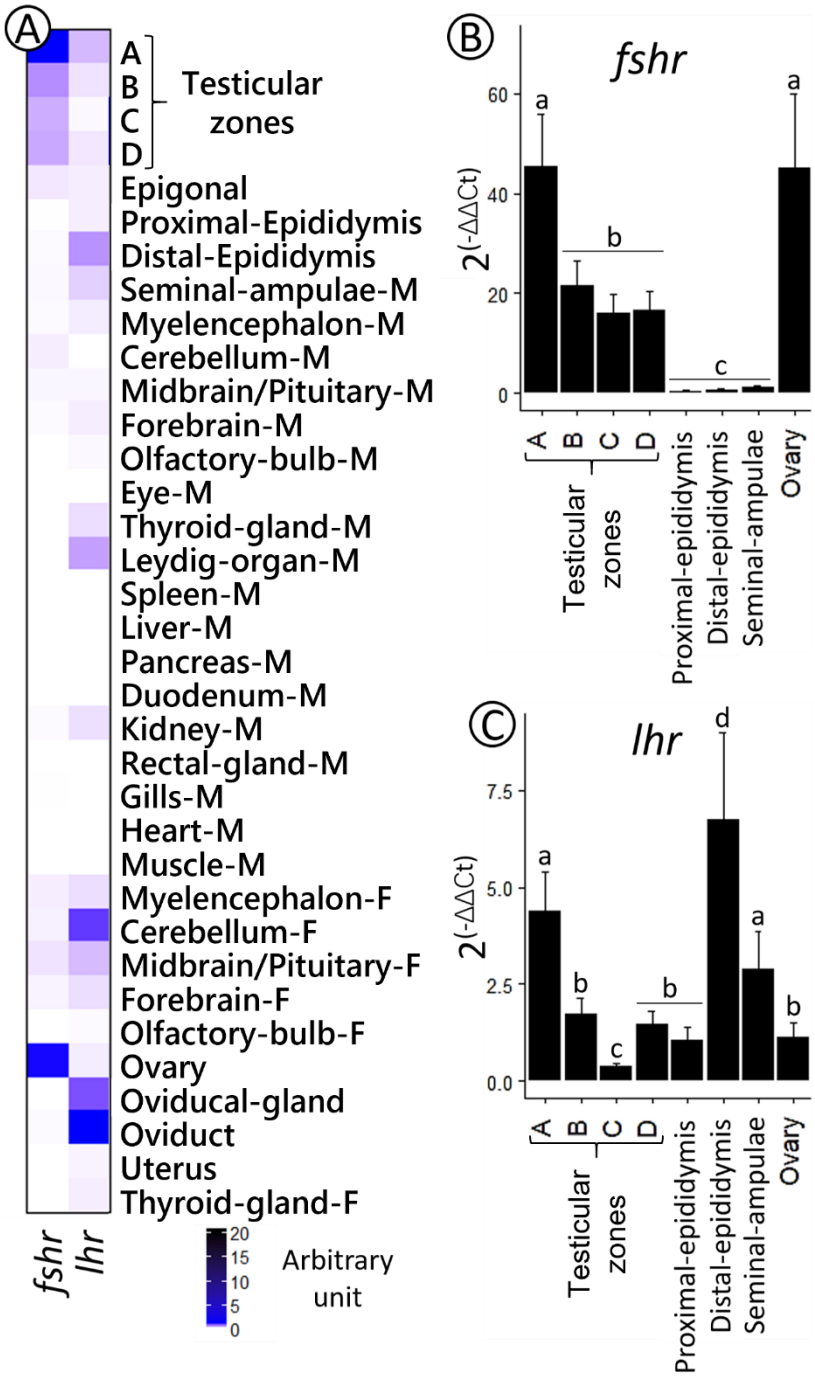


**Figure 4**. Relative expression profiles of *fshr* and *lhr* transcripts in *S. canicula* tissues focused on the testis (zones A-D), male genital tract and other male and female tissues. Messenger RNA levels were assayed by real-time PCR. Histology of testicular zones A, B, C and D, corresponding to the zone with spermatogonia, spermatocytes, early spermatids and late spermatids, respectively, is illustrated in Figure 6. (A) Warm map representation of relative gene expression in 35 different tissues. Relative gene expression of *fshr* (B) and *lhr* (C) along the male genital tract and in the ovary. Statistical analysis was performed using Mann-Whitney U test with P value < 0.05 between each statistical groups a, b, c and d. Testicular zones were assayed from six animals in triplicates (N=6; n=18) and other tissues from three animals in triplicates (N=3; n=9). The tissues from females corresponded to females caught in September (non-breeding period) whose ovaries contained a few early vitellogenic follicles. M, Male; F, Female.

The expression profiles of *fshr* and *lhr* transcripts in 35 different tissues showed that *fshr* expression was mainly observed in testicular zones and in ovary and at very low levels in epigonal tissue and in male and female parts of the brain (Fig. 4A). According to the spermatogenic wave, *fshr* was significantly higher expressed in the testicular zone A containing the germinative area and cysts with spermatogonia and was two-fold less expressed in the following stages of spermatogenesis (zones B, C and D) (Fig. 4B). Very low expressions were observed in epididymis and seminal ampullae. Levels of *fshr* transcripts in the ovary were of the same order of magnitude as in testicular zone A. With regard to *lhr*, a broader tissue-expression profile was observed with higher transcript levels in the testicular zone A, but at lower levels than *fshr*, the distal epididymis associated with leydig's gland, the seminal ampullae containing spermatozoa, the lymphomyeloid Leydig organ, the thyroid and kidney in males (Fig. 4A,C). In females, *lhr* was weakly expressed in the ovary but highly expressed in the nidamental gland and oviduct, as well as in the myelencephalon (Fig. 4A,C).

*3.7. Immunohistochemistry (IHC) and in situ hybridization (ISH) on S. canicula tissues, with a focus on the male genital tract*

*In situ* analyses were carried out in genital tract tissues, based on levels observed by real-time PCR, to identify the cell types expressing the receptors. In order to support the antibodies used, immunocytofluorescence was performed on HEK293T cells expressing *sc*FSHR or *sc*LHR (Fig. 5). The results showed that both the mouse monoclonal anti-human FSHR antibody and the rabbit polyclonal anti-human FSHR antibody exhibited a specific signal in the cytoplasm (probably in endoplasmic reticulum) and cell membrane of *sc*FSHR-expressing cells compared with the control corresponding to cells transfected with the empty plasmid. Similarly, the mouse monoclonal anti-human LHR antibody showed a specific signal in cytoplasm (probably in endoplasmic reticulum) and cell membrane of *sc*LHR-expressing cells compared with the control.

In function of the spermatogenetic waves, immunohistochemistry targeting FSHR (using the rabbit polyclonal anti-human FSHR antibody) showed a staining of individual spermatogonia (Fig. 6A1), corresponding to potential spermatogonial stem cells, and of spermatogonial progenitors (Fig. 6B1) in the germinative zone of the testis. Subsequently, spermatogonial staining, corresponding to differentiated spermatogonia, was still observed in the cysts formed, but basal and adluminal cystic staining also appeared, suggesting FSHR expression in

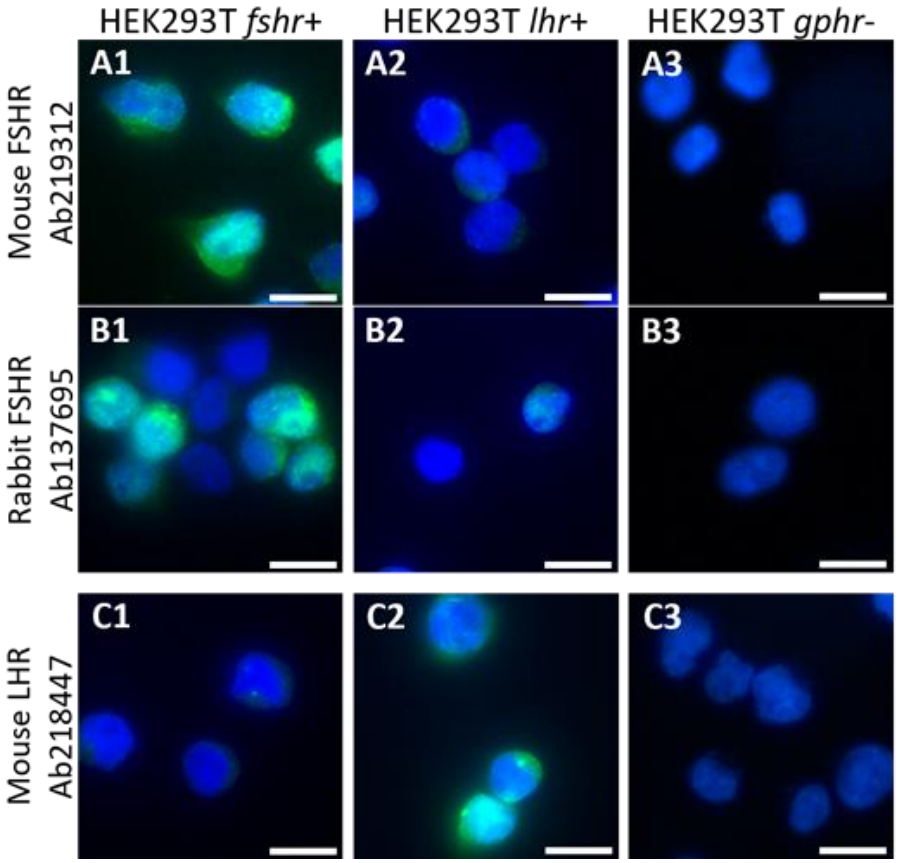


**Figure 5.** Immunocytofluorescence on HEK293T cells expressing *S. canicula gthrs.* HEKT293T cells were transfected with pTarget-*scfshr*, pTarget-*sclhr* or empty pTarget plasmids. After 24h, cells were fixed with 4% PFA, collected on polysine slides and immunocytofluorescence was performed with mouse monoclonal anti-human FSHR antibody (1:100, ab219312) (A1-A3), rabbit polyclonal anti-human FSHR antibody (1:100, ab137695) (B1-B3) or mouse monoclonal anti-human LHR antibody (1:100, ab218447) (C1-C3). Secondary antibodies used were anti-mouse goat IgI (H+L), Alexa Fluor™ 488 (1:250, A-11001) (A1-A3 and C1-C3) or anti-rabbit goat IgG (H+L) goat antibody, Alexa Fluor™ 488 (1:250, A-11008) (B1-B3). Merged pictures were aquired at 460 nm (DAPI, in blue) and 488 nm (Alexa fluor 488, in green). Scale bars: 5 µm.

Sertoli cells (Fig. 6C1). FSHR was further expressed in spermatocytes (Fig 6D1), round spermatids (Fig. 6E1) and their associated Sertoli cells. The staining observed in the cytoplasmic compartment surrounding the Sertoli cell nucleus in the basal position of the cyst at the round (Fig. 6E1) and elongated (Fig. 6F1) spermatid stages, allowed us to ensure the localization of FSHR in Sertoli cell. Furthermore, this stage- and cell-dependent FSHR expression pattern was consistent with ISH results which have shown the localization of *fshr* transcripts in early spermatogonia (Fig. 6A2) and, subsequently, when the cyst was formed (Fig. 6B2), in both Sertoli cells and germ cells (Fig. 6C2-E2) with the exception of late stages where only Sertoli cells remained stained, elongated spermatid bundles being unstained (Fig. 6F2). Analyses using mouse monoclonal anti-human FSHR antibody revealed very similar expression patterns (supplementary data Fig.S10).

Expression analyses of LHR by IHC showed similar localizations to those of FSHR. LHR staining was observed into undifferentiated spermatogonia and somatic precursors (Fig. 6A3-B3). Then, when cysts were formed, in Sertoli cells with adluminal (Fig. 6C3) and basal staining (Fig. 6C3-F3), and in germ cells (Fig. 6C3-F3). However, in cysts with bundles of elongated spermatids (Fig. 6F3) and at this level of observation, it remains difficult to determine whether the expression is located in sertolian projections between spermatids heads or in germ cells. In accordance with IHC results, ISH showed *lhr* transcripts in undifferentiated spermatogonia and their adjacent undifferentiated somatic cells (Fig. 6A4-B4). Expression of *lhr* was still observed in Sertoli cells and germ cells at the stages of differentiated spermatogonia (Fig. 6C4), spermatocytes (Fig. 6D4), round spermatids (Fig. 6E4), and elongated spermatid bundles (Fig. 6F4).

To partially conclude on these *in situ* results and taking into account the difficulty to certify more precisely the localization of expressions, it appeared that both *fshr* and *lhr* were expressed at all stages of spermatogenesis, reflecting a potential redundancy of functions associated with these receptors. For this reason, *in situ* expression analyses were extended to ovarian follicles containing differentiated granulosa and theca cells, used as a control rather than for in-depth study. In these follicles, FSHR protein and *fshr* mRNA were only expressed in granulosa cells (Fig. 7A4-A5), whereas LHR protein and *lhr* mRNA were only expressed in theca cells (Fig. 7A2-A3).

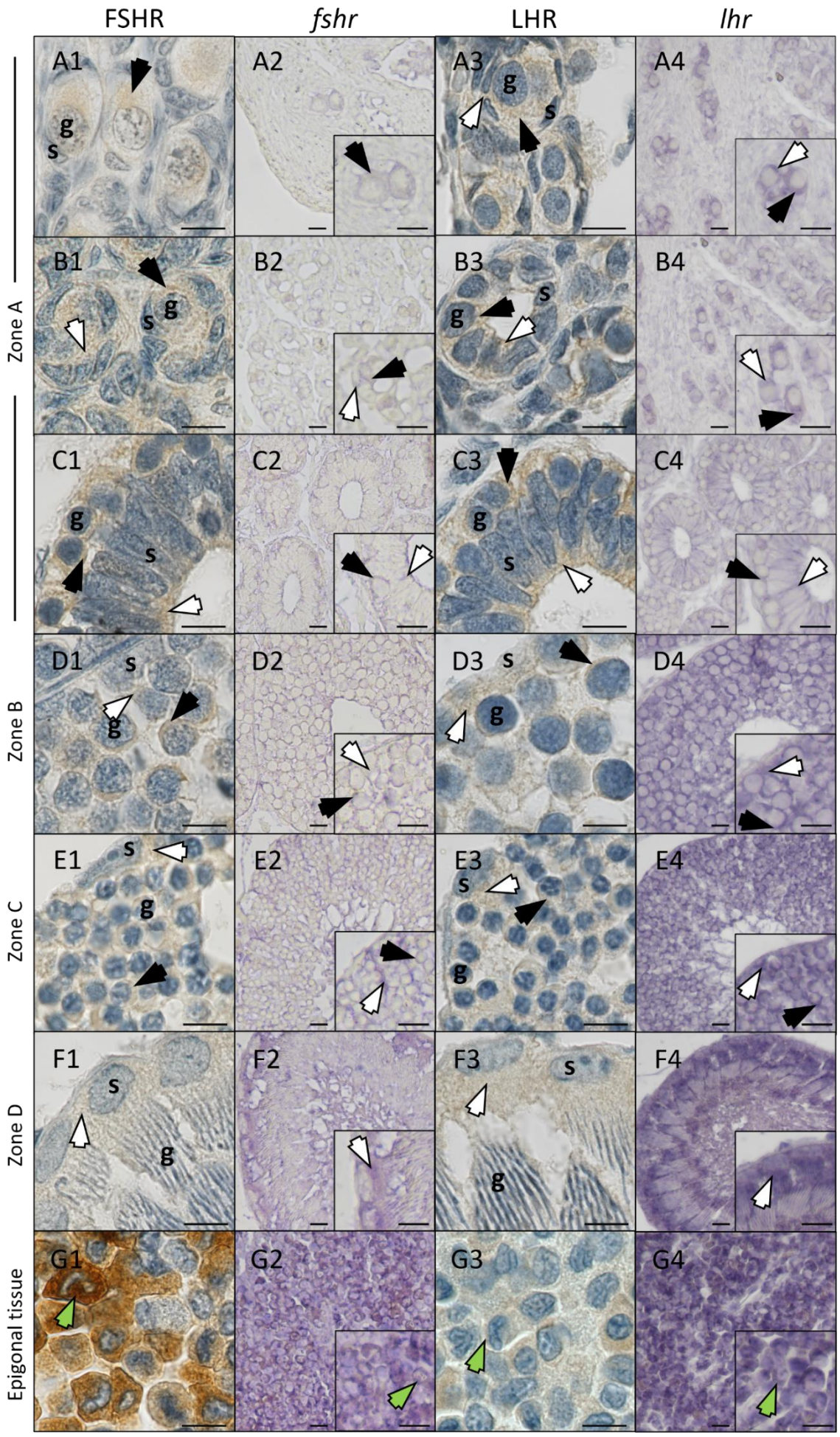
FSHR
fshr
LHR
lhr
Zone A
Zone B
Zone C
Zone D
Epigonal tissue
A1
A2
A3
A4
B1
B2
B3
B4
C1
C2
C3
C4
D1
D2
D3
D4
E1
E2
E3
E4
F1
F2
F3
F4
G1
G2
G3
G4
g
s

*In situ* analyses were completed with studies on the epigonal tissue, the testicular tubules (stem, branched and collecting tubules), the epididymis and its associated Leydig's gland. Surprisingly, strong staining was observed in the epigonal tissue for both *fshr*/FSHR and *lhr*/LHR, apparently associated with granulocytes and myelocytes but not lymphocytes and erythrocytes (Fig. 6G1-G4). In the following part of the male internal genital tract, the expressions of both *lhr*/LHR and *fshr*/FSHR were observed in epithelial cells of the stem and branched tubules (Fig. 7B2-B5), collecting tubules (Fig. 7C2-C5) and of *lhr*/LHR in the epithelial cells of the proximal (Fig. 7D2-D3) and distal epididymis (Fig. 7E2-E3) and Leydig's gland (Fig. 7F2-F3).

## 4. Discussion

### *4.1. Structures and interactions of gonadotropins with their receptors*

One of the aims of our study was to complete the characterization of gonadotropins and their receptors in elasmobranchs on the basis of a previous work that identified FSH, LH and receptors in *C. milii* (Buechi and Bridgham, 2017). The primary structures of the orthologs identified in elasmobranchs show that the CGA, FSHβ and LHβ subunits display the characteristic "seat" and "seat-belt" regions, the conserved cysteines, including the ones forming the 8-aa-ring cystine-knot, and the putative N-glycosylation sites. As highlighted in the human models, experimentally validated (Duan et al., 2021; Jiang et al., 2014a, 2014b),

---

**Figure 6.** Immunohistochemistry and RNA *in situ* hybridization of GTHRs and *gthrs* in *S. canicula* testicular sections. The testicular zone A corresponds to the germinative area (A1-A4), cysts in formation (B1-B4) and formed cysts with spermatogonia (C1-C4). The testicular zones B, C and D correspond to cysts with primary spermatocytes (D1-D4), cysts with young spermatids (E1-E4) and cysts with late spermatids (F1-F4), respectively. The lymphomyeloid epigonal tissue is illustrated (G1-G4). Immunohistochemistry was performed using rabbit polyclonal anti-human FSHR antibody (ab137695) (A1-G1) and mouse monoclonal anti-human LHR antibody (ab218447) (A3-G3). HRP-tagged secondary antibodies are then detected with DAB substrate kit. *In situ* hybridizations were performed using riboprobes targeting *Sc-fshr* mRNA (A2-G2) or *Sc-lhr* mRNA (A4-G4). For immunostaining and revelation, the DIG-Nucleic Acid Detection Kit was used. Black arrowheads, staining associated with germ cells; white arrowhead, staining associated with somatic precursors (A1-B4) or with Sertoli cells (C1-F4); green arrowhead, staining associated with myelocytes and granulocytes (G1-G4); g, germinal cell nuclei; s, sertolian precursor (A1-B4) or sertolian nuclei (C1-F4). Scale bars: 10 µm. Controls are presented in supplementary data (Fig. S10).

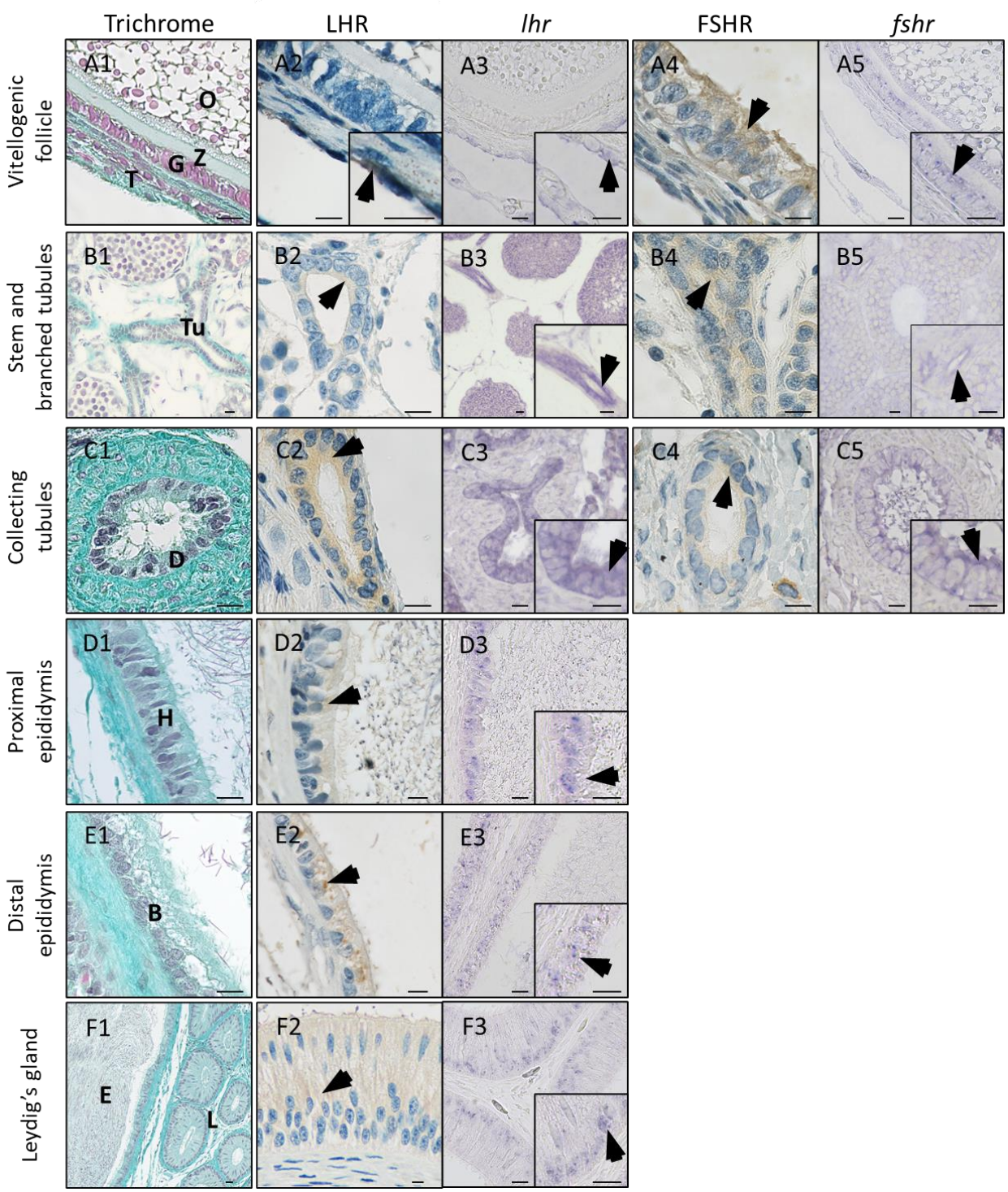
Trichrome
LHR
lhr
FSHR
fshr
Vitellogenic follicle
Stem and branched tubules
Collecting tubules
Proximal epididymis
Distal epididymis
Leydig's gland
A1
A2
A3
A4
A5
O
Z
G
T
B1
B2
B3
B4
B5
Tu
C1
C2
C3
C4
C5
D
D1
D2
D3
H
E1
E2
E3
B
F1
F2
F3
E
L

these conserved tertiary structures are essential for ligand-receptor interaction with the involvement of the “buckle”, the “seat-belt” and the potential interaction between the two “seat” regions of CGA and GTHβ. These results underline the high conservation of GTH structures from their emergence in chondrichthyes to mammals. Compared with the GTHRs of holocephalan *C. milii* (Buechi and Bridgham, 2017) and *H. sapiens* (Ulloa-Aguirre et al., 2018), the primary structures of the FSHR and LHR identified in elasmobranchs are highly conserved with the leucine-rich solenoid, hinge, N-glycosylation and sulfation sites and display the receptor family typical features in their ectodomain. On the basis of 3D models, while a high similarity in tertiary solenoid structures is observed between GTH receptors from *H. sapiens*, *C. milii* and *S. canicula*, a significant difference is observed between receptor hinges from the three species, both in size and conformation except for the potentially sulfated tyrosine which contributes greatly to hormone recognition and receptor activation (Jiang et al., 2014b, 2014a). Interestingly, a very recent work on the functional characterization of FSHR and LHR in the cloudy catshark *S. torazame* has shown that a LHR variant without exon 10, encoding part of the hinge and also corresponding to the *C. milii* and *S. canicula* LHRs used in our 3D modeling, exhibited basal cAMP activity (Arimura et al., 2024), reinforcing the role of the hinge in the receptor activation. For both receptors, FSHR and LHR, the primary structure of the seven transmembrane α- helixes is also conserved with APPL1, ERW, BXXBB, ubiquitin

---

**Figure 7**. Immunohistochemistry and RNA *in situ* hybridization of FSHR, LHR, *fshr* and *lhr* in *S. canicula* vitellogenic flollicle sections and other organs associated with the male genital tract. Histology of studied organs is presented (A1-F1) and corresppond to a vitellogenic follicle (A1-A5), intratesticular tubules (B1-B5), testicular collecting tubules (C1-C5), proximal and distal epididymis (D1-E3) and the Leydig’s gland adjacent to epididymis (F1-F3). Immunohistochemistry was performed using mouse monoclonal anti-human LHR antibody (ab218447) (A2-F2) or rabbit polyclonal anti-human FSHR antibody (ab137695) (A4-C4). *In situ* hybridizations were performed using riboprobes targeting *fshr* mRNA (A3-F3) or *lhr* mRNA (A5-B5). In the vitellogenic follicle, expressions of LHR/*lhr* and FSHR/*fshr* were observed in theca cells (white arrowhead) and granulosa cells (grey arrowhead), respectively (A2-A5). In the male genital tract, expressions of LHR/*lhr* and FSHR/*fshr* were observed in epithelial cells (black arroheads) of stem and branched tubules (B2-B5), collecting tubules (C2-C5) and expressions of LHR/*lhr* were observed in the epithelial cells of the proximal epididymis (D2-D3), distal epididymis (C2-C3) and of the leydig’s gland (F2-F3). T: theca layer; G: granulosa layer; Z: zona pellucida; O: ooplasm; Tu: intratesticular tubules; D: efferent duct; H: epithelium of the proximal epididymis; B: epithelium of the distal epididymis, E: epididymis ; L: Leydig’s gland D : Scale bars: 10 µm. Controls are presented in supplementary data (Fig. S11).

interacting and PKC2 binding domains in intracellular loops 1, 2 and 3, respectively. The second BXXBB, $F(X)_6LL$, L-palmitoylation and S/T motifs are also conserved in the intracellular Ct domain. Taken together, this suggests the ability of receptors to trigger downstream intracellular signaling, including the canonical Gs/adenylyl cyclase cAMP/protein kinase A (PKA) pathway through the conserved BXXBB and ERW motifs (Johnson and Jonas, 2020; Timossi et al., 2004). Effectively, activation of the cAMP pathway has been recently observed for FSHR and LHR stimulated by pituitary extracts in *S. torazame* (Arimura et al., 2024). In addition, the other conserved motifs could be involved in intracellular trafficking (i.e. export, endocytosis and degradation) *via* the $F(X)_6LL$ motif (Dong et al., 2007), receptor desensitization, recycling and $G_s$-independent ERK1/2-mediated signaling *via* beta-arrestin the class B serine/threonine (S/T) cluster (Kara et al., 2006; Marion et al., 2006; Troispoux et al., 1999; Wehbi et al., 2010).

Ligand-receptor interaction analyses, using transiently transfected HEK293T cells expressing *scfshr* or *sclhr* with the promiscuous *hs*$G\alpha_{16}$, showed that *sc*FSHR could be activated either by *sc*FSH or *sc*LH in the same range of efficiency, while *sc*LHR could be only activated by *sc*LH. The $EC_{50}$ obtained ranged from 103 to 383 pM, which is consistent with those obtained with human LH/CGR couples (Riccetti et al., 2017). Moreover, neither of the two receptors, *sc*FSHR and *sc*LHR, was activated by *sc*TSH. Interestingly, the *sc*FSHR could also be activated by *sc*FSH when transiently transfected in mLTC cells. Thus, using two types of *in vitro* functional assays, it appears that *sc*FSHR could be activated by *sc*FSH and cross-activated by *sc*LH while *sc*LHR could only be activated by *sc*LH in HEK293T cells. These results were supported by the similar structure observed between the receptor-binding site of *S canicula* LHβ and that of FSHβ from *S. canicula* and of FSHβ from *H. sapiens*. Cross-activation of FSHR by LH has been also observed in some actinopterygians such as the African catfish (García-López et al., 2009), Atlantic salmon (Andersson et al., 2009) or Japanese eel (Kazeto et al., 2008). However, *sc*LHR is not cross-activated by *sc*FSH, which is similar to the results in the Japanese eel (Suzuki et al., 2020) but differs from observations in zebrafish (Xie et al., 2017) and medaka (Burow et al., 2020) where both FSH and LH were able to activate FSHR or LHR, or in rainbow trout where LHR could be activated by FSH (Sambroni et al., 2007). Furthermore, the ligand-receptor binding results obtained in the catshark also differ from those of *C. milii* where each receptor is activated only by its own ligand (Buechi and Bridgham, 2017). However, the comparison

between the two species remains to be investigated since the assays used different detection systems (Ca-signaling in our study, CRE-activity in the study in *C. milii*). In our study, the HEK293T bioassay did not exhibit signal with the cAMP detection system, whereas the mLTC bioassay did when cells were transfected with *scfshr* and stimulated with *sc*FSH or *sc*LH. Unlike HEK293T cells, mLTC cells express endogenous murine LH receptors (mLHR) that are not activated by scLH (Figure S9) but that can potentially dimerize with the transfected *scfshr*. Such a dimerization in mLTCs would favor the cAMP signaling by adequately connecting the sc-FSHR/mLHR dimer with the downstream murine Gs protein. Moreover, in mLTC cells, we use a mix of IBMX, forskolin and oxytocin in the preincubation step which does not modifiy the basal cAMP level but considerably amplifies the cAMP response to GTHs relative to HEK293T cells, allowing detection of much lower amounts of gonadotropins. On the other hand, as the functional tests were carried out in heterologous mammalian cells at 37°C, the specificity of the receptors may be altered and our conclusions should be viewed with this limitation in mind.

From a structural point of view, the LH/FSH specificity, or lack of it, can be interpreted using the "negative specificity" model (Combarnous & Hengé, 1981; Combarnous, 1992) in which the high affinity of gonadotropins is largely due to their common α-subunit (i.e. not specific) whereas their specificities rely on the β-subunit-directed-binding inhibition to each other's receptor. In this model, specificity can be changed by modifying only a few amino-acid residues in the seatbelt without altering the high affinity towards the receptors. This view is in agreement with easy appearances and disappearances in FSH/LH specificity during Evolution.

*4.2. Expressions and functions of gonadotropins*

Since the initial purification of a gonadotropic fraction from the ventral lobe of the pituitary (VPD) in *S. canicula* (Sumpter et al., 1978) and the CGα, LHβ, FSHβ identification twenty years later (Quérat et al., 2001), the sequencing of the genomes of several chondrichthyes has allowed major advances in phylogeny of GpHs and their receptors. Orthologs of *cgα*, *lhβ* and *fshβ* have been identified in the genome of the three elasmobranchs *R. typus*, *C. punctatum* and *S. torazame* and are mainly expressed in the VPD for *S. torazame* (Arimura et al., 2024; Hara et al., 2018). In *S. canicula*, although we have not precisely studied their brain localization

by *in situ* analyses, our results show the highest expression of *fshβ* and *lhβ* in the midbrain/pituitary of males and females, which agrees with these previous data.

As previously observed in *S. torazame*, *fshr* is mainly expressed in ovaries and testes and *lhr* in ovaries and, surprisingly, in male Leydig organs, but not, or very weakly, in testes (Hara et al., 2018). In our present study, *fshr* and *lhr* are expressed in both gonads of *S. canicula*, but *lhr* is more weakly expressed than *fshr*. During spermatogenesis, the highest *fshr* expression level is associated with early stages where transcripts and proteins are localized in undifferentiated and differentiating spermatogonia. These results are consistent with the expression of FSHR by spermatogonial stem cells, recently demonstrated in humans and mice, which could regulate their differentiation (Bhartiya et al., 2021; Patel and Bhartiya, 2016). In the following stages of spermatogenesis, *fshr* expression decreases and is localized to germ cells and Sertoli cells, consistent with FSH function in supporting meiotic cell survival and spermiogenesis in sarcopterygians and actinopterygians (Huhtaniemi, 2015). With regard to *lhr* expression, higher levels of transcripts have also been found associated with the early stages of spermatogenesis, as for *fshr* mRNA. Here, *lhr* transcripts are apparently expressed by progenitor somatic cells and undifferentiated spermatogonia and could therefore be associated with their differentiation. Then, during the following stages of spermatogenesis, *lhr* expression decreases until the stage of cysts with round spermatids and increases again in the zone containing cysts with late spermatids and is instead associated with differentiated Sertoli cells, for both transcripts and proteins. In mammals, LH regulates the production of steroids by Leydig cells, enabling the completion of meiosis and spermiogenesis (Kumar, 2005; Ramaswamy and Weinbauer, 2014). In actinopterygians, one *fshr* and two *lhr* genes (*lhcgr1* and *lhcgr2*) have been identified (Maugars and Dufour, 2015). FSHR and LHR2 are expressed both in Leydig cells and Sertoli cells, in some species as for example in *Danio rerio*, and both gonadotropins stimulate steroid production (García-López et al., 2010; Ohta et al., 2007; Planas, 1995), with LH being primarily involved in spermiogenesis and spermiation (Chu et al., 2015; Xie et al., 2017). The expression of *fshr* and *lhr* in Sertoli cells of *S. canicula* may be associated with the fact that the main steroid-producing cell is the Sertoli cell in this species, based on its steroidal ultrastructural features and the fact that isolated cysts, as in *S. acanthias,* have the capacity to synthesize androgens in the absence of differentiated Leydig cells (Cuevas et al., 1993; Cuevas and Callard, 1992; Loir et al., 1995; Sourdaine and Garnier,

1993). However, previous studies of the pituitary VPD lobectomy showed no reduction in plasma testosterone concentration, and only total hypophysectomy resulted in a slight drop in testosterone levels, of around 18% (Dobson and Dodd, 1977a). Similarly, *in vitro* stimulation of steroidogenesis from testicular explants or isolated cysts with VPD extracts or dibutyryl cAMP showed only a 1.5-fold stimulation of testosterone (Sourdaine et al., 1990; Sourdaine and Garnier, 1993). These results suggest that gonadotropic hormones stimulate testicular steroidogenesis to a limited extent. However, ventral lobectomy induces disruption of spermatogenesis at the transition between the last mitosis of spermatogonia and the early stages of primary spermatocytes. This suggests an essential role for gonadotropins for entry into prophase (Dobson and Dodd, 1977b), in agreement with our observation of gonadotropin receptor expression at early stages (zone A).

Furthermore, we observed an unexpected expression of gonadotropin receptors in epigonal tissue. Even if functions of gonadotropins on this tissue remain to be explored, it is of interest to point them out as mammalian hematopoietic progenitors express functional LHR and FSHR and proliferate *in vivo* and *in vitro* in response to gonadotropins and prolactin (Abdelbaset-Ismail et al., 2016; Mierzejewska et al., 2015). In elasmobranchs, functional interactions between gonads and their associated lymphomyeloid epigonal tissue have been previously reported. The epigonal tissue has been described to play a role in cyst resorption after spermiation, to have an inhibitory effect on premeiotic stages DNA synthesis, and to be influenced by gonadal activity and steroids (Lutton and Callard, 2008, 2007; McClusky and Sulikowski, 2014; Piferrer and Callard, 1995).

In the male genital tract, *lhr*, but not *fshr*, is highly expressed in the distal epididymis, with expression localized in epithelial cells, but also in the Leydig's gland, unique to elasmobranchs. In mammals, *lhr* is also expressed in the epididymis of several species such as the rat (Shayu and Rao, 2006) or the squirrel (Wang et al., 2019) and participates in the regulation of the local steroidogenesis (Lei et al., 2001; Wang et al., 2018), resulting in the unique microenvironment necessary for sperm maturation (James et al., 2020; Johnston et al., 2005). Epididymis in elasmobranchs may carry out similar functions, creating a specific microenvironment and being involved in the acquisition of sperm motility (Dzyuba et al., 2019; Jones et al., 1984; Minamikawa' and Morisawa, 1996). Interestingly, a recent study on the stingray *Potamotrygon wallacei* showed the expression of the progesterone receptor in

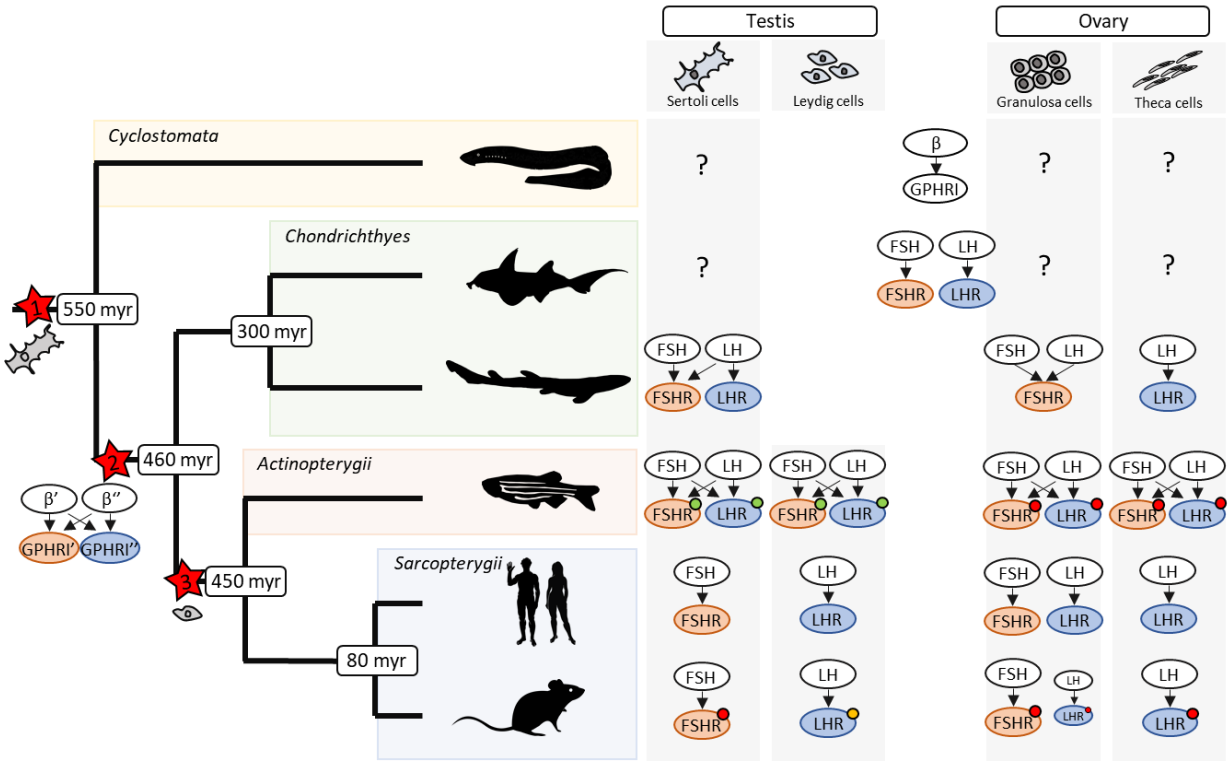


**Figure 8.** A proposed analysis of the co-evolution between gonadotropin hormones, their receptors and gonad structures in vertebrates. In cyclostomata, Sertoli cells have been identified and reproduction may be regulated by a single glycoprotein hormone GPA2/GpHβ activating the type I GpHR receptor. In the holocephalan *C. milii*, the two gonadotropins LH and FSH are differentiated, activating their cognate receptors, whose fuctions on gametaogenesis remain unexplored. In elasmobranchs, Sertoli cells are the main steroidogenic cells and functional Leydig cells are present or absent according to species. The present study showed that Sertoli cells express FSHR and LHR, theca cells LHR and Granulosa cells FSHR and that FSHR can be activeted by LH. In actinopterygians, according to species, FSHR and LHR can be expressed by both Leydig and Sertoli cells and FSHR and/or LHR are less discriminating for ligand, and as shown in D. rerio, expression of one of the receptors is sufficient to maintain complete spermatogenesis but not folliculogenesis. In sarcopterygians, Sertoli cells are specifically regulated by FSH, Leydig cells by LH, granulosa cells by FSH (untill maturation where granulosa cells also express LHR), and expression of FSHR alone may be sufficient to maintain spermatogeneis with high testosterone concentrations, but expression of both LHR and FSHR are required to suppport folliculogenesis. In the course of evolution, it could be hypothesized that the first differentiation of functional Sertoli cells was fundamental, while the Leydig cell differentiated later to support Sertoli cell functions with functional redundancy of gonadotropins. About folliculogenesis, cell-specific regulations were established earlier, with functional complementarity of gonadotropins. Green circles, knockout fully fertile; Red circles, knockout infertile; Orange circle, knockout infertile which could be partially compensate with a testosterone treatment; Red star 1, fully functional Sertoli cells; Red star 2, diversification event of ancestral genes encoding subunits of ancestral GTH (name β) and its cognate receptor, prior to GTH specification; Red star 3, fully functional Leydig cells.

epithelial cells of the epididymis and of the Leydig's gland, with a cell localization quite similar to those we determined for LHR (Morales-Gamba et al., 2023). All these results raise the question of the primitive role of the epididymis and its relationship with internal fertilization, which could be a primitive character of gnathostomes based on the observation of placoderm fossils (Long et al., 2015).

In contrast to the somatic cell composition of the testis in *S. canicula*, where Sertoli cells are differentiated and associated with steroidogenesis, while Leydig cells are rare and undifferentiated, ovarian follicles have differentiated granulosa cells and theca cells forming an inner and outer layer, respectively (Kousteni and Megalofonou, 2020; Lutton et al., 2011). Although the aim of our study was not a detailed study of gonadotropin receptor expression in the ovary, *in situ* analyses did indeed show specific expression of *fshr* and FSHR in the granulosa cells and *lhr* and LHR in theca cells. We also observed that *fshr* expression was higher than that of *lhr* in our sampled ovaries containing previtellogenic follicles and corresponding to postovulatory females. This result is in agreement with results obtained in *S. torazame* (Arimura et al., 2024), where *fshr* was more highly expressed in previtellogenic follicles, while *lhr* expression increased in vitellogenic and maturing follicles. Furthermore, it is interesting to note that *lhr*, but not *fshr,* is highly expressed in the *S. canicula*'s oviduct and oviducal gland whose basic functions are the egg capsule formation, initiated by progesterone in the cloudy catshark, and sperm storage (Marongiu et al., 2021; Shimoyama et al., 2023). Moreover, only *lhr* expression is found in the extragonadal parts of the female tracts, as in the male, underlining the function of LH in these locations.

*4.3. Evolution of the gonadal regulation by gonadotropins*

Our results can also be discussed in the light of the contribution of data from a chondrichthyan to our understanding of the evolution of gonadal regulation by gonadotropins (Fig. 8). In cyclostomes, reproduction is thought to be regulated by the single glycoprotein hormone GPA2/GpHβ, which activates the GpHRI receptor (Hausken et al., 2018). In these species Sertoli cells have been previously identified (Engel and Callard, 2007). Distinct LH and FSH have been identified in the holocephalan *C. milii* (Buechi and Bridgham, 2017), but their functions on gametogenesis remain unexplored. Moreover, testicular organization of holocephalans is poorly documented, although Sertoli cells have been mentioned (Stanley et al., 1984), whereas ovarian follicles have been better described and possess, as in other chondrichthyes,

granulosa cells and thecae (Díaz Andrade et al., 2018). In elasmobranchs, Sertoli cells are the main cellular site of steroid synthesis, with the contribution of Leydig cells, when present and differentiated according to species (Awruch, 2013; Loir et al., 1995; Prisco et al., 2002; Pudney and Callard, 1984). Sertoli cells therefore appear to be the main cells regulating spermatogenesis, under the control of FSH and LH. In actinopterygian teleosts, FSHR and LHR can be expressed by both Leydig and Sertoli cells, depending on the species, and FSHR and LHR are less discriminating for ligand, except for LHR in the eel, suggesting a functional redundancy of gonadotropins. This has been validated by knock-out approaches in the zebrafish where *lhr*;*fshr* double-KO males had underdeveloped testes and were infertile (Zhang et al., 2015), but the expression of only FSHR or LHR was sufficient to maintain complete spermatogenesis (Xie et al., 2017). Interestingly, in the medaka, the *lhr* KO, *fshr* KO and *lhr*;*fshr* double-KO phenotypes presented fertile males with histologically normal testes containing all stages of spermatogenesis and no marked differences in steroid hormone levels (Kitano et al., 2022). Finally, in tetrapods, Sertoli cells are specifically regulated by FSH and Leydig cells by LH, leading to functional complementarity; i.e. separation and complementarity of FSHR-bearing and LHR-bearing cells. This was also further supported by knock-out approaches showing that FSHR-KO or LHR-KO mice were infertile due to absent sertolian or leydigian functions, respectively (Oduwole et al., 2021; Pakarainen et al., 2005). But in the case of the LHR KO mice, strong FSH stimulation can maintain spermatogenesis without LH and high testosterone concentration, thus highlighting the central role of the Sertoli cells and the more marginal role of the Leydig cells (Oduwole et al., 2021; Pakarainen et al., 2005).

In conclusion, we postulate that during vertebrate evolution, the differentiation of functional Sertoli cells preceded that of the Leydig cell which essentially backed the Sertoli cell functions. Sertoli cells were initially regulated by a single gonadotropin, as in cyclostomes, before LH and FSH differentiated in chondrichthyans, and their receptors expressed in different cells in most bony vertebrates, except in some actinopterygians. Regarding folliculogenesis, the differentiation of granulosa and theca cells must have appeared before the divergence of cyclostomes and the differentiation of FSHR and LHR (Dziewulska and Domagala, 2009). But, once differentiated, both gonadotropins were necessary for functional folliculogenesis in gnathostomes (Chu et al., 2015; Murozumi et al., 2014; Oduwole et al., 2021; Xie et al., 2017). Overall, this suggests that folliculogenesis requires more specific regulation, than

spermatogenesis, with the emergence of the two gonadotropins to meet the needs of ovarian development and function, as previously hypothesized (Xie et al., 2017).

**Table 1**
Efficiency ($EC_{50}$) and efficacy (Emax) of *sc*FSHβ-*sc*CGA (*sc*FSH) and *sc*LHβ-*sc*CGA (*sc*LH) on *sc*FSHR and *sc*LHR.

| | Efficiency ($EC_{50}$) nM | | Efficacy (Emax) % | |
|---|---|---|---|---|
| | *sc*FSH | *sc*LH | *sc*FSH | *sc*LH |
| *sc*FSHR | 0.383 ± 0.019 | 0.103 ± 0.005 | 100.00 ± 3.58 | 78.18 ± 4.15 |
| *sc*LHR | N/A | 0.279 ± 0.014 | N/A | 100.00 ± 2.56 |

N/A: not applicable.

**Acknowledgments**

The authors are grateful to Didier Leroy from the CGFS (Channel Ground Fish Survey) campaign (IFREMER in the East Manche in September 2022) for providing the catsharks, and to Frédérique Guyon of the "Centre de Recherches en Environnement Côtier" (Luc sur Mer, France) for the care given to the animals.

**Author contributions: CRediT**

**Fabian Jeanne**: Conceptualization, Data curation, Formal analysis, Investigation, Methodology, Resources, Writing – original draft, Writing – review and editing; **Stanislas Pilet** Formal analysis, Investigation, Methodology, Resources; **Danièle Klett**: Conceptualization, Data curation, Formal analysis, Funding acquisition, Investigation, Methodology, Resources, Writing – review and editing; **Yves Combarnous**: Conceptualization, Data curation, Formal analysis, Funding acquisition, Investigation, Methodology, Resources, Writing – review and editing; **Benoît Bernay**: Conceptualization, Data curation, Formal analysis, Investigation, Methodology, Resources, Writing – review and editing; **Sylvie Dufour**: Formal analysis, Investigation; Writing – review and editing; **Pascal Favrel:** Conceptualization, Formal analysis, Investigation, Methodology, Resources, Writing – review and editing; **Pascal Sourdaine**: Conceptualization, Data curation, Formal analysis, Funding acquisition, Investigation, Methodology, Project administration, Resources, Writing – review and editing.

**Funding**

This work was supported by the "Ministère de l'Enseignement Supérieur et de la Recherche Scientifique" [F.J.'s PhD grant]; the European Regional Development Fund under the project "Manche 2021 – Plateformes d'exploitation de ressources marines" [Operational Programme ERDF/ESF 2014-2020]; the "Région Normandie" under the project "Emergent−CauSy" [grant number 22E02935/00126108]; the GIS FC3R on funds operated by Inserm (France) [grant number 22FC3R-008].

**Declaration of interests**

None.

**Associated content**

Supporting information

Supplementary figures corresponding to the 5sRNA validation as reference gene (Fig. S1), molecular phylogeny of gnathostomes CGA subunits (Fig. S2), GTHβ subunits (Fig. S3) and GTHRs (Fig. S4), alignment of elasmobranch CGA subunits (Fig. S5); GTH β subunits (Fig. S6); FSHR (Fig. S7); and LHR (Fig. S8); dose-dependent cAMP response to scFSH of mLTC cells transfected with *scfshr* (Fig. S9A), mLTC cells expressing endogenous murine LH receptors (mLHR) transfected with *scfshr* then stimulated by *sc*FSH, *sc*LH and *sc*TSH ligands (Fig. S9B); immunohistochemistry targeting FSHR using mouse monoclonal FSH-R (*H. sapiens*) antibody (ab219312) and controls associated to IHC and ISH, on *S. canicula* testicular sections (Fig. S10); controls associated to IHC and ISH, on *S. canicula* vitellogenic follicle and other organs of the male genital tract (Fig. S11) and supplementary tables corresponding to the primers used for real-time PCR and *in situ* hybridization (Table S1); supporting information for the predictive models of *S. canicula*, *C. milii* and *H. sapiens* GTHs/GTHRs interaction complexes (Table S2).

**References**

Abdelbaset-Ismail, A., Suszynska, M., Borkowska, S., Adamiak, M., Ratajczak, J., Kucia, M., Ratajczak, M.Z., 2016. Human haematopoietic stem/progenitor cells express several functional sex hormone receptors. Journal of cellular and molecular medicine 20, 134–146. https://doi.org/10.1111/jcmm.12712

Andersson, E., Nijenhuis, W., Male, R., Swanson, P., Bogerd, J., Taranger, G.L., Schulz, R.W., 2009. Pharmacological characterization, localization and quantification of expression of gonadotropin receptors in Atlantic salmon (Salmo salar L.) ovaries. General and Comparative Endocrinology 163, 329–339. https://doi.org/10.1016/j.ygcen.2009.05.001

Arimura, S., Wong, M.K.S., Inoue, R., Kawano, M., Shimoyama, K., Fujimori, C., Tokunaga, K., Takagi, W., Hyodo, S., 2024. Functional characterization of follicle-stimulating hormone and luteinizing hormone receptors in cloudy catshark, Scyliorhinus torazame. General and Comparative Endocrinology 354, 114542. https://doi.org/10.1016/j.ygcen.2024.114542

Awruch, C.A., 2013. Reproductive endocrinology in chondrichthyans: The present and the future. General and Comparative Endocrinology 192, 60–70. https://doi.org/10.1016/j.ygcen.2013.05.021

Belghazi, M., Klett, D., Cahoreau, C., Combarnous, Y., 2006. Nitro-thiocyanobenzoic acid (NTCB) reactivity of cysteines beta100 and beta110 in porcine luteinizing hormone: metastability and hypothetical isomerization of the two disulfide bridges of its beta-subunit seatbelt. Mol Cell Endocrinol. 247, 175-182. https://doi.org/10.1016/j.mce.2006.01.001.

Bhartiya, D., Patel, H., Kaushik, A., Singh, P., Sharma, D., 2021. Endogenous, tissue-resident stem/progenitor cells in gonads and bone marrow express FSHR and respond to FSH via FSHR-3. J Ovarian Res 14, 145. https://doi.org/10.1186/s13048-021-00883-0

Bosseboeuf, A., Gautier, A., Auvray, P., Mazan, S., Sourdaine, P., 2014. Characterization of spermatogonial markers in the mature testis of the dogfish (Scyliorhinus canicula L.). REPRODUCTION 147, 125–139. https://doi.org/10.1530/REP-13-0316

Buechi, H.B., Bridgham, J.T., 2017. Evolution of specificity in cartilaginous fish glycoprotein hormones and receptors. General and Comparative Endocrinology 246, 309–320. https://doi.org/10.1016/j.ygcen.2017.01.007

Burova, T., Lecompte, F., Galet, C., Monsallier, F., Delpech, S., Haertlé, T., Combarnous, Y., 2001. Conformational stability and in vitro bioactivity of porcine luteinizing hormone. Mol Cell Endocrinol. 176, 129-134. https://doi.org/10.1016/S0303-7207(01)00447-6.

Burow, S., Mizrahi, N., Maugars, G., Von Krogh, K., Nourizadeh-Lillabadi, R., Hollander-Cohen, L., Shpilman, M., Atre, I., Weltzien, F.-A., Levavi-Sivan, B., 2020. Characterization of gonadotropin receptors Fshr and Lhr in Japanese medaka, Oryzias latipes. General and Comparative Endocrinology 285, 113276. https://doi.org/10.1016/j.ygcen.2019.113276

Callard, G.V., 1991. Reproduction in male elasmobranch fishes. In: Kinne RKH, Kinne-Saffran E, and Beyenbach KW (eds) Oogenesis, Spermatogenesis and Reproduction.. Karger, Basel, pp 104–154.

Campbell, R., 2004. Piecing together evolution of the vertebrate endocrine system. Trends in Genetics 20, 359–366. https://doi.org/10.1016/j.tig.2004.06.005

Chauvigné, F., Tingaud-Sequeira, A., Agulleiro, M.J., Calusinska, M., Gómez, A., Finn, R.N., Cerdà, J., 2010. Functional and Evolutionary Analysis of Flatfish Gonadotropin Receptors Reveals Cladal- and Lineage-Level Divergence of the Teleost Glycoprotein Receptor Family. Biology of Reproduction 82, 1088–1102. https://doi.org/10.1095/biolreprod.109.082289

Chu, L., Li, J., Liu, Y., Cheng, C.H.K., 2015. Gonadotropin Signaling in Zebrafish Ovary and Testis Development: Insights From Gene Knockout Study. Molecular Endocrinology 29, 1743–1758. https://doi.org/10.1210/me.2015-1126

Cuevas, M.E., Callard, G., 1992. In vitro steroid secretion by staged spermatocysts (sertoli/germ cell units) of dogfish (Squalus acanthias) testis. General and Comparative Endocrinology 88, 151–165. https://doi.org/10.1016/0016-6480(92)90204-W

Cuevas, M.E., Collins, K., Callard, G.V., 1993. Stage-related changes in steroid-converting enzyme activities in Squalus testis: synthesis of biologically active metabolites via 3b-hydroxysteroid dehydrogenase/ isomerase and 5a-reductase. Steroids 58, 87–94. https://doi.org/10.1016/0039-128X(93)90058-U

Díaz Andrade, M.C., Moya, A.C., Wehitt, A., Di Giácomo, E.E., Galíndez, E.J., 2018. Observations of follicle cell processes in a holocephalan. Journal of Fish Biology 93, 424–427. https://doi.org/10.1111/jfb.13736

Dobson, S., Dodd, J.M., 1977a. Endocrine control of the testis in the dogfish Scyliorhinus canicula L. I. Effects of partial hypophysectomy on gravimetric, hormonal and biochemical aspects of testis function. General and Comparative Endocrinology 32, 41–52. https://doi.org/10.1016/0016-6480(77)90081-8

Dobson, S., Dodd, J.M., 1977b. The roles of temperature and photoperiod in the response of the testis of the dogfish, Scyliorhinus canicula L. to partial hypophysectomy (ventral

lobectomy). General and Comparative Endocrinology 32, 114–115. https://doi.org/10.1016/0016-6480(77)90088-0

Dong, C., Filipeanu, C.M., Duvernay, M.T., Wu, G., 2007. Regulation of G protein-coupled receptor export trafficking. Biochimica et Biophysica Acta (BBA) - Biomembranes 1768, 853–870. https://doi.org/10.1016/j.bbamem.2006.09.008

Duan, J., Xu, P., Cheng, X., Mao, C., Croll, T., He, X., Shi, J., Luan, X., Yin, W., You, E., Liu, Q., Zhang, S., Jiang, H., Zhang, Y., Jiang, Y., Xu, H.E., 2021. Structures of full-length glycoprotein hormone receptor signalling complexes. Nature 598, 688–692. https://doi.org/10.1038/s41586-021-03924-2

Dufour, S., Quérat, B., Tostivint, H., Pasqualini, C., Vaudry, H., Rousseau, K., 2020. Origin and Evolution of the Neuroendocrine Control of Reproduction in Vertebrates, With Special Focus on Genome and Gene Duplications. Physiological Reviews 100, 869–943. https://doi.org/10.1152/physrev.00009.2019

Dziewulska, K., Domagala, J., 2009. Ripening of the oocyte of the river lamprey (Lampetra fluviatilis L.) after river entry. Journal of Applied Ichthyology 25, 752–756. https://doi.org/10.1111/j.1439-0426.2009.01325.x

Dzyuba, V., Ninhaus-Silveira, A., Kahanec, M., Veríssimo-Silveira, R., 2019. Sperm motility in ocellate river stingrays: Evidence for post-testicular sperm maturation and capacitation in chondrichthyes. Journal of Zoology 307, 9–16. https://doi.org/10.1111/jzo.12610

Engel, K.B., Callard, G.V., 2007. Endocrinology of Leydig Cells in Nonmammalian Vertebrates, in: Payne, A.H., Hardy, M.P. (Eds.), The Leydig Cell in Health and Disease, Contemporary Endocrinology. Humana Press, Totowa, NJ, pp. 207–224. https://doi.org/10.1007/978-1-59745-453-7_15

Galet, C., Lecompte, F., Combarnous, Y., 2004. Association/dissociation of gonadotropin subunits involves disulfide bridge disruption which is influenced by carbohydrate moiety. Biochem Biophys Res Commun. 324, 868-873. https://doi.org/10.1016/j.bbrc.2004.09.143.

García-López, Á., Bogerd, J., Granneman, J.C.M., Van Dijk, W., Trant, J.M., Taranger, G.L., Schulz, R.W., 2009. Leydig Cells Express Follicle-Stimulating Hormone Receptors in African Catfish. Endocrinology 150, 357–365. https://doi.org/10.1210/en.2008-0447

García-López, Á., De Jonge, H., Nóbrega, R.H., De Waal, P.P., Van Dijk, W., Hemrika, W., Taranger, G.L., Bogerd, J., Schulz, R.W., 2010. Studies in Zebrafish Reveal Unusual Cellular Expression Patterns of Gonadotropin Receptor Messenger Ribonucleic Acids in the Testis and Unexpected Functional Differentiation of the Gonadotropins. Endocrinology 151, 2349–2360. https://doi.org/10.1210/en.2009-1227

Gautier, A., Bosseboeuf, A., Auvray, P., Sourdaine, P., 2014. Maintenance of Potential Spermatogonial Stem Cells In Vitro by GDNF Treatment in a Chondrichthyan Model (Scyliorhinus canicula L.). Biology of Reproduction 91, 91–105. https://doi.org/10.1095/biolreprod.113.116020

Gautron, J., 1978. Effet du calcium et de la stimulation sur les terminaisons nerveuses des fonctions nerf-électroplaque de la Torpille. Biol. Cell. 31, 31–44.

Giraldo, C., Le Roy, D., Martin-Baillet, V., 2022. CGFS2022 cruise, RV Thalassa. https://doi.org/10.17600/18001842

Hara, Y., Yamaguchi, K., Onimaru, K., Kadota, M., Koyanagi, M., Keeley, S.D., Tatsumi, K., Tanaka, K., Motone, F., Kageyama, Y., Nozu, R., Adachi, N., Nishimura, O., Nakagawa, R., Tanegashima, C., Kiyatake, I., Matsumoto, R., Murakumo, K., Nishida, K., Terakita, A., Kuratani, S., Sato, K., Hyodo, S., Kuraku, S., 2018. Shark genomes provide insights into elasmobranch evolution and the origin of vertebrates. Nat Ecol Evol 2, 1761–1771. https://doi.org/10.1038/s41559-018-0673-5

Hausken, K.N., Tizon, B., Shpilman, M., Barton, S., Decatur, W., Plachetzki, D., Kavanaugh, S., Ul-Hasan, S., Levavi-Sivan, B., Sower, S.A., 2018. Cloning and characterization of a second lamprey pituitary glycoprotein hormone, thyrostimulin (GpA2/GpB5). General and Comparative Endocrinology 264, 16–27. https://doi.org/10.1016/j.ygcen.2018.04.010

Helenius, A., Aebi, M., 2004. Roles of N-Linked Glycans in the Endoplasmic Reticulum. Annu. Rev. Biochem. 73, 1019–1049. https://doi.org/10.1146/annurev.biochem.73.011303.073752

Heyland, A., Plachetzki, D., Donelly, E., Gunaratne, D., Bobkova, Y., Jacobson, J., Kohn, A.B., Moroz, L.L., 2012. Distinct Expression Patterns of Glycoprotein Hormone Subunits in the Lophotrochozoan Aplysia: Implications for the Evolution of Neuroendocrine Systems in Animals. Endocrinology 153, 5440–5451. https://doi.org/10.1210/en.2012-1677

Hiro'oka, T., Maassen, D., Berger, P., Boime, I., 2000. Disulfide Bond Mutations in Follicle-Stimulating Hormone Result in Uncoupling of Biological Activity from Intracellular Behavior. Endocrinology 141, 4751–4756. https://doi.org/10.1210/endo.141.12.7821

Hsueh, A.J., He, J., 2018. Gonadotropins and their receptors: coevolution, genetic variants, receptor imaging, and functional antagonists. Biology of Reproduction 99, 3–12. https://doi.org/10.1093/biolre/ioy012

Hsueh, A.J.W., Feng, Y., 2020. Discovery of polypeptide ligand-receptor pairs based on their co-evolution. FASEB j. 34, 8824–8832. https://doi.org/10.1096/fj.202000779R

Huhtaniemi, I., 2015. A short evolutionary history of FSH-stimulated spermatogenesis. Hormones (Athens) 14, 468–478. https://doi.org/doi: 10.14310/horm.2002.1632

Irisarri, I., Baurain, D., Brinkmann, H., Delsuc, F., Sire, J.-Y., Kupfer, A., Petersen, J., Jarek, M., Meyer, A., Vences, M., Philippe, H., 2017. Phylotranscriptomic consolidation of the jawed vertebrate timetree. Nat Ecol Evol 1, 1370–1378. https://doi.org/10.1038/s41559-017-0240-5

James, E.R., Carrell, D.T., Aston, K.I., Jenkins, T.G., Yeste, M., Salas-Huetos, A., 2020. The Role of the Epididymis and the Contribution of Epididymosomes to Mammalian Reproduction. IJMS 21, 5377. https://doi.org/10.3390/ijms21155377

Jiang, X., Dias, J.A., He, X., 2014a. Structural biology of glycoprotein hormones and their receptors: Insights to signaling. Molecular and Cellular Endocrinology 382, 424–451. https://doi.org/10.1016/j.mce.2013.08.021

Jiang, X., Fischer, D., Chen, X., McKenna, S.D., Liu, H., Sriraman, V., Yu, H.N., Goutopoulos, A., Arkinstall, S., He, X., 2014b. Evidence for Follicle-stimulating Hormone Receptor as a Functional Trimer. Journal of Biological Chemistry 289, 14273–14282. https://doi.org/10.1074/jbc.M114.549592

Johansson, M.U., Zoete, V., Michielin, O., Guex, N., 2012. Defining and searching for structural motifs using DeepView/Swiss-PdbViewer. BMC Bioinformatics 13, 1–11. https://doi.org/10.1186/1471-2105-13-173

Johnson, G.P., Jonas, K.C., 2020. Mechanistic insight into how gonadotropin hormone receptor complexes direct signaling†. Biology of Reproduction 102, 773–783. https://doi.org/10.1093/biolre/ioz228

Johnston, D.S., Jelinsky, S.A., Bang, H.J., DiCandeloro, P., Wilson, E., Kopf, G.S., Turner, T.T., 2005. The Mouse Epididymal Transcriptome: Transcriptional Profiling of Segmental Gene Expression in the Epididymis. Biology of Reproduction 73, 404–413. https://doi.org/10.1095/biolreprod.105.039719

Jones, R.C., Jones, N., Djakiew, D., 1984. Luminal composition and maturation of spermatozoa in the male genital ducts of the Port Jackson shark, Heterodontus portusjacksoni. J. Exp. Zool. 230, 417–426. https://doi.org/10.1002/jez.1402300311

Kara, E., Crépieux, P., Gauthier, C., Martinat, N., Piketty, V., Guillou, F., Reiter, E., 2006. A Phosphorylation Cluster of Five Serine and Threonine Residues in the C-Terminus of the Follicle-Stimulating Hormone Receptor Is Important for Desensitization But Not for β-Arrestin-Mediated ERK Activation. Molecular Endocrinology 20, 3014–3026. https://doi.org/10.1210/me.2006-0098

Kazeto, Y., Kohara, M., Miura, T., Miura, C., Yamaguchi, S., Trant, J.M., Adachi, S., Yamauchi, K., 2008. Japanese Eel Follicle-Stimulating Hormone (Fsh) and Luteinizing Hormone (Lh): Production of Biologically Active Recombinant Fsh and Lh by Drosophila S2 Cells and Their Differential Actions on the Reproductive Biology. Biology of Reproduction 79, 938–946. https://doi.org/10.1095/biolreprod.108.070052

Kitano, T., Takenaka, T., Takagi, H., Yoshiura, Y., Kazeto, Y., Hirai, T., Mukai, K., Nozu, R., 2022. Roles of Gonadotropin Receptors in Sexual Development of Medaka.

Klett, D., Combarnous, Y., 2021. Highly sensitive in vitro bioassay for luteinizing hormone and chorionic gonadotropin allowing their measurement in plasma. Reproduction and Fertility 2, 300–307. https://doi.org/10.1530/RAF-21-0045

Kousteni, V., Megalofonou, P., 2020. Reproductive strategy of Scyliorhinus canicula (L., 1758): a holistic approach based on macroscopic measurements and microscopic observations of the reproductive organs. Mar. Freshwater Res. 71, 596. https://doi.org/10.1071/MF18474

Kudo, M., Chen, T., Nakabayashi, K., Hsu, S.Y., Hsueh, A.J.W., 2000. The Nematode Leucine-Rich Repeat-Containing, G Protein-Coupled Receptor (LGR) Protein Homologous to Vertebrate Gonadotropin and Thyrotropin Receptors is Constitutively Activated in Mammalian Cells 14, 272–284. https://doi.org/10.1210/mend.14.2.0422

Kumar, T.R., 2005. What have we learned about gonadotropin function from gonadotropin subunit and receptor knockout mice? Reproduction 130, 293–302. https://doi.org/10.1530/rep.1.00660

Lapthorn, A., Harris, D.C., Littlejohn, A., Lustbader, J.W., Canfield, R.E., Machin, K.J., Morgan, F.J., Isaacs, N.W., 1994. Crystal structure of human chorionic gonadotropin. Nature 369, 455–461. https://doi.org/10.1038/369455a0

Lei, Z.M., Mishra, S., Zou, W., Xu, B., Foltz, M., Li, X., Rao, C.V., 2001. Targeted Disruption of Luteinizing Hormone/Human Chorionic Gonadotropin Receptor Gene. Molecular Endocrinology 15, 184–200. https://doi.org/10.1210/mend.15.1.0586

Lemoine, F., Correia, D., Lefort, V., Doppelt-Azeroual, O., Mareuil, F., Cohen-Boulakia, S., Gascuel, O., 2019. NGPhylogeny.fr: new generation phylogenetic services for non-specialists. Nucleic Acids Research 47, 260–265. https://doi.org/10.1093/nar/gkz303

Letunic, I., Bork, P., 2021. Interactive Tree Of Life (iTOL) v5: an online tool for phylogenetic tree display and annotation. Nucleic Acids Research 49, 293–296. https://doi.org/10.1093/nar/gkab301

Livak, K.J., Schmittgen, T.D., 2001. Analysis of Relative Gene Expression Data Using Real-Time Quantitative PCR and the 2−ΔΔCT Method. Methods 25, 402–408. https://doi.org/10.1006/meth.2001.1262

Loir, M., Sourdaine, P., 1994. Testes cells: isolation and culture. In: Hochachka PW, Mommsen TP (eds) Biochemistry and molecular biology of fishes: analytical techniques. Elsevier, New York, pp. 219–272. https://doi.org/10.1016/B978-0-444-82033-4.50028-3

Loir, M., Sourdaine, P., Mendis-Handagama, S.M.L.C., Jégou, B., 1995. Cell-cell interactions in the testis of teleosts and elasmobranchs: CELL-CELL INTERACTIONS IN THE TESTIS. Microsc. Res. Tech. 32, 533–552. https://doi.org/10.1002/jemt.1070320606

Long, J.A., Mark-Kurik, E., Johanson, Z., Lee, M.S.Y., Young, G.C., Min, Z., Ahlberg, P.E., Newman, M., Jones, R., Blaauwen, J.D., Choo, B., Trinajstic, K., 2015. Copulation in antiarch placoderms and the origin of gnathostome internal fertilization. Nature 517, 196–199. https://doi.org/10.1038/nature13825

Loppion, G., Crespel, A., Martinez, A.-S., Auvray, P., Sourdaine, P., 2008. Study of the potential spermatogonial stem cell compartment in dogfish testis, Scyliorhinus canicula L. Cell and Tissue Research 332, 533–542. https://doi.org/10.1007/s00441-008-0590-z

Lutton, B.V., Callard, I.P., 2008. Influence of reproductive activity, sex steroids, and seasonality on epigonal organ cellular proliferation in the skate (Leucoraja erinacea). General and Comparative Endocrinology 155, 116–125. https://doi.org/10.1016/j.ygcen.2007.03.011

Lutton, B.V., Callard, I.P., 2007. Effects of reproductive activity and sex hormones on apoptosis in the epigonal organ of the skate (Leucoraja erinacea). General and Comparative Endocrinology 154, 75–84. https://doi.org/10.1016/j.ygcen.2007.06.014

Lutton, B.V., George, J.S., Murrin, C.R., Fileti, L.A., Callard, I.P., 2011. The elasmobranch ovary. In: Hamlett WC (ed) Reproductive Biology and Phylogeny of Chondrichthyes: Sharks, Batoids, and Chimaeras. SciencePublisher Inc, Einfeld, pp. 237–281.

Manca, R., Glomski, C., Pica, A., 2019. Hematopoietic stem cells debut in embryonic lymphomyeloid tissues of elasmobranchs. European Journal of Histochemistry 63. https://doi.org/10.4081/ejh.2019.3060

Marion, S., Oakley, R.H., Kim, K.-M., Caron, M.G., Barak, L.S., 2006. A β-Arrestin Binding Determinant Common to the Second Intracellular Loops of Rhodopsin Family G Protein-coupled Receptors. Journal of Biological Chemistry 281, 2932–2938. https://doi.org/10.1074/jbc.M508074200

Marongiu, M.F., Porcu, C., Pascale, N., Bellodi, A., Cau, A., Mulas, A., Pesci, P., Porceddu, R., Follesa, M.C., 2021. A Taxonomic Survey of Female Oviducal Glands in Chondrichthyes: A Comparative Overview of Microanatomy in the Two Reproductive Modes. Animals 11, 2653. https://doi.org/10.3390/ani11092653

Marra, N.J., Stanhope, M.J., Jue, N.K., Wang, M., Sun, Q., Pavinski Bitar, P., Richards, V.P., Komissarov, A., Rayko, M., Kliver, S., Stanhope, B.J., Winkler, C., O'Brien, S.J., Antunes, A.,

Jorgensen, S., Shivji, M.S., 2019. White shark genome reveals ancient elasmobranch adaptations associated with wound healing and the maintenance of genome stability. Proceedings of the National Academy of Sciences 116, 4446–4455. https://doi.org/10.1073/pnas.1819778116

Maston, G.A., Ruvolo, M., 2002. Chorionic Gonadotropin Has a Recent Origin Within Primates and an Evolutionary History of Selection. Molecular Biology and Evolution 19, 320–335. https://doi.org/10.1093/oxfordjournals.molbev.a004085

Maugars, G., Dufour, S., 2015. Demonstration of the Coexistence of Duplicated LH Receptors in Teleosts, and Their Origin in Ancestral Actinopterygians. PLoS ONE 10, e0135184. https://doi.org/10.1371/journal.pone.0135184

Maugars, G., Dufour, S., Cohen-Tannoudji, J., Quérat, B., 2014. Multiple Thyrotropin β-Subunit and Thyrotropin Receptor-Related Genes Arose during Vertebrate Evolution. PLoS ONE 9, e111361. https://doi.org/10.1371/journal.pone.0111361

McClusky, L.M., Sulikowski, J., 2014. The epigonal organ and mature pole of the testis in the recreationally fished blue shark (Prionace glauca): histochemico-functional correlates. Journal of Anatomy 225, 614–624. https://doi.org/10.1111/joa.12242

Mierzejewska, K., Borkowska, S., Suszynska, E., Suszynska, M., Poniewierska-Baran, A., Maj, M., Pedziwiatr, D., Adamiak, M., Abdel-Latif, A., Kakar, S.S., Ratajczak, J., Kucia, M., Ratajczak, M.Z., 2015. Hematopoietic Stem/Progenitor Cells Express Several Functional Sex Hormone Receptors—Novel Evidence for a Potential Developmental Link Between Hematopoiesis and Primordial Germ Cells. Stem Cells and Development 24, 927–937. https://doi.org/10.1089/scd.2014.0546

Minamikawa', S., Morisawa, M., 1996. Acquisition, Initiation and Maintenance of Sperm Motility in the Shark, Ttiakis scyllia. Comparative Biochemistry and Physiology Part A: Physiology 113, 387–392. https://doi.org/10.1016/0300-9629(95)02080-2

Morales-Gamba, R.D., Araújo, M.L.G., Barcellos, J.F.M., Rêgo, M.G., Dias, L.C., Marcon, J.L., 2023. Progesterone receptors in extratesticular ducts of the Amazonian stingray Potamotrygon wallacei: A potential role in sperm maturation and aggregate formation.

General and Comparative Endocrinology 344, 114375. https://doi.org/10.1016/j.ygcen.2023.114375

Murozumi, N., Nakashima, R., Hirai, T., Kamei, Y., Ishikawa-Fujiwara, T., Todo, T., Kitano, T., 2014. Loss of Follicle-Stimulating Hormone Receptor Function Causes Masculinization and Suppression of Ovarian Development in Genetically Female Medaka. Endocrinology 155, 3136–3145. https://doi.org/10.1210/en.2013-2060

Nechamen, C.A., Thomas, R.M., Dias, J.A., 2007. APPL1, APPL2, Akt2 and FOXO1a interact with FSHR in a potential signaling complex. Molecular and Cellular Endocrinology 260, 93–99. https://doi.org/10.1016/j.mce.2006.08.014

Oduwole, O.O., Huhtaniemi, I.T., Misrahi, M., 2021. The Roles of Luteinizing Hormone, Follicle-Stimulating Hormone and Testosterone in Spermatogenesis and Folliculogenesis Revisited. IJMS 22, 12735. https://doi.org/10.3390/ijms222312735

Ohta, T., Miyake, H., Miura, C., Kamei, H., Aida, K., Miura, T., 2007. Follicle-Stimulating Hormone Induces Spermatogenesis Mediated by Androgen Production in Japanese Eel, Anguilla japonica. Biology of Reproduction 77, 970–977. https://doi.org/10.1095/biolreprod.107.062299

Pakarainen, T., Zhang, F.-P., Mäkelä, S., Poutanen, M., Huhtaniemi, I., 2005. Testosterone Replacement Therapy Induces Spermatogenesis and Partially Restores Fertility in Luteinizing Hormone Receptor Knockout Mice. Endocrinology 146, 596–606. https://doi.org/10.1210/en.2004-0913

Park, J.-C., Lee, J.-H., Kodama, K., Urushitani, H., Ohta, Y., Horiguchi, T., 2013. Structure of the intratesticular duct system for sperm emission in the starspotted smooth-hound Mustelus manazo. Fish Sci 79, 203–211. https://doi.org/10.1007/s12562-012-0581-6

Patel, H., Bhartiya, D., 2016. Testicular Stem Cells Express Follicle-Stimulating Hormone Receptors and Are Directly Modulated by FSH. Reprod. Sci. 23, 1493–1508. https://doi.org/10.1177/1933719116643593

Piferrer, F.C., Callard, G.V., 1995. Inhibition of Deoxyribonucleic Acid Synthesis during Premeiotic Stages of Spermatogenesis by a Factor from Testis-Associated Lymphomyeloid

Tissue in the Dogfish Shark (Squalus Acanthias). Biology of Reproduction 53, 390–398. https://doi.org/10.1095/biolreprod53.2.390

Planas, J.V., 1995. Maturation-associated changes in the response of the salmon testis to the steroidogenic actions of gonadotropins (GTH I and GTH II) in vitro. Biology of Reproduction 52, 697–704. https://doi.org/10.1095/biolreprod52.3.697

Prisco, M., Loredana, R., Piero, A., 2002. Ultrastructural studies on developing follicles of the spotted rayTorpedo marmorata. Mol. Reprod. Dev. 61, 78–86. https://doi.org/10.1002/mrd.1133

Pudney, J., Callard, G.V., 1984. Development of agranular reticulum in Sertoli cells of the testis of the dogfishSqualus acanthias during spermatogenesis. Anat. Rec. 209, 311–321. https://doi.org/10.1002/ar.1092090309

Quérat, B., Tonnerre-Doncarli, C., Géniès, F., Salmon, C., 2001. Duality of Gonadotropins in Gnathostomes. General and Comparative Endocrinology 124, 308–314. https://doi.org/10.1006/gcen.2001.7715

Ramaswamy, S., Weinbauer, G.F., 2014. Endocrine control of spermatogenesis: Role of FSH and LH/ testosterone. Spermatogenesis 4, e996025. https://doi.org/10.1080/21565562.2014.996025

Read, T.D., Petit, R.A., Joseph, S.J., Alam, Md.T., Weil, M.R., Ahmad, M., Bhimani, R., Vuong, J.S., Haase, C.P., Webb, D.H., Tan, M., Dove, A.D.M., 2017. Draft sequencing and assembly of the genome of the world's largest fish, the whale shark: Rhincodon typus Smith 1828. BMC Genomics 18, 532. https://doi.org/10.1186/s12864-017-3926-9

Redon, E., Bosseboeuf, A., Rocancourt, C., Da Silva, C., Wincker, P., Mazan, S., Sourdaine, P., 2010. Stage-specific gene expression during spermatogenesis in the dogfish (Scyliorhinus canicula). Reproduction 140, 57–71. https://doi.org/10.1530/REP-10-0021

Riccetti, L., Yvinec, R., Klett, D., Gallay, N., Combarnous, Y., Reiter, E., Simoni, M., Casarini, L., Akli Ayoub, M., 2017. Human Luteinizing Hormone and Chorionic Gonadotropin Display Biased Agonism at the LH and LH/CG Receptors. Scientific Reports 7, 940. https://doi.org/10.1038/s41598-017-01078-8

Sambroni, E., Le Gac, F., Breton, B., Lareyre, J.-J., 2007. Functional specificity of the rainbow trout (Oncorhynchus mykiss) gonadotropin receptors as assayed in a mammalian cell line. Journal of Endocrinology 195, 213–228. https://doi.org/10.1677/JOE-06-0122

Schefe, J.H., Lehmann, K.E., Buschmann, I.R., Unger, T., Funke-Kaiser, H., 2006. Quantitative real-time RT-PCR data analysis: current concepts and the novel "gene expression's C T difference" formula. Journal of Molecular Medicine 84, 901–910. https://doi.org/10.1007/s00109-006-0097-6

Schwartz, J., Réalis-Doyelle E., Le Franc L., Favrel P., 2021. A Novel Dop2/Invertebrate-Type Dopamine Signaling System Potentially Mediates Stress, Female Reproduction, and Early Development in the Pacific Oyster (Crassostrea gigas). Mar Biotechnol (NY) 23, 683-694. https://doi.org/10.1007/s10126-021-10052-5

Shayu, D., Rao, A.J., 2006. Expression of functional aromatase in the epididymis: Role of androgens and LH in modulation of expression and activity. Molecular and Cellular Endocrinology 249, 40–50. https://doi.org/10.1016/j.mce.2006.01.016

Shimoyama, K., Kawano, M., Ogawa, N., Tokunaga, K., Takagi, W., Kobayashi, M., Hyodo, S., 2023. Progesterone initiates tendril formation in the oviducal gland during egg encapsulation in cloudy catshark (Scyliorhinus torazame). Zoological Lett 9, 13. https://doi.org/10.1186/s40851-023-00211-y

Sievers, F., Wilm, A., Dineen, D., Gibson, T.J., Karplus, K., Li, W., Lopez, R., McWilliam, H., Remmert, M., Söding, J., Thompson, J.D., Higgins, D.G., 2011. Fast, scalable generation of high-quality protein multiple sequence alignments using Clustal Omega. Molecular Systems Biology 7, 539. https://doi.org/10.1038/msb.2011.75

Sourdaine, P., Garnier, D.H., 1993. Stage-dependent modulation of Sertoli cell steroid production in dogfish (Scyliorhinus canicula). Reproduction 97, 133–142. https://doi.org/10.1530/jrf.0.0970133

Sourdaine, P., Garnier, D.H., Jégou, B., 1990. The adult dogfish (Scyliorhinus canicula L.) testis: a model to study stage-dependent changes in steroid levels during spermatogenesis. Journal of Endocrinology 127, 451–460. https://doi.org/10.1677/joe.0.1270451

Stanley, H.P., Kasinsky, H.E., Bols, N.C., 1984. Meiotic chromatin diminution in a vertebrate, the holocephalan fish Hydrolagus collie (Chondrichthyes, Holocephali). Tissue and Cell 16, 203–215. https://doi.org/10.1016/0040-8166(84)90045-4

Studer, G., Rempfer, C., Waterhouse, A.M., Gumienny, R., Haas, J., Schwede, T., 2020. QMEANDisCo—distance constraints applied on model quality estimation. Bioinformatics 36, 1765–1771. https://doi.org/10.1093/bioinformatics/btz828

Sumpter, J.P., Jenkins, N., Dodd, J.M., 1978. Gonadotrophic Hormone in the Pituitary Gland of the Dogfish (Scyliorhinus canicda L.): Distribution and Physiological Significance. General and Comparative Endocrinology 36, 275–285. https://doi.org/10.1016/0016-6480(78)90034-5

Sumpter, J.P. and Dodd, J.M., 1979. The annual reproductive cycle of the female lesser spotted dogfish, Scyliorhinus canicula L., and its endocrine control. Journal of Fish Biology 15, 687-695. https://doi.org/10.1111/j.1095-8649.1979.tb03678.x

Suzuki, H., Kazeto, Y., Gen, K., Ozaki, Y., 2020. Functional analysis of recombinant single-chain Japanese eel Fsh and Lh produced in FreeStyle 293-F cell lines: Binding specificities to their receptors and differential efficacy on testicular steroidogenesis. General and Comparative Endocrinology 285, 113241. https://doi.org/10.1016/j.ygcen.2019.113241

Timossi, C., Ortiz-Elizondo, C., Pineda, D.B., Dias, J.A., Conn, P.M., Ulloa-Aguirre, A., 2004. Functional significance of the BBXXB motif reversed present in the cytoplasmic domains of the human follicle-stimulating hormone receptor. Molecular and Cellular Endocrinology 223, 17–26. https://doi.org/10.1016/j.mce.2004.06.004

Troispoux, C., Guillou, F., Elalouf, J.-M., Firsov, D., Iacovelli, L., Blasi, A.D., Combarnous, Y., Reiter, E., 1999. Involvement of G protein-coupled receptor kinases and arrestins in desensitization to follicle-stimulating hormone action. Molecular endocrinology 13. https://doi.org/10.1210/mend.13.9.0342

Ulloa-Aguirre, A., Zariñán, T., Jardón-Valadez, E., Gutiérrez-Sagal, R., Dias, J.A., 2018. Structure-Function Relationships of the Follicle-Stimulating Hormone Receptor. Front. Endocrinol. 9, 707. https://doi.org/10.3389/fendo.2018.00707

Van Hiel, M.B., Vandersmissen, H.P., Van Loy, T., Vanden Broeck, J., 2012. An evolutionary comparison of leucine-rich repeat containing G protein-coupled receptors reveals a novel LGR subtype. Peptides 34, 193–200. https://doi.org/10.1016/j.peptides.2011.11.004

Vassart, G., 2004. A molecular dissection of the glycoprotein hormone receptors. Trends in Biochemical Sciences 29, 119–126. https://doi.org/10.1016/j.tibs.2004.01.006

Venkatesh, B., Lee, A.P., Ravi, V., Maurya, A.K., Lian, M.M., Swann, J.B., Ohta, Y., Flajnik, M.F., Sutoh, Y., Kasahara, M., Hoon, S., Gangu, V., Roy, S.W., Irimia, M., Korzh, V., Kondrychyn, I., Lim, Z.W., Tay, B.-H., Tohari, S., Kong, K.W., Ho, S., Lorente-Galdos, B., Quilez, J., Marques-Bonet, T., Raney, B.J., Ingham, P.W., Tay, A., Hillier, L.W., Minx, P., Boehm, T., Wilson, R.K., Brenner, S., Warren, W.C., 2014. Elephant shark genome provides unique insights into gnathostome evolution. Nature 505, 174–179. https://doi.org/10.1038/nature12826

Wang, J., Liu, Q., Wang, Z., Sheng, X., Zhang, H., Han, Y., Yuan, Z., Weng, Q., 2019. Seasonal expressions of luteinising hormone receptor, follicle-stimulating hormone receptor and prolactin receptor in the epididymis of the male wild ground squirrel (Spermophilus dauricus). Reprod. Fertil. Dev. 31, 735. https://doi.org/10.1071/RD18262

Wang, P., Liu, S., Yang, Q., Liu, Z., Zhang, S., 2018. Functional Characterization of Thyrostimulin in Amphioxus Suggests an Ancestral Origin of the TH Signaling Pathway. Endocrinology 159, 3536–3548. https://doi.org/10.1210/en.2018-00550

Wang, Q., Arighi, C.N., King, B.L., Polson, S.W., Vincent, J., Chen, C., Huang, H., Kingham, B.F., Page, S.T., Farnum Rendino, M., Thomas, W.K., Udwary, D.W., Wu, C.H., the North East Bioinformatics Collaborative Curation Team, 2012. Community annotation and bioinformatics workforce development in concert - Little Skate Genome Annotation Workshops and Jamborees. Database 2012, bar064. https://doi.org/10.1093/database/bar064

Waterhouse, A., Bertoni, M., Bienert, S., Studer, G., Tauriello, G., Gumienny, R., Heer, F.T., de Beer, T.A.P., Rempfer, C., Bordoli, L., Lepore, R., Schwede, T., 2018. SWISS-MODEL: homology modelling of protein structures and complexes. Nucleic Acids Research 46, 296–303. https://doi.org/10.1093/nar/gky427

Wehbi, V., Tranchant, T., Durand, G., Musnier, A., Decourtye, J., Piketty, V., Butnev, V.Y., Bousfield, G.R., Crépieux, P., Maurel, M.-C., Reiter, E., 2010. Partially Deglycosylated Equine

LH Preferentially Activates β-Arrestin-Dependent Signaling at the Follicle-Stimulating Hormone Receptor. Molecular Endocrinology 24, 561–573. https://doi.org/10.1210/me.2009-0347

Xie, Y., Chu, L., Liu, Y., Sham, K.W.Y., Li, J., Cheng, C.H.K., 2017. The highly overlapping actions of Lh signaling and Fsh signaling on zebrafish spermatogenesis. Journal of Endocrinology 234, 233–246. https://doi.org/10.1530/JOE-17-0079

Ye, J., Coulouris, G., Zaretskaya, I., Cutcutache, I., Rozen, S., Madden, T.L., 2012. Primer-BLAST: A tool to design target-specific primers for polymerase chain reaction. BMC Bioinformatics 13, 1–11. https://doi.org/10.1186/1471-2105-13-134

Zhang, Z., Lau, S.-W., Zhang, L., Ge, W., 2015. Disruption of Zebrafish Follicle-Stimulating Hormone Receptor (fshr) But Not Luteinizing Hormone Receptor (lhcgr) Gene by TALEN Leads to Failed Follicle Activation in Females Followed by Sexual Reversal to Males. Endocrinology 156, 3747–3762. https://doi.org/10.1210/en.2015-1039

# Annexes Chapitre II

# I. Annexes chapitre II : Données supplémentaires

**Supplementary material**

**Characterization of gonadotropins and their receptors in a chondrichthyan, *Scyliorhinus canicula*, fills a gap in the understanding of their coevolution.**

Fabian Jeanne[1], Stanislas Pilet[1], Danièle Klett[2], Yves Combarnous[2], Benoît Bernay[3], Sylvie Dufour[1], Pascal Favrel[1] and Pascal Sourdaine*[1]

[1] Université de Caen Normandie, MNHN, SU, UA, CNRS, IRD, Laboratoire de Biologie des Organismes et Ecosystèmes Aquatiques (BOREA), UMR 8067, 14032 Caen cedex 5, France.

[2] INRAE, CNRS, UMR Physiologie de la Reproduction & des Comportements, 37380 Nouzilly, France

[3] Université de Caen Normandie - Plateforme PROTEOGEN, US EMerode, 14032 Caen cedex 5, France.

*Corresponding Author: orcid.org/0000-0001-9811-2876; Email: pascal.sourdaine@unicaen.fr

**Table S1.** List of the primers used for real-time PCR and *in situ* hybridization

| Primer names | Experimentation | Sequence |
|---|---|---|
| S.ca-FSHR-RT | RT-qPCR | 5'-TTCACAAAGACGTTTCGGCG-3'; 5'-GCGATGAGTGGCTACCAGAA-3' |
| S.ca-LHR-RT | RT-qPCR | 5'-GCAGTTTGTCAGATGCACCA-3'; 5'-TCTCTCCAGGGAATCGCTTTG-3' |
| S.ca-CGA-RT | RT-qPCR | 5'- CGTGGTAGAACAGGGTGTACG-3'; 5'-CACTGGAAGATGGGCACTCC-3' |
| S.ca-FSHβ-RT | RT-qPCR | 5'-TCACCAAGGATCCAGTCTGC-3'; 5'-AGGGTTAACATTGGCAGGGC-3' |
| S.ca-LHβ-RT | RT-qPCR | 5'-CTATTCTGTCCAGGGCCGAC-3'; 5'-TGGACAGTAACCACCGCATATG-3' |
| S.ca-5SRNA-RT | RT-qPCR | 5'-TCGTCTGATCTCGGAAGCTA-3'; 5'-AGCCTACTGCACCTGGTATTC-3' |
| S.ca-FSHR-ISH | *in situ* hybridization | 5'-GCTCATAGCTCGGTCAACCA-3'; 5'-AGTGAAGAATCCAGCGGACG-3' |
| S.ca-LHR-ISH | *in situ* hybridization | 5'-CTTACTGCCCGCTTCACGTA-3'; 5'-TGAGGAAACGTGGGACTGTG-3' |

**Table S2**. Supporting information for the model prediction of *S. canicula*, *C. milii* and *H. sapiens* GTHs/GTHRs interaction complexes.

| | FSHβ-CGA/FSHR | LHβ-CGA/LHR |
|---|---|---|
| 3D model templates | 4mqw.1 | 7fii.1 |
| Global seq. identity with *H. sapiens* | 100.00% | 100.00% |
| Global Model Quality Estimate (GMQE) for *H. sapiens* models | 0.46 | 0.76 |
| QMEANDisCo Global for *H. sapiens* models | 0.73 ± 0.05 | 0.74 ± 0.05 |
| Global seq. identity with *C. milii* | 56.20% | 66.42% |
| Global Model Quality Estimate (GMQE) for *C. milii* models | 0.38 | 0.73 |
| QMEANDisCo Global for *C. milii* models | 0.65 ± 0.05 | 0.69 ± 0.05 |
| Global seq. identity with *S. canicula* | 51.55% | 67.07% |
| Global Model Quality Estimate (GMQE) for *S. canicula* models | 0.38 | 0.67 |
| QMEANDisCo Global for *S. canicula* models | 0.64 ± 0.05 | 0.64 ± 0.05 |

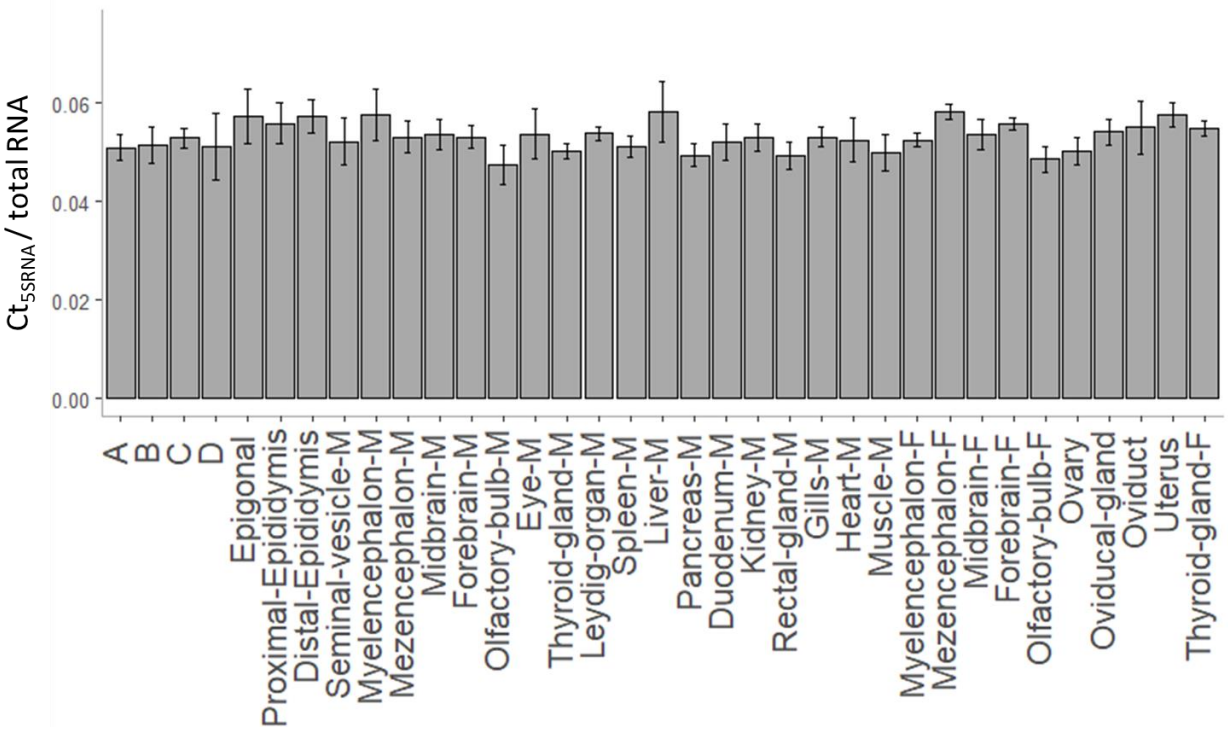


**Fig. S1**. Validation of the 5SRNA as reference gene for the real-time PCR normalization. Statistical analyze was performed using the none parametric Kruskal-Wallis test (based on the previous Shapiro-wilk test results) with a P-value of 0.11.

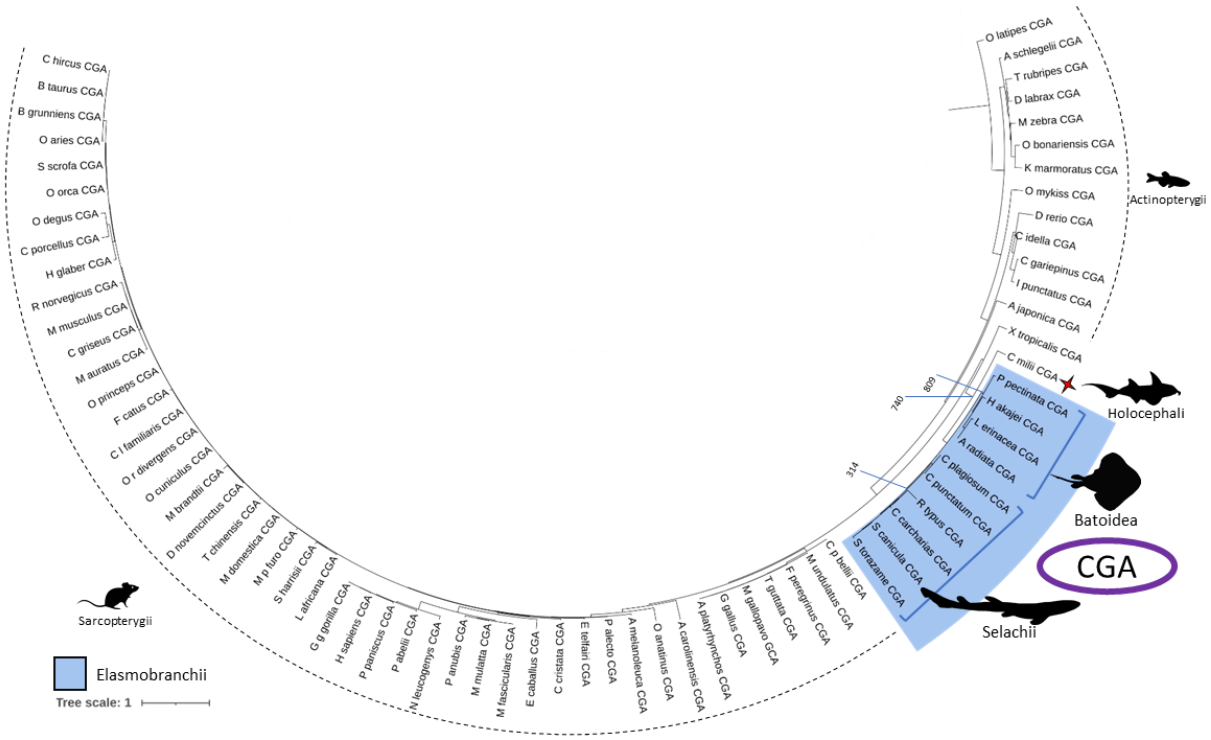


**Fig. S2.** Molecular phylogeny of gnathostomes CGA subunits. Identified elasmobranch CGAs are highlighted in blue. The *C. milii* sequence is highlighted by a red star. Support values shown for relevant node are bootstraps for 1000 replicates. Animal illustrations are used with permission from http://phylopic.org.

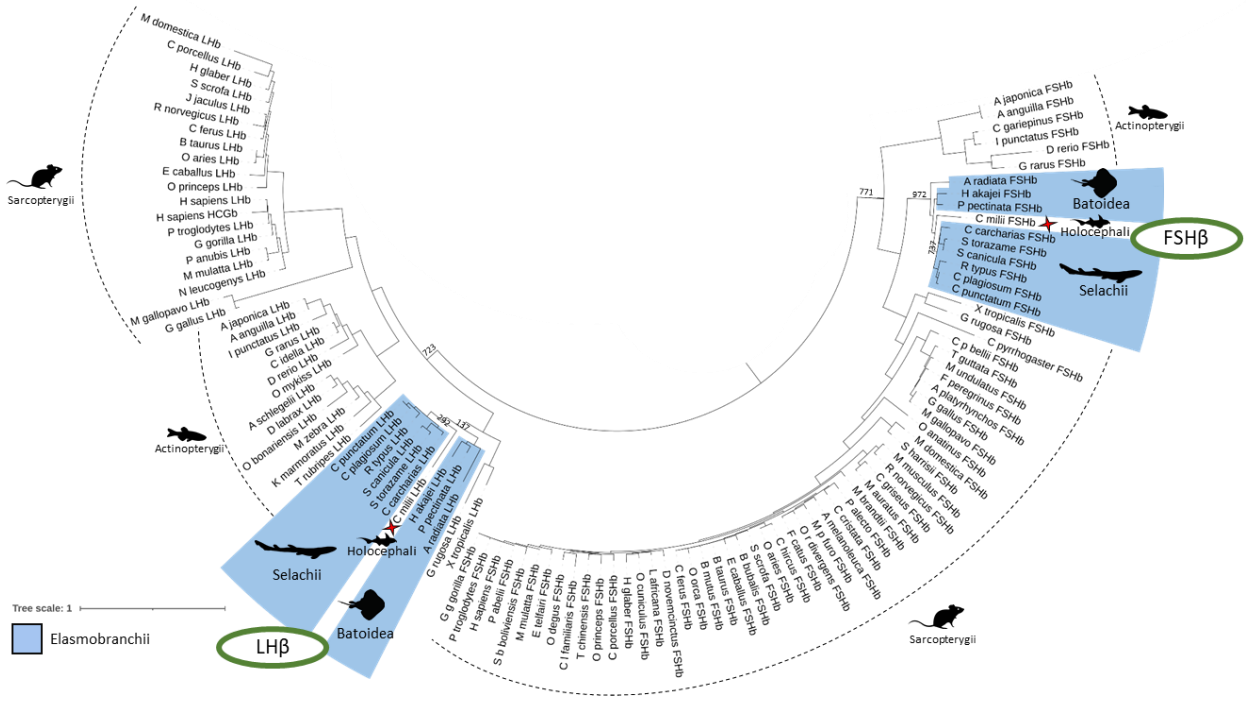


**Fig. S3.** Molecular phylogeny of gnathostomes GTHβ subunits. Identified elasmobranch LHβs and FSHβs are highlighted in blue. The *C. milii* sequences are highlighted by a red star. Support values shown for relevant node are bootstraps for 1000 replicates. Animal illustrations are used with permission from http://phylopic.org.

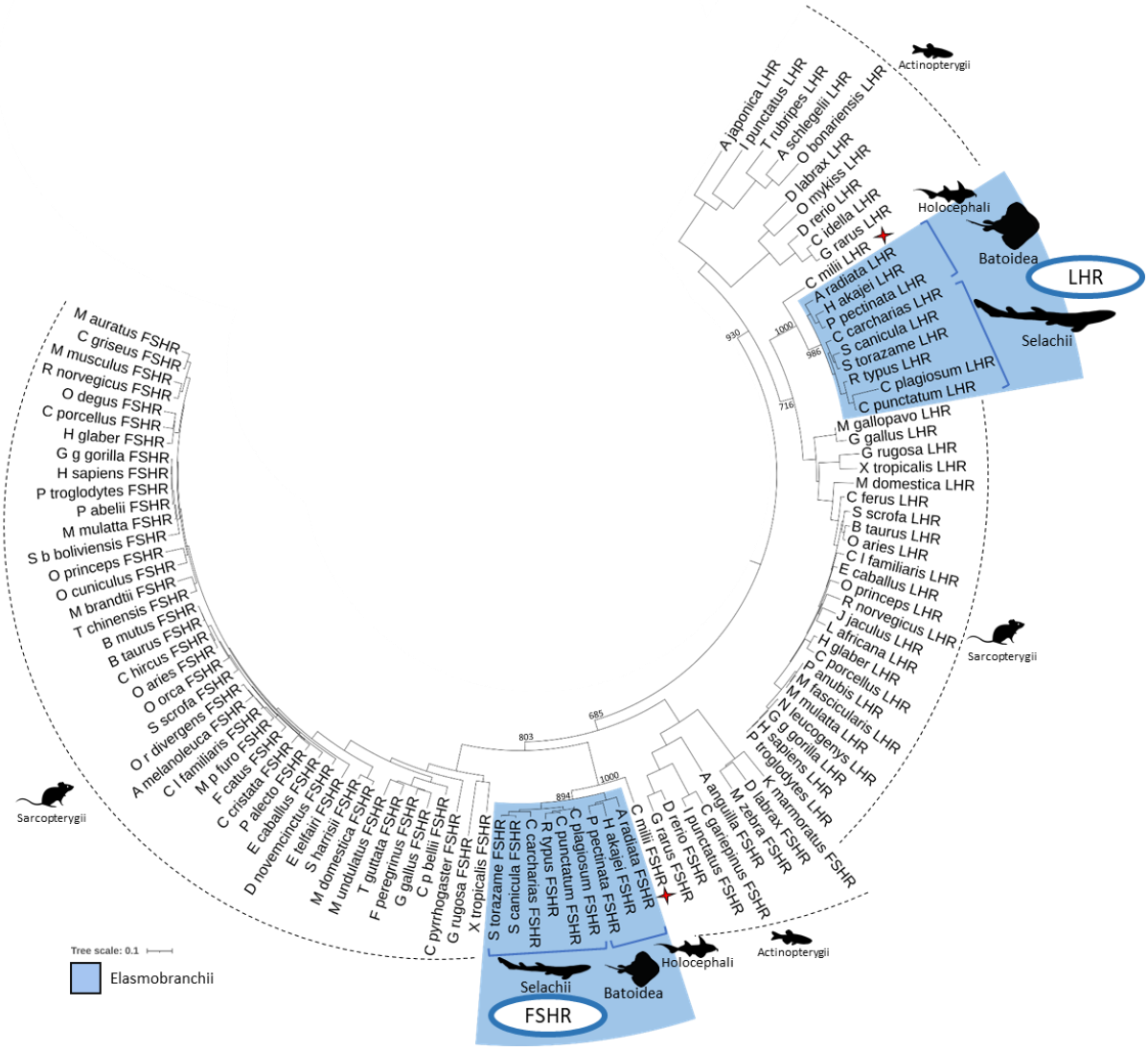


**Fig. S4.** Molecular phylogeny of gnathostomes GTHRs. Identified elasmobranch FSHRs and LHRs are highlighted in blue. The *C. milii* sequences are highlighted by a red star. Support values shown for relevant node are bootstraps for 1000 replicates. Animal illustrations are used with permission from http://phylopic.org.

```
                                                                  1  2
C.milii CGA        -------MIWYGKYAGLALVIFFVAEQGVHSFPDVEAATQGCPECRLKENKYFSRAGVPI      53
R.typus CGA        ---MFVLGLQHCQSEAKRKLEEQHLIFHLGSLQPNDLNSEGCPDCRLKENTRFSRTGVPI      57
C.carcharias CGA   -------MPRYMKCGGLALVVLLVIEQGVRSFPEVEAAALGCPDCRLKENTRFSKTGVPI      53
C.plagiosum CGA    -------MARYMKCGGLALVVLFVVEQGVRSFPEVEAAIPGCPDCRLKENTRFSRAGAPI      53
C.punctatum CGA    -------MARYMKCGGLALVVLFVVEQGVRSFPEVEAAIPGCPDCRLKENTRFSRAGAPI      53
S.canicula CGA     -------MARYMKYGGLAFVVLLVVEQGVRTFPEVEAAAPGCPDCRLKENTRFSRTGVPI      53
S.torazame CGA     -------MTRYMKCGGLALVVLLMVEQGVRSFPEVEASAPGCPDCRLKENTRFSRTGVPI      53
L.erinacea CGA     -------MLDCMKCGGLVLIVLLVMKHSFNSFPEVEAAAGGCPDCRLKENSRFSRPGIPI      53
A.radiata CGA      --MSVYKMLDYMKCGGLVLIVLLVVELSFHSFPEVEAAAGGCPDCRLKENSRFSRPGIPI      58
P.pectinata CGA    -------MFNYMKWGGLALVFFLVVEHSFHSFPEVEAATGGCPDCRLKENTRFSRPGKPI      53
H.akajei CGA       -------MFNYMKCGGLALIVLLIVELSFHSFPEVEAAPRGCPDCKLKENTRFSRPGKPI      53
                             :  . .   :        . ::   :    ***:*:****. **: * **
                    3  45                   G      67                 G   8 9
C.milii CGA        FQCVGCCFSRAYPTPMRSKRTMLVPKNITSEATCCVAKSFSRVI-VDNLKIENHTDCHCS     112
R.typus CGA        FQCKGCCFSRAYPTPMRSKKTMLVPKNITSEATCCVAKLFSRVTLMGNLKIENHTECHCS     117
C.carcharias CGA   FQCKGCCFSRAYPTPMRSKKTMLVPKNITSEATCCVAKLFSRVTLMGNLKIENHTECHCS     113
C.plagiosum CGA    FQCKGCCFSRAYPTPMRSKKTMLVPKNITSEATCCVAKLFSRVTLMGNLKIENHTECHCS     113
C.punctatum CGA    FQCKGCCFSRAYPTPMRSKKTMLVPKNITSEATCCVAKLFSRVTLMGNLKIENHTECHCS     113
S.canicula CGA     FQCKGCCFSRAYPTPMRSKKTMLVPKNITSEATCCVAKLFSRVTLMGNLKIENHTECHCS     113
S.torazame CGA     FQCKGCCFSRAYPTPMRSKKTMLVPKNITSEATCCVAKLFSRVRHFGNLKIENHTECHCS     113
L.erinacea CGA     FQCKGCCFSRAYPTPMRSKKTMLVPKNITSEATCCVAKLFSRVTLMGNLKIENHTDCHCG     113
A.radiata CGA      FQCKGCCFSRAYPTPMRSKKTMLVPKNITSEATCCVAKLFSRVTLMGNLKIENHTDCHCG     118
P.pectinata CGA    FQCKGCCFSRAYPTPMRSKKTMLVPKNITSEATCCVAKLFSRVTLMGNLKIENHTDCHCS     113
H.akajei CGA       FQCKGCCFSRAYPTPMRSKKTMLVPKNITSEATCCVAKLFSKVTLMGNLKVENHTDCHCS     113
                   *** ***************:****************** **:*  :.***:****:** .
                    10
C.milii CGA        TCYYHKS 119
R.typus CGA        TCYYHKS 124
C.carcharias CGA   TCYYHKS 120
C.plagiosum CGA    TCYYHKS 120
C.punctatum CGA    TCYYHKS 120
S.canicula CGA     TCYYHKS 120
S.torazame CGA     TCYYHKS 120
L.erinacea CGA     TCYYHKS 120
A.radiata CGA      TCYYHKS 125
P.pectinata CGA    TCYYHKS 120
H.akajei CGA       TCYYHKS 120
                   *******
```

**Fig. S5**. Multiple alignment of chondrichthyan CGA subunit protein sequences. Sequences of the putative peptide signal is highlighted in light orange, the 'seat' region in orange and conserved cysteines are numbered. G, putative N-glycosylation sites.

A

```
                                                1   G          2  3    G   4   5
C.milii FSHβ        MLLVMV-NRISAAHGFLLILCWVSIHCQNNCQLTNITMAVEKEECGYCGNVNVSWCSGYC        59
R.typus FSHβ        MLQIMV-TRSFVTYIFLILLSWMSVQSLNRCQLTNITISVEKEECGYCGMVNATWCAGYC        59
C.plagiosum FSHβ    MFQIMV-TRIFVIYIFIFLLSWMSVQSLNRCQLTNITISVEKEECGYCGMVNATWCAGYC        59
C.punctatum FSHβ    MFQIMV-TRIFVIYIFIFLLSWMSVQSLNRCQLTNITISVEKEECGYCGMVNATWCAGYC        59
C.carcharias FSHβ   MFQIMV-TKISTIHIFLFLLCWMSVQSLNRCQLSNITIAVEKEECGYCGMINVTWCAGYC        59
S.torazame FSHβ     MFEIMM-TKISTIHVFFFLLCWMSVQSLNRCQLTNITIAVEKEECGYCGMVNVTWCAGYC        59
S.canicula FSHβ     MFKIMM-TKISTFHVFFFLLCWMSVQSLNRCQLTNITIAVEKEECGYCGMVNVTWCAGYC        59
A.radiata FSHβ      MFQAMVPSKTFTIHLLLLVLCRASTVSMNKCQLTNITISVEREECGFCGTINVTWCSGYC        60
H.akajei FSHβ       MLQIMV-TKIITIHIFFLLLCWMSVKCQNRCQLTNVTIAVEKEECGYCSTVNVTWCSGYC        59
P.pectinata FSHβ    MLQIMV-TKNVAIHVFLLLLCWMSVESLHRCQLTNVTIAVEKEECGYCGTINVTWCSGYC        59
                    *:  *: .:  . : ::::*.  *  . :.***:*:*::**:****:*. :*.:**:***
                                    6              7               8 9  10
C.milii FSHβ        FTKDPVFKERMASIYQYICSYKEVIYQTITIPNCPSNVSPYYTYPVAISCQCGMCNTETT        119
R.typus FSHβ        FTKDPVSKNSLATIYQDICSYKEIVYETITIPNCPANVDPYYTYPVATGCQCGMCNTETT        119
C.plagiosum FSHβ    FTKDPVSKNSLASIYQDICSYKEIIYETITIPNCPANVDPYYTYPVAISCQCGMCNTETT        119
C.punctatum FSHβ    FTKDPVSKNSLASIYQDICSYREIIYETITIPNCPANVDPYYTYPVAISCQCGMCNTETT        119
C.carcharias FSHβ   FTKDPVCKHSLASIYQDICSYKEIIYESITIPNCPPNVDPYYTYPVAISCQCGMCNTETT        119
S.torazame FSHβ     FTKDPVCKHSMASIYQDICSYKEIIYETITIPNCPANVNPDYTYPVAISCQCGMCNTETT        119
S.canicula FSHβ     FTKDPVCKHSMASIYQDICSYKEIIYETITIPNCPANVNPYYTYPVAISCQCGMCNTETT        119
A.radiata FSHβ      FTKDPVCKHTLAFVYQEICSYKEIVYETMTIPNCPANVSPYYTYPVATSCQCGMCNTDTT        120
H.akajei FSHβ       FTKDPVCKHSLLFVYQEICSYKEIVYETITIPNCPPNVDPYFTYPVAISCQCGMCDTETT        119
P.pectinata FSHβ    FTKDPVCKHSLVFVYQEVCSYKEIVYETMTIPNCPANVDPYFTYPVAISCQCGMCNTETT        119
                    ****** *. :  :** :***:*::*:::****** **.* :***** .******:*:**
                     11       12
C.milii FSHβ        DCTVSALEPKYCSFTQQRKKRSLIMHSTLLH------RNI  153
R.typus FSHβ        DCTVSALEPTHCSLTP-------------------------  135
C.plagiosum FSHβ    DCTVSALEPTHCSLTP-------------------------  135
C.punctatum FSHβ    DCTVSALEPTHCSLKP-------------------------  135
C.carcharias FSHβ   DCTVSAMEPSHCSLTQQRTKDINKT----------------  144
S.torazame FSHβ     DCTVSAMEPTHCSLTQQRINDVNKT----------------  144
S.canicula FSHβ     DCTVSAMEPTHCSLTQQGIKDVNKT----------------  144
A.radiata FSHβ      DCTVSAMGPVHCSLEQPRRNDSSNSQITSNPSSRTNVKDI  160
H.akajei FSHβ       DCTVSALEPAHCSLTQQRGKDSNDVYLTSNPSSAPNEKNM  159
P.pectinata FSHβ    DCTVSAMEPAHCSLTQQRRKDIND-----------------  143
                    ******: * :**:
```

B

```
                                          1   G          2  3       4   5
C.milii LHβ         MVSPRLFLLALCLCCVQTRHFCRLTNITISAEKEECPTCITLTTSVCTGYCLTK----ES        56
S.canicula LHβ      MCLWQLFLLAMCFYSVQGRHLCHPTNVTISAEKDECPICVTLTTSICGGYCPTK----ES        56
S.torazame LHβ      MCLCQLFLLAMCFYSVQGRHLCHPTNVTISAEKDECPICVTLITSICSGYCPTK----ES        56
C.carcharias LHβ    MCSSQLFLLALCLCFVQSRHLCHPTNVTISAEKDECPICVSLTTSICSGYCPTK----ES        56
R.typus LHβ         MWWSQIFLLALSFAFVQSRHLCHPTNMTISAEKDECPICVALTTTVCSGYCPTK----ES        56
C.punctatum LHβ     MWWSQIFLLALCFPYVQNRHLCHPTNVTISAEKDECPICVTLTTSICSGYCPTK----ES        56
C.plagiosum LHβ     MWWSQIFLLALCFPYVQNRHLCHPTNVTISAEKDECPICVTLTTSICSGYCPTK----ES        56
A.radiata LHβ       MGP-TLLLLLVLTNLAQTHHLCRLTNATISAEKDGCPFCVSLTTTVCSGYCPTK----ES        55
H.akajei LHβ        MDCKRLLLLGLCILSVHSR-YCRLTNSTISAEKDNCPFCVVLTTTVCSGYCLTK----ES        55
P.pectinata LHβ     MDSTQLLLLGLCFSSVYSRYICHPTNSTISAEKDNCPFCVTLTTTVCSGYCLTKVMGQES        60
                    *    ::** :    .  :  *: ** ******: ** *: * *::* *** **    **
                                   6              7              8 9  10     11
C.milii LHβ         VYKSARLSMYQHVCTYGKIEYHSVKLQGCPKGVDPNYTFPVAISCECNRCRMDYTDCALQ        116
S.canicula LHβ      VYKSPLLSVYQHVCTYKEIRYETIRLPGCPTGVDSTYTYPVAVSCECNLCRMDYTDCTVQ        116
S.torazame LHβ      VYKSPLLSVYQHVCTYKEIRYETIRLPGCPAGVDSTYTYPVAVSCECNLCRMDYTDCTVQ        116
C.carcharias LHβ    VYKSPLLSVYQHVCTYKEIRYEAIRLPGCPLGVDSTYTYPVAVSCECNLCKMDYTDCTVQ        116
R.typus LHβ         VYKSPLLSVYQHVCTYKEIQYETIKLPGCPLGVDSTYTYPVAVSCECNLCKMDYTDCTVQ        116
C.punctatum LHβ     VYKSPLLSVYQHVCTYKEIQYETINLPGCPLGVDSTYTYPVAVSCECNLCKMDYTDCTVQ        116
C.plagiosum LHβ     VYKSPLLSVYQHVCTYKEIQYETINLPGCPLGVDSTYTYPVAVSCECNLCKMDYTDCTVQ        116
A.radiata LHβ       VYKSPLLSVYQHVCTYKALRYESIRLPGCGVRVEPTYTYPVALSCGCNLCKMHNTDCSRQ        115
H.akajei LHβ        VYKSPLLSVYQHVCTYREMRSETIKLPGCPKGVDPTYTYTVAVSCECNLCRLDYTDCSRQ        115
P.pectinata LHβ     VYKSPLLSVYQHVCTYKELRYESITLPGCPAGVDSTYTYPVAVSCECSLCKMDYTDCTRQ        120
                    ****  **:*******  :. .:: * **   *: .**: **:** *. *::. ***: *
                     12
C.milii LHβ         SIRPDFCSVRRGNQ  130
S.canicula LHβ      SIKPDFCIARRSSL  130
S.torazame LHβ      SIKPDFCIARRSSL  130
C.carcharias LHβ    SIKPDFCSARRVSL  130
R.typus LHβ         SIKPDFCSARRMSL  130
C.punctatum LHβ     SIKPDFCSARTLSL  130
C.plagiosum LHβ     SIKPDFCSARTLSS  130
A.radiata LHβ       SIMPDFCSSRRLLL  129
H.akajei LHβ        SIEPDFCSATRLLL  129
P.pectinata LHβ     SIMPDFCSARR---  131
                    ** ****
```

**Fig. S6**. Multiple alignment of chondrichthyan FSHβ and protein LHβ sequences. Sequence of the putative peptide signal is highlighted in light orange, the 'seat' region in orange, the 'seat-belt' region in green and conserved cysteines are numbered. G, putative N-glycosylation sites.

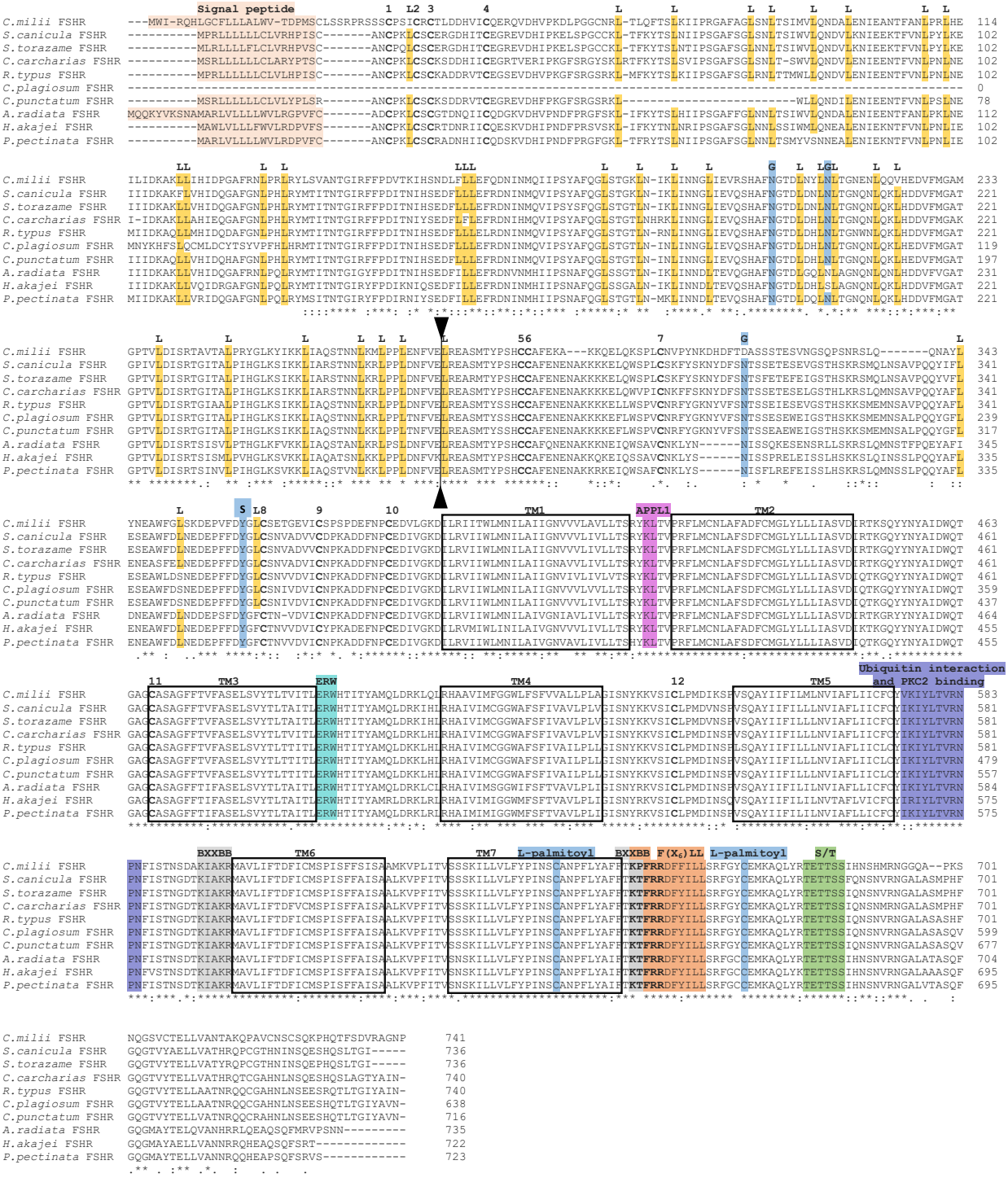


**Fig. S7**. Multiple alignment of chondrichthyan FSHR protein sequences. Sequence of the putative peptide signal is highlighted in light orange, conserved cysteines are numbered, leucine residues are highlighted in yellow, the putative N-glycosylation (G), sulfotyrosine (S) and L-palmitoyl sites are highlighted in blue, the vertical black bar corresponds to the putative limit between the solenoid and the hinge, putative intramembrane α-helixes are boxed and the putative interacting motifs colored.

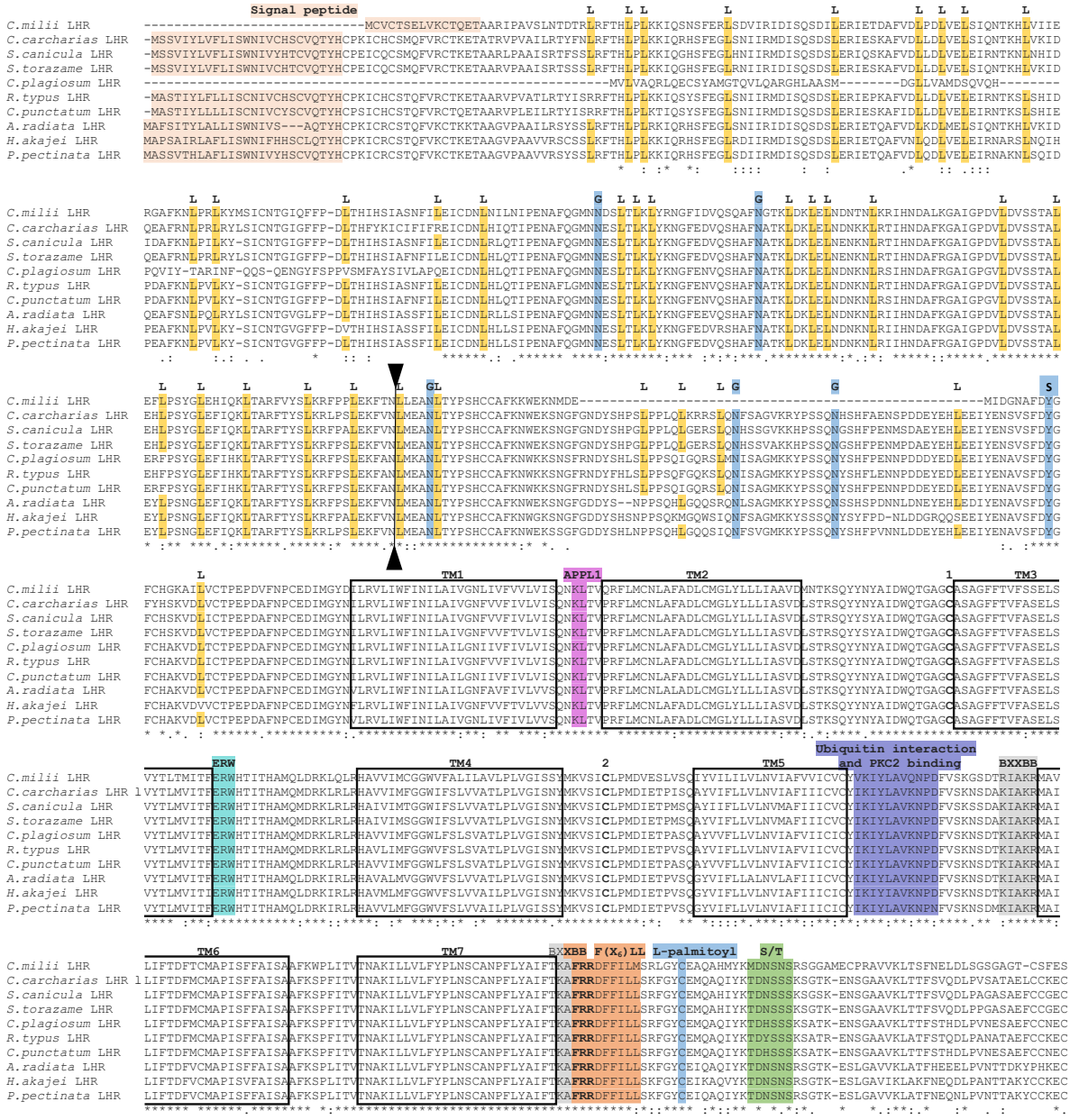


**Fig. S8.** Multiple alignment of chondrichthyan LHR protein sequences. Sequence of the putative peptide signal is highlighted in light orange, conserved cysteines are numbered, leucine residues are highlighted in yellow, the putative N-glycosylation (G), sulfotyrosine (S) and L-palmitoyl sites are highlighted in blue, the vertical black bar corresponds to the putative limit between the solenoid and the hinge, putative intramembrane α-helixes are boxed and the putative interacting motifs colored.

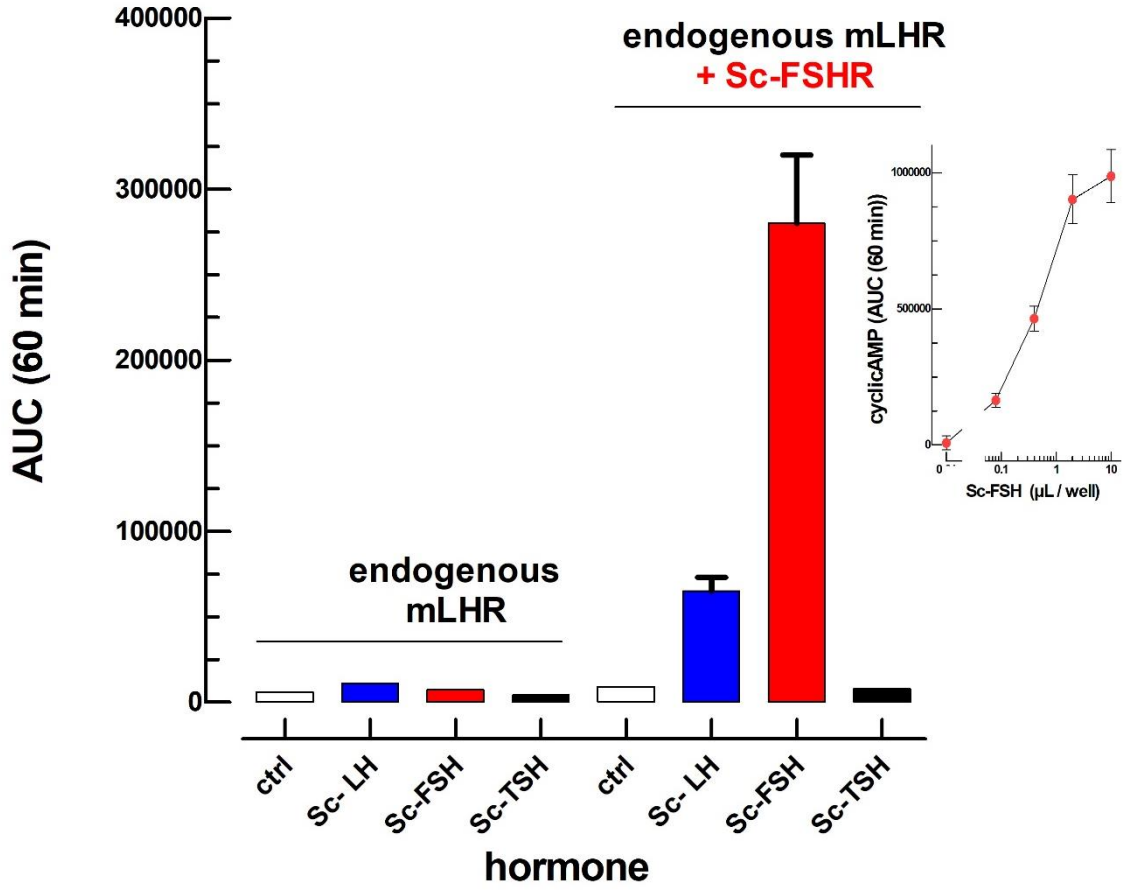


**Fig. S9.** In vitro mLTC bioassay. mLTC cells expressing endogeneous murine LH receptors (mLHR), were transfected with *scfshr* then stimulated by scFSH, scLH and scTSH ligands expressed in CHO cells (10µl of 5X concentrated supernatant). Non transfected mLTC cells were equally tested with the GTHs ligands and served as reference. Control (ctrl) refers to non transfected CHO cells surpernatants (10µl of 5X concentrated supernatant). The inserted graph shows the dose-dependent cAMP response to scFSH of mLTC cells transfected with *scfshr.*

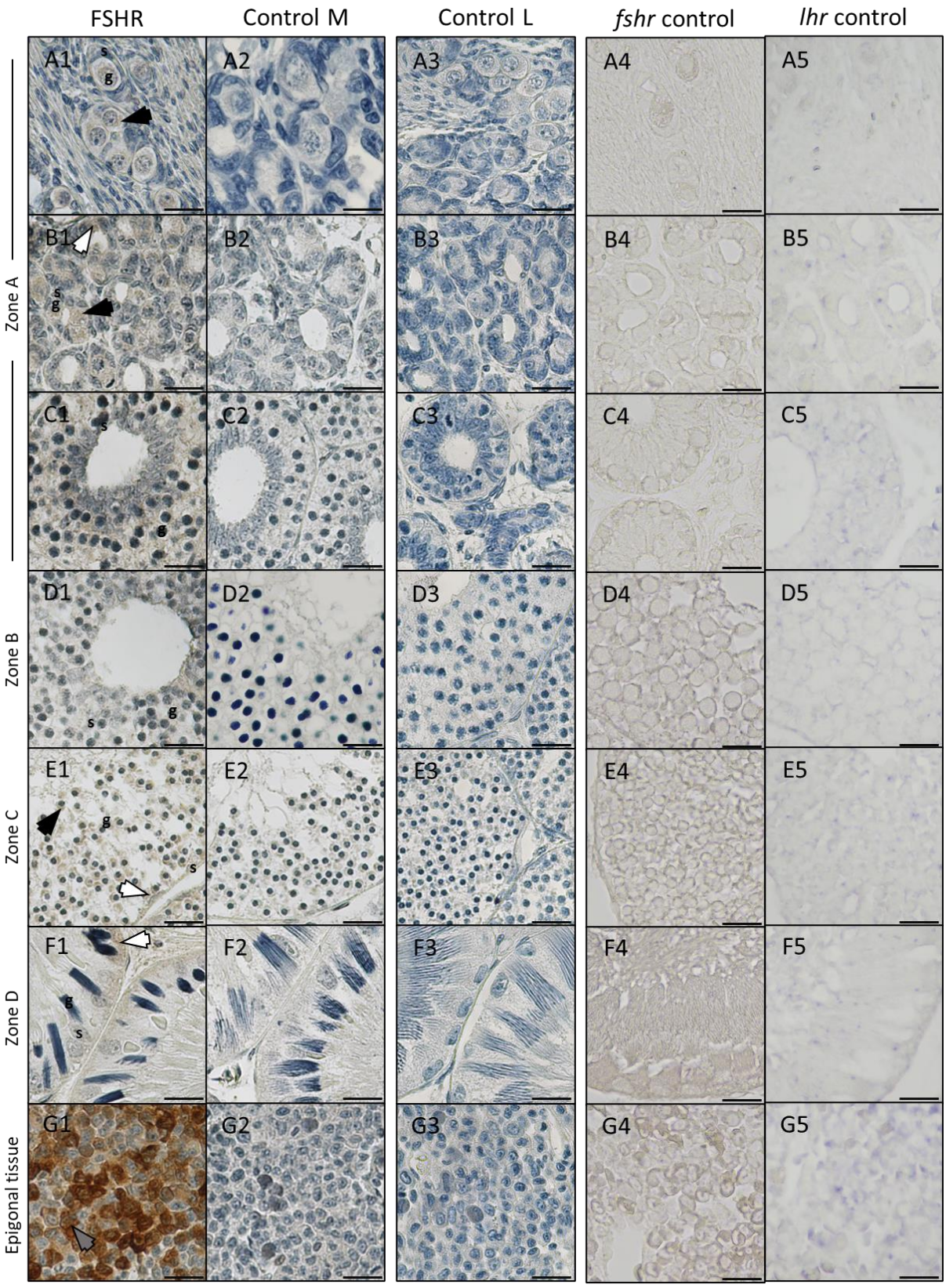


**Fig. S10.** Immunohistochemistry targeting FSHR and *in situ* control in *S. canicula* testicular sections. (A1-G1) Immunohistochemistry using mouse monoclonal anti-human FSH-R antibody (ab219312). (A2-G2) Immunohistochemistry controls using anti-mouse goat IgG H&L, horseradish peroxidase (HRP) polymer (1:1, Abcam, ab214879) and (A3-G3) anti-rabbit goat IgG H&L, HRP polymer (1:1, Abcam, ab214880). *In situ* hybridization controls using sense riboprobes of *fshr* (A4-G4) and *lhr* (A5-G5). (A),

germinative area; (B) cysts in formation; (C) cysts with spermatogonia; (D) cysts with spermatocytes; (E) cysts with young spermatids; (F) cysts with late spermatids and (G) epigonal tissu; g: germinal cell nuclei; s: sertolian precursor (A,B) or sertolian nuclei (C-F). Stain associated to FSHR IHC was observed in the cytoplasm of germ cells (black arrowhead), including undifferentiated spermatogonia (A1-B1) and young spermatids (E1) and in the cytoplasm of sertolian precurssors (B1) and differentiated Sertoli cells (E1-F1) (white arrowhead). Concerning the cysts with spermatogonia (C1) and cysts with spermatocytes (D1), stain was observed, but it was difficult to associate it with a type of cell. Stain was also well observed in the cytoplasm of epigonal tissu cells (G1) (gray arrowhead). *In situ* controls revealed no important background noise (A2-G2, A3-G3, A4-G4, A5-G5). Scale bars: normalized at 10 µm.

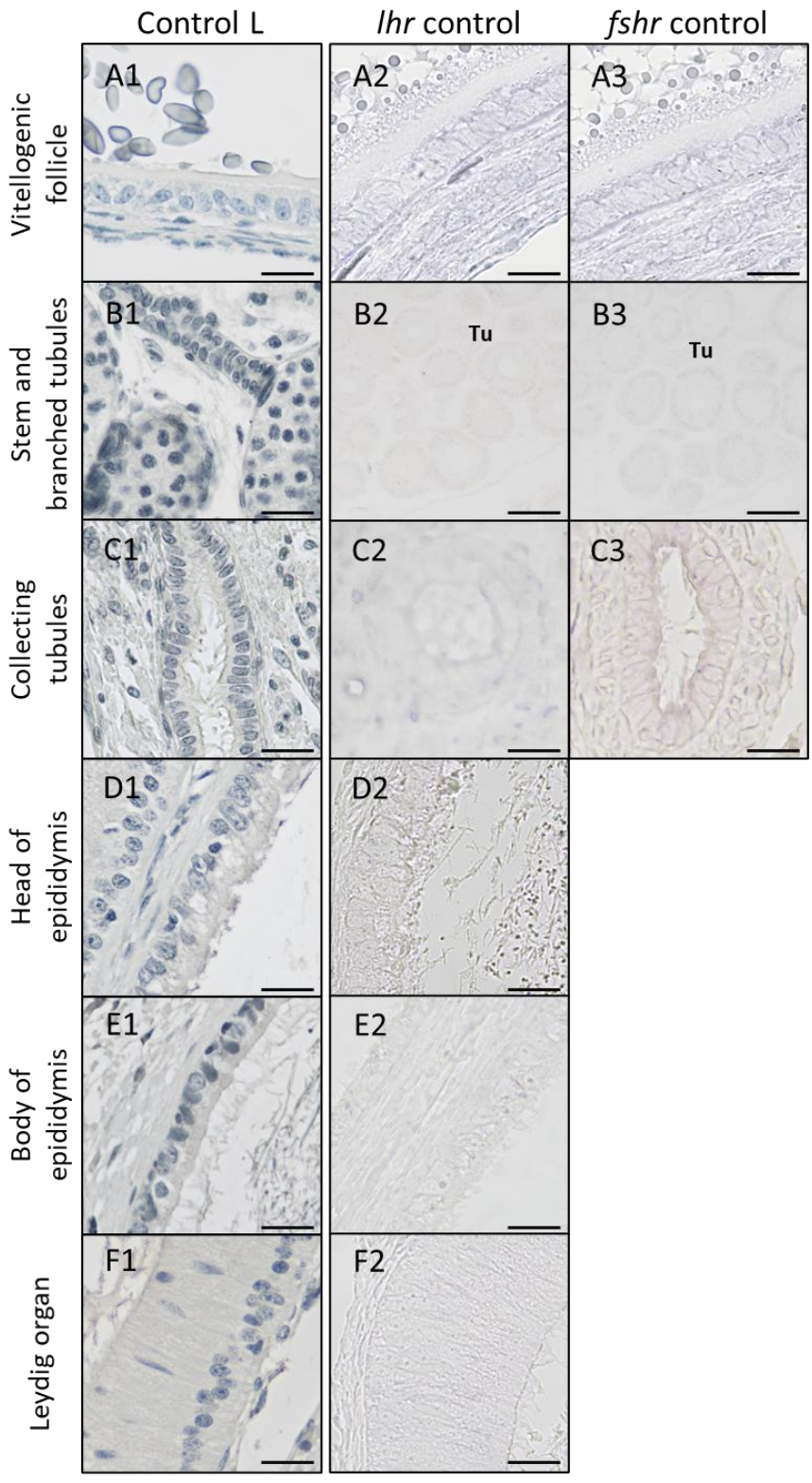


**Fig. S11**. *In situ* control in *S. canicula* vitellogenic follicle sections and other organs associated with the male genital tract. (A1-F1) Immunohistochemistry controls using anti-rabbit goat IgG H&L, HRP polymer (1:1, abcam, ab214880). *In situ* hybridization controls using sense riboprobes of *lhr* (A2-F2) and *fshr* (A3-C3). *In situ* controls revealed no significant background noise. Tu: epithelium of stem and branched tubules. Scale bars: normalized at 10 µm.

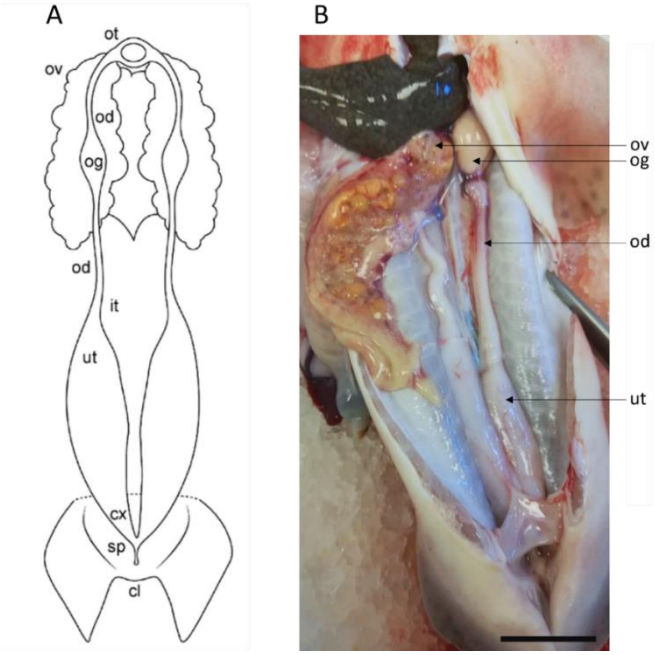


Fig. 1. **Le tractus génital femelle chez la petite roussette *Scyliorhinus canicula*. A.** Représentation schématique du tractus génital femelle (d'après García-Salinas et al., 2021). **B.** Photo anatomique correspondante (communication personnelle). cl, cloaque; cx, cervix; it, isthme; od, oviducte; og, glande de l'oviducte; ot, ostium; ov, ovaire; sp, sphincter; ut, utérus. Barre d'échelle : 2 cm.

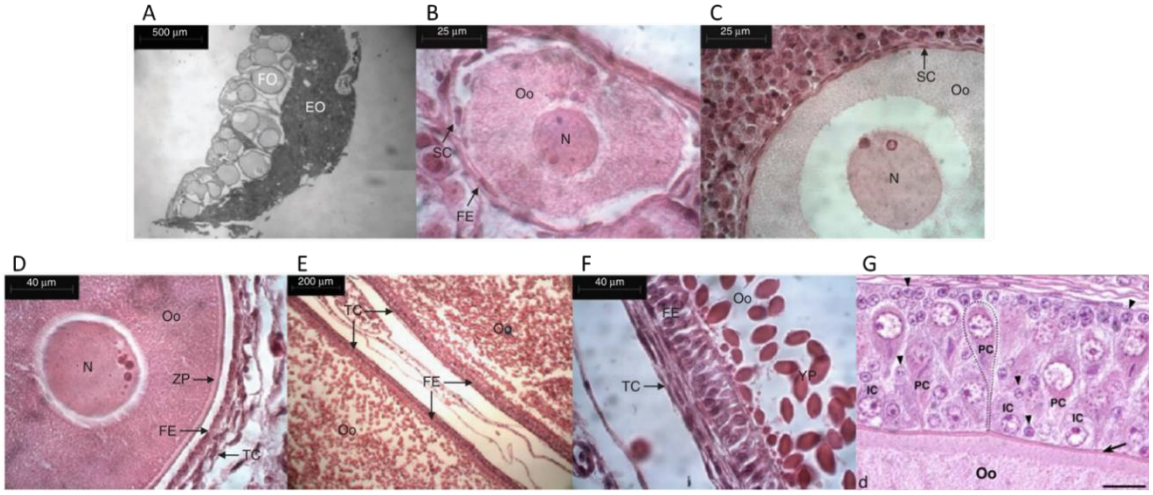


Fig. 2. **Histologie de l'ovaire et des différents stades folliculaires chez la petite roussette *Scyliorhinus canicula*. A.** Coupe transversale de l'ovaire, contenant des follicules ovariens à différents stades, associé au tissu épigonal (EO). **B.** Follicule primordial (0,095 mm de diamètre) composé d'un ovocyte (Oo) primaire avec son noyau (N) entouré d'une seule assise de cellules squameuses (SC) qui forme l'épithélium folliculaire (FE). **C.** Follicule primaire (0,23 mm de diamètre). **D.** Follicule secondaire (0,71 mm de diamètre) composé d'un Oo primaire entouré de la zone pellucide (ZP), du FE contenant des petites et grandes cellules de la granulosa et, plus extérieurement, des cellules thécales (TC). **E.** Follicules pré-vitellogènes voisins de 5 (à gauche) et 6 mm de diamètre (à droite). **F.** Gouttelettes vitellines (YP) positionnées à l'intérieur du cytoplasme entouré d'une granulosa épaisse d'un follicule vitellogène de 7 mm de diamètre. D'après Kousteni and Megalofonou, 2020. **G.** Follicule ovarien d'environ 1 cm de diamètre avec un épithélium folliculaire contenant des cellules pyriformes (PC) complètement différenciées dont l'apex est dirigé vers la surface de l'ovocyte (Oo) (pointillés). IC ; cellules intermédiaires. Barre d'échelle : 20 µm. D'après Maurizii et al., 2009.

## II. Annexes chapitre II : La folliculogenèse chez *Scyliorhinus canicula*

Le tractus génital femelle des Élasmobranches est élaboré (García-Salinas et al., 2021a) (Fig. 1). Les femelles possèdent une paire d'appareils reproducteurs répartie dans la cavité abdominale. Les ovaires sont associés au tissu épigonal et, selon l'espèce, ils peuvent être jumelés, fusionnés ou vestigiaux. Lors de l'ovulation, les ovules sont libérés dans le cœlome et captés au niveau de l'ostium puis transporté depuis l'oviducte jusqu'à la glande de l'oviducte, ou glande nidamentaire, par l'action des cellules ciliées de l'épithélium de l'oviducte. Cette glande est responsable du stockage des spermatozoïdes et est le lieu de la fécondation de l'ovocyte. Elle assure également la synthèse des différentes assises protectrices de l'œuf et de sa capsule. La présence de cette glande sépare l'oviducte en deux parties, l'oviducte antérieur et l'oviducte postérieur. Chez certaines espèces, une structure semblable à un sphincter, l'isthme, fait la jonction entre l'oviducte postérieur et l'utérus. Selon les espèces, un seul utérus peut être fonctionnel et les embryons s'y développent selon différents modes de viviparités (Cf introduction) ou, dans le cas des ovipares, les œufs y sont conservés jusqu'à la ponte. Les requins femelles possèdent un cloaque, situé entre les nageoires pelviennes, où convergent les systèmes urinaires, reproducteurs et digestif. À l'intérieur du cloaque, l'extrémité caudale des utérus peut être indépendante ou converger et fusionner en un col commun (García-Salinas et al., 2021a).

Chez les Élasmobranches, l'ovaire est associé au tissu épigonal et est constitué de follicules ovariens dont la structure est comparable à ceux des autres Vertébrés (Fig. 2A). Chez la roussette mature, l'ovaire présente des follicules à tous les stades de développement, avec des follicules primordiaux (< 1mm) (Fig. 2B), composés d'un ovocyte primaire entouré d'une seule assise de cellules fusiformes folliculaires ; des follicules primaires (de 1 à 2 mm) (Fig. 2C), composés d'un ovocyte primaire de plus grande taille entouré de la zone pellucide, de cellules de la granulosa et de cellules thécales ; les follicules en pré-vitellogenèse (de 2 à 8 mm) (Fig. 2E), de plus grande taille, composés d'un épithélium folliculaire plus épais contenant des cellules piriformes (Fig. 2G) formant des extensions cytoplasmiques dans le cytoplasme de l'ovocyte et pouvant servir au transfert des précurseurs du vitellus (Andreuccetti et al., 1999) ; et des follicules vitellogènes (de 8 à 13 mm) avec des plaquettes vitellines visibles à l'intérieur du cytoplasme de l'ovocyte (Fig. 2F), celui-ci est entouré d'une zone pellucide, d'un épithélium

folliculaire composé de plusieurs assises de cellules prismatiques de la granulosa, d'une thèque interne vascularisée et d'une thèque externe distante (Kousteni and Megalofonou, 2020).

# Chapitre III

## Pleiotropic signaling of thyrostimulin (GPA2/GPB5) on Glycoprotein Hormone Receptors (FSHR, LHR, TSHR) in the elasmobranch *Scyliorhinus canicula* reproduction

**Fabian Jeanne, Stanislas Pilet, Danièle Klett, Yves Combarnous, Benoît Bernay, Sylvie Dufour, Pascal Favrel et Pascal Sourdaine**

# Chapitre III

## Pleiotropic signaling of thyrostimulin (GPA2/GPB5) on Glycoprotein Hormone Receptors (FSHR, LHR, TSHR) in the elasmobranch *Scyliorhinus canicula* reproduction

**Fabian Jeanne, Stanislas Pilet, Danièle Klett, Yves Combarnous, Benoît Bernay, Sylvie Dufour, Pascal Favrel et Pascal Sourdaine**

## Signalisation pléiotrope de la thyrostimuline (GPA2/GPB5) sur les récepteurs des hormones glycoprotéiques (FSHR, LHR, TSHR) dans la reproduction de l'Élasmobranche *Scyliorhinus canicula*

Les hormones glycoprotéiques (GPHs) contrôlent de nombreux processus tels que la reproduction *via* l'hormone lutéinisante (LH) et l'hormone folliculo-stimulante (FSH) et le métabolisme *via* l'hormone thyroïdienne (TSH), et ce, par l'activation des récepteurs couplés aux protéines G (LGR), LHR, FSHR et TSHR. Chaque GPH se compose d'une sous-unité α commune et d'une sous-unité βFSH, βLH ou βTSH spécifique. Plus récemment, deux protéines GPH supplémentaires, GPA2 et GPB5, ont été identifiées chez les Vertébrés et correspondent aux orthologues des GPA et GPB identifiés chez presque tous les Bilatériens non-Vertébrés. Les Chondrichtyens (Holocéphales et Élasmobranches) constituent le groupe frère des Vertébrés osseux et c'est le premier clade à posséder des sous-unités GPH diversifiées, ce qui leur confère une position phylogénétique clef pour la compréhension de l'évolution des régulations endocrines. Cependant, à l'instar des GTHs, la caractérisation de GPA2, GPB5 et TSHβ demeure limitée chez les Chondrichtyens. C'est pourquoi l'objectif de cette étude a été de compléter l'identification de GPA2, GPB5, TSHβ et TSHR chez plusieurs Chondrichtyens, puis d'analyser leurs structures, leurs profils d'expression par PCR en temps réel et des approches *in situ*, notamment en fonction des stades de la spermatogenèse, chez *Scyliorhinus canicula*. Les spécificités des interactions hormone-récepteur ont été analysées à partir de l'expression dans des lignées de cellules embryonnaires de rein humain (HEK293T) des protéines *sc*GPA2 seule, *sc*GPB5 seule et des monocaténaires *sc*TSHβ2-*sc*CGA et *sc*GPB5-*sc*GPA2. Les protéines recombinantes ont ensuite été testées sur des lignées exprimant le récepteur à tester, *sc*TSHR, *sc*FSHR ou *sc*LHR, et la protéine $G\alpha_{16}$. Les activations des récepteurs ont été mesurées sur la base de la mobilisation calcique ou de la production d'AMPc.

Dans cette étude, les séquences protéiques de GPA2, GPB5, TSHβ2, mais pas TSHβ1, et TSHR ont été identifiées à partir des génomes d'Élasmobranches et leurs structures apparaissent conservées entre-elles et au cours de l'évolution, à l'exception de la région charnière du TSHR qui apparait plus divergente. Les essais fonctionnels ont montré que les $EC_{50}$ les plus faibles étaient associés au monocaténaire *sc*GPA2-*sc*GPB5, suivit par *sc*GPB5 puis *sc*GPA2, pour les

trois récepteurs *sc*FSHR, *sc*LHR et *sc*TSHR. Quant au monocaténaire *sc*CGA-*sc*TSHβ2, il est capable d'activer uniquement le *sc*TSHR avec un $EC_{50}$ compris entre ceux de *sc*GPA2-*sc*GPB5 et *sc*GPB5. Les analyses d'expression par PCR et *in situ* ont montré une distribution tissulaire plus large pour *tshr* et *gpa2* que pour *gpb5*. Au niveau testiculaire, *tshr* et *gpb5* sont exprimés par les cellules de Sertoli et *gpa2* par les cellules germinales, des spermatogonies précoces aux spermatides tardives.

Pris dans leur ensemble, ces résultats ont montré une co-expression de *gpa2*/*gpb5*/*tshr* qui est à rapporter à celles de *fshr*/FSHR et *lhr*/LHR (Cf chapitre II) au niveau testiculaire. Ces résultats suggèrent l'existence de régulations paracrines par GPA2/GPB5 et soulèvent la question de la redondance fonctionnelle entre GPA2, GPB5, GPA2-GPB5, CGA-LHβ et CGA-FSHβ ainsi que celle de la signification évolutive de GPA2 et GPB5. Dans le cas de l'expression d'une sous-unité seule, la question de savoir si les formes biologiquement actives sont sous formes de mono- et/ou homo-dimères reste ouverte.

Cette étude complète les données sur GPA2 et GPB5 en étudiant un Chondrichtyen qui, par sa position phylogénétique d'intérêt, pourrait être considéré comme ayant un système endocrinien intermédiaire entre le rôle pléiotrope de la signalisation GPA2-GPB5/GPHR identifié chez les Bilatériens et la signalisation spécifique GtH/GtHR identifiée chez les Mammifères.

**Pleiotropic signaling of thyrostimulin (GPA2/GPB5) on Glycoprotein Hormone Receptors (FSHR, LHR, TSHR) in the elasmobranch *Scyliorhinus canicula* reproduction.**

Fabian Jeanne[1], Stanislas Pilet[1], Danièle Klett[2], Yves Combarnous[2], Benoît Bernay[3], Sylvie Dufour[1], Pascal Favrel[1] and Pascal Sourdaine*[1]

[1] Université de Caen Normandie, Muséum national d'Histoire naturelle, Sorbonne Université, Université des Antilles, CNRS, IRD, Laboratoire de Biologie des Organismes et Ecosystèmes Aquatiques (BOREA), UMR 8067, 14032 Caen cedex 5, France.

[2] INRAE, CNRS, Université de Tours, UMR Physiologie de la Reproduction & des Comportements, 37380 Nouzilly, France

[3] Université de Caen Normandie - Plateforme PROTEOGEN, US EMerode, 14032 Caen cedex 5, France.

*Corresponding Author: orcid.org/0000-0001-9811-2876;
Email: pascal.sourdaine@unicaen.fr

**Abstract**

The pituitary glycoprotein hormones (GPHs) control several physiological processes in vertebrates such as reproduction and metabolism. They include the luteinizing hormone (LH), the follicle-stimulating hormone (FSH), and the thyroid-stimulating hormone (TSH), which activate their cognate leucine-rich repeat G protein-coupled receptors (LGRs), LHR, FSHR, and TSHR. Each pituitary GPH consists of a common α subunit and a specific βFSH, βLH or βTSH subunit. More recently, two supplementary GPH proteins, GPA and GPB, were identified in nearly all bilaterians and are the ancestors of the pituitary GPH α- and β-subunits, respectively. Chondrichthyans (holocephalans and elasmobranchs), the sister group of bony vertebrates, are the most ancient clade to possess diversified GPH subunits. In the present study, GPA2, GPB5, TSHβ2, but not TSHβ1, and TSHR sequences have been identified in several elasmobranch genomes, and structure and functional hormone-receptor interactions have been studied in the small-spotted catshark (*Scyliorhinus canicula*). Expression profiles were

analyzed by real-time PCR, *in situ* hybridization, and immunohistochemistry along the male genital tract, other tissues, and female tissues. Functional assays showed that conditioned media from cells expressing the recombinant *sc*GPB5/*sc*GPA2 were more effective than the independent subunit *sc*GPB5 in activating *sc*TSHR, *sc*FSHR, and scLHR. *Sc*GPA2 also appeared able to activate the three *sc*GPHRs, but only at high concentrations. Expression and *in situ* analyses showed a broader tissue distribution expression for *tshr* and *gpa2* than for *gpb5,* mainly observed in the testes. In testis, expression of *tshr* and *gpb5* by Sertoli cells and of *gpa2* by germ cells, from early spermatogonia to late spermatids, suggested paracrine/autocrine functions of GPA2/GPB5/GPHR signaling during spermatogenesis. This study complements the data on GPA2 and GPB5 by studying a chondrichthyan of phylogenetic interest for understanding the evolution of endocrine regulation in vertebrates.

Keywords: Thyrostimulin, GPA2, GPB5, Thyroid-stimulating hormone subunit β2 (TSHβ2), Thyroid-stimulating hormone receptor (TSHR), Glycoprotein hormone receptor (GPHR), Spermatogenesis, Chondrichthyes, Elasmobranchs, Shark, Evolution, Testis, Epididymis.

## Introduction

Glycoprotein hormones (GPHs) belong to the family of cystine-knot proteins and exert a wide range of physiological functions by activating their cognate leucine-rich repeat-containing G protein-coupled receptors (LGRs). In mammals, pituitary GPHs comprise two gonadotropins (GTHs), follicle-stimulating hormone (FSH) and luteinizing hormone (LH), as well as thyrotropin hormone (TSH). The pituitary GPHs comprise a common α-subunit (CGA) and a specific β-subunit (FSHβ, LHβ, TSHβ), forming non-covalent heterodimers. FSH and LH are produced by the anterior pituitary, under the regulation by the hypothalamic gonadotropin-releasing hormone (GnRH) signaling, and regulate gonadal functions by interacting with their receptors, FSHR and LHR, thus constituting the hypothalamic-pituitary-gonadal (HPG) axis. The pituitary TSH is regulated by the hypothalamic thyrotropin-releasing hormone (TRH) and regulates thyroid function by interacting with its receptor, TSHR, thus forming the hypothalamic-pituitary-thyroid (HPT) axis. These GPH subunits, with their cognate receptors, emerged before the gnathostome radiation (Heyland et al., 2012; Roch and Sherwood, 2014).

The β-subunits derived from an ancestral gene (*gpb*) through the two whole genome duplications, 1R and 2R, generating two gonadotropin β subunits, lhβ and fshβ, as well as two thyrotropin β subunits, *tshβ1* and *tshβ2*, present in some chondrichthyes, the holocephalan *Callorhinchus milii* and the batoidea *Leucoraja erinacea*, and in early lobe-finned fish, the coelacanth *Latimeria chalumnae* and the lungfish *Neoceratodus forsteri*, while *tshβ2* was lost in actinopterygians and tetrapods (Maugars et al., 2014; Dufour et al., 2020; Quérat, 2021). In the early 2000s, two supplementary GPH subunit-related genes, *gpa2,* and *gpb5*, were identified from the human genome (Hsu et al., 2002), and the ability of the recombinant GPA2/GPB5 heterodimer to activate TSHR in *Homo sapiens* and *Ratus norvegicus*, let to name the corresponding GPH as thyrostimulin, but also referred to as Corticotroph-derived glycoprotein hormone (CGH) (Nagasaki *et al*., 2006; Nakabayashi et al., 2002). *Gpa2* and *gpb5* orthologs were identified in several protostomia (Heyland et al., 2012; Kudo et al., 2000; Sudo et al., 2005; Wahl et al., 2022), primitive chordates (Dong et al., 2013; Wang et al., 2018; Yang et al., 2023), cyclostomata (Sower et al., 2015) and various vertebrates (Buechi and Bridgham, 2017; Cahoreau et al., 2015; Hara et al., 2018; Levavi-Sivan et al., 2010) but not in cnidaria (Dos Santos et al., 2009). Molecular ancestors of GPHRs have also been identified under different names and can be activated by recombinant GPA2/GPB5 heterodimers or recombinant single-chain GPB5-GPA2 proteins, such as in protostomia (Kenis et al., 2023; Rocco and Paluzzi, 2020; Sudo et al., 2005; Wang et al., 2018), primitive chordates (Dos Santos et al., 2009; Wang et al., 2018; Yang et al., 2023) and cyclostomata (Hausken et al., 2018); highlighting the coevolution of the GPH/GPHR signaling along bilateria evolution. However, the question of whether GPA2 and GPB5 are active *in vivo* as non-covalent heterodimers, homodimers, or monomers has been raised. Indeed, the absence of the seatbelt in GPB5, as well as the expression patterns of GPA2 and GPB5 in different cells, are not in favor of dimerization (Alvarez et al., 2009; Dufour et al., 2020; Yang et al., 2023). Concerning the roles of GPA2/GPB5, thyrostimulin would be involved in several biological functions through activation of TSHR, in addition to regulating thyroxine production (Nagasaki *et al*., 2006; Nakabayashi et al., 2002), such as bone formation (Bassett et al., 2015), immune response (Suzuki et al., 2009) and reproduction (Sun et al., 2010) in mammals, as well as development in protostomes (Heyland et al., 2012; Vandersmissen et al., 2014). The role of GPA2/GPB5 in reproduction have been highlighted in *H. sapiens* as a paracrine hormone secreted by the oocyte and activating granulosa and theca cells which express TSHR (Sun et al., 2010). In

males, the role of thyrostimulin has been demonstrated in studies using RNAi down expression of the GPHR of protostomia such as in the nematode, *Caenorhabditis elegans*, where down expression of its FSHR-1 results in the absence of germ cell renewal (Cho et al., 2007) and in the mosquito, *Aedes aegypti,* where down expression of its LGR1 results in abnormal spermatogenesis (Rocco et al., 2019, 2017). In addition, *gpa2*, *gpb5,* and their cognate receptors' gene are coexpressed in the gonads of several protostomia such as the fly, *Drosophila melanogaster* (Vandersmissen et al., 2014), the scallop, *Patinopecten yessoensis* (Zhang et al., 2020) and the prawn, *Macrobrachium rosenbergii* (Wahl et al., 2022). They are also coexpressed in the gonads of Chordata, such as the amphioxus, *Branchiostoma japonicum* (Wang et al., 2018), the ascidian, *Styela clava* (Yang et al., 2023), the lamprey, *Petromyzon marinus* (Hausken et al., 2018) and the catshark, *Scyliorhinus torazame* (Hara et al., 2018).

The study of the GPA2/GPB5 signaling in chondrichthyes is of interest because of their unique phylogenetic position. Indeed, the chondrichthyes are the sister group to osteichthyes (bony vertebrates), whose divergence occurred around 450 million years ago (Irisarri et al., 2017), and include the holocephalans (chimaeras) and elasmobranchs (sharks and rays). In terms of the comparative evolution of HPG and HPT endocrine axes, chondrichthyes could illustrate the first representatives of jawed vertebrates with specialized axes, positioned between cyclostomata, which have overlapping HPG and HPT axes with two GPHs (lGpH and thyrostimulin) and two GPHRs (lGpH-R I and –R II) (Sower and Hausken, 2017), and the bony vertebrates. The first study to examine the specificity of interactions between GPHs and GPHRs in a chondrichthyan was carried out on the holocephalan *C. milii*. It showed high specificity for FSH/FSHR, LH/LHR, and TSH/TSHR complexes, while recombinant GPB5-GPA2 activated no GPHR (Buechi and Bridgham, 2017). However, the GPA2/GPB5 signaling remains to be characterized in elasmobranchs which diverged early from holocephalans, around 380 million years ago. Interestingly, Hara's work, based on a global genome expression analysis of the shark *S. torazame*, showed that *gpa2* was expressed in several tissues, including testis, whereas *gpb5* expression appeared to be restricted to the testis (Hara et al., 2018). This result motivated us to develop a more comprehensive study during spermatogenesis in another chondrichthyan, the small-spotted catshark *Scyliorhinus canicula*, a nonendangered species belonging to the carcharhiniforms, which is the largest family of sharks.

Spermatogenesis is a highly conserved and orderly process under endocrine and paracrine regulations that allows the transformation of undifferentiated spermatogonia into spermatozoa. The testis of the small-spotted catshark *S. canicula* consists of spermatocysts (cysts), each made of spermatoblasts in which one Sertoli cell is associated with synchronously developing germ cells. On a cross-section of the testis, cysts originate from the germinative area, located on the dorsolateral edge of the testis. As new cysts are continuously formed, older cysts are moved to the opposite edge of the testis, leading to a zonal arrangement of cysts according to the spermatogenic wave. Thus, at least five testicular zones corresponding to the germinative area, the cysts with spermatogonia, the cysts with primary and secondary spermatocytes, the cysts with early spermatids, and the cysts with late spermatids, are easily distinguishable and accessible (Loir and Sourdaine, 1994). In addition, another particularity of the testis of *S. canicula* also observed in another shark, *Squalus acanthias*, is the absence of differentiated Leydig cells, Sertoli cells being the main steroidogenic cells (Cuevas and Callard, 1992; Pudney and Callard, 1984a, 1984b; Sourdaine and Garnier, 1993).

This study aimed to complete the identification of GPA2, GPB5, TSHβ and TSHR proteins in several chondrichthyes and to analyze their structures and expression profiles by real-time PCR and *in situ* detections in relation to spermatogenesis stages as well as in other tissues, including the male and female genital tracts of the small spotted catshark *S. canicula*. Using *in vitro* bioassays, specificities of hormone and receptor interactions were analyzed with *sc*GPA2, *sc*GPB5, and *sc*TSHβ as single-chain recombinant heterodimers or monomers as ligands, and with the recombinant receptors *sc*TSHR, *sc*FSHR, and *sc*LHR expressed in HEK293 cells for testing their respective activities. The results are discussed in an evolutionary perspective.

## Materials and Methods

### Animals and Tissue Sampling

The catshark *Scyliorhinus canicula* was assessed, in 2020, as least concern in the red list of threatened species by the IUCN (International Union for Conservation of Nature). Sexually mature male (608 ± 137 g; 58± 3 cm) and female (647 ± 90 g; 57 ± 4 cm) catsharks were fished during a CGFS (Channel Ground Fish Survey) campaign by IFREMER in the East Manche in September 2022 (Giraldo et al., 2022). Animals were maintained in natural seawater tanks at

the marine station of the University of Caen Normandy (Centre de Recherches en Environnement Côtier (CREC), Luc-sur-Mer, France). Under the A14384001 number, CREC facilities are approved by the council department of population care (Préfecture du Calvados, France). Sharks were acclimated 2 weeks before killing by percussive blow to the head followed by sectioning and pithing of the spinal cord and exsanguination according to the European directive 2010/63/UE. Testes, epigonal tissues, proximal and distal epididymis, seminal ampullae, myelencephalons, mesencephalons, midbrains/pituitaries, forebrains, olfactory bulbs, eyes, thyroid glands, Leydig organs, spleens, livers, pancreas, duodenums, kidneys, rectal glands, gills, hearts and muscles were sampled from 14 males and myelencephalons, mesencephalons, midbrains/pituitaries, forebrains, olfactory bulbs, ovaries, nidamental glands, oviducts, uterus and thyroid glands from 7 females and were transferred directly into liquid nitrogen before storage at -80°C with the exception of testes which were transferred in ice-cold Gautron's buffer (pH 7.8, 890 mosmol kg-1) (Gautron, 1978) with 58 mM trimethylamine-N-oxide (TMAO, Sigma, 317594) before dissection into the four zones (Loir and Sourdaine, 1994) corresponding to the zone containing the germinative area and cysts with spermatogonia (zone A), cysts with spermatocytes (zone B), cysts with early spermatids (zone C) and cysts with late spermatids (zone D). Other tissues such as testes, epididymis heads and bodies, ovaries, brains, thyroid glands and Leydig's gland were fixed in Gautron's buffer with paraformaldehyde 4% before alcoholic dehydration and stocked in butan-1-ol at -20°C.

**Sequence searches**

Protein sequences of GPA2, GBP5, TSHβ and TSHR were identified using BLAST searches, based on *C. milii* sequences (Buechi and Bridgham, 2017) against the following genomes and databases: *A. radiata* (sAmbRad1.1.pri), *C. carcharias* (Marra et al., 2019), *C. plagiosum* (ASM401019v1), *C. punctatum* (Hara et al., 2018), *P. pectinata* (sPriPec2.1.pri), *R. typus* (Read et al., 2017), *S. canicula* (sScyCan1.2) and *S. torazame* (Hara et al., 2018) on NCBI (https://www.ncbi.nlm.nih.gov/genome/); *H. akajei* (sHemAka1.1) on Squalomix Blast Server (https://transcriptome.riken.jp/squalomix/blast/); and *L. erinacea* (Wang et al., 2012) on Skatebase (http://skatebase.org). To verify the relationship between obtained sequences and their putative families, phylogenetic trees were built based on the previous work of Buechi and Bridgham, 2017 using the MAFFT (Multiple Alignment using Fast Fourier Transform)

program, BMGE (Block Mapping and Gathering with Entropy) alignment curation and PhylML tree inference on NGPhylogeny online services (https://ngphylogeny.fr/workflows/oneclick/, (Lemoine et al., 2019) with a bootstrap of 1000. Obtained trees were finalized using iTOL online tool (https://itol.embl.de/, (Letunic and Bork, 2021).

Synteny analyses of gnathostomes GPA2, GPB5, TSHβ1 and TSHβ2 genomic regions were performed to annotate the orthologs identified in the batoid *A. radiata* and the sharks *S. canicula* and *C. carcharias*. Species occupying key phylogenetic positions were selected, including the cyclostome P. marinus, the chondrichthyan *C. milii*, the actinopterygian *L. oculatus*, and the sarcopterygians *L. chalumnae*, *X. laevis* and *H. sapiens*. Genomic regions of *C. milii* were selected as templates. The genes were mapped using NCBI's Genome Data Viewer (https://www.ncbi.nlm.nih.gov/genome/gdv/) and, for unretrieved genes, tBlastn using orthologous protein sequences were performed.

**3D model building**

Multiple alignments were performed using Clustal Omega package (https://www.ebi.ac.uk/Tools/msa/clustalo/, (Sievers et al., 2011)) with manual corrections to identify conserved structures (based on the knowledge in *H. sapiens* sequences). Signal peptides were predicted using predisi software (http://www.predisi.de/). Predictive models of GPA2s, GPB5s, TSHβs and TSHRs were built using SWISS-MODEL (https://swissmodel.expasy.org/, (Waterhouse et al., 2018), using the Q96T91.1.A, Q86YW7.1.A and the 7utz.1 template of *H. sapiens*, and finalized using Swiss PDB Viewer program (Johansson et al., 2012). Obtained models were evaluated by retaining the global sequence identities against the template, the greatest GMQE score (Global Model Quality Estimate, (Waterhouse et al., 2018), which depends on coverage, and the highest QMEANDisCo Global score (Studer et al., 2020), which evaluates the model 'as is' without explicit coverage. The same procedure was performed with *H. sapiens* sequences, as control, and for *C. milii* sequences. Using Swiss-PdbViewer (Johansson et al., 2012), predicted models were superimposed and the Root Mean Square Deviation (RMSD) were calculated and averaged by GPH subunits and by GPHRs.

**Functional hormone-receptor interaction in *in vitro* assays**

Synthetic pTarget plasmids containing *S. canicula* cDNA sequences for *fshr* (s*c-fshr*), *lhr* (s*c-lhr*) or *tshr* (s*c-tshr*) were obtained from Twist Bioscience (San Francisco, USA) and synthetic pTarget plasmids containing fusion construct *sctshβ-sccga* and *scgpb5-scgpa2* were obtained from GenScript Biotech (Rijswijk, Netherlands), in addition to pTarget plasmids containing the *scgpa2* alone or the *scgpb5* alone. Human embryonic kidney (HEK293T) cells were transiently transfected with the synthetic plasmid using FuGENE HD (Promega) according to the manufacturer's instructions. Cotransfection was done with *gphr*/pTarget construct and a pTarget expression construct for the human $G\alpha_{16}$ subunit, a promiscuous G protein which can direct intracellular signaling of GPCRs to the release of calcium *via* the phospholipase Cβ pathway, regardless of the endogenous G protein coupling of the receptor. The pTarget ligand constructs were transfected in HEK293T cells around 80% of confluence in 75 $cm^2$ flasks, then after 24 h of culture, the media were collected and concentrated using Amicon® 3K filters (Millipore). Cells for negative control experiments were transfected with empty pTarget or Gα16 and empty pTarget. Activation of the *S. canicula* GPHRs by GPHs were monitored using a fluorescence-based calcium mobilization assay according to Schwartz et al., 2021. Briefly, transfected HEK293T cells were loaded with Fluo-4 Direct (Invitrogen) for 1 day at 37°C with 5% of $CO_2$. Excitation of the fluorophore was done at 488 nm. The calcium response was measured at 525 nm for 2 min using a Flexstation 3 (Molecular Devices) at 37°C and analyzed using SoftMax Pro (Molecular Devices). For analysis of the activation of the Gαs/adenylyl cyclase/cAMP/PKA pathway, transfected cells were incubated with Glosensor cAMP reagent (4% final concentration in media) (Promega) for 2 h at room temperature prior the injection of the ligands (sc-GPHBTSH-CGA, sc-GPB5-GPA2, sc-GPA2 or Sc-GPB5) and cAMP luminescence response was measured at 37°C for 30 min using the Flexstation 3.

To determine the absolute concentrations of the ligands produced, an initial proteomic analysis of the ligand-containing media was carried out using high-resolution nanoLC-ESI-MS/MS to identify peptides resulting from trypsin digestion of the α-subunit (scCGA), *sc*GPA2 and *sc*GPB5. The VTLMGNLK, EFTFLAK and EEIEIFTAK peptides were designed for CGA, GPB5 and GPA2, respectively, according to the following criteria: the absence of cysteine residue, the absence of post translational modifications and a number of amino acids superior to 5. Selected peptides were synthesized by CliniSciences (Nanterre, France) and used as internal

quantity markers. The standard curves were established, ranging from 16.3 pg/µl to 666 pg/µl, and the equations obtained were y=400.05x-6339.1 ($R^2$=0.9967), y=979.22x-3058.1 ($R^2$=0.9997) and y=231.1x+11558 ($R^2$=0.9747) for CGA, GPB5 and GPA2, respectively, where "y" was the peak area of the peptide and "x" the concentration. Efficiency ($EC_{50}$) and efficacy (Emax) were calculated with 95% confidence intervals (profile likelihood) from sigmoidal dose-response equations which were constructed with a nonlinear regression analysis using Prism 5.0 (GraphPad Software, USA).

**Reverse Transcription and RT-qPCR**

Total RNAs were extracted from *S. canicula* tissues using Tri-Reagent (Sigma-Aldrich, 93289) before purification with the NucleoSpin RNAII columns kit (Machery-Nagel). They were quantified with a NanoDrop™ 2000 (Thermo Scientific) and degradation analyses were performed with an Agilent 2100 Bioanalyzer (Agilent) for testes zones, epigonal tissues, male brains and ovaries. Obtained RNA integrity numbers were greater than 7. For tissue distribution, real-time PCR was performed independently for three animals (N=3) in triplicate (n=3) excepted for testes (zone A, B, C and D) and the epigonal tissue where six animals were used (N=6, n=18). The CFX Connect Detection System (Bio-Rad) was used for RT-qPCR analyses. Two hundred and seventy ng of total RNAs were treated with 1U of RQ1 DNase (Promega, M6101) (37°C/20min) following by the reverse transcription using 1 ng random hexanucleotide primers (Promega, C1181), 0.5 mM dNTPs and 200 U of M-MLV Reverse Transcriptase (Promega, M1701) then the reactions were stopped (70°C/5min). The gene-specific primers were designed using Primer-BLAST (https://www.ncbi.nlm.nih.gov/tools/primer-blast/, (Ye et al., 2012)) with manual corrections according to the following criteria: length between 18-22 bp, GC content over 50%, Tm close to 60°C and generation of an 150-200 bp amplicon. The real-time PCR (5 ng of cDNA, 40 cycles: 95°C/15s, 60°C/45s) was done with the GoTaq®qPCR Master Mix (Promega, A6001). Melt curve analysis and efficiency tests were carried out to ensure the primers amplified a single product with 90-110% efficiency. The Ct values were read at 200 relative fluorescence units and normalized against the 5S RNA (Redon et al., 2010) using the $\Delta C_t$ method (Schefe et al., 2006). The $2^{-\Delta\Delta Ct}$ method (Livak and Schmittgen, 2001) allowed to calculated the expression variations based on the mean $\Delta C_t$ of all tissues. Comparison of the Ct 5SRNA/total RNA ratio between tissues shown no significant difference using non-parametric Kruskal-Wallis test with

a P-value of 0.14 (Supplementary Figure S1). Statistical analyses were performed using a first Shapiro-wilk test analysis followed by the none parametric Mann-Whitney U test for P-value < 0.05.

***In situ* hybridization**

Digoxigenin-conjugated riboprobes were synthesized from cDNA clones produced with specific primers (Supplementary Table S2). The resulting amplicons were cloned in pCR™II-TOPO™ Vector by TA cloning and then transformed in chemically competent *E. coli* using the TOPO TA Cloning kit (Invitrogen, k461020). After cultures, plasmids were purified using the Wizard® Plus SV Minipreps (Promega, A1340) then the digoxigenin-conjugated riboprobes were generated using M13 PCR on 100 ng of plasmids with 1 mM $MgCl_2$, 0.2 mM of each dNTPs, 0.4 µM M13 primer and 0.625 U GoTaq® Flexi DNA Polymerase (Promega, M8291). The cycling parameters were as follows: 1X(95°C, 5min), 30X[(95°C, 30s), (60°C, 45s), (72°C, 1min30s)], 1X(72°C, 5min). PCR products were quantified using Nanodrop 2000 spectrophotometer (Thermo Scientific) and then purified using the NucleoSpin RNA Clean-up (Marcherey-Nagel, 740948.50). The size checking was done using gel migration. *In vitro* transcriptions were carried out for 3 h at 37°C on 1.2 µg PCR products with 25 U RNAsin, 25 U T7 or SP6 polymerase, 10 mM dithiothreitol, 1 mM rATP, rCTP and rGTP, 0.65 rUTP, and 0.35 digoxigenin-UTP (Roche, 03359247910) using the Riboprobe® Combination Systems (Promega, P1460). DNAs were digested with 2 U RQ1 DNAse (Promega, M6101) for 30 min at 37°C. Obtained riboprobes were purified and their qualities were checked by dot blots on PVDF membrane. Paraffin slices (5 µm) were incubated at 61°C to facilitate deparaffinization using Roti-histol (sigma, 6640.6). Hydration was achieved by successive ethanol baths (100%, 95% and 70%), then by PBS. Between each of the following treatments, slices were washed into PBS. Slices were treated with 4% PFA in PBS, with 5 µg/ml proteinase k in Tris buffer for 4 min, with 4% PFA in PBS, with 100 mM Triethanolamine in 25 % acetic acid, then with 100 mM glycine in tris buffer. Tissues were incubated for 1 h at 65°C with the hybridization mix (50% Deionised formamide, 1X Saline-sodium citrate (SSC), 0.5 M Ethylenediaminetetraacetic acid (EDTA), 10% Tween 20, 1X Denhardt'solution, 28 mg/ml Dextran sulphate, 0.1 mg/ml heparin, 10% Chaps, 0.5 mg/ml tRNA). Then, 0.1-0.4 ng/µl riboprobes in hybridization mix were incubated overnight at 65°C. Slices were washed using successive baths of SSC (1X and 1.5X at 65°C, 2X at 37°C, 2X with 0.2 µg/ml of RNAse A (Promega, A797C) at 37°C, 2X, and 0.2X

at 60°C) before maleic acid buffer baths with 0.3 % triton (MABT). For immunostaining and revelation, the DIG Nucleic Acid Detection kit (Roche, 11175041910) was used. Tissues were incubated 3 h in blocking solution then, overnight at 4°C, with 100 µl per slice of 1/2000 v/v anti-digoxigenin-AP-conjugated antibody 750 U/ml. According to the kit guidelines, slices were washed in MABT baths before being developed overnight at 4°C in NBT/BCIP. Finally, slices were mounted in Mowiol mounting medium and then dried for 48 h at 4°C, before being observed using a Nikon eclipse 80i microscope.

**Immunohistochemistry (IHC)**

Tissues embedded in paraffin were cut into 5 µm sections with a microtome (Leica, Histocore Autocut R). The slices were deparaffined in roti-histol baths (Roth, 6640.2), rehydrated using successive ethanol dilutions (100%, 96%, 75% and 50%) and washed in PBS before antigen unmasking (2x 90s, micro-waves 600W followed by a 1 h cooling period). Endogenous peroxidase activities were blocked using 3% hydrogen peroxide in PBS and non-specific labeling was blocked using 0.1% Triton in PBS with 1% BSA. Diluted primary antibodies in Antibody Diluent (Abcam, ab64211) were incubated overnight at 4°C, then washed in PBS before a 2h incubation with the corresponding secondary antibodies at room temperature. After washing, the DAB Substrate Kit (3.3'-Diaminobenzidine, Abcam, ab64238) was applied until staining (2-60 min). Then, the slices were counterstained with Groat's hematoxylin and rinsed with tap water. They were dehydrated into successive ethanol baths (50%, 75%, 96% and 100%), then into roti-histol (Roth, 6640.2) before to be mounted into roti®histokit media (Roth, 6638.1). Pictures were taken using an optical microscope (Nikon, eclipse 80i) equipped with NIS-Elements D 3.0 software (Nikon Instruments). The primary antibody targeting PCNA (proliferating cell nuclear antigen, anti-rat PCNA mouse monoclonal antibody, 1:500, Invitrogen, 13-3900 PC-10) was used as quality control for testes tissues and the same results as Loppion et al., 2008 were obtained (not shown). Primary antibodies were used at the indicated dilution: anti-human TSHR rabbit polyclonal antibody (1:2000, Abcam, ab202960) and, as control, the rabbit IgG polyclonal-isotype control (1:2000, Abcam, ab37415). Secondary antibodies were used at the indicated dilution: anti-rabbit goat H&L IgG, HRP polymer (1:1, Abcam, ab214880).

**Immunocytofluorescence (ICF)**

Immunocytofluorescence detections were performed to verify the expression of recombinant proteins and the antibodies' specificity used in IHC analyses. HEKT293T cells transfected with pTarget-*sctshr* plasmid were washed twice using PBS with 1% BSA, collected and fixed with 4% PFA for 15 min before attachment to polysine slides (Epredia). The cells were permeabilized with 0.1% Triton in PBS buffer with 1% BSA for 5 min then incubated with primary antibodies, overnight, at 4°C. The cells were then washed and incubated at room temperature for 2 h with the secondary antibodies. After washes, the cells were mounted in Prolong™ Gold Antifade Mountant with 40,6-diamidino-2-phenylindole (DAPI) (P36935). Pictures were taken using an optical microscope (Nikon, eclipse 80i) equipped with NIS-Elements D 3.0 software (Nikon Instruments) with the same exposure time for each antibody, independently of the sample tested. The same primary antibodies were used for both IHC and ICC experiments: anti-human TSHR rabbit polyclonal antibody (1:500, Abcam, ab202960) and, as control, the rabbit IgG polyclonal-isotype control (1:500, abcam, ab37415). The secondary antibody used was the goat anti-rabbit IgG (H&L), Alexa Fluor™ 488 (1:250, Invitrogen, A-11008).

**Western blot**

Frozen tissues from testicular zones A, B, C and D, proximal and distal segments of epididymis, ovary and thyroid gland were crushed in liquid nitrogen, extracted with 2.5 volumes of ice-cold lysis buffer (6M urea, 2M thiourea, 40 mM tris-base, 2% CHAPS, 1 mM EDTA, 0.5 mM DTT, 1 mM AEBSF and 10 µM E64 protease inhibitors), then sonicated and kept 1 h on ice before being centrifuged at 15 000 g for 30 min at 4°C. Supernatants were then centrifuged at 105 000 g for 1 h at 4 °C. Protein concentration of resulting supernatants was determined using the bicinchoninic acid (BCA) protein assay (Sigma-Aldrich, Merck, France). Purified proteins (500 ng) were resolved on 10% gel electrophoresis before blotting on a PVDF membrane (Cytiva Amersham, RPN303F). After a 1-h blocking step in PBS with 10% non-fat dried milk, the membranes were probed overnight at 4°C with the primary antibody at the following dilution: anti-human actin mouse monoclonal antibody (1:1000 dilution, Sigma, A3853), anti-human TSHR rabbit polyclonal antibody (1:500, Abcam, ab202960) and, as control, the rabbit IgG polyclonal-isotype control (1:500, Abcam, ab37415). After a 2-h incubation with the corresponding secondary, the goat anti-rabbit IgG (H&L), HRP polymer (1:1, Abcam, ab214880) or the goat anti-mouse IgG (H&L), horseradish peroxidase (HRP)

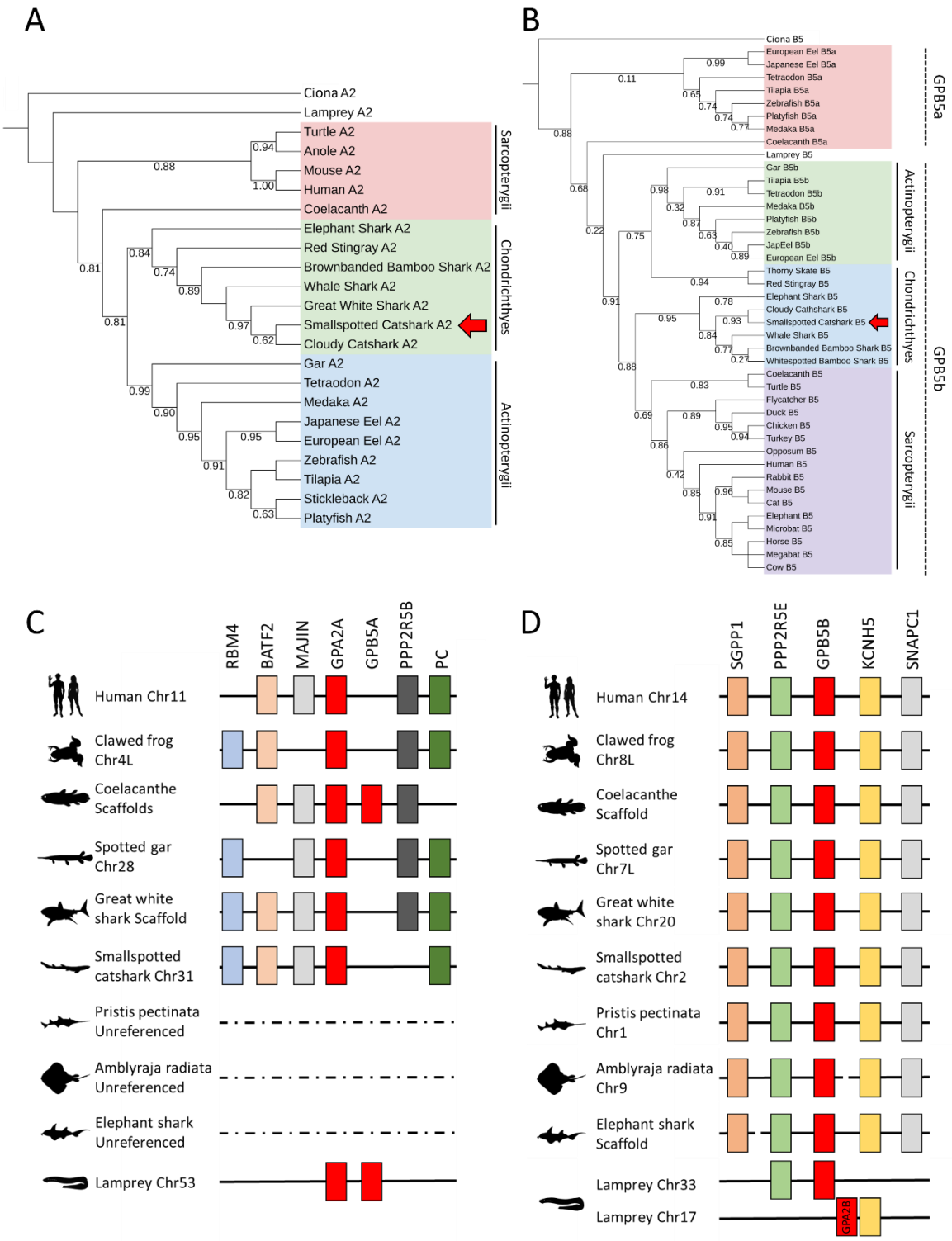


**Fig. 1.** *In silico* characterization of elasmobranchian GPA2 and GPB5. Molecular phylogeny of GPA2 (A) and GPB5 (B). *Scyliorhinus canicula* proteins are highlighted by red arrows. Support values shown are bootstraps for 1000 replicates. Synteny of the genomic region flanking *gpa2* and *gpb5a* genes (C) and *gpb5b* gene (D) in vertebrate species. The chromosome numbers are indicated. The coelacanth genomic regions were used as reference. Animal illustrations are used with permission from http://phylopic.org.

polymer (1:1, Abcam, ab214879), and washes, the DAB Substrate Kit (3.3'-Diaminobenzidine, Abcam, ab64238) was applied until staining (2-60 min). The bands' intensities in each PVDF membrane were normalized to their respective actin intensities using ImageJ software (https://imagej.net), and the relative expression values were compared.

## Results

### Searches for sequences of GPA2, GPB5, TSHβ and TSHRs in elasmobranch genomes

Sequence searches were carried out on the basis of sequences identified in *C. milii* and predicted sequences available in the NCBI database for *S. canicula*. Of the nine elasmobranch genomes analyzed, one TSHβ gene was identified for each, and *gpa2* and/or *gpb5* genes were identified in only 5 genomes and not in those of the batoid *A. radiata*, and of the sharks *C. carcharias*, *C. plagiosum*, and *P. pectinata*. The subsequent phylogenetic analysis including a maximum of GPH subunits and TSHRs sequences validated their annotations. Molecular phylogeny of the GPA2 subunits (Fig. 1.A) showed that the chondrichthyan sequences segregated in agreement with the phylogeny and that the holocephalan GPA2 rooted with the selachian sequences. Molecular phylogeny of the GPB5 subunits (Fig. 1.B) showed that the chondrichthyan sequences were grouped with GPB5b sequences and not with GPB5a sequences, and the holocephalan GPB5 rooted the shark sequences while batoidea sequences were grouped with actinopterygii sequences. Synteny analyses of *gpa2*- and *gpb5*-related gene regions confirmed the presence of *gpa2*, but not of *gpb5a*, in the genomes of *C. carcharias* and of *S. canicula* as well as the high conservation of the *gpb5b* gene region in the analyzed chondrichthyes (Fig. 2C,D). In addition, the *gpa2a-gpb5a* tandem and the *gpa2b*- and the *gpb5b*- related gene regions were conserved in the *P. marinus* genome. Genes coding protein phosphatase 2 regulatory subunit (PPP2R5) isoforms were located on the genomic fragments closed to *gpa2* and *gpb5* genes. Molecular phylogeny of the TSHR orthologs showed that the chondrichthyan sequences were grouped in agreement with the phylogeny, and the holocephalan TSHR rooted the batoidea and selachii groups (Fig. 2.A). The molecular phylogeny of TSHβs showed that elasmobranch orthologs segregated with the *C. milii* TSHβ2 while the *C. milii* TSHβ1 rooted the sarcopterygian sequences, which suggests the retention of *tshβ2* gene and the loss of *tshβ1* gene in elasmobranchs (Fig. 2B). Synteny analyses of *tshβ1*-

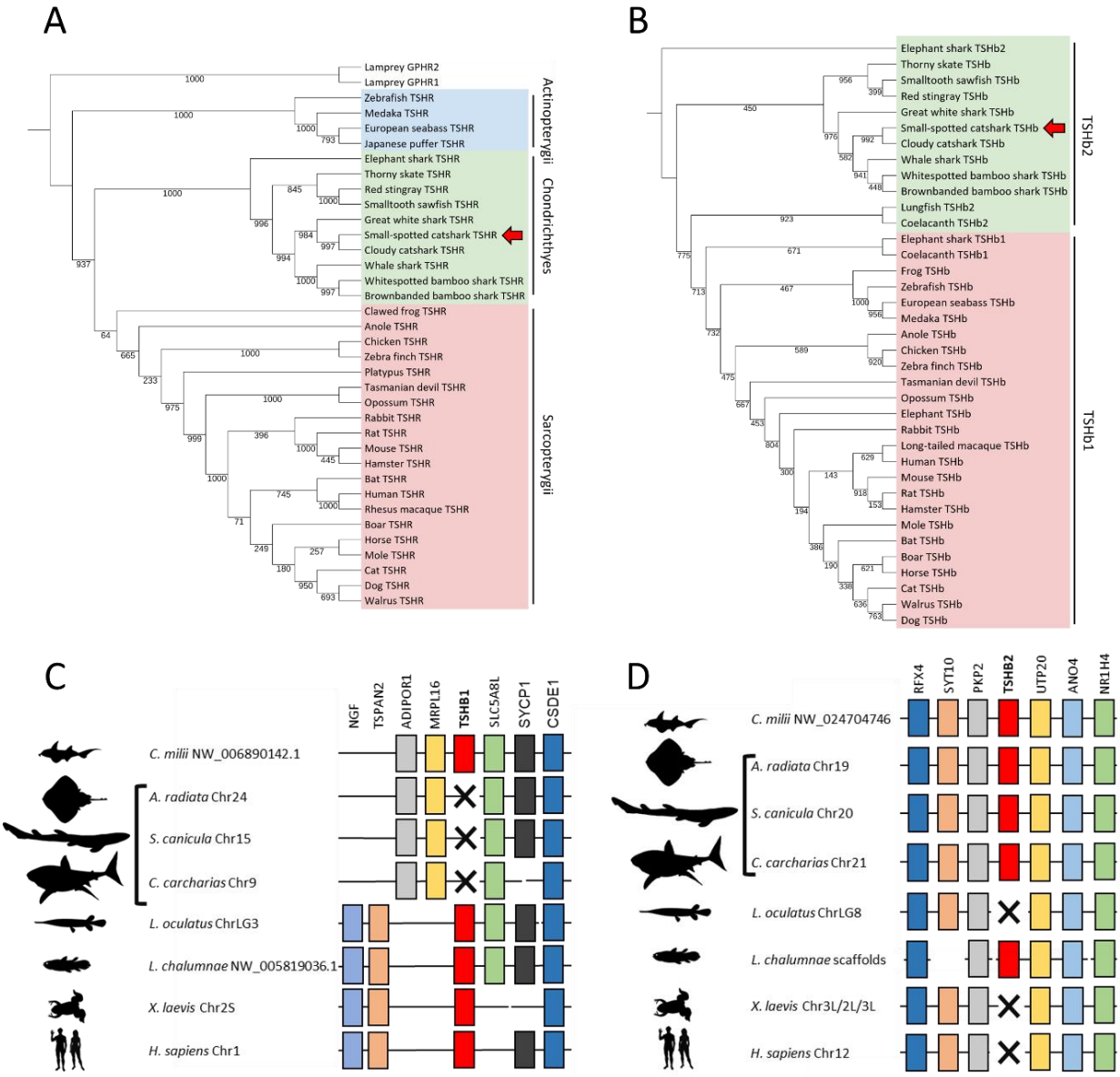


**Fig. 2.** *In silico* characterization of elasmobranchian TSHR and TSHβ2. Molecular phylogeny of TSHR (A) and TSHβ (TSHβ1 and TSHβ2) (B) *S. canicula* proteins are highlighted by red arrows. Support values shown are bootstraps for 1000 replicates. Synteny of the genomic region flanking *tshb1* (C) and *tshb2* genes (D) in representative species of vertebrate groups. The chromosome numbers are indicated. The *C. milii* genomic regions were used as reference. Animal illustrations are used with permission from http://phylopic.org.

and *tshβ2*-related genes regions in gnathostomes confirmed the absence of the *tshβ1* gene in the genomes of *A. radiata*, *C. carcharias* and *S. canicula* (Fig. 2C), while *tshβ2* gene was localized in a highly conserved region, also found in *C. milii* and *L. chalumanae* (Fig. 2B).

**Predicted structural domains of GPA2, GPB5, TSHβ2 and TSHRs**

The primary structures of elasmobranchs GPA2, GPB5, TSHβ2 and TSHRs were analyzed based on knowledges of human orthologs. Alignment of the Chondrichthyan GPA2 and GPB5 sequences has shown 10 conserved cysteines (C), 2 putative N-glycosylation sites, a "seat" region conserved in all Gpb5 and Gpa2 of elasmobranchs, except for *H. akajei* sequence with a histidine (H) instead of a tyrosine (Y), and the "seat-belt" region of GPB5 comprising only 2 conserved C (Supplementary Figure S2). Concerning alignment of the chondrichthyan TSHβ2 subunit sequences, it has shown 12 conserved C residues involved in disulfide bonds, including the three characteristic C of the "seat-belt" and 1 N-glycosylation site (Supplementary Figure S3). The "seat" region was conserved in elasmobranchs and diverged from the holocephalan sequence with a phenylalanine (F) instead of a tyrosine (Y). Multiple alignments of the protein sequences of TSHR (Supplementary Figure S4) have shown, in their large extracellular domains, 35 well-conserved leucine (L) residues, 2 N-glycosylation sites, and a conserved putatively sulfated tyrosine residue. The putative limit between the solenoid and the "hinge" region was predicted. The transmembrane region of the chondrichthyan TSHRs was composed of 7 putative α-helical transmembrane domains (TM), 2 conserved cysteines, one APPL1, one ERW, one Ubiquitin interaction, and PKC2 binding domain, and one BXXBB putative motif. The C-terminal region exhibits a putative $F(X)_6LL$ motif, a S/T cluster, a second BXXBB and a L-palmitoyl sites.

**Predicted models of GPA2, GPB5, TSHβ2 and the TSHR ectodomain**

The predicted models were constructed using the Q96T91.1.A template and the resulting pieces of information (Supplementary Table S2) reflected the fit between them. The closer GMQE and QMEANDisCo Global scores are to 1, the closer the predicted model is to the template. The TSHβ2 predicted models showed overall sequence identities relative to the Q96T91.1.A template of *H. sapiens* of 57.92% and 59.41% for *C. milii* and *S. canicula*, respectively. Despite these identities, the structural discrepancies were low since the GMQE

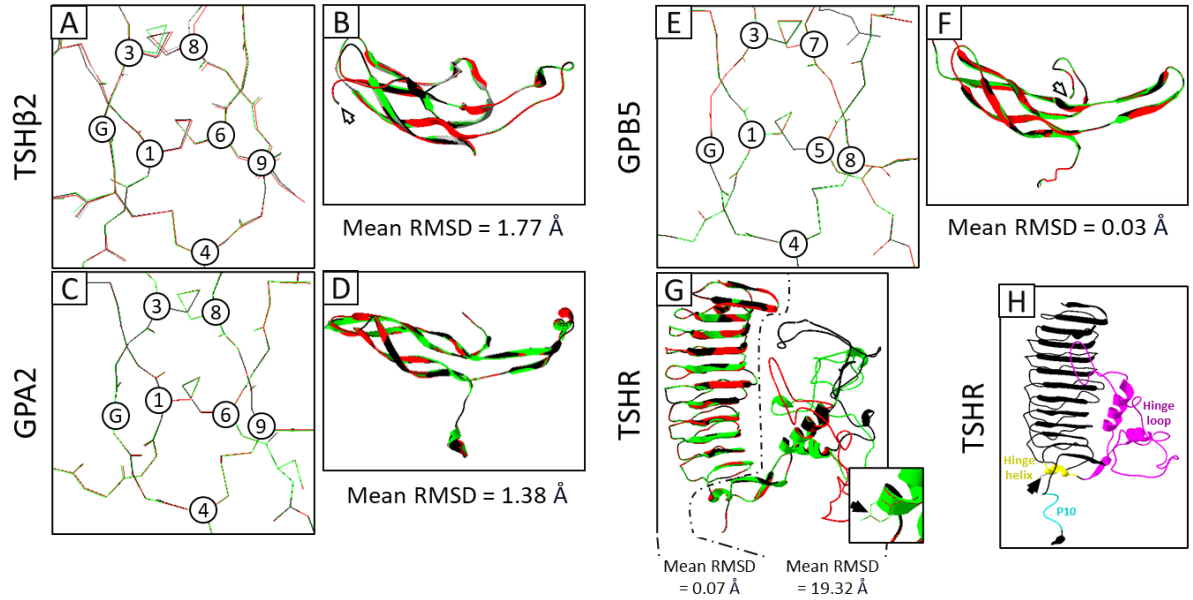


**Fig. 3.** *In silico* analysis of the 3D structures of *S. canicula, C. milii* and *H. sapiens* TSHβ, GPA2, GPB5 and TSHR. (A), (C), (E) Superpositions of the 8-aa-ring cystine-knot structure and (G) of the TSHR ectodomains, (H) TSHR model of *S. canicula* highlighting the hinge helix in yellow with the S280 (black arrowhead), the hinge loop in purple and the P10 loop in blue of the hinge region, (B, D, F) of the hormone subunits with RMSD means. The *H. sapiens* TSHβ model (used as template) and *C. milii* TSHβ1, *C. milii* TSHβ2 and *S. canicula* TSHβ2 predicted models are illustrated in green, grey, black and red, respectively. White arrowhead, C-terminal extremity with or without the "seat-belt" region; Black arrowhead, putative sulfotyrosine.

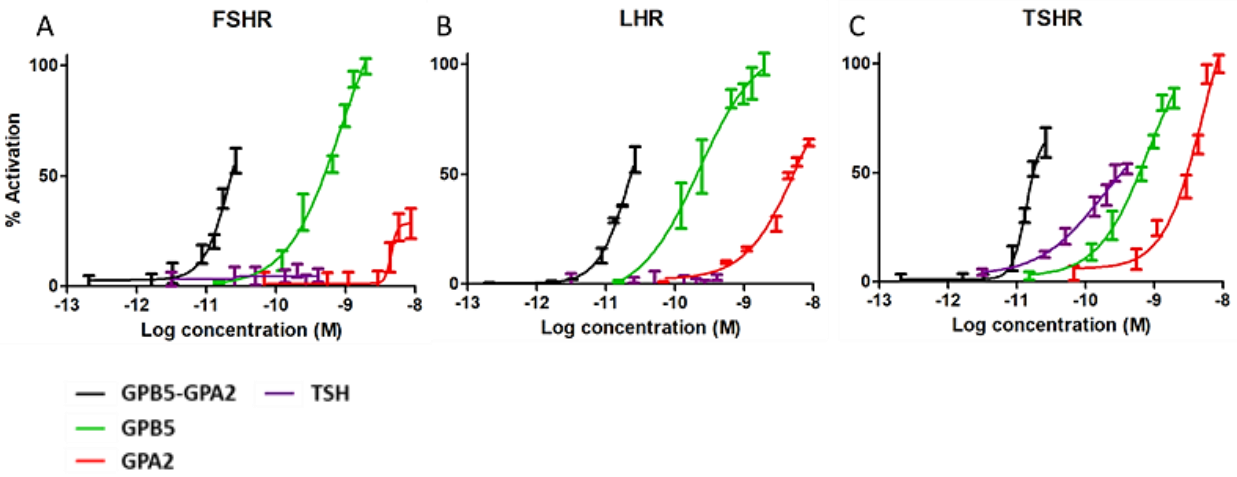


**Fig.4.** Dose-responses of cells expressing *sc*FSHR, *sc*LHR or *sc*TSHR induced by recombinant *sc*GPA2, *sc*GPB5 or single-chain *sc*GPB5-*sc*GPA2. (A-C) Dose-dependent calcium responses of HEK293T cells coexpressing *sc*GPHR/*hs*G$\alpha_{16}$ treated with serial dilutions of conditionned medium from HEK293T transfected with corresponding pTarget *gpa2*, *gpb5* or *gpb5-gpa2* plasmids. *Sc*TSH was used as control. All experiments were performed in duplicate and the most representative was selected for ligand absolute quantification using high-resolution nanoLC-ESI-MS/MS. Data are shown as relative (%) to the highest value (100% activation) for a given ligand and represent the mean of an experiment (n = 3).

and QMEANDisCo Global scores were only 0.06 to 0.08 lower for TSHβ2 predicted models of *C. milii* and *S. canicula* compared to the human control model (Supplementary Table S3). Scores obtained for TSHR models were relatively high with global sequence identities of 75.99% and 73,20%, GMQE and QMEANDisCo Global scores 0.02 to 0.06 lower than those of the human control template for *C. milii* and *S. canicula*, respectively. Compared to the human template, discrepancies of predicted models were slightly more important for GPA2 than for GPB5. For *C. milii* and *S. canicula* GPA2 models, respectively, global sequence identities were of 58.68% and 63,39%; GMQE scores were 0.41 and 0.42 lower and QMEANDisCo Global scores were 0.23 and 0.20 lower than the human template scores. For *C. milii* and *S. canicula* GPB5 models, respectively, global sequence identities were of 79.44% and 72,31%, GMQE scores 0.24 and 0.30 lower and QMEANDisCo Global scores 0.15 and to 0.21 lower than the human template scores. The predicted models of TSHβ, GPA2, and GPB5 obtained for *S. canicula* and *C. milii* proteins were superposable, including the cystine knot structures, and highlighted the shorter "seat-belt" domain of GPB5, with a very low mean RMSD ranging from 0.03 to 1.77Å (Fig. 2A-F). In contrast, the TSHR solenoid superposition had a very low mean RMSD of 0.07Å, which includes the hinge helix with the Serine scS280 (Fig. 3G-H), suggesting a conservation of the hinge helix and the solenoid structures between species. However, the mean RMSD of 19.32Å associated to the hinge loop and the P10 loop appeared much higher, suggesting their divergence. Furthermore, the putative sulfotyrosine site ($scY_{385}$) was highly conserved (Fig. 3G). This analysis showed structure conservations of GPA2, GPB5, and TSHβ, including the cystine knot, the absence of the third cysteine of the "seat-belt" in GPB5 orthologs, and conservation of the TSHR ectodomains, including hinge helix and sulfotyrosine site, while structural divergence was associated to hinge and P10 loops.

**Functional hormone-receptor interaction in *in vitro* assays**

HEK293T cells coexpressing scFSHR/$G\alpha_{16}$ subunit, scLHR/$G\alpha_{16}$ or scTSHR/$G\alpha_{16}$ were stimulated by serial dilutions of conditioned medium from cells expressing *sc*GPA2, *sc*GPB5, or the monocatenary recombinant *sc*GPB5-*sc*GPA2 or *sc*TSHβ2-*sc*CGA (Fig. 4). Dose-response analyses based on $Ca^{2+}$ detection have shown that *sc*GPA2, *sc*GPB5 and *sc*GPB5-*sc*GPA2 were able to activate *sc*FSHR-expressing cells over a picomolar to nanomolar concentration range, with higher potency for *sc*GPB5-*sc*GPA2 and *sc*GPB5 than for *sc*GPA2 (Fig. 4A, Table 1). For *sc*LHR-expressing cells, dose-response profiles were similar to those obtained with *sc*FSHR-

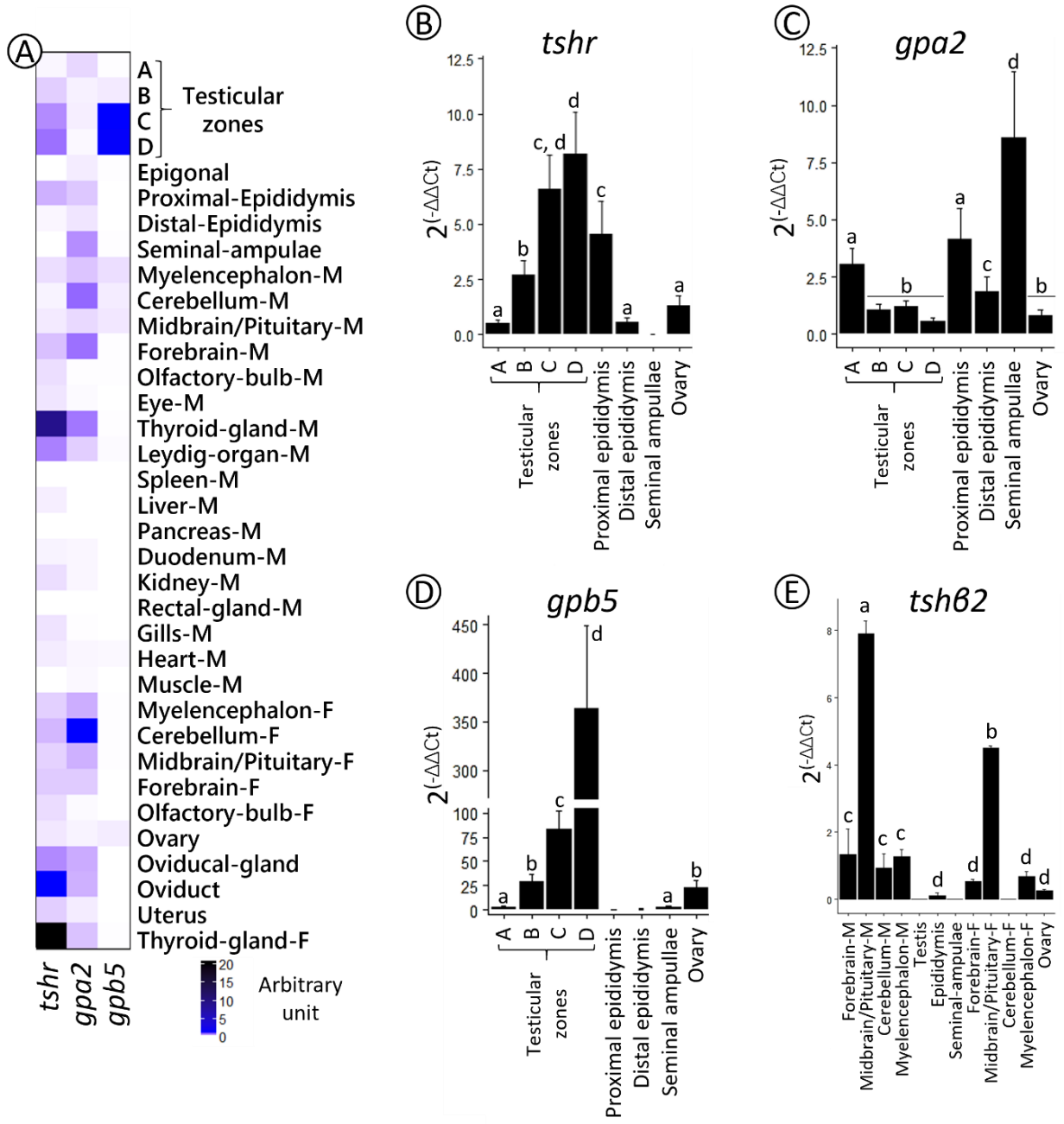


**Fig. 5.** Relative expression profiles of *tshr*, *gpa2*, *gpb5* and *tshβ* transcripts in *S. canicula* tissues with a focus on the male genital tract. Messenger RNA levels were assayed by real-time PCR. (A) Warm map representation of relative gene expression in 35 different tissues. Relative gene expression of *gpa2* (B), *gpb5* (C) and *tshr* (D) along the male genital tract and in the ovary. E. Relative gene expression of *tshβ2* in four different part of the brain and along the male genital tract. Statistical analysis was performed using Mann-Whitney U test with P value < 0.05 between each statistical groups a, b, c and d. A, B, C and D: testicular zones from six animals in triplicates (N=6; n=18); other tissues: from three animals in triplicates (N=3; n=9). The tissues from females correspond to females caught in September (non-breeding period) whose ovaries contained a few early vitellogenic follicles. M, Male; F, Female.

expressing cells, with potencies in the same order of magnitude (Fig. 4B, Table 1). For TSHR-expressing cells, the potency of *sc*GPB5-*sc*GPA2 was slightly higher than that of *sc*TSHβ2-*sc*CGA, which was used as control (Fig. 4C, Table 1). Analyses of cAMP production by HEK293T cells expressing *sc*FSHR, *sc*LHR or *sc*TSHR stimulated by conditioned media, without co-transfection with the human *hs*G$\alpha_{16}$ subunit, didn't allowed to detect significant responses.

**Relative expression profiles of *tshr*, *tshβ2*, *gpa2,* and *gpb5* mRNAs in *S. canicula* tissues with a focus on the male genital tract**

The expression profiles of transcripts were analyzed in 35 different tissues including the male and female genital tracts, brains and thyroids (Fig. 5). As expected, the highest level of *tshr* mRNA was observed in thyroids of males and females, but high levels were also observed in testis, with a 10-fold increase from the zone A to zone D, the proximal segment of the epididymis, and the Leydig organ of males (Fig. 5A,B). In females, high levels of *tshr* mRNA were observed in the brain and genital tract of females, particularly in the oviduct and oviducal gland (Fig. 5A). A broad tissue expression profile of the *gpa2* mRNA was observed with, in males and females, high levels in the different parts of brains, particularly the mesencephalons and the male forebrain, and thyroids (Fig. 5A). High levels were also observed in Leydig organ (Fig. 5A). In the male genital tract, the highest *gpa2* mRNA level was observed in seminal ampullae, high levels were observed in proximal and distal segments of the epididymis, and in testis, *gpa2* mRNA levels were three-fold higher in zone A, containing the germinative area and cysts with spermatogonia, than in the following stages of spermatogenesis (Fig. 5A,C). In the female genital tract, higher *gpa2* mRNA levels were observed in the oviduct and oviductal gland than in ovary and uterus (Fig. 5A). In contrast, the tissue expression profile for *gpb5* appeared more restricted than for *gpa2* with the highest levels observed in testis (Fig. 5A), with a 160-fold increase from the zone A to the zone D (Fig. 5D). During spermatogenesis, the two increases of *gpb5* and *tshr* mRNA levels were significantly correlated by a Spearman correlation test (P-value = 0.020). Outside the testis, *gpb5* appeared slightly expressed in the brain but not in the male tract, contrasting with the *gpa2* profile (Fig. 5A,D). In females, low levels of *gpb5* mRNA were observed in the ovary (Fig. 5A,D). For *tshβ2*, expression analysis showed the highest mRNA levels in males and female's midbrain/pituitary, lower levels in the male forebrain, mesencephalon, and myelencephalon and, at most, marginal expression with other tissues (Fig. 5E).

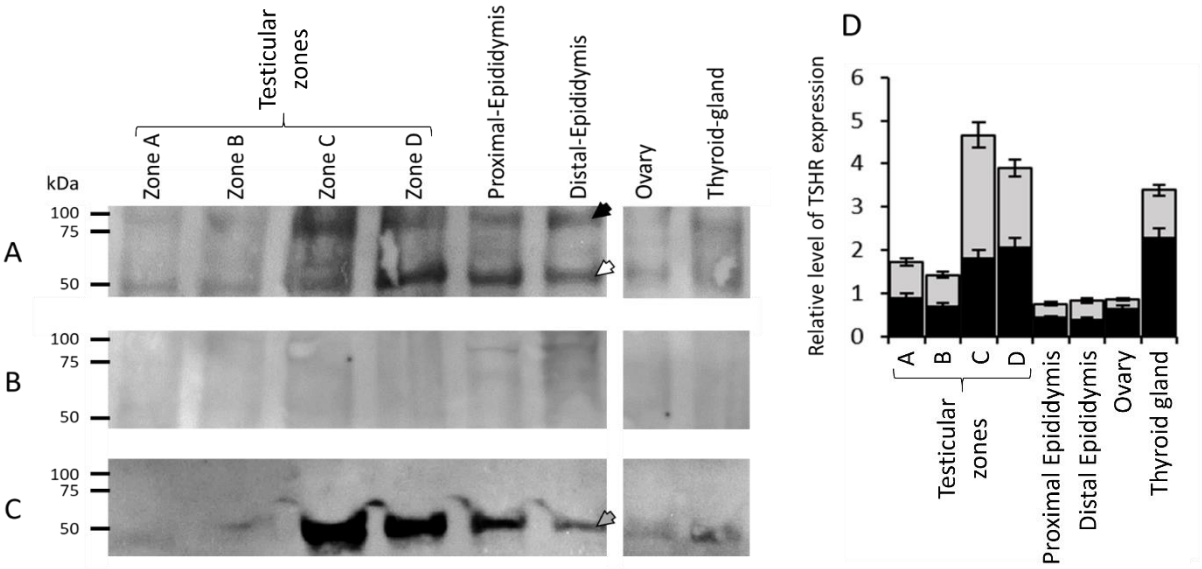


**Fig. 6**. Western blot analysis and relative quantification of TSHR in *S. canicula* tissues with a focus in the male genital tract. (A) Western blot detection using the anti-human TSHR rabbit polyclonal antibody (1:500, Abcam, ab202960) which reacted with two bands around 90 (black arrow) and 50 kDa (white arrow) and using the anti-human actin mouse monoclonal antibody (1:1000 dilution, Sigma, A3853) which reacted with one band around 45 kDa. (B) Western blot detection using the rabbit IgG polyclonal isotype control (human) antibody (1:500, Abcam, ab37415) which presented background for all tissues and reacted with bands around 75 kDa and 90 kDa in the zone C, D, proximal epididymis, distal epididymis and ovary. (C) Western blot detection using the mouse monoclonal anti-human actin antibody (1:1000 dilution, Sigma, A3853) which reacted with one band around 45 kDa (grey arrow). (D) Relative quantification of TSHR by measuring intensities of the two reactive bands, 50 kDa (black part of the histogramm) and 90 kDa (grey part of the histogramm), normalized to intensity of actin band. The tissues from females correspond to females caught in September (non-breeding period) whose ovaries contained a few early vitellogenic follicles. A, B, C and D: testicular zones.

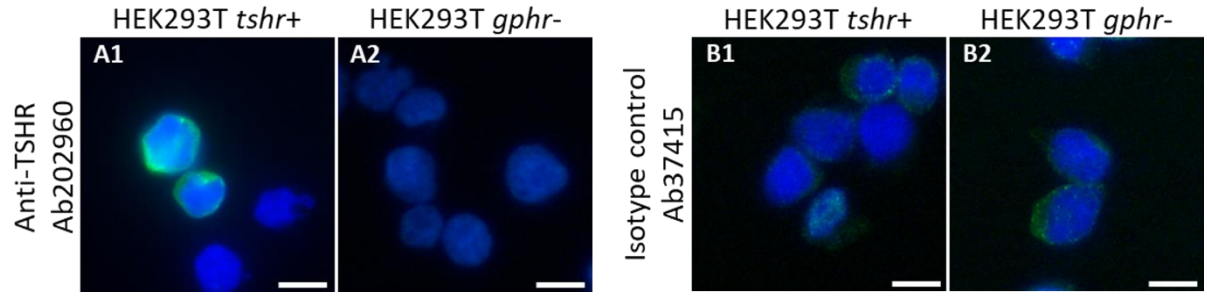


**Fig. 7**. Immunocytofluorescence on HEK293T cells expressing *S. canicula tshr*. HEK293T cells were transfected with p-target-*Sc-tshr* (HEK293T *tshr*+) or empty plasmids (HEK293T *gphr*-). After 24h, cells were fixed with 4% PFA4, collected on polysine slides and immunocytofluorescence was performed with the anti-human TSHR rabbit polyclonal antibody (1:500, Abcam, ab202960) (A1-A2) or with the rabbit IgG polyclonal isotype control (human) antibody (1:500, Abcam, ab37415) (B1-B2). Secondary antibodies used were anti-rabbit IgG (H+L) goat antibody, Alexa Fluor™ 488 (1:250, A-11008) (A1-B2). Merged pictures were acquired at 460 nm (DAPI, in blue) and 488 nm (Alexa fluor 488, in green) Scale bars: 10 µm.

**Immunoblotting**

Western blot analysis was performed in tissues expressing *tshr* according to real-time PCR results. Two bands of about 90 and 50 kDa were detected with the anti-human TSHR rabbit polyclonal antibody (Fig. 6A) in extracts of testicular zones (A, B, C, and D), proximal and distal epididymis, ovary and thyroid. The band of 90 kDa could correspond to the full-length receptor, based on its theoretical molecular weight of 85 kDa, and the band of 50 kDa to the extracellular domain of the receptor, based on its theoretical molecular weight of 46 kDa after cleavage at position 406 of the protein sequence (Supplementary Figure S4). The use of the rabbit IgG, polyclonal-isotype control revealed protein bands around 90 and 75 kDa but none corresponding to TSHR (Fig. 6B). Relative levels of TSHR to actin protein show that the two forms of TSHR (full-length or ectodomain only) evolved in parallel for all tissues (Fig. 6C) and that higher levels were associated to testicular zones C and D and thyroid than in zones A and B, ovary, proximal and distal segments of epididymis. These results agree with the levels of *tshr* transcripts, except for the proximal segment of the epididymis.

**Immunohistochemistry (IHC) and *in situ hybridization* (ISH) on *S. canicula* tissues, with a focus on the male genital tract**

*In situ* analyses were performed in genital tract tissues using real-time PCR results to identify the cell types expressing the transcripts and proteins of interest. In order to further validate the antibodies used, immunocytofluorescence was performed on HEK293T cells expressing scTSHR (Fig. 7). The results showed that the rabbit polyclonal TSHR antibody exhibited a specific signal in the cytoplasm and cell membrane of TSHR-expressing cells compared with the control corresponding to cells transfected with the empty plasmid. However, the rabbit IgG polyclonal-isotype control exhibited a low unspecific signal in the cytoplasm and cell membrane of both scTSHR-expressing cells and cells transfected with the empty plasmid. The immunohistochemistry of TSHR showed specific staining observed in the cytoplasmic extensions of differentiated Sertoli cells, localized between germ cells, in cysts with spermatogonia, with spermatocytes, with round spermatids, and in the basal cytoplasm, surrounding the nucleus of Sertoli cells in cysts with elongated spermatids (Fig. 8A1-F1). No

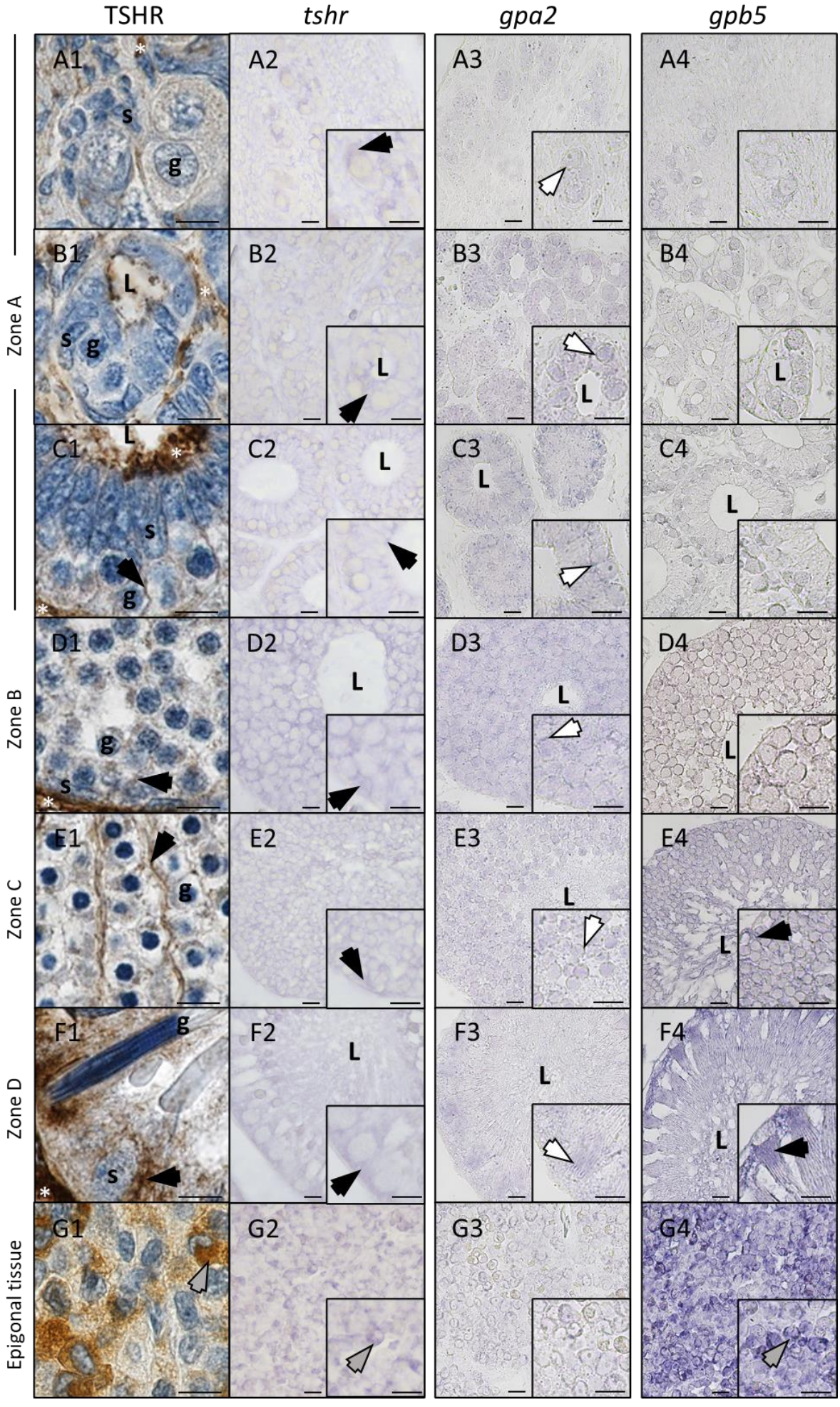
TSHR
tshr
gpa2
gpb5
Zone A
Zone B
Zone C
Zone D
Epigonal tissue
A1
A2
A3
A4
B1
B2
B3
B4
C1
C2
C3
C4
D1
D2
D3
D4
E1
E2
E3
E4
F1
F2
F3
F4
G1
G2
G3
G4
s
g
L
*

specific immunolabelling was observed in Sertoli cell precursors into the germinative area (Fig. 8A1-B1) and immunolabelling of the cyst lumen or interstitial tissue was unspecific according the results obtained with the rabbit IgG polyclonal-isotype control (Supplementary Figure S5). In agreement with the immunodetection of TSHR, the ISH results showed the localization of *tshr* transcripts in the cytoplasm of differentiated Sertoli cell (Fig. 8C2-F2) and was also observed in the cytoplasm of somatic precursors associated to early spermatogonia (Fig. 8A2) and cysts in formation (Fig. 8B2). The ISH of *gpa2* transcripts exhibited low staining associated to the cytoplasm of early spermatogonia, spermatogonia associated to cysts in formation, spermatocytes, rounds spermatids and associated to the head of elongated spermatids (Fig. 8A3-F3). In contrast, ISH of *gpb5* showed a first light staining in cysts containing spermatocytes (Fig. 8D4), which increased strongly in the cytoplasm of Sertoli cells in cysts containing round spermatids and elongated spermatids (Fig. 8E4-F4). In the last stage of spermatogenesis, the ISH signal was clearly localized in the basal cytoplasm of the Sertoli cells, surrounding nuclei, and in the thin cytoplasmic projections around head of spermatids (Fig. 8F4).

*In situ* analyses were completed by a study of the lymphomyeloid epigonal tissue associated to the testis, the testicular collecting tubules, the proximal and distal epididymis, the Leydig's gland and the thyroid. A strong staining was observed in the epigonal tissue for both *tshr*/TSHR and *gpb5*, apparently associated with granulocytes and myelocytes but not lymphocytes and erythrocytes (Fig. 8G1-G4). In the following part of the male genital tract, epithelial cells of the

---

**Fig. 8.** Immunohistochemistry and RNA *in situ* hybridization of TSHR, *tshr*, *gpa2* and *gpb5* in *S. canicula* testicular sections. The testicular zone A corresponds to the germinative area (A1-A4), cysts in formation (B1-B4) and formd cysts with spermatogonia (C1-C4). The testicular zones B, C and D correspond to cysts with primary spermatocytes (D1-D4), cysts with young spermatids (E1-E4) and cysts with late spermatids (F1-F4), respectively. The lymphomyeloid epigonal tissue is illustrated (G1-G4). Immunohistochemistry was perfomrd using anti-human TSHR rabbit polyclonal antibody (1:2000, Abcam, ab202960) (A1-G1). HRP-tagged secondary antibody is then detected with DAB substrate kit. *In situ* hybridization was performed using riboprobes targeting *Sc-tshr* mRNA (A2-G2), *Sc-gpa2* mRNA (A3-G3) or *Sc-gphb5* mRNA (A4-G4). For immunostaining and revelation, the DIG-Nucleic Acid Detection Kit was used. Black arrowhead, staining associated with somatic precursor (A1-B4) or with Sertoli cells (C1-F4); white arrowhead, staining associated with the germ cells; grey arrowhead, staining associated with myelocytes and granulocytes (G1-G4); g: germ cell nuclei; L: lumen; s: sertolian precursor (A1-B4) and sertolian nuclei (C1-F4). Asterix: unspecific staining. Scale bars: 10 µm. Controls are presented in supplementary date (Supplementary Figure S4).

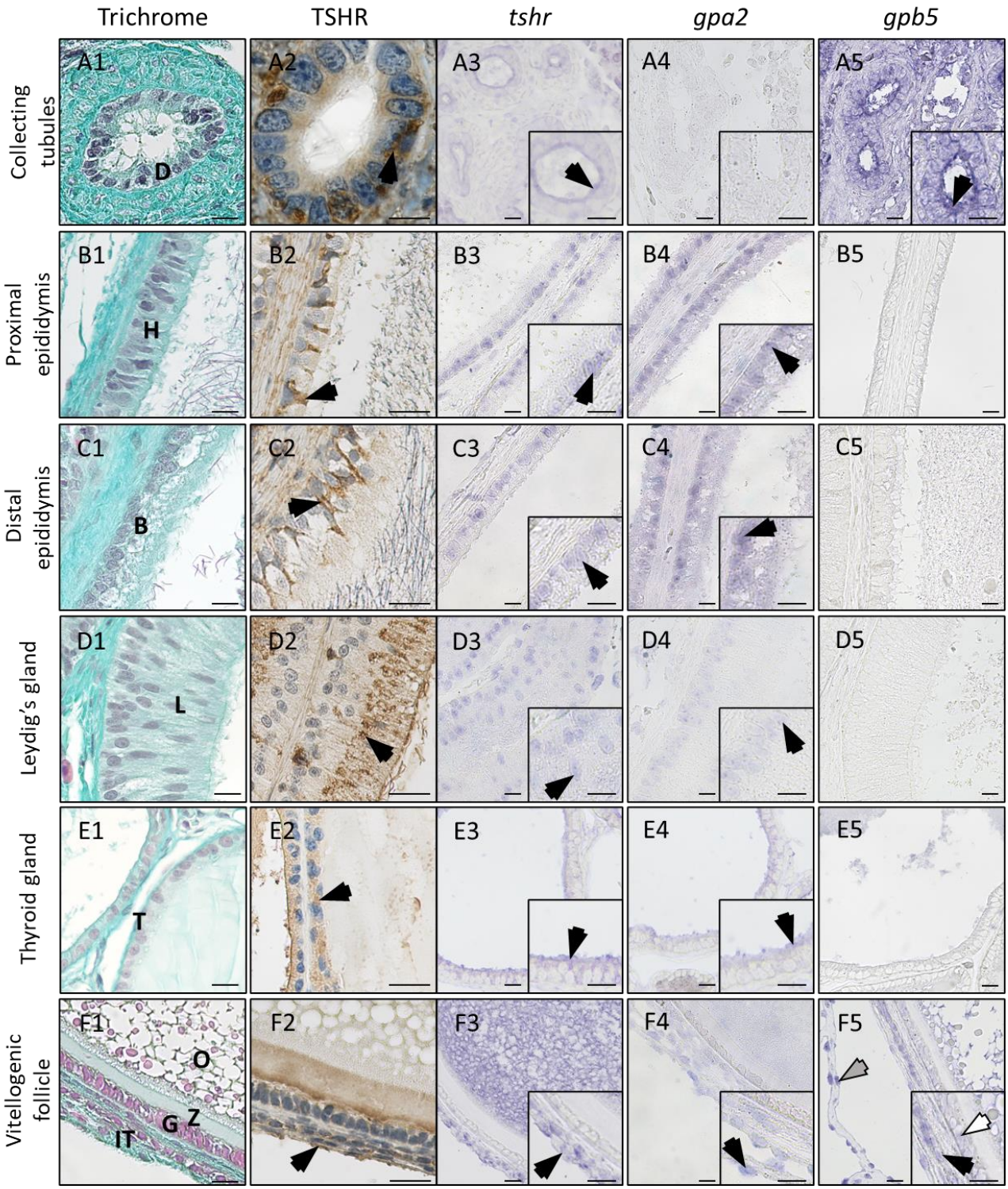
Trichrome
TSHR
tshr
gpa2
gpb5
Collecting tubules
Proximal epididymis
Distal epididymis
Leydig's gland
Thyroid gland
Vitellogenic follicle
A1
A2
A3
A4
A5
B1
B2
B3
B4
B5
C1
C2
C3
C4
C5
D1
D2
D3
D4
D5
E1
E2
E3
E4
E5
F1
F2
F3
F4
F5
D
H
B
L
T
O
G
Z
IT

collecting tubules expressed *tshr*/TSHR and *gpb5* (Fig. 9A2-A5), epithelial cells of the proximal (Fig. 9B2-B4) and distal (Fig. 9C2-C4) epididymis expressed *tshr*/TSHR and *gpa2*, and the epithelial cells of Leydig gland's expressed *tshr*/TSHR and *gpa2* (Fig. 9D2-D4). In the thyroid, *tshr*/TSHR-associated staining and *gpa2*-associated staining were observed in the follicular epithelium (Fig. 9E2-E4). Furthermore, *in situ* expression analyses were extended to ovarian follicles containing differentiated granulosa and theca cells, used as a control rather than for in-depth study since literature reported expressions of GPA2, GPB5 and TSHR in mammalian ovarian follicles. Here, theca cells and oocyte expressed *tshr*/TSHR, *gpa2* and *gpb5* while granulosa cells expressed only *gpb5* (Fig. 9F2-F5).

## Discussion

Recently, the sequencing of the genomes of several chondrichthyes has allowed significant advances in phylogeny of genes regulating reproduction in vertebrates, including those of the glycoprotein hormones (GpHs) and their receptors (GpHRs) such as in the holocephalan *C. milii* (Buechi and Bridgham, 2017) and the elasmobranchs *R. typus*, *C. punctatum* and *S. torazame* (Arimura et al., 2024; Hara et al., 2018). One of the aims of our study was to complete the characterization of GpHs and GpHRs in Elasmobranchs by analysis of more available genomes. Results allowed the identification of *gpa2* and/or *gpb5* genes in four additional species,

---

**Fig. 9**. Immunohistochemistry and RNA *in situ* hybridization of TSHR, t*shr*, *gpb5* and *gpa2* in the male genital tract and in vitellogenic follicle of *S. canicula*. Histology of testis collecting tubules (A1), proximal epididymis (B1), distal epididymis (C1), Leydig's gland (D1), thyroid gland (E1) and vitellogenic folicle (F1). Immunohistochemistry was performed using anti-human TSHR rabbit polyclonalantibody (1:2000, abcam, ab202960) (A2-F2). (A3-F3) *In situ* hybridization was performed using riboprobes targeting *tshr* mRNA, (A4-F4) *gpa2* mRNA or (A5-F5) *gpb5* mRNA. In the male genital tract, expressions of TSHR/*tshr*, *gpa2* and *gpb5* were observed in the epithelial cells of collecting tubules (A2-A5), ofTSHR/*tshr* and *gpa2* in epithelial cells of proximal epididymis (B2-B4), distal epididymis (C2-C4), Leydig's gland (D2-D4) and thyroid follicle (E1-E4) (black arrowhead). In the vitellogenic follicle, expressions of TSHR/*tshr*, *gpa2* and *gpb5* were observed in the theca cells (black arrowhead) and *gpb5* was additionally observed in the granulosa cells (white arrowhead) (F1-F5). B: epithelium of the distal of epididymis; D: epithelium of collecting tubules; G: granulosa layer; H: epithelium of the proximal of epididymis; IT: inner theca layer; L: Leydig's gland; T: epithelium of the thyoid gland follicle; O: ooplasm; Z: zona pellucida. Scale bars: 10 µm. Controls are presented in supplementary data (Supplementary Figure S5).

including the red stingray *H. akajei*, the thorny skate *A. radiata*, the great white shark *C. carcharias,* and the small-spotted catshark *S. canicula.* Furthermore, results confirmed that *tshβ2* gene, but not *tshβ1* gene, was retained in elasmobranch genomes, underlining the divergence with the holocephalan *C. milii* where both genes are present in its genome, as previously reported (Buechi and Bridgham, 2017; Maugars et al., 2014).

Outstanding predicted structures of GPHs were found conserved in the elasmobranch TSHβs, GPA2s, and GPB5s. Most importantly, the cysteine residues, all involved in disulfide bonds, were found in homologous positions thus allowing 1/ the formation of the cystine-knots in all GPH subunits as well as in GPA2 and GPB5 and 2/ the "seatbelt" fastening by C3-C12 bridge ("buckle") in all GPHβ subunits but not in GPB5s lacking these two cysteine residues. The absence of the seat-belt in GPB5 raised the question of the stability of the GPA2/GPB5 dimer in the peripheral circulation (Alvarez et al., 2009). The putative N-glycosylation sites and the characteristic "seat" region involved in α- and β-subunits interaction are also conserved.

Compared with the GTHR of *C. milii* (Buechi and Bridgham, 2017) and *H. sapiens* (Ulloa-Aguirre et al., 2018), the primary structures of the TSHR identified in elasmobranchs were highly conserved with the leucine-rich solenoid, hinge, N-glycosylation and sulfation sites in their ectodomains. In the human LHCGR, the hinge region includes a hinge helix (residues 276-282), a hinge loop (residues 284-340) and a P10 loop (residues 350-359), and hydrophobic mutations of the hinge helix, notably of the serine residue at position 277, alters the receptor activation property, as also noted for TSHR (He et al., 2022; Jaeschke et al., 2011; Mueller et al., 2009). In comparison, the TSHR sequence of *S. canicula* shows a highly conserved serine residue (scS280). At the same time, a significant conformational difference was observed for the hinge loop, possibly causing a conformational change in the P10 loop as observed in our model. However, the sequence and the 3D conformation of the potentially sulfated tyrosine $scY_{385}$ implied in a high-affinity ligand-receptor interaction must have been conserved. These results suggest that the hinge loop has diverged the most during evolution, although the consequence for ligand/receptor interaction specificity remains to be defined. Primary structures of the seven transmembrane α-helixes were also conserved with APPL1, ERW, BXXBB, ubiquitin interacting, and PKC2 binding domains in intracellular loops 1, 2, and 3, respectively. Interestingly, a Val/Ile variation was observed between chondrichthyes at position 595 of the *sc*TSHR corresponding to the Val597Ile variant in the transmembrane helix

5 of the hTSHR, which exhibits increased constitutive activity and dose-dependent increase in cAMP response to LH (Caron et al., 2020). The second BXXBB, $F(X)_6LL$, L-palmitoylation site, and S/T motifs were also conserved in the intracellular Ct domain.

In the present study, ligand-receptor interaction analyses using HEK293T cells transiently transfected to express *scfshr*, *sclhr* or *sctshr* with the promiscuous *hs*$G\alpha_{16}$ showed that the recombinant *sc*TSHβ2-*sc*CGA, as a single-stranded protein, could activate only *sc*TSHR, which is in agreement with the previous report concerning *C. milii* (Buechi and Bridgham, 2017). However, for the first time in an elasmobranch, it has been shown that the recombinant *sc*GPB5-*sc*GPA2 was able to activate *sc*TSHR, as it was previously observed in *R. norvegicus* and *H. sapiens* (Nagasaki *et al*., 2006; Nakabayashi et al., 2002). However, the $EC_{50}$ obtained with *sc*GPB5-*sc*GPA2 on *sc*TSHR appears ten times lower than those previously observed for human and rat thyrostimulins, but the efficiency of *sc*TSH on *sc*TSHR was similar to the bovine TSH (Nagasaki *et al*., 2006; Okajima et al., 2008).

Most interestingly, the recombinant single strand *sc*GPB5-*sc*GPA2 also activated *sc*FSHR and *sc*LHR in addition to TSHR. This apparently surprising result fits well with the previously proposed “negative specificity” model (Combarnous & Hengé, 1981; Combarnous, 1992). Indeed, in this model, the seatbelt sequence in the β-subunits wraps around their α-counterpart to stabilize the heterodimer formation but also determines specificity by inhibiting the binding (hence “negative specificity”) of each heterodimer to the other GPHRs. Since *sc*GPB5-*sc*GPA2 remains dimeric thanks to the β-α sequences’ fusion but lacks seatbelt sequence, there is no inhibition towards any of the GPHRs, thus leading to binding and activation of all of them.

This result suggests a more ancestral function or a specificity of the receptors not yet established, as it was described in the lamprey *Petromyzon marinus* where GPB5-GPA2 could activate both GPHRI and GPHRII (Hausken et al., 2018). In addition, recombinant *sc*GPB5 could also activate *sc*FSHR, *sc*LHR, and *sc*TSHR but with a tenfold lower efficiency than *sc*GPB5-*sc*GPA2. The recombinant *sc*GPA2 could also activate the three *sc*GPHRs, but probably only at a supraphysiological concentration. Observed efficacies also suggest agonist and partial agonist activities of *sc*GPB5 and *sc*GPA2-*sc*GPB5, respectively, on *sc*FSHR and *sc*LHR. Our results are, however, in contradiction with those obtained in the holocephalan *C. milii*, where GPA2/GPB5 failed to activate TSHR (Buechi and Bridgham, 2017). This lack of activation could

result from the use of a receptor with a truncated hinge loop (XP_007904236.1), whereas a full-length receptor (XP_042194080.1) was predicted later in 2021 by automated computational analysis. In our study, we were unable to determine if *sc*GPA2 or *sc*GPB5 were active as monomer or homodimer, which is a matter of debate in different species, along with the question of the endocrine or paracrine role of the GPA2/GPB5 heterodimer. In mammals, the fact that thyrostimulin can activate TSHR as a non-covalent heterodimer and that systemic blood concentrations of the subunits were below the Kd of dimerization suggest a paracrine role for the hormone but also raises the issue of the potential endocrine role of separate GPA2 and GPB5 units (Alvarez et al., 2009; Sun et al., 2010). In the basal chordate *B. japonicum*, each GPA2 or GPB5 monomers could bind the amphioxus GPHR (named as TSHR by the authors and also referred as LGR1) without activating it, only the recombinant single-chain GPB5-GPA2 was able to do so, suggesting a local role of monomers as antagonist of GPHR (Wang et al., 2018). In the ascidian *S. clava*, GPA2 and GPB5 are secreted by distinct secretory pathways and could activate, as recombinant single-chain GPB5-GPA2, HEK293T cells expressing GPHR (Yang et al., 2023); however, the separate GPA2 and GPB5 have not been tested. In the mosquito *A. aegypti*, it has also been suggested that GPA2 and GPB5 may form homodimers. Still, only the single-chain GPB5-GPA2 modulates the activity of the mosquito GPHR (LGR1) (Rocco and Paluzzi, 2020). In the lamprey, GPA2 heterodimerizes with GPB5 and the recombinant fusion protein GPB5-GPA2 can activate the lamprey GpH receptors I and II ; however, the separate GPA2 and GPB5 have not been tested (Hausken et al., 2018). Overall, heterodimerization of GPA2 and GPB5 seems necessary, and it has been suggested that they may have evolved from an ancestral homodimer consisting of two GPA2s in basal metazoans, based on the study of the crystal structure of the heterodimer GPA2/GPB5 of *Caenorhabditis elegans* secreted by transfected HEK293S cells (Gong et al., 2023). The dose-responses observed in our study when scGPA2 or scGPB5 are expressed alone would therefore not be incompatible with this evolutionary history from homodimers. This is also reinforced by synteny analysis where disruption of the GPA2a-GPB5a gene tandem, with the loss of GPB5a, and of the GPA2b-GPB5b gene tandem, with the loss of GPA2b, occurred after cyclostome divergence and favored the loss of common regulations and functions in gnathostomes.

Among the tissue expression profiles of the GPA2 and GPB5 subunits analyzed in several species, GPB5 exhibits a more restricted tissue expression than GPA2, and coexpression of

GPA2 and GPB5 was observed outside the brain and pituitary or pituitary-like organs; for example, in the gonads in ecdysozoans (Rocco et al., 2017; Rocco and Paluzzi, 2020; Vandersmissen et al., 2014), basal chordates (Wang et al., 2018; Yang et al., 2023); lamprey (Hausken et al., 2018) and mammals (Li et al., 2004; Nagasaki *et al*., 2006; Nakabayashi et al., 2002; Okada et al., 2006). Our results on the tissue expression profiles of the GPA2 and GPB5 subunits observed in *S. canicula* are in agreement with these previous studies since coexpression was observed in brains and gonads, notably testes. In *S. canicula*, although we did not precisely study its brain localization by *in situ* analyses, our results show the highest expression of *tshβ2* in the midbrain, including the hypothalamus and pituitary, of both males and females, which was in agreement with an expression in the ventral lobe of the pituitary of sharks (Hara et al., 2018). *Tshr*, *gpa2,* and *gpb5* genes were also coexpressed in the different parts, suggesting paracrine regulation of the central nervous system involving TSH/TSHR and/or GPA2-GPB5/TSHR signaling, as in the regulation of food intake in rats (Burgos et al., 2016) or seasonality in fishes, birds and mammals (Irachi et al., 2021; Yoshimura, 2010). Our results also show that *tshr* and TSHR were expressed in the epithelial cells of thyroid follicles, as expected. Still, extrathyroidal expressions of the receptor in addition to the brain, were also observed in the testis and epididymis, the lymphomyeloid Leydig organ, and the oviduct and oviducal gland. In testis, *tshr* mRNA and TSHR protein levels increased from early to late stages of spermatogenesis with localization in somatic precursors and differentiated Sertoli cells. These results are in agreement with TSHR expression observed in Sertoli cells of *R. norvegicus* (Fadlalla et al., 2017) and *H. sapiens* (Li et al., 2022) and in testis of some teleost as in the Walking catfish, *Clarias batrachus* (Bhat et al., 2017), Channel catfish, *Ictalurus punctatus* (Goto-Kazeto et al., 2009), striped bass, *Morone saxatilis* (Kumar et al., 2000), and European sea bass, *Dicentrarchus labrax* (Rocha et al., 2007). In *D. labrax*, it has been proposed involvement of TSHR signaling in gonadal development, spermiogenesis, and spermiation (Rocha et al., 2007). In the absence of *tshβ2* expression in the testis of *S. canicula* and based on functional assays, *sc*GPA2/*sc*GPB5 can be expected to exert a paracrine role in the regulation of spermatogenesis by activating testicular TSHR, without ruling out an endocrine action of circulating TSH. This is also reinforced by the correlation observed between *gpb5* and *tshr* mRNA levels during spermatogenesis. *In situ* analysis showed *gpa2* expression in germ cells while *gpb5* and *tshr* were expressed in the Sertoli cells, suggesting paracrine and/or autocrine regulations. Further studies will be needed to determine these regulations in

relation to testicular FSHR and LHR expressions recently studied in the catshark (Jeanne et al., accepted). Interestingly, the downregulation of the putative GPA2/GPB5 receptor (LGR1) in the mosquito *A. aegypti* impacted spermatozoa differentiation (Rocco et al., 2019), underlining the ancestral involvement of GPA2/GPB5 in spermiogenesis. However, the deletion of either GPB5 or GPA2 in mice did not produce an overt phenotype (Okada et al., 2006), raising the question of the biological role of GPA2 and GPB5 during spermatogenesis in organisms with differentiated gonadotropic hormones. Nevertheless, the double KO of both *gpa2* and *gpb5* genes has not been performed so that it cannot be excluded that GPA2 and GPB5 exert similar functions and can rescue each other.

In the male genital tract of *S. canicula*, significant *gpa2,* and *tshr* mRNA levels were observed in the proximal segment of the epididymis. *In situ* analyses localized *tshr* transcripts and protein in the epithelium of testicular collecting tubules, co-expressed with *gpb5* but not *gpa2*. Then, TSHR was localized in the epithelium of proximal and distal segments of the epididymis and in epithelial cells of Leydig's gland. In the epididymis, we show for the first time that *tshr* is co-expressed with *gpb5*. In mammals, spermatozoa acquire their motility and fertilizing properties during their epididymal transit (Dacheux and Dacheux, 2014; Sullivan et al., 2005) in relation to their internal fertilization mode (Gervasi and Visconti, 2017). In elasmobranchs, which also have internal fertilization, epididymis has been poorly studied despite its similarity to mammals. However, studies in sharks and batoids have shown that epididymis participates in luminal fluid modifications and that spermatozoa acquired their motility during their transit in the distal segment of the epididymis (Dzyuba et al., 2019; Jones et al., 1984). The Leydig gland, which is adjacent to epididymis and secretes part of the seminal fluid into the deferent duct, seems to be involved in spermatozoa aggregation, occurring into seminal ampullae, to form spermatozeugmata or spermatophores, according to species (Jones et al., 2005). Another specificity of elasmobranchs, is the presence of lymphomyeloid tissues forming the gonad-associated epigonal tissue and the gut-associated Leydig organ (different from Leydig gland). Our results show that the epigonal tissue expressed *tshr* and *gpb5* and the Leydig organ expressed *tshr* and *gpa2*. The biological significance of these expressions has to be clarified but previous studies have suggested a cross-talk between the epigonal tissue and the gonads in elasmobranchs (Lutton and Callard, 2007; Piferrer and Callard, 1995).

Expression analyses of *S. canicula* females showed high levels of *tshr* and *gpa2* transcripts in the oviduct and oviducal gland and lower levels in the ovary, as also observed for *gpb5* transcripts. Although the female tissues were taken from females outside their reproductive period and corresponded to ovaries with few vitellogenic follicles, *in situ* analyses showed an expression of TSHR/*tshr* in theca layers and oocyte, of *gpa2* in granulosa cells and of *gpb5* in theca and granulosa cells. Although our analysis remains limited, these follicular expressions are in agreement with a paracrine GPA2/GPB5/TSHR signaling as characterized in the *R. norvegicus* ovary (Sun et al., 2010).

In conclusion, our study shows that, *in vivo*, *gpb5* is highly expressed in *S. canicula* testis. *In vitro,* the recombinant single-chain *sc*GPB5-*sc*GPA2 dimer, as well as *sc*GPB5 alone, activate the three GPHRs (scFSHR, scLHR and scTSHR) in a same potency range, suggesting their implications in the paracrine regulation of spermatogenesis, an implication that remains to be to be clarified. Chondrichthyes, as the most ancient clade with differentiated GPHs and GPHRs, could exhibit a transitional endocrine system between the pleiotropic GPA2/GPB5/GPHR signaling found in the cyclostomes and early gnathostomes to the specific GtHs/GtHRs signaling found in mammals.

**Table 1**
Efficiency ($EC_{50}$) and efficacy (Emax) of *sc*GPA2, *sc*GPB5, *sc*GPB5-*sc*GPA2 or *sc*TSH on *sc*FSHR, *sc*LHR and *sc*TSHR.

| | Efficiency ($EC_{50}$) nM | | | | Efficacy (Emax) % | | | |
|---|---|---|---|---|---|---|---|---|
| | *scGPA2* | *scGPB5* | *scGPB5-scGPA2* | *scTSH* | *scGPA2* | *scGPB5* | *scGPB5-scGPA2* | *scTSH* |
| *sc*FSHR | 4.512 ± 0.226 | 0.837 ± 0.042 | 0.021 ± 0.004 | N/A | 27.64 ± 1.21 | 100.00 ± 4.29 | 48.51 ± 12.21 | N/A |
| *sc*LHR | 5.846 ± 0.292 | 0.221 ± 0.011 | 0.025 ± 0.003 | N/A | 59.96 ± 6.26 | 100.00 ± 6.19 | 46.15 ± 14.82 | N/A |
| *sc*TSHR | 5.164 ± 0.258 | 0.790 ± 0.040 | 0.014 ± 0.001 | 0.169 ± 0.008 | 100.00 ± 3.36 | 83.33 ± 1.44 | 58.00 ± 2.52 | 51.80 ± 4.59 |

N/A: not applicable.

## Associated content

### Supporting information

Supplementary figures corresponding to the 5sRNA validation as reference gene (Fig. S1), alignment of elasmobranch TSHβ2s (Fig. S2); GPA2s and GPB5s (Fig. S3) and TSHR (Fig. S4); Controls associated to IHC and ISH on *S. canicula* testis sections (Fig. S5); Controls associated to IHC and ISH on *S. canicula* vitellogenic follicle and other organs of the male genital tract (Fig. S6) and supplementary tables corresponding to the primers used for real-time PCR and *in situ* hybridization (Table S1); supporting information (Table S2) and their analysis for the predictive models of *S. canicula*, *C. milii* and *H. sapiens* TSHβ2, GPA2, GPB5 and TSHR ectodomain (Table S3).

## Author information

### Corresponding author

**Pascal Sourdaine –** *Université de Caen Normandie, MNHN, SU, UA, CNRS, IRD, Laboratoire de Biologie des Organismes et Ecosystèmes Aquatiques (BOREA), UMR 8067, 14032 Caen cedex 5, France ;* orcid.org/0000-0001-9811-2876; Email: pascal.sourdaine@unicaen.fr

### Authors

**Fabian Jeanne -** *Université de Caen Normandie, MNHN, SU, UA, CNRS, IRD, Laboratoire de Biologie des Organismes et Ecosystèmes Aquatiques (BOREA), UMR 8067, 14032 Caen cedex 5, France ;* ORCID; Email :

**Stanislas Pilet -** *Université de Caen Normandie, MNHN, SU, UA, CNRS, IRD, Laboratoire de Biologie des Organismes et Ecosystèmes Aquatiques (BOREA), UMR 8067, 14032 Caen cedex 5, France*

**Benoît Bernay -** *Université de Caen Normandie – Plateforme PROTEOGEN, US EMerode, 14032 Caen cedex 5, France* ; orcid.org/0000-0002-3624-1514; Email: benoit.bernay@unicaen.fr

**Yves Combarnous –** *Université de Tours, INRAE, CNRS, UMR Physiologie de la Reproduction & des Comportements, 37380 Nouzilly, France ;* orcid.org/0000-0002-0574-2025; Email: : yves.combarnous@inrae.fr

**Danièle Klett –** *Université de Tours, INRAE, CNRS, UMR Physiologie de la Reproduction & des Comportements, 37380 Nouzilly, France ;* Email: daniele.klett@inrae.fr

**Pascal Favrel –** *Université de Caen Normandie, MNHN, SU, UA, CNRS, IRD, Laboratoire de Biologie des Organismes et Ecosystèmes Aquatiques (BOREA), UMR 8067, 14032 Caen cedex 5, France ;* orcid.org/0000-0002-2504-9957; Email: pascal.favrel@unicaen.fr

**Sylvie Dufour –** *Université de Caen Normandie, MNHN, SU, UA, CNRS, IRD, Laboratoire de Biologie des Organismes et Ecosystèmes Aquatiques (BOREA), UMR 8067, 14032 Caen cedex 5, France ;* orcid.org/0000-0002-8646-4935; Email: sylvie.dufour@mnhn.fr

**Author Contributions**

All authors contributed to writing of the manuscript based on a first version of F.J. and have given approval to its final version. P.S. supervised and managed the study as well as performed dissection. B.B. performed mass spectrometry analysis. F.J. realized *in silico* analyses and, with S.P., real-time PCR, IHC, ISH and bioassay using the HEK293T under the expert guidance of P.F. Data analyses were performed by F.J., as well as analyzed and discussed the results with P.S., Y.C. and P.F. The bioassay using the mLTC were performed by Y.C. and D.K..

**Notes**

The authors declare no competing financial interest.

**Acknowledgments**

The authors are grateful to Didier Leroy from the CGFS (Channel Ground Fish Survey) campaign (IFREMER in the East Manche in September 2022) for providing the catsharks and to Frédérique Guyon of the “Centre de Recherches en Environnement Côtier” (Luc sur Mer, France) for the care given to the animals. The following are thanked for funding: “Ministère de l’Enseignement Supérieur et de la Recherche Scientifique” (F.J.’s PhD grant), European Regional Development Fund (Operational Programme ERDF/ESF 2014-2020) under the project “Manche 2021 – Plateformes d’exploitation de ressources marines”, Région Normandie under the project “Emergent−CauSy, and with financial support (contract 22FC3R-008) of the GIS FC3R on funds operated by Inserm (France).

**References**

Alvarez, E., Cahoreau, C., Combarnous, Y., 2009. Comparative structure analyses of cystine knot-containing molecules with eight aminoacyl ring including glycoprotein hormones (GPH) alpha and beta subunits and GPH-related A2 (GPA2) and B5 (GPB5) molecules. Reprod Biol Endocrinol 7, 90. https://doi.org/10.1186/1477-7827-7-90

Arimura, S., Wong, M.K.S., Inoue, R., Kawano, M., Shimoyama, K., Fujimori, C., Tokunaga, K., Takagi, W., Hyodo, S., 2024. Functional characterization of follicle-stimulating hormone and luteinizing hormone receptors in cloudy catshark, Scyliorhinus torazame. General and Comparative Endocrinology 354, 114542. https://doi.org/10.1016/j.ygcen.2024.114542

Bassett, J.H.D., Van Der Spek, A., Logan, J.G., Gogakos, A., Bagchi-Chakraborty, J., Murphy, E., Van Zeijl, C., Down, J., Croucher, P.I., Boyde, A., Boelen, A., Williams, G.R., 2015. Thyrostimulin Regulates Osteoblastic Bone Formation During Early Skeletal Development. Endocrinology 156, 3098–3113. https://doi.org/10.1210/en.2014-1943

Bhat, I.A., Rather, Mohd.A., Saha, R., Ganie, P.A., Sharma, R., 2017. Identification and Expression Analysis of Thyroid Stimulating Hormone Receptor (TSHR) in Fish Gonads Following LHRH Treatment. Proc. Natl. Acad. Sci., India, Sect. B Biol. Sci. 87, 719–726. https://doi.org/10.1007/s40011-015-0640-8

Bosseboeuf, A., Gautier, A., Auvray, P., Mazan, S., Sourdaine, P., 2014. Characterization of spermatogonial markers in the mature testis of the dogfish (Scyliorhinus canicula L.). REPRODUCTION 147, 125–139. https://doi.org/10.1530/REP-13-0316

Buechi, H.B., Bridgham, J.T., 2017. Evolution of specificity in cartilaginous fish glycoprotein hormones and receptors. General and Comparative Endocrinology 246, 309–320. https://doi.org/10.1016/j.ygcen.2017.01.007

Burgos, J.R., Iresjö, B.-M., Wärnåker, S., Smedh, U., 2016. Presence of TSH receptors in discrete areas of the hypothalamus and caudal brainstem with relevance for feeding controls—Support for functional significance. Brain Research 1642, 278–286. https://doi.org/10.1016/j.brainres.2016.04.007

Cahoreau, C., Klett, D., Combarnous, Y., 2015. Structureâ€“Function Relationships of Glycoprotein Hormones and Their Subunitsâ€TM Ancestors. Front. Endocrinol. 6. https://doi.org/10.3389/fendo.2015.00026

Caron, P., Broussaud, S., Galano-Frutos, J.J., Sancho, J., Savagner, F., 2020. New variant (Val597Ile) in transmembrane region of the TSH receptor with human chorionic gonadotropin hypersensitivity in familial gestational hyperthyroidism. Clin Endocrinol (Oxf) 93, 339-345. doi: 10.1111/cen.14215.

Cho, S., Rogers, K.W., Fay, D.S., 2007. The C. elegans Glycopeptide Hormone Receptor Ortholog, FSHR-1, Regulates Germline Differentiation and Survival. Current Biology 17, 203–212. https://doi.org/10.1016/j.cub.2006.12.027

Combarnous, Y., 1992. Molecular basis of the specificity of binding of glycoprotein hormones to their receptors. Endocr. Rev. 13, 670-691. doi: 10.1210/edrv-13-4-670.

Combarnous, Y., Hengé, M.H., 1981. Equine follicle-stimulating hormone. Purification, acid dissociation, and binding to equine testicular tissue. J. Biol. Chem. 256, 9567-9572.

Cuevas, M.E., Callard, G., 1992. In vitro steroid secretion by staged spermatocysts (sertoli/germ cell units) of dogfish (Squalus acanthias) testis. General and Comparative Endocrinology 88, 151–165. https://doi.org/10.1016/0016-6480(92)90204-W

Dacheux, J.-L., Dacheux, F., 2014. New insights into epididymal function in relation to sperm maturation. REPRODUCTION 147, R27–R42. https://doi.org/10.1530/REP-13-0420

Dong, J., Xin, M., Liu, H., Zhang, M., Pang, Q., Chen, L., Zhao, B., 2013. Identification, expression of a glycoprotein hormone receptor homolog in the amphioxus Branchiostoma belcheri with implications for origin of vertebrate GpHRs. General and Comparative Endocrinology 184, 35–41. https://doi.org/10.1016/j.ygcen.2012.08.006

Dos Santos, S., Bardet, C., Bertrand, S., Escriva, H., Habert, D., Querat, B., 2009. Distinct Expression Patterns of Glycoprotein Hormone-α2 and -β5 in a Basal Chordate Suggest Independent Developmental Functions. Endocrinology 150, 3815–3822. https://doi.org/10.1210/en.2008-1743

Dufour, S., Quérat, B., Tostivint, H., Pasqualini, C., Vaudry, H., Rousseau, K., 2020. Origin and Evolution of the Neuroendocrine Control of Reproduction in Vertebrates, With Special Focus on Genome and Gene Duplications. Physiological Reviews 100, 869–943. https://doi.org/10.1152/physrev.00009.2019

Dzyuba, V., Ninhaus-Silveira, A., Kahanec, M., Veríssimo-Silveira, R., 2019. Sperm motility in ocellate river stingrays: Evidence for post-testicular sperm maturation and capacitation in chondrichthyes. Journal of Zoology 307, 9–16. https://doi.org/10.1111/jzo.12610

Fadlalla, M.B., Wei, Q., Fedail, J.S., Mehfooz, A., Mao, D., Shi, F., 2017. Effects of hyper- and hypothyroidism on the development and proliferation of testicular cells in prepubertal rats. Anim Sci J 88, 1943–1954. https://doi.org/10.1111/asj.12883

Gautier, A., Bosseboeuf, A., Auvray, P., Sourdaine, P., 2014. Maintenance of Potential Spermatogonial Stem Cells In Vitro by GDNF Treatment in a Chondrichthyan Model (Scyliorhinus canicula L.). Biology of Reproduction 91, 91–105. https://doi.org/10.1095/biolreprod.113.116020

Gautron, J., 1978. Effet du calcium et de la stimulation sur les terminaisons nerveuses des fonctions nerf-électroplaque de la Torpille. Biol. Cell. 31, 31–44.

Gervasi, M.G., Visconti, P.E., 2017. Molecular changes and signaling events occurring in spermatozoa during epididymal maturation. Andrology 5, 204–218. https://doi.org/10.1111/andr.12320

Giraldo, C., Le Roy, D., Martin-Baillet, V., 2022. CGFS2022 cruise, RV Thalassa. https://doi.org/10.17600/18001842

Gong, Z., Wang, W., El Omari, K., Lebedev, A.A., Clarke, O.B., Hendrickson, W.A., 2023. Crystal structure of LGR ligand α2/β5 from Caenorhabditis elegans with implications for the evolution of glycoprotein hormones. Proceedings of the National Academy of Sciences. https://doi.org/10.1107/S205979832300102X

Goto-Kazeto, R., Kazeto, Y., Trant, J.M., 2009. Molecular cloning, characterization and expression of thyroid-stimulating hormone receptor in channel catfish. General and Comparative Endocrinology 161, 313–319. https://doi.org/10.1016/j.ygcen.2009.01.009

Hara, Y., Yamaguchi, K., Onimaru, K., Kadota, M., Koyanagi, M., Keeley, S.D., Tatsumi, K., Tanaka, K., Motone, F., Kageyama, Y., Nozu, R., Adachi, N., Nishimura, O., Nakagawa, R., Tanegashima, C., Kiyatake, I., Matsumoto, R., Murakumo, K., Nishida, K., Terakita, A., Kuratani, S., Sato, K., Hyodo, S., Kuraku, S., 2018. Shark genomes provide insights into elasmobranch evolution and the origin of vertebrates. Nat Ecol Evol 2, 1761–1771. https://doi.org/10.1038/s41559-018-0673-5

Hausken, K.N., Tizon, B., Shpilman, M., Barton, S., Decatur, W., Plachetzki, D., Kavanaugh, S., Ul-Hasan, S., Levavi-Sivan, B., Sower, S.A., 2018. Cloning and characterization of a second lamprey pituitary glycoprotein hormone, thyrostimulin (GpA2/GpB5). General and Comparative Endocrinology 264, 16–27. https://doi.org/10.1016/j.ygcen.2018.04.010

He, X., Duan, J., Ji, Y., Zhao, L., Jiang, H., Jiang, Y., Eric Xu, H., Cheng, X., 2022. Hinge region mediates signal transmission of luteinizing hormone and chorionic gonadotropin receptor. Computational and Structural Biotechnology Journal 20, 6503–6511. https://doi.org/10.1016/j.csbj.2022.11.039

Heyland, A., Plachetzki, D., Donelly, E., Gunaratne, D., Bobkova, Y., Jacobson, J., Kohn, A.B., Moroz, L.L., 2012. Distinct Expression Patterns of Glycoprotein Hormone Subunits in the Lophotrochozoan Aplysia: Implications for the Evolution of Neuroendocrine Systems in Animals. Endocrinology 153, 5440–5451. https://doi.org/10.1210/en.2012-1677

Hsu, S.Y., Nakabayashi, K., Bhalla, A., 2002. Evolution of Glycoprotein Hormone Subunit Genes in Bilateral Metazoa: Identification of Two Novel Human Glycoprotein Hormone Subunit Family Genes, GPA2 and GPB5.

Irachi, S., Hall, D.J., Fleming, M.S., Maugars, G., Björnsson, B.T., Dufour, S., Uchida, K., McCormick, S.D., 2021. Photoperiodic regulation of pituitary thyroid-stimulating hormone and brain deiodinase in Atlantic salmon. Molecular and Cellular Endocrinology 519, 111056. https://doi.org/10.1016/j.mce.2020.111056

Irisarri, I., Baurain, D., Brinkmann, H., Delsuc, F., Sire, J.-Y., Kupfer, A., Petersen, J., Jarek, M., Meyer, A., Vences, M., Philippe, H., 2017. Phylotranscriptomic consolidation of the jawed vertebrate timetree. Nat Ecol Evol 1, 1370–1378. https://doi.org/10.1038/s41559-017-0240-5

Jaeschke, H., Schaarschmidt, J., Günther, R., Mueller, S., 2011. The Hinge Region of the TSH Receptor Stabilizes Ligand Binding and Determines Different Signaling Profiles of Human and Bovine TSH. Endocrinology 152, 3986–3996. https://doi.org/10.1210/en.2011-1389

Johansson, M.U., Zoete, V., Michielin, O., Guex, N., 2012. Defining and searching for structural motifs using DeepView/Swiss-PdbViewer. BMC Bioinformatics 13, 1–11. https://doi.org/10.1186/1471-2105-13-173

Jones, C.J.P., Walker, T.I., Bell, J.D., Reardon, M.B., Ambrosio, C.E., Almeida, A., 2005. Male Genital Ducts and Copulatory Appendages in Chondrichthyans, in: Reproductive Biology and Phylogeny of Chondrichthyes: Sharks, Batoids and Chimaeras. W.C. Hamlett (Ed), pp. 371–387. https://doi.org/10.1201/9781439856000-27

Jones, R.C., Jones, N., Djakiew, D., 1984. Luminal composition and maturation of spermatozoa in the male genital ducts of the Port Jackson shark, Heterodontus portusjacksoni. J. Exp. Zool. 230, 417–426. https://doi.org/10.1002/jez.1402300311

Kenis, S., Istiban, M.N., Van Damme, S., Vandewyer, E., Watteyne, J., Schoofs, L., Beets, I., 2023. Ancestral glycoprotein hormone-receptor pathway controls growth in C. elegans. Front. Endocrinol. 14, 1200407. https://doi.org/10.3389/fendo.2023.1200407

Quérat, B., 2021. Unconventional Actions of Glycoprotein Hormone Subunits: A Comprehensive Review. Front. Endocrinol. 12, 731966. doi: 10.3389/fendo.2021.731966

Klett, D., Combarnous, Y., 2021. Highly sensitive in vitro bioassay for luteinizing hormone and chorionic gonadotropin allowing their measurement in plasma. Reproduction and Fertility 2, 300–307. https://doi.org/10.1530/RAF-21-0045

Kudo, M., Chen, T., Nakabayashi, K., Hsu, S.Y., Hsueh, A.J.W., 2000. The Nematode Leucine-Rich Repeat-Containing, G Protein-Coupled Receptor (LGR) Protein Homologous to Vertebrate Gonadotropin and Thyrotropin Receptors is Constitutively Activated in Mammalian Cells 14, 272–284. https://doi.org/10.1210/mend.14.2.0422

Kumar, R.S., Ijiri, S., Kight, K., Swanson, P., Dittman, A., Alok, D., Zohar, Y., Trant, J.M., 2000. Cloning and functional expression of a thyrotropin receptor from the gonads of a vertebrate (bony fish): potential thyroid-independent role for thyrotropin in reproduction. Molecular and Cellular Endocrinology 167, 1–9. https://doi.org/10.1016/S0303-7207(00)00304-X

Lemoine, F., Correia, D., Lefort, V., Doppelt-Azeroual, O., Mareuil, F., Cohen-Boulakia, S., Gascuel, O., 2019. NGPhylogeny.fr: new generation phylogenetic services for non-specialists. Nucleic Acids Research 47, 260–265. https://doi.org/10.1093/nar/gkz303

Letunic, I., Bork, P., 2021. Interactive Tree Of Life (iTOL) v5: an online tool for phylogenetic tree display and annotation. Nucleic Acids Research 49, 293–296. https://doi.org/10.1093/nar/gkab301

Levavi-Sivan, B., Bogerd, J., Mañanós, E.L., Gómez, A., Lareyre, J.J., 2010. Perspectives on fish gonadotropins and their receptors. General and Comparative Endocrinology 165, 412–437. https://doi.org/10.1016/j.ygcen.2009.07.019

Li, C., Habu, Y., Takagi, S., Gotoh, J., Nogimori, T., Hirooka, C., 2004. Distribution of thyrostimulin in the rat: an immunohistochemical study. Endocrine Regulations. Am J Cardiol 37, 223–230. https://doi.org/10.1016/0002-9149(76)90316-7

Li, H., Zhou, X., Wang, G., Hua, D., Li, S., Xu, T., Dong, M., Cui, X., Yang, X., Wu, Y., Cai, M., Liao, X., Zhang, T., Yang, Z., Du, Y., Li, X., 2022. CAR-T Cells Targeting TSHR Demonstrate Safety and Potent Preclinical Activity Against Differentiated Thyroid Cancer. The Journal of Clinical Endocrinology & Metabolism 107, 1110–1126. https://doi.org/10.1210/clinem/dgab819

Livak, K.J., Schmittgen, T.D., 2001. Analysis of Relative Gene Expression Data Using Real-Time Quantitative PCR and the 2−ΔΔCT Method. Methods 25, 402–408. https://doi.org/10.1006/meth.2001.1262

Loir, M., Sourdaine, P., 1994. Testes cells: isolation and culture. In: Hochachka PW, Mommsen TP (eds) Biochemistry and molecular biology of fishes: analytical techniques. Elsevier, New York, pp. 219–272.

Loppion, G., Crespel, A., Martinez, A.-S., Auvray, P., Sourdaine, P., 2008. Study of the potential spermatogonial stem cell compartment in dogfish testis, Scyliorhinus canicula L. Cell and Tissue Research 332, 533–542. https://doi.org/10.1007/s00441-008-0590-z

Lutton, B.V., Callard, I.P., 2007. Effects of reproductive activity and sex hormones on apoptosis in the epigonal organ of the skate (Leucoraja erinacea). General and Comparative Endocrinology 154, 75–84. https://doi.org/10.1016/j.ygcen.2007.06.014

Marra, N.J., Stanhope, M.J., Jue, N.K., Wang, M., Sun, Q., Pavinski Bitar, P., Richards, V.P., Komissarov, A., Rayko, M., Kliver, S., Stanhope, B.J., Winkler, C., O'Brien, S.J., Antunes, A., Jorgensen, S., Shivji, M.S., 2019. White shark genome reveals ancient elasmobranch adaptations associated with wound healing and the maintenance of genome stability. Proceedings of the National Academy of Sciences 116, 4446–4455. https://doi.org/10.1073/pnas.1819778116

Maugars, G., Dufour, S., Cohen-Tannoudji, J., Quérat, B., 2014. Multiple Thyrotropin β-Subunit and Thyrotropin Receptor-Related Genes Arose during Vertebrate Evolution. PLoS ONE 9, e111361. https://doi.org/10.1371/journal.pone.0111361

Mueller, S., Kleinau, G., Szkudlinski, M.W., Jaeschke, H., Krause, G., Paschke, R., 2009. The superagonistic activity of bovine thyroid-stimulating hormone (TSH) and the human TR1401 TSH analog is determined by specific amino acids in the hinge region of the human TSH receptor. J Biol Chem. 284,16317-16324. doi: 10.1074/jbc.M109.005710.

Nagasaki, H., Wang, Z., Jackson, V.R., Lin, S., Nothacker, H.P., Civelli, O., 2006. Differential expression of the thyrostimulin subunits, glycoprotein 2 and 5 in the rat pituitary. Journal of Molecular Endocrinology 37, 39–50. https://doi.org/10.1677/jme.1.01932

Nakabayashi, K., Matsumi, H., Bhalla, A., Bae, J., Mosselman, S., Hsu, S.Y., Hsueh, A.J.W., 2002. Thyrostimulin, a heterodimer of two new human glycoprotein hormone subunits, activates the thyroid-stimulating hormone receptor. J. Clin. Invest. 109, 1445–1452. https://doi.org/10.1172/JCI0214340

Okada, S.L., Ellsworth, J.L., Durnam, D.M., Haugen, H.S., Holloway, J.L., Kelley, M.L., Lewis, K.E., Ren, H., Sheppard, P.O., Storey, H.M., Waggie, K.S., Wolf, A.C., Yao, L.Y., Webster, P.J., 2006. A Glycoprotein Hormone Expressed in Corticotrophs Exhibits Unique Binding Properties on Thyroid-Stimulating Hormone Receptor. Molecular Endocrinology 20, 414–425. https://doi.org/10.1210/me.2005-0270

Okajima, Y., Nagasaki, H., Suzuki, C., Suga, H., Ozaki, N., Arima, H., Hamada, Y., Civelli, O., Oiso, Y., 2008. Biochemical roles of the oligosaccharide chains in thyrostimulin, a heterodimeric hormone of glycoprotein hormone subunits alpha2 (GPA2) and beta5 (GPB5). Regulatory Peptides 148, 62–67. https://doi.org/10.1016/j.regpep.2008.03.002

Piferrer, F.C., Callard, G.V., 1995. Inhibition of Deoxyribonucleic Acid Synthesis during Premeiotic Stages of Spermatogenesis by a Factor from Testis-Associated Lymphomyeloid Tissue in the Dogfish Shark (Squalus Acanthias). Biology of Reproduction 53, 390–398. https://doi.org/10.1095/biolreprod53.2.390

Pudney, J., Callard, G.V., 1984a. Development of agranular reticulum in Sertoli cells of the testis of the dogfishSqualus acanthias during spermatogenesis. Anat. Rec. 209, 311–321. https://doi.org/10.1002/ar.1092090309

Pudney, J., Callard, G.V., 1984b. Identification of Leydig-like cells in the testis of the dogfishSqualus acanthias. Anat. Rec. 209, 323–330. https://doi.org/10.1002/ar.1092090310

Read, T.D., Petit, R.A., Joseph, S.J., Alam, Md.T., Weil, M.R., Ahmad, M., Bhimani, R., Vuong, J.S., Haase, C.P., Webb, D.H., Tan, M., Dove, A.D.M., 2017. Draft sequencing and assembly of the genome of the world's largest fish, the whale shark: Rhincodon typus Smith 1828. BMC Genomics 18, 532. https://doi.org/10.1186/s12864-017-3926-9

Redon, E., Bosseboeuf, A., Rocancourt, C., Da Silva, C., Wincker, P., Mazan, S., Sourdaine, P., 2010. Stage-specific gene expression during spermatogenesis in the dogfish (Scyliorhinus canicula). Reproduction 140, 57–71. https://doi.org/10.1530/REP-10-0021

Rocco, D.A., Garcia, A.S.G., Scudeler, E.L., dos Santos, D.C., Nóbrega, R.H., Paluzzi, J.-P.V., 2019. Glycoprotein Hormone Receptor Knockdown Leads to Reduced Reproductive Success in Male Aedes aegypti. Front. Physiol. 10, 266. https://doi.org/10.3389/fphys.2019.00266

Rocco, D.A., Kim, D.H., Paluzzi, J.-P.V., 2017. Immunohistochemical mapping and transcript expression of the GPA2/GPB5 receptor in tissues of the adult mosquito, Aedes aegypti. Cell Tissue Res 369, 313–330. https://doi.org/10.1007/s00441-017-2610-3

Rocco, D.A., Paluzzi, J.-P.V., 2020. Expression Profiling, Downstream Signaling, and Inter-subunit Interactions of GPA2/GPB5 in the Adult Mosquito Aedes aegypti. Front. Endocrinol. 11, 158. https://doi.org/10.3389/fendo.2020.00158

Roch, G.J., Sherwood, N.M., 2014. Glycoprotein Hormones and Their Receptors Emerged at the Origin of Metazoans. Genome Biology and Evolution 6, 1466–1479. https://doi.org/10.1093/gbe/evu118

Rocha, A., Gómez, A., Galay-Burgos, M., Zanuy, S., Sweeney, G.E., Carrillo, M., 2007. Molecular characterization and seasonal changes in gonadal expression of a thyrotropin receptor in the European sea bass. General and Comparative Endocrinology 152, 89–101. https://doi.org/10.1016/j.ygcen.2007.03.001

Schefe, J.H., Lehmann, K.E., Buschmann, I.R., Unger, T., Funke-Kaiser, H., 2006. Quantitative real-time RT-PCR data analysis: current concepts and the novel "gene expression's C T difference" formula. Journal of Molecular Medicine 84, 901–910. https://doi.org/10.1007/s00109-006-0097-6

Schwartz, J., 2021. A Novel Dop2/Invertebrate-Type Dopamine Signaling System Potentially Mediates Stress, Female Reproduction, and Early Development in the Pacific Oyster (. Marine Biotechnology 12.

Sievers, F., Wilm, A., Dineen, D., Gibson, T.J., Karplus, K., Li, W., Lopez, R., McWilliam, H., Remmert, M., Söding, J., Thompson, J.D., Higgins, D.G., 2011. Fast, scalable generation of high-quality protein multiple sequence alignments using Clustal Omega. Molecular Systems Biology 7, 539. https://doi.org/10.1038/msb.2011.75

Sourdaine, P., Garnier, D.H., 1993. Stage-dependent modulation of Sertoli cell steroid production in dogfish (Scyliorhinus canicula). Reproduction 97, 133–142. https://doi.org/10.1530/jrf.0.0970133

Sower, S.A., Decatur, W.A., Hausken, K.N., Marquis, T.J., Barton, S.L., Gargan, J., Freamat, M., Wilmot, M., Hollander, L., Hall, J.A., Nozaki, M., Shpilman, M., Levavi-Sivan, B., 2015. Emergence of an Ancestral Glycoprotein Hormone in the Pituitary of the Sea Lamprey, a Basal Vertebrate. Endocrinology 156, 3026–3037. https://doi.org/10.1210/en.2014-1797

Sower, S.A., Hausken, K.N., 2017. A lamprey view on the origins of neuroendocrine regulation of the thyroid axis. Molecular and Cellular Endocrinology 459, 21–27. https://doi.org/10.1016/j.mce.2017.04.012

Studer, G., Rempfer, C., Waterhouse, A.M., Gumienny, R., Haas, J., Schwede, T., 2020. QMEANDisCo—distance constraints applied on model quality estimation. Bioinformatics 36, 1765–1771. https://doi.org/10.1093/bioinformatics/btz828

Sudo, S., Kuwabara, Y., Park, J.-I., Hsu, S.Y., Hsueh, A.J.W., 2005. Heterodimeric Fly Glycoprotein Hormone-α2 (GPA2) and Glycoprotein Hormone-β5 (GPB5) Activate Fly Leucine-Rich Repeat-Containing G Protein-Coupled Receptor-1 (DLGR1) and Stimulation of Human Thyrotropin Receptors by Chimeric Fly GPA2 and Human GPB5. Endocrinology 146, 3596–3604. https://doi.org/10.1210/en.2005-0317

Sullivan, R., Saez, F., Girouard, J., Frenette, G., 2005. Role of exosomes in sperm maturation during the transit along the male reproductive tract. Blood Cells, Molecules, and Diseases 35, 1–10. https://doi.org/10.1016/j.bcmd.2005.03.005

Sun, S.-C., Hsu, P.-J., Wu, F.-J., Li, S.-H., Lu, C.-H., Luo, C.-W., 2010. Thyrostimulin, but Not Thyroid-stimulating Hormone (TSH), Acts as a Paracrine Regulator to Activate the TSH Receptor in Mammalian Ovary. Journal of Biological Chemistry 285, 3758–3765. https://doi.org/10.1074/jbc.M109.066266

Suzuki, C., Nagasaki, H., Okajima, Y., Suga, H., Ozaki, N., Arima, H., Iwasaki, Y., Oiso, Y., 2009. Inflammatory Cytokines Regulate Glycoprotein Subunit β5 of Thyrostimulin through Nuclear Factor-κB. Endocrinology 150, 2237–2243. https://doi.org/10.1210/en.2008-0823

Ulloa-Aguirre, A., Zariñán, T., Jardón-Valadez, E., Gutiérrez-Sagal, R., Dias, J.A., 2018. Structure-Function Relationships of the Follicle-Stimulating Hormone Receptor. Front. Endocrinol. 9, 707. https://doi.org/10.3389/fendo.2018.00707

Vandersmissen, H.P., Van Hiel, M.B., Van Loy, T., Vleugels, R., Vanden Broeck, J., 2014. Silencing D. melanogaster lgr1 impairs transition from larval to pupal stage. General and Comparative Endocrinology 209, 135–147. https://doi.org/10.1016/j.ygcen.2014.08.006

Wahl, M., Levy, T., Manor, R., Aflalo, E.D., Sagi, A., Aizen, J., 2022. Genes Encoding the Glycoprotein Hormone GPA2/GPB5 and the Receptor LGR1 in a Female Prawn. Front. Endocrinol. 13, 823818. https://doi.org/10.3389/fendo.2022.823818

Wang, P., Liu, S., Yang, Q., Liu, Z., Zhang, S., 2018. Functional Characterization of Thyrostimulin in Amphioxus Suggests an Ancestral Origin of the TH Signaling Pathway. Endocrinology 159, 3536–3548. https://doi.org/10.1210/en.2018-00550

Wang, Q., Arighi, C.N., King, B.L., Polson, S.W., Vincent, J., Chen, C., Huang, H., Kingham, B.F., Page, S.T., Farnum Rendino, M., Thomas, W.K., Udwary, D.W., Wu, C.H., the North East

Bioinformatics Collaborative Curation Team, 2012. Community annotation and bioinformatics workforce development in concert - Little Skate Genome Annotation Workshops and Jamborees. Database 2012, bar064. https://doi.org/10.1093/database/bar064

Waterhouse, A., Bertoni, M., Bienert, S., Studer, G., Tauriello, G., Gumienny, R., Heer, F.T., de Beer, T.A.P., Rempfer, C., Bordoli, L., Lepore, R., Schwede, T., 2018. SWISS-MODEL: homology modelling of protein structures and complexes. Nucleic Acids Research 46, 296–303. https://doi.org/10.1093/nar/gky427

Yang, L.-K., Zhang, J., Liu, D., Han, T.-Y., Qin, Q.-S., Wang, A.-Q., Dong, B., 2023. Ancestral glycoprotein hormone and its cognate receptor present in primitive chordate ascidian: Molecular identification and functional characterization. International Journal of Biological Macromolecules 229, 401–412. https://doi.org/10.1016/j.ijbiomac.2022.12.297

Ye, J., Coulouris, G., Zaretskaya, I., Cutcutache, I., Rozen, S., Madden, T.L., 2012. Primer-BLAST: A tool to design target-specific primers for polymerase chain reaction. BMC Bioinformatics 13, 1–11. https://doi.org/10.1186/1471-2105-13-134

Yoshimura, T., 2010. Neuroendocrine mechanism of seasonal reproduction in birds and mammals. Animal Science Journal 81, 403–410. https://doi.org/10.1111/j.1740-0929.2010.00777.x

Zhang, M., Wei, H., Liu, T., Li, W., Li, Y., Wang, S., Xing, Q., Hu, X., Zhang, L., Bao, Z., 2020. Potential GnRH and steroidogenesis pathways in the scallop Patinopecten yessoensis. The Journal of Steroid Biochemistry and Molecular Biology 204, 105756. https://doi.org/10.1016/j.jsbmb.2020.105756

# Annexes Chapitre III

# I. Annexes chapitre III : Données supplémentaires

**Supplementary material**

**Pleiotropic signaling of thyrostimulin (GPA2/GPB5) on Glycoprotein Hormone Receptors (FSHR, LHR, TSHR) in the elasmobranch *Scyliorhinus canicula* reproduction**

Fabian Jeanne[1], Stanislas Pilet[1], Danièle Klett[2], Yves Combarnous[2], Benoît Bernay[3], Sylvie Dufour[1], Pascal Favrel[1] and Pascal Sourdaine*[1]

[1] Université de Caen Normandie, Muséum national d'Histoire naturelle, Sorbonne Université, Université des Antilles, CNRS, IRD, Laboratoire de Biologie des Organismes et Ecosystèmes Aquatiques (BOREA), UMR 8067, 14032 Caen cedex 5, France.

[2] INRAE, CNRS, Université de Tours, UMR Physiologie de la Reproduction & des Comportements, 37380 Nouzilly, France

[3] Université de Caen Normandie - Plateforme PROTEOGEN, US EMerode, 14032 Caen cedex 5, France.

*Corresponding Author: orcid.org/0000-0001-9811-2876; Email: pascal.sourdaine@unicaen.fr

**Table S1.** List of the primers used for RT-qPCR and *in situ* hybridization

| Primer names | Experimentation | Sequence |
|---|---|---|
| S.ca-TSHR-RT | RT-qPCR | 5'-GCTGTGCGTTCAAGAACTGG-3'; 5'-CTGCGTTGTTATCGTCAGCG-3' |
| S.ca-GPA2-RT | RT-qPCR | 5'-CTGACCATCAAGAGTGATCG-3'; 5'-GCAGGACAGCCTTACTCTCA-3' |
| S.ca-TSHβ2-RT | RT-qPCR | 5'-TCTCAGTGCTCGCTGACAAG-3'; 5'-CGCAAATGGTGGTGTTGATG-3' |
| S.ca-GPB5-RT | RT-qPCR | 5'-ACATCAGCTTGCGGACCTTC-3'; 5'-TCGATATACGGAGGGTCGAGA-3' |
| S.ca-5SRNA-RT | RT-qPCR | 5'-TCGTCTGATCTCGGAAGCTA-3'; 5'-AGCCTACTGCACCTGGTATTC-3' |
| S.ca-TSHR-ISH | *in situ* hybridization | 5'-GCTGTGCGTTCAAGAACTGG-3'; 5'-CGGTTCTGGTGTAGAGGTCC-3' |
| S.ca-GPB5-ISH | *in situ* hybridization | 5'- ACATCAGCTTGCGGACCTTC-3'; 5'-CAGTCACATCGAACTGCCAC-3' |
| S.ca-GPA2-ISH | *in situ* hybridization | 5'-CTGACCATCAAGAGTGATCG-3'; 5'-GCAGGACAGCCTTACTCTCA-3' |

**Table S2**. Supporting information for the model prediction of *S. canicula*, *C. milii* and *H. sapiens* TSHβ, GPA2, GPB5 and TSHR.

| | TSHβ | GPA2 | GPB5 | TSHR |
|---|---|---|---|---|
| 3D model templates | 7utz.1 | Q96T91.1.A | Q86YW7.1.A | 7utz.1 |
| Global seq. identity with *H. sapiens* sequence | ‘100.00% | 100.00% | 100.00% | 100.00% |
| Global Model Quality Estimate (GMQE) for *H. sapiens* models | ‘0.69 | 0.89 | 0.87 | 0.74 |
| QMEANDisCo Global for *H. sapiens* models | ‘0.76 ± 0.06 | 0.72± 0.06 | 0.75± 0.05 | 0.78 ± 0.05 |
| Global seq. identity with *C. milii* sequences | ’63.32%; ‘’57.92% | 58.68% | 79.44% | 75.99% |
| Global Model Quality Estimate (GMQE) for *C. milii* models | ‘0.63; ‘’0.62 | 0.48 | 0.63 | 0.72 |
| QMEANDisCo Global for *C. milii* models | ‘0.69 ± 0.06; ‘’0.68 ± 0.06 | 0.49 ± 0.08 | 0.60 ± 0.08 | 0.75 ± 0.05 |
| Global seq. identity with *S. canicula* sequences | 59.41% | 63.39% | 72.31% | 73.20% |
| Global Model Quality Estimate (GMQE) for *S. canicula* models | 0.62 | 0.47 | 0.57 | 0.68 |
| QMEANDisCo Global for *S. canicula* models | ‘’0.68 ± 0.06 | 0.52 ± 0.08 | 0.54 ± 0.07 | 0.75 ± 0.05 |

‘: TSHβ1; ‘’: TSHβ2

**Table S3**. Analysis of the supporting information for the model prediction of *S. canicula*, *C. milii* and *H. sapiens* TSHβ, GPA2, GPB5 and TSHR.

| | TSHb | | GPA2 | GPB5 | TSHR |
|---|---|---|---|---|---|
| | TSHb1 | TSHb2 | | | |
| $GMQE_{H.sap.}$ - $GMQE_{C.mil.}$ | 0.06 | 0.07 | 0.41 | 0.24 | 0.02 |
| $QMeanDisco_{H.sap.}$ - $QMeanDisco_{C.mil.}$ | 0.07 | 0.08 | 0.23 | 0.15 | 0.02 |
| $GMQE_{H.sap.}$ - $GMQE_{S.can.}$ | - | 0.06 | 0.42 | 0.30 | 0.06 |
| $QMeanDisco_{H.sap.}$ - $QMeanDisco_{S.can.}$ | - | 0.08 | 0.20 | 0.21 | 0.03 |

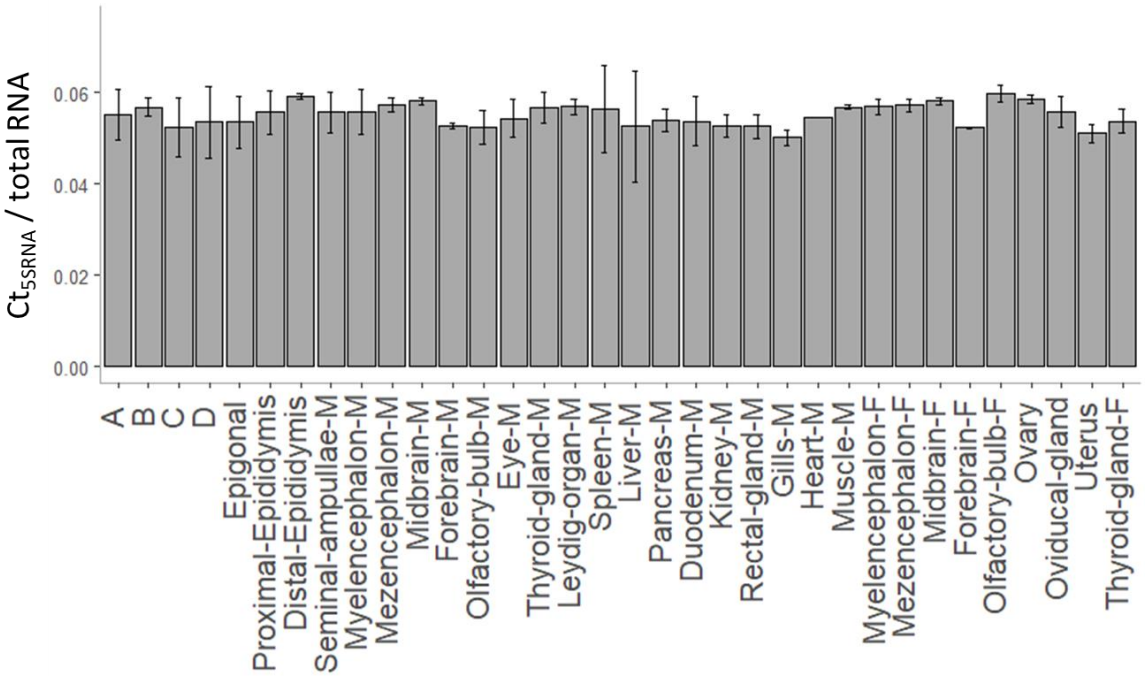


**Fig. S1**. Validation of the 5sRNA as reference gene for the real-time PCR. Statistical analyse was performed using the none parametric Kruskal-Wallis (based on the previous Shapiro-wilk test results) test for (P-value = 0.14).

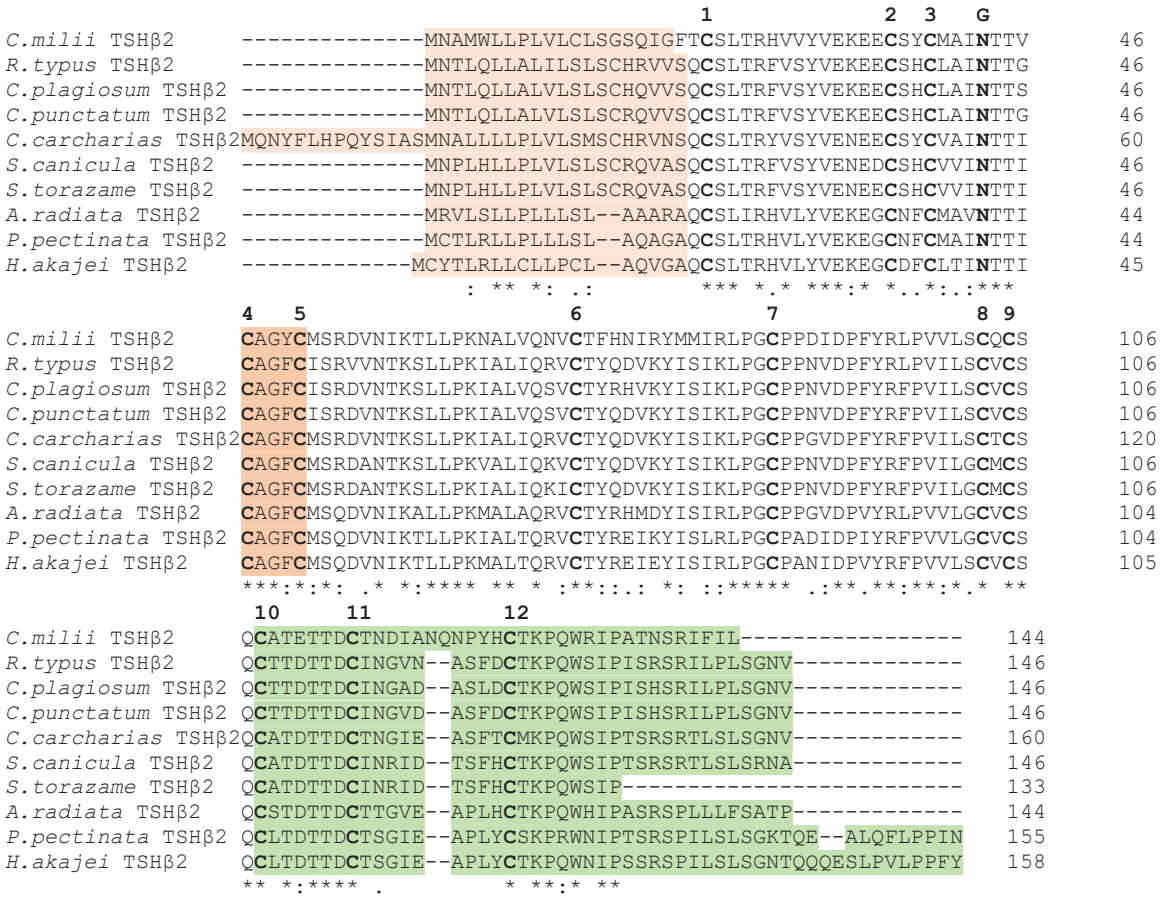


**Fig. S2.** Multiple alignment of chondrichthyan TSHβ2 subunit protein sequences. Sequences of the putative peptide signal is highlighted in light orange, the “seat” in orange, and conserved cysteines are numbered. G, putative N-glycosylation sites.

A

```
                                                        1     G          2        3
C.milii GPHA2      ----MSALRALALSVLTAVLASGGNGIQPLGPGCHLYPFNVTIRSDRRGTCQGMQSISAC       56
R.typus GPHA2      MPTVSK-MIPTVVLVLLLVSGALSPDPTDPEPGCHRYPFNVTIKSDRQGTCRGSQLIHAC       59
C.punctatum GPHA2  --------MPTIVVVLLLASGALSLDPTDPEPGCHLYRFNVTIKSDRQGTCLGSQLIHAC       52
S.canicula GPHA2   MPGVPELCGSGLILVLLLVSGGLSPDPGEPEPGCQLYPFNLTIKSDRRGTCRGSQLIQAC       60
S.torazame GPHA2   MPGLPELCGSGLILVLLLVSGGSSPDPGEPEPGCQLYPFNVTIKSDRQGTCQGSQLIQAC       60
C.carcharias GPHA2MSGLQDLSISGLILVLLLVSVSLSPDPAEPEPGCHLYPFNVTIKSDQRGTCRGSQLIQAC       60
H.akajei GPHA2     -------MSGIRLFFLTGLVIGSFAQSPEPAAGCRLYPFNVTIRSDGPGSCRGRHASHAC       53
                                .  .   :      **: * **:**:**  *:* * :   **

                     4                 G      56            7
C.milii GPHA2      VGYCESSAFPSKYSVLLASNFKRNITSVSQCCTINKMQKVRVKLFCGARKEEVDIFTARS       116
R.typus GPHA2      VGYCESSAFPSKSSVLLASGYKHNITSVSQCCTISKMLKVRVSLFCGPRREEIEIFTAGS       119
C.punctatum GPHA2  VGYCESSAFPSKFSVLLASEFKHNITSVSQCCTISKMLKVRVSLFCGPRREDIEIFTARS       112
S.canicula GPHA2   VGYCESSAFPSKYSVLKASGFKHNITSVSQCCTISKMQKVRVRLSCGNRREEIEIFTAKS       120
S.torazame GPHA2   VGYCESSAFPSKYSVLMASGFKHNITSVSQCCTITKMQKVRVRLSCGIRREEIEIFTAKS       120
C.carcharias GPHA2VGYCESSAFPSKYSVLMASGFKHNITSVSQCCIIRKMQKVRVRLFCGPRREEIEIFTAKS       120
H.akajei GPHA2     VGHCESSAFPSKFSVLRASGFRHITTSVSQCCTIGRLEKVRVSLSCGERTEELEIFTARS       113
                   **:********* *** ** :::  ******* * :: **** * ** * *:::**** *

                   8 9  10
C.milii GPHA2      CRCDMCRLSRY     127
R.typus GPHA2      CRCDMCRLSRY     130
C.punctatum GPHA2  CRCDMCRLSRY     123
S.canicula GPHA2   CRCDMCRLSRY     131
S.torazame GPHA2   CHCDMCRLSRY     131
C.carcharias GPHA2CSCDMCRLSRY     131
H.akajei GPHA2     CRCDMCRQSRY     124
                   * ***** ***
```

B

```
                                                          G        1            2
C.milii GPHB5      ---------------------------MYVSVLPASNISLRTFIGCAVREFTFLAKKPGC       33
S.canicula GPHB5 -----MLSYRLNLHHIIWGSLILQLLVVYVNILPASNISLRTFIGCAVREFTFLAKKPGC       55
S.torazame GPHB5 --------MLLNLHHIIWGSLILQLLVVYVNILPASNISLRTFIGCAVREFTFLAKKPGC       52
C.punctatum GPHB5MSVTGEREELLNHHHVIWGSLILQLLVVYVNVLPASNMSLRTFIGCAVREFTFLAKKPGC       60
C.plagiosum GPHB5-----MWSHRLNHHHIIWGSLLLQLLVVYVNVLPASNISLRTFIGCAVREFTFLAKKPGC       55
R.typus GPHB5      -----MWSHRLNHHHIIWGSLILQLLVVYVNVLPASNISLRTFIGCAVREFTFLAKKPGC       55
A.radiata GPHB5    -----MSSHRLNLHRLIWGSLILQLLVVYEHALPASNISLQTFIGCAVREFRFMARKPGC       55
H.akajei GPHB5     ----MCICLRLNLHHLLWGSIILQFLVFYENALPASSISLQTFIGCAVREFRFLARKPGC       56
                                          .*   ****.:**:********** *:*:****

                         3   4                    5  G           6
C.milii GPHB5      KGLRISTDACWGRCETWEKPVLDPPYVDAHHRVCTYNETRLATVKLPNCRPNVDPYYTYP       93
S.canicula GPHB5 KGLRISTDACWGRCETWEKPVLDPPYIDGHHRVCTYNETRFITVKLPNCRPGTDPYYTYP       115
S.torazame GPHB5 KGLRVSTDACWGRCETWEKPVLDPPYIDGHHRVCTYNETRFITVKLPNCRPGIDPYYTYP       112
C.punctatum GPHB5KGLRINTDACWGRCETWEKPVLDPPYIEAHHRVCTYNETRFITVKLPNCRAGIDPYYTYP       120
C.plagiosum GPHB5KGLRINTDACWGRCETWEKPVLDPPYIEAHHRVCTYNETRFITVKLPNCRAGIDPYYTYP       115
R.typus GPHB5      KGLRISTDACWGRCETWEKPVLDPPYIEAHHRVCTYNETRFITVKLPNCQAGIDPYYTYP       115
A.radiata GPHB5    KKLRITTDACWGRCETWERPILDPPYIEAYHRVCTYNETKSVTVKMPNCLPDVDPFYTYP       115
H.akajei GPHB5     KGLRITTDACWGRCETWERPILDPPYVEAYHRVCTYNETRFVTVKLPNCRADVDPFYTYP       116
                   * **:.************:*:*****::.:*********:  ***:***  . **:****

                       7 8  9      10
C.milii GPHB5      VALRCDCSGCSTASTECETL      113
S.canicula GPHB5 VAVRCDCGVCSTATTECETL      135
S.torazame GPHB5 VAVRCDCGVCSTATTECETL      132
C.punctatum GPHB5VAIRCDCGVCSTATTECETL      140
C.plagiosum GPHB5VAMRCDCGVCSTATTECETL      135
R.typus GPHB5      VAMRCECGVCSTATTECETL      135
A.radiata GPHB5    MALRCDCDLCSTTTTECVTL      135
H.akajei GPHB5     VAVRCDCGICSTTTTECETL      136
                   :*:**:*. ***::*** **
```

**Fig. S3.** Multiple alignment of chondrichthyan GPA2 and GPB5 protein sequences. Sequences of the putative peptide signal is highlighted in light orange, the “seat” region in orange, the “seat-belt” region in green and conserved cysteines are numbered. G, putative N-glycosylation sites.

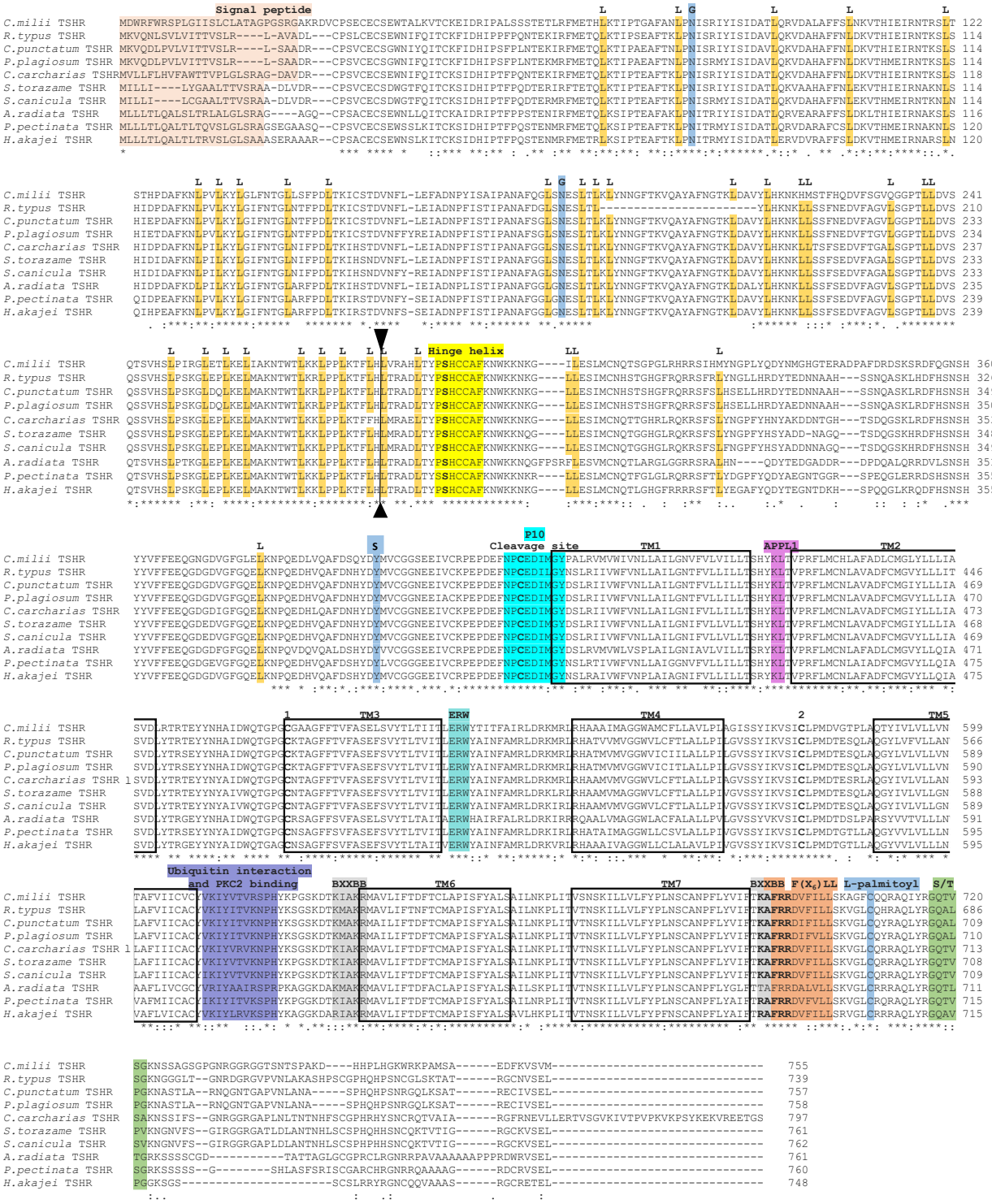


**Fig. S4.** Multiple alignment of chondrichthyan TSHR protein sequences. Sequence of the putative peptide signal is highlighted in light orange, conserved cysteines of the transmembrane region are numbered, leucine residues are highlighted in dark yellow, the putative N-glycosylation (G), sulfotyrosine (S) and L-palmitoyl sites are highlighted in dark blue, the hinge helix (with the Serine ScS280 highlighted in bold) and P10 loop are highlighted in light yellow and light blue respectively, the vertical black bar corresponds to the putative limit between the solenoid and the diverse putative transmembrane α-helixes (TM) are boxed and the putative interacting motifs highlighted with different color.

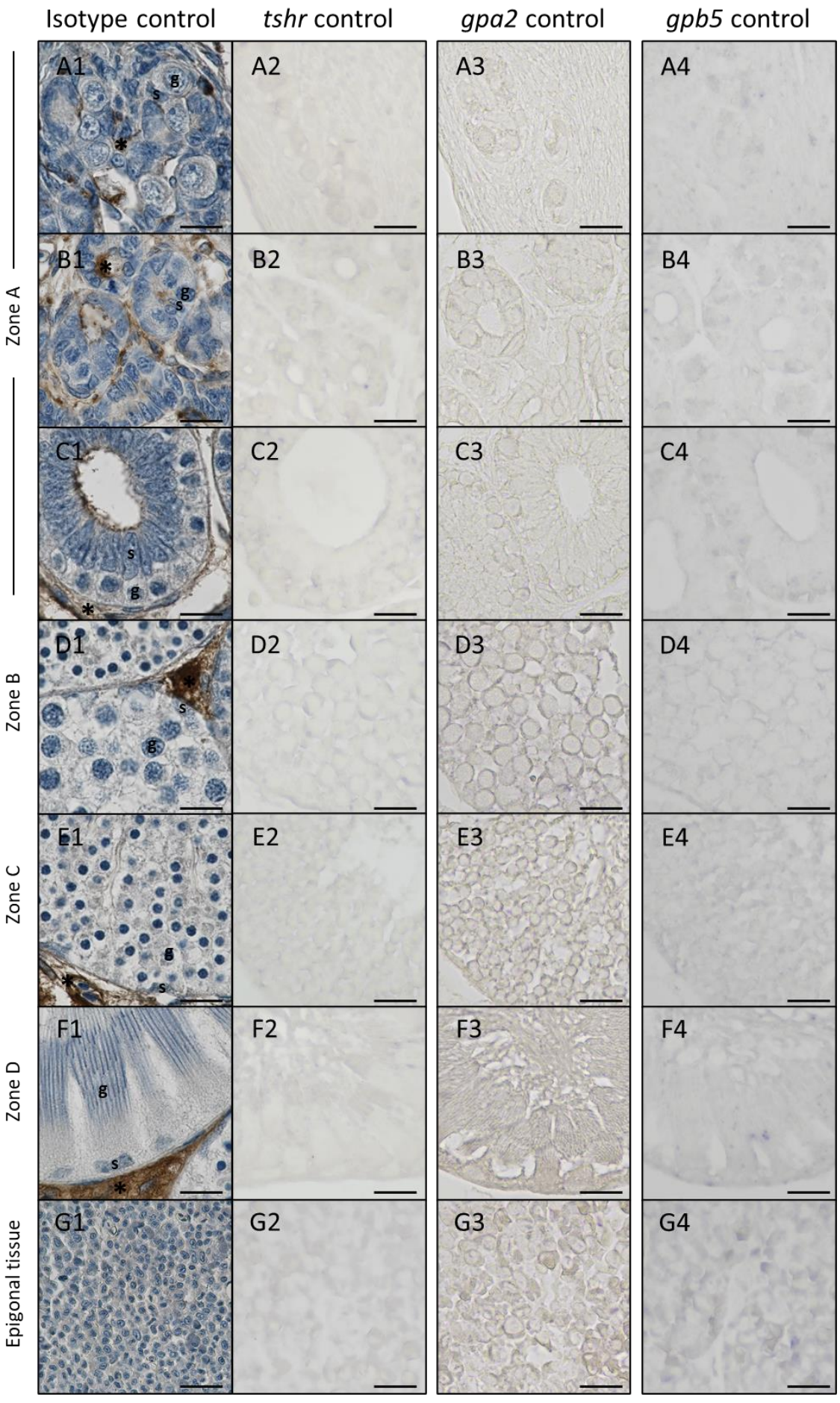
Isotype control
tshr control
gpa2 control
gpb5 control
Zone A
Zone B
Zone C
Zone D
Epigonal tissue
A1
A2
A3
A4
B1
B2
B3
B4
C1
C2
C3
C4
D1
D2
D3
D4
E1
E2
E3
E4
F1
F2
F3
F4
G1
G2
G3
G4
g
s
*

**Fig. S5.** (A1-G2) Immunohistochemistry controls were performed with using the rabbit IgG polyclonal isotype control (human) antibody (1:2000, Abcam, ab37415). Secondary antibodies were used at the indicated dilution: goat anti-rabbit IgG H&L, HRP polymer (1:1, Abcam, ab214880). *In situ* hybridization control was performed using sense riboprobes of *tshr* (A2-G2), *gpa2* (A3-G3) or *gpb5* (A4-G4). (A), germinative area; (B) cysts in formation; (C) cysts with spermatogonia; (D) cysts with spermatocytes; (E) cysts with young spermatids; (F) cysts with late spermatids and (G) epigonal tissu; g: germinal cell nuclei; s: sertolian precursor (A,B) or sertolian nuclei (C-F). Immunohistochemistry performed with the rabbit IgG polyclonal isotype control (human) antibody presented unspecific staining associated to the interstitial compartment (highlighted with an asterisk) (A1-G1). *In situ* hybridization controls revealed no important background noise (A2-G4). Scale bars: normalized at 10 µm.

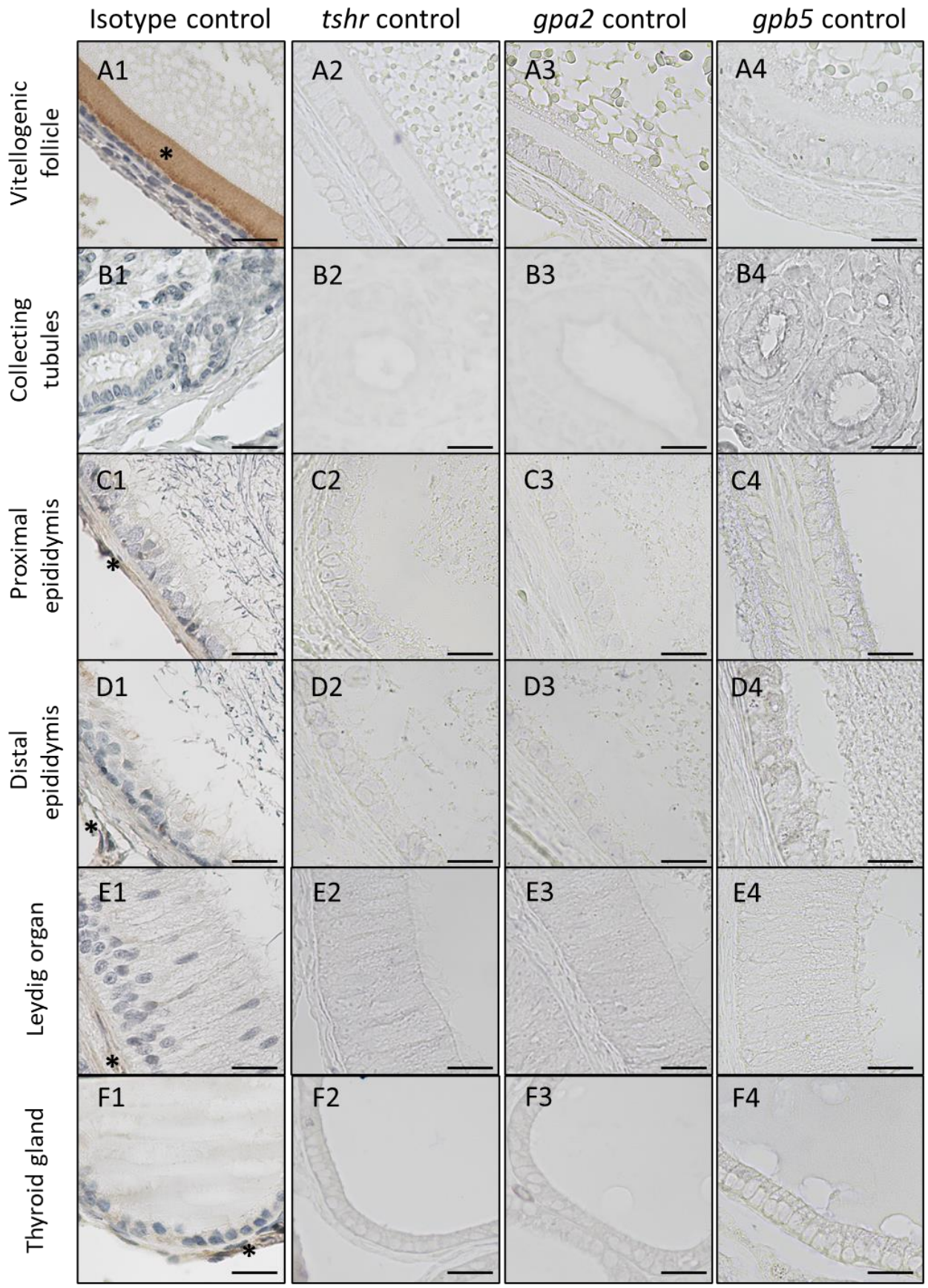
Isotype control
tshr control
gpa2 control
gpb5 control
Vitellogenic follicle
Collecting tubules
Proximal epididymis
Distal epididymis
Leydig organ
Thyroid gland
A1
A2
A3
A4
B1
B2
B3
B4
C1
C2
C3
C4
D1
D2
D3
D4
E1
E2
E3
E4
F1
F2
F3
F4

**Fig. S6**. *In situ* control in *S. canicula* vitellogenic follicle sections and other organs of the male genital tract. (A1-F1) Immunohistochemistry controls were performed using the rabbit IgG polyclonal isotype control (human) antibody (1:2000, Abcam, ab37415). Secondary antibodies were used at the indicated dilution: goat anti-rabbit IgG H&L, HRP polymer (1:1, Abcam, ab214880). *In situ* hybridization control was performed using sense riboprobes of *tshr* (A2-F2), *gpa2* (A3-F3) or *gpb5* (A4-F4). Immunohistochemistry performed with the rabbit IgG polyclonal isotype control (human) antibody presented unspecific staining only associated to the zona pellucida of the ovarian follicles (A1-F1). *In situ* controls revealed no important background noise. Tu: epithelium of stem and branched tubules. Scale bars: normalized at 10 µm.

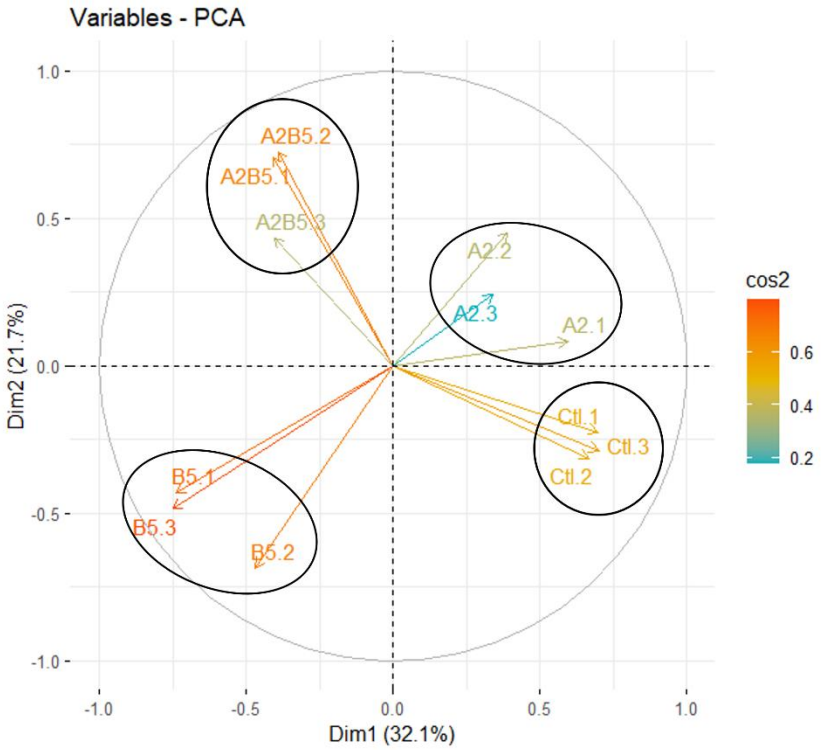


Fig. 1 **Contrôle de l'homogénéité des réplicats expérimentaux (N = 3)**. Seules les 500 protéines présentant les plus fortes modifications en abondance ont été analysées par analyse des composantes principales puis par *k-clustering*. Le gradient de couleur Cos2 indique les qualités de représentation des échantillons en considérant les deux dimensions sélectionnées pour la représentation. Les cercles noirs représentent les clusters obtenus pour les réplicats expérimentaux des explants de la zone D traités avec *Sc*GPA2 (A2), *Sc*GPB5 (B5) et *Sc*GPB5-*Sc*GPA2 (A2B5) et des contrôles (Ctl) non traités.

## II. Annexes chapitre III : Perspectives et analyses préliminaires

Sur la base des résultats précédents, montrant que la zone D pouvait être la plus sensible aux GPA2, GPB5 et GPB5-GPA2 du fait, notamment, d'une très forte expression de *gpb5* et de *tshr* au niveau de cette zone, une stimulation *in vitro* des explants correspondants avec des protéines recombinantes a été réalisée pendant 22 h.

Les concentrations molaires (1 concentration testée en triplicat) des protéines recombinantes *Sc*GPA2, *Sc*GPB5 et *Sc*GPB5-*Sc*GPA2 utilisées sont à déterminer (Dosage en spectrométrie de masse). Les protéomes des explants incubés ont été caractérisés par NanoLC-ESI-MS/MS.

Les explants de la zone testiculaire D de *S. canicula* ont été préparés d'une façon similaire à l'expérimentation *in silico* présentée dans le chapitre IV et les ligands *Sc*GPA2, *Sc*GPB5 et *Sc*GPB5-*Sc*GPA2 ont été produits comme présenté précédemment dans le chapitre III. Une analyse en composante partielle (ACP) suivit d'un *k-clustering* utilisant les 500 protéines présentant les plus fortes modifications de leurs abondances a mis en évidence une homogénéité des triplicats expérimentaux ainsi qu'une forte distinction des différentes conditions expérimentales (Fig. 1).

Un total de 7619 protéines a été identifié. Une approche préliminaire a été d'analyser en un seul groupe les protéines qui présentaient des abondances significativement différentes des contrôles en réponse à au moins un traitement, ce qui correspond à 933 protéines (Fig. 2A). Un *k-clustering* a mis en évidence quatre clusters de 39 (C1), 348 (C2), 467 (C3) et 79 (C4) protéines. Les variations des niveaux en protéines en fonction des quatre clusters et des traitements ont été représentées par une carte de chaleur. Pour estimer les variations globales des niveaux des protéines induites par les différents traitements, les log2ratios ont été moyennés par cluster et par traitement. Les clusters C1 et C4 sont apparus très sensibles aux traitements par *Sc*GPA2, *Sc*GPB5 et *Sc*GPB5-*Sc*GPA2, tandis que les clusters C2 et C3 sont apparus moins sensibles aux traitements. Par ailleurs, comme les concentrations molaires utilisées de *Sc*GPA2, *Sc*GPB5 et *Sc*GPB5-*Sc*GPA2 n'ont pas encore été caractérisées, les différences d'abondances en protéines entre les traitements ne peuvent être interprétées, par conséquent les analyses statistiques ont seulement été réalisées pour comparer la condition contrôle aux différentes conditions traitées. La base de données String

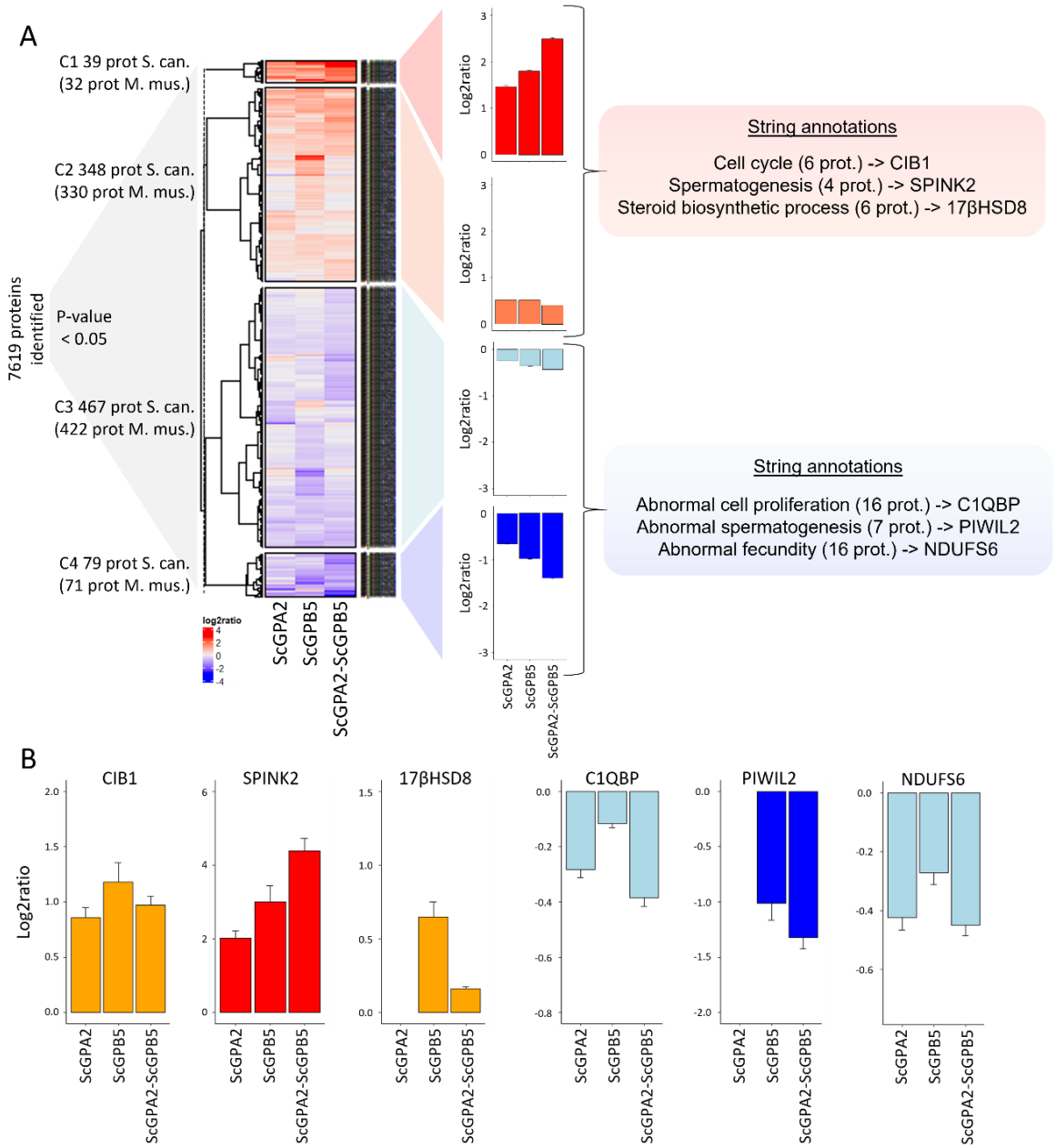


Fig. 2 **Analyse protéomique des explants de la zone testiculaire D de *S. canicula* stimulés par les protéines recombinantes *Sc*GPA2, *Sc*GPB5 ou *Sc*GPB5-*Sc*GPA2.** **A.** L'analyse protéomique a permis d'identifier 7619 protéines dont 933 différentiellement régulées dans au moins une condition stimulée, en comparaison avec le contrôle. L'analyse statistique a été réalisée à l'aide du test ANOVA avec une valeur P < 0,05. Le profil d'expression des 933 protéines différentiellement exprimées a été analysé par k-clustering (k=4) pour obtenir les clusters C1, C2, C3 et C4 comprenant respectivement 39, 348, 467 et 79 protéines et représentés par une carte de chaleur. Par la méthodologie blastp utilisant les protéines de *S. canicula*, 32, 330, 422 et 71 orthologues de *M. musculus* ont été associés aux clusters C1, C2, C3 et C4, respectivement. Ensuite, pour chaque condition stimulée et par groupe, les moyennes de toutes les abondances relatives des protéines associées ont été calculées. L'annotation fonctionnelle a été réalisée avec la base de données STRING (https://string-db.org) et 6 termes d'intérêts ont été illustrés. **B.** Profiles d'expression relatifs de 6 protéines impliquées dans les 6 termes précédemment identifiés et connues pour avoir un rôle crucial dans le bon déroulement de la spermatogenèse.

(https://string-db.org) a été utilisée pour annoter les clusters et 6 termes d'intérêts ont été mis en avant, ce qui a permis d'associer les termes « Cell cycle », « Spermatogenesis » et « Steroid biosynthetic process » aux clusters C1 et C2, et les termes « Abnormal cell proliferation », « Abnormal spermatogenesis » et « Abnormal fecundity » aux clusters C3 et C4. Ces résultats suggèrent que les traitements avec *Sc*GPA2, *Sc*GPB5 et *Sc*GPB5-*Sc*GPA2 favoriseraient la spermiogenèse, la stéroïdogenèse et la qualité des spermatides. À titre d'exemples pour les protéines présentant une augmentation : la protéine CIB1 (*calcium and integrin binding 1*), qui est associée au terme « Cell cycle », régule la prolifération et la survie cellulaire (Leisner et al., 2016) et l'invalidation de son gène *cib1* induit une stérilité chez la souris (Yuan et al., 2006) ; la protéine SPINK2 (*serine peptidase inhibitor, Kazal type 2*), qui est un inhibiteur de protéases ciblant notamment l'acrosine, est associée au terme «Spermatogenesis» et l'invalidation de son gène *spink2* induit une azoospermie chez la souris (Kherraf et al., 2017); la 17βHSD8 a été associée au terme « Steroid biosynthetic process » et pourrait avoir un rôle d'inactivateur de l'œstradiol au niveau des testicules d'homme et de souris en métabolisant l'œstradiol en estrone (Ohno et al., 2008).

À l'inverse, parmi les protéines présentant une diminution, la protéine C1QBP (*Complement C1q binding protein*), qui a été associée au terme « Abnormal cell proliferation », est l'une des protéines cibles de la kinase HASPIN et serait impliquée dans la réaction acrosomique (Maeda et al., 2022). De même, la protéine PIWIL2 (*Piwi-like RNA-mediated gene silencing 2*), qui a été associée au terme « Abnormal spermatogenesis», régule le traitement primaire des piARNs sens jusqu'aux stades des spermatocytes pachytènes et l'invalidation de son gène *Mili* induit une infertilité chez les souris (Bak et al., 2011). En dernier exemple, la protéine NDUFS6 (*NADH:ubiquinone oxidoreductase core subunit S6*) a été associée au terme « Abnormal fecundity » et elle compose le complexe I de la NADH déshydrogénase (ubiquinone) impliqué dans le transport d'électrons dans la chaîne respiratoire ; la diminution de son expression au niveau des spermatozoïdes de souris induit une altération du métabolisme, de la motilité et de la réaction acrosomique (Bae and Kwon, 2024).

Ces résultats préliminaires suggèrent que GPA2, GPB5 et GPB5-GPA2 sont des régulateurs des fonctions testiculaires chez *S. canicula* en condition *in vitro*, notamment en modulant la spermiogenèse et la stéroïdogenèse. Ces résultats soulignent également la nécessité d'étudier davantage l'importance de la thyrostimuline (GPA2/GPB5) dans la régulation de la

spermatogenèse et/ou dans le cadre des perturbations de la fertilité chez l'homme, sachant que son action paracrine a été mise en évidence au niveau de l'ovaire chez la femme (Sun et al., 2010).

# Chapitre IV

## Characterization of a direct endocrine role of GnRHs in testicular regulation in the small-spotted catshark *Scyliorhinus canicula*: a GnRH signaling in the control of spermiogenesis and steroidogenesis in early gnathostomes

**Fabian Jeanne, Stanislas Pilet, Benoît Bernay, Stéphanie Lagadu, Raphaël Delépée, Sylvie Dufour, and Pascal Sourdaine**

# Chapitre IV

## Characterization of a direct endocrine role of GnRHs in testicular regulation in the small-spotted catshark *Scyliorhinus canicula*: a GnRH signaling in the control of spermiogenesis and steroidogenesis in early gnathostomes

**Fabian Jeanne, Stanislas Pilet, Benoît Bernay, Stéphanie Lagadu, Raphaël Delépée, Sylvie Dufour and Pascal Sourdaine**

# Caractérisation d'un rôle endocrine direct des GnRHs dans la régulation testiculaire de la roussette *Scyliorhinus canicula* : une signalisation GnRH dans le contrôle de la spermiogenèse et de la stéroïdogenèse chez les premiers Gnathostomes.

Chez les Vertébrés, les gonadolibérines (GnRHs) hypothalamiques sont des régulateurs de la production des gonadotrophines adénohypophysaires qui contrôlent les gonades, et par conséquent la reproduction des organismes. Chez les Élasmobranches, les cellules gonadotropes sont localisées dans le lobe ventral hypophysaire et, en l'absence de système vasculaire porte et de projections axonales directes vers ce lobe, les GnRHs sont libérées directement dans la circulation systémique. Chez les requins, les GnRHs systémiques ont été dosées chez *Scyliorhinus canicula* et l'expression des ARNm des GnRHRs a été observée dans le testicule chez *Scyliorhinus torazame*. L'objectif de ce chapitre est d'explorer le rôle régulateur direct qu'exercerait les GnRHs systémiques dans la régulation de la spermatogenèse chez *Scyliorhinus canicula*.

Les séquences des précurseurs des GnRHs et des GnRHRs d'Élasmobranches ont été identifiées et validées par synténie avant l'analyse des profils d'expression des ARNm par RT-PCR et hybridation *in situ* (ISH), notamment au cours de la spermatogenèse. De plus, des explants testiculaires de *S. canicula* contenant les stades tardifs de la spermiogenèse ont été traités avec 0, 10 et 100 nM de *sc*GnRH2 ou de *sc*GnRH3 synthétiques. Les protéines différentiellement exprimées ont été identifiées par analyse protéomique en NanoLC-ESI-MS/MS à haute résolution. L'expression d'ARNm correspondant à des protéines différentiellement exprimées a ensuite été analysée par PCR en temps réel et hybridation *in situ*. Enfin, les milieux des explants traités ont fait l'objet d'un dosage de quinze stéroïdes, dont la progestérone, la testostérone, l'œstradiol et l'œstrone.

Les recherches de séquences ont permis d'identifier trois sous-familles de GnRHs et quatre sous-familles de GnRHRs chez plusieurs Élasmobranches. Chez *S. canicula*, l'expression des *gnrhs* apparait spécifique au cerveau, ce qui est cohérent avec la littérature, et permet d'écarter leur rôle paracrine au niveau testiculaire. Les quatre *gnrhrs* sont exprimés au niveau testiculaire avec cependant une expression spécifique du testicule de *gnrhrI1* et une expression plus élevée du *gnrhrIIb2*, par rapport aux autres formes, au niveau testiculaire. Les

ARNm *gnrhrI1* sont localisés dans les cellules somatiques associées aux spermatides dont les cellules de Sertoli et les cellules interstitielles. Les ARNm *gnrhrIIb2* sont quant à eux localisés plus largement, notamment dans les précurseurs somatiques de la zone germinative, les cellules germinales, et les cellules somatiques associées à la spermiogenèse dont les cellules de Sertoli et les cellules interstitielles. L'analyse des protéomes des explants testiculaires stimulés par les *sc*GnRHs ont montré une augmentation de l'abondance de dix-neuf protéines impliquées dans le métabolisme du cholestérol et des stéroïdes, dont plusieurs 17βHSD (17βHSD2, 17βHSD3, 17βHSD7 et 17βHSD12). Les niveaux des ARNm des *17ϐhsd3* et *17ϐhsd12* sont également augmentés en réponse aux GnRHs et ils sont localisés dans les cellules de Sertoli, renforçant le fait qu'elles sont les principales cellules stéroïdogènes testiculaires chez *S. canicula*. Ces résultats sont en accord avec une augmentation des niveaux d'œstrone (E1) et d'œstradiol (E2), ce qui serait cohérent avec les expressions des *17ϐhsd*. De plus, l'annotation par ontologie génétique des protéines régulées à la baisse a montré des termes liés à la transcription, à la modification de la structure de l'ADN et du cytosquelette. En conclusion, en utilisant une approche sans *a priori* basée sur des données -omiques, notre étude a montré que les GnRHs pourraient avoir un rôle direct dans la régulation testiculaire chez les Élasmobranches en stimulant la spermiogenèse et en modulant la stéroïdogenèse.

**Characterization of a direct endocrine role of GnRHs in testicular regulation in the small-spotted catshark *Scyliorhinus canicula*: a GnRH signaling in the control of spermiogenesis and steroidogenesis in early gnathostomes.**

Fabian Jeanne[1], Stanislas Pilet[1], Benoît Bernay[2], Stéphanie Lagadu[3], Raphaël Delépée[3], Sylvie Dufour[1] and Pascal Sourdaine*[1]

[1] Université de Caen Normandie, MNHN, SU, UA, CNRS, IRD, Laboratoire de Biologie des Organismes et Ecosystèmes Aquatiques (BOREA), UMR 8067, 14032 Caen cedex 5, France.

[2] Université de Caen Normandie - Plateforme PROTEOGEN, US EMerode, 14032 Caen cedex 5, France.

[3] INSERM U1086 "ANTICIPE" Unité de Recherche Interdisciplinaire pour la Prévention et le Traitement des Cancers, Centre de Lutte Contre le Cancer Francois Baclesse, 3 Av. Général Harris, 14076 CAEN cedex 05, France.

*Corresponding Author: orcid.org/0000-0001-9811-2876; Email: pascal.sourdaine@unicaen.fr

**Abstract**

Gonadotropin-releasing hormones (GnRH) are hypothalamic regulators of vertebrate reproduction. They regulate the production of gonadotropins by the gonadotropic cells of the pituitary, which control gonad functions. In elasmobranchs, gonadotropic cells are located in the ventral lobe of the pituitary. However, differently from other gnastostomes, in absence of portal vessels and direct axonal projection, GnRHs are released into the systemic circulation. This study aimed at exploring the potential role of systemic GnRH on the regulation of the testis in an elasmobranch, the small-spotted catshark, *Scyliorhinus canicula.* Phylogenic and synteny analyses of *gnrh* and *gnrhr* genes in several elasmobranchs were carried out, identifying three GnRHs and four GnRHRs subfamilies. Their expression profiles were then

analyzed by Real Time quantitative-PCR in a large range of tissues, including male and female genital tractus. In *S. canicula*, the three *gnrh* were expressed in the nervous central system with the *gnrh2* also expressed in the thyroid and the lymphomyeloid Leydig organ. The expression profiles of *gnrhr* genes varied according to tissues: *gnrhrI1 was* testis-specific; *gnrhrIIb2* was ubiquitously expressed and was the most highly expressed *gnrhr* in the testis; *gnrhrIIa1 was expressed in brain* and *gnrhrIIa2* was expressed in brain, male genital tract and oviduct. *In situ* hybridization analyses showed that *gnrhrI1* transcripts were localized in Sertoli cells of cysts containing spermatids and in interstitial cells surrounding these cysts. *GnrhrIIb2* mRNAs were localized more largely, in somatic precursors of the germinative area, germ cells, Sertoli cells at all stages of spermatogenesis and in interstitial cells associated with spermiogenesis stages. Based on these results, testicular explants at stages of spermiogenesis were treated with *Sc*GnRH2 or *Sc*GnRH3 and tissular proteins analyzed by high-resolution NanoLC-ESI-MS/MS. In response to GnRHs, 1677 proteins were significantly differentially expressed with, notably, increased levels of the growth hormone receptor (GHR) and of nineteen proteins involved in cholesterol and steroid metabolism, including, among others, 17βHSD2, 17βHSD3, 17βHSD7 and 17βHSD12. *In situ* hybridization analyses showed that *17ϐhsd3*, *17ϐhsd12* and *ghr* transcripts were localized in Sertoli cells, which are the main testicular steroidogenic cells in *S. canicula*. Finally, the media of treated explants were assayed for fifteen different steroids, using mass spectrometry analysis. The results showed an increase in estrone and 17β-oestradiol levels which would be consistent with *17ϐhsd* expressions. Furthermore, gene ontology annotation of down-regulated proteins in response to GnRHs showed terms related to transcription and modification of DNA structure. In conclusion, using an *a priori*-free approach based on omics data, our study showed that *Sc*GnRH could have a direct role in testicular regulation in elasmobranchs by promoting spermiogenesis and modulating steroidogenesis.

Key words: GnRH, GnRH receptors, Spermatogenesis, Steroidogenesis, Chondrichthyes, Elasmobranchs, Shark, Evolution, Testis.

## Introduction

Gonadotropin-releasing hormones (GnRH) are highly conserved neuropeptides and, at least, three major types of GnRH decapeptides have been identified in vertebrates on the basis of their localization and phylogenetic analyses. Globally, the *gnrh1* gene, conserved in all gnathostomes with the exception of some teleosts as the zebrafish or the medaka, is expressed in the diencephalon, the *gnrh2* gene, conserved in all vertebrates, is expressed in the mesencephalon and the *gnrh3* gene, lost in tetrapods, some teleosts such as the anguilla and in the holocephalan *Callorhinchus milii*, is expressed in the telencephalon and diencephalon (Dufour et al., 2020; Gaillard et al., 2018; Hara et al., 2018; Kanda, 2019; Ogawa et al., 2022). In lamprey, three members of the GnRH family have been identified with the lGnRH-I (ortologous to gnathostome GnRH2) and the two cyclostome paralogs lGnRH-II and lGnRH-III (co-orthologous to gnathostome GnRh3) (Gaillard et al., 2018). In chondrichthyes (chimeras, rays and sharks), the holocephalan *C. milii* has the *gnrh2* and two paralogs of *gnrh1* (*gnrh1a* and *gnrh1b*), while *gnrh1*, *gnrh2* and *gnrh3* have been found in elasmobranchs (Gaillard et al., 2018; Roch et al., 2014). In vertebrates, GnRH1 synthesized by hypothalamic neurons plays a central role in the control of reproduction through the hypothalamic-pituitary-gonadal (HPG) axis. In mammals, GnRH1 is released into the hypophyseal portal system, which limits its diffusion to the pituitary only, where it regulates the production of the luteinizing hormone (LH) and the follicle-stimulating hormone (FSH). In teleosts, GnRH neurons directly project to the pituitary and GnRH1 is the main hypophysiotropic peptide, except in some fishes such as the zebrafish where this role is assumed by GnRH3 (Abraham et al., 2010; Spicer et al., 2016). Several neuromodulators are also involved in the control of GnRH and gonadotropins, including the gonadotropin-inhibiting hormone (GnIH), a RF-amide peptide first identified in the quail (Tsutsui and Ubuka, 2021) and having an inhibitory role on GnRH neurons and a direct inhibitory role on gonadotropic cells (For review: Dufour et al., 2020). In Elasmobranchs, a particularity is the ventral lobe of the pars distalis (VPD), at the base of pituitary, which is the main site expressing genes encoding glycoprotein hormone subunits (Hara et al., 2018). The absence of a portal vessel and of a direct axonal pathway toward the VPD, together with the presence of GnRH in the blood at physiological concentrations, led to the hypothesis that gonadotropic cells were regulated via the systemic circulation (D'antonio et al., 1995; Knowles

et al., 1975; Sherwood and Lovejoy, 1993). Presently, GnIH has not been identified in Chondrichthyes.

GnRH functions are mediated by GnRH receptors (GnRHR), which derived from an ancestral *gnrhr* gene that gave rise to six GnRHR types in vertebrates as a result of local gene duplications, whole genome duplications and multiple gene losses. Evolutionarily retained GnRHR types have been classified into two groups, GnRHR type-I and type-II, with six subfamilies (types-I1, -IIb2, -IIb3, -IIa1, -IIa2 and -IIa3). Subsequently, further gene losses occurred in different vertebrate lineages, leading to the retention of one functional *GNRHR* gene in humans, five in coelacanths, two in *C. milii* and four in the elasmobranch *Scyliorhinus torazame*, as examples (Hara et al., 2018; Ogawa et al., 2022). All three types of GnRH are generally able of activating all GnRH receptors, sometimes with preferential ligand-receptor selectivity (Flanagan et al., 2007; Li et al., 2022; Roch et al., 2011; Tello et al., 2008; Wang et al., 2003). GnRHRs are expressed in different parts of the brain and by gonadotropic cells in tetrapods (Bjelobaba et al., 2016; Janjic et al., 2019; Miao et al., 2024; Schang et al., 2011; Wang et al., 2001), teleost fishes (Ciani et al., 2020; Levavi-Sivan and Avitan, 2005) and elasmobranchs (Hara et al., 2018). In addition, GnRHRs, with GnRHs, are also expressed in peripheral tissues such as the testis in several species (Chianese et al., 2012; Ciaramella et al., 2015; Fallah et al., 2020), where they may be involved in paracrine regulations. For example, GnRH *in vitro* treatments have been shown to mediate testosterone secretion in the boar (Desaulniers et al., 2015) and increase the number of undifferentiated spermatogonia and spermatozoa in an *ex vivo* zebrafish testis culture system (Fallah et al., 2020). In addition, GnRH signaling pathway was found in the Sertoli cells of the black rockfish *Sebastes schlegelii*, highlighting its importance in maintaining spermatogenesis (Jin et al., 2024). In elasmobranchs, previous studies showed that *in vitro* treatment with GnRH stimulated ovarian steroidogenesis in the little skate (Callard et al., 1993), but no data were yet available for spermatogenesis. Moreover, the functional significance of the various GnRHs and GnRHRs in elasmobranchs and their roles on the gonads remain to be analyzed. Given the key phylogenetic position of chondrichthyes, this would contribute to understanding the evolutionary innovations of the endocrine and paracrine systems that characterize jawed vertebrates (Santiago-Andres et al., 2021; Venkatesh et al., 2014).

As *Scyliorhinus canicula* has been catalogued as "Least Concern" on the IUCN Red List, this species represents a useful and relevant model for studying physiological functions, including reproduction, in order to develop breeding programs for the conservation of threatened elasmobranchs (García-Salinas et al., 2021; Muñoz-Baquero et al., 2021). In addition to their phylogenetic position of interest, elasmobranchs exhibit several features in their male genital tract: the polarized and cystic organization of testes, allowing gene and protein expression analyses during spermatogenesis (Bosseboeuf et al., 2014; Gribouval et al., 2018; Jeanne et al., 2023); the Sertoli cells are the main testicular steroidogenic cells in *S. canicula* and other sharks (Loir et al., 1995); the presence of an epigonal lymphomyeloid tissue (Manca et al., 2019); and a complex male genital tract, including epididymis (Jones et al., 1984).

In order to explore the potential direct role of circulating GnRH on testis, the GnRHs and GnRHRs protein sequences were identified from several elasmobranchs and annotated using synteny. Their expression profiles were explored by real-time PCR and *in situ* hybridization, during spermatogenesis and in different tissues. In addition, *in vitro* functional assays were carried out on *S. canicula* testicular explants containing spermiogenesis stages treated with 0, 10 or 100 nM of *Sc*GnRH2 or *Sc*GnRH3. Differentiated expressed proteins were then identified by proteome analysis using high-resolution NanoLC-ESI-MS/MS before being completed by RT-PCR and *in situ* hybridization analyses targeting the key regulators identified. Furthermore, media from GnRH-treated testicular explants were assayed for several steroids using LC-ESI-HRMS/MS profiling. In the present study we also investigated GnIH, using genome search and synteny analyses, and our results supported the loss of GnIH in chondrichtyans.

## Materials and Methods

### *Animals and tissue Sampling*

In 2020, the catshark *Scyliorhinus canicula* was assessed as a least concern species in the red list of threatened species by the IUCN (International Union for Conservation of Nature). Adult male (608 ± 137 g; 58± 3 cm) and female (647 ± 90 g; 57 ± 4 cm) catsharks were fished during a CGFS (Channel Ground Fish Survey) campaign by IFREMER in the East Manche in September 2022 (Giraldo et al., 2022). Animals were maintained in natural seawater tanks at the marine station of the University of Caen Normandy (*Centre de Recherches en Environnement Côtier*

(CREC), Luc-sur-Mer, France). The CREC experimental facilities were approved by the council department of population care under the A14384001 number (*Préfecture du Calvados*, France). Catsharks were allowed to acclimate at least 2 weeks before collection of the samples. Animals were killed by percussive blow to the head followed by sectioning and pithing of the spinal cord and exsanguination according to the European directive 2010/63/UE for care and use of animals. Sampled tissues were transferred directly into liquid nitrogen before being stored at -80°C until RNA extractions. Fresh testicular cross sections were transferred into ice-cold Gautron's buffer (pH 7.8, 890 mosmol $kg^{-1}$) (Gautron, 1978) completed by 58 mM trimethylamine-N-oxide (TMAO, Sigma, 317594), then microdissected into the zone of undifferentiated spermatogonia and cysts with spermatogonia (zone A), the zone of cysts with spermatocytes (zone B), the zone of cysts with early spermatids (zone C) and the zone of cysts with late spermatids (zone D) (Loir and Sourdaine, 1994). Tissues used for *in situ* hybridization (ISH) were fixed in Gautron's buffer with paraformaldehyde 4% before alcoholic dehydration and stocked in butan-1-ol at -20°C.

*Sequence searches*

Protein sequences of GnRH1, 2, 3 and GnRHR type I1, IIa1, IIa2 and IIb2 were identified using Blast searches, based on multiple vertebrate sequences, against genomes of *A. radiata* (sAmbRad1.1.pri), *C. carcharias* (Marra et al., 2019), *C. plagiosum* (ASM401019v1), *C. punctatum* (Hara et al., 2018), *P. pectinata* (sPriPec2.1.pri), *R. typus* (Read et al., 2017), *S. canicula* (sScyCan1.2) and *S. torazame* (Hara et al., 2018) on NCBI (https://www.ncbi.nlm.nih.gov/genome/); of *H. akajei* (sHemAka1.1) on Squalomix Blast Server (https://transcriptome.riken.jp/squalomix/blast/); and of *L. erinacea* (Wang et al., 2012) on Skatebase (http://skatebase.org). To verify the relationship between obtained sequences and their putative families, chordate trees were built based on the previous work of Williams et al., 2014 and Gaillard et al., 2018 using the MAFFT (Multiple Alignment using Fast Fourier Transform) program, BMGE (Block Mapping and Gathering with Entropy) alignment curation and PhylML tree inference on NGPhylogeny online services (https://ngphylogeny.fr/workflows/oneclick/, Lemoine et al., 2019) with a bootstrap of 1000. Obtained trees were finalized using iTOL online tool (https://itol.embl.de/, Letunic and Bork, 2021).

To validate the annotation of GnRHR genes identified and the absence of the GnIH in chondrichthyan genomes, conserved synteny analyses of gnathostome genomic regions were performed in *A. radiata*, *S. canicula* and *C. carcharias* genomes. Species occupying key phylogenetic positions were selected, including the actinopterygian *L. oculatus*, the sarcopterygians *L. chalumnae*, *X. laevis* and *H. sapiens*. Genomic regions of the chondrichthyan *C. milii* were selected as template. The genes were mapped using NCBI's Genome Data Viewer (https://www.ncbi.nlm.nih.gov/genome/gdv/) and, for unretrieved genes, tBlastn using orthologous protein sequences were performed.

*Reverse Transcription and real-time PCR*

Total RNAs were extracted from *S. canicula* tissues using Tri-Reagent (Sigma-Aldrich, 93289) before purification with the NucleoSpin RNAII columns kit (Machery-Nagel). They were quantified on a NanoDrop™ 2000 (Thermo Scientific) and their qualities were analysed on an Agilent 2100 Bioanalyzer (Agilent). Obtained RINs (RNA integrity number) were greater than 7. For tissue distribution, real-time PCR was performed independently for three animals (N=3) in triplicate (n=3) except for testes (zone A, B, C and D) and epigonal tissues where six animals were used (N=6, n=18). The CFX Connect Detection System (Bio-Rad) was used for real-time PCR analysis. Two hundred and seventy ng of total RNAs were treated with 1U of RQ1 Dnase (Promega, M6101) (37°C/20min) following by the reverse transcription using 1 ng random hexanucleotide primers (Promega, C1181), 0.5 mM dNTPs and 200 U of M-MLV Reverse Transcriptase (Promega, M1701) then the reactions were stopped (70°C/5min). The gene specific primers were designed using Primer-BLAST (https://www.ncbi.nlm.nih.gov/tools/primer-blast/, Ye et al., 2012) with manual corrections according to the following criteria: length between 18-22 bp, GC content over 50%, Tm close to 60°C and generation of an 150-200 bp amplicon (Supplementary Table S1). The real-time PCR (5 ng of cDNA, 40 cycles: 95°C/15s, 60°C/45s) was done with the GoTaq®qPCR Master Mix (Promega, A6001) was used. Melt curve analysis and efficiency tests were carried out to ensure the primers amplified a single product with 90-110% efficiency. The Ct values were read at 200 relative fluorescence units and normalized against the 5S RNA gene (Redon et al., 2010) using the $\Delta C_t$ method (Schefe et al., 2006). Comparison of the Ct 5SRNA/total RNA ratio between tissues shown no significant difference using none parametric Kruskal-Wallis test with a P-value of 0.24 (Supplementary data Fig. S1). The $2^{-\Delta\Delta Ct}$ method (Livak and Schmittgen,

2001) allowed to calculated the expression variations based on the mean $\Delta C_t$ of all tissues. Statistical analyses were performed using non-parametric Mann-Whitney U (based on the previous Shapiro-wilk test results) test for P-value < 0.05.

*In situ hybridization*

Digoxigenin-conjugated riboprobes were synthesized from synthetic cDNA (Twist Bioscience) with specific primers (Supplementary Table S1). Obtained amplicons were cloned in pCR™II-TOPO™ Vector by TA cloning and then transformed in chemically competent *E. coli* using the TOPO TA Cloning kit (Invitrogen, k461020). After cultures, plasmids were purified using the Wizard® Plus SV Minipreps (Promega, A1340) then the digoxigenin-conjugated riboprobes were generated using M13 PCR on 100 ng of plasmids with 1 mM $MgCl_2$, 0.2 mM of each dNTPs, 0.4 µM M13 primer and 0.625 U GoTaq® Flexi DNA Polymerase (Promega, M8291). The cycling parameters were as follows: 1X(95°C, 5min), 30X[(95°C, 30s), (60°C, 45s), (72°C, 1min30s)], 1X(72°C, 5min). PCR products were quantified using Nanodrop 2000 spectrophotometer (Thermo Scientific) and then purified using the NucleoSpin RNA Clean-up (Marcherey-Nagel, 740948.50). The size checking was done using gel migration. *In vitro* transcriptions were carried out for 3 h at 37°C on 1.2 µg PCR products with 25 U RNAsin, 25 U T7 or SP6 polymerase, 10 mM dithiothreitol, 1 mM rATP, rCTP and rGTP, 0.65 rUTP, and 0.35 digoxigenin-UTP (Roche, 03359247910) using the Riboprobe® Combination Systems (Promega, P1460). DNAs were digested with 2 U RQ1 DNAse (Promega, M6101) for 30 min at 37°C. Obtained riboprobes were purified and their qualities were checked by Dot Blots on PVDF membrane. Paraffin slices (7 µm) were incubated at 61°C before deparaffinization using Roti-histol (sigma, 6640.6). Hydration was done into successive ethanol baths (100%, 95% and 70%), then into PBS. Between each of the following treatments, slices were washed into PBS. Slices were treated with PFA 4% in PBS, with 5 µg/ml proteinase k in Tris buffer for 4 min, with PFA 4% in PBS, with 100 mM Triethanolamine in 25 % acetic acid, then with 100 mM glycine in tris buffer. Tissues were incubated for 1 h at 65°C with the hybridization mix (50% Deionised formamide, 1X Saline-sodium citrate (SSC), 0.5 M Ethylenediaminetetraacetic acid (EDTA), 10% Tween 20, 1X Denhardt'solution, 28 mg/ml Dextran sulphate, 0.1 mg/ml heparin, 10% Chaps, 0.5 mg/ml tRNA). Then, 0.1-0.5 ng/µl riboprobes in hybridization mix were incubated overnight at 65°C. Slices were washed using successive baths of SSC (1X and 1.5X at 65°C, 2X at 37°C, 2X with 0.2 µg/ml of RNAse A (Promega, A797C) at 37°C, 2X, and 0.2X at 60°C) before

maleic acid buffer baths with 0.3 % triton (MABT). For immunostaining and revelation, the DIG Nucleic Acid Detection kit (Roche, 11175041910) was used. Tissues were incubated 3 h in blocking solution then, overnight at 4°C, with 100 µl per slice of 1/2000 v/v anti-digoxigenin-AP-conjugate antibody 750 U/ml. According to the kit guidelines, slides were washed in MABT baths before being developed 24 h at 4°C in NBT/BCIP according to the kit guidelines. Finally, slides were mounted in Mowiol mounting medium and then dried for 48 h at 4°C, before being observed using a Nikon eclipse 80i microscope.

*Primary culture of explants from zone D of* S. canicula *testis.*

After they were decapsulated, testes of four *Scyliorhinus canicula* were cut into 2-mm slices. Then, the zone D was taken from each slice and pooled in Gautron buffer (pH 7.8, 890 mosmol kg-1) (Gautron, 1978) completed by 58 mM trimethylamine-N-oxide (TMAO, Sigma, 317594), 60 mg/ml penicillin, 100 mg-ml streptomycin and 250 µg/ml amphotericin. Areas were then cut in 1 $mm^3$ explants and regroup by 10 in L-15, 20 mM Hepes, 0.5% bovin serum albumin, 1% FBS, 0.25% heat-decomplemented *S. canicula* serum, 4.6 mM D(+) glucose, 280 mM NaCl, 330 mM urea, 58 mM TMAO, 60 mg/ml penicillin, 100 mg-ml streptomycin and 250 µg/ml amphotericin. Treatments with 0, 10 or 100 nM of synthetic ScGnRH2 (pGlu-HWSHGWYPG-amide) or ScGnRH3 (pGlu-HWSHGWLPG-amide) (Proteogenix) were performed independently for four groups of explants (n=4). After an incubation of 24 h at 17°C, explants and media were independently collected and stored at -80°C. RNAs extraction, reverse transcription and real-time PCR of explants were performed as presented above, tissue proteins and media steroids were analyzed as describe below.

*Protein extraction*

Protein extraction was performed on zone D explants treated with *Sc*GnRHs, from the independent quadruplicate for each condition. Frozen tissues were crushed using the T 25 digital Ultra-Turrax®, extracted with 2.5 volumes of ice-cold lysis buffer (Urea 6M, Thiourea 2M, Tris-Base 40mM, CHAPS 2%, EDTA 1 mM, DTT 0.5 mM, AEBSF 1 mM and E64 10 µM protease inhibitors), then sonicated and stayed 1 h on ice before being centrifuged at 15000 g for 30 min at 4 °C. Supernatants were then ultracentrifuged at 105000 g for 1 h at 4 °C. Protein concentration of resulting supernatants was determined using the bicinchoninic acid protein assay (Sigma-Aldrich, Merck, France).

*NanoLC-ESI-MS/MS analysis*

From each sample, 5 µg of proteins were prepared using a modified GASP protocol (Gel-aided sample preparation with a gel plug cut into two pieces only) (Fischer and Kessler, 2015) before an overnight hydrolysis at 37°C with a mix solution of trypsin/lysine-C (400 ng per sample; V5073 Promega). Resulting peptides samples were first desalted and concentrated onto a C18 microcolumn (Omix C18 10 µl, Agilent) then fractionated onto a NanoElute ultrahigh-pressure nanoflow chromatography system (nanoLC, Bruker Daltonics) with a C18 pepmap 100 (5 mm x 300 µm i.d.) precolumn (Thermo Scientific) and separated at 50°C onto a reversed phase Reprosil column (25 cm x 75 µm i.d.) packed with 1.6 µm C18 coated porous silica beads (Ionopticks). The mobile phases consisted of 0.1% formic acid in water (solvent A) and 0.1% formic acid in acetonitrile (solvent B). The nanoflow rate was set at 250 nL/min with a gradient profile from 2% to 30% solvent B within 70 min, then an increase to 37% solvent B within 5 min, followed by a 85% solvent B washing step before reequilibration. MS experiments were carried out on an TIMS-TOF pro mass spectrometer (Bruker Daltonics) with a modified nano electrospray ion source (CaptiveSpray, Bruker Daltonics). A 1400 spray voltage with a capillary temperature of 180°C was typically employed for ionizing. MS spectra were acquired in the positive mode in the mass range from 100 to 1700 m/z and 0.60 to 1.60 1/k0 window. In the experiments described here, the mass spectrometer was operated in PASEF DIA mode with exclusion of single charged peptides. The DIA acquisition scheme consisted of 16 variable windows ranging from 400 to 1200 m/z.

*Database Searching*

Database searching and LFQ quantification (using XIC) was performed using DIA-NN (version 1.8.2) (https://www.nature.com/articles/s41592-019-0638-x). An updated UniProt *Crassostrea gigas* database was used for library-free search / library generation. For RT prediction and extraction mass accuracy, we used the default parameter 0.0, which means DIA-NN performed automatic mass and RT correction. Top six fragments (ranked by their library intensities) were used for peptide identification and quantification. The variable modifications allowed were as follows: Nterm-acetylation and Oxidation (M). In addition, C-Propionoamide was set as fix modification. “Trypsin/P” was selected. Data were filtering according to a false discovery rate (FDR) of 1% at the peptide level. Cross-run normalization

was performed using RT-dependent. From database search results, 7379 protein accession numbers were retrieved in all replicates of all conditions.

*Bioinformatics and Functional Annotation*

Based on the previous work of Jeanne et al., 2023 and still due to the limited number of correctly-annotated proteins (50 774 sequences, as of 01/2024), the limited number of gene ontologies (4 137 annotations, as of 01/2024) and the absence of kegg pathways in *S. canicula*, identified proteins were blasted against *Mus musculus* proteome (Proteome ID: UP000000589), uploaded from Uniprot (https://www.uniprot.org/), due to the richness of available databases (54 822 sequences for proteome, 1 130 838 GO annotations with 62 773 annotations validated by mutant phenotypes and 353 kegg pathways; as of 01/2024). BLASTp were carried out using the Galaxy web resource (https://usegalaxy.org/) with hits filtering proteins showing more than 40% of identity and coverage, and e-value below $1e^{-05}$. For each catshark protein, hits with lowest e-value and higher percentage of identity were retained.

To quantify the relative levels of protein abundance between different groups, datas from DIA-NN were then analyzed using DEP package from R. Briefly, proteins that are identified in 2 out of 3 replicates of at least one condition were filtered, missing data were imputed from PERSEUS using a normal distribution and differential enrichment analysis was based on linear models and empirical Bayes statistic. A 1.2-fold increase in relative abundance and a 0.05 P-value were used to determine enriched proteins. ANOVA were performed from PERSEUS to determine those enriched proteins. A 0.05 P-value was used.

The quantification values of the 7379 proteins identified were converted into log2ratio (abundance values of proteins in a sample divided by the mean abundance value of the control corresponding to 0 nM *Sc*GnRH). The protein abundances of the quadruplicates were then averaged by condition. Finally, 1677 proteins had abundances significantly different from the control (0 nM *Sc*GnRH), in at least one condition (10 nM *Sc*GnRH2, 100 nM *Sc*GnRH2, 10 nM *Sc*GnRH3 and 100 nM *Sc*GnRH3), and were treated by k-mean clustering to obtained 4 clusters representative of the proteins with the most important increase in abundance (cluster 1) or decrease (cluster 4) and with low increase (cluster 2) or decrease (cluster 3) in abundance. Each cluster contains 231, 248, 537 or 661 proteins, respectively, and their corresponding abundances were represented using the Heatmap package (Gu et al., 2016). All protein abundances for each group and condition were averaged. Functional annotation was

performed by gene ontology (GO) supplemented by the reactome pathway and wiki pathway databases and using Cluego, a Cytoscape plug-in (https://apps.cytoscape.org/apps/cluego), for mouse homolog accessions of clusters 1 and 4 (Bindea et al., 2009). The following parameters were applied: GO tree between 3 and 8; cluster with a minimum of 3 accessions associated by term; genes association higher than 4%; Term P-value corrected with Bonferroni step down < 0.05; GO Term fusion parameter selected. Corrected P-value were converted into -log2(P-value) and the 5 most interesting terms, according to the literature, were kept.

*Steroids analyses*

Stock solutions of separate steroids and analog stable isotopes were prepared in methanol at a concentration of 1 g/L. A mixture of the unlabeled steroids stock solutions was prepared in water achieving final concentration of 10 mg/L for each steroid corresponding to the higher concentration working solution. This solution was diluted in water to prepare 12 other working solutions at 0.5-1-2.5-5-10-25-50-100-250-500-1000-5000 µg/L. A steroids internal standard (IS) working solution was prepared in water at a final concentration of 5 mg/L for each steroid. All stock and working solutions were stored at −80 °C until further use. QC's at four different concentrations were prepared by addition of steroids to medium of treated explant at reach the concentration corresponding to the limit of quantification (LOQ), 2 times the LOQ, the middle of the linearity range and 80% of the highest standard concentration.

The medium of treated explant (250 µL) was mixed with 5 µL of steroids IS at 5mg/L and 10 µL of 125 mM tetrabutyl ammonium aqueous solutions prior to the application to the supported liquid extraction (SLE). Concerning calibrators, 5µL of unlabeled of steroids working solutions was added to reach concentrations of 0.01-0.02-0.05-0.1-0.2-0.5-1-2-5-10-20-100 and 200 µg/L. SLE 96-well plate 400 µL (Biotage) was selected to proceed with the sample and standard extraction procedure. The combined standards solutions were loaded onto the SLE sorbent and were allowed to flow through the sorbent under monitored positive pressure of 20 psi using Waters Positive Pressure-96 Processor manifold (Waters) to facilitate the flow of the sample, meanwhile achieving proper contact time with the sorbent (5 min between each step). After the complete drainage of the sample or standard from SLE, elution of the analytes was performed with 2 x 500 µL ethyl acetate. The eluates were dried at 30°C using nitrogen then reconstituted with 50 µL of methanol by sonication and centrifugated for 5 min at 16900 g before injection.

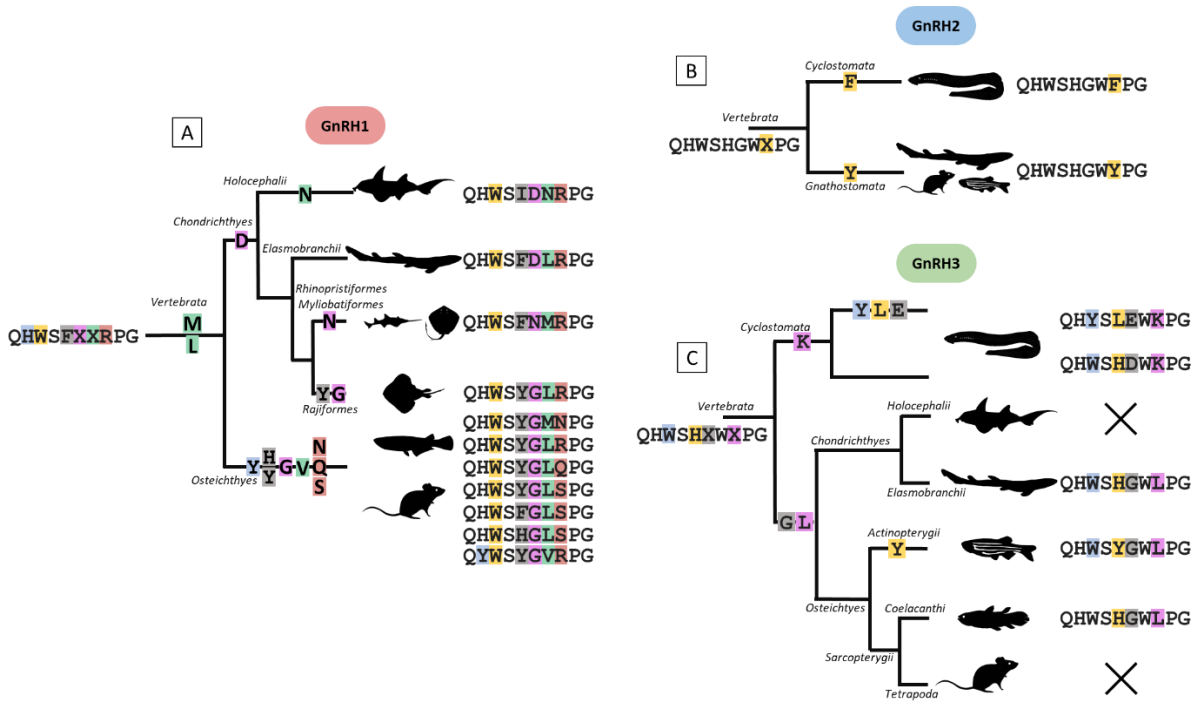


**Fig. 1.** A schematic diagram showing the evolution model of GnRHs orthologs. A. GnRH1 evolved extensively along vertebrate evolution, giving rise to at least 10 orthologs, including 3 specifics to holocephali, selachii and batoidea, respectively. B. GnRH2 was highly conserved with two orthologs, one unique to cyclostomata and a second conserved in all gnathostomata. C. GnRH3 evolution gave rise to two orthologs specific to cyclostomata, one ortholog specific to Actinopterygii, and one common to chondrichthyes and coelacanthi, while GnRH3 was lost in tetrapoda. Animal illustrations are used with permission from http://phylopic.org.

LC-HRMS analyses were carried out on a ExionLC Binary UHPLC system (Sciex) connected with a X500R QTOF mass spectrometer Sciex (Singapore) equipped with an ESI source in both positive and negative modes. Chromatographic separation was achieved by injecting 5 µL sample extract on a Kinetex 1.7 µm Biphenyl, LC column 100 × 1 mm Phenomenex (Torrance).

Mobile phase A consisted of 20 µM ammonium fluoride dissolved in water and mobile phase B consisted of 20 µM ammonium fluoride dissolved in methanol. The flow rate remained constant at 0.1 mL $min^{-1}$, column temperature was maintained at 40°C and the autosampler at 10°C. Mobile phase gradient for steroids analyses was as follows: 0–5.0 min linear gradient from 43% B to 85% B; 5.0–5.3 min linear gradient from 85% B to 100% B; 5.3–7.5 min isocratic at 100% B. Then the mobile phase composition was set to the initial conditions and the column was equilibrated for 3 min. The media of treated explants samples were analyzed using multiple reaction monitoring (MRM) acquisition in positive or negative ESI modes, depending of the steroids, at a resolution of 30000 (at *m/z* 200). The scan was obtained from m/z100 to m/z=1000 and accumulation time was set to 0.25s. ESI source and gas parameters were as follows: ion source gas 1: 35 psi, ion source gas 3: 70 psi, curtain gas: 40 psi, CAD gas: 9 and temperature: 500 °C. The spray voltage was set to +5500V and -4500V in positive and negative mode, respectively. Two MRM transitions were used for each steroid. The first one (quantifier), with the best signal to noise ratio was used for quantification, and the second (qualifier) was used for the confirmation. The precursor MRM ion was the mass corresponding to the molecular weight in low resolution, and the formed fragmented ion from a collision induced dissociation (CID) was detected at its exact mass (+/- 0.005 Da) (Supplementary Table S2).

SciexOS software, current version: 3.3.1.43 was used for instrument control, data acquisition and data processing. Accuracy was studied by the 4 QC's repeated at least 3 times. Mean accuracy (in %) at different concentrations is reported. Precision of the method was studied by calculating the CV% and was considered acceptable if CV was below 20% for QC at LOQ and 15 % for the other QC concentrations. Each steroid is quantified with an analog stable isotope IS. Specificity was evaluated using extracted blank medium of treated explant samples. Specificity was controlled in samples, calibrators and QC's by checking the quantifier to qualifier intensities ratio compared to analytical standards in water.For each steroid, the calibration curve was plotted as the unlabeled to labeled compounds area ratio. The

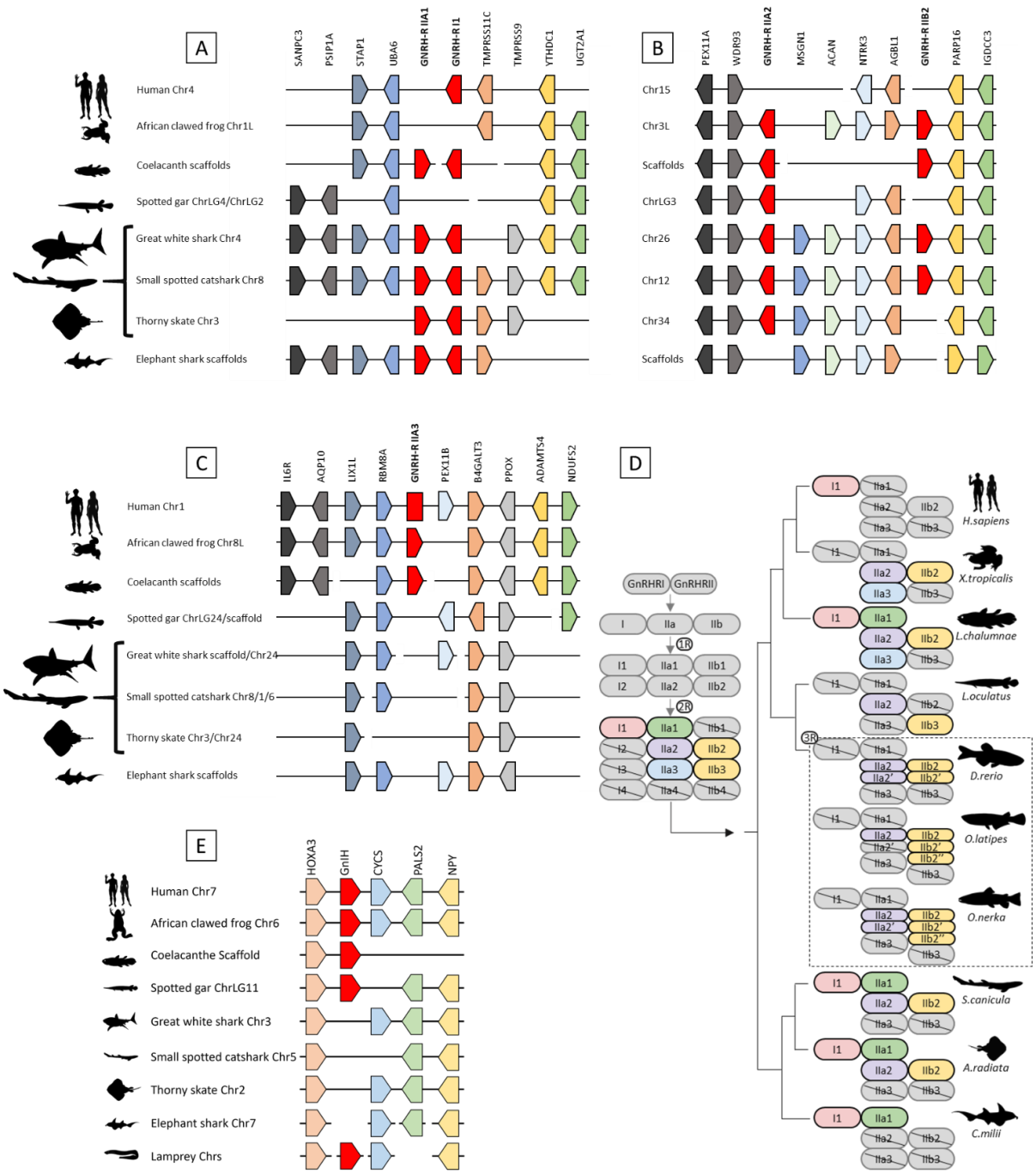


**Fig. 2.** *In silico* characterization of elasmobranch GnRHRs and GnIH. A. Synteny analysis of vertebrate GnRHRI1 and GnRHRIIA1 genomic regions. The *C. milii* genomic regions were used as templates. B. Synteny analysis of vertebrate GnRHRIIA2 and GnRHRIIB2 genomic regions. The coelacanth genomic regions were used as templates. C. Synteny analysis of vertebrate GnRHRIIA3 genomic regions. The human genomic regions were used as templates. D. A schematic diagram showing an evolution model of GnRH receptors. From the six GnRH receptor orthologs identified, GnRHRI1, GnRHRIIA1, GnRHRIIA2 and GnRHRIIB2 were retained in sharks and rays, by opposition to *C. milii* where only GnRHRI1 and GnRHRIIA1 were retained. Teleost fishes are boxed with dotted line and whole genome duplication (1R, 2R and 3R) are illustrated. Modified from Dufour et al., 2020 and Ogawa et al., 2022. E. Synteny analysis of vertebrate GnIH genomic regions. The human genomic region was used as templates. Animal illustrations are used with permission from http://phylopic.org.

quadratic regression weighted by 1/C was used. For each steroid, at least 8 calibrators among the 13 injected were selected. The lowest calibrator allowing an accuracy of 20% was defined as the LOQ.

## Results

*Genome searches have identified 3 types of GnRH and 4 types of GnRHR in elasmobranchs*

Sequence searches identified four GnRHR and three GnRH sequences in elasmobranch genomes. Molecular phylogeny of GnRHs (Supplementary data Fig. S2A) showed segregation of chondrichthyan GnRH1, GnRH2 and GnRH3 sequences in accordance with phylogeny, with the exception of GnRH1 from *A. radiata* and *L. erinacea* (two rays), which segregated with actinopterygian GnRH1. A model for the evolution of GnRH orthologs in vertebrates has been proposed, highlighting significant divergence from GnRH1 with 10 orthologs identified, including one specific to selachii (QHWSFDLRPG) and one to rhinopristiformes and myliobatiformes (QHWSFNMRPG) (Fig. 1A), a single GnRH2 (QHWSHGWYPG) conserved in all gnathostomes (Fig. 1B), and 4 orthologs of GnRH3 (Fig. 1C). Molecular phylogeny of GnRHR sequences presented segregation in accordance with the phylogeny. The four elasmobranch GnRHR were grouped with gnathostome GnRHRI1, GnRHRIIA1, GnRHRIIA2 and GnRHRIIB2, respectively (Supplementary data Fig. S2B). To validate their annotations and include elasmobranch homologs in the evolutionary history of *gnrhr* genes, synteny analyses were performed and supported the conservation of GnRHRI1, GnRHRIIA1 (Fig. 2A), GnRHRIIA2 and GnRHRIIB2 (Fig. 2B) and the loss of GnRHRIIA3 (Fig. 2C) in elasmobranchs. Elasmobranchs are the second vertebrate group with the highest number of conserved GnRHR subfamilies, after the basal sarcopterygian, *L. chalumnae* which possess five GnRHR subfamilies, and diverged from holocephalans, which retain only the two GnRHRIIA2 and GnRHRIIB2 subfamilies (Fig. 2D).

*Genome and synteny searches of* gnih

The genome search, using vertebrate GnIH sequences, failed to identify homologs from the 10 elasmobranch genomes analyzed. A synteny of *gnih* genomic regions was performed and suggested the loss of *gnih* homologs in chondrichthyes (Fig. 2E).

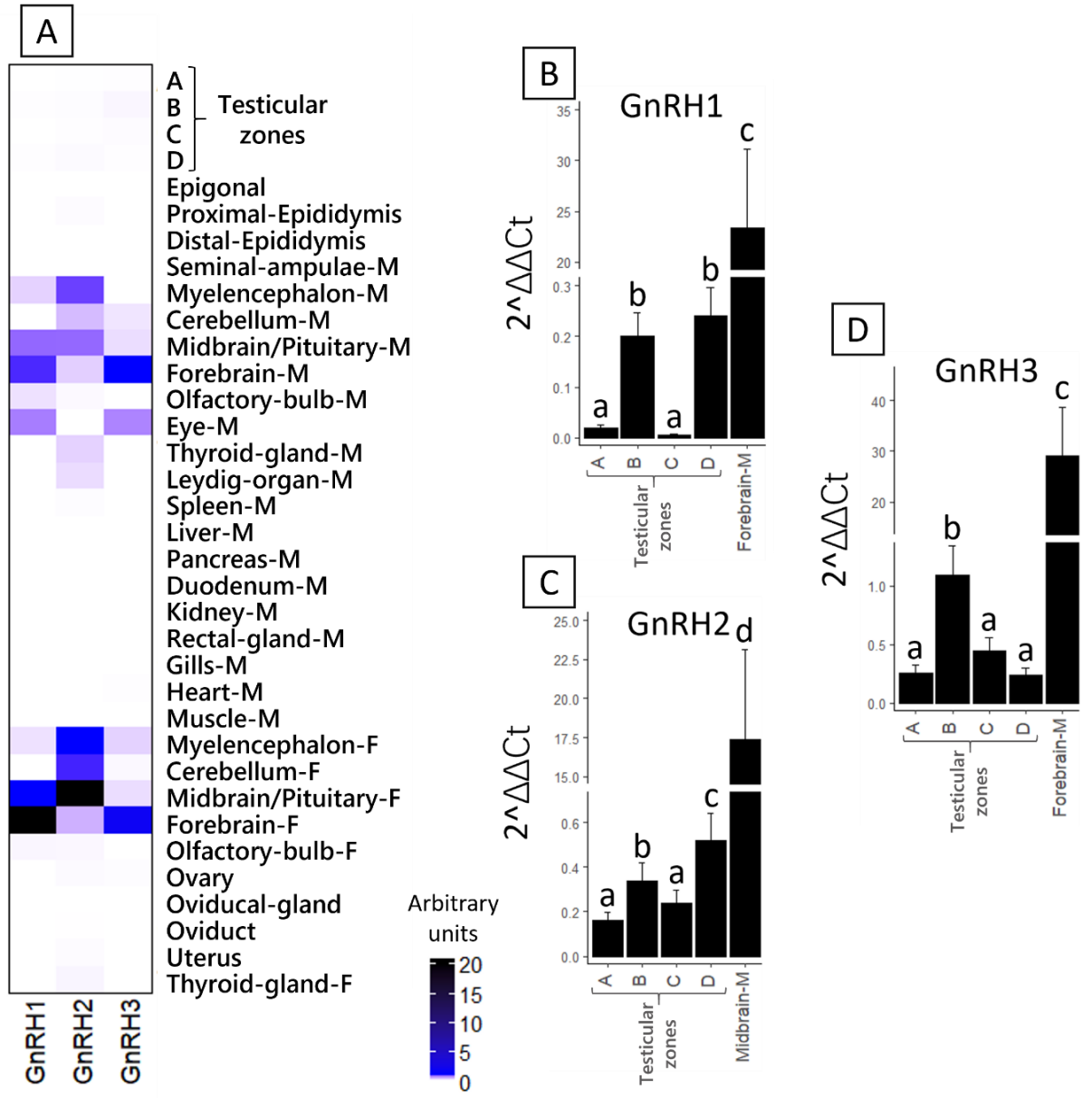


**Fig. 3.** Relative expression profiles of *gnrh1*, *gnrh2* and *gnrh3* transcripts in *S. canicula* tissues with a focus on stages of spermatogenesis. Messenger RNA levels were assayed by real-time PCR. A. Warm map representation of relative expression profiles of *gnrh1*, *gnrh2* and *gnrh3* transcripts in 35 different tissues of *S. canicula*. The tissues from females correspond to females caught in September (non-breeding period) whose ovaries contained previtellogenic follicles and corresponding to females in postovulatory stage. M, Male; F, Female. B-D. Relative gene expression of *gnrh1*, *gnrh2* and *gnrh3* transcripts in testicular zones and epigonal tissue. Statistical analysis was performed using Mann-Whitney U test with P value < 0.05 between each statistical groups a, b, c and d.

*Relative expression profiles of* gnrh1*,* gnrh2 *and* gnrh3 *transcripts in* S. canicula *tissues*

Expression profiles of *gnrh1*, *gnrh2* and *gnrh3* transcripts in 35 different tissues of *S. canicula* showed the highest *gnrhs* expression levels, in the different parts of the male and female brains, with *gnrh1* transcripts in the midbrain, forebrain and eyes, *gnrh2* transcripts in myelencephalon, cerebellum, midbrain and forebrain and *gnrh3* transcripts in the forebrain and eyes (Fig. 3A). Outside the brain, expressions of *gnrh2* were also observed in the thyroid gland and the lymphomyeloid Leydig organ. Although very low levels of *gnrh* transcripts were observed in the testicular zones, a targeted analysis was carried out to assess the potential roles of peptides in paracrine regulation (Fig. 3B-D). All three mRNA types were found in all four zones, with higher levels of GnRH1 and GnRH2 transcripts in zones B and D, and GnRH3 in zone B.

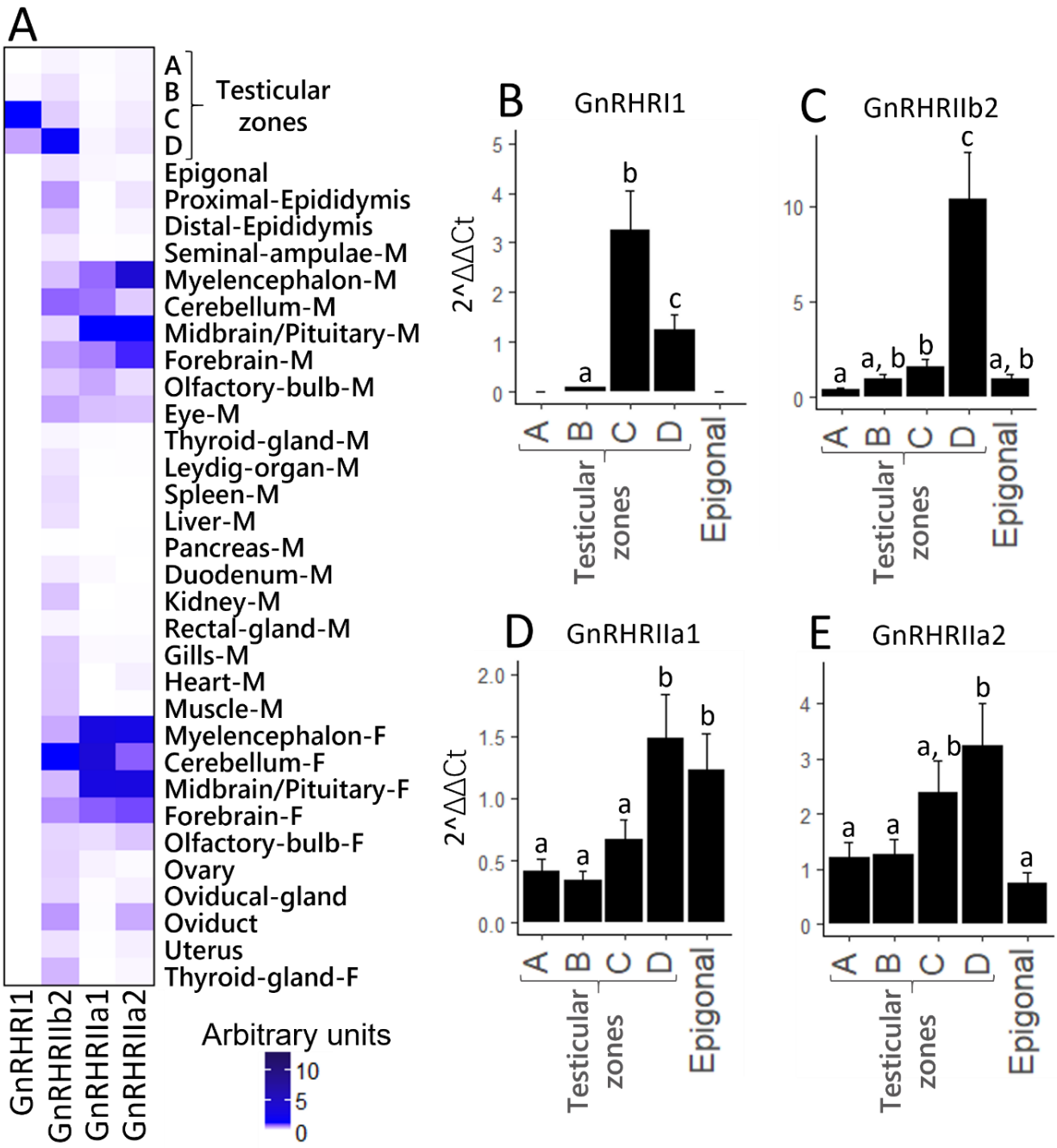


**Fig. 4.** Relative expression profiles of *gnrhrI1*, *gnrhrIIb2*, *gnrhrIIa1* and *gnrhrIIa2* transcripts in *S. canicula* tissues with a focus on stages of spermatogenesis. Messenger RNA levels were assayed by real-time PCR. A. Warm map representation of relative gene expression in 35 different tissues. Relative gene expression of *gnrhrI1* (B), *gnrhrIIb2* (C), *gnrhrIIa1* (D), and *gnrhrIIa2* (D) at different stages of spermatogenesis. Statistical analysis was performed using Mann-Whitney U test with P value < 0.05 between each statistical groups a, b, c and d. A, B, C and D: testicular zones from six different animals in triplicates (N=6; n=18); other tissues: from three different animals in triplicates (N=3; n=9). The tissues from females correspond to females caught in September (non-breeding period) whose ovaries contained previtellogenic follicles and corresponding to females in postovulatory stage. M, Male; F, Female.

*Expression profiles of* gnrhrI1, gnrhrIIb2, gnrhrIIa1 and gnrhrIIa2 *transcripts in* S. canicula *tissues with a focus on spermatogenesis*

Expression profiles of the four *gnrhr* transcripts showed tissue-specific expression of *gnrhrI1* in testicular zones C and D, a ubiquitous expression of *gnrhrIIb2*, including in the testicular zone D, a preferential expression of *gnrhrIIa1* in the brain, including eyes, and a preferential expression of *gnrhrIIa2* in the brain, with also lower expression in various peripheral tissues, including testicular zones, the epididymis, and the female reproductive tract, notably the oviduct (Fig. 4A). According to the spermatogenetic wave, all four transcripts were highly expressed in the stages of spermiogenesis (zones C and/or D), with the highest level associated with *gnrhrIIb2* (Fig. 4B-E). Low levels of transcripts were also observed in the epigonal tissue.

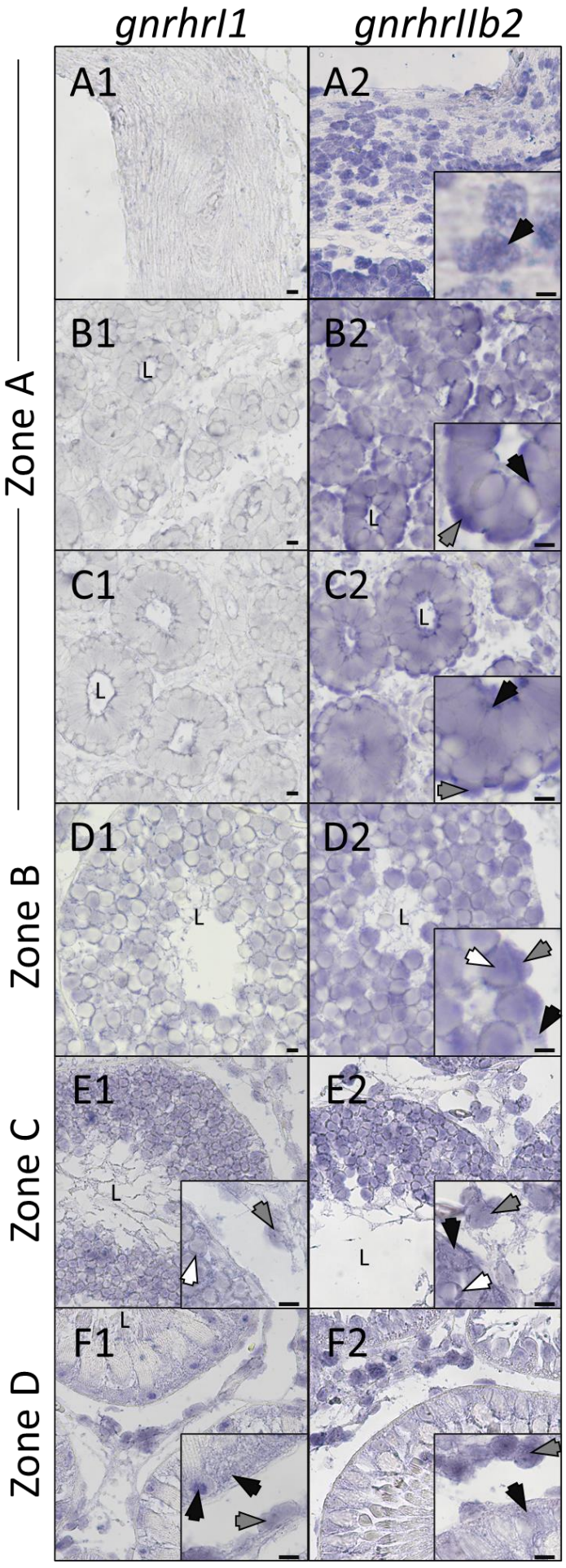
gnrhrl1
gnrhrllb2
A1
A2
B1
B2
C1
C2
D1
D2
E1
E2
F1
F2
L
Zone A
Zone B
Zone C
Zone D

*In situ hybridization (ISH) targeting* gnrhrI1 *and* gnrhrIIb2 *transcripts on S. canicula testis*

Based on RT-PCR results, ISH analyses were carried out targeting *gnrhrI1* transcripts, which appeared testis-specific, and *gnrhrIIb2* transcripts, which appeared to be the most abundant *gnrhr* transcripts in testis. According to the spermatogenetic wave, slight *gnrhrI1*-associated staining was observed in Sertoli cells associated to spermatogonia, but not in the germinative area (Fig. 5A1-C1), in Sertoli cells associated to spermatocytes (Fig. 5D1) and an increase in signal was observed in cysts with round spermatids, probably including a germ cell labelling, which is in accordance with the previous results showing the highest mRNA levels in zone C (Fig. 5E1). In the zone of cysts with elongated spermatids, ISH staining for *gnrhrI1* transcripts decreased and appeared to be associated with interstitial cells (Fig. 5F1). The ISH signal corresponding to *gnrhrIIb2* transcripts was observed throughout the spermatogenic wave (Fig. 5A2-F2) from somatic precursors (Fig. 5A2-B2) to Sertoli cells (Fig. 5C2-F2), spermatocytes (Fig. 5D2), round spermatids and interstitial cells (Fig. 5E2). These results are consistent with ubiquitous expression of *gnrhrIIb2* mRNA as observed by real-time PCR. Controls revealed no background noise (Supplementary data Fig. S3).

**Fig. 5.** *In situ* hybridization of *gnrhrI1* and *gnrhrIIb2* mRNAs in *S. canicula* testicular sections. The testicular zone A corresponds to the germinative area (A1, A2), the cysts in formation (B1, B2) and formed cysts with spermatogonia (C1, C2). The testicular zones B, C and D correspond to cysts with primary spermatocytes (D1, D2), cysts with young spermatids (E1, E2) and cysts with late spermatids (F1, F3), respectively. *In situ* hybridization was performed using riboprobes targeting *Sc-gnrhrI1* mRNA (A1-F1) and *Sc-gnrhrIIb2* (A2-F2). White arrowhead, staining associated to germ cell (A-B); Black arrowhead, staining associated to somatic precursor (A) and Sertoli cells (B-E); grey arrowhead, staining associated to interstitial cell. L: lumen. Scale bars: 10µm. Controls are presented in supplementary data (Supplementary Figure S4).

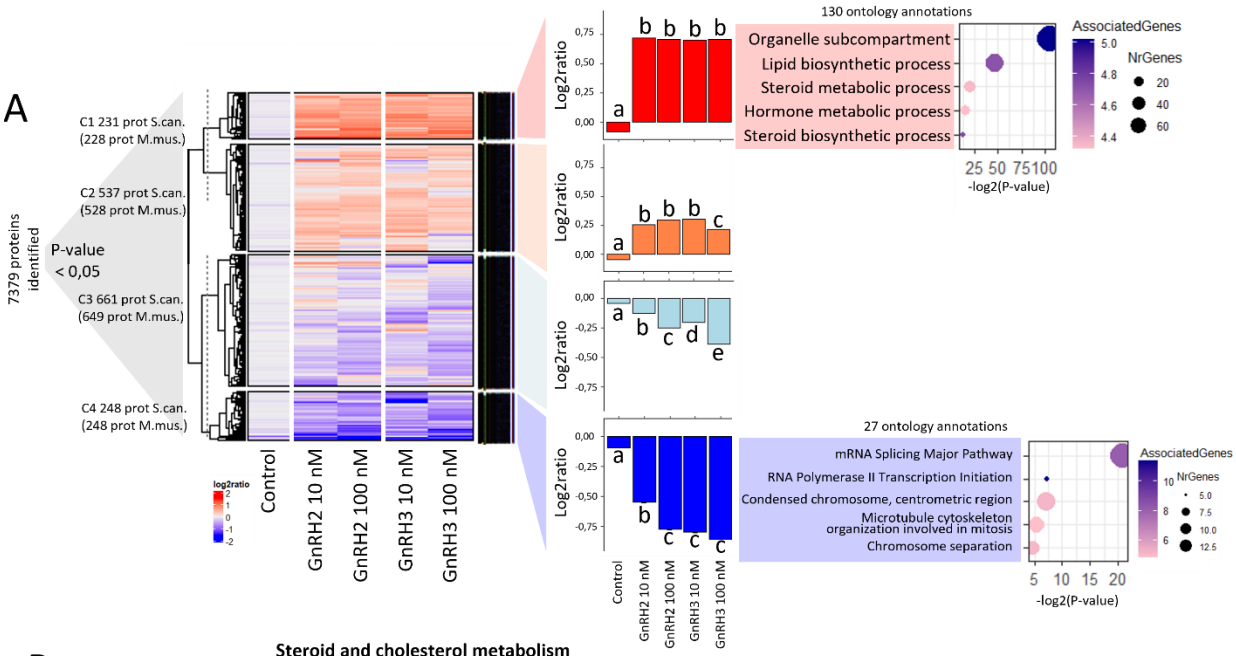
A
7379 proteins identified
P-value < 0,05
C1 231 prot S.can. (228 prot M.mus.)
C2 537 prot S.can. (528 prot M.mus.)
C3 661 prot S.can. (649 prot M.mus.)
C4 248 prot S.can. (248 prot M.mus.)
log2ratio
Control
GnRH2 10 nM
GnRH2 100 nM
GnRH3 10 nM
GnRH3 100 nM
130 ontology annotations
Organelle subcompartment
Lipid biosynthetic process
Steroid metabolic process
Hormone metabolic process
Steroid biosynthetic process
-log2(P-value)
AssociatedGenes
NrGenes
27 ontology annotations
mRNA Splicing Major Pathway
RNA Polymerase II Transcription Initiation
Condensed chromosome, centrometric region
Microtubule cytoskeleton organization involved in mitosis
Chromosome separation

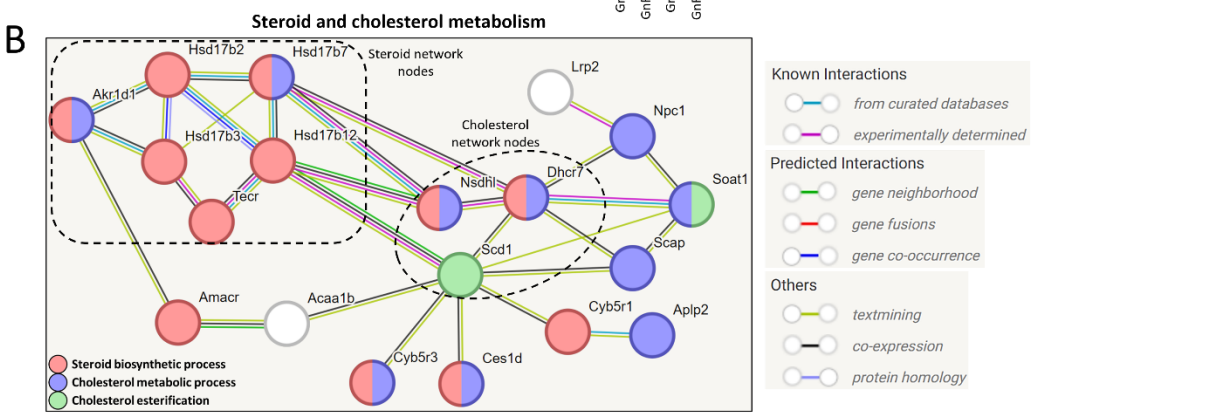
B
Steroid and cholesterol metabolism
Steroid network nodes
Cholesterol network nodes
Hsd17b2
Hsd17b7
Akr1d1
Hsd17b3
Hsd17b12
Tecr
Lrp2
Npc1
Nsdhl
Dhcr7
Soat1
Scd1
Scap
Amacr
Acaa1b
Cyb5r1
Aplp2
Cyb5r3
Ces1d
Steroid biosynthetic process
Cholesterol metabolic process
Cholesterol esterification
Known Interactions
from curated databases
experimentally determined
Predicted Interactions
gene neighborhood
gene fusions
gene co-occurrence
Others
textmining
co-expression
protein homology

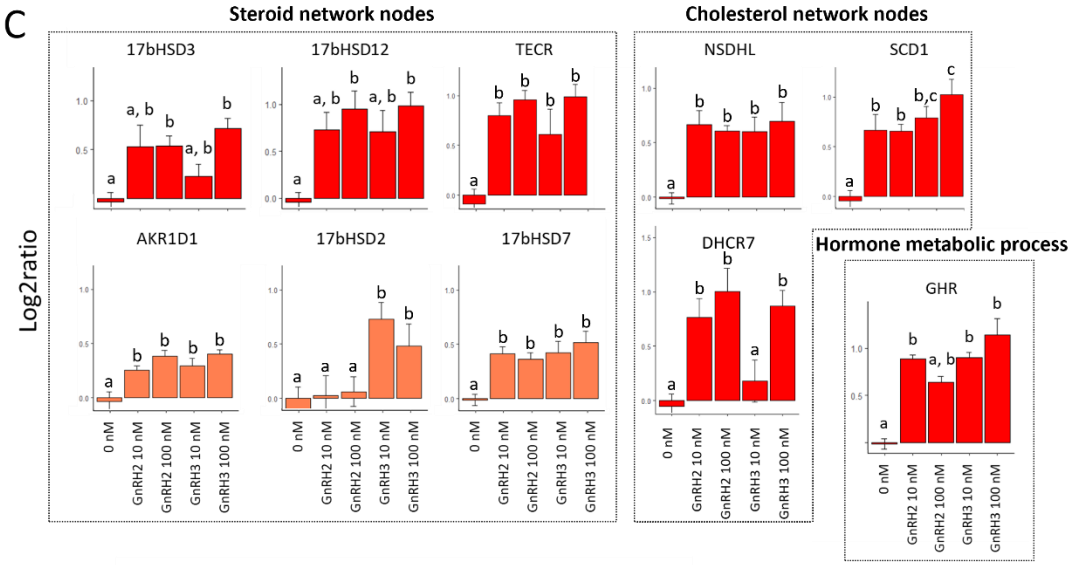
C
Steroid network nodes
Cholesterol network nodes
Log2ratio
17bHSD3
17bHSD12
TECR
NSDHL
SCD1
AKR1D1
17bHSD2
17bHSD7
DHCR7
Hormone metabolic process
GHR
0 nM
GnRH2 10 nM
GnRH2 100 nM
GnRH3 10 nM
GnRH3 100 nM

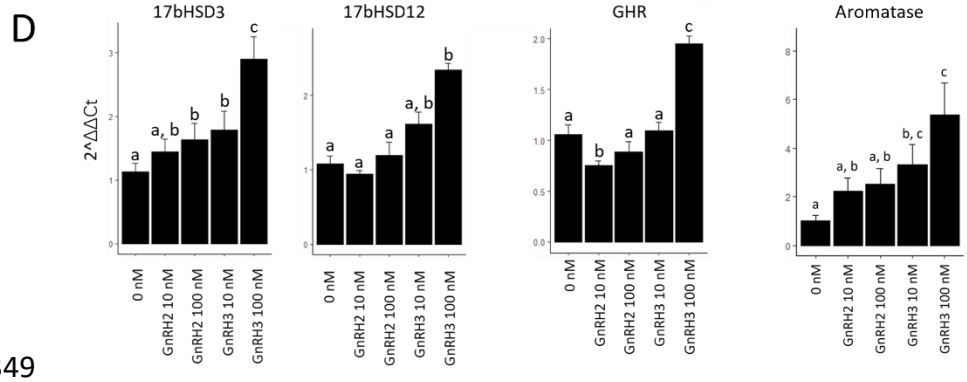
D
17bHSD3
17bHSD12
GHR
Aromatase
2^ΔΔCt
0 nM
GnRH2 10 nM
GnRH2 100 nM
GnRH3 10 nM
GnRH3 100 nM

*Effects of ScGnRH2 and ScGnRH3 treatments on the proteome of* S. canicula *testicular zone D explants*

Based on the results reported above, showing that zone D could be the most sensitive to GnRH, *in vitro* incubation of testicular explants from the zone D was performed with synthetic *Sc*GnRH2 or *Sc*GnRH3 at 0 nM, 10 nM or 100 nM during 24 h. NanoLC-ESI-MS/MS analysis identified 7379 proteins and an anova test (P-value < 0.05) showed that 1677 proteins (representing 22.74% of total proteins) were significantly differentially expressed in at least one treatment, compared with the 0 nM condition. Using the k-clustering method (k=4), four clusters of 231 (C1), 537 (C2), 661 (C3) and 248 (C4) proteins were obtained. Proteins from each cluster were blasted against the mouse proteome, yielding 228 (C1), 528 (C2), 649 (C3) and 248 (C4) homologs (Fig. 6A). Variations in protein levels according to the 4 clusters and treatments were represented by a heatmap. To estimate the overall variations in protein levels induced by the different treatments, log2ratios were averaged by cluster and treatment.

---

**Fig. 6.** Proteomic analysis of *S. canicula* testicular zone D explants stimulated with 0 nM, 10 nM or 100 nM of ScGnRH2 or ScGnRH3. A. The proteomic analysis allowed to identified 7379 proteins including 1677 differentially regulated in at least one stimulated condition, by comparison to the control. Statistical analysis was performed using ANOVA test with P-value < 0.05. The expression profile of the 1677 differentially expressed proteins were analyzed by k-clustering (k=4) to obtain clusters C1, C2, C3 and C4 comprising 231, 537, 661 and 248 proteins respectively and represented with a heatmap. By blastp methodology using the *S. canicula* proteins, 228, 528, 649 and 248 *M. musculus* orthologs were associated to the cluster C1, C2, C3 and C4 respectively. Then, for each stimulated condition and by cluster, the means of all associated protein relative abundances were calculated and statistical analysis was performed using Tukey's Honest Significant difference (HSD) test with P-value < 0.05 between each statistical groups a, b, c, d and e. By gene ontology functional annotation, 130 and 27 terms were obtained for C1 and C4, respectively, and the five most representative terms are shown. B. Proteins involved in steroid metabolism terms and showing increased abundances were visualized as a functionally grouped network. Three groups were identified including "Steroid biosynthetic process", "Cholesterol metabolic process" and "Cholesterol esterification", illustrated in red, blue and green respectively. C. Relative expression profile of proteins found in the steroid and cholesterol network nodes are shown. GHR was also identified in the C1-associated "Hormone metabolic process" and the corresponding relative expression profile was illustrated. Statistical analysis was performed using ANOVA test with P value < 0.05 between each statistical groups a, b, c and d. D. Relative expression profiles of *ghr*, *17ϐhsd3*, *17ϐhsd12* and *cyp19a1* transcripts in zone D explants treated with ScGnRH. Statistical analysis was performed using Mann-Whitney U test with P value < 0.05 between each statistical groups a, b, c and d.

The C1 and C4 clusters appeared highly sensitive to *Sc*GnRH treatments, achieving a maximum variation in protein levels of 0.75 log2ratio with 10 and 100 nM of ScGnRH2 and ScGnRH3, while the C2 and C3 clusters appeared less sensitive to *Sc*GnRH treatments, achieving a variation in protein levels of 0.25 log2ratio with 10 nM and 100 nM of *Sc*GnRH2 and *Sc*GnRH3. Functional annotation was performed on C1 and C4 clusters, and 130 and 27 terms were identified, respectively. Five terms linked to critical regulations were selected. They were related, for C1, to cellular component with “organelle subcompartement”, to steroid regulation with “lipid biosynthetic process”, “steroid metabolic process” and “steroid biosynthetic process” and other hormone regulations with “hormone metabolic process”.For C4, terms were related to transcription with “mRNA splicing major pathway” and “RNA polymerase II transcription initiation” and to DNA structure modification with “condensed chromosome centromeric region”, “microtubule cytoskeleton organization involved in mitosis” and “chromosome separation”. The proteins involved in these terms were further analyzed, highlighting: the growth hormone receptor (GHR) linked to the hormone metabolic processes term; the hydroxysteroid 17β dehydrogenases 3 (17βHSD3) and 12 (17βHSD12) linked to the steroidal processes term. Analysis of the C2 cluster revealed also a 1.2-fold increase of the hydroxysteroid (17-beta) dehydrogenase 2 (17βHSD2), the hydroxysteroid (17-beta) dehydrogenase 7 (17βHSD7) and of the aldo-keto reductase family 1, member D1 (Akr1d1) proteins in response to GnRH treatments. Analysis of the C3 cluster revealed also a 1.19-fofd decrease of the serine and arginine-rich splicing factor 5 (Srsf5). Overall, it appeared that GnRH treatments modulated steroid biosynthesis and metabolism, and further reduced factors no longer required for spermiogenesis. The 19 highlighted proteins linked to steroid biosynthesis and metabolism were visualized as a functionally clustered network (Fig. 6B). Three functional clusters were identified, corresponding to “Steroid biosynthetic process”, “Cholesterol metabolic process” and “Cholesterol esterification”. Two network nodes were then highlighted with the steroid network nodes involving Akr1d1, 17βHSD2, 17βHSD3, 17βHSD7, 17βHSD12 and Tecr and the cholesterol network nodes involving Dhcr7 (7-dehydrocholesterol reductase), Nsdhl, (NAD(P) dependent steroid dehydrogenase-like) and Scd1 (sterol coenzymeA desaturase).

*Relative expression profiles of actors involved in steroid and cholesterol network nodes*

For the steroid network nodes, the protein levels of 17βHSD3 and 17βHSD12 increased accordingly to a dose-response profile, while TECR level importantly increased after all GnRH treatments (Fig. 6C). The protein levels of Akr1D1 and 17βHSD7 increased similarly after all treatments, while the level of17βHSD2 level increased only with *Sc*GnRH3 treatments. For the cholesterol network nodes, NSDHL and SCD1 protein levels increased after all GnRH treatments, with the highest levels of SCD1 observed with 100 nM *Sc*GnRH3, while DHCR7 protein levels remained low with 10 nM *Sc*GnRH3. For the biological metabolic process, the GHR protein level increased after all GnRH treatments. This analysis was completed by real-time PCR analyses targeting *17βhsd3*, *17βhsd12* and *ghr* transcripts (Fig. 6D). The transcript levels of *17βhsd3* increased slightly with 100 nM *Sc*GnRH2 and 10 nM *Sc*GnRH3 and up to 3-fold with 100 nM *Sc*GnRH3, illustrating a better efficiency of *Sc*GnRH3. A better efficiency of ScGnRH3 than ScGnRH2 was also observed on the transcript levels of *17βhsd12*, with a 2-fold increase observed with 100 nM *Sc*GnRH3. As for the transcript levels of *Ghr*, they decreased slightly with 10 nM of ScGnRH2 but increased 2-fold with 100 nM of ScGnRH3. Overall, the increases of 17βHSD3, 17βHSD12 and GHR proteins were also found at the transcriptional level.

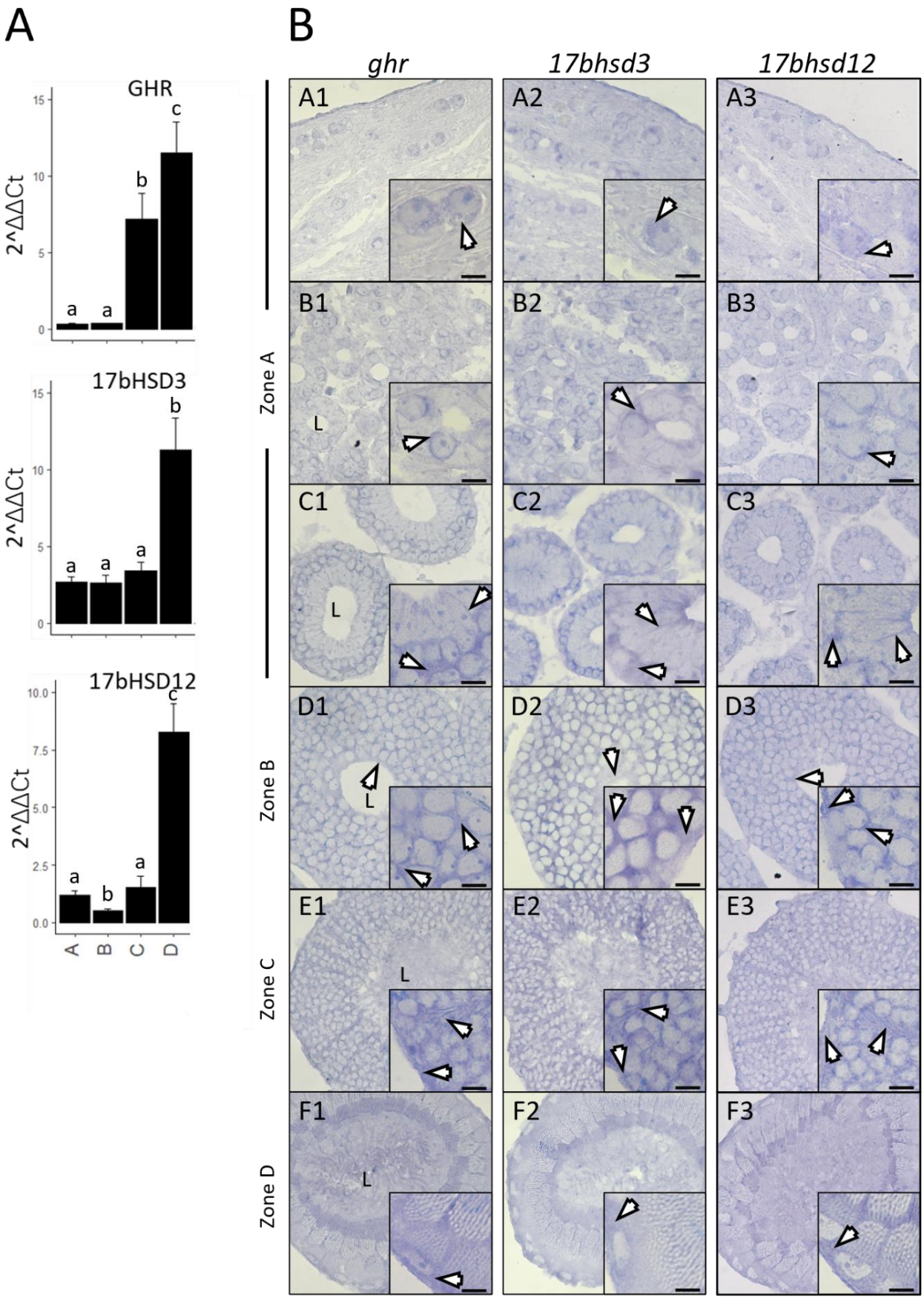
A
GHR
2^ΔΔCt
a
a
b
c
17bHSD3
a
a
a
b
17bHSD12
a
b
a
c
A
B
C
D
B
ghr
17bhsd3
17bhsd12
Zone A
Zone B
Zone C
Zone D
A1
A2
A3
B1
B2
B3
C1
C2
C3
D1
D2
D3
E1
E2
E3
F1
F2
F3
L

Expression of *ghr, 17ϐhsd3*, *17ϐhsd12* transcripts in the testis of *S. canicula*

To further explore the roles of *17ϐhsd3*, *17ϐhsd12* and *ghr* in the regulation of spermatogenesis, expression analysis of transcripts was carried out. According to the spermatogenetic wave, *ghr* mRNA levels were low in zones A and B, increased strongly in zone C and were the highest in zone D (Fig. 7A). The mRNA levels of *17ϐHSD3* and *17ϐHSD12* were the highest in zone D compared with earlier stages (Fig. 7A). ISH targeting *ghr* transcripts presented staining in somatic cell precursors surrounding undifferentiated spermatogonia (Fig. 7B. A1, B1) and in Sertoli cells of cysts containing spermatogonia, spermatocytes, early and late spermatids (Fig.7B. C1-F1). Transcripts of *17ϐhsd3* and *17ϐhsd12* were also localized in somatic precursors surrounding undifferentiated spermatogonia (Fig.7B. A2-B3) and in the cytoplasm of Sertoli cells at the apical part, basal part and around germ cells in cysts with spermatogonia (Fig.7B. C2, C3), cysts with spermatocytes (Fig.7B. D2, D3), cysts with round spermatids (Fig.8B. E2, E3) and cysts with elongated spermatids (Fig.7B. F2, F3). Controls showed no background noise (Supplementary data Fig. S4).

**Fig. 7.** Expression analyses of *ghr*, *17ϐhsd3* and *17ϐhsd12* transcripts in spermatogenesis stages. A. Relative gene expression of *ghr*, *17ϐhsd3* and *17ϐhsd12* transcripts at different stages of spermatogenesis. Statistical analysis was performed using Mann-Whitney U test with P value < 0.05 between each statistical groups a, b, c and d. B. *In situ* hybridization of *ghr* and *17ϐhsd3* and *17ϐhsd12* mRNAs in *S. canicula* testicular sections. The testicular zone A corresponds to the germinative area (A1-A3), cysts in formation (B1-B3), and formed cysts with spermatogonia (C1-C3). The testicular zones B, C and D correspond to cysts with primary spermatocytes (D1-D3), cysts with young spermatids (E1-E3) and cysts with late spermatids (F1-F3), respectively. *In situ* hybridization was performed using riboprobes targeting *Sc-ghr* (A1-F1), *Sc-17ϐhsd3* (A2-F2) and *Sc-17ϐhsd12* mRNAs (A3-F3). White arrowhead, staining associated to sertolian precursor (A-B) and Sertoli cells (C-F); L: lumen. Scale bars: 10µm. Controls are presented in supplementary data (Supplementary Figure S5).

*Steroid levels in response to GnRH*

Analysis of steroids in culture media of testicular explants from the late spermatide zone (Zone D) stimulated with 10nM and 100 nM of GnRH2 or GnRH3 allowed the assay of the following steroids: pregnenolone (Preg), progesterone (Prog), androstenedione (A4), testosterone (T), 11-ketotestosterone (11-KT), 17α-hydroxyprogesterone (17OHProg), estrone (E1), estrone 3-sulfate (E1S), 17β-oestradiol (E2), cortisone (E), aldosterone (Aldo), corticosterone (B), 11-deoxycorticosterone (DOC), dehydroepiandrosterone (DHEA) and dehydroepiandrosterone sulfate (DHEAS) (Table 1). The highest concentrations were observed for DHEAS followed by Preg and Prog. However, only a significant decrease in estrone (E1) levels at 100 nM *Sc*GnRH2 and a significant increase in estradiol (E2) levels at 10 nM *Sc*GnRH2, 100 nM *Sc*GnRH2 and 100 nM *Sc*GnRH3 were observed. In absence of aromatase (CYP19) detection during the proteomic analysis, *cyp19a1* gene expression analysis was performed in GnRH-stimulated explants. The corresponding real-time RT-PCR results showed that *cyp19a1* transcript levels were increased 2- fold with 10 and 100 nM *Sc*GnRH2, and 3- and 5-fold with 10 and 100 nM *Sc*GnRH3, respectively (Fig.6D).

## Discussion

The present study completed the identification of the GnRH1, GnRH2 and GnRH3 protein sequences in multiple elasmobranchs, which is in agreement with the previous identification of the three *gnrh* genes in *S. canicula* and *R. typus* (Gaillard et al., 2018). Elasmobranch GnRHs were structurally conserved, with a sequence of 10 amino acids, the retention of residues in positions 1-4, 9 and 10, the N-terminal pyroglutamate site and the C-terminal glycinamide site. Along vertebrate phylogeny, GnRH2 sequence was conserved in all gnathostomes, including elasmobranchs. The GnRH3 was conserved in actinopterygians, coelacanths and elasmobranchs, with the amino-acid residue diverging at position 5, and was lost in tetrapods and holocephali. GnRH1, on the other hand, diverged markedly during vertebrate evolution, with 10 different sequences highlighted, including the shark specific isoform (QHWSFDLRPG), the rhinopristiforme rays and myliobatiforme rays isoform (QHWSFNMRPG), while rajiforme rays possess an isoform common to some bony vertebrates. Elasmobranch GnRH isoforms have diverged from those of holocephalan, which have lost *gnrh3* and possess two copy of the

*gnrh1* gene (*gnrh1a* and *gnrh1b*) (Gaillard et al., 2018). Additional GnRHs were suggested in ancient biochemical analyses that identified the dogfish GnRH (currently GnRH3) and chicken GnRH-II (currently GnRH2) (Lovejoy et al., 1992), as well as multiple forms of immunoreactive GnRH in elasmobranchs, up to 4 or 5 (D'antonio et al., 1995; Forlano et al., 2000; Sherwood and Lovejoy, 1993). However, during our *in silico* analysis, we found no additional sequences related to GnRHs or their precursors, excepted a potential decapeptide, with a Q residue at the Nt and a PG at the Ct, from the KCNH5 (potassium voltage-gated channel subfamily H member 5) gene. We found no potential GnIH sequence and the synteny showed the absence of the *gnih* gene in chondrichthyes, raising the question of its loss in holocephalans and elasmobranchs during the course of evolution, since GnIH peptides have been identified in cyclostomes (lamprey), suggesting that GnIH may have emerged in ancestral vertebrates before the split between cyclostomes and gnathostomes (Osugi et al., 2014).

In *S. canicula*, although we have not studied their brain localization by *in situ* analyses, our results showed specific expression of the three *gnrh* genes in different part of the brain, which is in agreement with previous reports (Gaillard et al., 2018). The highest *gnrh1* mRNA levels were associated to forebrain, those of *gnrh2* to midbrain and those of *gnrh3* to forebrain, in agreement with the three main GnRH neural systems in bony vertebrates, corresponding respectively to the ventral forebrain (expressing GnRH1), the midbrain (expressing GnRH2) and the terminal nerve (expressing GnRH3) (Dubois et al., 2002). Furthermore, these results highlighted the absence or very low expression of *gnrh* in extra-brain tissues, including the testes, in contrast to the testicular *gnrh* expression observed in zebrafish (*gnrh2* and *gnrh3*) (Fallah et al., 2020) and rat (*gnrh1*) (Ciaramella et al., 2015). This suggests that the potential paracrine/autocrine role of GnRH in *S. canicula* gonads is marginal at best.

The present study reports the identification of four GnRHR subfamilies in all elasmobranch genomes analyzed and conserved synteny revealed the conservation of the *gnrhrl1*, *gnrhrIIa1*, *gnrhrIIa2* and *gnrhrIIb2*. This makes elasmobranchs the second clade of vertebrates with the highest number of conserved GnRHR subfamilies, after the coelacanth with five GnRHR subfamilies (Ogawa et al., 2022). However, the difference observed with the holocephalan *C. milii*, in which two GnRHR subfamilies (*gnrhrl1* and *gnrhrIIa1*) have been identified, underlines the evolutionary divergence resulting from 300-million years of independent evolution between holocephalans and elasmobranchs (Irisarri et al., 2017).

In *S. canicula*, the analysis of the *gnrhrs* expression showed: a testis-specific expression for *gnrhrI1;* an expression in all tissues analyzed, except pancreas, for *gnrhrIIb2*; an expression principally associated to the different parts of the brain for *gnrhrIIa1*; and an expression in the brain and in the reproductive organs, at lower levels, for *gnrhrIIb2*. These results are in agreement with the previous tissue-expression profile obtained in a limited number of *S. torazame* sharks (Hara et al., 2018). Stage-related expression analyses of the four *gnrhr* genes during spermatogenesis in *S. canicula* have shown higher levels in zones corresponding to cysts with spermatids (Zone C and D). Using *in situ* hybridization, *gnrhrI1* was localized in Sertoli cells with increased signal in cysts with early spermatids, in which the localization of *gnrhrI1* in spermatids cannot be excluded, and in interstitial cells associated with cysts containing elongated spermatids. *GnrhrIIb2* was more widely localized, in somatic precursors of the germinative area, Sertoli cells, germ cells and interstitial cells, the latter being associated with late stages of spermiogenesis. These results are in agreement with the expression of *gnrhr* genes observed in zebrafish (Fallah et al., 2020), frog (Chianese et al., 2012), boar (Desaulniers et al., 2015) and rat testes, in which localization in haploid cells was observed in addition to somatic cells (Ciaramella et al., 2015).

The direct role of *Sc*GnRH was investigated on explants from the testicular zone D (late stages of spermatogenesis) of *S. canicula* treated with synthetic *Sc*GnRHs. The choice of *Sc*GnRH2 and *Sc*GnRH3 was based on their previous identification, at physiological concentrations, in the systemic circulation of *S. canicula* (D'antonio et al., 1995; Knowles et al., 1975; Sherwood and Lovejoy, 1993). In response, the proteome analyzes of explants identified 231 highly up-regulated and 248 highly down-regulated proteins, with a maximum variation in average protein level of 0.75 log2ratio for both ScGnRH2 and ScGnRH3 treatments at 10 and 100 nM. The functional annotation was performed on highly up- and down-regulated proteins. Terms associated with down-regulated proteins were related to transcription and modification of DNA structure, consistent with the decrease in transcriptional activity during spermiogenesis as spermatids nuclei remodel with the replacement of histones by protamines (Tanaka and Baba, 2005). Terms associated to up-regulated proteins were related to hormone regulation and steroid synthesis, including several *17ϐHSD* enzymes. An increase in *17ϐhsd3* and *17ϐhsd12* mRNA levels was also observed and they were localized by ISH in Sertoli cells which are the main steroidogenic cells in the testis of *S. canicula*, as in another shark, *S. acanthias*.

The *17βHSD* enzymes metabolize, among others, for *17βHSD3* the synthesis of androstenedione into testosterone (Luu-The et al., 2006), for *17βHSD12* and *17βHSD7* the synthesis of estrone into 17β-oestradiol and for *17βHSD2* the synthesis of 17β-oestradiol into estrone (Gilligan et al., 2017; Luu-The et al., 2006). This analysis was extended to aromatase, whose activity was previously assayed in the testis of *S. acanthias* (Callard et al., 1985) and which metabolizes testosterone and androstenedione into 17β-oestradiol and estrone, respectively. The aromatase was not identified by our proteomic analysis but *cyp19a1* transcript levels increased in response to stimulation of the testicular explants by *Sc*GnRH2 and *Sc*GnRH3. Variations in estrone and estradiol levels in response to scGnRHs appeared to correspond to variations in steroidogenic enzymes, as observed, for example, for 17β-estradiol levels which appeared lower for 100 nM *Sc*GnRH3 than for 100 nM *Sc*GnRH2, in agreement with the increase in *17βHSD2* proteins observed only with 100 nM *Sc*GnRH3.

Thirteen other steroids than estrone and 17β-estradiol were assayed, and the non-significative differences in abundance observed might suggest that other reactions in steroid and cholesterol metabolism could be modulated. These steroids have been previously assayed in cultures of testicular explants or isolated cysts in *S. canicula* (Sourdaine et al., 1990; Sourdaine and Garnier, 1993) and in plasma of other chondrichthyans, including also corticosteroids (for review: Becerril-García et al., 2020). The fact that GnRHs act directly on gonadal tissue to stimulate steroidogenesis has previously been observed in the female skate *Raja erinacea* (Callard et al., 1993) and in other species, where GnRHs stimulated testicular testosterone release with an order of magnitude of about 2-fold in boar (Desaulniers et al., 2015), and stimulated spermiogenesis with an increase of spermatozoid number in zebrafish (Fallah et al., 2020).

Among other proteins whose levels increased in response to *Sc*GnRH treatments, we noted the Growth Hormone receptor (GHR) protein whose mRNA levels were localized in spermatogonia and Sertoli cells. This result is in agreement with an expression of *ghr* gene in the testis of the shark *S. torazame* (Hara et al., 2018), and of the rainbow trout, (Gomez et al., 1998), in testis germ cells of the Japanese eels (Miura et al., 2011), in spermatogonia of the rooster (Harvey et al., 2004) and in Sertoli cells of the rat (Hull and Harvey, 2000). The increase in ScGHR protein levels is also consistent with the strong interconnection between the GH/IGF-1 pathway and gonadal hormones characterized in the testis (Tenuta et al., 2021). This

suggests that the crosstalk between the neuroendocrine gonadotropic and somatotropic axes may be evolutionarily ancient, as early as in elasmobranchs. Furthermore, the GH is also produced locally in the testes of the sharks *S. torazame* (Hara et al., 2018) and *S. canicula* (Mayeur et al., 2024), by the Sertoli cells of the Japanese eel (Miura et al., 2011), as well as by Sertoli and Leydig cells in humans, where GH is thought to generate paracrine and autocrine signals involved in both spermatogenesis and steroidogenesis (Tenuta et al., 2021).

In conclusion, our study completed the data on GnRHs and GnRHRs in elasmobranchs and showed that GnRH may have a direct endocrine role in testis regulation. Using an omics-based without *a priori* approach, we observed that GnRH could promote spermiogenesis and modulate steroidogenesis, notably increasing estradiol synthesis and/or release.

**Table 1.** Concentrations (pg/mL/mg tissue) of steroids in culture media of testicular explants treated with GnRH2 or GnRH3.

| Steroids | Abbreviation | GnRH 0 nM | GnRH 2 10 nM | GnRH 2 100 nM | GnRH 3 10 nM | GnRH 3 100 nM |
|---|---|---|---|---|---|---|
| Pregnenolone | Preg | 63.9 ± 12.0 | 20.2 ± 2.5 | 42.0 ± 5.2 | 54.4 ± 6.8 | 15.6 ± 2.0 |
| Progesterone | Prog | 68.0 ± 5.5 | 83.5 ±3.3 | 82.7 ± 6.6 | 62.9 ± 4.3 | 61.9 ± 3.4 |
| 17α-hydroxyprogesterone | 17OHProg | 26.2 ± 2.5 | 30.8 ± 1.1 | 28.0 ± 3.8 | 31.2 ± 2.7 | 28.1 ± 3.5 |
| 4-androstenedione | A4 | 31.7 ± 1.5 | 35.5 ± 2.4 | 36.6 ± 3.0 | 31.8 ± 1.0 | 35.1 ± 2.0 |
| Testosterone | T | 25.3 ± 1.4 | 22.4 ± 0.8 | 21.6 ± 1.5 | 22.4 ± 1.1 | 29.3 ± 4.0 |
| *11-ketotestosterone* | *11-KT* | 6.7 ± 0.9 | n.d. | *9.8 ± 1.5* | n.d. | *7.0 ± 1.0* |
| **Estrone** | **E1** | **13.7 ± 0.4** | **14.1 ± 1.7** | **13.1 ± 0.6**** | **12.6 ± 1.6** | **14.9 ± 2.2** |
| Estrone 3-sulfate | E1S | 2.5 ± 0.38 | 1.6 ± 0.2 | 2.2 ± 0.3 | 1.8 ± 0.3 | 1.9 ± 0.1 |
| **17β-estradiol** | **E2** | **2.0 ± 0.5** | **5.2 ± 1.0*** | **7.3 ± 1.6**** | **3.4 ± 0.8** | **4.7 ± 0.9**** |
| 11-deoxycorticosterone | DOC | 21.6 ± 2.8 | 22.1 ± 2.7 | 22.4 ± 2.9 | 21.6 ± 3.0 | 21.4 ± 0.6 |
| Corticosterone | B | 5.6 ± 0.8 | 6.3 ± 0.8 | 5.5 ± 0.8 | 7.0 ± 1.0 | 10.8 ± 1.9 |
| *Cortisone* | *E* | *24.1 ± 4.1* | *9.3 ± 1.4* | n.d. | *9.1 ± 1.6* | n.d. |
| Aldosterone | Aldo | 28.8 ± 1.8 | 26.3 ± 3.3 | 26.3 ± 1.6 | 25.4 ± 3.4 | 25.6 ± 1.2 |
| Dehydroepiandrosterone | DHEA | 27.4 ± 3.8 | 36.0 ± 7.1 | 32.8 ± 5.6 | 17.4 ± 3.1 | 34.7 ± 7.6 |
| Dehydroepiandrosterone sulfate | DHEAS | 128.6 ± 10.8 | 113.2 ± 9.7 | 115.1 ± 10.1 | 110.5 ± 12.6 | 112.0 ± 9.9 |

Concentrations of 15 different steroids in culture media of testicular explants at spermiogenesis stages treated with ScGnRH. Steroids were assayed by LC-MS/MS. Statistical analysis was performed using Mann-Whitney U test. n.d.: not detected (Steroid concentration below the sensitivity of the assay). * P<0.05; **P<0.005

## Associated content

### Supporting information

Supplementary figures corresponding to the 5sRNA validation as reference gene (Fig. S1), molecular phylogeny of gnathostome GnRHs and GnRHRs (Fig. S2), control associated to ISH on *S. canicula* testicular section targeting *gnrhrI1* and *gnrhrIIb2* transcripts (Fig. S3) and *ghr*, *17ϐhsd3* and *17ϐhsd12* (Fig. S4). Supplementary tables corresponding to the primers used for real-time PCR and *in situ* hybridization (Table S1) and details of all steroids assayed from cultured explant media (Table S2).

## Author information

### Corresponding author

**Pascal Sourdaine** – Université de Caen Normandie, MNHN, SU, UA, CNRS, IRD, Laboratoire de Biologie des Organismes et Ecosystèmes Aquatiques (BOREA), UMR 8067, 14032 Caen cedex 5, France; orcid.org/0000-0001-9811-2876; Email: pascal.sourdaine@unicaen.fr

### Authors

**Fabian Jeanne** - Université de Caen Normandie, MNHN, SU, UA, CNRS, IRD, Laboratoire de Biologie des Organismes et Ecosystèmes Aquatiques (BOREA), UMR 8067, 14032 Caen cedex 5, France; Email : fabian.jeanne@unicaen.fr

**Stanislas Pilet** - Université de Caen Normandie, MNHN, SU, UA, CNRS, IRD, Laboratoire de Biologie des Organismes et Ecosystèmes Aquatiques (BOREA), UMR 8067, 14032 Caen cedex 5, France

**Benoît Bernay** - Université de Caen Normandie – Plateforme PROTEOGEN, US EMerode, 14032 Caen cedex 5, France; orcid.org/0000-0002-3624-1514; Email: benoit.bernay@unicaen.fr

**Sylvie Dufour** – Université de Caen Normandie, MNHN, SU, UA, CNRS, IRD, Laboratoire de Biologie des Organismes et Ecosystèmes Aquatiques (BOREA), UMR 8067, 14032 Caen cedex 5, France; orcid.org/0000-0002-8646-4935; Email: sylvie.dufour@mnhn.fr

**Stéphanie Lagadu** – Université de Caen Normandie, 14032 Caen cedex 5, France; Email: stephanie.daon@unicaen.fr

**Raphaël Delépée** – Université de Caen Normandie, INSERM, CCC Baclesse, ANTICIPE, UMR 1086, US PLATON, Plateforme PRISMM, 14032 Caen cedex 5, France; orcid.org/0000-0002-9894-1268; Email: raphael.delepee@unicaen.fr

**Notes**

The authors declare no competing financial interest.

**Acknowledgments**

The authors are grateful to Didier Leroy from the CGFS (Channel Ground Fish Survey) campaign (IFREMER in the East Manche in September 2022) for providing the catsharks, and to Frédérique Guyon of the “Centre de Recherches en Environnement Côtier” (Luc sur Mer, France) for the care given to the animals. The following are thanked for funding: University of Caen Normandy (F.J.’s PhD grant), European Regional Development Fund (Operational Program ERDF/ESF 2014-2020) under the project “Manche 2021 – Plateformes d’exploitation de ressources marines”, Région Normandie under the project “Emergent−CauSy”. UHPLC-MS/MS equipment was acquired as part of the Equip'innov Caen 2022 project - PRISMM V2.0 sub-project, co-financed by the European Union, the Normandy Region as part of the ERDF/ESF 2014-2020 operational program and by the French State, as part of the 2015-2020 State-Bas-Normandy Region Plan Contract.

**References**

Abraham, E., Palevitch, O., Gothilf, Y., Zohar, Y., 2010. Targeted Gonadotropin-Releasing Hormone-3 Neuron Ablation in Zebrafish: Effects on Neurogenesis, Neuronal Migration, and Reproduction. Endocrinology 151, 332–340. https://doi.org/10.1210/en.2009-0548

Becerril-García, E.E., Arellano-Martínez, M., Bernot-Simon, D., Hoyos-Padilla, E.M., Galván-Magaña, F., Godard-Codding, C., 2020. Steroid hormones and chondrichthyan reproduction:

physiological functions, scientific research, and implications for conservation. PeerJ 8, e9686. https://doi.org/10.7717/peerj.9686

Bindea, G., Mlecnik, B., Hackl, H., Charoentong, P., Tosolini, M., Kirilovsky, A., Fridman, W.-H., Pagès, F., Trajanoski, Z., Galon, J., 2009. ClueGO: a Cytoscape plug-in to decipher functionally grouped gene ontology and pathway annotation networks. Bioinformatics 25, 1091–1093. https://doi.org/10.1093/bioinformatics/btp101

Bjelobaba, I., Janjic, M.M., Tavcar, J.S., Kucka, M., Tomić, M., Stojilkovic, S.S., 2016. The relationship between basal and regulated Gnrhr expression in rodent pituitary gonadotrophs. Molecular and Cellular Endocrinology 437, 302–311. https://doi.org/10.1016/j.mce.2016.08.040

Bosseboeuf, A., Gautier, A., Auvray, P., Mazan, S., Sourdaine, P., 2014. Characterization of spermatogonial markers in the mature testis of the dogfish (Scyliorhinus canicula L.). Reproduction 147, 125–139. https://doi.org/10.1530/REP-13-0316

Callard, G.V., Pudney, J.A., Mak, P., Canick, J.A., 1985. Stage-Dependent Changes in Steroidogenic Enzymes and Estrogen Receptors during Spermatogenesis in the Testis of the Dogfish, Squalus acanthias*. Endocrinology 117, 1328–1335. https://doi.org/10.1210/endo-117-4-1328

Callard, T.J., Fileti, L.A., Koob, T.J., 1993. Ovarian steroid synthesis and the hormonal control of the elasmobranch reproductive tract. Environ Biol Fishes 175–185. https://doi.org/10.1007/978-94-017-3450-9_16

Chianese, R., Ciaramella, V., Scarpa, D., Fasano, S., Pierantoni, R., Meccariello, R., 2012. Anandamide regulates the expression of GnRH1, GnRH2, and GnRH-Rs in frog testis. Am J Physiol Endocrinol Metab 303, E475–E487. https://doi.org/10.1152/ajpendo.00086.2012

Ciani, E., Fontaine, R., Maugars, G., Nourizadeh-Lillabadi, R., Andersson, E., Bogerd, J., Von Krogh, K., Weltzien, F.-A., 2020. Gnrh receptor gnrhr2bbα is expressed exclusively in lhb-expressing cells in Atlantic salmon male parr. General and Comparative Endocrinology 285, 113293. https://doi.org/10.1016/j.ygcen.2019.113293

Ciaramella, V., Chianese, R., Pariante, P., Fasano, S., Pierantoni, R., Meccariello, R., 2015. Expression Analysis of Gnrh1 and Gnrhr1 in Spermatogenic Cells of Rat. Int J Endocrinol 2015, 1–8. https://doi.org/10.1155/2015/982726

D'antonio, M., Vallarino, M., Lovejoy, D.A., Vandesande, F., King, J.A., Pierantoni, R., Peter, R.E., 1995. Nature and distribution of gonadotropin-releasing hormone (GnRH) in the brain, and GnRH and GnRH binding activity in serum of the spotted dogfish Scyliorhinus canicula. Gen Comp Endocrinol 98, 35–49. https://doi.org/10.1006/gcen.1995.1042

Desaulniers, A.T., Cederberg, R.A., Mills, G.A., Ford, J.J., Lents, C.A., White, B.R., 2015. LH-Independent Testosterone Secretion Is Mediated by the Interaction Between GNRH2 and Its Receptor Within Porcine Testes. Biol Reprod 93. https://doi.org/10.1095/biolreprod.115.128082

Dubois, E.A., Zandbergen, M.A., Peute, J., Goos, H.J., 2002. Evolutionary development of three gonadotropin-releasing hormone (GnRH) systems in vertebrates. BRB 57, 413–418. https://doi.org/10.1016/S0361-9230(01)00676-1

Dufour, S., Quérat, B., Tostivint, H., Pasqualini, C., Vaudry, H., Rousseau, K., 2020. Origin and Evolution of the Neuroendocrine Control of Reproduction in Vertebrates, With Special Focus on Genome and Gene Duplications. Physiol Rev 100, 869–943. https://doi.org/10.1152/physrev.00009.2019

Fallah, H.P., Rodrigues, M.S., Corchuelo, S., Nóbrega, R.H., Habibi, H.R., 2020. Role of GnRH Isoforms in Paracrine/Autocrine Control of Zebrafish (Danio rerio) Spermatogenesis. Endocrinology 161, bqaa004. https://doi.org/10.1210/endocr/bqaa004

Fischer, R., Kessler, B.M., 2015. Gel-aided sample preparation (GASP)—A simplified method for gel-assisted proteomic sample generation from protein extracts and intact cells. Proteomics 15, 1224–1229. https://doi.org/10.1002/pmic.201400436

Flanagan, C.A., Chen, C.-C., Coetsee, M., Mamputha, S., Whitlock, K.E., Bredenkamp, N., Grosenick, L., Fernald, R.D., Illing, N., 2007. Expression, Structure, Function, and Evolution of Gonadotropin-Releasing Hormone (GnRH) Receptors GnRH-R1SHS and GnRH-R2PEY in the Teleost, Astatotilapia burtoni. Endocrinology 148, 5060–5071. https://doi.org/10.1210/en.2006-1400

Forlano, P.M., Maruska, K.P., Sower, S.A., King, J.A., Tricas, T.C., 2000. Differential Distribution of Gonadotropin-Releasing Hormone-Immunoreactive Neurons in the Stingray Brain: Functional and Evolutionary Considerations. General and Comparative Endocrinology 118, 226–248. https://doi.org/10.1006/gcen.2000.7467

Gaillard, A.-L., Tay, B.-H., Pérez Sirkin, D.I., Lafont, A.-G., De Flori, C., Vissio, P.G., Mazan, S., Dufour, S., Venkatesh, B., Tostivint, H., 2018. Characterization of Gonadotropin-Releasing Hormone (GnRH) Genes From Cartilaginous Fish: Evolutionary Perspectives. Front. Neurosci. 12, 607. https://doi.org/10.3389/fnins.2018.00607

García-Salinas, P., Gallego, V., Asturiano, J.F., 2021. Reproductive Anatomy of Chondrichthyans: Notes on Specimen Handling and Sperm Extraction. I. Rays and Skates. Animals 11, 1888. https://doi.org/10.3390/ani11071888

Gautron, J., 1978. Effet du calcium et de la stimulation sur les terminaisons nerveuses des fonctions nerf-électroplaque de la Torpille. Biol. Cell. 31, 31–44. https://doi.org/10.1007/BF00495387

Gilligan, L.C., Rahman, H.P., Hewitt, A.-M., Sitch, A.J., Gondal, A., Arvaniti, A., Taylor, A.E., Read, M.L., Morton, D.G., Foster, P.A., 2017. Estrogen Activation by Steroid Sulfatase Increases Colorectal Cancer Proliferation via GPER. The Journal of Clinical Endocrinology & Metabolism 102, 4435–4447. https://doi.org/10.1210/jc.2016-3716

Giraldo, C., Le Roy, D., Martin-Baillet, V., 2022. CGFS2022 cruise, RV Thalassa. https://doi.org/10.17600/18001842

Gomez, J.M., Loir, M., Le Gac , F. 1998. Growth hormone receptors in testis and liver during the spermatogenetic cycle in rainbow trout (Oncorhynchus mykiss). Biology of Reproduction 58, 483-491.

Gribouval, L., Sourdaine, P., Lareyre, J.-J., Bellaiche, J., Le Gac, F., Mazan, S., Guiardiere, C., Auvray, P., Gautier, A., 2018. The nanos1 gene was duplicated in early Vertebrates and the two paralogs show different gonadal expression profiles in a shark. Sci Rep 8, 6942. https://doi.org/10.1038/s41598-018-24643-1

Gu, Z., Eils, R., Schlesner, M., 2016. Complex heatmaps reveal patterns and correlations in multidimensional genomic data. Bioinformatics 32, 2847–2849. https://doi.org/10.1093/bioinformatics/btw313

Hara, Y., Yamaguchi, K., Onimaru, K., Kadota, M., Koyanagi, M., Keeley, S.D., Tatsumi, K., Tanaka, K., Motone, F., Kageyama, Y., Nozu, R., Adachi, N., Nishimura, O., Nakagawa, R., Tanegashima, C., Kiyatake, I., Matsumoto, R., Murakumo, K., Nishida, K., Terakita, A., Kuratani, S., Sato, K., Hyodo, S., Kuraku, S., 2018. Shark genomes provide insights into elasmobranch evolution and the origin of vertebrates. Nat Ecol Evol 2, 1761–1771. https://doi.org/10.1038/s41559-018-0673-5

Harvey, S., Baudet, M.-L., Murphy, A., Luna, M., Hull, K.L., Aramburo, C., 2004. Testicular growth hormone (GH): GH expression in spermatogonia and primary spermatocytes. General and Comparative Endocrinology 139, 158–167. https://doi.org/10.1016/j.ygcen.2004.08.002

Hull, K.L., Harvey, S., 2000. Growth Hormone: Roles in Male Reproduction. Endocrine 13, 243–250. https://doi.org/10.1385/ENDO:13:3:243

Irisarri, I., Baurain, D., Brinkmann, H., Delsuc, F., Sire, J.-Y., Kupfer, A., Petersen, J., Jarek, M., Meyer, A., Vences, M., Philippe, H., 2017. Phylotranscriptomic consolidation of the jawed vertebrate timetree. Nat Ecol Evol 1, 1370–1378. https://doi.org/10.1038/s41559-017-0240-5

Janjic, M.M., Prévide, R.M., Fletcher, P.A., Sherman, A., Smiljanic, K., Abebe, D., Bjelobaba, I., Stojilkovic, S.S., 2019. Divergent expression patterns of pituitary gonadotropin subunit and GnRH receptor genes to continuous GnRH in vitro and in vivo. Scientific Reports 9, 20098. https://doi.org/10.1038/s41598-019-56480-1

Jeanne, F., Bernay, B., Sourdaine, P., 2023. Comparative Proteome Analysis of Four Stages of Spermatogenesis in the Small-Spotted Catshark (Scyliorhinus canicula), Using High-Resolution NanoLC-ESI-MS/MS. J Proteome Res 22, 2477–2492. https://doi.org/10.1021/acs.jproteome.3c00206

Jin, C., Yan, K., Wang, M., Song, W., Wang, B., Men, Y., Niu, J., He, Y., Zhang, Q., Qi, J., 2024. Dissecting the dynamic cellular transcriptional atlas of adult teleost testis development

throughout the annual reproductive cycle. Development 151, dev202296. https://doi.org/10.1242/dev.202296

Kanda, S., 2019. Evolution of the regulatory mechanisms for the hypothalamic-pituitary-gonadal axis in vertebrates–hypothesis from a comparative view. Gen Comp Endocrinol 284, 113075. https://doi.org/10.1016/j.ygcen.2018.11.014

Knowles, F., Vollrath, L., Meurling, P., 1975. Cytology and neuroendocrine relations of the pituitary of the dogfish, Scyliorhinus canicula. Proceedings of the Royal Society of London. Series B. Biological Sciences 191, 507–525. https://doi.org/10.1098/rspb.1975.0141

Lemoine, F., Correia, D., Lefort, V., Doppelt-Azeroual, O., Mareuil, F., Cohen-Boulakia, S., Gascuel, O., 2019. NGPhylogeny.fr: new generation phylogenetic services for non-specialists. Nucleic Acids Research 47, 260–265. https://doi.org/10.1093/nar/gkz303

Letunic, I., Bork, P., 2021. Interactive Tree Of Life (iTOL) v5: an online tool for phylogenetic tree display and annotation. Nucleic Acids Research 49, 293–296. https://doi.org/10.1093/nar/gkab301

Levavi-Sivan, B., Avitan, A., 2005. Sequence analysis, endocrine regulation, and signal transduction of GnRH receptors in teleost fish. General and Comparative Endocrinology 142, 67–73. https://doi.org/10.1016/j.ygcen.2005.01.019

Li, W., Du, R., Xia, C., Zhang, H., Xie, Y., Gao, X., Ouyang, Y., Yin, Z., Hu, G., 2022. Novel pituitary actions of GnRH in teleost: The link between reproduction and feeding regulation. Front. Endocrinol. 13, 982297. https://doi.org/10.3389/fendo.2022.982297

Livak, K.J., Schmittgen, T.D., 2001. Analysis of Relative Gene Expression Data Using Real-Time Quantitative PCR and the 2−ΔΔCT Method. Methods 25, 402–408. https://doi.org/10.1006/meth.2001.1262

Loir, M., Sourdaine, P., 1994. Testes cells: isolation and culture. In: Hochachka PW, Mommsen TP (eds) Biochemistry and molecular biology of fishes: analytical techniques. New York, pp. 219–272.

Loir, M., Sourdaine, P., Mendis-Handagama, S.M.L.C., Jégou, B., 1995. Cell-cell interactions in the testis of teleosts and elasmobranchs. Microsc. Res. Tech. 32, 533–552. https://doi.org/10.1002/jemt.1070320606

Lovejoy, D.A., Fischer, W.H., Ngamvongchon, S., Craig, A.G., Nahorniak, C.S., Peter, R.E., Rivier, J.E., Sherwood, N.M., 1992. Distinct sequence of gonadotropin-releasing hormone (GnRH) in dogfish brain provides insight into GnRH evolution. Proc. Natl. Acad. Sci. U.S.A. 89, 6373–6377. https://doi.org/10.1073/pnas.89.14.6373

Luu-The, V., Tremblay, P., Labrie, F., 2006. Characterization of Type 12 17β-Hydroxysteroid Dehydrogenase, an Isoform of Type 3 17β-Hydroxysteroid Dehydrogenase Responsible for Estradiol Formation in Women. Molecular Endocrinology 20, 437–443. https://doi.org/10.1210/me.2005-0058

Manca, R., Glomski, C., Pica, A., 2019. Hematopoietic stem cells debut in embryonic lymphomyeloid tissues of elasmobranchs. European Journal of Histochemistry 63. https://doi.org/10.4081/ejh.2019.3060

Marra, N.J., Stanhope, M.J., Jue, N.K., Wang, M., Sun, Q., Pavinski Bitar, P., Richards, V.P., Komissarov, A., Rayko, M., Kliver, S., Stanhope, B.J., Winkler, C., O'Brien, S.J., Antunes, A., Jorgensen, S., Shivji, M.S., 2019. White shark genome reveals ancient elasmobranch adaptations associated with wound healing and the maintenance of genome stability. PNAS 116, 4446–4455. https://doi.org/10.1073/pnas.1819778116

Mayeur, H., Leyhr, J., Mulley, J., Leurs, N., Michel, L., Sharma, K., Lagadec, R., Aury, J.-M., Osborne, O.G., Mulhair, P., Poulain, J., Mangenot, S., Mead, D., Smith, M., Corton, C., Oliver, K., Skelton, J., Betteridge, E., Dolucan, J., Dudchenko, O., Omer, A.D., Weisz, D., Aiden, E.L., McCarthy, S., Sims, Y., Torrance, J., Tracey, A., Howe, K., Baril, T., Hayward, A., Martinand-Mari, C., Sanchez, S., Haitina, T., Martin, K., Korsching, S.I., Mazan, S., Debiais-Thibaud, M., 2024. The sensory shark: high-quality morphological, genomic and transcriptomic data for the small-spotted catshark Scyliorhinus canicula reveal the molecular bases of sensory organ evolution in jawed vertebrates. bioRxiv. https://doi.org/10.1101/2024.05.23.595469

Miao, D.Z., Liu, C., Deng, Z.Y., Zhang, C., Guo, Z.Y., Li, W.Q., Wang, Y., Yang, H.M., Wang, Z.Y., 2024. Characterization of reproductive hormones and related gene expression in the

hypothalamus and pituitary gland in the egg-laying interval in White King pigeon. Poultry Science 103, 103422. https://doi.org/10.1016/j.psj.2024.103422

Miura, C., Shimizu, Y., Uehara, M., Ozaki, Y., Young, G., Miura, T. 2011. Gh is produced by the testis of Japanese eel and stimulates proliferation of spermatogonia. Reproduction, 142 869–877. DOI: 10.1530/REP-11-0203

Muñoz-Baquero, M., Marco-Jiménez, F., García-Domínguez, X., Ros-Santaella, J.L., Pintus, E., Jiménez-Movilla, M., García-Párraga, D., García-Vazquez, F.A., 2021. Comparative Study of Semen Parameters and Hormone Profile in Small-Spotted Catshark (Scyliorhinus canicula): Aquarium-Housed vs. Wild-Captured. Animals 11, 2884. https://doi.org/10.3390/ani11102884

Ogawa, S., Yamamoto, N., Hagio, H., Oka, Y., Parhar, I.S., 2022. Multiple gonadotropin-releasing hormone systems in non-mammalian vertebrates: Ontogeny, anatomy, and physiology. J Neuroendocrinol 34, e13068. https://doi.org/10.1111/jne.13068

Osugi, T., Ubuka, T., Tsutsui, K., 2014. Review: evolution of GnIH and related peptides structure and function in the chordates. Front. Neurosci. 8. https://doi.org/10.3389/fnins.2014.00255

Pudney, J., Callard, G.V., 1984b. Development of agranular reticulum in Sertoli cells of the testis of the dogfishSqualus acanthias during spermatogenesis. Anat Rec 209, 311–321. https://doi.org/10.1002/ar.1092090309

Pudney, J., Callard, G.V., 1984a. Identification of Leydig-like cells in the testis of the dogfish Squalus acanthias. Anat. Rec. 209, 323–330. https://doi.org/10.1002/ar.1092090310

Read, T.D., Petit, R.A., Joseph, S.J., Alam, Md.T., Weil, M.R., Ahmad, M., Bhimani, R., Vuong, J.S., Haase, C.P., Webb, D.H., Tan, M., Dove, A.D.M., 2017. Draft sequencing and assembly of the genome of the world's largest fish, the whale shark: Rhincodon typus Smith 1828. BMC Genomics 18, 532. https://doi.org/10.1186/s12864-017-3926-9

Redon, E., Bosseboeuf, A., Rocancourt, C., Da Silva, C., Wincker, P., Mazan, S., Sourdaine, P., 2010. Stage-specific gene expression during spermatogenesis in the dogfish (Scyliorhinus canicula). Reproduction 140, 57–71. https://doi.org/10.1530/REP-10-0021

Roch, G.J., Busby, E.R., Sherwood, N.M., 2014. GnRH receptors and peptides: Skating backward. General and Comparative Endocrinology 209, 118–134. https://doi.org/10.1016/j.ygcen.2014.07.025

Roch, G.J., Busby, E.R., Sherwood, N.M., 2011. Evolution of GnRH: Diving deeper. Gen Comp Endocrinol 171, 1–16. https://doi.org/10.1016/j.ygcen.2010.12.014

Santiago-Andres, Y., Golan, M., Fiordelisio, T., 2021. Functional Pituitary Networks in Vertebrates. Front. Endocrinol. 11, 619352. https://doi.org/10.3389/fendo.2020.619352

Schang, A.-L., Ngô-Muller, V., Bleux, C., Granger, A., Chenut, M.-C., Loudes, C., Magre, S., Counis, R., Cohen-Tannoudji, J., Laverrière, J.-N., 2011. GnRH Receptor Gene Expression in the Developing Rat Hippocampus: Transcriptional Regulation and Potential Roles in Neuronal Plasticity. Endocrinology 152, 568–580. https://doi.org/10.1210/en.2010-0840

Schefe, J.H., Lehmann, K.E., Buschmann, I.R., Unger, T., Funke-Kaiser, H., 2006. Quantitative real-time RT-PCR data analysis: current concepts and the novel "gene expression's C T difference" formula. Journal of Molecular Medicine 84, 901–910. https://doi.org/10.1007/s00109-006-0097-6

Sherwood, N.M., Lovejoy, D.A., 1993. Gonadotropin-releasing hormone in cartilaginous fishes: structure, location, and transport In: Demski, L.S., Wourms, J.P. (eds) The reproduction and development of sharks, skates, rays and ratfishes. Developments in environmental biology of fishes, vol 14. Springer, Dordrecht. https://doi.org/10.1007/978-94-017-3450–9_18.

Sourdaine, P., Garnier, D.H., 1993. Stage-dependent modulation of Sertoli cell steroid production in dogfish (Scyliorhinus canicula). Reproduction 97, 133–142. https://doi.org/10.1530/jrf.0.0970133

Sourdaine, P., Garnier, D.H., Jégou, B., 1990. The adult dogfish (Scyliorhinus canicula L.) testis: a model to study stage-dependent changes in steroid levels during spermatogenesis. J Endocrinol 127, 451–460. https://doi.org/10.1677/joe.0.1270451

Spicer, O.S., Wong, T.-T., Zmora, N., Zohar, Y., 2016. Targeted Mutagenesis of the Hypophysiotropic Gnrh3 in Zebrafish (Danio rerio) Reveals No Effects on Reproductive Performance. PLoS ONE 11, e0158141. https://doi.org/10.1371/journal.pone.0158141

Tanaka, H., Baba, T., 2005. Gene expression in spermiogenesis. CMLS Cellular and Molecular Life Sciences 62, 344–354. https://doi.org/10.1007/s00018-004-4394-y

Tello, J.A., Wu, S., Rivier, J.E., Sherwood, N.M., 2008. Four functional GnRH receptors in zebrafish: analysis of structure, signaling, synteny and phylogeny. Integrative and Comparative Biology 48, 570–587. https://doi.org/10.1093/icb/icn070

Tenuta, M., Carlomagno, F., Cangiano, B., Kanakis, G., Pozza, C., Sbardella, E., Isidori, A.M., Krausz, C., Gianfrilli, D., 2021. Somatotropic-Testicular Axis: A crosstalk between GH/IGF-I and gonadal hormones during development, transition, and adult age. Andrology 9, 168–184. https://doi.org/10.1111/andr.12918

Tsutsui, K., Ubuka, T., 2021. Gonadotropin-inhibitory hormone (GnIH): A new key neurohormone controlling reproductive physiology and behavior. Front Neuroendocrinol 61, 100900. https://doi.org/10.1016/j.yfrne.2021.100900

Venkatesh, B., Lee, A.P., Ravi, V., Maurya, A.K., Lian, M.M., Swann, J.B., Ohta, Y., Flajnik, M.F., Sutoh, Y., Kasahara, M., Hoon, S., Gangu, V., Roy, S.W., Irimia, M., Korzh, V., Kondrychyn, I., Lim, Z.W., Tay, B.-H., Tohari, S., Kong, K.W., Ho, S., Lorente-Galdos, B., Quilez, J., Marques-Bonet, T., Raney, B.J., Ingham, P.W., Tay, A., Hillier, L.W., Minx, P., Boehm, T., Wilson, R.K., Brenner, S., Warren, W.C., 2014. Elephant shark genome provides unique insights into gnathostome evolution. Nature 505, 174–179. https://doi.org/10.1038/nature12826

Wang, A.F., Li, J.H., Maiti, K., Kim, W.P., Kang, H.M., Seong, J.Y., Kwon, H.B., 2003. Preferential ligand selectivity of the monkey type-II gonadotropin-releasing hormone (GnRH) receptor for GnRH-2 and its analogs. Molecular and Cellular Endocrinology 209, 33–42. https://doi.org/10.1016/j.mce.2003.08.004

Wang, L., Bogerd, J., Choi, H.S., Seong, J.Y., Soh, J.M., Chun, S.Y., Troskie, B.E., Millar, R.P., Yu, W.H., McCann, S.M., Kwon, H.B., 2001. Three distinct types of GnRH receptor characterized in the bullfrog. Proceedings of the National Academy of Sciences 98, 361–366. https://doi.org/10.1073/pnas.98.1.361

Wang, Q., Arighi, C.N., King, B.L., Polson, S.W., Vincent, J., Chen, C., Huang, H., Kingham, B.F., Page, S.T., Farnum Rendino, M., Thomas, W.K., Udwary, D.W., Wu, C.H., the North East Bioinformatics Collaborative Curation Team, 2012. Community annotation and bioinformatics

workforce development in concert - Little Skate Genome Annotation Workshops and Jamborees. Database 2012, bar064. https://doi.org/10.1093/database/bar064

Williams, B.L., Akazome, Y., Oka, Y., Eisthen, H.L., 2014. Dynamic evolution of the GnRH receptor gene family in vertebrates. BMC Evolutionary Biology 14, 215. https://doi.org/10.1186/s12862-014-0215-y

Ye, J., Coulouris, G., Zaretskaya, I., Cutcutache, I., Rozen, S., Madden, T.L., 2012. Primer-BLAST: A tool to design target-specific primers for polymerase chain reaction. BMC Bioinformatics 13, 1–11. https://doi.org/10.1186/1471-2105-13-134

# Annexes Chapitre IV

## I. Annexes chapitre IV : Données supplémentaires

**Supplementary material**

**Characterization of a direct endocrine role of GnRHs in testicular regulation in the small-spotted catshark *Scyliorhinus canicula*: a GnRH signaling in the control of spermiogenesis and steroidogenesis in early gnathostomes**

Fabian Jeanne[1], Stanislas Pilet[1], Benoît Bernay[2], Stéphanie Lagadu[3], Raphaël Delépée[3], Sylvie Dufour[1], and Pascal Sourdaine*[1]

[1] Université de Caen Normandie, MNHN, SU, UA, CNRS, IRD, Laboratoire de Biologie des Organismes et Ecosystèmes Aquatiques (BOREA), UMR 8067, 14032 Caen cedex 5, France.

[2] Université de Caen Normandie - Plateforme PROTEOGEN, US EMerode, 14032 Caen cedex 5, France.

[3] INSERM U1086 "ANTICIPE" Unité de Recherche Interdisciplinaire pour la Prévention et le Traitement des Cancers, Centre de Lutte Contre le Cancer Francois Baclesse, 3 Av. Général Harris, 14076 CAEN cedex 05, France.

*Corresponding Author: orcid.org/0000-0001-9811-2876; Email: pascal.sourdaine@unicaen.fr

**Table S1.** List of the primers used for real-time PCR and *in situ* hybridization

| Primer names | Experimentation | Sequence |
|---|---|---|
| S.ca-GnRH1-RT | RT-qPCR | 5'-GTCGCAACCAGACAAGCTC-3'; 5'-AGTCCCTCGCAAACAATCAG-3' |
| S.ca-GnRH2-RT | RT-qPCR | 5'- CGCTCTTCCTGATCTTTCTGC-3'; 5'-GCATCAACATATCAGTCACAATGC-3' |
| S.ca-GnRH3-RT | RT-qPCR | 5'- ACTGGTCTCATGGTTGGCTG-3'; 5'-TGTCTGGGATATAGGCTGGAG-3' |
| S.ca-GnRHRI1-RT | RT-qPCR | 5'-TCATCCCTCTATTCATCATGCTG-3'; 5'-CCAGCTCCATCATACTGTTATC-3' |
| S.ca-GnRHRIIA1-RT | RT-qPCR | 5'-CTCCAAGGTCAGGGTAGTCG-3'; 5'-TCACGATGAAAGTCACCAGC-3' |
| S.ca-GnRHRIIA2-RT | RT-qPCR | 5'-ACGGCCACCCAGAATCG-3'; 5'-ATGAGCAGCCGACAGGC-3' |
| S.ca-GNRHRIIb2-RT | RT-qPCR | 5'-AAGGAAACAGAGCAAGAGCAC-3'; 5'-TCCTTCAGTATTCCCGGCTTG-3' |
| S.ca-GHR-RT | RT-qPCR | 5'-GCGAATTCAGCAGCTTCCAG-3'; 5'-GCTGCGATTTACTGCCATCG-3' |
| S.ca-HSD17b3-RT | RT-qPCR | 5'-GAAATTGGGCAAGCCACAGG-3'; 5'-ATGCCAACGTTGTTCACCAG-3' |
| S.ca- HSD17b2-RT | RT-qPCR | 5'-GGCTGGACTCGAAATTGGTG-3'; 5'-TCCACCATAGCAGGCAACAC-3' |
| S.ca-5SRNA-RT | RT-qPCR | 5'-TCGTCTGATCTCGGAAGCTA-3'; 5'-AGCCTACTGCACCTGGTATTC-3' |
| S.ca-GnRHRI1-ISH | *in situ* hybridization | 5'- GAATCACGCGTTAGGTTGCTG-3'; 5'-CGGCCCAGCTCCATCATAC-3' |
| S.ca-GnRHRIIb2-ISH | *in situ* hybridization | 5'-TTCGCCGTGTCCATGTTCAG-3'; 5'-CTGTAAGAGGCGTGACATAC-3' |
| S.ca-GHR-ISH | *in situ* hybridization | 5'- GCGAATTCAGCAGCTTCCAG-3'; 5'-GACGTGTAGGCGTTGTCTGA-3' |
| S.ca- HSD17b3-ISH | *in situ* hybridization | 5'-GAAATTGGGCAAGCCACAGG-3'; 5'-TCCCAGGCATAACACGTGAC-3' |
| S.ca- HSD17b12-ISH | *in situ* hybridization | 5'GGCTGGACTCGAAATTGGTG -3'; 5'-CCCATTACAGCATGTGGCAG-3' |

**Table S2.** Data on steroids assayed by LC-HRMS

| Analyte | ESI mode | LOQ (ng/mL) | MRM precursor (m/z) | MRM product ion (m/z) | Collision energy (V) |
|---|---|---|---|---|---|
| Cortisone (E) | + | 0.5 | 360.95 | 163.1086 (283.1665) | -27 (-23) |
| Aldosterone (Aldo) | + | 0.2 | 361.2 | 343.1859 (315.1923) | -18 (-22) |
| 11-ketotestosterone (11-KT) | + | 0.02 | 303.09 | 121.0630 (259.1657) | -31 (-31) |
| Estrone (E1) | - | 0.02 | 269.08 | 145.0654 (143.0499) | 49 (80) |
| 17β-estradiol (E2) | - | 0.02 | 271.09 | 145.0657 (183.0814) | 51 (52) |
| Cortisone (B) | + | 0.5 | 347.1 | 329.2058 (121.0629) | -17 (-23) |
| Testosterone (T) | + | 0.01 | 289.11 | 97.0626 (109.0628) | -28 (-41) |
| Dehydroepiandrosterone (DHEA) | + | 0.2 | 271 | 253.1905 (213.1624) | -11 (-11) |
| 11-deoxycorticosterone (DOC) | + | 0.1 | 331.06 | 96.0629 (109.0627) | -26 (-26) |
| 17α-hydroxyprogesterone (17OHProg) | + | 0.1 | 331.05 | 109.0631 (97.0631) | -29 (-24) |
| 4-androstenedione (A4) | + | 0.02 | 287.1 | 97.0625 (109.0625) | -23 (-27) |
| Pregnenolone (Preg) | + | 2 | 299.05 | 281.2350 (161.1307) | -19 (-24) |
| Progesterone (Prog) | + | 0.2 | 315.08 | 97.0629 (109.0630) | -24 (-47) |
| Estrone 3-sulfate (E1S) | - | 0.02 | 349.09 | 269.1542 (145.0659) | 51 (52) |
| Dehydroepiandrosterone sulfate (DHEAS) | - | 0.02 | 367.14 | 96.9595 (79.9570) | 71 (100) |

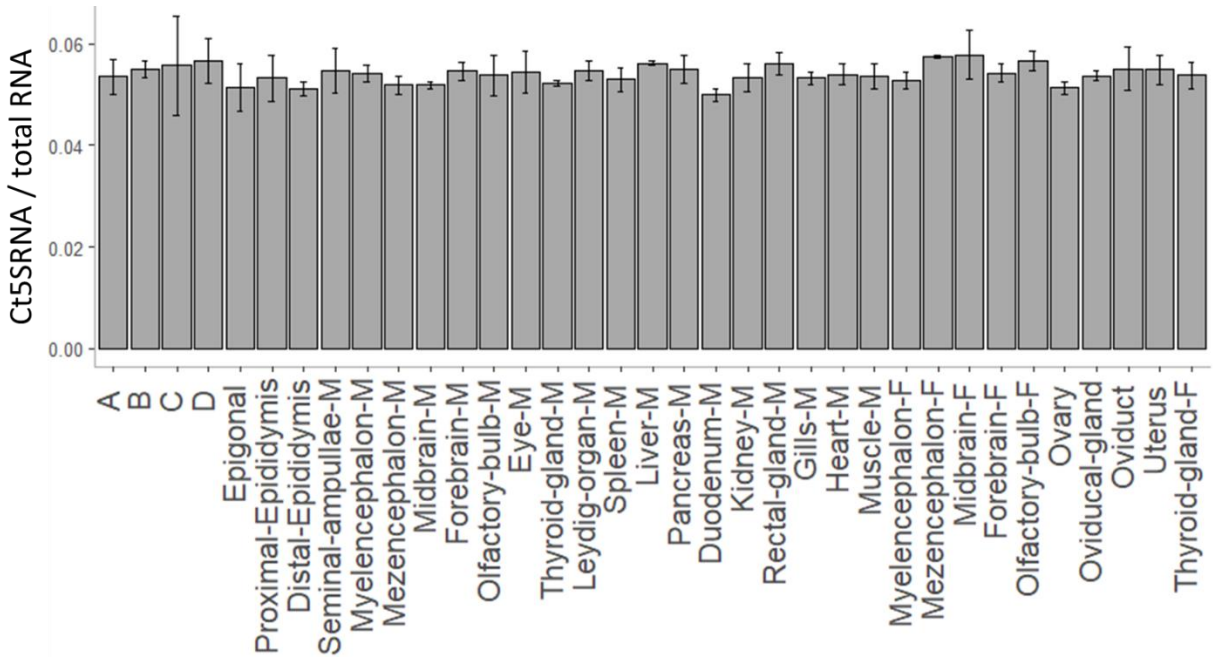


**Fig. S1**. Validation of the 5sRNA as reference gene for the real-time PCR. Statistical analysis was performed using the non-parametric Kruskal-Wallis (based on the previous Shapiro-wilk test results) test for (P-value = 0.24).

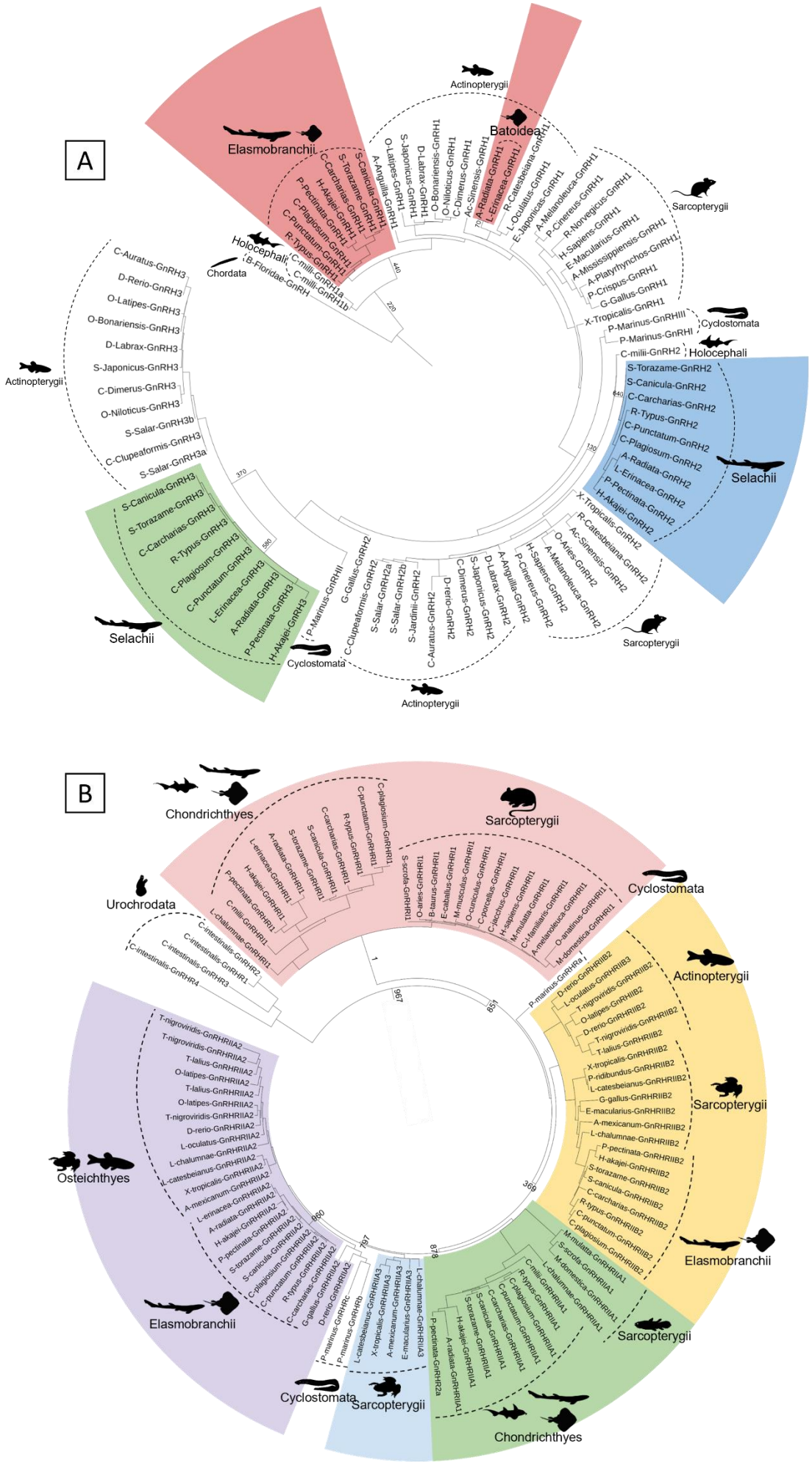
A
Actinopterygii
Elasmobranchii
Batoidea
Sarcopterygii
Holocephali
Chordata
Cyclostomata
Selachii
B
Chondrichthyes
Sarcopterygii
Cyclostomata
Urochrodata
Actinopterygii
Osteichthyes
Elasmobranchii
Sarcopterygii
Cyclostomata
Sarcopterygii
Chondrichthyes

**Fig. S2.** Molecular phylogeny of gnathostomes GnRHs and GnRHRs. A. Identified elasmobranch GnRH1s, GnRH2s and GnRH3s are highlighted in red, blue and green respectively. B. The six GnRHR subfamilies are represented, including GnRHR1I (red), GnRHRIIA1 (green), GnRHRIIA2 (purple), GnRHRIIA3 (blue), GnRHRIIB2 and GnRHRIIB3 (yellow). In elasmobranchs, four GnRHRs were identified including GnRHR1I, GnRHRIIA1, GnRHRIIA2 and GnRHRIIB2 homologs. Support values shown for relevant node are bootstraps. Animal illustrations are used with permission from http://phylopic.org.

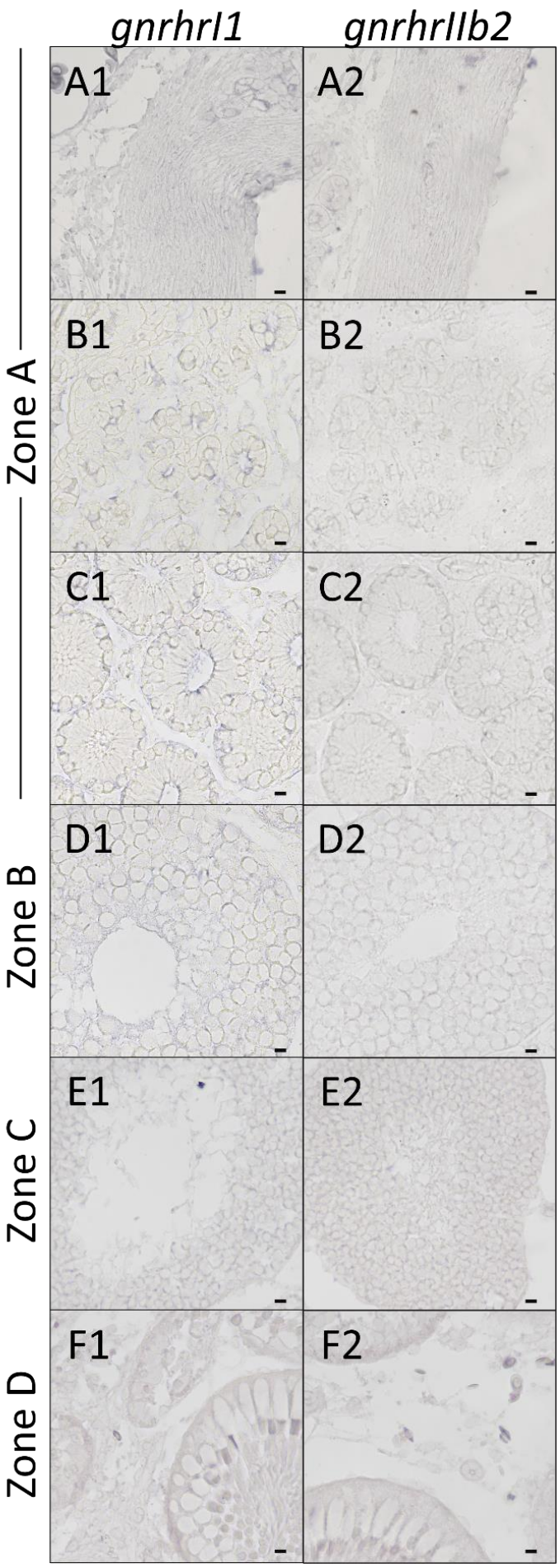
gnrhrI1
gnrhrIIb2
A1
A2
B1
B2
C1
C2
D1
D2
E1
E2
F1
F2
Zone A
Zone B
Zone C
Zone D

**Fig. S3.** *In situ* hybridization controls were performed using sense riboprobes of *gnrhrI1* (A1-F1) and *gnrhrIIb2* (A2-F2). (A), germinative area; (B), cysts in formation; (C), cysts with spermatogonia; (D), cysts with spermatocytes; (E), cysts with young spermatids; (F), cysts with late spermatids. No significant background was revealed. Scale bars: 10 µm.

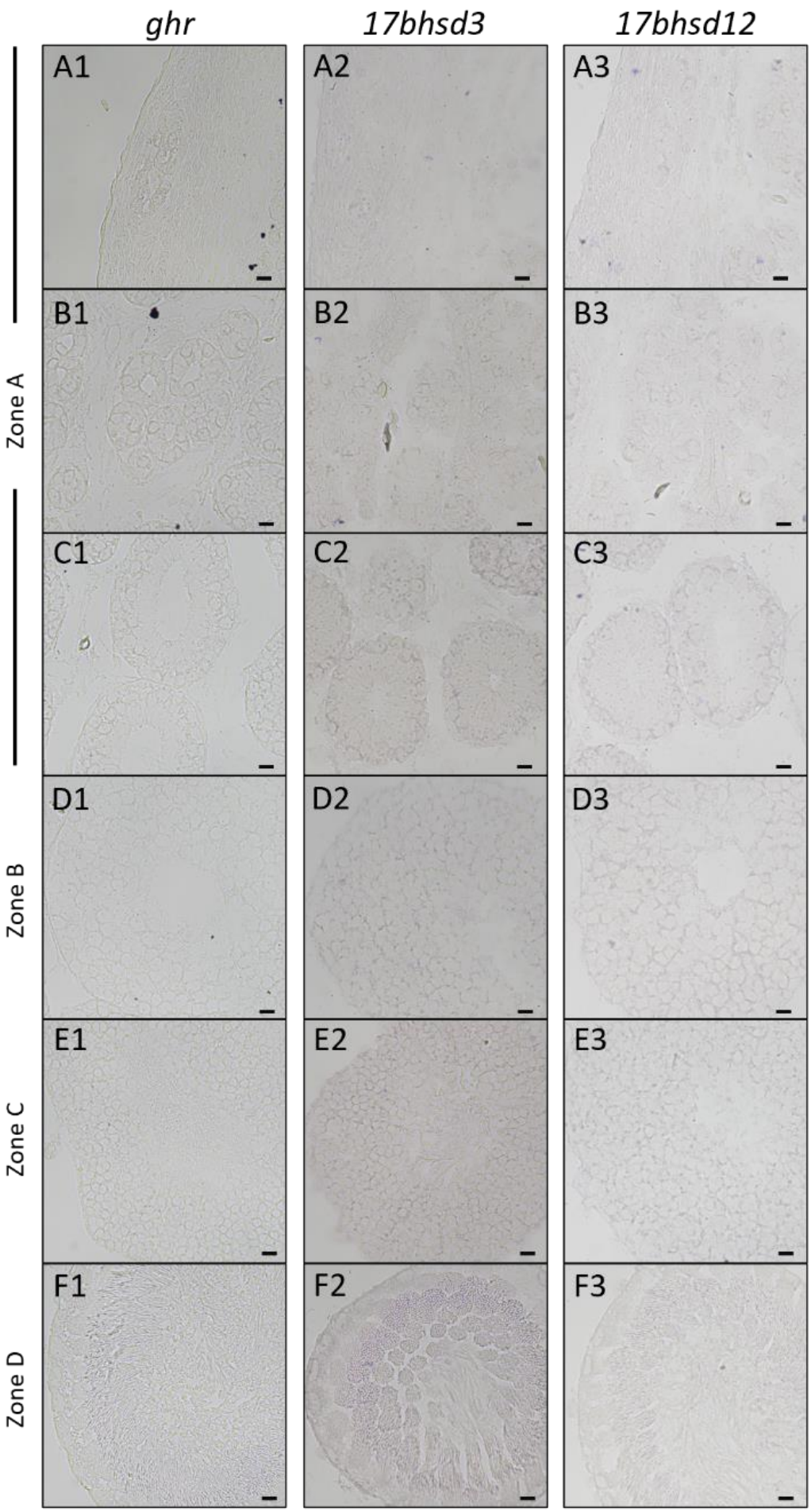
ghr
17bhsd3
17bhsd12
A1
A2
A3
B1
B2
B3
C1
C2
C3
D1
D2
D3
E1
E2
E3
F1
F2
F3
Zone A
Zone B
Zone C
Zone D

**Fig. S4.** *In situ* hybridization controls were performed using sense riboprobes of *ghr* (A1-F1), *17βhsd3* (A2-F2) and *17βhsd12* (A3-F3). (A), germinative area; (B), cysts in formation; (C), cysts with spermatogonia; (D), cysts with spermatocytes; (E), cysts with young spermatids; (F), cysts with late spermatids. *In situ* hybridization revealed no important background noise. Scale bars: 10 µm.

# Discussion générale et perspectives

# Discussion générale et perspectives

# Discussion générale et perspectives

Le clade des Vertébrés cartilagineux (chimères, raies et requins) n'a pas fait l'objet de beaucoup d'études ces dernières décennies, malgré leur intérêt évolutif, leur physiologie unique et la crise massive d'extinction qu'ils subissent. Par conséquent, les processus les plus fondamentaux de leurs cycles de vie restent largement inexplorés, ce qui inclut le processus de reproduction. Ce travail de thèse avait pour objectif d'explorer les régulations endocrines et paracrines exercées par les acteurs de l'axe hypothalamo-hypophyso-ganodique et les hormones glycoprotéiques GPA2 et GPB5 sur la spermatogenèse chez un modèle Élasmobranche, la petite roussette *Scyliorhinus canicula*. L'ensemble des résultats obtenus sera discuté selon deux principaux axes : la régulation de la spermatogenèse chez *S. canicula* et l'insertion d'un modèle Élasmobranche dans l'histoire évolutive des systèmes endocrines chez les Vertébrés, ce qui comble partiellement le fossé des connaissances à la base de l'arbre phylogénétique des Gnathostomes.

## II. Caractérisation de processus moléculaires et de voies de signalisation au cours de la spermatogenèse chez *S. canicula*

Le testicule est l'organe qui exprime le plus grand nombre de gènes enrichis au niveau tissulaire (Djureinovic et al., 2014) et des efforts sont actuellement déployés pour caractériser les fonctions de ces gènes (Vandenbrouck et al., 2020). Dans ce but, l'analyse des expressions spécifiques aux types cellulaires et dépendantes des stades spermatogénétiques est fondamentale pour caractériser les événements se déroulant au cours de la spermatogenèse. Dans ce contexte, la caractérisation de processus moléculaires et de voies de signalisation au niveau du testicule de *S. canicula* présente des intérêts du fait de sa position phylogénétique unique à la racine des Gnathostomes (Irisarri et al., 2017) et de la possession des répertoires de gènes régulant l'homéostasie et la reproduction (Hara et al., 2018).

Lors de l'analyse protéomique sans *a priori* des différents stades de la spermatogenèse chez la roussette (Chapitre 1), quatre voies de signalisation ont été analysées plus en détail sur la base des résultats d'ontologie ou de leur importance présumée au cours de la spermatogenèse. Ces voies étaient celles du protéasome, de la protéolyse ubiquitine

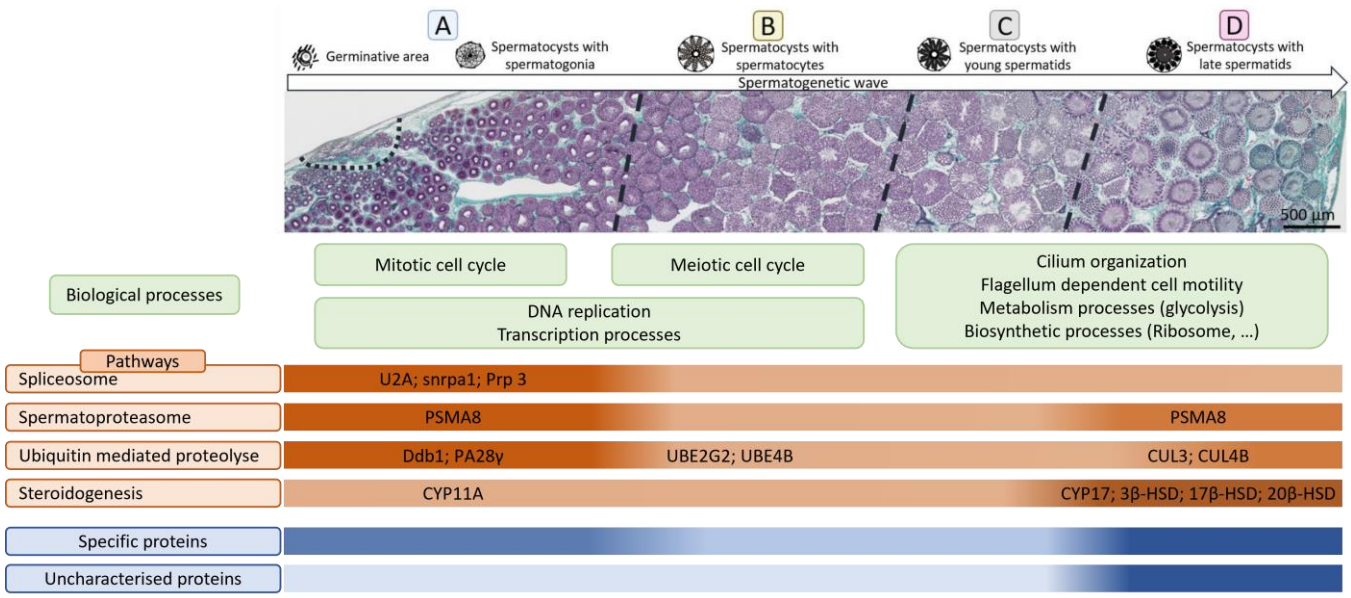


Fig. 31 **Représentation schématique de la dynamique de plusieurs processus biologiques et voies de signalisation au cours de la spermatogenèse de *S. canicula*.** En haut figure une coupe histologique transversale colorée d'un testicule de *S. canicula*. Les principales annotations fonctionnelles sont illustrées en vert. Le nombre et le niveau d'abondance des protéines pour les quatre voies de signalisations caractérisées sont représentés par un gradient de couleur (avec une couleur plus foncée correspondant à un nombre de protéines et des abondances plus forts). Les acteurs protéiques d'intérêt sont illustrés dans les zones où ils sont les plus abondants. L'abondance des protéines est représentée par un gradient de couleur (avec une couleur plus foncée correspondant à un nombre plus important de protéines).

dépendante, du splicéosome et de la stéroïdogenèse.

Au niveau de la zone A, où se produit 13 cycles de division mitotique des spermatogonies indifférenciées et différenciées (Bosseboeuf et al., 2014), notre étude a mis en évidence des processus biologiques en accord avec l'activité mitotique tels la réplication de l'ADN, le cycle cellulaire mitotique et une forte activité transcriptionnelle (Fig. 31). Cette dernière a notamment été illustrée par le splicéosome qui est impliqué dans l'épissage des ARNm et qui joue un rôle dans l'auto-renouvellement des cellules souches spermatogoniales et la différenciation des spermatogonies, notamment au travers des acteurs U2A/snrpa1 (Wu et al., 2016) et Prp 3 (Chen et al., 2019; Qin et al., 2023). Par ailleurs, un large répertoire d'acteurs impliqués dans différents processus moléculaires et voies de signalisation ont présenté des abondances plus importantes en zone A. Parmi ceux-ci, certains présentent un intérêt particulier comme la sous-unité α4s (PSMA8) caractéristique du spermatoprotéasome (particule s20S) qui, en ciblant les composants du complexe synaptonémal, régulerait la méiose des spermatocytes primaires chez la souris (Gómez-H et al., 2019; Živković et al., 2022) et PSMA8 serait également impliquée dans la dégradation des histones lors de la réparation de l'ADN des spermatocytes (Zhang et al., 2021). Cette expression précoce au niveau de la zone A, correspondant aux cystes à spermatogonies et non à spermatocytes, pose la question de cette expression précoce qui pourrait être en prévision du stade suivant ou suggérer un rôle du spermatoprotéasome lors de la prolifération mitotique des spermatogonies ; ce qui reste à explorer. D'autres protéines retrouvées en abondance dans la zone A sont impliquées dans la protéolyse médiée par l'ubiquitine comme l'adaptateur Ddb1 de CUL4 dont les différents facteurs associés à ce complexe, les facteurs DCAF (*DDB1-CUL4-Associated Factor*), sont exprimés préférentiellement au niveau testiculaire chez différentes espèces (Mistry et al., 2020), seraient importants dans le développement et la fertilité chez le nématode (Durkan et al., 2022) et impacterait la prolifération des gonocytes et la formation de la niche des spermatogonies souches chez les souris avec une invalidation conditionnelle des gènes *Cul4* (*Cul4a* et *Cul4b*) (Yin et al., 2021). De même, l'abondance du régulateur PA28ɣ, également appelé REGɣ ou PSME3, dans la zone A est associé à la régulation de la spermatogenèse chez la souris chez qui l'invalidation de l'expression de PA28ɣ entrainerait une diminution du nombre de spermatogonies PLZF+ (Gao et al., 2019).

Au niveau de la zone B, l'activité méiotique a été mise en évidence avec les processus biologiques liés aux traitements des ARNm, la réplication de l'ADN et le cycle méiotique. Aucun autre acteur n'est apparu majoritairement associé à la zone B, à l'exception des ligases d'ubiquitine UBE2G2 et UBE4B, associées respectivement à E2 et E3, qui restent peu étudiées mais qui présentent des niveaux d'abondance différents au niveau du testicule d'hommes subfertiles pour UBE2G2 (Laqqan and Hammadeh, 2018) ou une surexpression dans les spermatides allongées de souris (M. Li et al., 2020), pour UBE4B.

Concernant les zones C et D, correspondant aux stades précoces et tardifs de la spermiogenèse, les processus biologiques mis en évidence illustrent le développement et l'activité du flagelle des spermatides. De plus, en zone C, un nombre important de processus métaboliques et de biosynthèses ont été mis en évidence ce qui est en accord avec le remodelage cellulaire profond qui se produit pendant la spermiogenèse. Par ailleurs, comme pour la zone A, c'est également au niveau de la zone D qu'ont été retrouvés un plus large répertoire et une plus forte abondance d'acteurs impliqués dans différents processus moléculaires et voies de signalisation. Ainsi, il a été mis en évidence : le métabolisme du glucose, qui est l'une des principales voies de production d'ATP dans les spermatozoïdes (Amaral, 2022) ; de nombreuses protéines associées au protéasome en cohérence avec le rôle de ce dernier dans la maturation et la réponse au stress oxydatif des spermatozoïdes (Dietrich et al., 2019; Huang et al., 2016) ; les ligases d'ubiquitine CUL3 et CUL4B, associées à E3, en accord avec le profil de CUL3 chez la souris (Richburg et al., 2014) et le rôle de CUL4B au cours de la spermatogenèse (Yin et al., 2021) où l'invalidation de l'expression germinale de *Cul4b* entraine des anomalies dans la structure du flagelle (Yin et al., 2016).

Ce travail s'inscrit dans la continuité de la caractérisation et de l'étude de l'évolution moléculaire de la spermatogenèse chez les Vertébrés, comme précédemment étudié chez les primates et les amniotes par Murat et al., 2023. Notre étude a mis en évidence une forte conservation de certains processus biologiques et voies de signalisation au niveau des stades mitotiques (Zone A) et méiotiques (Zone B). Ces résultats sont en accord avec le faible taux d'évolution de l'expression génique au niveau des spermatogonies et des spermatocytes chez les amniotes (Murat et al., 2023), ce qui suggère une mise en place précoce des profils d'expressions géniques à ces stades. Notre étude a également montré que les nombres les plus élevés de protéines spécifiques à une zone ont été trouvés dans les zones A et D,

correspondant aux étapes fondamentales de la spermatogenèse contrôlant la phase d'amplification cellulaire qui déterminera le nombre final de gamètes produits (zone A) et contrôlant l'étape finale de différenciation et de libération des gamètes (zone D). Ces deux étapes correspondent à des traits variables d'une espèce à l'autre, tels que le taux de production de spermatozoïdes et la morphologie des spermatozoïdes. De plus, le plus grand nombre de protéines non caractérisées a été trouvé dans la zone D et il est intéressant de le mettre en relation avec le fait que l'évolution du testicule a été guidée, au moins en partie, par l'émergence de nouveaux gènes associés à la spermiogenèse (Murat et al., 2023).

En ce qui concerne la mise en évidence des enzymes de la stéroïdogenèse, qui sera discutée plus loin, il a été observé une abondance de CYP11A dans la zone A, suggérant une synthèse préférentielle de prégnénolone dans cette zone, et une abondance des autres enzymes au niveau de la zone D telles la 3β-HSD, CYP17, la 17β-HSD et la 20β-HSD, suggérant une synthèse préférentielle de la 17α-20β-dihydroxyprogestérone (DHP) et de la testostérone dans cette zone.

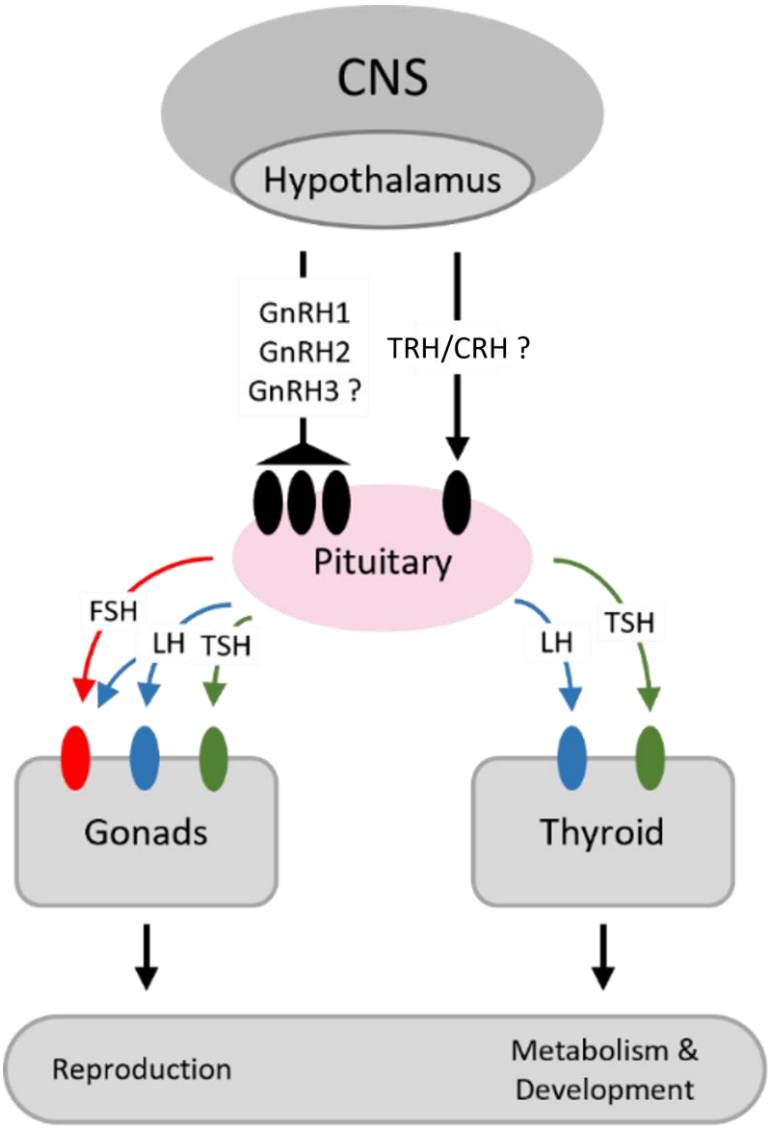


Fig. 32 **Représentation schématique des axes neuroendocrines chez la roussette *S. canicula*.** CNS, système nerveux central ; FSH, hormone folliculostimulante ; GnRH, hormone de libération des gonadotrophines ; LH, hormone lutéinisante ; TRH, thyréolibérine; TSH, thyréotrophine; TSHR, récepteur à la thyréotrophine.

## III. Les axes hypothalamo-hypophyso-gonadique et hypothalamo-hypophyso-thyroïdien chez *S. canicula*, une lacune comblée dans l'histoire évolutive des Vertébrés

Ce travail de thèse a caractérisé et exploré les fonctions des acteurs de l'axe hypothalamo-hypophyso-gonadique (HHG) et hypothalamo-hypophyso-thyroïdien (HHT) chez *S. canicula*. Ainsi, l'identification des GnRHs et de leurs récepteurs (GnRHRs) (Chapitre IV), des sous-unités des hormones glycoprotéiques (GPHs) gonadotropes (GtHs) (CGA, FSHβ et LHβ) et thyréotrope (TSHβ) et de leurs récepteurs respectifs FSHR et LHR (Chapitre II) et TSHR (Chapitre III) et des sous-unités ancestrales (GPA2 et GPB5) (Chapitre III) a été effectuée chez plusieurs Élasmobranches. Pris dans leur ensemble, nos résultats mettent en évidence la présence d'un axe hypothalamo-hypophyso-gonadique chez *S. canicula* (Fig. 32), dont l'étude avait débuté cinquante ans plus tôt avec la purification d'une fraction gonadotrope à partir du lobe ventral de l'hypophyse chez *S. canicula* (Sumpter et al., 1978). Bien que l'étude de l'axe hypothalamo-hypophyso-thyroïdien n'était pas un sujet central de notre thèse, il a été exploré du fait de l'appartenance de la TSH aux GPHs et de la possible interaction de la thyrostimuline (GPA2/GPB5) avec TSHR et dans le cadre de la différenciation des axes HHG et HHT à la base de l'arbre phylogénétique des Vertébrés.

D'un point de vue évolutif, les axes HHG et HHT les plus primitifs ont été identifiés chez les Cyclostomes (Sower, 2018). En effet, chez ces derniers, trois GnRHs ont été identifiées et la GnRH hypophysiotrope diffuserait de l'hypothalamus vers l'hypophyse (Gorbman, 1995; Sower, 2015). De plus, des administrations de lGnRHI et lGnRHIII stimulent l'expression hypophysaire de *gphβ* ou *gphβ*, *gpa2* et *gpb5*, respectivement, les gènes *cga*, *fshβ* et *lhβ* étant absent chez les Cyclostomes (Hausken et al., 2018). Ces résultats suggèrent une action hypophysiotrope des GnRHs de Lamproie, une caractéristique qui a été conservée chez tous les Gnathostomes (Sower, 2018). Chez les Élasmobranches, les GnRHs hypothalamiques seraient sécrétées dans la circulation générale pour stimuler le lobe ventral de l'hypophyse, en l'absence d'innervation ou de vascularisation directe depuis l'hypothalamus (D'antonio et

al., 1995; Knowles et al., 1975; Sherwood and Lovejoy, 1993). Dans notre étude, l'identification

de trois GnRHs (GnRH1, GnRH2 et GnRH3) et de quatre GnRHRs (GnRHRI1, GnRHRIIb2, GnRHRIIa1 et GnRHRIIa2) est en accord avec les précédentes identifications chez *S. canicula, S. torazame* et *R. typus* (Gaillard et al., 2018; Hara et al., 2018). De même, les niveaux d'expression retrouvés dans nos travaux, avec une expression plus importante des *gnrh1, gnrh2, gnrhrIIa1*, *gnrhrIIa2*, *gnrhrIIb2* au niveau de la partie du cerveau moyen comprenant le diencéphale et une partie du mésencéphale (que nous avons appelé *midbrain* dans nos publications) suggèrent une expression des *gnrhs* au niveau hypothalamique et des *gnrhrs* au niveau de l'hypophyse de *S. canicula* et sont en accord avec les résultats précédemment obtenus (Gaillard et al., 2018; Hara et al., 2018). Chez les Ostéichtyens, la diffusion du GnRH hypothalamique serait limitée à la communication hypothalamo-hypophysaire par le système porte *via* l'éminence médiane, comme observé chez les Tétrapodes, ou *via* une innervation directe, comme observé chez les Téléostéens (Gorbman, 1995; Sower, 2015). Pris dans leur ensemble, ces résultats suggèrent la mise en place progressive d'une spécialisation du rôle des GnRHs dans la communication hypothalamo-hypophysaire pour réguler la production d'hormones gonadotropes. En parallèle, deux autres systèmes neuronaux GnRH-dépendants se sont mis en place avec le système GnRH2 mésencéphalique et le système GnRH3 du nerf terminal, présents ou absents selon les clades de Vertébrés (Dubois et al., 2002). Les niveaux d'expression de *gnrh2*, au niveau du myélencéphale et du mésencéphale, et de *gnrh3*, au niveau du cerveau antérieur, que nous avons observé chez *S. canicula* suggèrent que ces deux systèmes sont en place chez les Élasmobranches, ce qui est en accord avec des résultats précédents (Gaillard et al., 2018).

Ancestralement, chez les Protostomiens, les peptides apparentés aux GnRHs sont synthétisés par le système nerveux et possèdent des fonctions associées à la reproduction avec les GnRH-*like* qui induisent, d'une façon directe, la prolifération des cellules germinales précoces (gonies) chez le Gastéropode *Haliotis discus hannai* et le Bivalve *Mizuhopecten yessoensis* (Sakai et al., 2020), et la méiose ovocytaire chez le Malacostracé *Eriocheir sinensis* (Luo et al., 2023). Chez les Pro-chordés, les GnRH-*like* induisent la contraction du corps de *C. intestinalis* responsable de la libération des gamètes (Terakado, 2001) ou la croissance et la maturation ovarienne chez la cione *Ciona robusta* (Osugi et al., 2017). Depuis quelques années, une

thématique émergente se concentre sur le rôle paracrine des GnRHs au niveau des gonades chez les Vertébrés. En effet, il a été mis en évidence une expression testiculaire des *gnrh* et *gnrhr* chez le verrat (Desaulniers et al., 2015) et le poisson zèbre (Fallah et al., 2020). Chez ces derniers, l'action paracrine des GnRHs augmente la sécrétion de testostérone chez le verrat et le nombre de spermatogonies indifférenciées et de spermatozoïdes chez le poisson zèbre. Chez *S. canicula,* notre étude a mis en évidence qu'un traitement par la GnRH2 et la GnRH3 d'explants testiculaires pourrait avoir un impact sur la spermiogenèse et modulerait la stéroïdogenèse, notamment la synthèse et/ou la sécrétion d'œstradiol, ce qui est en accord avec une étude antérieure qui a montré que la GnRH stimule la stéroïdogenèse de l'ovaire de la raie *Leucoraja erinacea* (Callard et al., 1993). Une expression plus faible des *gnrhr* a également été observée au niveau des autres stades de la spermatogenèse, de l'épididyme et des ampoules séminales, ce qui suggère un rôle plus large, qui reste à être caractérisé, des GnRHs dans la fertilité mâle.

Pris dans leur ensemble, ces données suggèrent que le rôle régulateur direct qu'exerce la GnRH sur la reproduction était présent chez l'ancêtre commun des Bilatériens et qu'il a été maintenu chez les Protostomiens et les Deutérostomiens. Chez les Vertébrés, en parallèle de l'acquisition de l'axe HHG, la GnRH circulante des Élasmobranches aurait gardé une fonction de régulation directe des gonades qui aurait été remplacé, en l'absence de GnRH circulante, par une expression gonadique paracrine des *gnrhs* chez les Vertébrés osseux. Il y aurait donc un double rôle de la GnRH circulante chez *S. canicula* avec un rôle direct sur la modulation des gonades et un rôle indirect *via* l'axe HHG, ce qui constituerait un système unique aux Élasmobranches. Cela pose cependant la question des fonctions spécifiques ou de la redondance du rôle de la GnRH dans la régulation de la fonction testiculaire en plus des régulations par les hormones gonadotropes, voire par la thyréostimuline.

Comme mentionné précédemment, notre analyse fragmentaire de l'axe hypothalamo-hypophyso-thyroïdien nous a permis de montrer la perte du gène *tshβ1,* alors que le *tshβ2* a été maintenu, chez les Élasmobranches. Ce résultat souligne la divergence entre l'holocéphale *C. milii*, qui possède *tshβ1* et *tshβ2*, et les Élasmobranches mais aussi avec les Ostéichthyens, où seul *tshβ1* a été maintenu (Buechi and Bridgham, 2017; Maugars et al., 2014), à l'exception des dipneustes et du cœlacanthe qui ont conservé les deux gènes (Dos Santos et al., 2011;

Dufour et al., 2020; Maugars et al., 2014). Nos résultats ont également mis en évidence une expression de *tshβ2* au niveau du cerveau moyen (*midbrain*), une expression de *tshr* au niveau de l'épithélium folliculaire thyroïdien et une activation de TSHR par la TSH en système *in vitro* (Fig. 32). Ces résultats sont en accord avec les données obtenues chez *S. torazame* (Hara et al., 2018) qui avaient également présenté une expression du *trh* et des *trhr* au niveau de l'hypothalamus et de l'hypophyse, respectivement. Ces résultats permettent d'étayer la présence d'un axe hypothalamo-hypophyso-thyroïdien chez les Élasmobranches. Le rôle de la TSH sur la production et la sécrétion des hormones thyroïdiennes, la thyroxine (T4) et la triiodothyronine (T3), reste à être caractérisé.

Chez les Cyclostomes, la différenciation des axes HHG et HHT reste partielle au regard de l'absence d'hormones gonadotropes et thyréotropes différenciées, une hormone glycoprotéine commune (lGPH) étant présente en plus de la thyrostimuline (GPA2/GPB5) (Sower, 2018). Chez la lamproie, les deux récepteurs lGpH-RI et lGpH-RII sont exprimés au niveau testiculaire et thyroïdien (Freamat et al., 2006; Freamat and Sower, 2008) et peuvent être activés par GPA2-GPB5 et GPA2-GPHβ, pour lGpH-RI, ou seulement GPA2-GPB5, pour lGpH-RII (Hausken et al., 2018) ; ce qui suggère la présence d'une régulation appariée des fonctions métaboliques et de reproduction médiées par GPA2-GPB5 et GPA2-GPHβ (Sower, 2018). Chez *S. canicula*, les axes HHG et HHT possèderaient une organisation intermédiaire comprise entre le système plus primitif des Cyclostomes et celui des Sarcoptérygiens. En effet, la principale innovation évolutive observée chez les Vertébrés cartilagineux est l'acquisition des gènes codants pour les hormones gonadotropes (FSH et LH) et thyréotrope (TSH) en plus de leurs récepteurs associés (FSHR, LHR et TSHR), une diversité de gènes qui a été maintenue chez tous les Gnathostomes (Buechi and Bridgham, 2017). Chez *S. canicula*, nous avons montré que la TSH active spécifiquement le TSHR, comme chez l'holocéphale C. milii (Buechi and Bridgham, 2017), suggérant que la spécificité de l'interaction TSH-TSHR aurait été acquise chez l'ancêtre commun des Gnathostomes. En plus d'une action de la TSH sur la thyroïde, une régulation directe des fonctions gonadiques peut être envisagée du fait de l'expression testiculaire du TSHR chez *S. canicula*, expression qui a également été observé au niveau des gonades de Vertébrés osseux (Bhat et al., 2017; Rocha et al., 2007; Sun et al., 2010; Yang et al., 2024). Nos résultats ont également montré que le TSHR pouvait être activé par

l'hétérodimère recombinant scGPB5-scGPA2 (voir plus loin), ce qui pose encore une fois la question des fonctions spécifiques ou de la redondance des hormones glycoprotéiques dans la régulation de la fonction testiculaire chez les Élasmobranches.

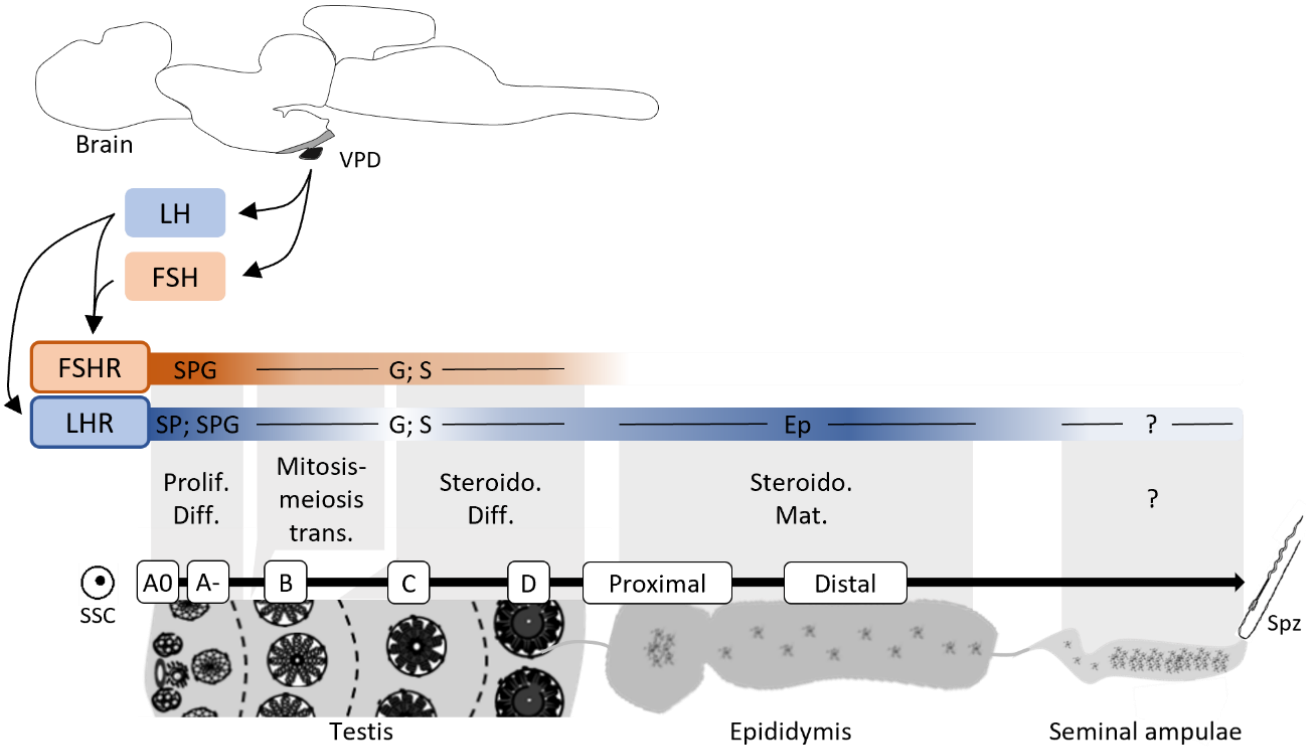


Fig. 33 **Représentation schématique de l'axe hypophyso-tractus génital mâle chez *S. canicula*.** Les niveaux d'ARNm de *fshr* et *lhr* sont représentés par un gradient de couleur orange et bleu, respectivement, où les couleurs plus foncées correspondent aux plus fortes abondances. Les localisations des expressions sont notées à l'intérieur des gradients de couleurs correspondant. A0, zone contenant la zone germinative ; A-, zone contenant les cystes à spermatogonies différenciées ; B, zone contenant les cystes à spermatocytes ; C, zone contenant les cystes à spermatides rondes ; D, zone contenant les cystes à spermatides allongées ; Diff., différenciation ; Ep, cellules épithéliales épididymaires ; FSH, hormone folliculostimulante ; FSHR, récepteur à l'hormone folliculostimulante ; G, cellules germinales ; LH, hormone lutéinisante ; LHR, récepteur à l'hormone lutéinisante ; Mat., maturation ; Prolif., prolifération ; S, cellule de Sertoli ; SP, précurseur somatique ; SPG, spermatogonies indifférenciées et en cours de différenciation ; Spz, spermatozoïdes ; SSC, cellules souches spermatogoniales ; Steroido., stéroïdogenèse ; Trans., transition ; VPD, lobe ventral hypophysaire.

L'analyse de l'expression des récepteurs aux hormones gonadotropes a mis en évidence de fortes expressions de *fshr* et *lhr* au niveau du testicule et de l'ovaire de *S. canicula*, comme précédemment observé chez *S. torazame* (Arimura et al., 2024; Hara et al., 2018). Chez cette dernière espèce, il a été montré récemment que des extraits hypophysaires activeraient FSHR et LHR, renforçant la présence d'un axe HHG fonctionnel chez les requins (Arimura et al., 2024). Au cours de la spermatogenèse de *S. canicula*, *fshr* est exprimé à tous les stades avec une expression majoritaire aux stades précoces avec une première localisation dans les spermatogonies indifférenciées puis dans les cellules de Sertoli, en plus des cellules germinales, dans les cystes formés et correspondant aux stades ultérieurs de la spermatogenèse (Fig. 33). Ces résultats sont cohérents avec l'expression de *FSHR* par les cellules souches spermatogoniales (SSCs), récemment observée chez l'homme et la souris, qui pourrait réguler la différenciation des spermatogonies (Bhartiya et al., 2021; Patel and Bhartiya, 2016). Cette action directe de FSH pourrait être explorée dans notre modèle de culture des SSCs et comparé à l'action du GDNF qui permet le maintien de la pluripotence et de la formation de colonies de cellules souches (Gautier et al., 2014). L'expression sertolienne de FSHR est, quant à elle, en accord avec la fonction indirecte de FSH dans le soutien de la survie des cellules méiotiques et de la spermiogenèse décrite chez les Sarcoptérygiens et les Actinoptérygiens (Huhtaniemi, 2015). Quant à *lhr*, il est majoritairement exprimé aux premiers stades et aux derniers stades de la spermatogenèse avec une localisation au niveau des progéniteurs somatiques, des spermatogonies indifférenciées et des cellules de Sertoli différenciées. Chez les Mammifères, la LH régule la production de stéroïdes par les cellules de Leydig, permettant l'achèvement de la méiose et de la spermiogenèse (Kumar, 2005; Ramaswamy and Weinbauer, 2014). Chez les Actinoptérygiens, un gène *fshr* et deux gènes *lhr* (*lhcgr1* et *lhcgr2*) ont été identifiés (Maugars and Dufour, 2015) et FSHR et LHR2 sont exprimés à la fois dans les cellules de Leydig et les cellules de Sertoli, comme chez *D. rerio*, et les deux gonadotrophines stimulent la production de stéroïdes (García-López et al., 2010; Ohta et al., 2007; Planas, 1995). Chez les poissons téléostéens, la LH est principalement impliquée dans la spermiogenèse et la spermiation (Chu et al., 2015; Xie et al., 2017). L'ensemble de ces données suggère qu'aux stades précoces, la FSH et la LH réguleraient la prolifération et la différentiation des spermatogonies indifférenciées alors que la LH seule régulerait la prolifération et la différenciation des précurseurs somatiques. Une fois les cystes à spermatogonies formés au stade IIIA de la spermatogenèse, *fshr* et *lhr* sont tous les deux

exprimés au niveau des cellules germinales et de Sertoli avec cependant une plus forte expression de *lhr* au niveau des cystes à spermatides âgées, suggérant un rôle potentiellement majoritaire de la LH au niveau de la spermiation. Cependant, l'importance essentielle des hormones gonadotropes en tant que support des différents stades de la spermatogenèse peut être discutée au regard des expériences anciennes de ventralobectomie de l'hypophyse, couplée à une augmentation de la température, qui induisaient un arrêt de la spermatogenèse uniquement au niveau de la transition entre la dernière mitose des spermatogonies et les premiers stades des spermatocytes primaires, ce qui suggère un rôle essentiel des gonadotrophines seulement pour l'entrée en prophase de méiose (Dobson and Dodd, 1977a, 1977b), alors qu'aux autres stades leurs rôles seraient de soutenir une spermatogenèse pleinement quantitative et qualitative.

L'utilisation des protéines recombinantes de roussette dans des tests fonctionnels en culture de cellules mammaliennes nous a permis de montrer que LHR était activé seulement par LH alors que FSHR pouvait être activé par FSH et LH. Cette redondance et/ou compensation fonctionnelle a également été identifiée chez certains poissons téléostéens comme *D. rerio* et *O. latipes* (Burow et al., 2020; Xie et al., 2017). L'activation spécifique de LHR par LH serait une caractéristique retrouvée chez la majorité des Vertébrés osseux (Buechi and Bridgham, 2017), à l'exception de certains poissons téléostéens où LHR peut également être activé par FSH, comme observé chez la truite arc-en-ciel *Oncorhynchus mykiss* (Sambroni et al., 2007), le medaka *Oryzias latipes* (Burow et al., 2020) et *D. rerio* (Xie et al., 2017).

L'expression de *fshr* et *lhr* dans les cellules de Sertoli de *S. canicula* peut être associée au fait qu'en l'absence de cellules de Leydig différenciées, la cellule de Sertoli est considérée comme la cellule stéroïdogène principale chez cette espèce sur la base de ses caractéristiques ultrastructurales et du fait que les cystes isolés ont la capacité de synthétiser des androgènes, comme observé également chez *S. acanthias* (Cuevas et al., 1993; Cuevas and Callard, 1992a; Loir et al., 1995; Sourdaine and Garnier, 1993). Notre analyse protéomique a montré une expression constitutive des enzymes de la stéroïdogenèse, à l'exception de CYP11A, plus élevée au niveau de la zone D ce qui apparait en accord avec des concentrations en androgènes plus élevées retrouvées au niveau de cette zone (Sourdaine et al., 1990) et des cystes isolés correspondants (Sourdaine and Garnier, 1993). L'expression préférentielle de CYP11A au niveau de la zone A suggère une synthèse préférentielle de prégnénolone dans

cette zone alors que les concentrations les plus élevées en progestérone ont été reportées au niveau de la zone D et des cystes correspondants (Sourdaine et al., 1990; Sourdaine and Garnier, 1993). Il y aurait donc un métabolisme des stéroïdes selon l'onde spermatogénétique qui impliquerait des sécrétions et des rétentions différentes selon les stades (Awruch, 2013; Cuevas and Callard, 1992a). En terme de stimulation de la stéroïdogenèse, il a été montré que des extraits du lobe ventral de l'hypophyse, ainsi que l'utilisation d'un analogue de l'AMPc, stimulaient la synthèse des stéroïdes testiculaires (Sourdaine et al., 1990; Sourdaine and Garnier, 1993) et que des extraits hypophysaires activaient FSHR et LHR en système cellulaire *in vitro* (Arimura et al., 2024) *;* ce qui va dans le sens d'une stimulation par les hormones gonadotropes. Cependant, nous avons également montré au cours de cette thèse que des explants de la zone D stimulés par les GnRHs présentaient une augmentation des niveaux de différentes 17βHSD (17βHSD2, 17βHSD3, 17βHSD7 et 17βHSD12), suggérant également une modulation du métabolisme des androgènes par la GnRH circulante.

En plus de l'expression gonadique, nous avons également observé une expression de LHR et de FSHR au niveau des tractus génitaux, laissant supposer l'existence d'un axe hypothalamo-hypophyso-tractus génital chez *S. canicula*. Dans le tractus génital mâle de *S. canicula*, seul *lhr* est exprimé au niveau des cellules épithéliales des épididymes proximale et distale et des ampoules séminales (Fig. 33). Chez les Mammifères, *lhr* est également exprimé dans l'épididyme de plusieurs espèces comme le rat (Shayu and Rao, 2006) ou l'écureuil (Wang et al., 2019), et participe à la régulation de la stéroïdogenèse locale (Lei et al., 2001; Wang et al., 2019), résultant en la mise en place d'un microenvironnement unique et nécessaire à la maturation des spermatozoïdes (James et al., 2020; Johnston et al., 2005). L'épididyme des Élasmobranches peut remplir des fonctions similaires, par la mise en place d'un microenvironnement spécifique impliqué dans l'acquisition de la motilité des spermatozoïdes (Dzyuba et al., 2019; Jones et al., 1984; Minamikawa' and Morisawa, 1996). De manière intéressante, une étude récente sur la raie *Potamotrygon wallacei* a montré l'expression du récepteur à la progestérone dans les cellules épithéliales de l'épididyme et de la glande de Leydig (Morales-Gamba et al., 2023), avec une localisation cellulaire assez similaire à celles que nous avons déterminées pour LHR. Tous ces résultats soulèvent la question du rôle primitif de l'épididyme et de sa relation avec la fécondation interne, qui pourrait être un caractère primitif des Gnathostomes d'après l'observation de placodermes fossiles (Long et

al., 2015). Par ailleurs, chez les roussettes femelles, *lhr* est également exprimé au niveau de la glande de l'oviducte, de l'oviducte et de l'utérus dont les fonctions de base sont la formation de la capsule de l'œuf, initiée par la progestérone, et le stockage des spermatozoïdes (Marongiu et al., 2021; Shimoyama et al., 2023). Ces résultats sont en accord avec une expression de *lhr* au niveau de l'oviducte et de l'utérus chez la souris (Zheng et al., 2001), le yak (Yin et al., 2016) et la truie (Liang et al., 2012). L'ensemble de ces résultats suggère l'existence d'un axe hypothalamo-hypophyso-tractus génital chez les Gnathostomes. Cet axe pourrait faire l'objet d'une thématique d'étude à part entière.

Les gènes appartenant aux familles des LGRs et des GPHs ont été identifiés au sein de tous les principaux clades de Bilatériens (Roch and Sherwood, 2014). Une hypothèse de l'origine évolutive des GpHRs a été proposée avec un récepteur ancestral qui interagirait avec une GpH ancestrale monomérique ou homodimérique (Gong et al., 2023). Chez de nombreux Bilatériens non Vertébrés, les gènes *gpa2* et *gpb5* ont été identifiés et récemment renommés *gpa* et *gpb*, sur la base leurs histoires évolutives (Dufour et al., 2020; Querat, 2021). De plus, leurs récepteurs associés ont également été identifiés et différents noms leur ont été attribués selon les espèces et les auteurs. Ces LGRs sont activés par l'hétérodimère recombinant GPA/GPB, comme observé chez les Protostomiens (Kenis et al., 2023; Rocco and Paluzzi, 2020; Sudo et al., 2005) et les Chordés primitifs (Dos Santos et al., 2009; P. Wang et al., 2018; Yang et al., 2023). Cependant, la question de savoir si cet hétérodimère est actif *in vivo* en tant qu'hétérodimères, homodimères ou monomères non covalents a été soulevée (Alvarez et al., 2009; Dufour et al., 2020; Yang et al., 2023) ainsi que la question du rôle endocrine ou paracrine de l'hétérodimère GPA2/GPB5 en condition physiologique. (Alvarez et al., 2009; Sun et al., 2010), questions qui restent irrésolues.

La caractérisation des protéines GPA2 et de GPB5, précédemment identifiées chez le requin *S. torazame* (Hara et al., 2018) et l'holocéphale *C. milii* (Buechi and Bridgham, 2017), a été complétée au cours de notre travail de thèse chez plusieurs espèces d'Élasmobranches (requins et raies). De plus, les tests fonctionnels que nous avons réalisés ont montré, pour la première fois chez un Élasmobranche, que l'hormone recombinante monocaténaire *sc*GPB5-*sc*GPA2 était capable d'activer le *sc*TSHR, avec une efficacité qui serait supérieure à celle de *sc*TSH, comme cela avait été observé précédemment chez *R. norvegicus* et *H. sapiens* pour la thyrostimuline (Nagasaki *et al*., 2006; Nakabayashi et al., 2002). Il est également remarquable

que le recombinant *sc*GPB5-*sc*GPA2 ait montré une activité agoniste sur *sc*FSHR et *sc*LHR dans notre système *in vitro*. Ces résultats apparemment surprenants s'accordent bien avec le modèle de « spécificité négative » de l'interaction ligand-récepteur des hormones gonadotropes proposé précédemment (Combarnous, 1992; Combarnous and Hengé, 1981) (cf : chapitre IV) et suggèrent une fonction plus ancestrale de GPA2/GPB5 et/ou une spécificité des récepteurs qui n'est pas encore établie, comme cela a été décrit chez la lamproie où GPB5-GPA2 pouvait activer à la fois GPHR I et GPHR II (Hausken et al., 2018). De plus, nous avons observé que le *sc*GPB5 recombinant pouvait également activer *sc*FSHR, *sc*LHR et *sc*TSHR, mais avec une efficacité dix fois inférieure à celle du *sc*GPB5-*sc*GPA2, suggérant une activité agoniste partielle de *sc*GPB5 sur *sc*FSHR et *sc*LHR. Dans notre étude, nous n'avons pas pu déterminer si les protéines *sc*GPA2 ou *sc*GPB5 étaient actives en tant que monomère ou homodimère.

GPA et GPB possèdent de nombreuses fonctions (Bassett et al., 2015; Heyland et al., 2012; Nagasaki *et al*., 2006; Nakabayashi et al., 2002; Suzuki et al., 2009; Vandersmissen et al., 2014), dont celle de moduler les fonctions gonadiques. En effet, le récepteur de GPA/GPB serait impliqué chez *Caenorhabditis elegans* dans le renouvellement des cellules germinales (Cho et al., 2007) et chez le moustique tigre *Aedes aegypti* dans le maintien qualitatif et quantitatif de la spermatogenèse (Rocco et al., 2017, 2019). Par ailleurs, un rôle régulateur de la reproduction a été suggéré chez d'autres Protostomiens comme *Drosophila melanogaster* (Vandersmissen et al., 2014), *Patinopecten yessoensis* (M. Zhang et al., 2020) et *Macrobrachium rosenbergii* (Wahl et al., 2022) sur la base de la coexpression de *gpa*, *gpb* et des *lgrs* au niveau des gonades. Chez les Prochordés, cette coexpression au niveau gonadique a également été observée chez *Branchiostoma japonicum* et *Styela clava*, où le recombinant GPA/GPB active les LGRs associés (P. Wang et al., 2018; Yang et al., 2023). Chez les Vertébrés, la coexpression gonadique de *gpa2*, *gpb5* et des récepteurs associés suggère également un rôle régulateur de la reproduction (Hara et al., 2018; Hausken et al., 2018; Sun et al., 2010). Chez les Mammifères, GPA2/GPB5 serait sécrété par l'ovocyte et exercerait une action paracrine sur les cellules de la granulosa et de la thèque qui expriment TSHR (Sun et al., 2010). Les résultats que nous avons obtenus au cours de cette thèse suggèrent également un rôle paracrine de GPA2/GPB5 chez la roussette (Fig. 34). En l'absence d'expression de *tshβ2* dans

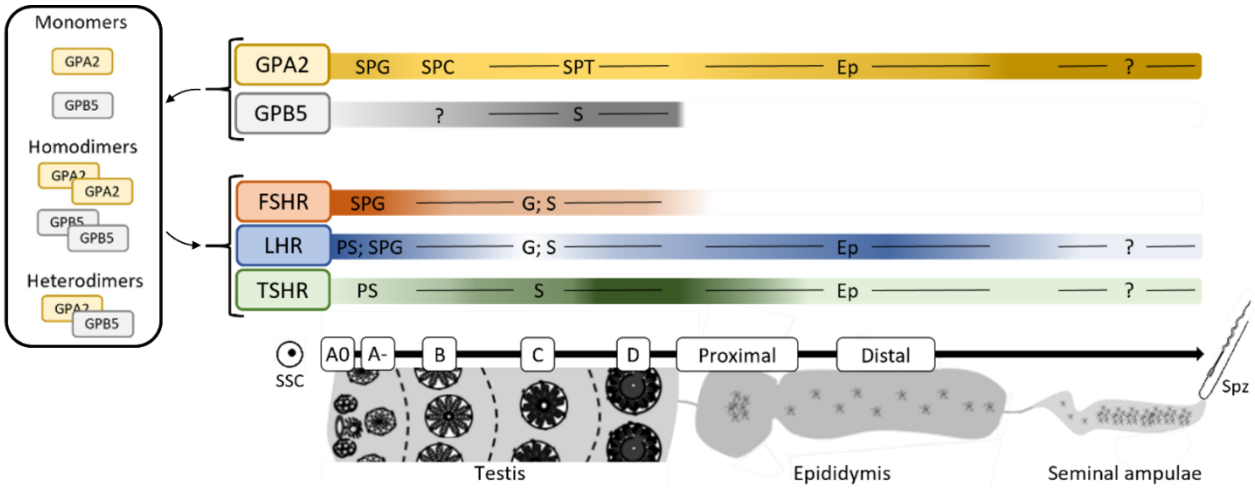


Fig. 34 **Représentation schématique de la régulation paracrine GPA2/GPB5 au niveau du tractus génital mâle chez *S. canicula*.** Les niveaux d'ARNm de *gpa2*, *gpb5*, *fshr*, *lhr* et *tshr* sont représentés par des gradients de couleur où les couleurs plus foncées correspondent aux plus fortes abondances. Les localisations des expressions sont notées à l'intérieur des gradients de couleurs correspondant. A0, zone contenant la zone germinative ; A-, zone contenant les cystes à spermatogonies différenciées ; B, zone contenant les cystes à spermatocytes ; C, zone contenant les cystes à spermatides rondes ; D, zone contenant les cystes à spermatides allongées ; Ep, cellules épithéliales épididymaires ; FSHR, récepteur à l'hormone folliculostimulante ; G, cellules germinales ; LHR, récepteur à l'hormone lutéinisante ; S, cellule de Sertoli ; PS, précurseur somatique ; SPG, spermatogonies indifférenciées et en cours de différenciation ; Spz, spermatozoïdes.

le testicule de *S. canicula*, nous nous attendions à ce que *sc*GPA2/*sc*GPB5 exerce un rôle paracrine dans la régulation de la spermatogenèse en activant le TSHR testiculaire. Cette hypothèse était notamment renforcée par la corrélation observée entre les niveaux d'ARNm de *gpb5* et de *tshr* au cours de la spermatogenèse. L'analyse *in situ* a également montré l'expression de *gpa2* dans les cellules germinales mâles alors que *gpb5* et *tshr* étaient exprimés dans les cellules de Sertoli, suggérant des régulations paracrines et/ou autocrines. Bien que notre étude sur les ovaires de roussette reste limitée, les analyses *in situ* ont montré une expression de TSHR/*tshr* au niveau de la thèque et de l'ovocyte, de *gpa2* au niveau de la granulosa et de *gpb5* au niveau de la granulosa et de la thèque ; suggérant également un rôle paracrine de GPA2/GPB5 au niveau de l'ovaire. Cependant, la possible activation de FSHR et de LHR par la protéine recombinante *sc*GPB5-*sc*GPA2 pose à nouveau la question des fonctions spécifiques ou de la redondance des hormones glycoprotéiques dans la régulation de la fonction testiculaire chez les Élasmobranches ou celle de la persistance de fonctions ancestrales. Afin d'appréhender le rôle de GPA2/GPB5 dans la régulation de la spermatogenèse chez la roussette, nous avons initié une étude protéomique d'explants testiculaires des zones à spermatides en réponse à un traitement par la protéine recombinante *sc*GPB5-*sc*GPA2, résultats qui restent à être interprétés.

L'ensemble de ces données suggère l'existence d'un rôle régulateur de la reproduction exercé par GPA et GPB chez les premiers Bilatériens et qui aurait été conservé jusqu'aux Vertébrés, dont l'humain, au travers des orthologues GPA2 et GPB5.

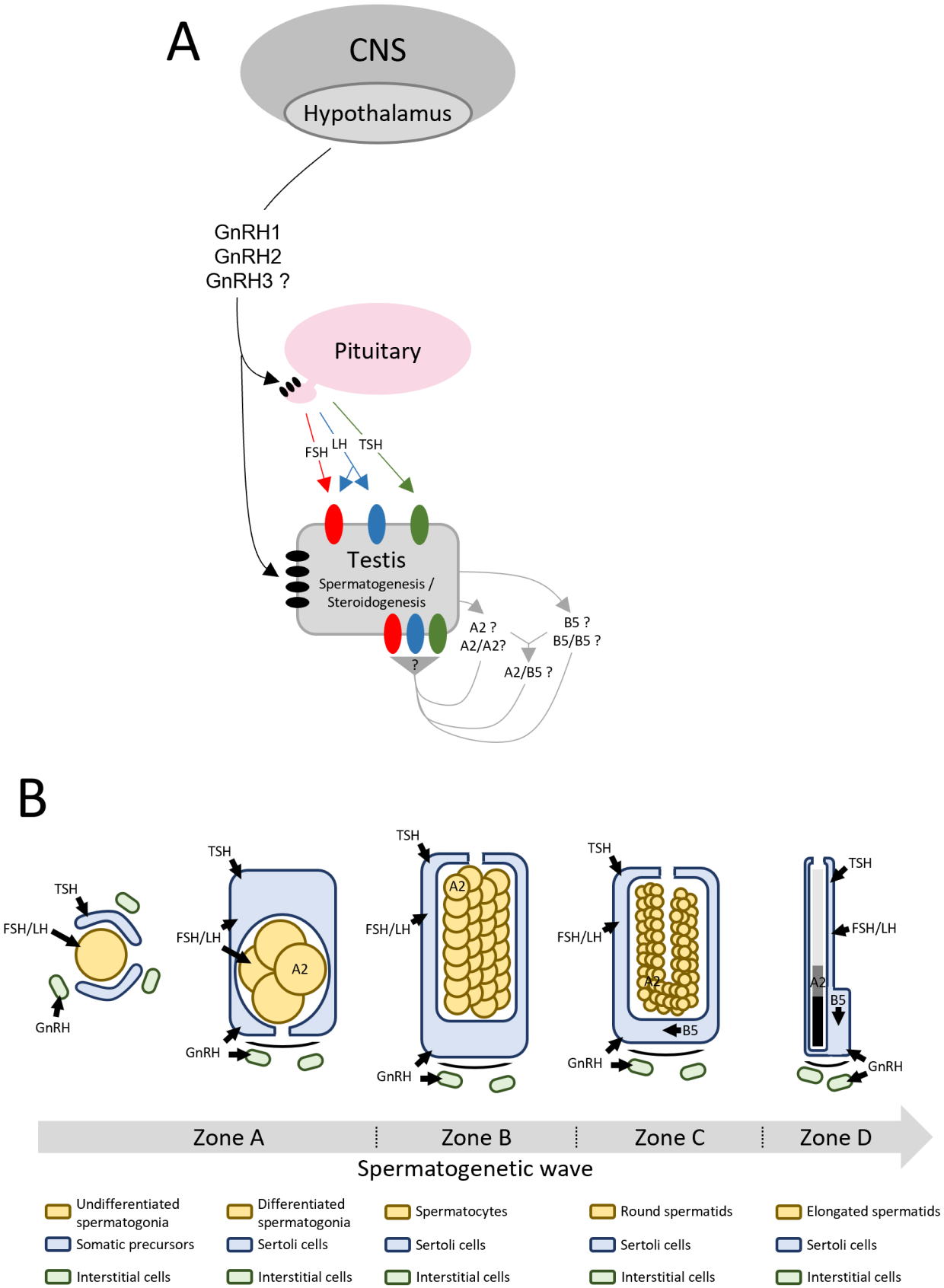


Fig. 35 **Proposition d'un modèle de régulation de la spermatogenèse couplant les régulations endocrine et paracrine au cours de la spermatogenèse chez *S. canicula*.** A. Système de régulation des fonctions testiculaires impliquant les GnRHs et les GpHs chez *S. canicula*. B. Rôles des GnRHs et GpHs dans la régulation des différents types cellulaires au cours de la spermatogenèse chez la roussette *S. canicula*.

## IV. Proposition d'un modèle couplant les régulations endocrine et paracrine de la spermatogenèse chez *S. canicula* : une redondance et/ou une compensation fonctionnelle dans la modulation d'une spermatogenèse relativement indépendante

Dans ce travail de thèse, les signalisations GnRH et GpH de *S. canicula* ont été discutées individuellement, afin de mettre en exergue leurs particularités et leurs origines évolutives apparentées. Cependant, en condition physiologique, la spermatogenèse est initiée et maintenue en continu par l'orchestration de facteurs endocrines, paracrines et autocrines (Sengupta et al., 2019). L'ensemble des résultats obtenus suggérerait que les signalisations paracrine et endocrine associées aux GnRHs, GtHs et à GPA2/GPB5 feraient partie d'un unique système complexe de régulations multiples qui contrôle la gamétogenèse et la stéroïdogenèse chez *S. canicula* (Fig. 35). Cependant, la spermatogenèse de *S. canicula* peut montrer peu ou pas de changements saisonniers, avec une spermatogenèse qui est continue tout au long de l'année (Garnier et al., 1999; Sourdaine et al., 2018). Cela suggère que, chez les mâles mâtures, les voies de signalisation régulant la spermatogenèse pourraient également présenter peu ou pas de changements saisonniers, comme cela a été observé pour certains stéroïdes à l'exception d'un pic de production de testostérone testiculaire en février associé à une augmentation des réserves spermatiques (Garnier et al., 1999). De plus, tout au long de la spermatogenèse, les cellules de Sertoli expriment FSHR, LHR, TSHR et GPB5, les cellules germinales, GPA2, et les cellules interstitielles les GnRHRs. Par ailleurs, les profils d'interaction ligand/récepteur montrent des redondances fonctionnelles chez *S. canicula*, ce qui a également était observé chez des poissons téléostéens (Burow et al., 2020; Xie et al., 2017). Ces redondances pourraient avoir permis l'acquisition d'une forte capacité d'adaptation et d'acclimatation qui peut être intéressant de mettre en lien avec l'importante diversité écologique de ces clades (Dulvy et al., 2014; Helfman et al., 2009; Weigmann, 2016). Lors des expériences de ventralectomie de l'hypophyse chez *S. canicula*, une zone de dégénérescence limitée au niveau des stades d'entrée en prophase méiotique n'a été observée que si une augmentation de la température de 13°C à 18°C était également appliquée aux animaux (Dobson and Dodd, 1977a, 1977b) ; soulignant à la fois une relative indépendance de la spermatogenèse par rapport aux hormones du lobe ventral de l'hypophyse (les stades pré- et

post-méiotiques n'étant pas affectés) et un impact relativement limité de la température. Il semblerait donc que la seule fonction essentielle associée aux signalisations du lobe ventral hypophysaire (GpH) soit de faciliter l'entrée en méiose. Cette relative autonomie du testicule par rapport à une régulation centrale pourrait être liée à la prépondérance d'une régulation paracrine, du fait notamment d'une expression locale de GPB5 et des GnRHs et d'une activité stéroïdogène basale des cystes. Cette spermatogenèse relativement indépendante et sans fluctuation saisonnière majeure soulève la question de la force évolutive qui a permis le maintien et le développement des différentes voies de signalisation des GnRHs et GpHs chez les Vertébrés. Une hypothèse serait que le développement et la mise en place des voies de signalisation impliquant les GnRHs et GpHs ont répondu, en premier lieu, aux besoins d'une régulation plus spécifique de la folliculogenèse comme cela a été précédemment supposé par Xie et al., 2017. Cette hypothèse s'accorde bien avec les différents profils d'expression de *fshr* et *lhr* qui présentent des fluctuation en fonction des stades de la folliculogenèse chez *S. torazame* (Arimura et al., 2024) et avec ce qui a été observé chez les femelles *S. canicula* qui présentent une folliculogenèse avec de légères fluctuations saisonnières (Capapé et al., 2008b, 2008a; Ellis and Shackley, 1997; Rodrigtjez-Cabello et al., 1998), où le FSHR est exprimé par les cellules de la granulosa et le LHR et le TSHR par les cellules de la thèque des follicules ovariens, alors que ces trois récepteurs sont coexprimés par la cellule de Sertoli au niveau testiculaire.

À travers ce travail, une question récurrente demeure à propos des fonctions spécifiques des différents acteurs étudiés et la balance entre des fonctions ancestrales persistantes (rôle de GPA2/GPB5) et des fonctions associées à des hormones (FSH, LH) qui ont émergé au niveau de ce clade des Chondrichtyens. Les perspectives que nous pouvons envisager pour répondre à cette question seraient l'approfondissement des approches *in vitro* par la mise en place de cultures d'explants testiculaires ou de cystes isolés co-traités avec des GPHs et/ou des GnRHs, comme cela a pu être réalisé au niveau d'un système de culture *ex-vivo* de testicules de *D. rerio* (Fallah et al., 2020), la mise en place de méthodologie d'inhibition de l'expression de gènes codant pour des GPHRs ou des GnRHRs par RNAi au niveau de cultures *in vitro*, comme réalisé sur des cellules de Sertoli d'hommes (Wang et al., 2018) et de souris (González-González et al., 2008), la mise en place d'approches *in vivo* impliquant des injections d'agonistes ou d'antagonistes des GPHRs ou des GnRHRs, comme cela a été réalisé avec des

implants de GnRH chez les raies Potamotrygon sp. (Sailler et al., 2023), ou par des méthodologies d'édition de gènes qui se développent depuis peu chez les Vertébrés cartilagineux (Fujimori et al., 2022), voir par des méthodologies émergentes utilisant le système de recombinaison par pont IS110 (Durrant et al., 2024).

## Conclusion générale

Pour conclure, ce travail de thèse a permis l'acquisition de nombreuses données obtenues pour la première fois chez un modèle Élasmobranche, la petite roussette *Scyliorhinus canicula*. La caractérisation moléculaire des protéomes au cours de la spermatogenèse et la caractérisation de voies de signalisation impliquées dans la régulation endocrine et paracrine de la spermatogenèse répondent parfaitement aux challenges actuels que sont : l'extinction de masse que subissent les espèces de Vertébrés cartilagineux ainsi que le développement des technologies permettant le maintien d'individus et la reproduction en captivité. *S. canicula* présente une spermatogenèse modulée par un système complexe, multifactoriel et unique aux Élasmobranches qui implique des régulations endocrines, tels les axes HHG, HHT et *via* les GnRHs circulantes, et paracrine et/ou autocrine *via* GPA2 et GPB5 ainsi que les stéroïdes. Du fait de la redondance fonctionnelle de certaines hormones, de la potentielle action de compensation entre des voies de signalisation endocrine et paracrine, du maintien d'une spermatogenèse après une hypophysectomie partielle et du maintien d'une stéroïdogenèse active dans des cultures de cystes isolés, il a été suggéré que la spermatogenèse de *S. canicula* pouvait être relativement indépendante, ce qui suggère sa potentielle résistance et résilience aux changements physiologiques et environnementaux.

Finalement, l'acquisition des axes HHG et HHT, qui sont des intégrateurs des informations d'origines physiologiques et environnementales permettant de coordonner les grandes fonctions biologiques (Levine, 2000), pourrait avoir été l'un des leviers clefs, dès leurs mises en place chez l'ancêtre commun des Gnathostomes, qui aurait permis la domination des Gnathostomes en tant que principal groupe (99,9 %) de Vertébrés vivants (Venkatesh et al., 2014).

# Références bibliographiques

# Références bibliographiques

# Références bibliographiques

A. Soares, K.D., 2020. Comparative anatomy of the clasper of catsharks and its phylogenetic implications (Chondrichthyes: Carcharhiniformes: Scyliorhinidae). Journal of Morphology 281, 591–607. https://doi.org/10.1002/jmor.21123

Acevedo-Rodriguez, A., Kauffman, A.S., Cherrington, B.D., Borges, C.S., Roepke, T.A., Laconi, M., 2018. Emerging insights into hypothalamic-pituitary-gonadal axis regulation and interaction with stress signalling. J Neuroendocrinology 30, e12590. https://doi.org/10.1111/jne.12590

Ahn, J., Park, Y.-J., Chen, P., Lee, T.J., Jeon, Y.-J., Croce, C.M., Suh, Y., Hwang, S., Kwon, W.-S., Pang, M.-G., Kim, C.-H., Lee, S.S., Lee, K., 2017. Comparative expression profiling of testis-enriched genes regulated during the development of spermatogonial cells. PLoS ONE 12, e0175787. https://doi.org/10.1371/journal.pone.0175787

Almeida, F.F.L., Kristoffersen, C., Taranger, G.L., Schulz, R.W., 2008. Spermatogenesis in Atlantic Cod (Gadus morhua): A Novel Model of Cystic Germ Cell Development. Biol. Reprod. 78, 27–34. https://doi.org/10.1095/biolreprod.107.063669

Almeida, T., Ohta, Y., Gaigher, A., Muñoz-Mérida, A., Neves, F., Castro, L.F.C., Machado, A.M., Esteves, P.J., Veríssimo, A., Flajnik, M.F., 2021. A Highly Complex, MHC-Linked, 350 Million-Year-Old Shark Nonclassical Class I Lineage. The Journal of Immunology 207, 824–836. https://doi.org/10.4049/jimmunol.2000851

Alvarez, E., Cahoreau, C., Combarnous, Y., 2009. Comparative structure analyses of cystine knot-containing molecules with eight aminoacyl ring including glycoprotein hormones (GPH) alpha and beta subunits and GPH-related A2 (GPA2) and B5 (GPB5) molecules. Reprod Biol Endocrinol 7, 90. https://doi.org/10.1186/1477-7827-7-90

Amaral, A., 2022. Energy metabolism in mammalian sperm motility. WIREs Mechanisms of Disease 14. https://doi.org/10.1002/wsbm.1569

Amaral, C.R.L., Pereira, F., Silva, D.A., Amorim, A., de Carvalho, E.F., 2018. The mitogenomic phylogeny of the Elasmobranchii (Chondrichthyes). Mitochondr DNA 29, 867–878. https://doi.org/10.1080/24701394.2017.1376052

Anbazhagan, R., Kavarthapu, R., Dufau, M.L., 2022. Chromatoid Bodies in the Regulation of Spermatogenesis: Novel Role of GRTH. Cells 11, 613. https://doi.org/10.3390/cells11040613

Andreuccetti, P., Iodice, M., Prisco, M., Gualtieri, R., 1999. Intercellular bridges between granulosa cells and the oocyte in the elasmobranch Raya asterias. Anat. Rec. 255, 180–187. https://doi.org/10.1002/(SICI)1097-0185(19990601)255:2<180::AID-AR8>3.0.CO;2-S

Arimura, S., Wong, M.K.S., Inoue, R., Kawano, M., Shimoyama, K., Fujimori, C., Tokunaga, K., Takagi, W., Hyodo, S., 2024. Functional characterization of follicle-stimulating hormone and luteinizing hormone receptors in cloudy catshark, Scyliorhinus torazame. Gen Comp Endocrinol 354, 114542. https://doi.org/10.1016/j.ygcen.2024.114542

Atake, O.J., Eames, B.F., 2021. Mineralized Cartilage and Bone-Like Tissues in Chondrichthyans Offer Potential Insights Into the Evolution and Development of Mineralized Tissues in the Vertebrate Endoskeleton. Front. Genet. 12, 762042. https://doi.org/10.3389/fgene.2021.762042

Awider-Al-Amawi, M., Marchlewicz, M., Kolasa, A., Wenda-Rozewicka, L., Wiszniewska, B., 2007. Rat epididymal epithelial cells and 17beta-estradiol synthesis under hCG stimulation in vitro. Folia Histochem Cyto 45, 255–263.

Awruch, C.A., 2013. Reproductive endocrinology in chondrichthyans: The present and the future. Gen Comp Endocrinol 192, 60–70. https://doi.org/10.1016/j.ygcen.2013.05.021

Baba, T., Hoff III, H.B., Nemoto, H., Lee, H., Orth, J., Arai, Y., Gerton, G.L., 1993. Acrogranin, an acrosomal cysteine-rich glycoprotein, is the precursor of the growth-modulating peptides, granulins, and epithelins, and is expressed in somatic as well as male germ cells. Mol. Reprod. Dev 34, 233–243. https://doi.org/10.1002/mrd.1080340302

Backe, S.J., Sager, R.A., Regan, B.R., Sit, J., Major, L.A., Bratslavsky, G., Woodford, M.R., Bourboulia, D., Mollapour, M., 2022. A specialized Hsp90 co-chaperone network regulates steroid hormone receptor response to ligand. Cell Reports 40, 111039. https://doi.org/10.1016/j.celrep.2022.111039

Bae, J.-W., Kwon, W.-S., 2024. Proteomic analysis of fipronil-induced molecular defects in spermatozoa. Sci Rep 14, 7668. https://doi.org/10.1038/s41598-024-57876-4

Bak, C.W., Yoon, T.-K., Choi, Y., 2011. Functions of PIWI proteins in spermatogenesis. Clin Exp Reprod Med 38, 61. https://doi.org/10.5653/cerm.2011.38.2.61

Bakke, F.K., Gundappa, M.K., Matz, H., Stead, D.A., Macqueen, D.J., Dooley, H., 2022. Exploration of the Nurse Shark (Ginglymostoma cirratum) Plasma Immunoproteome Using High-Resolution LC-MS/MS. Front. Immunol. 13, 873390. https://doi.org/10.3389/fimmu.2022.873390

Ballard, W.W., Mellinger, J., Lechenault, H., 1993. A series of normal stages for development of Scyliorhinus canicula, the lesser spotted dogfish (Chondrichthyes: Scyliorhinidae). J. Exp. Zool. 267, 318–336. https://doi.org/10.1002/jez.1402670309

Bassett, J.H.D., Van Der Spek, A., Logan, J.G., Gogakos, A., Bagchi-Chakraborty, J., Murphy, E., Van Zeijl, C., Down, J., Croucher, P.I., Boyde, A., Boelen, A., Williams, G.R., 2015. Thyrostimulin Regulates Osteoblastic Bone Formation During Early Skeletal Development. Endocrinology 156, 3098–3113. https://doi.org/10.1210/en.2014-1943

Becerril-García, E.E., Arellano-Martínez, M., Bernot-Simon, D., Hoyos-Padilla, E.M., Galván-Magaña, F., Godard-Codding, C., 2020. Steroid hormones and chondrichthyan reproduction: physiological functions, scientific research, and implications for conservation. PeerJ 8, e9686. https://doi.org/10.7717/peerj.9686

Bhartiya, D., Patel, H., Kaushik, A., Singh, P., Sharma, D., 2021. Endogenous, tissue-resident stem/progenitor cells in gonads and bone marrow express FSHR and respond to FSH via FSHR-3. J Ovarian Res 14, 145. https://doi.org/10.1186/s13048-021-00883-0

Bhat, I.A., Rather, Mohd.A., Saha, R., Ganie, P.A., Sharma, R., 2017. Identification and Expression Analysis of Thyroid Stimulating Hormone Receptor (TSHR) in Fish Gonads Following LHRH Treatment. Proc. Natl. Acad. Sci., India, Sect. B Biol. Sci. 87, 719–726. https://doi.org/10.1007/s40011-015-0640-8

Bindea, G., Mlecnik, B., Hackl, H., Charoentong, P., Tosolini, M., Kirilovsky, A., Fridman, W.-H., Pagès, F., Trajanoski, Z., Galon, J., 2009. ClueGO: a Cytoscape plug-in to decipher functionally grouped gene ontology and pathway annotation networks. Bioinformatics 25, 1091–1093. https://doi.org/10.1093/bioinformatics/btp101

Blackburn, D.G., Hughes, D.F., 2024. Phylogenetic analysis of viviparity, matrotrophy, and other reproductive patterns in chondrichthyan fishes. Biol Rev 99, 1314–1356. https://doi.org/10.1111/brv.13070

Boehm, T., 2011. Design principles of adaptive immune systems. Nat Rev Immunol 11, 307–317. https://doi.org/10.1038/nri2944

Bosseboeuf, A., Gautier, A., Auvray, P., Mazan, S., Sourdaine, P., 2014. Characterization of spermatogonial markers in the mature testis of the dogfish (Scyliorhinus canicula L.). Reproduction 147, 125–139. https://doi.org/10.1530/REP-13-0316

Brauns, A.-K., Heine, M., Tödter, K., Baumgart-Vogt, E., Lüers, G.H., Schumacher, U., 2019. A defect in the peroxisomal biogenesis in germ cells induces a spermatogenic arrest at the round spermatid stage in mice. Sci Rep 9, 9553. https://doi.org/10.1038/s41598-019-45991-6

Browne, J.A., Leir, S., Yin, S., Harris, A., 2019. Transcriptional networks in the human epididymis. Andrology 7, 741–747. https://doi.org/10.1111/andr.12629

Buechi, H.B., Bridgham, J.T., 2017. Evolution of specificity in cartilaginous fish glycoprotein hormones and receptors. General and Comparative Endocrinology 246, 309–320. https://doi.org/10.1016/j.ygcen.2017.01.007

Burger, J., Merlet, J., Tavernier, N., Richaudeau, B., Arnold, A., Ciosk, R., Bowerman, B., Pintard, L., 2013. CRL2LRR-1 E3-Ligase Regulates Proliferation and Progression through Meiosis in the Caenorhabditis elegans Germline. PLoS Genet 9, e1003375. https://doi.org/10.1371/journal.pgen.1003375

Burlibaşa, L., Ionescu, A.C., Dragusanu, D.-M., 2019. Histone hyperacetylation and DNA methylation interplay during murine spermatogenesis. Zygote 27, 305–314. https://doi.org/10.1017/S0967199419000303

Burow, S., Mizrahi, N., Maugars, G., Von Krogh, K., Nourizadeh-Lillabadi, R., Hollander-Cohen, L., Shpilman, M., Atre, I., Weltzien, F.-A., Levavi-Sivan, B., 2020. Characterization of gonadotropin receptors Fshr and Lhr in Japanese medaka, Oryzias latipes. Gen Comp Endocrinol 285, 113276. https://doi.org/10.1016/j.ygcen.2019.113276

Cahoreau, C., Klett, D., Combarnous, Y., 2015. Structure-Function Relationships of Glycoprotein Hormones and Their Subunits' Ancestors. Front. Endocrinol. 6. https://doi.org/10.3389/fendo.2015.00026

Callard, G.V., 1991. Reproduction in male elasmobranch fishes, in: Oogenesis, Spermatogenesis and Reproduction, pp. 104–154. Edited by R.K.H. Kinne, E. Kinne-Saffran and K.W. Beyenbach. Karger, Basel.

Callard, G.V., Pudney, J.A., Mak, P., Canick, J.A., 1985. Stage-Dependent Changes in Steroidogenic Enzymes and Estrogen Receptors during Spermatogenesis in the Testis of the Dogfish, Squalus acanthias*. Endocrinology 117, 1328–1335. https://doi.org/10.1210/endo-117-4-1328

Callard, T.J., Fileti, L.A., Koob, T.J., 1993. Ovarian steroid synthesis and the hormonal control of the elasmobranch reproductive tract. Environ Biol Fishes 175–185. https://doi.org/10.1007/978-94-017-3450-9_16

Capapé, C., Mnasri-Sioudi, N., El Kamel-Moutalibi, O., Boumaïza, M., Amor, M.M.B., Reynaud, C., 2014. Production, maturity, reproductive cycle and fecundity of small-spotted catshark, Scyliorhinus canicula (Chondrichthyes: Scyliorhinidae) from the northern coast of Tunisia (Central Mediterranean). J. Ichthyol. 54, 111–126. https://doi.org/10.1134/S0032945214010020

Capapé, C., Reynaud, C., Vergne, Y., Quignard, J.-P., 2008a. Biological observations on the smallspotted catshark Scyliorhinus canicula (Chondrichthyes: Scyliorhinidae) off the Languedocian coast (southern France, northern Mediterranean). Pan-Am J Aquat 3, 282–289.

Capapé, C., Vergne, Y., Reynaud, C., Guélorget, O., Quignard, J.P., 2008b. Maturity, fecundity and occurrence of the smallspotted catshark Scyliorhinus canicula (chondrichthyes: scyliorhinidae) off the Languedocian coast (southern France, north-western Mediterranean). Life & Environment 47–55.

Cascio, P., 2021. PA28γ: New Insights on an Ancient Proteasome Activator. Biomolecules 11, 228. https://doi.org/10.3390/biom11020228

Chana-Munoz, A., Jendroszek, A., Sønnichsen, M., Kristiansen, R., Jensen, J.K., Andreasen, P.A., Bendixen, C., Panitz, F., 2017. Multi-tissue RNA-seq and transcriptome characterisation of the spiny dogfish shark (Squalus acanthias) provides a molecular tool for biological research and reveals new genes involved in osmoregulation. PLoS ONE 12, e0182756. https://doi.org/10.1371/journal.pone.0182756

Chandrashekar, V., Bartke, A., Coschigano, K.T., Kopchick, J.J., 1999. Pituitary and Testicular Function in Growth Hormone Receptor Gene Knockout Mice. Endocrinology 140. https://doi.org/1082-1088. doi: 10.1210/endo.140.3.6557

Chapman, D.D., Shivji, M.S., Louis, E., Sommer, J., Fletcher, H., Prodöhl, P.A., 2007. Virgin birth in a hammerhead shark. Biol. Lett. 3, 425–427. https://doi.org/10.1098/rsbl.2007.0189

Chatelain, P.G., Sanchez, P., Saez, J.M., 1991. Growth Hormone and Insulin-Like Growth Factor I Treatment Increase Testicular Luteinizing Hormone Receptors and Steroidogenic Responsiveness of Growth Hormone Deficient Dwarf Mice. Endocrinology 128, 1857–1862. https://doi.org/10.1210/endo-128-4-1857

Chen, X., Luan, X., Zheng, Q., Qiao, C., Chen, W., Wang, M., Yan, Y., Xie, B., Shen, C., He, Z., Zhang, J., Liu, M., Hu, X., Li, H., Zheng, B., Fang, J., Yu, J., 2019. Precursor RNA processing 3 is required for male fertility, and germline stem cell self-renewal and differentiation via regulating spliceosome function in Drosophila testes. Sci Rep 9, 9988. https://doi.org/10.1038/s41598-019-46419-x

Chianese, R., Ciaramella, V., Scarpa, D., Fasano, S., Pierantoni, R., Meccariello, R., 2012. Anandamide regulates the expression of GnRH1, GnRH2, and GnRH-Rs in frog testis. Am J Physiol Endocrinol Metab 303, E475–E487. https://doi.org/10.1152/ajpendo.00086.2012

Cho, S., Rogers, K.W., Fay, D.S., 2007. The C. elegans Glycopeptide Hormone Receptor Ortholog, FSHR-1, Regulates Germline Differentiation and Survival. Curr Biol 17, 203–212. https://doi.org/10.1016/j.cub.2006.12.027

Choi, D., 2018. Evolutionary Viewpoint on GnRH (gonadotropin-releasing hormone) in Chordata - Amino Acid and Nucleic Acid Sequences. Dev. Reprod. 22, 119–132. https://doi.org/10.12717/DR.2018.22.2.119

Chu, L., Li, J., Liu, Y., Cheng, C.H.K., 2015. Gonadotropin Signaling in Zebrafish Ovary and Testis Development: Insights From Gene Knockout Study. J Mol Endocrinol 29, 1743–1758. https://doi.org/10.1210/me.2015-1126

Ciaramella, V., Chianese, R., Pariante, P., Fasano, S., Pierantoni, R., Meccariello, R., 2015. Expression Analysis of *Gnrh1* and *Gnrhr1* in Spermatogenic Cells of Rat. Int J Endocrinol 2015, 1–8. https://doi.org/10.1155/2015/982726

Collenot, G., Damas, D., 1980. Étude ultrastucturale de la cellule de Sertoli au cours de la spermiogenèse chez Scyliorhinus canicula L. Cah Biol Mar 21.

Combarnous, Y., 1992. Molecular basis of the specificity of binding of glycoprotein hormones to their receptors. Endocr Rev 13, 670–670. https://doi.org/10.1210/edrv-13-4-670

Combarnous, Y., Hengé, M.H., 1981. Equine follicle-stimulating hormone. Purification, acid dissociation, and binding to equine testicular tissue. JBC 256, 9567–9572. https://doi.org/10.1016/S0021-9258(19)68799-5

Criswell, K.E., Roberts, L.E., Koo, E.T., Head, J.J., Gillis, J.A., 2021. *hox* gene expression predicts tetrapod-like axial regionalization in the skate, *Leucoraja erinacea*. Proc Natl Acad Sci USA 118, e2114563118. https://doi.org/10.1073/pnas.2114563118

Cuevas, M.E., Callard, G., 1992a. In vitro steroid secretion by staged spermatocysts (sertoli/germ cell units) of dogfish (Squalus acanthias) testis. Gen Comp Endocrinol 88, 151–165. https://doi.org/10.1016/0016-6480(92)90204-W

Cuevas, M.E., Callard, G., 1992b. Androgen and progesterone receptors in shark (Squalus) testis: characteristics and stage-related distribution. Endocrinology 130, 2173–2182. https://doi.org/10.1210/endo.130.4.1547734

Cuevas, M.E., Collins, K., Callard, G.V., 1993. Stage-related changes in steroid-converting enzyme activities in Squalus testis: synthesis of biologically active metabolites via 3b-

hydroxysteroid dehydrogenase/ isomerase and 5a-reductase. Steroids 58, 87–94. https://doi.org/10.1016/0039-128X(93)90058-U

Dahia, C.L., Rao, A.J., 2006. Demonstration of Follicle-Stimulating Hormone Receptor in Cauda Epididymis of Rat. Biol Reprod 75, 98–106. https://doi.org/10.1095/biolreprod.105.047704

Dai, L., Tsai-Morris, C.-H., Sato, H., Villar, J., Kang, J.-H., Zhang, J., Dufau, M.L., 2011. Testis-specific miRNA-469 up-regulated in gonadotropin-regulated testicular RNA helicase (GRTH/DDX25)-null mice silences transition protein 2 and protamine 2 messages at sites within coding region. JBC 286, 44306–44318. https://doi.org/10.1074/jbc.M111.282756

D'antonio, M., Vallarino, M., Lovejoy, D.A., Vandesande, F., King, J.A., Pierantoni, R., Peter, R.E., 1995. Nature and distribution of gonadotropin-releasing hormone (GnRH) in the brain, and GnRH and GnRH binding activity in serum of the spotted dogfish Scyliorhinus canicula. Gen Comp Endocrinol 98, 35–49. https://doi.org/10.1006/gcen.1995.1042

De Oliveira Camilo, L., Maganhe, B.L., Gallo Neto, H., Crusco, S.E., Malavasi-Bruno, C.E., Sanches, E.G., 2023. Andrology of shortnose guitarfish *Zapteryx brevirostris* (Müller & Henle, 1841) (Chondrichthyes, Trygonorrhinidae). J Fish Biol 103, 635–645. https://doi.org/10.1111/jfb.15479

Del Mar Pedreros-Sierra, T., Ramírez-Pinilla, M.P., 2015. Morphology of the reproductive tract and acquisition of sexual maturity in males of Potamotrygon magdalenae (Elasmobranchii: Potamotrygonidae): Male reproductive tract of Potamotrygon magdalenae. J Morphol 276, 273–289. https://doi.org/10.1002/jmor.20337

Desaulniers, A.T., Cederberg, R.A., Mills, G.A., Ford, J.J., Lents, C.A., White, B.R., 2015. LH-Independent Testosterone Secretion Is Mediated by the Interaction Between GNRH2 and Its Receptor Within Porcine Testes. Biol Reprod 93, 1-9. https://doi.org/10.1095/biolreprod.115.128082

Dietrich, M.A., Nynca, J., Ciereszko, A., 2019. Proteomic and metabolomic insights into the functions of the male reproductive system in fishes. Theriogenology 132, 182–200. https://doi.org/10.1016/j.theriogenology.2019.04.018

Djureinovic, D., Fagerberg, L., Hallström, B., Danielsson, A., Lindskog, C., Uhlén, M., Pontén, F., 2014. The human testis-specific proteome defined by transcriptomics and antibody-based profiling. MHR: Basic science of reproductive medicine 20, 476–488. https://doi.org/10.1093/molehr/gau018

Dobson, S., Dodd, J.M., 1977a. Endocrine control of the testis in the dogfish Scyliorhinus canicula L. I. Effects of partial hypophysectomy on gravimetric, hormonal and biochemical aspects of testis function. Gen Comp Endocrinol 32, 41–52. https://doi.org/10.1016/0016-6480(77)90081-8

Dobson, S., Dodd, J.M., 1977b. The roles of temperature and photoperiod in the response of the testis of the dogfish, Scyliorhinus canicula L. to partial hypophysectomy (ventral lobectomy). Gen Comp Endocrinol 32, 114–115. https://doi.org/10.1016/0016-6480(77)90088-0

Dong, J., Xin, M., Liu, H., Zhang, M., Pang, Q., Chen, L., Zhao, B., 2013. Identification, expression of a glycoprotein hormone receptor homolog in the amphioxus Branchiostoma belcheri with implications for origin of vertebrate GpHRs. Gen Comp Endocrinol 184, 35–41. https://doi.org/10.1016/j.ygcen.2012.08.006

Dos Santos, S., Bardet, C., Bertrand, S., Escriva, H., Habert, D., Querat, B., 2009. Distinct Expression Patterns of Glycoprotein Hormone-α2 and -β5 in a Basal Chordate Suggest Independent Developmental Functions. Endocrinology 150, 3815–3822. https://doi.org/10.1210/en.2008-1743

Dos Santos, S., Mazan, S., Venkatesh, B., Cohen-Tannoudji, J., Quérat, B., 2011. Emergence and evolution of the glycoprotein hormone and neurotrophin gene families in vertebrates. BMC Evol Biol 11, 332. https://doi.org/10.1186/1471-2148-11-332

Dubois, E.A., Zandbergen, M.A., Peute, J., Goos, H.J., 2002. Evolutionary development of three gonadotropin-releasing hormone (GnRH) systems in vertebrates. BRB 57, 413–418. https://doi.org/10.1016/S0361-9230(01)00676-1

Dufau, M.L., Kavarthapu, R., 2019. Gonadotropin Regulated Testicular RNA Helicase, Two Decades of Studies on Its Structure Function and Regulation From Its Discovery Opens a Window for Development of a Non-hormonal Oral Male Contraceptive. Front. Endocrinol. 10, 576. https://doi.org/10.3389/fendo.2019.00576

Dufour, S., Quérat, B., Tostivint, H., Pasqualini, C., Vaudry, H., Rousseau, K., 2020. Origin and Evolution of the Neuroendocrine Control of Reproduction in Vertebrates, With Special Focus on Genome and Gene Duplications. Physiol Rev 100, 869–943. https://doi.org/10.1152/physrev.00009.2019

Dulvy, N.K., Fowler, S.L., Musick, J.A., Cavanagh, R.D., Kyne, P.M., Harrison, L.R., Carlson, J.K., Davidson, L.N., Fordham, S.V., Francis, M.P., Pollock, C.M., Simpfendorfer, C.A., Burgess, G.H., Carpenter, K.E., Compagno, L.J., Ebert, D.A., Gibson, C., Heupel, M.R., Livingstone, S.R., Sanciangco, J.C., Stevens, J.D., Valenti, S., White, W.T., 2014. Extinction risk and conservation of the world's sharks and rays. eLife 3, e00590. https://doi.org/10.7554/eLife.00590

Dulvy, N.K., Pacoureau, N., Rigby, C.L., Pollom, R.A., Jabado, R.W., Ebert, D.A., Finucci, B., Pollock, C.M., Cheok, J., Derrick, D.H., Herman, K.B., Sherman, C.S., VanderWright, W.J., Lawson, J.M., Walls, R.H.L., Carlson, J.K., Charvet, P., Bineesh, K.K., Fernando, D., Ralph, G.M., Matsushiba, J.H., Hilton-Taylor, C., Fordham, S.V., Simpfendorfer, C.A., 2021. Overfishing drives over one-third of all sharks and rays toward a global extinction crisis. Curr Biol 31, 4773-4787.e8. https://doi.org/10.1016/j.cub.2021.08.062

Durkan, A., Byrnes, C., Cooper, E., Hally, A., Sullivan-Brown, J., Sowa, J., 2022. DCAF-13 is required for C. elegans growth, development, and fertility. microPubl. biol. https://doi.org/10.17912/micropub.biology.000641

Durrant, M.G., Perry, N.T., Pai, J.J., Jangid, A.R., Athukoralage, J.S., Hiraizumi, M., McSpedon, J.P., Pawluk, A., Nishimasu, H., Konermann, S., Hsu, P.D., 2024. Bridge RNAs direct programmable recombination of target and donor DNA. Nature 630, 984–993. https://doi.org/10.1038/s41586-024-07552-4

Dzyuba, V., Ninhaus-Silveira, A., Kahanec, M., Veríssimo-Silveira, R., 2019. Sperm motility in ocellate river stingrays: Evidence for post-testicular sperm maturation and capacitation in chondrichthyes. J Zool 307, 9–16. https://doi.org/10.1111/jzo.12610

Ellis, J.R., Shackley, S.E., 1997. The reproductive biology of *Scyliorhinus canicula* in the Bristol Channel, U.K. J Fish Biol 51, 361–372. https://doi.org/10.1111/j.1095-8649.1997.tb01672.x

Engel, K.B., Callard, G.V., 2007. Endocrinology of Leydig Cells in Nonmammalian Vertebrates, in: Payne, A.H., Hardy, M.P. (Eds.), The Leydig Cell in Health and Disease, Contemporary Endocrinology. Humana Press, Totowa, NJ, pp. 207–224. https://doi.org/10.1007/978-1-59745-453-7_15

Fallah, H.P., Rodrigues, M.S., Corchuelo, S., Nóbrega, R.H., Habibi, H.R., 2020. Role of GnRH Isoforms in Paracrine/Autocrine Control of Zebrafish (Danio rerio) Spermatogenesis. Endocrinology 161, bqaa004. https://doi.org/10.1210/endocr/bqaa004

Feng, J., He, Y., Shen, Y., Zhang, G., Ma, S., Zhao, X., Zhang, Y., 2020. Protective effects of nuclear factor erythroid 2-related factor on oxidative stress and apoptosis in the testis of mice before adulthood. Theriogenology 148, 112–121. https://doi.org/10.1016/j.theriogenology.2020.03.002

Field, I.C., Meekan, M.G., Buckworth, R.C., Bradshaw, C.J., 2009. Susceptibility of sharks, rays and chimaeras to global extension. Adv Org 275–363. https://doi.org/10.1016/S0065-2881(09)56004-X

Finotto, L., Gristina, M., Garofalo, G., Riginella, E., Mazzoldi, C., 2015. Contrasting life history and reproductive traits in two populations of Scyliorhinus canicula. Mar Biol 162, 1175–1186. https://doi.org/10.1007/s00227-015-2659-z

Fischer, R., Kessler, B.M., 2015. Gel-aided sample preparation (GASP)—A simplified method for gel-assisted proteomic sample generation from protein extracts and intact cells. Proteomics 15, 1224–1229. https://doi.org/10.1002/pmic.201400436

Fitzpatrick, J.L., Kempster, R.M., Daly-Engel, T.S., Collin, S.P., Evans, J.P., 2012. Assessing the potential for post-copulatory sexual selection in elasmobranchs. J Fish Biol 80, 1141–1158. https://doi.org/10.1111/j.1095-8649.2012.03256.x

Freamat, M., Kawauchi, H., Nozaki, M., Sower, S.A., 2006. Identification and cloning of a glycoprotein hormone receptor from sea lamprey, Petromyzon marinus. J Mol Endocrinol 37, 135–146. https://doi.org/10.1677/jme.1.02064

Freamat, M., Sower, S.A., 2008. A sea lamprey glycoprotein hormone receptor similar with gnathostome thyrotropin hormone receptor. J Mol Endocrinol 41, 219–228. https://doi.org/10.1677/JME-08-0030

Fricke, R., Eschmeyer, W.N., Van Der Laan, R., 2024. Eschmeyer's catalog of Fishes: Genera, Species, References.

Fujimori, C., Umatani, C., Chimura, M., Ijiri, S., Bando, H., Hyodo, S., Kanda, S., 2022. In vitro and in vivo gene transfer in the cloudy catshark *Scyliorhinus torazame*. Dev Growth Differ 64, 558–565. https://doi.org/10.1111/dgd.12824

Gaillard, A.-L., Tay, B.-H., Pérez Sirkin, D.I., Lafont, A.-G., De Flori, C., Vissio, P.G., Mazan, S., Dufour, S., Venkatesh, B., Tostivint, H., 2018. Characterization of Gonadotropin-Releasing Hormone (GnRH) Genes From Cartilaginous Fish: Evolutionary Perspectives. Front. Neurosci. 12, 607-620. https://doi.org/10.3389/fnins.2018.00607

Gao, X., Chen, H., Liu, J., Shen, S., Wang, Q., Clement, T.M., Deskin, B.J., Chen, C., Zhao, D., Wang, L., Guo, L., Ma, X., Zhang, B., Xu, Y., Li, X., Li, L., 2019. The REGγ-Proteasome Regulates Spermatogenesis Partially by P53-PLZF Signaling. Curr Stem Cell Rep 13, 559–571. https://doi.org/10.1016/j.stemcr.2019.07.010

García-López, Á., Bogerd, J., Granneman, J.C.M., Van Dijk, W., Trant, J.M., Taranger, G.L., Schulz, R.W., 2009. Leydig Cells Express Follicle-Stimulating Hormone Receptors in African Catfish. Endocrinology 150, 357–365. https://doi.org/10.1210/en.2008-0447

García-López, Á., De Jonge, H., Nóbrega, R.H., De Waal, P.P., Van Dijk, W., Hemrika, W., Taranger, G.L., Bogerd, J., Schulz, R.W., 2010. Studies in Zebrafish Reveal Unusual Cellular Expression Patterns of Gonadotropin Receptor Messenger Ribonucleic Acids in the Testis and Unexpected Functional Differentiation of the Gonadotropins. Endocrinology 151, 2349–2360. https://doi.org/10.1210/en.2009-1227

García-Salinas, P., Gallego, V., Asturiano, J.F., 2021a. Reproductive Anatomy of Chondrichthyans: Notes on Specimen Handling and Sperm Extraction. I. Rays and Skates. Animals 11, 1888. https://doi.org/10.3390/ani11071888

García-Salinas, P., Gallego, V., Asturiano, J.F., 2021b. Reproductive Anatomy of Chondrichthyans: Notes on Specimen Handling and Sperm Extraction. II. Sharks and Chimaeras. Animals 11, 2191. https://doi.org/10.3390/ani11082191

Garnier, D.H., Sourdaine, P., Jégou, B., 1999. Seasonal Variations in Sex Steroids and Male Sexual Characteristics in Scyliorhinus canicula. General and Comparative Endocrinology 116, 281–290. https://doi.org/10.1006/gcen.1999.7369

Gautier, A., Bosseboeuf, A., Auvray, P., Sourdaine, P., 2014. Maintenance of Potential Spermatogonial Stem Cells In Vitro by GDNF Treatment in a Chondrichthyan Model

(Scyliorhinus canicula L.). Biology of Reproduction 91, 91–105. https://doi.org/10.1095/biolreprod.113.116020

Gautron, J., 1978. Effet du calcium et de la stimulation sur les terminaisons nerveuses des fonctions nerf-électroplaque de la Torpille. Biol. Cell. 31, 31–44. https://doi.org/10.1007/BF00495387

Gilbert, P.W., Heath, G.W., 1972. The clasper-siphon sac mechanism in Squalus acanthias and Mustelus canis. Comp Biochem Physiol A Comp Physiol 42, 97–119. https://doi.org/doi: 10.1016/0300-9629(72)90371-4

Girard, M., Rivalan, P., Sinquin, G., 2000. Testis and sperm morphology in two deep-water squaloid sharks, *Centroscymnus coelolepis* and *Centrophorus squamosus*. J Fish Biol 57, 1575–1589. https://doi.org/10.1111/j.1095-8649.2000.tb02233.x

Gomes do Rêgo, M., Fitzpatrick, J.L., Hissa V. Hazin, F., Araujo, M.Lucia.G., Barros, M.E.G., Evêncio Neto, J., 2016. Comparison of the Morphology and Histomorphometry of Spermatogenic Cyst of Three Sharks Species With Diametric Testes: Morphology of Cysts of three sharks. Anat. Rec. 299, 759–768. https://doi.org/10.1002/ar.23326

Gómez-H, L., Felipe-Medina, N., Condezo, Y.B., Garcia-Valiente, R., Ramos, I., Suja, J.A., Barbero, J.L., Roig, I., Sánchez-Martín, M., de Rooij, D.G., Llano, E., Pendas, A.M., 2019. The PSMA8 subunit of the spermatoproteasome is essential for proper meiotic exit and mouse fertility. PLoS Genet 15, e1008316. https://doi.org/10.1371/journal.pgen.1008316

Gong, Z., Wang, W., El Omari, K., Lebedev, A.A., Clarke, O.B., Hendrickson, W.A., 2023. Crystal structure of LGR ligand α2/β5 from Caenorhabditis elegans with implications for the evolution of glycoprotein hormones. PNAS 120, e2218630120. https://doi.org/10.1107/S205979832300102X

Gonzalez De Acevedo, M., Frazier, B.S., Belcher, C., Gelsleichter, J., 2020. Reproductive cycle and fecundity of the bonnethead Sphyrna tiburo from the northwest Atlantic Ocean. J Fish Biol 97, 1733–1747. https://doi.org/10.1111/jfb.14537

González-González, E., López-Casas, P.P., Del Mazo, J., 2008. Gene silencing by RNAi in mouse Sertoli cells. Reprod Biol Endocrinol 6, 29. https://doi.org/10.1186/1477-7827-6-29

Goodman, H.M., 2009. Hormonal control of reproduction in the male. Basic Medical Endocrinology 239–256. https://doi.org/10.1016/b978-0-12-373975-9.00012-4

Gorbman, A., 1995. Olfactory origins and evolution of the brain-pituitary endocrine system: facts and speculation. Gen Comp Endocrinol 97, 171–178. https://doi.org/10.1006/gcen.1995.1016

Grier, H.J., 1992. Chordate testis: The extracellular matrix hypothesis. J. Exp. Zool. 261, 151–160. https://doi.org/10.1002/jez.1402610206

Grier, H.J., Uribe, M.C., Lo Nostro, F.L., Mims, S.D., Parenti, L.R., 2016. Conserved form and function of the germinal epithelium through 500 million years of vertebrate evolution: Vertebrate Germinal Epithelium. J Morphol 277, 1014–1044. https://doi.org/10.1002/jmor.20554

Grogan, E.D., Lund, R., Greenfest-Allen, E., 2012. The origin and relationships of early chondrichthyans, in: Biology of Sharks and Their Relatives. M. R. Heithaus, J. A. Musick, and J. C. Carrier, (CRC Press: Boca Raton, FL), pp. 3–29.

Gu, Z., Eils, R., Schlesner, M., 2016. Complex heatmaps reveal patterns and correlations in multidimensional genomic data. Bioinformatics 32, 2847–2849. https://doi.org/10.1093/bioinformatics/btw313

Guo, F., Huang, X., Li, S., Sun, L., Li, Y., Li, H., Zhou, Y., Chu, Y., Zhou, T., 2007. Identification of Prosaposin as a Novel Interaction Partner for Rhox5. Journal of Genetics and Genomics 34, 392–399. https://doi.org/10.1016/S1673-8527(07)60042-3

Hall, B.K., 2005. Bones and Cartilage: developmental and evolutionary skeletal biology. Elsevier.

Hara, Y., Yamaguchi, K., Onimaru, K., Kadota, M., Koyanagi, M., Keeley, S.D., Tatsumi, K., Tanaka, K., Motone, F., Kageyama, Y., Nozu, R., Adachi, N., Nishimura, O., Nakagawa, R., Tanegashima, C., Kiyatake, I., Matsumoto, R., Murakumo, K., Nishida, K., Terakita, A., Kuratani, S., Sato, K., Hyodo, S., Kuraku, S., 2018. Shark genomes provide insights into elasmobranch evolution and the origin of vertebrates. Nat Ecol Evol 2, 1761–1771. https://doi.org/10.1038/s41559-018-0673-5

Hausken, K., Levavi-Sivan, B., 2019. Synteny and phylogenetic analysis of paralogous thyrostimulin beta subunits (GpB5) in vertebrates. PLoS ONE 14, e0222808. https://doi.org/10.1371/journal.pone.0222808

Hausken, K.N., Tizon, B., Shpilman, M., Barton, S., Decatur, W., Plachetzki, D., Kavanaugh, S., Ul-Hasan, S., Levavi-Sivan, B., Sower, S.A., 2018. Cloning and characterization of a second lamprey pituitary glycoprotein hormone, thyrostimulin (GpA2/GpB5). Gen Comp Endocrinol 264, 16–27. https://doi.org/10.1016/j.ygcen.2018.04.010

Helfman, G.S., Collette, B.B., Facey, D.E., Bowen, B.W., 2009. The diversity of fishes: biology, evolution, and ecology. John Wiley & Sons, Ltd.

Henke, A., Gromoll, J., 2008. New insights into the evolution of chorionic gonadotrophin. Molecular and Cellular Endocrinology 291, 11–19. https://doi.org/10.1016/j.mce.2008.05.009

Heyland, A., Plachetzki, D., Donelly, E., Gunaratne, D., Bobkova, Y., Jacobson, J., Kohn, A.B., Moroz, L.L., 2012. Distinct Expression Patterns of Glycoprotein Hormone Subunits in the Lophotrochozoan Aplysia: Implications for the Evolution of Neuroendocrine Systems in Animals. Endocrinology 153, 5440–5451. https://doi.org/10.1210/en.2012-1677

Holstein, A.-F., 1968. Zur Frage der lokalen Steuerung der Spermatogenese beim Dornhai (Squalus acanthias L.). Z. Zellforsch. 93, 265–281. https://doi.org/10.1007/BF00336694

Hsu, S.Y., Nakabayashi, K., Bhalla, A., 2002. Evolution of Glycoprotein Hormone Subunit Genes in Bilateral Metazoa: Identification of Two Novel Human Glycoprotein Hormone Subunit Family Genes, GPA2 and GPB5. J Mol Endocrinol 16, 1538–1551. https://doi.org/10.1210/mend.16.7.0871

Hsueh, A.J., He, J., 2018. Gonadotropins and their receptors: coevolution, genetic variants, receptor imaging, and functional antagonists. Biology of Reproduction 99, 3–12. https://doi.org/10.1093/biolre/ioy012

Hsueh, A.J.W., Feng, Y., 2020. Discovery of polypeptide ligand-receptor pairs based on their co-evolution. FASEB j. 34, 8824–8832. https://doi.org/10.1096/fj.202000779R

Huang, L., Haratake, K., Miyahara, H., Chiba, T., 2016. Proteasome activators, PA28γ and PA200, play indispensable roles in male fertility. Sci Rep 6, 23171. https://doi.org/10.1038/srep23171

Huhtaniemi, I., 2015. A short evolutionary history of FSH-stimulated spermatogenesis. Hormones (Athens) 14, 468–478. https://doi.org/doi: 10.14310/horm.2002.1632

Irisarri, I., Baurain, D., Brinkmann, H., Delsuc, F., Sire, J.-Y., Kupfer, A., Petersen, J., Jarek, M., Meyer, A., Vences, M., Philippe, H., 2017. Phylotranscriptomic consolidation of the jawed vertebrate timetree. Nat Ecol Evol 1, 1370–1378. https://doi.org/10.1038/s41559-017-0240-5

Ivory, P., Jeal, F., Nolan, C.P., 2004. Age Determination, Growth and Reproduction in the Lesser-spotted Dogfish, *Scyliorhinus canicula* (L.). J. Northw. Atl. Fish. Sci. 35, 89–106. https://doi.org/10.2960/J.v35.m504

Iwai, T., Yoshii, A., Yokota, T., Sakai, C., Hori, H., Kanamori, A., Yamashita, M., 2006. Structural components of the synaptonemal complex, SYCP1 and SYCP3, in the medaka fish Oryzias latipes. Exp Cell Res 312, 2528–2537. https://doi.org/10.1016/j.yexcr.2006.04.015

James, E.R., Carrell, D.T., Aston, K.I., Jenkins, T.G., Yeste, M., Salas-Huetos, A., 2020. The Role of the Epididymis and the Contribution of Epididymosomes to Mammalian Reproduction. IJMS 21, 5377. https://doi.org/10.3390/ijms21155377

Jeanne, F., Bernay, B., Sourdaine, P., 2023. Comparative Proteome Analysis of Four Stages of Spermatogenesis in the Small-Spotted Catshark (Scyliorhinus canicula), Using High-Resolution NanoLC-ESI-MS/MS. J Proteome Res 22, 2477–2492. https://doi.org/10.1021/acs.jproteome.3c00206

Jiang, S., Katz, T.A., Garee, J.P., DeMayo, F.J., Lee, A.V., Oesterreich, S., 2015. Scaffold attachment factor B2 (SAFB2) null mice reveal non-redundant functions compared to its paralog SAFB1. Model. Mec. 8, 1121–1127. https://doi.org/10.1242/dmm.019885

Johnson, G.P., Jonas, K.C., 2020. Mechanistic insight into how gonadotropin hormone receptor complexes direct signaling. Biol Reprod 102, 773–783. https://doi.org/10.1093/biolre/ioz228

Johnston, D.S., Jelinsky, S.A., Bang, H.J., DiCandeloro, P., Wilson, E., Kopf, G.S., Turner, T.T., 2005. The Mouse Epididymal Transcriptome: Transcriptional Profiling of Segmental Gene Expression in the Epididymis. Biol Reprod 73, 404–413. https://doi.org/10.1095/biolreprod.105.039719

Jones, C.J., Hamlett, W.C., 2002. Glycosylation of the male genital ducts and spermatozeugmata formation in the clearnose skate Raja eglanteria. Histochem J 34, 601–615. https://doi.org/doi: 10.1023/a:1026093902502

Jones, C.J.P., Hamlett, William.C., 2006. Ultrastructure of the male genital ducts of the clearnose skate Raja eglanteria. J. Exp. Zool. 305A, 1018–1029. https://doi.org/10.1002/jez.a.329

Jones, C.J.P., Walker, T.I., Bell, J.D., Reardon, M.B., Ambrosio, C.E., Almeida, A. (Eds.), 2005. Male Genital Ducts and Copulatory Appendages in Chondrichthyans, in: Reproductive Biology and Phylogeny of Chondrichthyes: Sharks, Batoids and Chimaeras. W.C. Hamlett, pp. 371–387. https://doi.org/10.1201/9781439856000-27

Jones, R.C., Jones, N., Djakiew, D., 1984. Luminal composition and maturation of spermatozoa in the male genital ducts of the Port Jackson shark, *Heterodontus portusjacksoni*. J. Exp. Zool. 230, 417–426. https://doi.org/10.1002/jez.1402300311

Joyce, W., Ripley, D.M., Gillis, T., Black, A.C., Shiels, H.A., Hoffmann, F.G., 2023. A Revised Perspective on the Evolution of Troponin I and Troponin T Gene Families in Vertebrates. Genome Biology and Evolution 15, evac173. https://doi.org/10.1093/gbe/evac173

Kanda, S., 2019. Evolution of the regulatory mechanisms for the hypothalamic-pituitary-gonadal axis in vertebrates–hypothesis from a comparative view. Gen Comp Endocrinol 284, 113075. https://doi.org/10.1016/j.ygcen.2018.11.014

Kanzaki, M., Morris, P.L., 1999. Growth Hormone Regulates Steroidogenic Acute Regulatory Protein Expression and Steroidogenesis in Leydig Cell Progenitors. Endocrinology 140, 1681–1686. https://doi.org/doi: 10.1210/endo.140.4.6661

Kara, E., Crépieux, P., Gauthier, C., Martinat, N., Piketty, V., Guillou, F., Reiter, E., 2006. A Phosphorylation Cluster of Five Serine and Threonine Residues in the C-Terminus of the Follicle-Stimulating Hormone Receptor Is Important for Desensitization But Not for β-Arrestin-Mediated ERK Activation. J Mol Endocrinol 20, 3014–3026. https://doi.org/10.1210/me.2006-0098

Kassambara, A., Mundt, F., 2020. Factoextra: Extract and Visualize the Results of Multivariate Data Analyses R Package Version 1.0.7.

Katona, G., Szabó, F., Végvári, Z., Székely, T., Liker, A., Freckleton, R.P., Vági, B., Székely, T., 2023. Evolution of reproductive modes in sharks and rays. J Evol Biol 36, 1630–1640. https://doi.org/10.1111/jeb.14231

Kavanaugh, S.I., Root, A.R., Sower, S.A., 2005. Distribution of gonadotropin-releasing hormone (GnRH) by in situ hybridization in the tunicate Ciona intestinalis. J Evol Biol 141, 76–83. https://doi.org/10.1016/j.ygcen.2004.11.012

Kavarthapu, R., Anbazhagan, R., Raju, M., Morris, C.-H.T., Pickel, J., Dufau, M.L., 2019. Targeted knock-in mice with a human mutation in GRTH/DDX25 reveals the essential role of phosphorylated GRTH in spermatid development during spermatogenesis. Hum. Mol. Genet. 28, 2561–2572. https://doi.org/10.1093/hmg/ddz079

Kawada, T., Aoyama, M., Sakai, T., Satake, H., 2013. Structure, Function, and Evolutionary Aspects of Invertebrate GnRHs and their Receptors, in: Gonadotropin-Releasing Hormone (GnRH): Production, Structure and Functions, Endocrinology Research and Clinical Developments. Nova Biomedical, New York, pp. 1–15.

Kenis, S., Istiban, M.N., Van Damme, S., Vandewyer, E., Watteyne, J., Schoofs, L., Beets, I., 2023. Ancestral glycoprotein hormone-receptor pathway controls growth in C. elegans. Front. Endocrinol. 14, 1200407. https://doi.org/10.3389/fendo.2023.1200407

Kherraf, Z., Christou-Kent, M., Karaouzene, T., Amiri-Yekta, A., Martinez, G., Vargas, A.S., Lambert, E., Borel, C., Dorphin, B., Aknin-Seifer, I., Mitchell, M.J., Metzler-Guillemain, C., Escoffier, J., Nef, S., Grepillat, M., Thierry-Mieg, N., Satre, V., Bailly, M., Boitrelle, F., Pernet-Gallay, K., Hennebicq, S., Fauré, J., Bottari, S.P., Coutton, C., Ray, P.F., Arnoult, C., 2017. SPINK2 deficiency causes infertility by inducingsperm defects in heterozygotes and azoospermiain homozygotes. EMBO Mol Med 9, 1132–1149. https://doi.org/10.15252/emmm.201607461

Kil, Y.J., Becker, C., Sandoval, W., Goldberg, D., Bern, M., 2011. Preview: A Program for Surveying Shotgun Proteomics Tandem Mass Spectrometry Data. Analytical Chemistry 83, 5259–5267. https://doi.org/10.1021/ac200609a

King, B.L., Gillis, J.A., Carlisle, H.R., Dahn, R.D., 2011. A Natural Deletion of the HoxC Cluster in Elasmobranch Fishes. Science 334, 1517–1517. https://doi.org/10.1126/science.1210912

King, J.A., Steneveld, A.A., Millar, R.P., Fasano, S., Romano, G., Spagnuolo, A., Zanetti, L., Pierantoni, R., 1992. Gonadotropin-releasing hormone in elasmobranch (electric ray, Torpedo marmorata) brain and plasma: Chromatographic and immunological evidence for chicken GnRH II and novel molecular forms. Peptides 13, 27–35. https://doi.org/10.1016/0196-9781(92)90136-Q

Knowles, F., Vollrath, L., Meurling, P., 1975. Cytology and neuroendocrine relations of the pituitary of the dogfish, Scyliorhinus canicula. Proceedings of the Royal Society of London. Series B. Biological Sciences 191, 507–525. https://doi.org/10.1098/rspb.1975.0141

Kopanja, D., Roy, N., Stoyanova, T., Hess, R.A., Bagchi, S., Raychaudhuri, P., 2011. Cul4A is essential for spermatogenesis and male fertility. Developmental Biology 352, 278–287. https://doi.org/10.1016/j.ydbio.2011.01.028

Kousteni, V., Kontopoulou, M., Megalofonou, P., 2010. Sexual maturity and fecundity of *Scyliorhinus canicula* (Linnaeus, 1758) in the Aegean Sea. Mar Biol Res 6, 390–398. https://doi.org/10.1080/17451000903233771

Kousteni, V., Megalofonou, P., 2020. Reproductive strategy of Scyliorhinus canicula (L., 1758): a holistic approach based on macroscopic measurements and microscopic

observations of the reproductive organs. Mar. Freshwater Res. 71, 596. https://doi.org/10.1071/MF18474

Krishnaswamy Gopalan, T., Gururaj, P., Gupta, R., Gopal, D.R., Rajesh, P., Chidambaram, B., Kalyanasundaram, A., Angamuthu, R., 2014. Transcriptome Profiling Reveals Higher Vertebrate Orthologous of Intra-Cytoplasmic Pattern Recognition Receptors in Grey Bamboo Shark. PLoS ONE 9, e100018. https://doi.org/10.1371/journal.pone.0100018

Kudo, M., Chen, T., Nakabayashi, K., Hsu, S.Y., Hsueh, A.J.W., 2000. The Nematode Leucine-Rich Repeat-Containing, G Protein-Coupled Receptor (LGR) Protein Homologous to Vertebrate Gonadotropin and Thyrotropin Receptors is Constitutively Activated in Mammalian Cells. J Mol Endocrinol 14, 272–284. https://doi.org/10.1210/mend.14.2.0422

Kumar, T.R., 2005. What have we learned about gonadotropin function from gonadotropin subunit and receptor knockout mice? Reproduction 130, 293–302. https://doi.org/10.1530/rep.1.00660

Kunduri, G., Le, S.-H., Baena, V., Vijaykrishna, N., Harned, A., Nagashima, K., Blankenberg, D., Yoshihiro, I., Narayan, K., Bamba, T., Acharya, U., Acharya, J.K., 2022. Delivery of ceramide phosphoethanolamine lipids to the cleavage furrow through the endocytic pathway is essential for male meiotic cytokinesis. PLoS Biol 20, e3001599. https://doi.org/10.1371/journal.pbio.3001599

Kuraku, S., 2021. Shark and ray genomics for disentangling their morphological diversity and vertebrate evolution. Developmental Biology 477, 262–272. https://doi.org/10.1016/j.ydbio.2021.06.001

Laqqan, M., Hammadeh, M.E., 2018. Alterations in DNA methylation patterns and gene expression in spermatozoa of subfertile males. Andrologia 50, e12934. https://doi.org/10.1111/and.12934

Laxson, C.J., Condon, N.E., Drazen, J.C., Yancey, P.H., 2011. Decreasing Urea:Trimethylamine N-Oxide Ratios with Depth in Chondrichthyes: A Physiological Depth Limit? Physiol Biochem Zool 84, 494–505. https://doi.org/10.1086/661774

Lê, S., Josse, J., Husson, F., 2008. FactoMineR: An R Package for Multivariate Analysis. J. Stat. Softw. 25, 1–18. https://doi.org/10.18637/jss.v025.i01

Leal, M.C., Cardoso, E.R., Nóbrega, R.H., Batlouni, S.R., Bogerd, J., França, L.R., Schulz, R.W., 2009. Histological and Stereological Evaluation of Zebrafish (Danio rerio) Spermatogenesis with an Emphasis on Spermatogonial Generations. Biol Reprod 81, 177–187. https://doi.org/10.1095/biolreprod.109.076299

Lei, Z.M., Mishra, S., Zou, W., Xu, B., Foltz, M., Li, X., Rao, C.V., 2001. Targeted Disruption of Luteinizing Hormone/Human Chorionic Gonadotropin Receptor Gene. J Mol Endocrinol 15, 184–200. https://doi.org/10.1210/mend.15.1.0586

Leisner, T.M., Freeman, T.C., Black, J.L., Parise, L.V., 2016. CIB1: a small protein with big ambitions. FASEB j. 30, 2640–2650. https://doi.org/10.1096/fj.201500073R

Leuzinger, L., Cuny, G., Popov, E., Billon-Bruyat, J., 2017. A new chondrichthyan fauna from the Late Jurassic of the Swiss Jura (Kimmeridgian) dominated by hybodonts, chimaeroids and guitarfishes. Papers in Palaeontology 3, 471–511. https://doi.org/10.1002/spp2.1085

Levavi-Sivan, B., Bogerd, J., Mañanós, E.L., Gómez, A., Lareyre, J.J., 2010. Perspectives on fish gonadotropins and their receptors. Gen Comp Endocrinol 165, 412–437. https://doi.org/10.1016/j.ygcen.2009.07.019

Levine, J.E., 2000. The hypothalamus as a major integrating center, in: Neuroendocrinology in Physiology and Medicine. NJ: Humana Press, Totowa, pp. 75–93.

Li, J., Ge, W., 2020. Zebrafish as a model for studying ovarian development: Recent advances from targeted gene knockout studies. Mol Cell Endocrinol 507, 110778. https://doi.org/10.1016/j.mce.2020.110778

Li, M., Li, H., Yang, H., Cheng, R., Zheng, P., Guo, R., 2020. Comparative proteomic analysis of round and elongated spermatids during spermiogenesis in mice. BMC 34. https://doi.org/10.1002/bmc.4799

Li, Q., Li, T., Xiao, X., Ahmad, D.W., Zhang, N., Li, H., Chen, Z., Hou, J., Liao, M., 2020. Specific expression and alternative splicing of mouse genes during spermatogenesis. Mol. Omics 16, 258–267. https://doi.org/10.1039/C9MO00163H

Li, W., Du, R., Xia, C., Zhang, H., Xie, Y., Gao, X., Ouyang, Y., Yin, Z., Hu, G., 2022. Novel pituitary actions of GnRH in teleost: The link between reproduction and feeding regulation. Front. Endocrinol. 13, 982297. https://doi.org/10.3389/fendo.2022.982297

Liang, H., Chen, L., Liu, Z., Zhou, X., 2012. Expression of functional follicle-stimulating hormone receptor and luteinizing hormone/chorionic gonadotrophin receptor in oviduct and uterus in prepubertal gilts. Livest Sci 148, 74–80. https://doi.org/10.1016/j.livsci.2012.05.012

Lin, C.-J., Jeng, S.-R., Lei, Z.-Y., Yueh, W.-S., Dufour, S., Wu, G.-C., Chang, C.-F., 2021. Involvement of Transforming Growth Factor Beta Family Genes in Gonadal Differentiation in Japanese Eel, Anguilla japonica, According to Sex-Related Gene Expressions. Cells 10, 3007. https://doi.org/10.3390/cells10113007

Liu, X., Teng, Z., Wang, Z., Zhu, P., Song, Z., Liu, F., 2022. Expressions of HSPA1L and HSPA9 are associated with poor sperm quality of low-motility spermatozoa in fertile men. Andrologia 54, e14321. https://doi.org/10.1111/and.14321

Loir, M., Sourdaine, P., 1994. Testes cells: isolation and culture. In: Hochachka PW, Mommsen TP (eds) Biochemistry and molecular biology of fishes: analytical techniques. New York, pp. 219–272.

Loir, M., Sourdaine, P., Mendis-Handagama, S.M.L.C., Jégou, B., 1995. Cell-cell interactions in the testis of teleosts and elasmobranchs. Microsc. Res. Tech. 32, 533–552. https://doi.org/10.1002/jemt.1070320606

Long, J.A., Mark-Kurik, E., Johanson, Z., Lee, M.S.Y., Young, G.C., Min, Z., Ahlberg, P.E., Newman, M., Jones, R., Blaauwen, J.D., Choo, B., Trinajstic, K., 2015. Copulation in antiarch placoderms and the origin of gnathostome internal fertilization. Nature 517, 196–199. https://doi.org/10.1038/nature13825

Loppion, G., Crespel, A., Martinez, A.-S., Auvray, P., Sourdaine, P., 2008. Study of the potential spermatogonial stem cell compartment in dogfish testis, Scyliorhinus canicula L. Cell Tissue Res 332, 533–542. https://doi.org/10.1007/s00441-008-0590-z

Lu, J.-Y., Schneider, R.J., 2004. Tissue Distribution of AU-rich mRNA-binding Proteins Involved in Regulation of mRNA Decay. Journal of Biological Chemistry 279, 12974–12979. https://doi.org/10.1074/jbc.M310433200

Luer, C.A., Walsh, C.J., Bodine, A.B., Wyffels, J.T., 2007. Normal embryonic development in the clearnose skate, Raja eglanteria, with experimental observations on artificial insemination. Environ Biol Fish 80, 239–255. https://doi.org/10.1007/s10641-007-9219-4

Luo, B.-Y., Fang, X., Wang, C.-Z., Yao, C.-J., Li, Z., He, X.-Y., Xiong, X.-Y., Xie, C.-Z., Lai, X.-L., Zhang, Z.-H., Qiu, G.-F., 2023. Identification of GnRH-like peptide and its potential signaling pathway involved in the oocyte meiotic maturation in the Chinese mitten crab, Eriocheir sinensis. Int J Biol Macromol 239, 124326. https://doi.org/10.1016/j.ijbiomac.2023.124326

Machado, A.M., Almeida, T., Mucientes, G., Esteves, P.J., Verissimo, A., Castro, L.F.C., 2018. De novo assembly of the kidney and spleen transcriptomes of the cosmopolitan blue

shark, Prionace glauca. Marine Genomics 37, 50–53. https://doi.org/10.1016/j.margen.2017.11.009

Maeda, N., Tsuchida, J., Nishimune, Y., Tanaka, H., 2022. Analysis of Ser/Thr Kinase HASPIN-Interacting Proteins in the Spermatids. IJMS 23, 9060. https://doi.org/10.3390/ijms23169060

Marion, S., Oakley, R.H., Kim, K.-M., Caron, M.G., Barak, L.S., 2006. A β-Arrestin Binding Determinant Common to the Second Intracellular Loops of Rhodopsin Family G Protein-coupled Receptors. JBC 281, 2932–2938. https://doi.org/10.1074/jbc.M508074200

Marongiu, M.F., Porcu, C., Pascale, N., Bellodi, A., Cau, A., Mulas, A., Pesci, P., Porceddu, R., Follesa, M.C., 2021. A Taxonomic Survey of Female Oviducal Glands in Chondrichthyes: A Comparative Overview of Microanatomy in the Two Reproductive Modes. Animals 11, 2653. https://doi.org/10.3390/ani11092653

Marra, N.J., Stanhope, M.J., Jue, N.K., Wang, M., Sun, Q., Pavinski Bitar, P., Richards, V.P., Komissarov, A., Rayko, M., Kliver, S., Stanhope, B.J., Winkler, C., O'Brien, S.J., Antunes, A., Jorgensen, S., Shivji, M.S., 2019. White shark genome reveals ancient elasmobranch adaptations associated with wound healing and the maintenance of genome stability. PNAS 116, 4446–4455. https://doi.org/10.1073/pnas.1819778116

Martin, C.S., Vaz, S., Ellis, J.R., Lauria, V., Coppin, F., Carpentier, A., 2012. Modelled distributions of ten demersal elasmobranchs of the eastern English Channel in relation to the environment. J Exp Mar Biol 418–419, 91–103. https://doi.org/10.1016/j.jembe.2012.03.010

Marvel, M., Spicer, O.S., Wong, T.-T., Zmora, N., Zohar, Y., 2018. Knockout of the Gnrh genes in zebrafish: effects on reproduction and potential compensation by reproductive and feeding-related neuropeptides†. Biol Reprod 99, 565–577. https://doi.org/10.1093/biolre/ioy078

Maston, G.A., Ruvolo, M., 2002. Chorionic Gonadotropin Has a Recent Origin Within Primates and an Evolutionary History of Selection. MBE 19, 320–335. https://doi.org/10.1093/oxfordjournals.molbev.a004085

Matz, H., Dooley, H., 2019. Shark IgNAR-derived binding domains as potential diagnostic and therapeutic agents. DCI 90, 100–107. https://doi.org/10.1016/j.dci.2018.09.007

Matz, H., Munir, D., Logue, J., Dooley, H., 2021. The immunoglobulins of cartilaginous fishes. Developmental & Comparative Immunology 115, 103873. https://doi.org/10.1016/j.dci.2020.103873

Maugars, G., Dufour, S., 2015. Demonstration of the Coexistence of Duplicated LH Receptors in Teleosts, and Their Origin in Ancestral Actinopterygians. PLoS ONE 10, e0135184. https://doi.org/10.1371/journal.pone.0135184

Maugars, G., Dufour, S., Cohen-Tannoudji, J., Quérat, B., 2014. Multiple Thyrotropin β-Subunit and Thyrotropin Receptor-Related Genes Arose during Vertebrate Evolution. PLoS ONE 9, e111361. https://doi.org/10.1371/journal.pone.0111361

Maurizii, M.G., Cavaliere, V., Gamberi, C., Lasko, P., Gargiulo, G., Taddei, C., 2009. Vasa protein is localized in the germ cells and in the oocyte-associated pyriform follicle cells during early oogenesis in the lizard Podarcis sicula. Dev Genes Evol 219, 361–367. https://doi.org/10.1007/s00427-009-0295-7

Mayeur, H., Leyhr, J., Mulley, J., Leurs, N., Michel, L., Sharma, K., Lagadec, R., Aury, J.-M., Osborne, O.G., Mulhair, P., Poulain, J., Mangenot, S., Mead, D., Smith, M., Corton, C., Oliver, K., Skelton, J., Betteridge, E., Dolucan, J., Dudchenko, O., Omer, A.D., Weisz, D., Aiden, E.L., McCarthy, S., Sims, Y., Torrance, J., Tracey, A., Howe, K., Baril, T., Hayward, A., Martinand-Mari, C., Sanchez, S., Haitina, T., Martin, K., Korsching, S.I., Mazan, S., Debiais-Thibaud, M., 2024. The sensory shark: high-quality morphological,

genomic and transcriptomic data for the small-spotted catshark *Scyliorhinus canicula* reveal the molecular bases of sensory organ evolution in jawed vertebrates. bioRxiv. https://doi.org/10.1101/2024.05.23.595469

McClusky, L.M., 2022. Several routes of cell death to secondary necrosis in the elasmobranch testis. Apoptosis 27, 454–464. https://doi.org/10.1007/s10495-022-01733-0

McClusky, L.M., 2013. The caspase-dependent apoptosis gradient in the testis of the blue shark, Prionace glauca. Reproduction 145, 297–310. https://doi.org/10.1530/REP-12-0216

McClusky, L.M., 2012. Coordination of spermatogenic processes in the testis: lessons from cystic spermatogenesis. Cell Tissue Res 349, 703–715. https://doi.org/10.1007/s00441-011-1288-1

McClusky, L.M., 2006. Stage-dependency of apoptosis and the blood-testis barrier in the dogfish shark (Squalus acanthias): cadmium-induced changes as assessed by vital fluorescence techniques. Cell Tissue Res 325, 541–553. https://doi.org/10.1007/s00441-006-0184-6

McClusky, L.M., 2005. Stage and season effects on cell cycle and apoptotic activities of germ cells and Sertoli cells during spermatogenesis in the spiny dogfish (Squalus acanthias). Reproduction 129, 89–102. https://doi.org/10.1530/rep.1.00177

McClusky, L.M., Sulikowski, J., 2014. The epigonal organ and mature pole of the testis in the recreationally fished blue shark (Prionace glauca): histochemico-functional correlates. J Anat 225, 614–624. https://doi.org/10.1111/joa.12242

Mellinger, J., 1994. L'œuf de roussette (scyliorhinus canicula) incubé au laboratoire: un matériel de recherche pour l'embryologiste, l'éthologiste, le physiologiste. Ichtyophysiologica Acta 9–27.

Millar, R.P., 2005. GnRHs and GnRH receptors. Anim Reprod Sci 88, 5–28. https://doi.org/10.1016/j.anireprosci.2005.05.032

Millar, R.P., 2003. GnRH II and type II GnRH receptors. TEM 14, 35–43. https://doi.org/10.1016/S1043-2760(02)00016-4

Minamikawa', S., Morisawa, M., 1996. Acquisition, Initiation and Maintenance of Sperm Motility in the Shark, Ttiakis scyllia. Comp Biochem Physiol A Mol Integr Physiol 113, 387–392. https://doi.org/10.1016/0300-9629(95)02080-2

Mistry, B.V., Alanazi, M., Fitwi, H., Al-Harazi, O., Rajab, M., Altorbag, A., Almohanna, F., Colak, D., Assiri, A.M., 2020. Expression profiling of WD40 family genes including DDB1- and CUL4- associated factor (DCAF) genes in mice and human suggests important regulatory roles in testicular development and spermatogenesis. BMC Genomics 21, 602. https://doi.org/10.1186/s12864-020-07016-9

Miyaso, H., Ogawa, Y., Itoh, M., 2022. Microenvironment for spermatogenesis and sperm maturation. Histochem Cell Biol 157, 273–285. https://doi.org/10.1007/s00418-021-02071-z

Mohammadzadeh, S., Moradian, F., Yeganeh, S., Falahatkar, B., Milla, S., 2020. Design, production and purification of a novel recombinant gonadotropin-releasing hormone associated peptide as a spawning inducing agent for fish. Protein Expr Purif 166, 105510. https://doi.org/10.1016/j.pep.2019.105510

Morales-Gamba, R.D., Araújo, M.L.G., Barcellos, J.F.M., Rêgo, M.G., Dias, L.C., Marcon, J.L., 2023. Progesterone receptors in extratesticular ducts of the Amazonian stingray Potamotrygon wallacei: A potential role in sperm maturation and aggregate formation. Gen Comp Endocrinol 344, 114375. https://doi.org/10.1016/j.ygcen.2023.114375

Muciaccia, B., Boitani, C., Berloco, B.P., Nudo, F., Spadetta, G., Stefanini, M., De Rooij, D.G., Vicini, E., 2013. Novel Stage Classification of Human Spermatogenesis Based on Acrosome Development. Biol Reprod 89. https://doi.org/10.1095/biolreprod.113.111682

Mulley, J.F., Hargreaves, A.D., Hegarty, M.J., Heller, R.S., Swain, M.T., 2014. Transcriptomic analysis of the lesser spotted catshark (Scyliorhinus canicula) pancreas, liver and brain reveals molecular level conservation of vertebrate pancreas function. BMC genomics 15, 1–18. https://doi.org/10.1186/1471-2164-15-1074

Muñoz-Baquero, M., Lorenzo-Rebenaque, L., García-Domínguez, X., Valdés-Hernández, J., García-Párraga, D., Marin, C., García-Vázquez, F.A., Marco-Jiménez, F., 2024. Proteomic Insights into Seminal Plasma and Spermatozoa Proteins of Small-Spotted Catsharks, Scyliorhinus canicula: Implications for Reproductive Conservation in Aquariums. Animals 14, 1281. https://doi.org/10.3390/ani14091281

Murat, F., Mbengue, N., Winge, S.B., Trefzer, T., Leushkin, E., Sepp, M., Cardoso-Moreira, M., Schmidt, J., Schneider, C., Mößinger, K., Brüning, T., Lamanna, F., Belles, M.R., Conrad, C., Kondova, I., Bontrop, R., Behr, R., Khaitovich, P., Pääbo, S., Marques-Bonet, T., Grützner, F., Almstrup, K., Schierup, M.H., Kaessmann, H., 2023. The molecular evolution of spermatogenesis across mammals. Nature 613, 308–316. https://doi.org/10.1038/s41586-022-05547-7

Nagasaki, H., Wang, Z., Jackson, V.R., Lin, S., Nothacker, H.P., Civelli, O., 2006ential expression of the thyrostimulin subunits, glycoprotein α2 and β5 in the rat pituitary. J Mol Endocrinol 37, 39–50. https://doi.org/10.1677/jme.1.01932

Nakabayashi, K., Matsumi, H., Bhalla, A., Bae, J., Mosselman, S., Hsu, S.Y., Hsueh, A.J.W., 2002. Thyrostimulin, a heterodimer of two new human glycoprotein hormone subunits, activates the thyroid-stimulating hormone receptor. J. Clin. Invest. 109, 1445–1452. https://doi.org/10.1172/JCI0214340

Nakamura, M., Okinaga, shoichi, ARAI, K., 1984. Metabolism of pachytene primary spermatocytes from rat testes: pyruvate maintenance of adenosine triphosphate level. Biol Reprod 30, 1187–1197.

Naro, C., Jolly, A., Di Persio, S., Bielli, P., Setterblad, N., Alberdi, A.J., Vicini, E., Geremia, R., De la Grange, P., Sette, C., 2017. An Orchestrated Intron Retention Program in Meiosis Controls Timely Usage of Transcripts during Germ Cell Differentiation. Developmental Cell 41, 82-93.e4. https://doi.org/10.1016/j.devcel.2017.03.003

Nazarian, J., Hathout, Y., Vertes, A., Hoffman, E. P, 2007. The Proteome Survey of an Electricity-Generating Organ (*Torpedo Californica* Electric Organ). Proteomics 7, 617–627. https://doi.org/10.1002/pmic.200600686.

Nelson, J.S., Grande, T.C., Wilson, M.V., 2016. Fishes of the World, Fifth Edition. ed. John Wiley & Sons, Inc.

Neves, F., Muñoz-Mérida, A., Machado, A.M., Almeida, T., Gaigher, A., Esteves, P.J., Castro, L.F.C., Veríssimo, A., 2022. Uncovering a 500 million year old history and evidence of pseudogenization for TLR15. Front. Immunol. 13, 1020601. https://doi.org/10.3389/fimmu.2022.1020601

Nielsen, J., Hedeholm, R.B., Heinemeier, J., Bushnell, P.G., Christiansen, J.S., Olsen, J., Ramsey, C.B., Brill, R.W., Simon, M., Steffensen, K.F., Steffensen, J.F., 2016. Eye lens radiocarbon reveals centuries of longevity in the Greenland shark ( *Somniosus microcephalus* ). Science 353, 702–704. https://doi.org/10.1126/science.aaf1703

Nóbrega, R.H., Greebe, C.D., Van De Kant, H., Bogerd, J., De França, L.R., Schulz, R.W., 2010. Spermatogonial Stem Cell Niche and Spermatogonial Stem Cell Transplantation in Zebrafish. PLoS ONE 5, e12808. https://doi.org/10.1371/journal.pone.0012808

Norman, M., Rivers, C., Lee, Y.-B., Idris, J., Uney, J., 2016. The increasing diversity of functions attributed to the SAFB family of RNA-/DNA-binding proteins. Biochemical Journal 473, 4271–4288. https://doi.org/10.1042/BCJ20160649

Nosenko, T., Schreiber, F., Adamska, M., Adamski, M., Eitel, M., Hammel, J., Maldonado, M., Müller, W.E.G., Nickel, M., Schierwater, B., Vacelet, J., Wiens, M., Wörheide, G.,

2013. Deep metazoan phylogeny: When different genes tell different stories. Mol Phylogenet Evol 67, 223–233. https://doi.org/10.1016/j.ympev.2013.01.010

Oduwole, O.O., Huhtaniemi, I.T., Misrahi, M., 2021. The Roles of Luteinizing Hormone, Follicle-Stimulating Hormone and Testosterone in Spermatogenesis and Folliculogenesis Revisited. IJMS 22, 12735. https://doi.org/10.3390/ijms222312735

Ogawa, S., Yamamoto, N., Hagio, H., Oka, Y., Parhar, I.S., 2022. Multiple gonadotropin-releasing hormone systems in non-mammalian vertebrates: Ontogeny, anatomy, and physiology. J Neuroendocrinol 34, e13068. https://doi.org/10.1111/jne.13068

Ogórek, M., Herman, S., Pierzchała, O., Bednarz, A., Rajfur, Z., Baster, Z., Grzmil, P., Starzyński, R.R., Szudzik, M., Jończy, A., Lipiński, P., Lenartowicz, M., 2019. Molecular machinery providing copper bioavailability for spermatozoa along the epididymial tubule in mouse. Biology of Reproduction 100, 1505–1520. https://doi.org/10.1093/biolre/ioz028

Ohno, S., Nishikawa, K., Honda, Y., Nakajin, S., 2008. Expression in E. coli and tissue distribution of the human homologue of the mouse Ke 6 gene, 17β-hydroxysteroid dehydrogenase type 8. Mol Cell Biochem 309, 209–215. https://doi.org/10.1007/s11010-007-9637-9

Ohta, T., Miyake, H., Miura, C., Kamei, H., Aida, K., Miura, T., 2007. Follicle-Stimulating Hormone Induces Spermatogenesis Mediated by Androgen Production in Japanese Eel, Anguilla japonica. Biol Reprod 77, 970–977. https://doi.org/10.1095/biolreprod.107.062299

Okubo, K., Nagahama, Y., 2008. Structural and functional evolution of gonadotropin-releasing hormone in vertebrates. Acta Physiologica 193, 3–15. https://doi.org/10.1111/j.1748-1716.2008.01832.x

Onimaru, K., Tatsumi, K., Shibagaki, K., Kuraku, S., 2018. A de novo transcriptome assembly of the zebra bullhead shark, Heterodontus zebra. Sci Data 5, 180197. https://doi.org/10.1038/sdata.2018.197

Onoda, M., Djakiew, D., 1990. Modulation of Sertoli cell secretory function by rat round spermatid protein(s). Molecular and Cellular Endocrinology 73, 35–44. https://doi.org/10.1016/0303-7207(90)90042-7

O'Shaughnessy, K.L., Dahn, R.D., Cohn, M.J., 2015. Molecular development of chondrichthyan claspers and the evolution of copulatory organs. Nat Commun 6, 6698. https://doi.org/10.1038/ncomms7698

Osugi, T., Sasakura, Y., Satake, H., 2017. The nervous system of the adult ascidian Ciona intestinalis Type A (Ciona robusta): Insights from transgenic animal models. PLoS ONE 12, e0180227. https://doi.org/10.1371/journal.pone.0180227

Parenti, L.R., Grier, H.J., 2004. Evolution and Phylogeny of Gonad Morphology in Bony Fishes. ICB 44, 333–348. https://doi.org/10.1093/icb/44.5.333

Park, J., Kim, S.W., Cho, M.C., 2021. The Role of LIM Kinase in the Male Urogenital System. Cells 11, 78. https://doi.org/10.3390/cells11010078

Park, J.-C., Lee, J.-H., Kodama, K., Urushitani, H., Ohta, Y., Horiguchi, T., 2013. Structure of the intratesticular duct system for sperm emission in the starspotted smooth-hound Mustelus manazo. Fish Sci 79, 203–211. https://doi.org/10.1007/s12562-012-0581-6

Paronetto, M.P., Sette, C., 2010. Role of RNA-binding proteins in mammalianspermatogenesis. Cancer research 70, 229–239. https://doi.org/10.1111/j.1365-2605.2009.00959.x

Patel, H., Bhartiya, D., 2016. Testicular Stem Cells Express Follicle-Stimulating Hormone Receptors and Are Directly Modulated by FSH. Reprod. Sci. 23, 1493–1508. https://doi.org/10.1177/1933719116643593

Pawlicki, P., Yurdakok-Dikmen, B., Tworzydlo, W., Kotula-Balak, M., 2024. Toward understanding the role of the interstitial tissue architects: Possible functions of telocytes

in the male gonad. Theriogenology 217, 25–36. https://doi.org/10.1016/j.theriogenology.2024.01.013
Pecio, A., 2019. Testis structure, Spermatogenesis, and spermatozoa in teleost fishes, in: The Histology of Fishes. CRC Press, pp. 177–206.
Penfold, L.M., Wyffels, J.T., 2019. Reproductive Science in Sharks and Rays In: Comizzoli, P., Brown, J., Holt, W. (eds) Reproductive Sciences in Animal Conservation. Advances in Experimental Medicine and Biology, vol 1200. Springer, pp. 465–488. https://doi.org/10.1007/978-3-030-23633-5_15
Perey, B., Clermont, Y., Leblond, C., 1960. The wave of the seminiferous epithelium in the rat. Am J Anat.
Piferrer, F.C., Callard, G.V., 1995. Inhibition of Deoxyribonucleic Acid Synthesis during Premeiotic Stages of Spermatogenesis by a Factor from Testis-Associated Lymphomyeloid Tissue in the Dogfish Shark (Squalus Acanthias). Biol Reprod 53, 390–398. https://doi.org/10.1095/biolreprod53.2.390
Plain, Z., Voliotis, M., McArdle, C.A., Tsaneva-Atanasova, K., 2022. Modelling KNDy neurons and gonadotropin-releasing hormone pulse generation. Curr Opin Endocrinol Diabetes Obes 27, 100407. https://doi.org/10.1016/j.coemr.2022.100407
Planas, J.V., 1995. Maturation-associated changes in the response of the salmon testis to the steroidogenic actions of gonadotropins (GTH I and GTH II) in vitro. Biol Reprod 52, 697–704. https://doi.org/10.1095/biolreprod52.3.697
Poulakis, G.R., Grier, H.J., 2014. Ontogenetic testicular development and spermatogenesis in rays: the Cownose Ray, Rhinoptera bonasus, as a model. Environ Biol Fish 97, 1013–1029. https://doi.org/10.1007/s10641-014-0267-2
Pratt, H.L., 1988. Elasmobranch Gonad Structure: A Description and Survey. Copeia 1988, 719. https://doi.org/10.2307/1445394
Pratt, H.L., Carrier, J.C., 2001. A Review of Elasmobranch Reproductive Behavior with a Case Study on the Nurse Shark, Ginglymostoma Cirratum. Environ Biol Fishes 157–188. https://doi.org/10.1023/A:1007656126281
Pratt, H.L., Tanaka, S., 1994. Sperm storage in male elasmobranchs: A description and survey. J. Morphol. 219, 297–308. https://doi.org/10.1002/jmor.1052190309
Prisco, M., Donizetti, A., Aniello, F., Locascio, A., Del Giudice, G., Agnese, M., Angelini, F., Andreuccetti, P., 2009. Expression of Prothymosin alpha during the spermatogenesis of the spotted ray Torpedo marmorata. General and Comparative Endocrinology 164, 70–76. https://doi.org/10.1016/j.ygcen.2009.05.005
Prisco, M., Liguoro, A., Comitato, R., Cardone, A., D'Onghia, B., Ricchiari, L., Angelini, F., Andreuccetti, P., 2003. Apoptosis during spermatogenesis in the spotted rayTorpedo marmorata. Mol. Reprod. Dev. 64, 341–348. https://doi.org/10.1002/mrd.10267
Prisco, M., Liguoro, A., Ricchiari, L., Del Giudice, G., Angelini, F., Andreuccetti, P., 2008. Immunolocalization of 3β-HSD and 17β-HSD in the testis of the spotted ray Torpedo marmorata. Gen Comp Endocrinol 155, 157–163. https://doi.org/10.1016/j.ygcen.2007.04.016
Prisco, M., Loredana, R., Piero, A., 2002. Ultrastructural studies on developing follicles of the spotted rayTorpedo marmorata. Mol. Reprod. Dev. 61, 78–86. https://doi.org/10.1002/mrd.1133
Pudney, J., 1995. Spermatogenesis in nonmammalian vertebrates. Microsc Res Tech 32, 459–497. https://doi.org/10.1002/jemt.1070320602
Pudney, J., Callard, G.V., 1986. Sertoli cell cytoplasts in the semen of the spiny dogfish Squalus acanthias. Cell Tissue Res 375–382. https://doi.org/10.1016/0040-8166(86)90057-1
Pudney, J., Callard, G.V., 1984a. Identification of Leydig-like cells in the testis of the dogfish Squalus acanthias. Anat. Rec. 209, 323–330. https://doi.org/10.1002/ar.1092090310

Pudney, J., Callard, G.V., 1984b. Development of agranular reticulum in Sertoli cells of the testis of the dogfish *Squalus* acanthias during spermatogenesis. Anat Rec 209, 311–321. https://doi.org/10.1002/ar.1092090309

Pudney, J., Callard, G.V., 1984b. Development of agranular reticulum in Sertoli cells of the testis of the dogfishSqualus acanthias during spermatogenesis. Anat Rec 209, 311–321. https://doi.org/10.1002/ar.1092090309

Qin, J., Huang, T., Wang, Z., Zhang, X., Wang, J., Dang, Q., Cui, D., Wang, X., Zhai, Y., Zhao, L., Lu, G., Shao, C., Li, S., Liu, H., Liu, Z., 2023. Bud31-mediated alternative splicing is required for spermatogonial stem cell self-renewal and differentiation. Cell Death Differ 30, 184–194. https://doi.org/10.1038/s41418-022-01057-1

Querat, B., 2021. Unconventional Actions of Glycoprotein Hormone Subunits: A Comprehensive Review. Front. Endocrinol. 12, 731966. https://doi.org/10.3389/fendo.2021.731966

Rabionet, M., Bayerle, A., Jennemann, R., Heid, H., Fuchser, J., Marsching, C., Porubsky, S., Bolenz, C., Guillou, F., Gröne, H.-J., Gorgas, K., Sandhoff, R., 2015. Male meiotic cytokinesis requires ceramide synthase 3-dependent sphingolipids with unique membrane anchors. Hum. Mol. Genet. 24, 4792–4808. https://doi.org/10.1093/hmg/ddv204

Ramaswamy, S., Weinbauer, G.F., 2014. Endocrine control of spermatogenesis: Role of FSH and LH/ testosterone. Spermatogenesis 4, e996025. https://doi.org/10.1080/21565562.2014.996025

Read, T.D., Petit, R.A., Joseph, S.J., Alam, Md.T., Weil, M.R., Ahmad, M., Bhimani, R., Vuong, J.S., Haase, C.P., Webb, D.H., Tan, M., Dove, A.D.M., 2017. Draft sequencing and assembly of the genome of the world's largest fish, the whale shark: Rhincodon typus Smith 1828. BMC Genomics 18, 532. https://doi.org/10.1186/s12864-017-3926-9

Ricchiari, L., Liguoro, A., Andreuccetti, P., Angelini, F., Prisco, M., 2006. The Fas/FasL system is a possible regulator of germ cell apoptosis in the testis of Torpedo marmorata. J Fish Biology 69, 1779–1787. https://doi.org/10.1111/j.1095-8649.2006.01248.x

Richburg, J.H., Myers, J.L., Bratton, S.B., 2014. The role of E3 ligases in the ubiquitin-dependent regulation of spermatogenesis. Semin Cell Dev Biol 30, 27–35. https://doi.org/10.1016/j.semcdb.2014.03.001

Rocco, D.A., Garcia, A.S.G., Scudeler, E.L., dos Santos, D.C., Nóbrega, R.H., Paluzzi, J.-P.V., 2019. Glycoprotein Hormone Receptor Knockdown Leads to Reduced Reproductive Success in Male Aedes aegypti. Front. Physiol. 10, 266. https://doi.org/10.3389/fphys.2019.00266

Rocco, D.A., Kim, D.H., Paluzzi, J.-P.V., 2017. Immunohistochemical mapping and transcript expression of the GPA2/GPB5 receptor in tissues of the adult mosquito, Aedes aegypti. Cell Tissue Res 369, 313–330. https://doi.org/10.1007/s00441-017-2610-3

Rocco, D.A., Paluzzi, J.-P.V., 2020. Expression Profiling, Downstream Signaling, and Inter-subunit Interactions of GPA2/GPB5 in the Adult Mosquito Aedes aegypti. Front. Endocrinol. 11, 158. https://doi.org/10.3389/fendo.2020.00158

Roch, G.J., Busby, E.R., Sherwood, N.M., 2011. Evolution of GnRH: Diving deeper. Gen Comp Endocrinol 171, 1–16. https://doi.org/10.1016/j.ygcen.2010.12.014

Roch, G.J., Sherwood, N.M., 2014. Glycoprotein Hormones and Their Receptors Emerged at the Origin of Metazoans. Genome Biol Evol 6, 1466–1479. https://doi.org/10.1093/gbe/evu118

Roch, G.J., Tello, J.A., Sherwood, N.M., 2014. At the Transition from Invertebrates to Vertebrates, a Novel GnRH-Like Peptide Emerges in Amphioxus. Mol Biol Evol 31, 765–778. https://doi.org/10.1093/molbev/mst269

Rocha, A., Gómez, A., Galay-Burgos, M., Zanuy, S., Sweeney, G.E., Carrillo, M., 2007. Molecular characterization and seasonal changes in gonadal expression of a thyrotropin receptor in the European sea bass. Gen Comp Endocrinol 152, 89–101. https://doi.org/10.1016/j.ygcen.2007.03.001

Rodrigtjez-Cabello, C., de la Gándara, F., Sánchez, F., 1998. Preliminary results on growth and movements of dogfish Scyliorhinus canicula (Linnaeus, 1758) in the Cantabrian Sea. Oceanologica Acta 21, 363–370. https://doi.org/10.1016/S0399-1784(98)80023-6

Rupik, W., Huszno, J., Klag, J., 2011. Cellular organisation of the mature testes and stages of spermiogenesis in Danio rerio (Cyprinidae; Teleostei)—Structural and ultrastructural studies. Micron 42, 833–839. https://doi.org/10.1016/j.micron.2011.05.006

Sahin, Z., Szczepny, A., McLaughlin, E.A., Meistrich, M.L., Zhou, W., Ustunel, I., Loveland, K.L., 2014. Dynamic Hedgehog signalling pathway activity in germline stem cells. Andrology 2, 267–274. https://doi.org/10.1111/j.2047-2927.2014.00187.x

Sailler, A., Laidebeure, S., Lécu, A., 2023. Effects of a GnRH vaccine and deslorelin acetate implants in male freshwater stingrays (Potamotrygon sp.). J Zoo Wildl Med 54, 40–48. https://doi.org/10.1638/2022-0090

Sakai, T., Yamamoto, T., Matsubara, S., Kawada, T., Satake, H., 2020. Invertebrate Gonadotropin-Releasing Hormone Receptor Signaling and Its Relevant Biological Actions. IJMS 21, 8544. https://doi.org/10.3390/ijms21228544

Sambroni, E., Lareyre, J.-J., Le Gac, F., 2013. Fsh Controls Gene Expression in Fish both Independently of and through Steroid Mediation. PLoS ONE 8, e76684. https://doi.org/10.1371/journal.pone.0076684

Sambroni, E., Le Gac, F., Breton, B., Lareyre, J.-J., 2007. Functional specificity of the rainbow trout (Oncorhynchus mykiss) gonadotropin receptors as assayed in a mammalian cell line. J Endocrinol 195, 213–228. https://doi.org/10.1677/JOE-06-0122

Santiago-Andres, Y., Golan, M., Fiordelisio, T., 2021. Functional Pituitary Networks in Vertebrates. Front. Endocrinol. 11, 619352. https://doi.org/10.3389/fendo.2020.619352

Sato, H., Tsai-Morris, C.-H., Dufau, M.L., 2010. Relevance of gonadotropin-regulated testicular RNA helicase (GRTH/DDX25) in the structural integrity of the chromatoid body during spermatogenesis. Biochim Biophys Acta 1803, 534–543. https://doi.org/10.1016/j.bbamcr.2010.02.004

Schmidt, P., Leman, E., Lagadec, R., Schubert, M., Mazan, S., Reshef, R., 2022. Evolutionary Transition in the Regulation of Vertebrate Pronephros Development: A New Role for Retinoic Acid. Cells 11, 1304. https://doi.org/10.3390/cells11081304

Schulz, R.W., de França, L.R., Lareyre, J.-J., LeGac, F., Chiarini-Garcia, H., Nobrega, R.H., Miura, T., 2010. Spermatogenesis in fish. Gen Comp Endocrinol 165, 390–411. https://doi.org/10.1016/j.ygcen.2009.02.013

Sefideh, F.A., Moon, M.J., Yun, S., Hong, S.I., Hwang, J.-I., Seong, J.Y., 2014. Local Duplication of Gonadotropin-Releasing Hormone (GnRH) Receptor before Two Rounds of Whole Genome Duplication and Origin of the Mammalian GnRH Receptor. PLoS ONE 9, e87901. https://doi.org/10.1371/journal.pone.0087901

Seidel, R., Lyons, K., Blumer, M., Zaslansky, P., Fratzl, P., Weaver, J.C., Dean, M.N., 2016. Ultrastructural and developmental features of the tessellated endoskeleton of elasmobranchs (sharks and rays). J Anat 229, 681–702. https://doi.org/10.1111/joa.12508

Sengupta, P., Arafa, M., Elbardisi, H., 2019. Hormonal regulation of spermatogenesis, in: Molecular Signaling in Spermatogenesis and Male Infertility. CRC Press, pp. 41–49.

Shang, G., Peng, X., Ji, C., Zhai, G., Ruan, Y., Lou, Q., Jin, X., He, J., Wang, H., Yin, Z., 2019. Steroidogenic acute regulatory protein and luteinizing hormone are required for normal

ovarian steroidogenesis and oocyte maturation in zebrafish†. Biol Reprod 101, 760–770. https://doi.org/10.1093/biolre/ioz132

Shayu, D., Rao, A.J., 2006. Expression of functional aromatase in the epididymis: Role of androgens and LH in modulation of expression and activity. Mol Cell Endocrinol 249, 40–50. https://doi.org/10.1016/j.mce.2006.01.016

Sherwood, N.M., Lovejoy, D.A., 1993. Gonadotropin-releasing hormone in cartilaginous fishes: structure, location, and transport In: Demski, L.S., Wourms, J.P. (eds) The reproduction and development of sharks, skates, rays and ratfishes. Developments in environmental biology of fishes, vol 14. Springer, Dordrecht. https://doi.org/10.1007/978-94-017-3450–9_18.

Shimoyama, K., Kawano, M., Ogawa, N., Tokunaga, K., Takagi, W., Kobayashi, M., Hyodo, S., 2023. Progesterone initiates tendril formation in the oviducal gland during egg encapsulation in cloudy catshark (Scyliorhinus torazame). Zool Lett 9, 13. https://doi.org/10.1186/s40851-023-00211-y

Simpson, T.H., Wardle, C.S., 1967. A Seasonal Cycle in the Testis of the Spurdog, Squalus Acanthias, and the Sites of 3β-Hydroxysteroid Dehydrogenase Activity. J. Mar. Biol. Ass. 47, 699–708. https://doi.org/10.1017/S0025315400035281

Somoza, G.M., Mechaly, A.S., Trudeau, V.L., 2020. Kisspeptin and GnRH interactions in the reproductive brain of teleosts. Gen Comp Endocrinol 298, 113568. https://doi.org/10.1016/j.ygcen.2020.113568

Song, H., Park, H.-J., Lee, W.-Y., Lee, K.H., 2022. Models and Molecular Markers of Spermatogonial Stem Cells in Vertebrates: To Find Models in Nonmammals. Stem Cells Int 2022, 1–11. https://doi.org/10.1155/2022/4755514

Sonigo, C., Binart, N., 2012. Overview of the impact of kisspeptin on reproductive function. Annales d'Endocrinologie 73, 448–458. https://doi.org/10.1016/j.ando.2012.07.680

Soumillon, M., Necsulea, A., Weier, M., Brawand, D., Zhang, X., Gu, H., Barthès, P., Kokkinaki, M., Nef, S., Gnirke, A., Dym, M., de Massy, B., Mikkelsen, T.S., Kaessmann, H., 2013. Cellular Source and Mechanisms of High Transcriptome Complexity in the Mammalian Testis. Cell Reports 3, 2179–2190. https://doi.org/10.1016/j.celrep.2013.05.031

Sourdaine, P., Garnier, D.H., 1993. Stage-dependent modulation of Sertoli cell steroid production in dogfish (Scyliorhinus canicula). Reproduction 97, 133–142. https://doi.org/10.1530/jrf.0.0970133

Sourdaine, P., Garnier, D.H., Jégou, B., 1990. The adult dogfish (Scyliorhinus canicula L.) testis: a model to study stage-dependent changes in steroid levels during spermatogenesis. J Endocrinol 127, 451–460. https://doi.org/10.1677/joe.0.1270451

Sourdaine, P., Gautier, A., Gribouval, L., 2018. Spermatogenesis and Spermiogenesis in Elasmobranchs, a Short Overview, in: Encyclopedia of Reproduction. Elsevier, pp. 305–312. https://doi.org/10.1016/B978-0-12-809633-8.20572-4

Sourdaine, P., Jeanne, F., 2024. Spermatogenesis in Elasmobranchs, in: Encyclopedia of Reproduction, 3d Edition. Elsevier, pp. 1–13. https://doi.org/10.1016/B978-0-443-21477-6.00014-6

Sower, S.A., 2018. Landmark discoveries in elucidating the origins of the hypothalamic-pituitary system from the perspective of a basal vertebrate, sea lamprey. Gen Comp Endocrinol 264, 3–15. https://doi.org/10.1016/j.ygcen.2017.10.016

Sower, S.A., 2015. Breaking Dogma on the Hypothalamic-Pituitary Anatomical Relations in Vertebrates. Endocrinology 156, 3882–3884. https://doi.org/10.1210/en.2015-1778

Sower, S.A., Decatur, W.A., Hausken, K.N., Marquis, T.J., Barton, S.L., Gargan, J., Freamat, M., Wilmot, M., Hollander, L., Hall, J.A., Nozaki, M., Shpilman, M., Levavi-Sivan, B., 2015. Emergence of an Ancestral Glycoprotein Hormone in the Pituitary of the Sea

Lamprey, a Basal Vertebrate. Endocrinology 156, 3026–3037. https://doi.org/10.1210/en.2014-1797

Stanley, H.P., 1971. Fine structure of spermiogenesis in the elasmobranch fish Squalus suckleyi. II. Late stages of differentiation and structure of the mature spermatozoon. J Ultrastruct Res 36, 103–118. https://doi.org/10.1016/S0022-5320(71)80091-6

Stanley, H.P., 1966. The structure and development of the seminiferous follicle in Scyliorhinus caniculus and Torpedo marmorata (Elasmobranchii). Zeitschrift für Zellforschung und Mikroskopische Anatomie 75, 453–468. https://doi.org/10.1007/BF00336875

Stavrianakou, M., Perez, R., Wu, C., Sachs, M.S., Aramayo, R., Harlow, M., 2017. Draft de novo transcriptome assembly and proteome characterization of the electric lobe of Tetronarce californica: a molecular tool for the study of cholinergic neurotransmission in the electric organ. BMC Genomics 18, 611. https://doi.org/10.1186/s12864-017-3890-4

Sudo, S., Kuwabara, Y., Park, J.-I., Hsu, S.Y., Hsueh, A.J.W., 2005. Heterodimeric Fly Glycoprotein Hormone-α2 (GPA2) and Glycoprotein Hormone-β5 (GPB5) Activate Fly Leucine-Rich Repeat-Containing G Protein-Coupled Receptor-1 (DLGR1) and Stimulation of Human Thyrotropin Receptors by Chimeric Fly GPA2 and Human GPB5. Endocrinology 146, 3596–3604. https://doi.org/10.1210/en.2005-0317

Sullivan, R., Mieusset, R., 2016. The human epididymis: its function in sperm maturation. Hum. Reprod. Update 22, 574–587. https://doi.org/10.1093/humupd/dmw015

Sumpter, J.P., Jenkins, N., Dodd, J.M., 1978. Gonadotrophic Hormone in the Pituitary Gland of the Dogfish (Scyliorhinus canicda L.): Distribution and Physiological Significance. Gen Comp Endocrinol 36, 275–285. https://doi.org/10.1016/0016-6480(78)90034-5

Sun, S.-C., Hsu, P.-J., Wu, F.-J., Li, S.-H., Lu, C.-H., Luo, C.-W., 2010. Thyrostimulin, but Not Thyroid-stimulating Hormone (TSH), Acts as a Paracrine Regulator to Activate the TSH Receptor in Mammalian Ovary. J Biol Chem 285, 3758–3765. https://doi.org/10.1074/jbc.M109.066266

Suzuki, C., Nagasaki, H., Okajima, Y., Suga, H., Ozaki, N., Arima, H., Iwasaki, Y., Oiso, Y., 2009. Inflammatory Cytokines Regulate Glycoprotein Subunit β5 of Thyrostimulin through Nuclear Factor-κB. Endocrinology 150, 2237–2243. https://doi.org/10.1210/en.2008-0823

Świder-Al-Amawi, M., Kolasa, A., Sikorski, A., Marchlewicz, M., Baranowska-Bosiacka, I., Wiszniewska, B., 2010. The Immunoexpression of FSH-R in the Ductuli Efferentes and the Epididymis of Men and Rat: Effect of FSH on the Morphology and Steroidogenic Activity of Rat Epididymal Epithelial Cells In Vitro. J Biomed Biotechnol 2010, 1–8. https://doi.org/10.1155/2010/506762

Tan, M., Redmond, A.K., Dooley, H., Nozu, R., Sato, K., Kuraku, S., Koren, S., Phillippy, A.M., Dove, A.D., Read, T., 2021. The whale shark genome reveals patterns of vertebrate gene family evolution. eLife 10, e65394. https://doi.org/10.7554/eLife.65394

Tello, J.A., Rivier, J.E., Sherwood, N.M., 2005. Tunicate Gonadotropin-Releasing Hormone (GnRH) Peptides Selectively Activate Ciona intestinalis GnRH Receptors and the Green Monkey Type II GnRH Receptor. Endocrinology 146, 4061–4073. https://doi.org/10.1210/en.2004-1558

Tena-Sempere, M., 2005. Exploring the role of ghrelin as novel regulator of gonadal function. Growth Horm IGF Res 15, 83–88. https://doi.org/10.1016/j.ghir.2005.02.001

Tenuta, M., Carlomagno, F., Cangiano, B., Kanakis, G., Pozza, C., Sbardella, E., Isidori, A.M., Krausz, C., Gianfrilli, D., 2021. Somatotropic-Testicular Axis: A crosstalk between GH/IGF-I and gonadal hormones during development, transition, and adult age. Andrology 9, 168–184. https://doi.org/10.1111/andr.12918

Terakado, K., 2001. Induction of Gamete Release by Gonadotropin-Releasing Hormone in a Protochordate, Ciona intestinalis. Gen Comp Endocrinol 124, 277–284. https://doi.org/10.1006/gcen.2001.7728

Thompson, I.R., Kaiser, U.B., 2014. GnRH pulse frequency-dependent differential regulation of LH and FSH gene expression. Mol Cell Endocrinol 385, 28–35. https://doi.org/10.1016/j.mce.2013.09.012

Tong, J., Xie, J., Ren, H., Liu, J., Zhang, Weijia, Wei, C., Xu, J., Zhang, Wen, Li, X., Wang, W., Lv, D., He, J.C., Chen, N., 2015. Comparison of Glomerular Transcriptome Profiles of Adult-Onset Steroid Sensitive Focal Segmental Glomerulosclerosis and Minimal Change Disease. PLoS ONE 10, e0140453. https://doi.org/10.1371/journal.pone.0140453

Tricas, T.C., Maruska, K.P., Rasmussen, L.E.L., 2000. Annual Cycles of Steroid Hormone Production, Gonad Development, and Reproductive Behavior in the Atlantic Stingray. General and Comparative Endocrinology 118, 209–225. https://doi.org/10.1006/gcen.2000.7466

Tsutsui, K., Ubuka, T., 2021. Gonadotropin-inhibitory hormone (GnIH): A new key neurohormone controlling reproductive physiology and behavior. Front Neuroendocrinol 61, 100900. https://doi.org/10.1016/j.yfrne.2021.100900

Tyminski, J.P., Gelsleichter, J.J., Motta, P.J., 2015. Androgen receptors in the bonnethead, Sphyrna tiburo: cDNA cloning and tissue-specific expression in the male reproductive tract. Gen Comp Endocrinol 224, 235–246. https://doi.org/10.1016/j.ygcen.2015.08.018

Ubuka, T., Son, Y.L., Tobari, Y., Tsutsui, K., 2012. Gonadotropin-inhibitory hormone action in the brain and pituitary. Front. Endocrin. 3, 148. https://doi.org/10.3389/fendo.2012.00148

Ulloa-Aguirre, A., Zariñán, T., Jardón-Valadez, E., Gutiérrez-Sagal, R., Dias, J.A., 2018. Structure-Function Relationships of the Follicle-Stimulating Hormone Receptor. Front. Endocrinol. 9, 707. https://doi.org/10.3389/fendo.2018.00707

Vandenbrouck, Y., Pineau, C., Lane, L., 2020. The Functionally Unannotated Proteome of Human Male Tissues: A Shared Resource to Uncover New Protein Functions Associated with Reproductive Biology. J. Proteome Res. 19, 4782–4794. https://doi.org/10.1021/acs.jproteome.0c00516

Vandersmissen, H.P., Van Hiel, M.B., Van Loy, T., Vleugels, R., Vanden Broeck, J., 2014. Silencing D. melanogaster lgr1 impairs transition from larval to pupal stage. Gen Comp Endocrinol 209, 135–147. https://doi.org/10.1016/j.ygcen.2014.08.006

Venditti, M., Minucci, S., 2017. Prothymosin alpha expression in the vertebrate testis: a comparative review. Zygote 25, 760–770. https://doi.org/10.1017/S096719941700065X

Venkatesh, B., Kirkness, E.F., Loh, Y.-H., Halpern, A.L., Lee, A.P., Johnson, J., Dandona, N., Viswanathan, L.D., Tay, A., Venter, J.C., Strausberg, R.L., Brenner, S., 2007. Survey Sequencing and Comparative Analysis of the Elephant Shark (Callorhinchus milii) Genome. PLoS Biol 5, e101. https://doi.org/10.1371/journal.pbio.0050101

Venkatesh, B., Lee, A.P., Ravi, V., Maurya, A.K., Lian, M.M., Swann, J.B., Ohta, Y., Flajnik, M.F., Sutoh, Y., Kasahara, M., Hoon, S., Gangu, V., Roy, S.W., Irimia, M., Korzh, V., Kondrychyn, I., Lim, Z.W., Tay, B.-H., Tohari, S., Kong, K.W., Ho, S., Lorente-Galdos, B., Quilez, J., Marques-Bonet, T., Raney, B.J., Ingham, P.W., Tay, A., Hillier, L.W., Minx, P., Boehm, T., Wilson, R.K., Brenner, S., Warren, W.C., 2014. Elephant shark genome provides unique insights into gnathostome evolution. Nature 505, 174–179. https://doi.org/10.1038/nature12826

Vizziano, D., Fostier, A., Loir, M., Le Gac, F., 2008. Testis development, its hormonal regulation and spermiation induction in teleost fish., in: Fish Spermatology. Oxford, Alpha Science International Ltd, pp. 103–140.

Wahl, M., Levy, T., Manor, R., Aflalo, E.D., Sagi, A., Aizen, J., 2022. Genes Encoding the Glycoprotein Hormone GPA2/GPB5 and the Receptor LGR1 in a Female Prawn. Front. Endocrinol. 13, 823818. https://doi.org/10.3389/fendo.2022.823818

Wang, J., Liu, Q., Wang, Z., Sheng, X., Zhang, H., Han, Y., Yuan, Z., Weng, Q., 2019. Seasonal expressions of luteinising hormone receptor, follicle-stimulating hormone receptor and prolactin receptor in the epididymis of the male wild ground squirrel (Spermophilus dauricus). Reprod. Fertil. Dev. 31, 735. https://doi.org/10.1071/RD18262

Wang, P., Al Azad, M.A.R., Yang, X., Martelli, P.R., Cheung, K.Y., Shi, J., Shen, Y., 2021. Self-adaptive and efficient propulsion of Ray sperms at different viscosities enabled by heterogeneous dual helixes. Proc. Natl. Acad. Sci. U.S.A. 118, e2024329118. https://doi.org/10.1073/pnas.2024329118

Wang, P., Liu, S., Yang, Q., Liu, Z., Zhang, S., 2018. Functional Characterization of Thyrostimulin in Amphioxus Suggests an Ancestral Origin of the TH Signaling Pathway. Endocrinology 159, 3536–3548. https://doi.org/10.1210/en.2018-00550

Wang, P., Wang, M., Ji, G., Yang, S., Zhang, S., Liu, Z., 2017. Demonstration of a Functional Kisspeptin/Kisspeptin Receptor System in Amphioxus With Implications for Origin of Neuroendocrine Regulation. Endocrinology 158, 1461–1473. https://doi.org/10.1210/en.2016-1848

Wang, Q., Arighi, C.N., King, B.L., Polson, S.W., Vincent, J., Chen, C., Huang, H., Kingham, B.F., Page, S.T., Farnum Rendino, M., Thomas, W.K., Udwary, D.W., Wu, C.H., the North East Bioinformatics Collaborative Curation Team, 2012. Community annotation and bioinformatics workforce development in concert - Little Skate Genome Annotation Workshops and Jamborees. Database 2012, bar064. https://doi.org/10.1093/database/bar064

Wang, X., Xie, W., Yao, Y., Zhu, Y., Zhou, J., Cui, Y., Guo, X., Yuan, Y., Zhou, Z., Liu, M., 2020. The heat shock protein family gene *Hspa1l* in male mice is dispensable for fertility. PeerJ 8, e8702. https://doi.org/10.7717/peerj.8702

Wang, Yuang, Q., Niu, M., Wen, L., Fu, H., Zhou, F., Zhang, W., He, Z., 2018. Gene Silencing of Human Sertoli Cells Utilizing Small Interfering RNAs, in: Sertoli Cells: Methods and Protocols. Alves MG, Oliveira PF, editors. Sertoli Cells. 1748: Humana Press, pp. 191–202.

Weber, J.A., Park, S.G., Luria, V., Jeon, S., Kim, H.-M., Jeon, Y., Bhak, Y., Jun, J.H., Kim, S.W., Hong, W.H., Lee, S., Cho, Y.S., Karger, A., Cain, J.W., Manica, A., Kim, S., Kim, J.-H., Edwards, J.S., Bhak, J., Church, G.M., 2020. The whale shark genome reveals how genomic and physiological properties scale with body size. Proc. Natl. Acad. Sci. U.S.A. 117, 20662–20671. https://doi.org/10.1073/pnas.1922576117

Weigmann, S., 2016. Annotated checklist of the living sharks, batoids and chimaeras (Chondrichthyes) of the world, with a focus on biogeographical diversity. J Fish Biol 88, 837–1037. https://doi.org/10.1111/jfb.12874

Wetsel, W.C., Srinivasan, S., 2002. Pro-GnRH processing, in: Progress in Brain Research. Elsevier, pp. 221–241. https://doi.org/10.1016/S0079-6123(02)41096-5

Whitney, N.M., Pratt, H.L., Carrier, J.C., 2004. Group courtship, mating behaviour and siphon sac function in the whitetip reef shark, Triaenodon obesus. Anim Behav 68, 1435–1442. https://doi.org/10.1016/j.anbehav.2004.02.018

Widlak, W., Vydra, N., 2017. The Role of Heat Shock Factors in Mammalian Spermatogenesis. Adv. Anat. Embryol. Cell Biol., Advances in Anatomy, Embryology and Cell Biology 222, 45–65. https://doi.org/10.1007/978-3-319-51409-3_3

Wong, E.W.P., Cheng, C.Y., 2009. Chapter 7 Polarity Proteins and Cell–Cell Interactions in the Testis, in: International Review of Cell and Molecular Biology. Elsevier, pp. 309–353. https://doi.org/10.1016/S1937-6448(09)78007-4

Wu, H., Sun, L., Wen, Y., Liu, Y., Yu, J., Mao, F., Wang, Y., Tong, C., Guo, X., Hu, Z., Sha, J., Liu, M., Xia, L., 2016. Major spliceosome defects cause male infertility and are associated with nonobstructive azoospermia in humans. Proc. Natl. Acad. Sci. U.S.A. 113, 4134–4139. https://doi.org/10.1073/pnas.1513682113

Wu, J.-T., Lin, H.-C., Hu, Y.-C., Chien, C.-T., 2005. Neddylation and deneddylation regulate Cul1 and Cul3 protein accumulation. Nat Cell Biol 7, 1014–1020. https://doi.org/10.1038/ncb1301

Wyffels, J.T., George, R., Adams, L., Adams, C., Clauss, T., Newton, A., Hyatt, M.W., Yach, C., Penfold, L.M., 2020. Testosterone and semen seasonality for the sand tiger shark Carcharias taurus†. Biol Reprod 102, 876–887. https://doi.org/10.1093/biolre/ioz221

Xiaodong, S., Yehua, G., Jing, M., Zuoren, Y., Sai, L., Yongchao, W., Shepu, X., Daishu, H., 2002. The cloning and expression characterization of the centrosome protein genes family (centrin genes) in rat testis. Science in China. Series C, Life Sciences 45, 655 662. https://doi.org/10.1007/BF02879754

Xie, Q., Kang, Y., Zhang, C., Xie, Y., Wang, C., Liu, J., Yu, C., Zhao, H., Huang, D., 2022. The Role of Kisspeptin in the Control of the Hypothalamic-Pituitary-Gonadal Axis and Reproduction. Front. Endocrinol. 13, 925206. https://doi.org/10.3389/fendo.2022.925206

Xie, Y., Chu, L., Liu, Y., Sham, K.W.Y., Li, J., Cheng, C.H.K., 2017. The highly overlapping actions of Lh signaling and Fsh signaling on zebrafish spermatogenesis. J Endocrinol 234, 233–246. https://doi.org/10.1530/JOE-17-0079

Xing, Y., Myers, R.V., Cao, D., Lin, W., Jiang, M., Bernard, M.P., Moyle, W.R., 2004. Glycoprotein Hormone Assembly in the Endoplasmic Reticulum. J Biol Chem 279, 35437–35448. https://doi.org/10.1074/jbc.M403053200

Xiong, Y., Yu, C., Zhang, Q., 2022. Ubiquitin-Proteasome System–Regulated Protein Degradation in Spermatogenesis. Cells 11, 1058. https://doi.org/10.3390/cells11061058

Yan, L., 2021. Ggvenn: Draw Venn Diagram by Ggplot2 R package version 0.1.9.

Yang, L.-K., Zhang, J., Liu, D., Han, T.-Y., Qin, Q.-S., Wang, A.-Q., Dong, B., 2023. Ancestral glycoprotein hormone and its cognate receptor present in primitive chordate ascidian: Molecular identification and functional characterization. Int J Biol Macromol 229, 401–412. https://doi.org/10.1016/j.ijbiomac.2022.12.297

Yang, X., Wu, Y., Zhang, S., Gan, R., Wang, Z., Zhang, L., Zhang, W., 2024. Expression of Tshb and Tshr in the ricefield eel Monopterus albus: Potential paracrine/autocrine roles in gonads. Gen Comp Endocrinol 114580. https://doi.org/10.1016/j.ygcen.2024.114580

Yin, Y., Liu, L., Yang, C., Lin, C., Veith, G.M., Wang, C., Sutovsky, P., Zhou, P., Ma, L., 2016. Cell Autonomous and Nonautonomous Function of CUL4B in Mouse Spermatogenesis. J Biol Chem 291, 6923–6935. https://doi.org/10.1074/jbc.M115.699660

Yin, Y., Zhu, L., Li, Q., Zhou, P., Ma, L., 2021. Cullin4 E3 Ubiquitin Ligases Regulate Male Gonocyte Migration, Proliferation and Blood-Testis Barrier Homeostasis. Cells 10, 2732. https://doi.org/10.3390/cells10102732

Young, B.A., Bryan, M.B., Glenn, J.R., Yun, S.S., Scott, A.P., Li, W., 2007. Dose–response relationship of 15α-hydroxylated sex steroids to gonadotropin-releasing hormones and pituitary extract in male sea lampreys (Petromyzon marinus). Gen Comp Endocrinol 151, 108–115. https://doi.org/10.1016/j.ygcen.2006.12.005

Yuan, W., Leisner, T.M., McFadden, A.W., Clark, S., Hiller, S., Maeda, N., O'Brien, D.A., Parise, L.V., 2006. CIB1 Is Essential for Mouse Spermatogenesis. Molecular and Cellular Biology 26, 8507–8514. https://doi.org/10.1128/MCB.01488-06

Zeng, R., Wang, Z., Li, X., Chen, Y., Yang, S., Dong, J., 2020. Cyclin-dependent kinase 1-mediated phosphorylation of protein kinase N1 promotes anchorage-independent growth and migration. Cell Signal 69, 109546. https://doi.org/10.1016/j.cellsig.2020.109546

Zhang, M., Wei, H., Liu, T., Li, W., Li, Y., Wang, S., Xing, Q., Hu, X., Zhang, L., Bao, Z., 2020. Potential GnRH and steroidogenesis pathways in the scallop Patinopecten yessoensis. J Steroid Biochem Mol Biol 204, 105756. https://doi.org/10.1016/j.jsbmb.2020.105756

Zhang, Y., Gao, H., Li, H., Guo, J., Ouyang, B., Wang, M., Xu, Q., Wang, Jiahao, Lv, M., Guo, X., Liu, Q., Wei, L., Ren, H., Xi, Y., Guo, Y., Ren, B., Pan, S., Liu, C., Ding, X., Xiang, H., Yu, Y., Song, Y., Meng, L., Liu, Shanshan, Wang, Jun, Jiang, Y., Shi, J., Liu, Shiping, Sabir, J.S.M., Sabir, M.J., Khan, M., Hajrah, N.H., Ming-Yuen Lee, S., Xu, X., Yang, H., Wang, Jian, Fan, G., Yang, N., Liu, X., 2020. The White-Spotted Bamboo Shark Genome Reveals Chromosome Rearrangements and Fast-Evolving Immune Genes of Cartilaginous Fish. iScience 23, 101754. https://doi.org/10.1016/j.isci.2020.101754

Zhang, Z.-H., Jiang, T.-X., Chen, L.-B., Zhou, W., Liu, Y., Gao, F., Qiu, X.-B., 2021. Proteasome subunit α4s is essential for formation of spermatoproteasomes and histone degradation during meiotic DNA repair in spermatocytes. JBC 296, 100130. https://doi.org/10.1074/jbc.RA120.016485

Zhao, C., Zhang, Z., Qu, X., Bai, X., Liu, X., Tao, W., Zhou, L., Wang, D., Wei, J., 2022. Desert hedgehog mediates the proliferation of medaka spermatogonia through Smoothened signaling. Reproduction 163, 209–218. https://doi.org/10.1530/REP-21-0468

Zheng, B., Zhou, Q., Guo, Y., Shao, B., Zhou, T., Wang, L., Zhou, Z., Sha, J., Guo, X., Huang, X., 2014. Establishment of a proteomic profile associated with gonocyte and spermatogonial stem cell maturation and differentiation in neonatal mice. Proteomics 14, 274–285. https://doi.org/10.1002/pmic.201300395

Zheng, M., Shi, H., Segaloff, D.L., Van Voorhis, B.J., 2001. Expression and Localization of Luteinizing Hormone Receptor in the Female Mouse Reproductive Tract. Biol Reprod 64, 179–187. https://doi.org/10.1093/biolreprod/64.1.179

Zirkin, B.R., Papadopoulos, V., 2018. Leydig cells: formation, function, and regulation†. Biol Reprod 99, 101–111. https://doi.org/10.1093/biolre/ioy059

Živković, D., Sanchez Dafun, A., Menneteau, T., Schahl, A., Lise, S., Kervarrec, C., Toste Rêgo, A., da Fonseca, P.C.A., Chavent, M., Pineau, C., Burlet-Schiltz, O., Marcoux, J., Bousquet, M.-P., 2022. Proteasome complexes experience profound structural and functional rearrangements throughout mammalian spermatogenesis. Proc. Natl. Acad. Sci. U.S.A. 119, e2116826119. https://doi.org/10.1073/pnas.2116826119

Zubeyde, B.-W., Sienz, M.A., Knight, J., 2021. Endocrine system 2: hypothalamus and pituitary gland. Nurs Times 117, 49. https://doi.org/PMID: 17951176

## Évolution des systèmes GnRH et des hormones glycoprotéiques dans les contrôles endocrine et paracrine de la spermatogenèse chez la roussette, *Scyliorhinus canicula*

**Résumé**

La spermatogenèse est un processus hautement spécialisé de prolifération et de différenciation cellulaire conduisant à la production de spermatozoïdes haploïdes à partir de cellules souches spermatogoniales diploïdes. Chez les Gnathostomes, les fonctions testiculaires sont principalement contrôlées de façon endocrine par l'axe hypothalamo-hypophyso-gonadique (HHG) impliquant notamment les GnRHs hypothalamiques et les hormones gonadotropes, FSH et LH, dont l'émergence s'est produite à la racine des Vertébrés cartilagineux. De plus, des fonctions paracrines des GnRHs et de la thyrostimuline ont été explorées au niveau gonadique chez des Vertébrés osseux. L'objet de cette thèse était de caractériser les régulations endocrines et paracrines de la spermatogenèse médiées par les GnRHs et les hormones gonadotropes chez un modèle Élasmobranche, la roussette *Scyliorhinus canicula*. Ce travail a été étendu à la caractérisation de GPA2 et GPB5, constituant la thyrostimuline, qui correspondent aux orthologues des ancêtres moléculaires des sous-unités des hormones glycoprotéiques. Dans ce travail, l'évolution du protéome testiculaire au cours de la spermatogenèse de *S. canicula* a été décrite, les neuropeptides GnRHs, les hormones glycoprotéiques FSH, LH, TSH, GPA2 et GPB5, et leurs récepteurs associés ont fait l'objet d'analyses *in silico* et d'expressions dans différents tissus avec un focus au cours de la spermatogenèse. Il a été observé une expression à tous les stades de la spermatogenèse de *fshr*, *lhr* et des récepteurs aux GnRHs au niveau germinale et sertolien, de *tshr* et *gpb5* au niveau sertolien et de *gpa2* au niveau germinal, avec des abondances plus importantes associées aux stades spermatides. Ce travail a été complété par des tests fonctionnels *in vitro* qui ont montré que FSHR pouvait être activé par FSH et LH, LHR uniquement par LH, et que GPB5-GPA2 pouvait activer les trois récepteurs FSHR, LHR et TSHR, suggérant ainsi un rôle paracrine de la thyrostimuline au niveau testiculaire. L'ensemble de ce travail permet de proposer un modèle de régulation de la spermatogenèse chez les Élasmobranches qui associe des hormones endocrines, avec les GnRHs et gonadotropines circulantes, et des hormones paracrines, avec GPA2, GPB5 et les stéroïdes. Ce modèle apparaît cohérent et intermédiaire dans l'évolution des systèmes régulateurs de la spermatogenèse qui seraient passés d'une régulation paracrine prépondérante chez les Bilatériens non-Vertébrés à une régulation endocrine prépondérante chez les Vertébrés osseux avec la mise en place de l'axe hypothalamo-hypophyso-gonadique.

**Mots-clefs : Spermatogenèse, Stéroïdogenèse, *Scyliorhinus canicula*, Régulations endocrine et paracrine, Hormones glycoprotéiques, Gonadolibérines, Évolution**

---

## Evolution of GnRH and glycoprotein hormone systems in endocrine and paracrine controls of spermatogenesis in the catshark, *Scyliorhinus canicula*

**Abstract**

Spermatogenesis is a highly specialized process of cell proliferation and differentiation leading to the production of haploid spermatozoa from diploid spermatogonial stem cells. In Gnathostomes, testicular functions are mainly controlled by the endocrine hypothalamic-pituitary-gonadal (HHG) axis, involving hypothalamic GnRHs and the gonadotropic hormones FSH and LH, which emerged at the root of cartilaginous vertebrates. In addition, paracrine functions of GnRHs and thyrostimulin have been explored at the gonadic level in bony vertebrates. The aim of this thesis was to characterize the endocrine and paracrine regulation of spermatogenesis exerted by GnRHs and gonadotropic hormones in an Elasmobranch model, the catshark *Scyliorhinus canicula*. This work has been extended to the characterization of GPA2 and GPB5, constituting thyrostimulin, which correspond to orthologs of the molecular ancestors of glycoprotein hormone subunits. In this work, the evolution of the testicular proteome during spermatogenesis in *S. canicula* was described, and the neuropeptides GnRHs, the glycoprotein hormones FSH, LH, TSH, GPA2 and GPB5, as well as their associated receptors were studied by *in silico* and expression analyses in different tissues, with a focus on spermatogenesis. Expressions were observed at all stages of spermatogenesis for *fshr*, *lhr* and GnRH receptors associated at germinal and sertolian levels, for *tshr* and *gpb5* at sertolian level and for *gpa2* at germinal level, with higher abundances associated with spermatid stages. This work was complemented by *in vitro* functional tests which showed that FSHR could be activated by FSH and LH, LHR only by LH, and that GPB5-GPA2 could activate all three receptors FSHR, LHR and TSHR, suggesting a paracrine role for thyrostimulin at the testicular level. Taken together, this work proposes a model for the regulation of spermatogenesis in Elasmobranchs that combines endocrine hormones, with circulating GnRHs and gonadotropins, and paracrine hormones, with GPA2, GPB5 and steroids. This model appears consistent and intermediate in the evolution of spermatogenesis regulating systems, which has shift from predominantly paracrine regulation in non-vertebrate bilaterians to predominantly endocrine regulation in bony vertebrates, with the establishment of the hypothalamic-pituitary-gonadal axis.

**Keywords: Spermatogenesis, Steroidogenesis, *Scyliorhinus canicula*, Endocrine and paracrine regulations, Glycoprotein hormones, Gonadotropin-releasing hormones, Evolution**

Discipline : Aspects moléculaires et cellulaires de la biologie

Université de Caen Normandie, MNHN, SU, UA, CNRS, IRD, Laboratoire de Biologie des Organismes et Ecosystèmes Aquatiques (BOREA), UMR 8067, 14032 Caen cedex 5, France.